University of Huddersfield Repository

Manchester, Kieran R.

The Physicochemical and Pharmacokinetic Properties of Benzodiazepines Appearing as New Psychoactive Substances

Original Citation

Manchester, Kieran R. (2019) The Physicochemical and Pharmacokinetic Properties of Benzodiazepines Appearing as New Psychoactive Substances. Doctoral thesis, University of Huddersfield.

This version is available at http://eprints.hud.ac.uk/id/eprint/34997/

University of Huddersfield

School of Applied Sciences

The Physicochemical and Pharmacokinetic Properties of Benzodiazepines Appearing as New Psychoactive Substances

Kieran Manchester

A thesis submitted to the University of Huddersfield in
partial fulfilment of the requirements for the degree of
Doctor of Philosophy, January 2019

Copyright Statement

(i) The author of this thesis (including any appendices and/or schedules to this thesis) owns any copyright in it (the "Copyright") and s/he has given The University of Huddersfield the right to use such Copyright for any administrative, promotional, educational and/or teaching purposes.

(ii) Copies of this thesis, either in full or in extracts, may be made only in accordance with the regulations of the University Library. Details of these regulations may be obtained from the Librarian. Details of these regulations may be obtained from the Librarian. This page must form part of any such copies made.

(iii) The ownership of any patents, designs, trademarks and any and all other intellectual property rights except for the Copyright (the Intellectual Property Rights) and any reproductions of copyright works, for example graphs and tables (Reproductions), which may be described in this thesis, may not be owned by the author and may be owned by third parties. Such Intellectual Property Rights and Reproductions cannot and must not be made available for use without permission of the owner(s) of the relevant Intellectual Property Rights and/or Reproductions.

Acknowledgements

I would like to express my sincere gratitude to my supervisors, Dr Peter Maskell and Professor Laura Waters, firstly for the opportunity to complete a PhD and secondly for all the help, support and encouragement I have received from them over the past three years.

I would also like to thank Dr Fiona Dempsey for the large amount of time she set aside to train me in cell culture and for answering my many queries about cells and to Dr Jack Blackburn for the hours he contributed towards running my analytical samples and compiling results.

I would like to thank my family, firstly my fianceé Jeanna for her understanding and patience during the long days and evenings I spent writing my thesis and also for her constant support. I would also like to thank my parents, brother and grandad for their encouragement and also for their concern about whether I was going to remain a student forever.

I would also like to thank my three cats, Oscar, Max and Nala for the company and the near-constant source of entertainment that they provided me during the course of writing my thesis.

Abstract

Benzodiazepines are a class of compounds that were initially developed for medicinal purposes. Multiple benzodiazepines have appeared as 'new psychoactive substances' on the illicit drug market and have never been developed for medicinal use. Very little pharmacokinetic data exists regarding them. This information is valuable as it allows the prediction and interpretation of their effects in humans and aids with forensic and toxicological work.

In this work the lipophilicity ($\log D_{7.4}$), the pK_a and the plasma protein binding were determined for benzodiazepines appearing as new psychoactive substances and these were compared to theoretical values from software packages. ACD/I-LAB returned the most accurate values for $\log D_{7.4}$ and plasma protein binding while ADMET Predictor returned the most accurate values for pK_a. None of the software packages were able to predict parameters to a sufficient degree of accuracy and *in vitro* data is currently preferable.

An improved relationship to calculate the volume of distribution at steady state (Vd_{ss}) by using the Øie-Tozer equation, the $\log D_{7.4}$, the pK_a and the plasma protein binding of benzodiazepines was developed. The Vd_{ss} of benzodiazepines could be predicted to within a 1.11-fold accuracy.

The blood to plasma concentration ratios of six benzodiazepines appearing as new psychoactive substances were determined. Despite the small dataset a large variation in ratios was observed, from 0.57 for phenazepam to 1.18 for pyrazolam, highlighting the need for accurate pharmacokinetic data.

The metabolic characterisation of illicit compounds is an important aid in toxicological interpretations. This is commonly performed *in vitro* using human hepatocellular carcinoma cell lines and the choice of cell line is crucial in order to obtain reliable results. The C3A and HepaRG cell lines were characterised with respect to six major phase I metabolic enzymes. HepaRG was shown to have a greater expression of these enzymes and thus have a superior utility in a metabolic study.

The metabolism of 12 benzodiazepines appearing as new psychoactive substances was investigated with the HepaRG cell line. Some of the benzodiazepines were observed to have different metabolic pathways to those previously reported. This again highlights the need for accurate experimental data in order to assess the pharmacokinetics of new psychoactive substances.

Publications and Conference Presentations Arising From This Thesis

Publications Arising from this Thesis

Portions of this work have been published and these publications are listed henceforth. The publications can be found in full in the Appendix.

- K R Manchester, E C Lomas, L Waters, F C Dempsey, P D Maskell, The emergence of new psychoactive substance (NPS) benzodiazepines: A review., Drug Testing and Analysis, 2018, 10, 37-53, doi: 10.1002/dta.2211

- L Waters, K R Manchester, P D Maskell, C Haegeman, S Haider, The use of a quantitative structure-activity relationship (QSAR) model to predict $GABA_A$ receptor binding of newly emerging benzodiazepines, Science & Justice, 2018, doi: 10.1016/j.scijus.2017.12.004

- K R Manchester, L Waters, P D Maskell, Experimental versus theoretical log $D_{7.4}$, pK_a and plasma protein binding values for benzodiazepines appearing as new psychoactive substances, Drug Testing and Analysis, 2018, doi: 10.1002/dta.2387

Conference Presentations Arising from this Thesis

- 2018 United Kingdom and Ireland Association of Forensic Toxicologists (UKIAFT) London conference: Benzodiazepines as new psychoactive substances: a history and pharmacokinetic perspective.

Contents

List of Tables

List of Figures

Chapter 1

Introduction

1.1 Substance abuse

The term 'substances of abuse' commonly refers to three categories of compounds; specific drugs of abuse, medications and toxins [1]. Substances have been abused for hundreds if not thousands of years as a result of their psychoactive effects [2]. Psychoactive substances are broadly defined as:

"compounds that when consumed can affect the central nervous system of a person by stimulation or depression resulting in hallucinations or a significant disturbance, or significant change to, motor function, thinking, behaviour, perception, awareness or mood." [3,4]

The earliest substances of abuse were plant-based, for example; alcohol, opium, cocaine and cannabis [2]. Various cooperative international attempts have been made to control the trade and supply of illicitly-used compounds as a result of their damaging effects upon health. The Single Convention on Narcotic Drugs of 1961 aimed to control cannabis and a variety of opioids [5]. This was followed by the Convention on Psychotropic Substances of 1971 which aimed to control compounds not specified in the previous convention such as; phenethylamines, tryptamines, cathinones, synthetic cannabinoids, barbiturates and benzodiazepines [6]. All of

these substances are commonly abused [1]. In order to circumvent and evade these international controls, a variety of compounds have emerged and are abused that are not regulated under either convention [7]. This circumvention of existing legislation is often known as a 'cat and mouse game' and is exemplified by the appearance of compounds differing by a single atom from those that are controlled substances [8]. Compounds that appear as substances of abuse and that are not under international control are known as 'new psychoactive substances' (NPS) [9]. In terms of the control of new psychoactive substances in the United Kingdom; the Psychoactive Substances Bill became law in 2016 [7]. This law aimed to control any substances which were not under control of the Misuse of Drugs Act 1971 and were capable of producing a psychoactive effect, with exemptions for compounds such as caffeine, alcohol and tobacco [7].

1.2   The Rise of New Psychoactive Substances

NPS are defined by the United Nations Office on Drugs and Crime (UNODC) as being:

"substances of abuse, either in a pure form or a preparation, that are not controlled by the 1961 Single Convention on Narcotic Drugs or the 1971 Convention on Psychotropic Substances, but which may pose a public health threat."[9]

The word 'new' refers to the substance appearing on the illicit drug market and not whether it is an entirely new compound. Many of these compounds have been previously synthesised and patented during the early stages of drug development [9]. NPS are usually grouped by similarity in structure and pharmacological mechanism of action. These include synthetic cannabinoids, cathinones, opioids, phenylethylamines, piperazines, tryptamines, benzodiazepines and plant derivatives such as khat [10-19].

In Europe, the European Monitoring Centre for Drugs and Drug Addiction (EMCDDA) is responsible for monitoring the availability and illicit use of NPSs [20]. The number of NPSs has increased markedly in recent years and peaked in 2014 with 101 compounds being reported to the EMCDDA. This total then decreased to 98 compounds in 2015, to 66 compounds in

2016 and to 51 compounds in 2017 [21-24]. This increase and decrease can be seen in Figure 1.1 with the data obtained from the EMCDDA [20-22,25-31]. In total over 620 compounds are currently monitored in Europe by the EMCDDA as NPS [31].
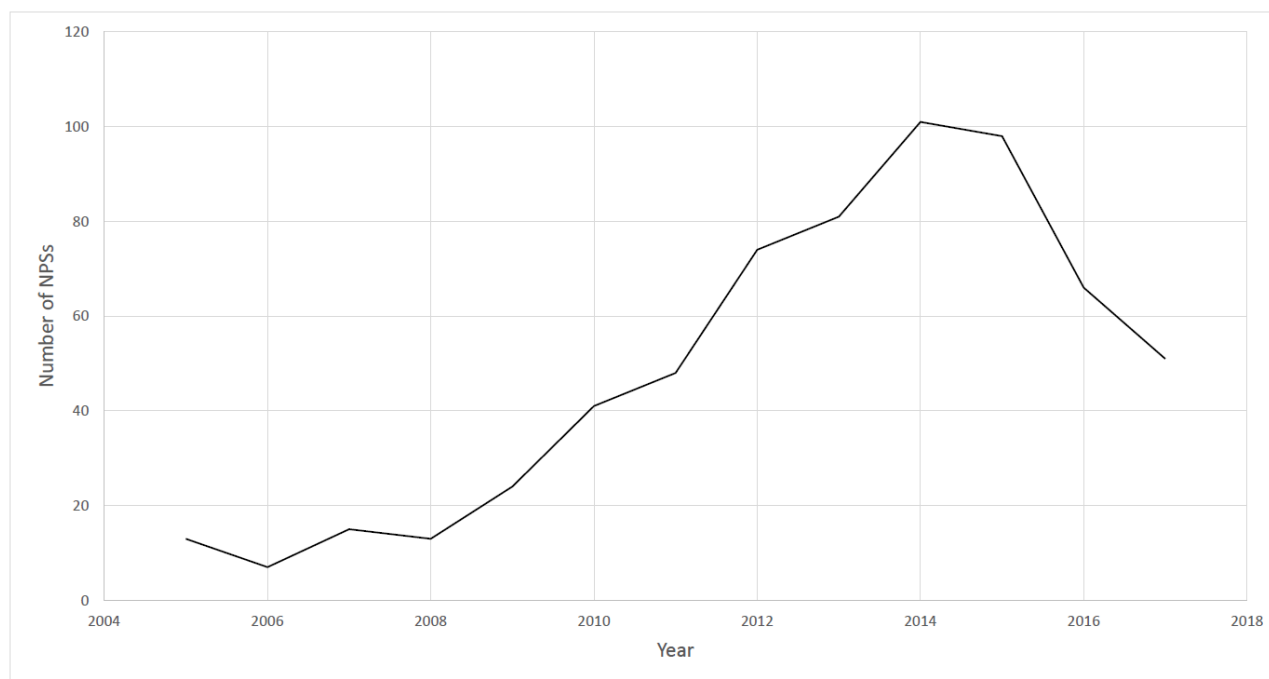
Figure 1.1: Number of NPSs reported to the EU Early Warning System by year since 2005 [20-22,25-31].

1.3 Benzodiazepines as Medicinally-Important Compounds

One group of NPSs to emerge are the benzodiazepines which were initially developed for medicinal use [16,32]. Benzodiazepines have sedative, anticonvulsant and anxiolytic properties and are medicinally important for the treatment of epilepsy, anxiety, muscle spasms and alcohol withdrawal syndrome [33-38]. Benzodiazepines are typically prescribed on a short-term basis as longer durations of use can lead to cognitive problems such as amnesia, tolerance and dependence [38-41]. Severe withdrawal symptoms can occur with abrupt discontinuation of use [42,43]. Benzodiazepines succeeded the use of barbiturates in most medicinal areas as their lower addictive nature purportedly left them less open to abuse [44].

1.4   Benzodiazepines as Drugs of Abuse

Despite having a lower abuse liability and being less addictive than the barbiturates, the anxiolytic and sedative effects of benzodiazepines still cause them to be misused [45,46]. Benzodiazepines are often misused concurrently with opioids, often to increase the effects gained from the use of either of these drugs in isolation [47-52]. It is thought that rather than affect the pharmacokinetics of opioids, co-ingestion of benzodiazepines with opioids instead affects the pharmacodynamics of opioids [48]. Research suggests that at least some of the analgesic, anxiolytic effects of benzodiazepines are as a result of their binding to opioid receptors [53-56]. It is suggested that benzodiazepines increase the 'high' or rewarding effects of opioid ingestion [57,58]. The pharmacodynamics of benzodiazepines will be discussed in greater detail in Section 1.9.

The co-ingestion of benzodiazepines and opioids can lead to respiratory depression and death [59-61]. The main binding site for benzodiazepines, the $GABA_A$ receptor (see Section 1.9), is co-expressed in the central nervous system (CNS) with opioid receptors [62]. It is thought that both receptors are co-expressed in areas of the CNS that are responsible for ventilatory control and interactions of opioids and benzodiazepines at these sites may contribute to respiratory depression [60]. Benzodiazepine use in combination with alcohol is known to lead to excessive sedation and it has also been reported that high levels of alcohol and benzodiazepine intake can also cause respiratory depression [63,64].

Benzodiazepines are widely misused in the UK. For example, one report indicated that benzodiazepines (including prescription diazepam and the new psychoactive substance etizolam, see Section 1.6) were implicated or involved in 552 drug-related deaths (DRDs) in Scotland in 2017 (59 % of the total). In 336 out of 552 DRDs, the only drugs found to be present were benzodiazepines which were also new psychoactive substances. In the majority of these the benzodiazepine was etizolam [65]. In England and Wales, benzodiazepines were involved in 6383 DRDs from 1993 - 2016 [66]. The benzodiazepine found in the majority of these cases was diazepam (53 %) and DRDs involving benzodiazepines were noted to be increasing [66].

Another form of misuse for benzodiazepines comes from attempted self-medication by users [67,68]. Research conducted in the UK using an online questionnaire suggests that the most common reasons given by users for self-medication were to help with sleep (66 % of respondents) and to cope with stress (37 %) [69].

The side-effects caused by benzodiazepine use when under prescription was recognised very early on in the 1960s [70,71]. Dependence and addiction were reported when using benzodiazepines long-term, as was severe withdrawal syndrome following abrupt discontinuation of use [72]. Their side-effects and their potential for misuse led to 35 benzodiazepines and their closely-related derivatives being placed under control by the United Nations (UN) Convention on Psychotropic Substances of 1971 [6].

In terms of comparison to other substances of abuse, benzodiazepines are held to have a greater potential for physical harm than drugs such as alcohol, cannabis, LSD and ecstasy, a greater potential for dependence than drugs such as ketamine, amphetamine, cannabis, LSD and ecstasy and a greater potential for social harm than amphetamine, cannabis, LSD and ecstasy [73].

1.5   The Structure of Benzodiazepines

The most common benzodiazepines are the 1,4-benzodiazepines. Their basic structure is a fused benzene ring and a diazepine ring with an additional phenyl ring typically being present at position 5 (Figure 1.2A). Other benzodiazepines exist, such as 1,5-benzodiazepines and 2,3-benzodiazepines but their use is outside the scope of this research as they are not thought to be illicitly used in a widespread manner, possibly as a result of their lack of sedative effects when compared to 1,4-benzodiazepines [74-76]. In addition to 1,4-benzodiazepines, a number of derivatives exist that are often grouped under the generic umbrella of 'benzodiazepines' as they have similar structures and they act on the same pharmacological target [16]. These include triazolobenzodiazepines (Figure 1.2B), oxazolobenzodiazepines (Figure 1.2C) and thienotriazolodiazepines (Figure 1.2D). Despite the thienotriazolodiazepines not being 'true' benzodiazepines in the sense that they contain a thiophene ring rather than a benzene ring, they are

often grouped together as 'benzodiazepines' as they have the same pharmacological mechanism of action and similar pharmacokinetics [77]. For simplicity this trend will be continued in this work.

Benzodiazepines are often substituted with functional groups at various positions. These typically take the form of a halogen atom (Cl, Br, F) or nitro group (NO_2) substitution at position 2 (Figure 1.2D), position 7 (Figures 1.2A and 1.2E) or position 8 (Figure 1.2B). Substitution on position 1 (Figure 1.2A and Figure 1.2B) by an amine-, alkane- or alkene-containing group is common. Less common but still observed is substitution at position 3 (Figure 1.2A) with a hydroxyl or methyl group. The R2' position on the phenyl ring often has a substituent, usually a halogen atom. The majority of benzodiazepines that do not have an additional triazole ring (i.e. 1,4-benzodiazepines) contain a carbonyl group on position 2 (Figure 1.2A).
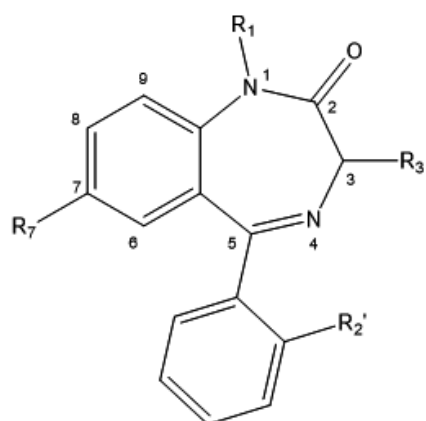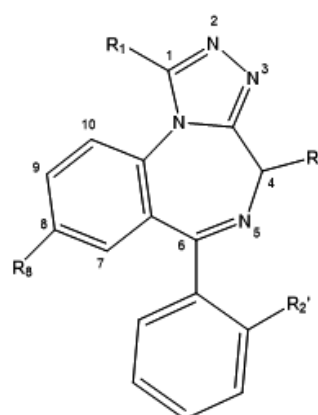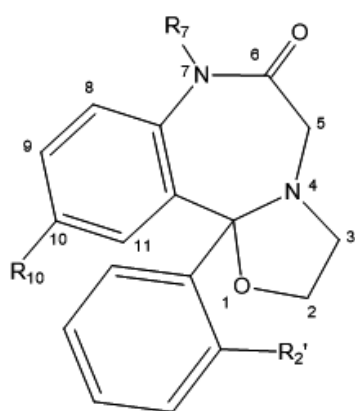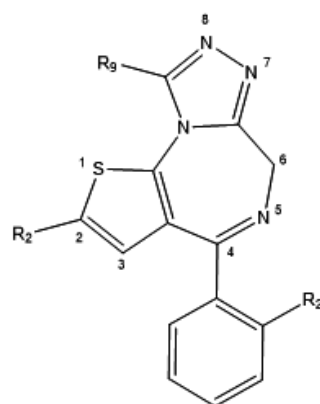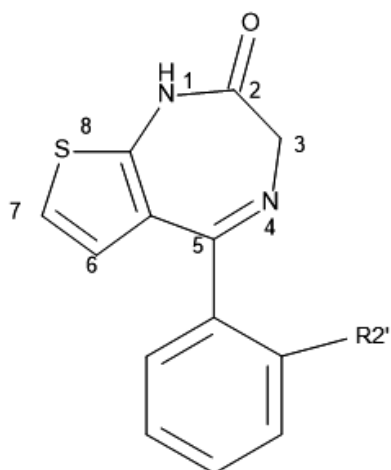
Figure 1.2: Structures of a 1,4-benzodiazepine, a triazolobenzodiazepine, an oxazolobenzodiazepine, a thienotriazolodiazepine and a thienodiazepine.

1.6   Benzodiazepines as New Psychoactive Substances

There are currently 27 benzodiazepines that have emerged on the illicit drug market as NPSs (Table 1.1, data collected from the EMCDDA). To distinguish these benzodiazepines from those that are used medicinally, the term "NPS-benzodiazepine(s)" will be used from here onwards to refer to them.

In addition to the benzodiazepines controlled under the UN Convention on Psychotropic Substances 1971, there are other benzodiazepines that are medically-licensed and prescribed in various countries around the world. By virtue of existing outside of this legislation, when they are used illicitly in countries where they are not licensed they are denoted as being NPS. Three of these to appear as NPSs are phenazepam (originally prescribed in Russia), etizolam (originally prescribed in Japan and India) and flutazolam (originally prescribed in Japan) [78-80]. Other NPS-benzodiazepines to appear were simply patented and not developed further into marketable drugs (e.g. pyrazolam), are metabolites of medically-used benzodiazepines (e.g. desalkylflurazepam) or never gained marketing approval (e.g. adinazolam) [16,81,82]. A summary of the names of these compounds, the year that they were patented (if any) and the year that they were reported to the EMCDDA is shown in Table 1.1 [20-22,25-31].

In Europe, 1,4-benzodiazepines, triazolobenzodiazepines, oxazolobenzodiazepines, thienodiazepines and thienotriazolodiazepines have all appeared as NPSs [16]. Their names and structures are listed in Tables 1.2 to 1.6.

Table 1.1: NPS-benzodiazepine, year patented and year reported to the EMCDDA

Compound	Year patented	Year reported to the EMCDDA	References
3-Hydroxyphenazepam	Not reported	2016	[31]
4'-Chlorodiazepam	1964	2016	[31,83]
Adinazolam	1976	2015	[22,84]
Bentazepam	1978	2018	[85,86]
Bromazolam	1976	2016	[31,87]
Clonazolam	1971	2015	[22,88]
Cloniprazepam	Not reported	2016	[31]
Desalkylflurazepam	Not reported	2016	[89]
Deschloroetizolam	1998	2014	[21,89]
Desmethylflunitrazepam	1963	2016	[31,91]
Diclazepam	1964	2013	[29,83]
Difludiazepam	1970	2017	[92,93]
Etizolam	1978	2011	[27,94]
Flualprazolam	Not reported	2018	[95]
Flubromazepam	1962	2013	[29,96]
Flubromazolam	1978	2014	[21,97]
Fluclotizolam	1979	2018	[95,98]
Flunitrazolam	Not reported	2016	[31]
Flutazolam	1970	2014	[86,99]
Meclonazepam	1975	2014	[21,100]
Methyl-clonazepam	Not reported	2018	[95]
Metizolam	1988	2015	[22,101]
Nifoxipam	1985	2015	[22,91]
Nitrazolam	1971	2015	[22,102]
Phenazepam	1974	2007	[20,78]
Pyrazolam	1979	2012	[28,103]
Thionordazepam	1972	2017	[104,105]

Table 1.2: The substitutions of 1,4-benzodiazepines appearing as NPSs (From Figure 1.2A)

Compound	R1	R2'	R3	R7	R4'	R6'
3-Hydroxyphenazepam	H	Cl	OH	Br	H	H
4'-Chlorodiazepam	CH_3	H	H	Cl	Cl	H
Adinazolam	CH_3	H	H	Cl	Cl	H
Cloniprazepam	Methylcyclopropane	Cl	H	NO_2	H	H
Desalkylflurazepam	H	F	H	Cl	H	H
Desmethylflunitrazepam	H	F	H	NO_2	H	H
Diclazepam	CH_3	Cl	H	Cl	H	H
Difludiazepam	CH_3	F	H	Cl	H	F
Flubromazepam	H	F	H	Br	H	H
Meclonazepam	H	Cl	CH_3	NO_2	H	H
Methyl-clonazepam	CH_3	Cl	H	NO_2	H	H
Nifoxipam	H	F	OH	NO_2	H	H
Phenazepam	H	Cl	H	Br	H	H
Thionordazepam[1]	H	H	H	Cl	H	H

[1]Thionordazepam has a sulphur atom rather than an oxygen atom at the R2 position

Table 1.3: The substitutions of triazolobenzodiazepines appearing as NPSs (From Figure 1.2B)

Compound	R1	R2'	R8
Adinazolam	$CH_2N(CH_3)_3$	H	Cl
Bromazolam	CH_3	H	Br
Clonazolam	CH_3	Cl	NO_2
Flualprazolam	CH_3	F	Cl
Flubromazolam	CH_3	F	Br
Flunitrazolam	CH_3	F	NO_2
Nitrazolam	CH_3	H	NO_2
Pyrazolam[1]	CH_3	None	Br

[1]Pyrazolam has a pyridine ring rather than a phenyl ring at position 6

Table 1.4: The substitutions of thienotriazolobenzodiazepines appearing as NPSs (From Figure 1.2C)

Compound	R2	R2'	R9
Deschloroetizolam	CH_2CH_3	H	CH_3
Etizolam	CH_2CH_3	Cl	CH_3
Fluclotizolam	Cl	F	CH_3
Metizolam	CH_2CH_3	Cl	H

Table 1.5: The substitutions and name of a thienodiazepine appearing as an NPS (From Figure 1.2D)

Compound	R2'	R7	R10
Bentazepam[1]	H	H	H

[1]Bentazepam has an additional benzene ring (part of a benzothiophene system) attached to its thiophene ring

Table 1.6: The substitutions and name of an oxazolobenzodiazepine appearing as an NPS (From Figure 1.2E)

Compound	R2'	R7	R10
Flutazolam[1]	F	CH_2CH_2OH	Cl

1.7   Physicochemical Properties of Benzodiazepines

The physicochemical properties of compounds affect their pharmacokinetics and pharmaco-dynamics. Therefore knowledge of physicochemical properties is an important prerequisite in pharmaceutical development and is also important for the prediction of pharmacokinetic properties [106,107]. This will be expanded upon in the relevant Sections (1.7.1 and 1.7.2) of this work. Two physicochemical properties will be discussed here with regards to benzodiazepines; their lipophilicity and their pK_a.

1.7.1   Lipophilicity

The lipophilicity of a compound is commonly measured by the partition constant (P), a ratio of the distribution between two phases; water and an organic phase such as octanol [105]. Compounds interact with organic phases via Van der Waals forces and with a water phase via hydrogen bonding or dipolar forces [108]. When the partition coefficient is measured with an aqueous phase other than water, it is known as the distribution coefficient (D). The most common aqueous phase for the measurement of D is a buffer with a pH mimicking the pH of physiological system, for example 7.4 for the human body [109]. This will be referred to henceforth as the log $D_{7.4}$. The values for P and D are usually given as the base-10 logarithm and denoted as log P or log $D_{7.4}$ respectively for ease of comparison between different molecules.

The lipophilicity of a molecule affects its absorption within the body. Highly lipophilic drugs are hydrophobic and poorly soluble in aqueous solutions which can have implications for their absorption inside the body in gastrointestinal fluid or blood [110]. Cell membranes are commonly accepted to consist of phospholipids arranged in a bilayer formation [111]. The transfer of drugs across the cell membrane is mediated by two processes, active transport and passive diffusion. For most drugs, passage across the cell membrane occurs by passive diffusion and the effect of lipophilicity on this process has been well-reviewed [112]. Drugs that are too lipophilic typically exhibit a preferential association with the cell membrane and have poor absorption across the membrane into target tissues [112].

Following absorption into the body, the distribution of a compound within the body is also affected by its lipophilicity. Drugs that are very lipophilic can engage in off-target binding to other structures within the body which is generally referred to as drug promiscuity [113]. Drug promiscuity is undesirable as exemplified by the propensity of highly-lipophilic compounds to bind to the human ether-a-go-go related gene (hERG)-encoded potassium channel and cause fatal cardiac arrhythmias [114,115]. A higher lipophilicity is also typically associated with increased plasma protein binding which will be discussed in further detail in Section 1.8.1 [116]. As a general rule the more lipophilic a compound is, the easier it is for the compound to cross the blood-brain barrier (BBB) and distribute within the brain [117]. However many highly-lipophilic drugs often experience a lower than expected BBB partition as a result of them being substrates for ATP-binding cassette (ABC) transporters which are highly-efficient proteins capable of quickly removing compounds from the central nervous system [117,118].

The majority of drugs are metabolised in the liver by the oxidative CYP450 enzyme family and this pharmacokinetic process will be discussed in greater detail in Section 1.8.4 [119,120]. Lipophilicity affects CYP450 enzyme metabolism and the relationship generally follows a parabolic arc; compound affinity increases for CYP450 enzymes up to a certain value for lipophilicity and thereafter the affinity rapidly decreases as a result of the compound being too hydrophobic [121,122].

The excretion of a compound also has the potential to be affected by its lipophilicity. As many drugs are excreted via the kidneys in a process known as glomerular filtration they require a reasonable degree of water solubility. Drugs that are highly lipophilic may not be adequately metabolised into hydrophilic compounds and must be reabsorbed and metabolised into more hydrophilic compounds in order to facilitate their excretion [123].

The previously-discussed effects of lipophilicity on absorption, distribution, metabolism and excretion means that it is an important parameter in the initial stages of drug development [110,124].

Attempts are often made to relate physicochemical parameters and/or molecular descriptors to pharmacokinetics or other biological activity of compounds, this is known as quantitative-

structure-activity-relationship (QSAR) modelling [125,126]. This allows for basic measurements regarding physicochemical properties to be conducted and then utilised to predict more complex parameters thus allowing for rapid screening of compounds and a theoretical assessment of their potential activity in the body [127]. The importance of lipophilicity measurements for QSAR has been well-reviewed and it is often regarded as one of the most important parameters in QSAR models [121,126]

Benzodiazepines typically have reasonably high values for lipophilicity and thus they undergo rapid absorption into the body, accumulate in lipid-high areas of the body, partition with ease across cell membranes, experience a high distribution within the brain and have a high volume of distribution [128-133].

The log P values of ten NPS-benzodiazepines were recently published in 2017 with a view to making them available for the estimation of pharmacological and toxicological properties of NPS-benzodiazepines [134].

The lipophilicity of a compound, as well as other parameters such as plasma protein binding and pK_a can be used to predict a pharmacokinetic parameter known as the volume of distribution and this has been previously demonstrated for some benzodiazepines [135]. This is described in further detail in Section 1.8.2.

Various methods exist for measuring the log $D_{7.4}$ but the most common is the so-called 'shake-flask' method [136]. Here a known mass of the compound is dissolved and allowed to equilibrate in equal volumes of octanol and a buffer at pH 7.4 [136]. Following equilibration the concentrations in each phase are determined, typically with HPLC-DAD or LC-MS. Further discussion of analytical methods such as these will take place in Section 1.10. This process is depicted in Figure 1.3. Although this experimental measurement of log $D_{7.4}$ can be time-consuming as it requires equilibration of the two phases followed by separation and analysis it is generally considered the 'gold-standard' for determining lipophilicity as it is accurate, precise and repeatable measurements can also be obtained [136,137].

To reduce the time taken to generate log $D_{7.4}$ values a variety of software packages exist in order

to provide theoretical values [109]. A common method of predicting log $D_{7.4}$ relies on totalling the individual contributions to lipophilicity from each atom or fragment of a molecule [125,138]. However lipophilicity is not a simple addition and therefore corrections are often included; for example some approaches assess how these fragments or atoms interact in an intramolecular manner along with their lipophilicity descriptors [136]. More complex approaches exist which involve topological and molecular orbital descriptors and these have been well-reviewed [139,140].

$$Log\ D_{7.4} = 10^{\frac{Concentration\ in\ octanol}{Concentration\ in\ buffer}}$$
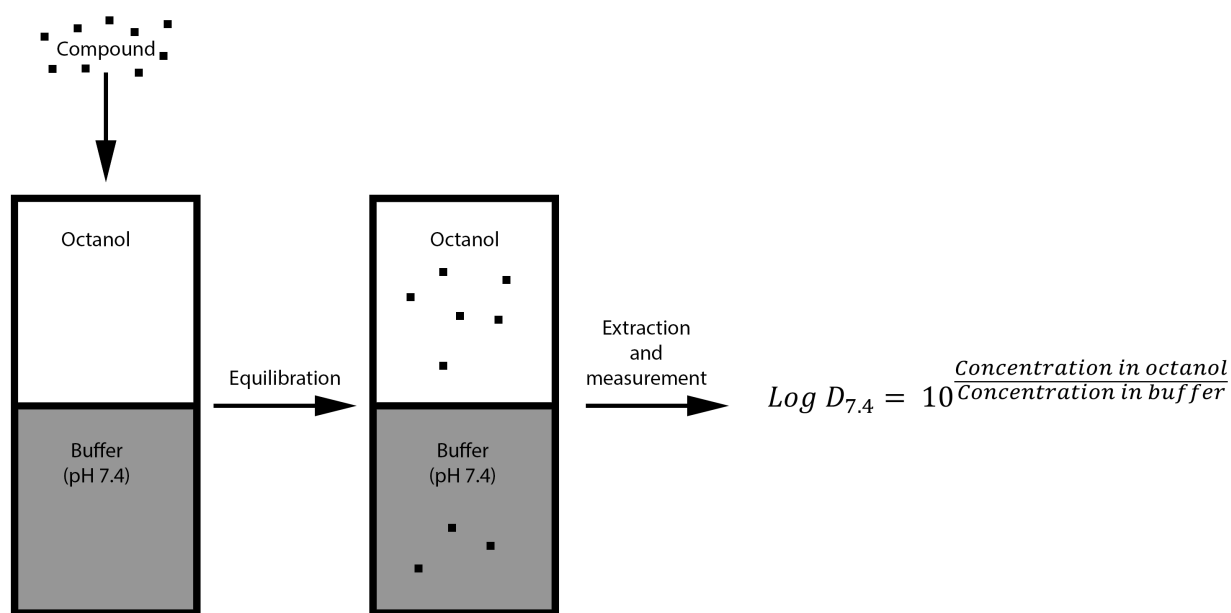
Figure 1.3: The shake-flask method for measuring log $D_{7.4}$ [133].

1.7.2   pK$_a$

The pK$_a$ of a compound is the base-10 logarithm of its acid dissociation constant (K$_a$) [141]. It is essentially a measure of the strength of an acid or base in solution; in other words its propensity to dissociate into a proton and an anion. Compounds can have multiple pK$_a$ values for each ionisable site that they contain [142].

Knowledge of the pK$_a$ of a compound is important during pharmaceutical development especially when used in conjunction with other parameters such as molecular weight and lipophilicity [106,141,143]. pK$_a$ directly influences physicochemical parameters such as the log D$_{7.4}$ and solubility and hence indirectly influences pharmacokinetic parameters such as absorption and distribution [141,144]. Ionised compounds have a greater solubility in aqueous solutions as a result of their increased polarity. This increased solubility and hydrophilicity comes at a cost of reduced lipophilicity. The effect of this reduced lipophilicity is that the permeability of compounds through biological membranes is decreased and hence ionised compounds tend to have a lower permeability compared to neutral compounds [145]. Ionised drugs are not able to diffuse easily across hepatocyte membranes in the liver and as a result are more likely to undergo renal clearance [146,147].

The pK$_a$ of compounds has been used in pharmacokinetic modelling for predicting the volume of distribution [107,148]. This is discussed in greater detail in Section 1.8.2. The pK$_a$ of benzodiazepines has also been postulated to be important in determining the extent of their distribution into adipose tissue as well as predicting their post-mortem distribution [149,150]. A model capable of predicting post-mortem distribution with an R^2 of 0.98 has been reported for benzodiazepines where ionisation (i.e. pK$_a$) exerted significant impact [149]. Benzodiazepine distribution into adipose tissue was found to be significantly related to pK$_a$ but unrelated to lipophilicity (as log P) [150].

Benzodiazepines either have one pK$_a$ value (e.g. flunitrazepam with 1.8) or two pK$_a$ values (e.g. clonazepam with 1.5 and 10.5) [151,152]. As mentioned previously each pK$_a$ value refers to a separate site of ionisation on the molecule. The first pK$_a$ value for benzodiazepines refers

to the deprotonation of the nitrogen cation at position 4 and the second pK_a refers to the deprotonation of the nitrogen atom at position 1 (from Figure 1.2A) [153]. The deprotonation of the nitrogen atom at position 1 is thought to be resonance-stabilised with the negatively-charged oxygen atom [153]. This can be visualised in Figure 1.4 for clonazepam.
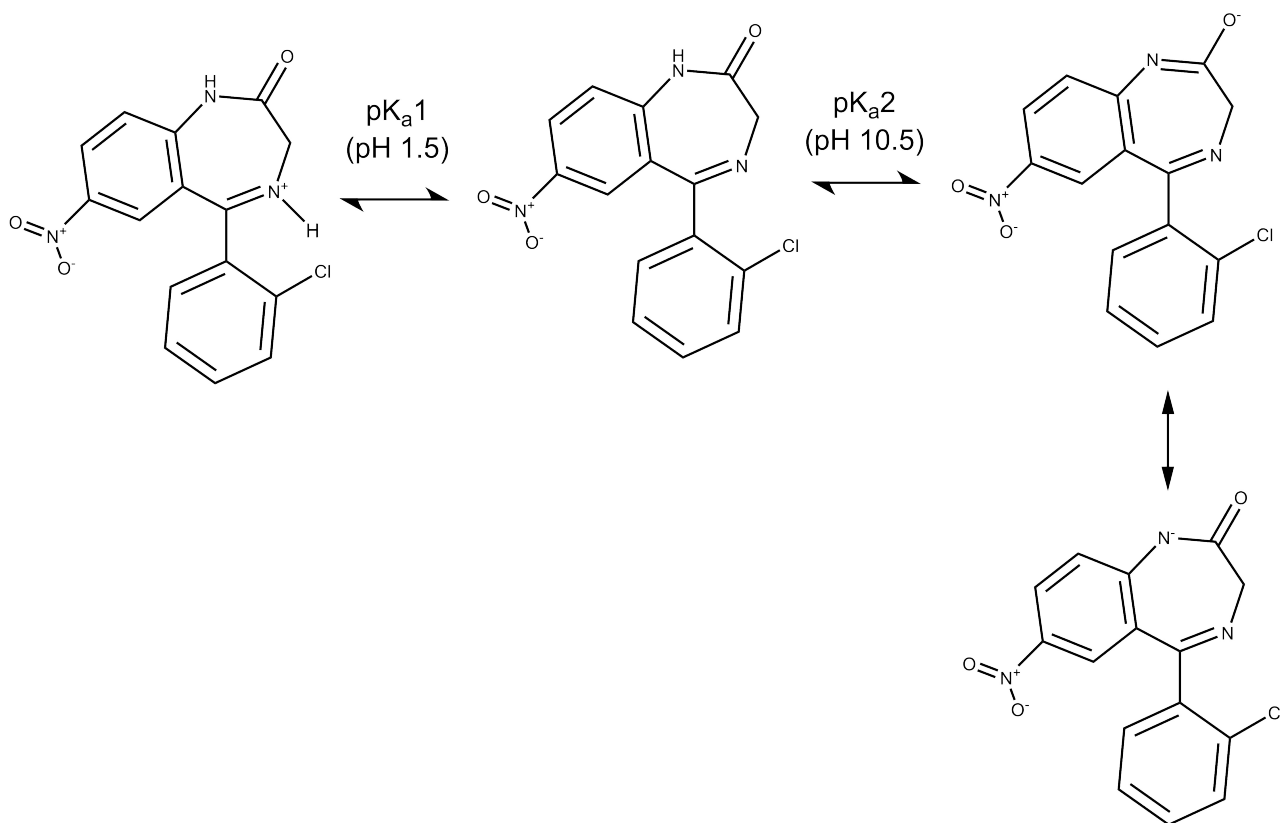
Figure 1.4: pK$_a$ values and structures for clonazepam [148,149].

A variety of methods exist for measuring pK$_a$ such as potentiometry, calorimetry and electrophoresis and these have been well-reviewed [154,155]. A commonly used method is capillary electrophoresis because of its efficiency, ease of use and the low concentrations (in the order of ng mL^{-1}) that are required [156,157]. In this technique, ions are separated using an applied electrical voltage as a result of their differing electrophoretic mobilities [158]. The electrophoretic mobility of a compound describes its rate of movement when an electrical field is applied in a specific solution [159]. A compound in its unionised state has no electrophoretic mobility. Once an electrical voltage is applied and the compound is fully ionised then its electrophoretic mobility is at its maximum [160]. Between this minimum and maximum electrophoretic mobility there exist various intermediate mobilities that are dependent on the pH of the solution. The effective electrophoretic mobility of a compound can be calculated with knowledge of the difference in migration time between the test compound and a neutral marker compound (Equation 1.1) [156].

$$\mu_{\text{eff}} = (\frac{L_{\text{d}}L_{\text{t}}}{V})(\frac{1}{t_{\text{a}}} - \frac{1}{t_{\text{m}}}) \tag{1.1}$$

Equation 1.1 Determination of effective mobility where μ_{eff} is the effective mobility, t_{a} is the migration time for the test compound (in seconds), t_{m} is the migration time for the neutral marker (in seconds), L_{d} is the total length from the capillary inlet to the detection window (cm), L_{t} is the total capillary length (in cm) and V is the applied voltage.

Once the effective mobility of a compound has been determined at a specific pH, it can be related to the pK$_{\text{a}}$ of a compound through Equations 1.2 and 1.3.

$$\mu_{\text{eff}} = \frac{\alpha \times 10^{\text{-pH}}}{10^{\text{-pK}_{\text{a}}} + 10^{\text{-pH}}} \tag{1.2}$$

Equation 1.2 Relationship between effective mobility at a specific pH and the pK$_{\text{a}}$ of a compound where μ_{eff} is the effective mobility, pH is the pH of the buffer solution, pK_a is the compound pK$_{\text{a}}$ and α is a fitting constant for acidic compounds equal to the electrophoretic mobility of the ionised form of the compound with the subscript denoting to the order of ionization.

$$\mu_{\text{eff}} = \frac{b_1(10^{\text{-pH}})^2 + a_1 10^{\text{-pK}_{\text{a1}}} 10^{\text{-pK}_{\text{a2}}}}{(10^{\text{-pH}})^2 + a_1 10^{\text{-pK}_{\text{a1}}} 10^{\text{-pH}} + 10^{\text{-pK}_{\text{a1}}} 10^{\text{-pK}_{\text{a2}}}} \tag{1.3}$$

Equation 1.3 Relationship between effective mobility at a specific pH and the pK$_{\text{a}}$ of a compound where μ_{eff} is the effective mobility, pH is the pH of the buffer solution, pK_a is the compound pK$_{\text{a}}$ and α and β are a fitting constants equal to the electrophoretic mobilities of the ionised forms of the compound with the subscript denoting to the order of ionization for acidic and basic compounds respectively.

Equation 1.2 describes the relationship between the effective electrophoretic mobility of a compound and its pK$_{\text{a}}$ when it contains one ionisable basic group and Equation 1.3 describes the relationship between the effective electrophoretic mobility of a compound and its pK$_{\text{a}}$ when it contains both an ionisable basic and acidic group [161]. In equations 1.2 and 1.3, a and b are constants.

As determination of pK_a by capillary electrophoresis requires measurement of the electrophoretic mobility of a compound at a range of pH values, often in triplicate, it can be time-consuming even with automated equipment. Therefore multiple theoretical approaches exist. Some of these are similar to those used for predicting $\log D_{7.4}$ in that they take into account the contributions of individual atoms and fragments in a compound or use training datasets of compounds with known pK_a values [162]. Linear free-energy relationships, often based on Hammett-Taft methods are commonly used [142]. A linear free-energy relationship describes two parallel sets of reactions where changes to the first reaction affect the second reaction in the same manner [159]. Hammett-Taft equations take into account the electronic effects of substituents in a compound, namely their ability to donate and withdraw electrons [163]. The use of different software packages to predict pK_a values has been well-reviewed [162].

1.8   Pharmacokinetics of Benzodiazepines

Benzodiazepines have various routes of administration, however oral is the most common route of administration overall, with injective routes of administration being more common amongst opiate users [47,164,165]. The pharmacokinetics of NPS-benzodiazepines have been previously reviewed [16]. Three pharmacokinetic parameters;the plasma protein binding, the volume of distribution at steady state and the blood to plasma ratio will be discussed here along with the pharmacokinetic phase of metabolism.

1.8.1   Plasma Protein Binding

Whole blood consists of blood cells (45 % by volume) and a liquid component known as plasma (55 % by volume) [166]. The plasma can be subdivided into water (92 %), proteins (7 %) and inorganic ions (1 %) [167]. Following absorption, compounds in the body typically bind in a reversible manner to plasma proteins [168]. Important plasma proteins for binding include human serum albumin (HSA), alpha-1 acid glycoprotein (α1AGp) and lipoproteins [169]. Acidic and neutral compounds preferentially bind to human serum albumin and basic compounds to alpha-1 acid glycoprotein although this is a simplistic description and many compounds bind to both human serum albumin and α1AGp as well as additional proteins or components within the blood such as lipoproteins or erythrocytes [168,170174].

The fraction that is not bound to plasma proteins (known as the unbound or free fraction) is responsible for a pharmacological effect of a compound and undergoes metabolism and excretion [168]. Therefore plasma protein binding directly affects the pharmacokinetics of a compound and this has been well-reviewed [168]. The clearance of a compound (the rate at which it is removed from a specific volume of blood) from the body can be affected by plasma protein binding as only the free fraction of a compound is metabolised and excreted, therefore compounds with high plasma protein binding generally have a lower clearance from the body and thus an increased half-life ($t_{1/2}$) [175,176]. High protein binding is generally defined as being greater than 95 % [177]. Plasma protein binding is highly correlated with cerebrospinal fluid

concentrations for benzodiazepines [178]. Plasma protein binding is an important determinant of the volume of distribution along with tissue binding and this will be discussed in more detail in Section 1.8.2 [168,179]. Knowledge of plasma protein binding is therefore important to help characterise the pharmacokinetics of drugs as it allows predictions to be made prior to, or in the absence of, *in vivo* studies.

As mentioned previously, the majority of plasma protein binding is to human serum albumin and alpha-1 acid glycoprotein. Human serum albumin is a globular protein that consists of three domains (I, II and III), with each domain further separated into two subdomains (A and B) [180-183]. Diazepam and other benzodiazepines have been observed to bind to a site known as the IIIA subdomain [172-186]. It has been observed that flunitrazepam does not generally bind to the IIIA site and that benzodiazepines which do not bind to the IIA site are unlikely to experience a large binding affinity to HSA [187]. Several benzodiazepines have also been shown to bind to alpha-1 acid glycoprotein although at a lower affinity than human serum albumin [188]. The majority of benzodiazepines are highly protein-bound such as diazepam which is 96.8 - 99 % bound [189,190]. Some benzodiazepines experience lower plasma protein binding such as alprazolam which is 68.9 - 76.7 % bound [191,192].

Plasma protein binding has been reported to be concentration-independent for a number of benzodiazepines within the concentration ranges found during typical therapeutic use [189,193]. For example the plasma protein binding of diazepam, alprazolam and flunitrazepam remains unchanged in the concentration of 10 ng mL^{-1} to 10000 ng mL^{-1} [189].

A number of methods exist for the measurement of the plasma protein binding of a compound such as equilibrium dialysis, ultracentrifugation and ultrafiltration [194]. Equilibrium dialysis is often referred to as the 'gold standard' for measuring plasma protein binding because of its accuracy and reproducibility [195]. In equilibrium dialysis, plasma and an appropriate buffer are placed into two chambers separated by a semi-permeable membrane with a specific molecular-weight-cut-off for proteins (Figure 1.5). The compound is then spiked into the plasma or buffer and left to equilibrate. Following equilibration the resultant concentrations are measured and the plasma protein binding calculated using Equation 1.4.

$$f_u = 1 - \frac{C_{\text{plasma}} - C_{\text{buffer}}}{C_{\text{plasma}}} \tag{1.4}$$

Equation 1.4 Determination of plasma protein binding where f_u is the fraction unbound in plasma, C_{plasma} is the compound concentration in plasma and C_{buffer} is the compound concentration in buffer.
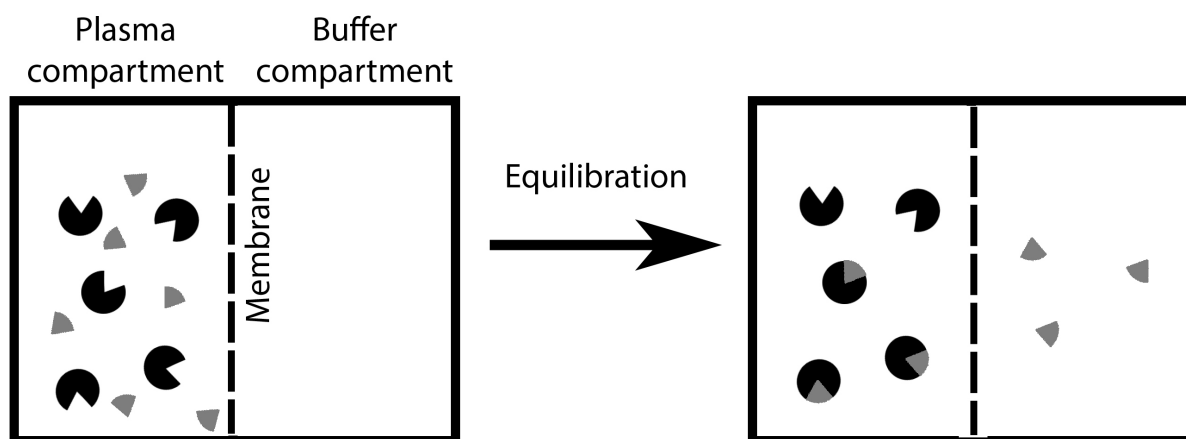
Figure 1.5: Equilibrium dialysis procedure for determining plasma protein binding where the plasma and buffer are separated by a membrane with a specific molecular cut-off and are left to equilibrate [173].

As with pK_a and log $D_{7.4}$, various theoretical approaches have attempted to predict the plasma protein binding of compounds. However plasma protein binding is extremely complex as a result of the multiple proteins and different sites that compounds can bind to as well as physicochemical factors affecting binding [196]. Many of the most precise models focus upon predicting plasma protein binding for small, structurally-related compounds as a result of the errors when analysing large, diverse datasets [167]. Models are generally complex with multiple molecular descriptors requiring a reasonable amount of computational power to generate plasma protein binding values [197,198]. Lipophilicity correlates well with plasma protein binding and thus theoretical approaches often attempt to utilise this relationship as well as other molecular descriptors [176,196]. In the most basic sense, compounds with a greater lipophilicity typically experience a greater plasma protein binding [113]. Lipophilicity is thought to be one of the most important factors in determining compound binding to human serum albumin, especially

for binding at the site responsible for the binding of diazepam [199,200].

1.8.2   Volume of Distribution at Steady State

The volume of distribution at steady state (Vd_{ss}) is a pharmacokinetic parameter that describes the theoretical volume that would be required to contain a drug so that the concentration of this would be equal to the concentration of the drug in the plasma under steady-state equilibrium [141]. Therefore, it does not relate to a physical volume, rather it is a proportionality factor. Steady-state equilibrium conditions can take the form of intravenous or multiple drug administration [201].

The distribution of a drug is another important parameter during pharmaceutical development as it relates to the half-life of a drug and therefore its duration of action [144]. If two compounds are ingested at the same dose, the compound with a lower Vd_{ss} could require more frequent dosing to produce the same concentrations in the body and thus pharmacological effect [201]. A greater Vd_{ss} means that less of the compound is actually present in the plasma and instead it is distributed into the tissues and therefore unavailable for elimination from the body. Therefore compounds with a greater Vd_{ss} have a reduced clearance.

Compounds with a Vd_{ss} that is lower than 0.6 L kg^{-1} (the approximate total body water content in humans) are termed as having a low volume of distribution, those with a Vd_{ss} greater than 5 L kg^{-1} have a high volume of distribution and those compounds in between these values have a moderate volume of distribution [144].

The benzodiazepine lorazepam has a longer duration of action compared to diazepam and it is thought that this is as a result of its vastly lower volume of distribution as well as a slow diffusion across the blood-brain-barrier [202-204].

The experimental Vd_{ss} is typically calculated from the intravenous administration of a compound into the body and then measurement of the concentrations of the compound in the plasma [205]. As a result of the time-consuming methodology and difficulty of intravenous studies as well as debates around the ethics of the use of animals in experiments, theoretical

approaches exist to predict the volume of distribution such as QSAR modelling [206,207]. It should be noted that the Vd$_{ss}$ can also be calculated from a plot of plasma concentration versus time but this must be corrected for bioavailability; another pharmacokinetic parameter not widely measured and requiring *in vivo* data [144].

The volume of distribution at steady state is related to both the plasma protein binding (V$_p$) and the tissue binding of a compound (V$_t$) (Equation 1.5).

$$Vd_{ss} = V_p + V_T \frac{f_u}{f_{ut}} \tag{1.5}$$

Equation 1.5 Relationship between the volume of distribution, tissue binding and plasma protein binding where V_p is the plasma volume, V_T is the tissue volume, f_u is the fraction unbound in plasma and f_{ut} is the fraction unbound in tissues.

Tissues are defined as any part of the body in which drug can be contained [144]. Basic and neutral compounds typically experience binding to tissues and thus have a low f_{ut} [144]. Changes in the plasma protein binding do not always affect the tissue binding of a compound and therefore there is often no direct relationship between a change in the plasma protein binding and the volume of distribution [179]. Where two compounds have identical plasma protein binding, a compound that experiences a higher binding to the tissues will also have a higher volume of distribution [148].

One approach to predict the volume of distribution at steady state is the use of the Øie-Tozer equation which utilises a number of physiological parameters [104,145]. Compared to other methods such as allometric scaling, use of the Øie-Tozer equation is generally held to be one of the more accurate models and is reasonably straightforward to use as the required datasets are easy to gather [204]. The Øie-Tozer equation is displayed in Equation 1.6.

$$Vd_{ss} = V_p(1 + R_{E/I} + (f_u V_p (\frac{V_E}{V_p} - R_{E/I}) + \frac{V_R f_u}{f_u} \tag{1.6}$$

Equation 1.6 Øie-Tozer equation for the calculation of the volume of distribution at steady

state where f_u is the fraction of the compound unbound in plasma, f_{ut} is the fraction of the compound unbound in tissues, V_p is the plasma volume, V_E is the extracellular fluid volume and $R_{E/I}$ is the ratio of extravascular to intravascular proteins.

Multiple forms of compound-tissue binding occur within the body and as such these small contributions are not experimentally determinable, therefore it is assumed that these are non-specific [1074,148]. The plasma volume (V_p) is 0.0436 L kg^{-1} for humans), the extracellular fluid volume (V_E) 0.151 L kg^{-1} for humans and the ratio of extravascular to intravascular proteins ($R_{E/I}$) is 1.4 for humans. These are all averaged values and the $R_{E/I}$ ratio only describes human serum albumin distribution [107,148].

The fraction unbound in tissues can only be obtained from *in vivo* experiments which are often unfeasible and it is not a routine measurement in pharmacokinetic studies [209]. However other measurements are routine in pharmacokinetic studies such as the Vd_{ss} and f_u. If these two values are experimentally known then Equation 1.6 can be rearranged to calculate f_{ut} in Equation 1.7.

$$f_{ut} = \frac{V_R f_u}{Vd_{ss} - V_p - f_u V_E - (1 - f_u)R_{E/I}V_p} \tag{1.7}$$

Equation 1.7 Rearranged Øie-Tozer equation for the calculation of the fraction unbound in tissues

The fraction unbound in tissues is related to the fraction unbound in plasma (i.e. the plasma protein binding). If experimental values exist for a series of compounds that have known values for the plasma protein binding and tissue binding as well as other physicochemical descriptors such as log $D_{7.4}$ and pK_a then the relationship between the aforementioned parameters can be derived using multiple linear regression. Once this relationship has been determined, the fraction unbound in tissues can be theoretically calculated with knowledge of plasma protein binding, log $D_{7.4}$ and pK_a which are relatively easy to measure *in vitro*. After the fraction unbound in tissues has been calculated, this value of f_{ut} can then be substituted into Equation 1.7 along with the value for f_u to give a value for Vd_{ss}. This process is summarised in Figure

1.6.
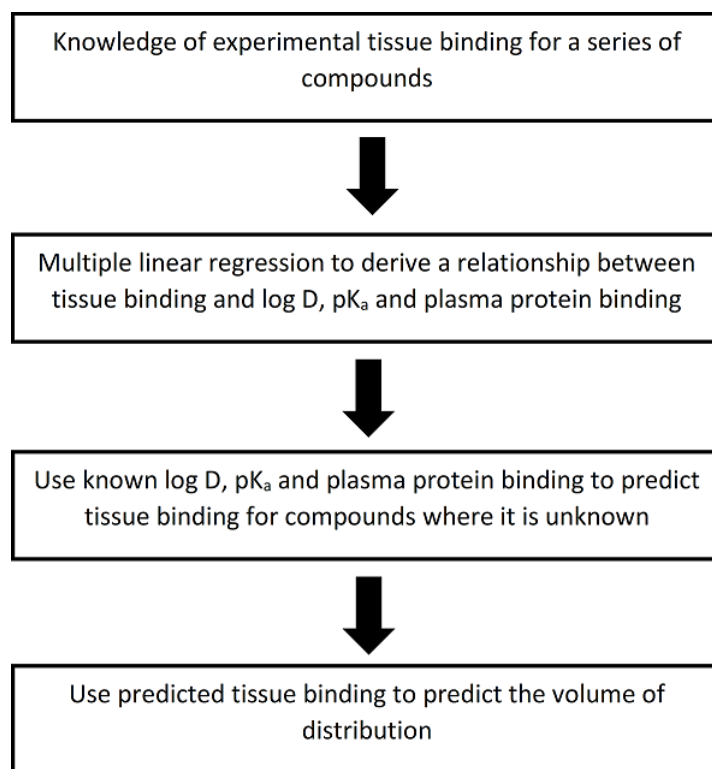
Figure 1.6: Process for determining volume of distribution from log $D_{7.4}$, pK_a and plasma protein binding [104,145].

This process has previously been reported for sets of 64 and 120 compounds obtaining good correlations between Vd_{ss}, the log $D_{7.4}$ and the fraction of a compound ionised at pH 7.4 ($f_{i7.4}$) [107,148]. In particular the use of f_u, $f_{i7.4}$ and log $D_{7.4}$ has been reported to give an R^2 of 0.8737 with a 1.86 mean-fold error for 12 benzodiazepines [107,148]. Hence, accurate values for the log $D_{7.4}$, pK_a and plasma protein binding of NPS-benzodiazepines can allow predictions to be made about their Vd_{ss}. The pK_a is necessary for the calculation of the fraction ionised at pH 7.4 as these parameters are related by the Hendelson-Hasselbalch equation (Equation 1.8).

$$pH = pK_a + log\frac{ionised}{unionised} \tag{1.8}$$

Equation 1.8 The Hendelson-Hasselbalch equation

1.8.3   Blood to Plasma Ratio

As discussed in Section 1.8.1, compounds bind to plasma proteins. However, they can also experience binding to blood cells (which consist of 45 % of the total volume of whole blood) [167]. The blood to plasma concentration ratio describes the ratio of the concentrations of an administered compound in the blood and the plasma at equilibrium.

A closely-related parameter is the blood to plasma partition coefficient ($K_{e/p}$), which describes the ratio between the concentration of a compound in red blood cells to the concentration of a compound in plasma.

If a compound experiences extensive binding to components in the blood then any pharmacokinetic parameters calculated solely from plasma concentrations are likely to be incorrect [210]. Compounds that have a blood to plasma concentration ratio in favour of them partitioning into the blood will have a lower sensitivity to an analytical method that is purely analysing the plasma [211]. Therefore, knowledge of a compound's blood to plasma concentration ratio allows an informed decision to be made regarding analysis of the blood or plasma.

Clinical laboratories and medical evaluations typically analyse compound concentrations within the plasma. Forensic laboratories and post-mortem investigations will often measure concentrations solely in whole blood [212]. Reliable interpretations from these analyses and any equivalences drawn will therefore require knowledge of the blood to plasma concentration ratio [213].

Blood to plasma concentration ratios have been previously published in the literature for a range of illicitly-used compounds that are of toxicological interest and significance. These include 3,4-methylenedioxymethamphetamine (MDMA), $\delta 9$-Tetrahydrocannabinol (THC), γ-hydroxybutyric acid (GHB), phencyclidine (PCP), zopiclone and opiates such as morphine, oxycodone and fentanyl [210,214-218].

Although the main use of blood to plasma concentration ratios has been the interpretation of toxicological analyses, the ratios have still found utility in predicting concentration-time profiles for some drugs [219]. The blood to plasma concentration ratio can also be used to calculate the

clearance of a drug from the plasma [220]. The hepatic clearance *in vivo* can be estimated using *in vitro* experiments with human hepatocytes [221]. This has been demonstrated for the NPS-benzodiazepine flubromazolam [222]. For the calculation of the hepatic clearance, knowledge of the blood to plasma concentration ratio of a compound is required [221].

A common method for the measurement of the blood to plasma partition coefficient has been well-described in the literature [223]. In this method the compound is spiked into equal volumes of plasma and whole blood and allowed to equilibrate. The blood is then centrifuged to yield the plasma. The concentrations of the compound in both volumes of plasma are then analysed and with this knowledge the blood to plasma partition coefficient can be calculated with Equation 1.9.

$$K_{\text{e/p}} = \frac{1}{H} \times (\frac{C_{\text{Pref}}}{C_{\text{P}}} - 1) + 1 \tag{1.9}$$

Equation 1.9 Calculation of the red blood cell partition coefficient where $K_{\text{E/P}}$ is the red blood cell partition coefficient, H is the haematocrit, C_{Pref} is the concentration of the test analyte in the reference plasma and C_{P} is the concentration of the test analyte in the plasma separated from the whole blood.

The blood to plasma partition coefficient and the blood to plasma concentration ratio can be interconverted with Equation 1.10.

$$K_{\text{b/p}} = (K_{\text{e/p}} \times H) + (1 - H) \tag{1.10}$$

Equation 1.10 Conversion between the blood to plasma partition coefficient ($K_{\text{e/p}}$) and the blood to plasma concentration ratio ($K_{\text{b/p}}$) with the haematocrit (H).

1.8.4 Metabolism

Metabolism, also known as biotransformation, is an important pharmacokinetic phase for xenobiotics prior to their elimination or excretion from the body [224]. The majority of metabolic

processes occur in the liver [224]. The main purpose of metabolism is to remove the compound from the body - typically by increasing its aqueous solubility. One additional effect of metabolism is the conversion of compounds that are pharmacologically inactive into those that have a pharmacological effect, a process known as bioactivation [225]. The metabolic processes is divided into two phases; phase I and phase II [226-228].

Phase I metabolism involves the introduction of a polar or reactive functional group into the compound in order to increase its water solubility. The most common phase I reactions are oxidation, reduction and hydrolysis [227]. The cytochrome P450 enzyme family is a large group of haemoproteins responsible for the majority of phase I oxidative metabolism of compounds within the liver [229]. Cytochrome P450 enzymes are named with the letters 'CYP' denoting the enzyme superfamily (cytochrome) and then a number, letter and number denoting the family, subfamily and individual gene respectively [230]. The majority of compound metabolism is mediated by a small group of cytochrome (CYP) enzymes (CYP 1A2, 2C9, 2C19, 2D6, 2E1 and 3A4/5) [119,120,231]. Other enzymes are involved in phase I metabolism such as aldo-keto reductases and esterases responsible for catalysing hydrolytic reactions [232,233].

The metabolism of benzodiazepines is mainly mediated by CYP3A4/A5 and CYP2C19 enzymes [234-242]. CYP1A2, CYP2B6 and CYP2D6 are also thought to contribute to the metabolism of some benzodiazepines [241,243-246]. The specific metabolic reactions are typically hydroxylation at position 3 (Figure 1.2A) or position 4 (Figure 1.2B). Dealkylation at position 1 (Figure 1.2A) is also common. This is exemplified for diazepam where both hydroxylation and demethylation occur, leading to the presence of three different metabolites within the body; nordiazepam, temazepam and oxazepam (Figure 1.7). This effect has also been observed for NPS-benzodiazepines such as diclazepam, which is metabolised to the prescription benzodiazepines lorazepam, lormetazepam and delorazepam [247]. These metabolites often known as 'active metabolites' as they are responsible for the majority of the observed pharmacological activity for a compound [225].

In terms of specific metabolic pathways for benzodiazepines, hydroxylation on alkyl groups present at position 1 (Figure 1.2B) for triazolobenzodiazepines and position 9 for thienotria-

zolodiazepines (Figure 1.2C) often occurs [248,249]. Reduction of the nitro group to an amine occurs for those benzodiazepines with substituted nitro groups, typically at position R7 (Figure 1.2A) or position R8 (Figure 1.2B) [249]. Some benzodiazepines, such as lorazepam and oxazepam, do not undergo phase I metabolism and instead progress directly to phase II metabolic processes as a result of the presence of a hydroxyl group on position 3 (Figure 1.2A) [250]. Debromination has been reported for one NPS-benzodiazepine, flubromazepam [251]. Demethylation and hydroxylation reactions, and a demonstration of how benzodiazepines are metabolised into other benzodiazepines, can be seen in Figure 1.7.
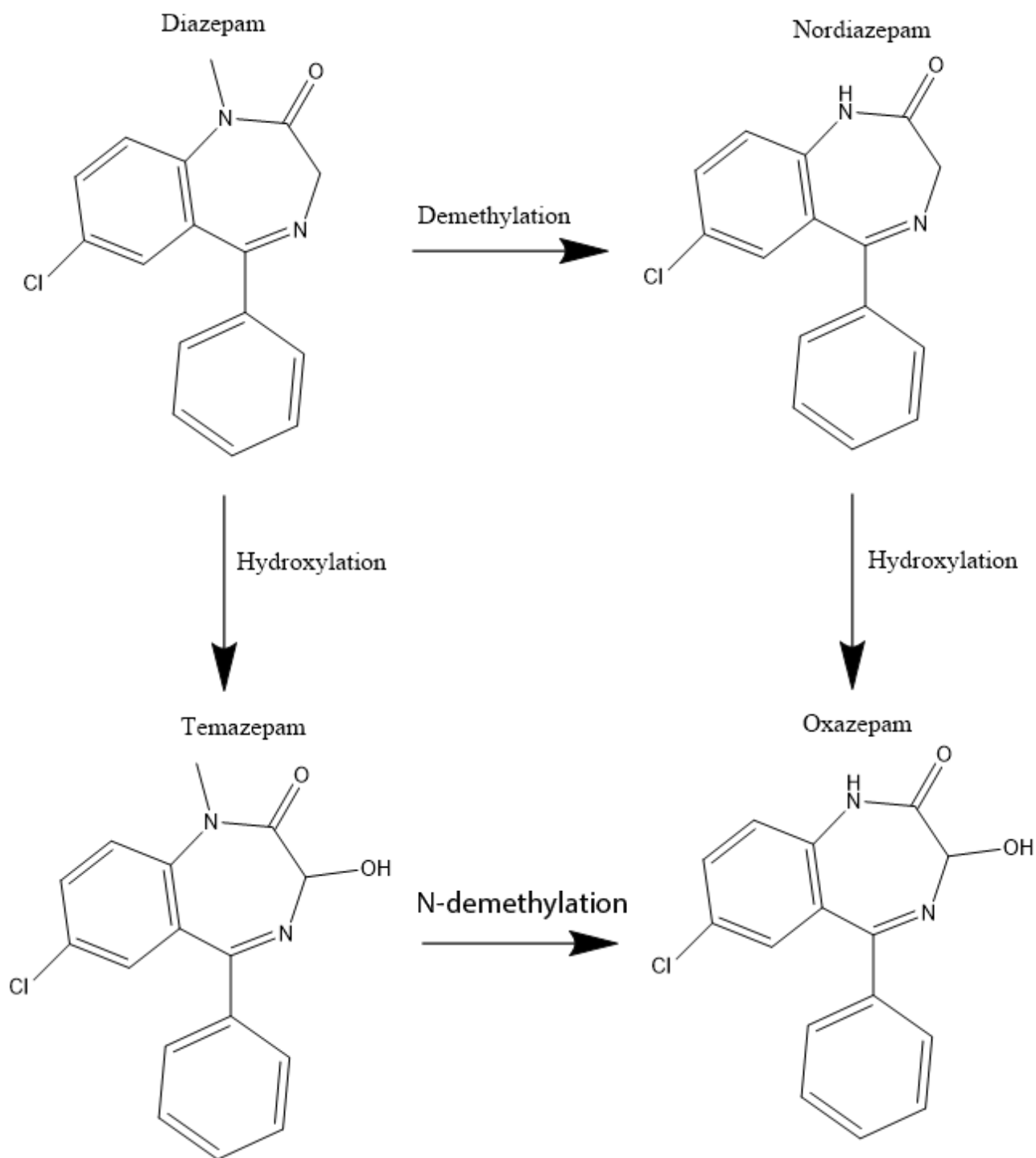
Figure 1.7: Phase I metabolism of diazepam [230-238].

Phase II metabolism is generally performed by a class of enzymes known as transferases [228]. Uridine 5'-diphospho-glucuronosyltransferases (UGTs) are thought to be responsible for the majority of phase II metabolism [252]. Their metabolic role is the addition of a molecule of glucuronic acid to compounds in a process known as glucuronidation [228]. The end result is an increase in the aqueous solubility of a compound so that it can be efficiently excreted. Glucuronidation of benzodiazepines by UGTs is typical on hydroxyl groups such as position R3 for oxazepam (Figure 1.8) [253].

Certain benzodiazepines experience metabolic contributions from other enzymes such as N-acetyltransferase 2 (NAT2) which acetylates the phase I metabolite of clonazepam, 7-aminoclonazepam (Figure 1.9) [254].
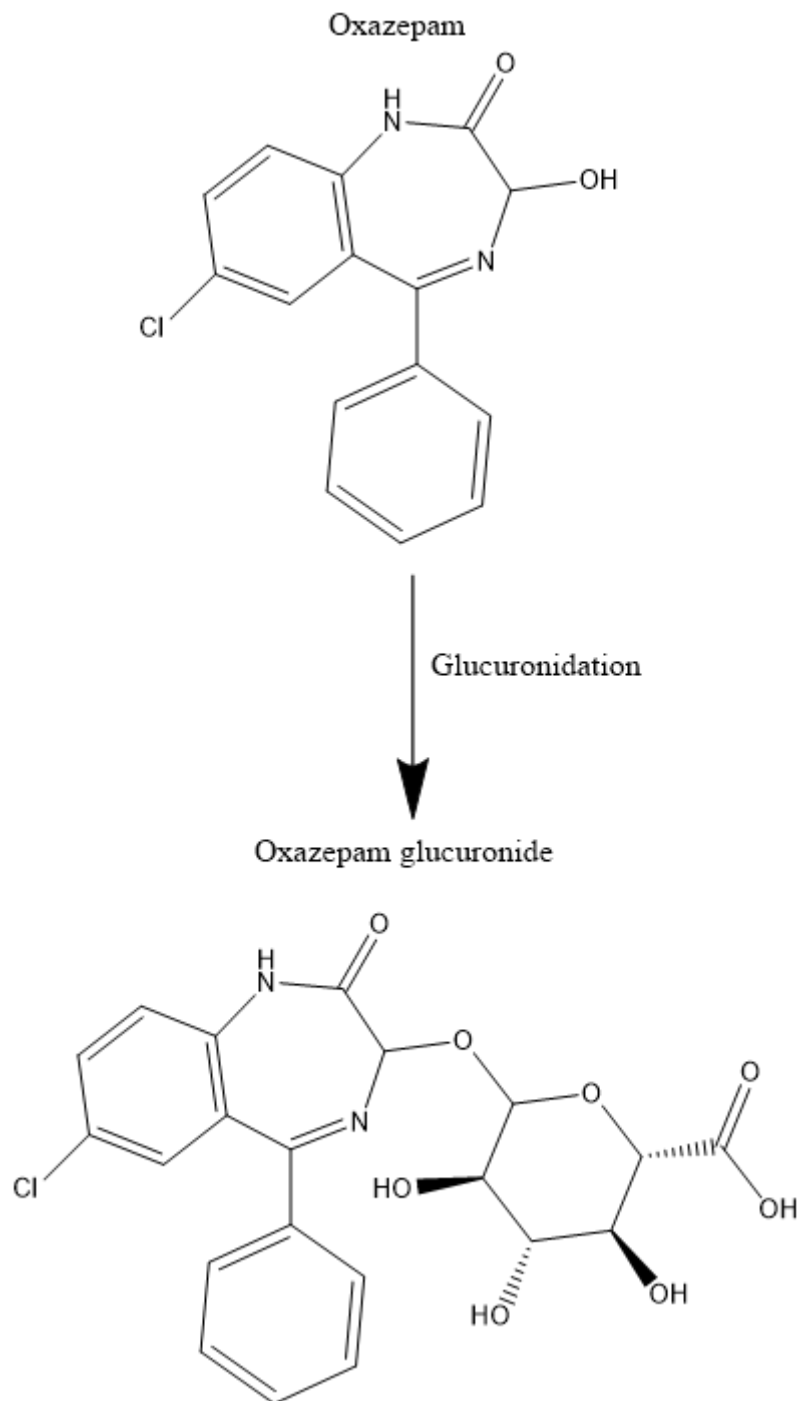
Figure 1.8: Phase II metabolism of oxazepam [249].
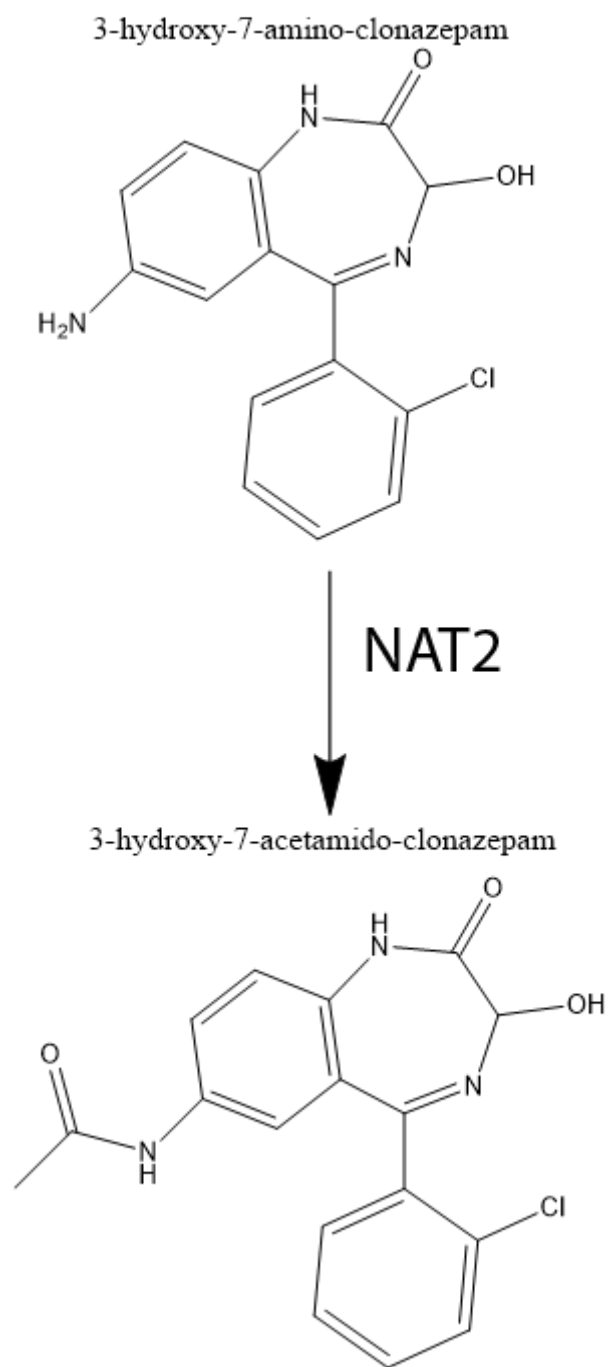
Figure 1.9: Phase II metabolism of clonazepam [250].

Characterising the metabolic pathways of compounds *in vitro* is an important aspect of pharmaceutical development in a forensic and chemical toxicology context, such methods allow identification of the use of illict drugs even if the parent compound is no longer detectable [255]. As mentioned previously, benzodiazepines are metabolised in phase I reactions by CYP450 enzymes and in phase II reactions by UGTs, NAT2 and other enzymes. Therefore, it is important for any *in vitro* method to allow compounds to be exposed to sufficient levels of enzymatic activity.

The metabolic pathways of many of these NPS-benzodiazepines have been previously assessed *in vivo* as a result of self-ingestion experiments and collection of forensic samples from criminal cases and intoxicated patients in hospitals as well as *in vitro* experiments using cryopreserved primary human hepatocytes (PHHs), human liver microsomes (HLMs) and isolated phase II metabolic enzymes [256-260]. Authentic toxicological samples are often unavailable and the use of animals is often undesirable and subject to ethical restrictions hence the use of *in vitro* investigations.

One form of *in vitro* experiments to determine metabolism is the use of primary human hepatocytes; they are often the 'first-choice' or 'gold-standard' for the metabolic characterisation of compounds [261]. They express a full complement of phase I and II enzymes and generate metabolites in an extremely similar manner to those produced *in vivo* [262]. However their use can be cost-prohibitive and loss of metabolic function during incubation is often observed [263]. Primary human hepatocytes are extracted from human livers and can be cultured in an appropriate environment or cryopreserved for later use. HLMs are another technique also commonly used to study metabolic pathways as these subcellular fractions often have a good expression of CYP450 enzymes [264]. However these levels can be variable and they lack expression of phase II enzymes [264]. Another method of identifying metabolic pathways *in vitro* is the use of human hepatocellular carcinoma cell lines [261].

The human hepatocellular carcinoma cell line HepG2 is often used as an *in vitro* model to identify metabolic pathways as it contains a variety of CYP450 enzymes although typically with lower expressions compared to primary human hepatocytes and human liver microsomes

[265,266]. The C3A cell line is a patented clonal derivative of the human hepatocellular carcinoma cell line HepG2 [267]. The C3A cell line derivative was selected for strong contact inhibition of growth, high albumin production, high production of alpha fetoprotein and an ability to grow in glucose-deficient medium [268]. It is also reported to be more metabolically active than its parent cell line and also to express a phenotype closer to that of primary human hepatocytes [269,270]. Without the use of tissue engineering methods, metabolic characterisation has only been conducted for the C3A cell line with regards to the CYP3A4/5 and CYP1A2 [269]. It was reported that they have a much lower turnover of metabolic substrates (testosterone for CYP3A4/5, phenacetin for CYP1A2) than the another cell line known as HepaRG [269].

The levels of CYP enzymes in hepatoma cell lines are known to be inducible following treatment of the cell culture with 1 % DMSO (v/v in typical cell culture medium). This inductive potential has been observed for the parent line of the C3A cells, HepG2, as well as other cell lines such as Huh7 [271,272].

The HepaRG cell line is a human hepatocellular carcinoma cell line that has been well-characterised [261,273277]. It is provided as a differentiated single-use cell line [269]. The HepaRG cell line is reported to express high levels of CYP1A2, CYP2B6, CYP2C9, CYP2C19 and CYP3A4 [269,275,277]. The HepaRG cell line is derived from an individual who had a low expression of CYP2D6 resulting in a relatively low proportion of this enzyme compared to the other CYP enzymes it expresses [274,277].

The expression of CYP450 enzymes can vary markedly in HepG2 and other human hepatocellular carcinoma cell lines and thus it is recommended that the levels of these enzymes should be characterised before use [278]. One commonly-used set of guidelines for the characterisation of enzyme levels *in vitro* are those published by the Food and Drug Administration (FDA) [279]. The FDA recommend that six enzymes be expressed; CYP1A2, CYP2B6, CYP2C19, CYP2C9, CYP2D6, CYP3A4/5, as these are responsible for the phase I metabolism of the majority of pharmaceutical compounds [119,120,231]. Recommended substrates for specific enzymes are phenacetin for CYP1A2, bupropion for CYP2B6, S-mephenytoin for CYP2C19, diclofenac for

CYP2C9, dextromethorphan for CYP2D6 and testosterone for CYP3A4/5 [279].

Various computer programs are available both commercially and as freeware to attempt prediction of the metabolic pathways of compounds [280]. Their methods are typically based upon identifying structural features that are suitable as sites of metabolism by the relevant enzymes. These structural features are often based upon those found on experimentally determined metabolic pathways of compounds. Studies on the metabolism of NPS-benzodiazepines conducted using HLMs often attempt to predict the expected metabolites from comparison with clinically-used benzodiazepines. This allows their structures to be input into software which can then search the resultant mass spectra for signs of these metabolites [251].

1.9   The Pharmacodynamics of Benzodiazepines

Although no work in this thesis has been directly conducted upon the pharmacodynamics of benzodiazepines, a brief overview will be given here in order to add context to their use as new psychoactive substances.

Benzodiazepines exert their effects through reversible binding to gamma-Aminobutyric acid A (GABA$_A$) receptors in the brain [281]. The GABA$_A$ receptor is pentameric and its isoform can vary as a result of the seven subunit groups (α 1-6, β 1-3 γ 1-3, δ, ϵ, π, ω) that it can consist of [281]. However in the human brain the most common GABA$_A$ receptor isoform contains two α subunits, two β subunits and a single γ subunit (Figure) [281,282]. There are two binding sites for the neurotransmitter gamma-Aminobutyric acid (GABA) [283]. These sites exist between the α1 and β2 subunits and an allosteric benzodiazepine binding site (BZD site) also exists between the α1 and γ2 subunits [284-286]. A number of other binding sites also exist on the GABA$_A$ receptor however benzodiazepines are not known to bind to any of these and they are not depicted on Figure 1.10 [287,288].
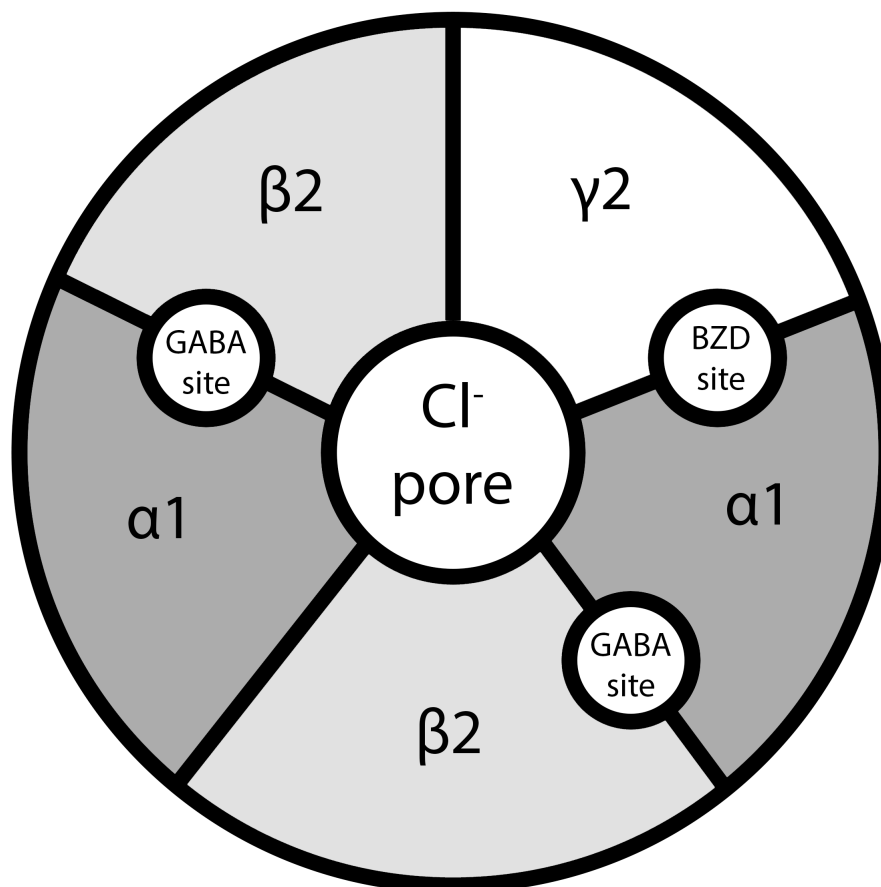
Figure 1.10: Example composition of an $\alpha 2\beta 2\gamma 1$ GABA$_A$ receptor [277,278].

GABA$_A$ receptors are ligand-gated ion channels; they open to selectively allow chloride (Cl-) ions through following the binding of a ligand (in this case GABA) [289]. A membrane potential exists in the GABA$_A$ receptor as a result of the difference in electric potentials on each side of the receptor. Binding of GABA to the receptor causes an influx of Cl- ions through the central pore which results in the membrane potential becoming more electrically negative (known as hyperpolarisation) [289]. A reduction in neurotransmission is observed and this is known as an inhibitory postsynaptic potential [[290]. When benzodiazepines bind to the benzodiazepine site the conformation of the whole GABA$_A$ receptor is transformed into one that allows GABA to bind with a greater affinity [291,292]. The result of this is an increased frequency in the opening of the Cl- pore and thus an increase in number of the hyperpolarisation events mentioned earlier [[293]. This decreases the likelihood of a successful action potential occurring as the excitatory threshold is too great to be reached by depolarisation [294].

The structure of benzodiazepines greatly affects their binding affinity to GABA$_A$ receptors. For 1,4-benzodiazepines the carbonyl group at position 2 is essential for binding affinity. Other functional groups important for binding affinity are; lipophilic or electronically-charged groups at position 7, electrophilic or bulky groups at position 2' and molar refractivity (i.e. polarisability, or the propensity of a molecule to form dipoles) combined with a low steric bulk at position 1 (Figure 1.2A) [285]. The substitution of a triazole ring onto a 1,4-benzodiazepine that previously possessed a low affinity for the GABA$_A$ receptor typically increases the affinity of the compound. However the same is not true for compounds that already possess a high affinity for the GABA$_A$ receptor [285]. Benzodiazepines containing substitutions at the R6' or R8 positions experience a lower binding affinity to GABA$_A$ receptors (Figure 1.2B) [295].

A recent NPS-benzodiazepine to emerge in 2017 was 4'-chlorodiazepam. The phenyl ring is substituted at the 4' position rather than the 2' position (Figure 1.2A); the former substitution is more common amongst benzodiazepines. Instead of binding to the GABA$_A$ receptor, 4'-chlorodiazepam binds to the translocator protein (TSPO) which was previously known as the peripheral benzodiazepine receptor [292,293]. TSPO is distributed in various regions of the body and has been investigated as a therapeutic drug target [296,297]. While 1,4-benzodiazepines such as diazepam also experience some limited binding to TSPO, their pharmacological effects

are believed to occur from their interaction with $GABA_A$ receptors [301303].

1.10 Analytical Methods for the Detection of Benzodiazepines

As a result of their widespread use, a large number of analytical methods to detect and quantify benzodiazepines in a variety of matrices are available and have been described in the literature [304]. Benzodiazepines are prominent in both forensic cases and toxicological investigations in a medical setting and therefore careful analysis and quantitation is often necessary [305307].

1.10.1 Benzodiazepine Extraction from Biological Samples

The complex nature of matrices such as blood, plasma, cell culture or human liver microsomes means that compounds must often be extracted in order to decrease interferences in analytical equipment. These interferences can occur as a result of the presence of various proteins and inorganic materials in the samples [308]. Matrix interference can cause signal suppression or enhancement in mass spectrometry therefore decreasing the accuracy and precision of this analytical method for certain samples [209]. Types of extraction include solid-phase extraction (SPE), liquid-liquid extraction (LLE) and protein precipitation [308].

SPE is usually based upon SPE cartridges which consist of an internally-lined cylinder containing a specific sorbent [310]. Firstly, the cartridge is conditioned (typically with an organic solvent) to reduce interferences and increase the surface area available for solute retention [311]. The sample solution is then passed through the cartridge and the solute adsorbs onto the sorbent. An organic solvent or water is then often passed through the cartridge to remove interferences. Finally the solute is desorbed with another organic solvent and collected [311].

Protein precipitation is another common extraction method. This is facilitated by the addition of an organic solvent such as acetonitrile that has been ice-cooled, causing the proteins to de-

nature and precipitate. Centrifugation is then applied to pelletise proteins and the supernatant is collected and analysed.

Protein precipitation has been demonstrated for NPS-benzodiazepines incubated with human liver microsomes or primary human hepatocytes [312315]. However benzodiazepine extractions also often take place with the use of solid-phase extraction cartridges [316,317]. Careful evaluation of the most suitable method for extraction is often necessary [318].

1.10.2   Liquid chromatography (LC)

In the most basic sense, liquid chromatography is an analytical technique to separate compounds. LC is used to separate and quantify compounds based on their hydrophobicity [319]. It is based on the theory of a stationary phase and a mobile phase that have different hydrophobicities. Compounds with a hydrophobicity closer in nature to that of the stationary phase will be attracted to the stationary phase and thus elute more slowly. The converse is also true; compounds with a hydrophobicity more similar to the mobile phase will not interact to a great degree with the stationary phase and elute in a quicker fashion [320]. The volume ratio of organic solvent flowing through the chromatographic system is often increased over time which is known as gradient elution. Elution at a constant volume ratio of organic solvent is known as isocratic elution [320].

It is often utilised in a technique known as high-performance liquid chromatography (HPLC) where samples are passed through a column at high pressure. The most common is reversed-phase HPLC. In this technique, the mobile phase is polar and the stationary phase (i.e. the internal column) is non-polar. The polar mobile phase causes hydrophilic compounds to typically be retained in the mobile phase and therefore elute first while hydrophobic compounds bind or interact with the non-polar stationary phase and experience a later elution. The polar mobile phase is typically formulated of a buffer and a solvent such as acetonitrile. The point at which a compound elutes is known as its retention time [320].

HPLC is typically coupled to a diode array detector (DAD). Diode array detectors are capable

of recording absorbance over the ultraviolet-visible wavelength range of 190 - 800 nm [321]. The absorbance of a compound depends upon its molecular structure as it is determined by the excitation of electrons in molecular orbitals as a result of the excess energy gifted by the electromagnetic radiation [322]. Compounds with different structures will produce different absorbance readings and differentiation between them is therefore possible. HPLC is also often coupled to a mass spectrometer, the theory of which will be discussed in Section 1.10.4.

1.10.3 Gas chromatography (GC)

Gas-chromatography (GC) is a widely-used method for the detection and quantitation of compounds. Gas-chromatography works in a similar manner to LC in that a stationary phase and a mobile phase are used to separate analytes. However in gas-chromatography the stationary phase is liquid (a non-volatile liquid internally contained upon a column) and the mobile phase is a gas. gas-chromatography can be used to analyse gases, volatile solids or liquids. Only the analysis of compounds dissolved in liquids is of interest here.

Upon injection onto the system the liquid sample is thermally vaporised. The vaporised sample is then eluted through the column by applying a carrier gas. The carrier gas is typically inert such as helium [323]. The column is contained within an oven, the temperature of which can be programmed to adjust with time. Splitless injection is often used in GC and in this method all the analyte present in a sample will be injected onto the column. This allows for the analysis of low concentrations (ng mL^{-1}).

Some benzodiazepines are thermally labile and this can potentially cause problems when attempting to analyse them with GC-MS [324]. To improve their thermal stability and the sensitivity of a GC-MS method towards them, benzodiazepines are often derivatised prior to analysis [324]. This is typically achieved by the addition of a silyl group to the compound [325].

1.10.4   Mass spectrometry (MS)

Mass spectrometry is an analytical technique that can differentiate between ions based on their mass to charge (m/z) ratio. The m/z is calculated by dividing the mass number of an ion by its charge [108].

Mass spectrometry consists of a number of steps. Firstly, the compound is ionised with an appropriate ion source. The ion source will differ depending on the nature of the analysis and type of analytical instrument (LC vs GC). The ion source for gas-chromatography is most commonly electron ionisation (EI). Here, a filament is heated to produce electrons which are then accelerated with an electric field to form an electron beam. The vaporised sample is then bombarded with the electron beam, causing ionisation and fragmentation [326]. The ion source for liquid chromatography is often electrospray ionisation (ESI). In this process the solution containing the sample is sprayed from the capillary via a nebulising nozzle. The nozzle has a strong electrical potential applied and serves to create a fine spray of charged droplets [327]. These charged droplets undergo evaporation of the mobile phase, eventually resulting in molecular ions with no solvent remaining [328]. The evaporation of the solvent is typically facilitated by heat or the application of a gas [328].

The second step, following the production of the ions is mass separation. Ions are separated according to their m/z ratios by the application of electric or magnetic fields [329]. A mass analyser (quadrupole) is commonly used for this purpose. In this method four parallel metal rods are contained equidistant from one another. Voltages (direct current and a superimposed radio frequency) are applied to diagonally-opposite pairs of rods. The applied voltages cause the ions to traverse through the quadrupole and oscillate. With the variation of the applied voltages only ions of a specific m/z will successfully pass through the quadrupole; other ions will experience large oscillations, collide with the metal rods and will not reach the detector [328].

Another form of mass separation is from the use of time-of-flight (TOF) mass spectrometry (TOF-MS). The TOF analyser applies an electrical field to accelerate all ions in an equal

manner. Once the ions have equal kinetic energies they enter a flight tube that does not contain any applied electrical fields. The kinetic energy of the ions can be described by ½ mv, where m is the mass and v is the velocity of the specific ion [330]. Therefore two ions with different masses but the same kinetic energy will have different velocities through the flight tube [330]. Ions with a lower mass will have a greater velocity and thus a shorter flight time. The time taken to reach the detector through the flight tube can be related to the m/z ratio of each individual ion which has been well described and is computed automatically [330-332].

TOF-MS is an example of high-resolution mass spectrometry (HRMS). HRMS is a term often used to describe mass spectrometers that can distinguish between compounds with a high mass-accuracy and a high resolution. HRMS is capable of detecting analytes to 0.001 atomic mass units. An advantage of this method is that it is extremely selective because of high mass-accuracy. However two compounds with the same molecular mass and charge and may produce two peaks of the same m/z and differentiation between them may not be possible. The two compounds would have to separated chromatographically and their different retention times would have to be matched to those of a standard of these compounds. This a disadvantage when analysing multiple compounds in the same chromatographic analysis and can necessitate the use of (often costly) standards.

To combat this problem, the quadrupole mass analyser is itself often contained within a system known as a triple quadrupole (TQ). In this system, as the name suggests, there are three quadrupoles connected in a linear fashion. The first quadrupole serves to select an ion of interest based upon its m/z. The selected ion then enters the second quadrupole where it is exposed to a collision gas causing further fragmentation. The second quadrupole contains only an applied radio frequency rather than both an applied direct current and radio frequency. The third quadrupole can then further select ions by their m/z and they can enter the detector. This analytical method is known as LC-MS/MS. In the second quadrupole, compounds that have the same m/z will fragment into product ions in a different manner to each other. This allows differentiation between these compounds and can also provide structural information about the compound. A TOF analyser can also be included as part of this system; the third quadrupole on the TQ is replaced by a TOF analyser to give a quantitative TOF (QTOF)

instrument [333].

The third step in mass spectrometry is analysis of the separated ions as they enter a detector capable of differentiating between the ions and recording the observed response [329].

Liquid chromatography coupled to time of flight mass spectrometry (TOF-MS) is one of the most common methods used to analyse NPS-benzodiazepines because of its reliability and its ability to detect low concentrations (in the order of ng mL^{-1}) [134,333].

1.11   Research Aims

It is clear that there is a deficit of physicochemical and pharmacokinetic data for benzodiazepines [16]. Knowledge of the plasma protein binding of benzodiazepines has been shown to help correlate their *in vitro* receptor binding potential to their EC_{50} values (the concentration of a drug that produces a half-maximal response) therefore illustrating how pharmacokinetics can aid the prediction of pharmacodynamic properties [334]. The collection and collation of this data will allow the development of more accurate and precise modelling of the effects of benzodiazepines within the body and also aid in toxicological interpretations regarding the illicit use of benzodiazepines.

As mentioned in Section 1.10, a variety of methods have been used for the detection and quantitation of benzodiazepines. Therefore one aim was to develop and validate analytical methods capable of quantitating NPS-benzodiazepines.

A series of interlinked research aims have also been devised which are the determination of two physicochemical parameters (pK_a and log $D_{7.4}$) and a pharmacokinetic parameter (plasma protein binding) and the use of these three parameters to predict a pharmacokinetic parameter (Vd_{ss}) using the Øie-Tozer equation.

As many physicochemical and pharmacokinetic parameters can be theoretically estimated, another aim of this work is to compare experimental values (to be determined in this work) to theoretical values and judge whether theoretical values are a suitable replacement.

An important pharmacokinetic parameter discussed was the blood to plasma concentration ratio (Section 1.8.3) and an aim of this work is to determine this parameter for a series of NPS-benzodiazepines.

Knowledge of the metabolism of a compound is extremely important in knowing the fate of a compound and its metabolites within the body. The need for characterisation of cell cultures before using them to investigate the unknown metabolism of compounds was discussed previously (Section 1.8.4). Therefore another aim is to characterise two cell lines (C3A and HepaRG) and to use the most appropriate of these to investigate the metabolism of a series of NPS-benzodiazepines.

Investigation of the above pharmacokinetic and physicochemical parameters will add to the knowledge of NPS-benzodiazepines and allow more accurate and reliable predictions to be made about their pharmacokinetics.

Chapter 2

Experimental

2.1 Materials

2.1.1 Compounds and Reagents

Alprazolam, clonazepam, diazepam, flunitrazepam, nitrazepam, oxazepam, prazepam, temazepam, dextromethorphan, diclofenac, omeprazole, phenacetin, testosterone, chlorpromazine and quinine were obtained from Sigma-Aldrich (Dorset, UK).

3-Hydroxyphenazepam, 4'-chlorodiazepam, desalkylflurazepam, deschloroetizolam, diclazepam, etizolam, flubromazepam, flubromazolam, meclonazepam, nitrazolam, phenazepam and pyrazolam were obtained from Chiron AS (Trondheim, Norway). All compounds were received as powdered solids.

Dimethyl sulfoxide (DMSO), methanol, phosphoric acid, sodium hydrogen phosphate heptahydrate, sodium dihydrogen phosphate, disodium hydrogen phosphate, acetic acid, sodium acetate trihydrate, boric acid, sodium hydroxide, hydrochloric acid, sodium chloride and octan-1-ol were obtained from Fisher Scientific (Leicestershire, UK). Phosphate buffered saline (PBS) tablets were obtained from Sigma-Aldrich (Dorset, UK).

2.1.2 Biological Samples

Human plasma and blood (pooled, from three male donors and three female donors) was obtained from Seralab (West Sussex, UK). Plasma was received frozen with sodium citrate as an anticoagulant and kept frozen (-20 °C) until use. Blood was received chilled with sodium citrate as an anticoagulant and kept chilled (4 °C) until use. Both plasma and blood were used prior to their expiration dates.

2.1.3 Cell Cultures

The human hepatocellular carcinoma cell line C3A was obtained frozen from Heriot-Watt University (Edinburgh, UK) at passage 29 and kept frozen (-80 °C, liquid nitrogen) until use. The human hepatocellular carcinoma cell line HepaRG was obtained frozen from Fisher Scientific (Loughborough, UK) and kept frozen (-80 °C, liquid nitrogen) until use.

2.2 HPLC-DAD

The HPLC-DAD analysis discussed in this Section was used for analysis and quantitation of benzodiazepine concentrations for the log $D_{7.4}$ experiments and the plasma protein binding experiments.

2.2.1 Equipment

Analysis was carried out using a Dionex (Surrey, UK) UltiMate 3000 HPLC system equipped with an UltiMate 3000 Pump, UltiMate 3000 Autosampler, UltiMate 3000 Column Compartment, UltiMate 3000 Photodiode Array Detector and Chromeleon software. Separation was achieved with a Waters (Hertfordshire, UK) Spherisorb analytical column, C18 5 μM 80 Å (4.6 × 150 mm) with an attached guard column identically packed to the analytical column.

2.2.2   Conditions

The internal column temperature was kept constant at 25 °C and a flow rate of 0.8 mL min^{-1} was set. Injection volumes for the log D$_{7.4}$ experiments were 25 μL for the octanol phase and 100 μL for the phosphate buffer phase so that a dilution step was not necessary. Compound concentrations were retrospectively corrected. Injection volumes of 100 μL were used for the plasma protein binding experiments. A 46:54 (v/v) ratio of acetonitrile and sodium phosphate buffer (pH 3.0, 25 mM) was applied for 25 minutes. All compounds eluted within this time. The eluent was monitored by UV detection at 230 nm.

2.2.3   Validation

The method was validated in terms of linearity, limit of quantitation (LOQ), limit of detection (LOD), accuracy and precision. This was performed according to the ICH guidelines [335].

Linearity

The linearity of this method was measured by constructing a five-point calibration plot of the area under the curve (AUC) of each compound against its concentration which spanned from 0.0004 to 0.25 mg mL^{-1} (n=3).

LOQ and LOD

The limits of detection and quantitation were determined from the signal-to-noise ratio. The baseline response of the blank samples was recorded. The peak heights on the spectra at the retention time of the compound were compared to the peak heights at that same time on blank samples. A ratio of 10:1 for the compound response to the baseline response was used for the LOQ and a ratio of 3:1 for the LOD.

Accuracy

Accuracy was determined through comparison of the percentage recovery at three concentrations (0.25, 0.01 and 0.0004 mg mL^{-1}).

Precision

Precision was determined from the calculation of the standard deviation and relative standard deviation (RSD) of the compound peak areas at three concentrations (0.25, 0.01 and 0.0004 mg mL^{-1}).

2.3 GC-MS

The GC-MS analysis discussed in this Section was used for analysis and quantitation of benzodiazepine concentrations for the blood/plasma ratio experiments.

2.3.1 Equipment

The GC-MS method used an Agilent 7890B GC instrument with a 7693 autosampler and a 5977A MSD mass spectrometer. The column was a HP-5 MS 5 % phenyl 95 % methylpolysiloxane fused silica capillary column (30 m × 0.25 mm, thickness 0.25 mm).

2.3.2 Conditions

The inlet port temperature was set at 280 ℃, transfer line temperature was set at 250 ℃. The carrier gas was helium and the flow rate was a constant flow of 1.2 mL min^{-1}. Splitless injection volumes of 1 - 2 μL were used. The temperature program consisted of an initial temperature of 60 ℃ for two minutes followed by a 30 ℃/min ramp to 280 ℃ and a 10-minute hold at 280 ℃. The MS was operated in positive electron impact mode and the electron energy was 70.0 eV. Source temperature was 230 ℃ and the quadrupole temperature was 150 ℃.

2.3.3 Data Analysis

Qualitative data analysis was conducted using ChemStation version F.01.01.2317 to confirm the presence of the analytes using their respective m/z values for qualifier ions (Table 2.1). One quantifier ion was selected for quantification of the analyte (underlined in Table 2.1).

Table 2.1: Compound, retention time and target ions (quantification ion underlined) for GC-MS

Compound	Retention Time (minutes)	Target Ions
Chlorpromazine	9.66	$\underline{58}, 86, 272, 318$
Diazepam	9.50	$165, 221, \underline{256}, 283$
Nitrazepam	13.20	$206, 234, \underline{253}, 280$
Quinine	10.76	$96, \underline{136}, 215, 287$
Deschloroetizolam	13.71	$77, 239, \underline{279}, 308$
Diclazepam	9.93	$255, \underline{283}, 291, 318$
Etizolam	14.40	$239, 266, \underline{313}, 342$
Flubromazolam	13.97	$181, \underline{222}, 341, 370$
Meclonazepam	11.72	$240, 286, \underline{294}, 328$
Phenazepam	9.80	$75, 285, \underline{321}, 350$
Pyrazolam	8.23	$78, \underline{205}, 274, 353$

2.3.4   Validation

The method was validated in terms of linearity, limit of quantitation (LOQ), limit of detection (LOD), accuracy and precision according to ICH guidelines [335].

Linearity

Five concentrations (250, 100, 50, 25, 10 μM) were used to assess the relationship between concentration and instrument response. Three replicate injections were performed for each concentration.

Weighting factors (1/x or $1/x^2$) are often applied to transform the data in order to obtain a suitable fit [336,337]. The appropriateness of using a weighting factor was determined by conducting a two-sample F-test for variances to assess the variance in instrument response between the highest and lowest concentrations. The two-sample F-test for variances was conducted using the Data Analysis tools in Microsoft Excel. If the resultant p value was greater than 0.05 then there was no statistical difference between the two variances. If the resultant p value was lower than 0.05 then a statistically-significant difference existed between the two variances and a weighting factor was applied.

If a weighting factor was required, the use of a 1/x or $1/x^2$ transformation was assessed by means of a plot of the variance at each concentration versus the concentration. If the variance at each concentration followed a linear relationship with concentration, then this meant that

a 1/x weighting factor was used. If the variance at each concentration followed a non-linear parabolic relationship with concentration, then this meant that a $1/x^2$ weighting factor was required.

With knowledge of the appropriate weighting factor, the most appropriate model could then be assessed. Two models are typically used to describe data in GC-MS; linear and quadratic (Equations 2.1 and 2.2 respectively)

$$y = mx + c \tag{2.1}$$

Equation 2.1 Equation for a linear relationship between concentration and instrumental response

$$y = ax^2 + bx + c \tag{2.2}$$

Equation 2.2 Equation for a quadratic relationship between concentration and instrumental response

The model that adequately describes the relationship between concentration and instrument response while remaining the simplest model is the one preferred. To assess the appropriateness of a linear or quadratic model, a two-way analysis of variance (ANOVA) test was performed using the Data Analysis tools in Microsoft Excel. Both linear and quadratic models were used to generate theoretical values. The variance (square of the standard deviation) of these theoretical values when compared to the experimental values was calculated. The two-way ANOVA test was performed on the variances and generated a p value to compare the models. If the p-value was greater than 0.05 then this indicated that the change in variance when changing from a linear to a quadratic model was significant and that a quadratic model was most suitable. However, if the converse was true and the p value was less than 0.05 then this indicated that the increase in variance was not significant and a linear model was the most suitable.

LOQ and LOD

The limits of detection and quantitation were determined from the signal-to-noise ratio. The baseline response of blank samples was recorded. The peak heights on the spectra at the retention time of the compound were compared to the peak heights at that same time on blank samples. A ratio of 10:1 for the compound response to the baseline response was used for the LOQ and a ratio of 3:1 for the LOD.

Accuracy

Accuracy assessed for each compound through three replicate injections of three concentrations; 10, 50 and 250 μM and experimental instrument response was compared to theoretical instrument response from the calibration plot.

Precision

The inter-day and intra-day precision were measured at three concentrations which spanned the analytical range of the method; 10, 50 and 250 μM. Three replicate injections at each concentration were used and the standard deviation and relative standard deviation were calculated.

2.4   Extraction Procedure Development

Four benzodiazepines were chosen as test benzodiazepines for the methods; alprazolam, diazepam, nitrazepam and oxazepam. Stock solutions of these four benzodiazepines were formulated to yield a concentration of 20 mM in DMSO. Benzodiazepines were spiked into plasma at a concentration of 10 μM (final DMSO concentration 0.2 %). The extraction procedure was as follows; ice-cold acetonitrile was added (4:1 ratio), samples were centrifuged (10,000 rpm, 20 minutes) and the supernatant was then collected and evaporated using a flow of nitrogen (TurboVap). Blank controls were also performed where the benzodiazepines were spiked into acetonitrile rather than plasma. Three repetitions were performed for each benzodiazepine and all samples analysed using the HPLC-DAD method detailed in Section 2.2. The extraction efficiency was calculated from Equation 2.3.

$$Extraction \quad efficiency \quad (\%) = \frac{Plasma \quad concentration}{Control \quad concentration} \times 100 \qquad (2.3)$$

Equation 2.3 Calculation of extraction efficiency for protein precipitation.

2.5   Log D$_{7.4}$

2.5.1   Experimental Log D$_{7.4}$ Measurements

Sodium phosphate buffer (0.01 M) was formulated using deionised water (Barnstead UltraPure) and filtered through a 0.45 μM Nylon Phenex filter membrane (Phenomenex, Cheshire, UK) using a Millipore filtration apparatus (Merck Millipore, Hertfordshire, UK).

Compounds were dissolved in methanol at a concentration of 1 mg mL^{-1}. Aliquots of compound solution were evaporated with a flow of nitrogen using a TurboVap to yield 0.20 mg of compound. Equal volumes (700 μL) of sodium phosphate buffer (0.01 M, pH 7.4) and octanol were added and the samples were vortexed for 30 seconds.

The samples were transferred into 1.5 mL Eppendorf microcentrifuge tubes and placed on a Stuart SB3 rotator (Bibby Scientific, Staffordshire UK) and rotated at 40 rpm for four hours. Samples were then centrifuged at 10,000 rpm for 20 minutes. The octanol and buffer phases were separated and collected. Each log D$_{7.4}$ determination was repeated in triplicate.

2.5.2   Sample Analysis

Analysis of the octanol and buffer phases was achieved on an HPLC-DAD, details of which can be found in Section 2.2.

2.5.3   Calculation of Log D$_{7.4}$

Values for log D$_{7.4}$ were calculated from Equation 2.4.

$$logD_{7.4} = \frac{Compound \quad Concentration \quad in \quad Buffer}{Compound \quad Concentration \quad in \quad Octanol} \qquad (2.4)$$

Equation 2.4 Calculation of log D$_{7.4}$.

2.5.4   Method Development

Aliquots of 200 μL were evaporated to yield 0.2 mg of compound. This was then dissolved in equal volumes of octanol and phosphate buffer (pH 7.4, 0.01 M); 700 μL of each phase. These were then rotated to facilitate equilibration for a set period of time; 2 hours, 4 hours or 6 hours.

2.5.5   Theoretical Log D$_{7.4}$ Predictions

Theoretical log D$_{7.4}$ were generated using the free, online software ACD/I-Lab (which makes use of the EPSRC funded National Chemical Database Service hosted by the Royal Society of Chemistry) and two commercial software packages; MarvinSketch (version 17.28.0) (ChemAxon) and ADMET Predictor (Simulations Plus) [334-336].

2.6   pK$_a$ Measurements

2.6.1   Equipment

Compound migration times were determined using a Beckman Coulter P/ACE MDQ Capillary Electrophoresis System with a diode array detector (Beckman-Coulter, High Wycombe, UK). The internal capillary temperature was set at 25 °C using the liquid cooling system. Sample injection was conducted at 1.0 psi for 10 seconds and then 20 kV voltage was applied during separations. The capillary was rinsed between each run in the following manner; NaOH applied at 20 psi for 1.0 minute followed by the appropriate buffer for the next repeat at 20 psi for 2.0 minutes.

2.6.2   Experimental pK$_a$ Measurements

Phosphate, acetate and borate buffers were utilised as described elsewhere with a pH spacing of 0.5 pH units (Table 2.2) [341]. All buffers had an ionic strength of I=0.05 and a concentration of 0.05 M. Sodium chloride was used to adjust the ionic strength and hydrochloric acid (0.1 M) or sodium hydroxide (0.1 M) were used to adjust the pH values if necessary. The pH was measured with a Jenway 3505 pH meter (Jenway, Essex, UK) which was calibrated before use. Buffers were filtered prior to use through a 0.45 μM Nylon Phenex filter membrane (Phenomenex, Cheshire, UK) using a Millipore filtration apparatus (Merck Millipore, Hertfordshire, UK).

Table 2.2: Reagents used for each pH

pH	Reagent Masses, Volumes and Concentrations
1.5	22.30 g Na$_4$P$_2$O$_7$ ·10H$_2$O, 818.59 mL H$_3$PO$_4$ (1 M)
2.0	22.30 g Na$_4$P$_2$O$_7$ ·10H$_2$O, 287.69 mL H$_3$PO$_4$ (1 M)
2.5	22.30 g Na$_4$P$_2$O$_7$ ·10H$_2$O, 154.54 mL H$_3$PO$_4$ (1 M), 0.3247 g NaCl
3.0	6.22 mL H$_3$PO$_4$ (1 M), 5.25 g NaH$_2$PO$_4$
3.5	2.06 mL H$_3$PO$_4$ (1 M), 5.75 g NaH$_2$PO$_4$, 0.1076 g NaCl
4.0	40.96 mL CH$_3$COOH, 0.7413 g CH$_3$COONa, 2.39 g NaCl
5.0	15.42 mL CH$_3$COOH, 2.84 g CH$_3$COONa, 0.8956 g NaCl
6.0	2.13 mL CH$_3$COOH, 3.93 g CH$_3$COONa, 0.1248 g NaCl
7.0	2.72 g NaH$_2$PO$_4$, 3.88 g Na$_2$HPO$_4$
8.0	0.4595 g NaH$_2$PO$_4$, 6.55 g Na$_2$HPO$_4$
9.0	3.09 g H$_3$BO$_3$, 24.11 mL NaOH (1 M), 1.51 g NaCl
10.0	3.09 g H$_3$BO$_3$, 44.13 mL NaOH (1 M)
10.5	0.9247 g NaH$_2$CO$_3$, 4.13 g Na2CO3
11.0	0.2514 g NaH$_2$CO$_3$, 4.98 g Na2CO3
11.5	3.09 g H$_3$BO$_3$, 58.81 mL NaOH (1 M)
12.0	3.09 g H$_3$BO$_3$, 76.39 mL NaOH (1 M)

Compounds were dissolved in methanol at a concentration of 1 mg mL^{-1}. Solutions were diluted to 0.25 mg mL^{-1} with deionised water (Barnstead UltraPure) and contained DMSO as the electroosmotic flow marker (1 % v/v). DMSO (1 % v/v) in deionised water (Barnstead UltraPure) was run at each pH before experimental repeats to ensure that an expected electrophoretic mobility was obtained.

2.6.3   Calculation of pK$_a$ Values

Experimentally determined values for the effective mobility (μ_{eff}) were obtained using Equations 2.5 and 2.6.

$$\mu_{\text{eff}} = \frac{\alpha \times 10^{\text{-pH}}}{10^{\text{-pK}_a} + 10^{\text{-pH}}} \tag{2.5}$$

Equation 2.5 Relationship between effective mobility at a specific pH and the pK$_a$ of a compound.

$$\mu_{\text{eff}} = \frac{b_1(10^{\text{-pH}})^2 + a_1 10^{\text{-pK}_{a1}} 10^{\text{-pK}_{a2}}}{(10^{\text{-pH}})^2 + a_1 10^{\text{-pK}_{a1}} 10^{\text{-pH}} + 10^{\text{-pK}_{a1}} 10^{\text{-pK}_{a2}}} \tag{2.6}$$

Equation 2.6 Relationship between effective mobility at a specific pH and the pK$_a$ of a compound.

The Microsoft Excel add-in, Solver, was used to calculate the pK$_a$ value using least-squares regression. Initial best-guess estimates for the pK$_a$ and α values were used to calculate theoretical effective mobilities and the squared difference (the residuals) between these theoretical values and experimental values was then calculated and then this was minimised by varying the values for pK$_a$ and α. Each pK$_a$ measurement was repeated in triplicate.

2.6.4   Theoretical Prediction of the pK$_a$ Values of Benzodiazepines

Theoretical pK$_a$ values were generated using the free, online software ACD/I-Lab (which makes use of the EPSRC funded National Chemical Database Service hosted by the Royal Society of Chemistry) and two commercial software packages; MarvinSketch (version 17.28.0) (ChemAxon) and ADMET Predictor (Simulations Plus) [338-340].

2.7   Plasma Protein Binding Measurements

2.7.1   Experimental Plasma Protein Binding Measurements

Plasma protein binding values were determined using the commonly-used method of equilibrium dialysis [342]. Frozen plasma was thawed at room temperature prior to the experiments. The pH was measured with a Jenway 3505 pH meter (Jenway, Essex, UK) which was calibrated before use. Plasma pH was found to be within the physiological range of 7.38 - 7.42 and adjustment was not required [343].

PBS tablets were dissolved in deionised water (Barnstead UltraPure) to yield a buffer solution that contained 0.01 M phosphate, 0.0027M KCl, and 0.137 M NaCl, pH 7.4 at 25 °C. Stock solutions of compounds in DMSO at a concentration of 10 mM were created and were diluted with PBS prior to the experiments to yield working solutions at a concentration of 200 μM.

Reusable Single-Sample Fast Micro-Equilibrium Dialyzers (500 μL volume) were obtained from Harvard Apparatus (Cambridge, UK), as were cellulose acetate membranes with a molecular weight cut-off (MWCO) of 10,000 Da.

The membranes were soaked for 30 minutes in deionised water (Barnstead UltraPure) and rinsed thoroughly. 30 μL of compound working solution was added to 270 μL of plasma to yield a final concentration of 20 μM of compound (final DMSO concentration 0.2 %). This was placed in one chamber and 500 μL of PBS was placed in the second chamber. The Micro-Equilibrium Dialyzers were then placed into a shaking waterbath held at 37 °C for 24 hours.

The temperature was monitored with a Sentry Thermometer (Fisher Scientific, Leicestershire, UK). After 24 hours had elapsed, the samples were extracted from each chamber, matrix matched (with blank plasma or blank buffer). Ice-cold acetonitrile at a 4:1 ratio was then added to precipitate proteins. The samples were centrifuged at 10,000 rpm for 20 minutes and the supernatant was recovered and evaporated using a flow of nitrogen with a TurboVap. Each plasma protein binding measurement was repeated in triplicate.

2.7.2   HPLC-DAD Analysis

The evaporated samples were reconstituted in 200 μL of acetonitrile and analysed using HPLC-DAD. Details of this analysis are given in Section 2.2.

2.7.3   Calculation of Plasma Protein Binding

Plasma protein binding (PPB) was calculated using the experimental plasma concentration (P_{exp}) and the experimental buffer concentration (B_{exp}) according to Equation 2.7.

$$PPB \quad (\%) = 100 \times \frac{P_{\mathrm{exp}} - B_{\mathrm{exp}}}{P_{\mathrm{exp}}} \tag{2.7}$$

Equation 2.7 Calculation of plasma protein binding .

For those benzodiazepines that were highly protein bound and had a concentration in the buffer phase that was below the limit of quantitation (LOQ), the buffer concentration was calculated indirectly using Equation 2.8 which involved the experimental plasma concentration and the total expected concentration (P_{tot}), determined using a calibration plot. The total expected concentration was adjusted using a previously-determined correction factor (CF) for the extraction efficiency (95 %). This indirectly-calculated buffer concentration was then input into Equation 2.7 to generate plasma protein binding values.

$$B_{\mathrm{exp}} = P_{\mathrm{tot}} CF - P_{\mathrm{exp}} \tag{2.8}$$

Equation 2.8 Indirect calculations of the concentration of drugs in the buffer phase.

2.7.4   Method Development

Eight benzodiazepines were used to determine the appropriate length of equilibration (alprazolam, clonazepam, diazepam, flunitrazepam, nitrazepam, oxazepam, prazepam and temazepam). They had literature plasma protein binding values of 60 - 99 %.

2.7.5   Theoretical Prediction of Plasma Protein Binding

Theoretical plasma protein binding values were obtained from two sources used for $\log D_{7.4}$ and pK_a; ACD/I-Lab Lab (which makes use of the EPSRC funded National Chemical Database Service hosted by the Royal Society of Chemistry) and ADMET Predictor (Simulations Plus) and one source available as a free online resource, PreADMET (version 2.0) [338,340,344].

2.8   Volume of Distribution at Steady State

Values for Vd_{ss}, f_u, $\log D_{7.4}$ and $f_{i7.4}$ for 18 benzodiazepines were obtained from a variety of literature sources. No $\log D_{7.4}$ and pK_a data was available for some benzodiazepines and these were predicted using ACD/I-lab software online. For nine benzodiazepines (alprazolam, clonazepam, desmethyldiazepam, diazepam, flunitrazepam, nitrazepam, oxazepam, temazepam and triazolam) $\log D_{7.4}$, pK_a and plasma protein binding values were determined within this research and those values were used in the prediction of Vd_{ss}.

Multiple linear regression was performed using the R language programming environment [345].

2.9   Blood to Plasma Ratio

2.9.1   Experimental Determination of the Blood to Plasma Ratio

Whole blood was centrifuged at 2500 rpm for 20 minutes to separate the plasma from other blood components. This was performed on the day of the experiments. The resultant plasma was extracted and stored at 4 °C until use (typically within 2 hours).

Test analytes were dissolved in DMSO to yield stock solutions at a concentration of 5 mM. These stock solutions were subsequently diluted with PBS (pH 7.4) to produce working solutions at a concentration of 50 μM. Appropriate volumes of working solutions were added to blood or plasma to yield a final compound concentration of 5 μM (final solvent concentrations were 0.1 %). The treated whole blood or plasma samples were incubated for 1 hour at 37 °C.

Following incubation, the blood sample was centrifuged at 2500 rpm for 20 minutes and the plasma extracted. Ice-cold acetonitrile was added to extracted plasma and reference plasma (4:1 ratio) to induce protein precipitation. The plasma was centrifuged at 10,000 rpm to 20 minutes, the supernatant collected and evaporated to dryness under a stream of nitrogen using a TurboVap.

2.9.2   Sample Analysis

The evaporated samples were reconstituted in 50 - 150 μL acetonitrile and analysed using GC-MS. Details of the analysis with GC-MS can be found in Section 2.3.

2.9.3   Calculation of the Blood to Plasma Partition Coefficient

Once concentrations had been determined with GC-MS, the blood to plasma partition coefficient was calculated using Equation 2.9.

$$K_{e/p} = \frac{1}{H} \times (\frac{C_{Pref}}{C_P} - 1) + 1 \qquad (2.9)$$

Equation 2.9 Calculation of the red blood cell partition coefficient where $K_{E/P}$ is the red blood cell partition coefficient, H is the haematocrit, C_{Pref} is the concentration of the analyte in the reference plasma and C_P the concentration of the analyte in the plasma separated from the whole blood.

The haematocrit of the pooled blood was given as 41 % by the supplier Seralab.

2.10   Metabolic Studies

2.10.1   C3A Cell Line

Stock solutions of the substrates (phenacetin, bupropion, omeprazole, diclofenac, dextromethorphan and testosterone) were formulated in DMSO and subsequently diluted with the cell culture medium to obtain the desired concentrations for their K_m values (Table 2.4). The final concentration of the DMSO in these solutions did not exceed 0.1 %.

The C3A cells were maintained as an adherent cell line in 75 cm^2 Nunc EasYFlasks (Fisher Scientific, Leicestershire, UK) with the use of Gibco Minimum Essential Medium supplemented with 10 % fetal bovine serum, 1 × non-essential amino acids and 1 × sodium pyruvate in a 37 °C, 5 % CO_2 atmosphere. Medium was replaced every two to three days. Cells were passaged as required by using TrypLE Express enzyme. The C3A cells were seeded in 96-well microplates at a density of 3.3 × 10^5 cells per mL. At 60 % confluence the medium was replaced with one containing the test substrates at their respective K_m values (Table 2.4). The cells were then incubated with the substrates for 24 hours. The cell culture medium was collected for each substrate. Ice-cold acetonitrile was added at a 4:1 ratio and the samples centrifuged at 10,000 rpm for 20 minutes. The supernatant was extracted and evaporated with a flow of nitrogen using a TurboVap. All samples were stored at -20 °C until analysis.

Table 2.3: Substrates and their K_m values for CYP450 enzymes

CYP450 enzyme	Substrate	Concentration (μM)	Metabolite	Reference
CYP1A2	Phenacetin	50	Paracetamol	[346]
CYP2B6	Bupropion	100	2-OH-bupropion	[346]
CYP2C19	Omeprazole	20	5-OH-omeprazole	[346]
CYP2C9	Diclofenac	5	4-OH-diclofenac	[347]
CYP2D6	Dextromethorphan	5	Dextrorphan	[346]
CYP3A4/5	Testosterone	100	6-OH-testosterone	[346]

2.10.2   C3A Cells Treated with DMSO

The same procedure was conducted as described for the C3A cells other than that at 60 % confluence the medium was replaced with one containing 1 % (v/v) DMSO. Cultures were incubated for 20 days and the culture medium was replaced every 2 - 3 days. Cells were passaged upon reaching 60 % confluence. Following 20 days the cells were incubated with the test substrates; phenacetin, bupropion, diclofenac, dextromethorphan, testosterone and omeprazole at their respective K_m values. Following 24 hours of incubation the cell culture medium was collected for each substrate. Ice-cold acetonitrile was added at a 4:1 ratio and the samples centrifuged at 10,000 rpm for 20 minutes. The supernatant was extracted and evaporated with a flow of nitrogen using a TurboVap. All samples were stored at -20 °C until analysis.

2.10.3   Cell Counts

Estimations of the number of cells in culture for the C3A cells and DMSO-treated cells were performed by removing the cell culture medium and adding an appropriate volume of TrypLE Express Enzyme (1X) to remove the adherent cells. 100 μL of the resulting suspension was then stained with Tryphan Blue. The cells were counted using a haemocytometer.

2.10.4   HepaRG Cells

The HepaRG cells were seeded at 1.20×10^6 cells/mL in 24-well Collagen I coated microplates. Cell medium was Williams Medium E with 1 % to which HepaRG Thaw, Plate and General

Purpose Working Medium was added. The cells were cultured at 37 °C in a 5 % CO_2 atmosphere. Four hours after plating, the media was removed and replaced with one containing the substrates at their respective K_m values (Table 2.10.1). The cell culture medium was collected for each substrate after 24 hours of incubation. Ice-cold acetonitrile was added at a 4:1 ratio and the samples centrifuged at 10,000 rpm for 20 minutes. The supernatant was extracted and evaporated with a flow of nitrogen using a TurboVap. All samples were stored at -20 °C until analysis.

2.10.5   The Metabolism of NPS-Benzodiazepines

The NPS-benzodiazepines were incubated with HepaRG cells at a concentration of 10 μM. The same procedure for extraction was followed as is described in Section 2.10.4.

2.10.6   LC-MS/MS Analysis of Metabolites

Samples were processed by the internal mass spectrometry service at the University of Huddersfield. The supernatant that was collected in the previous sections was analysed using an Agilent 6530 Quadrupole Time-of-Flight (QTOF) LC/MS in the positive ionisation mode (ESI) attached to an Agilent 1290 Infinity HPLC instrument.

Two chromatographic methods were used. The first analysed the compounds incubated with the C3A and C3A-DMSO cell lines (bupropion, dextromethorphan, diclofenac, omeprazole, phenacetin and testosterone).

The mobile phases consisted of 0.1 % formic acid in acetonitrile (mobile phase A) and 0.1 % formic acid in water (mobile phase B). The flow rate was set at 0.5 mL min^{-1} and the proportions of the mobile phases at 0, 6, 12, 18, 36, 43, 43.1 and 46 minutes were 90/10, 90/10, 70/30, 70/30, 10/90, 10/90, 90/10 and 90/10 respectively. Separation was achieved with an ACE C18-AR column (250 × 4.6 mm, 5 μM) (Advanced Chromatography Technologies Ltd, Aberdeen, Scotland). The optimised V_{Cap} voltage and temperature were set at 3000 V and

300 °C. Octopole OCT 1 RF V_{pp} voltage was 750 V and the fragmentor voltage was 175 V. Nebuliser pressure was 35 psi and drying gas flow rate was 8 L min^{-1}.

Following this, method optimisation took place for the analysis of the compounds incubated with the HepaRG cell lines (bupropion, dextromethorphan, diclofenac, omeprazole, phenacetin, testosterone, 3-hydroxyphenazepam, 4'-chlorodiazepam, desalkylflurazepam, deschloroetizolam, diclazepam, etizolam, flubromazepam, flubromazolam, meclonazepam, nitrazolam, phenazepam and pyrazolam).

For this method mobile phases consisted of 0.1 % formic acid in acetonitrile (mobile phase A) and 0.1 % formic acid in water (mobile phase B). The flow rate was set at 0.5 mL min^{-1} and the proportions of the mobile phases at 0, 6, 12, 18, 36, 48, 48.1, 55 minutes were 90/10, 90/10, 70/30, 70/30, 10/90, 10/90, 90/10 and 90/10 respectively. Separation was achieved with an ACE C18-AR column (250 × 4.6 mm, 5 μM) (Advanced Chromatography Technologies Ltd, Aberdeen, Scotland). The optimised V_{Cap} voltage and temperature were set at 3000 V and 300 °C. Octopole OCT 1 RF V_{pp} voltage was 750 V and the fragmentor voltage was 150 V. Nebuliser pressure was 40 psi and drying gas flow rate was 8 L min^{-1}.

The main differences between the methods are a lower fragmentor voltage for the second method (150 V compared to 175 V) and a higher nebuliser pressure (40 psi compared to 35 psi).

The extracted cell culture media for omeprazole, a pure standard of omeprazole sulfide (0.01 mg mL^{-1}) and a pure standard omeprazole sulfone (0.01 mg mL^{-1}) were analysed using an Agilent 6210 Time-of-Flight (TOF) mass spectrometer (MS) operating in positive ionisation (Dual ESI) mode. Gas temperature was 350 °C, fragmentor voltage was 150 V, Octopole OCT 1 RF V_{pp} was 250 V, nebuliser pressure was 40 psi and the drying gas flow rate was 10 L min^{-1}. Skimmer voltage was 65 V and V_{Cap} voltage was 5000 V.

Chapter 3

Method Development and Validation

3.1 Validation of an HPLC-DAD Analytical Method

3.1.1 Introduction

HPLC-DAD was chosen to determine NPS-benzodiazepine concentrations for the log $D_{7.4}$ and plasma protein binding experiments as it is a common laboratory instrument and the development of methods and operation of instrumentation is generally held to be easier than that of mass spectrometry methods [348,349]. In addition many modern HPLC-DAD instruments are automated through the use of autosamplers so that multiple samples can be programmed to run in one sequence [350]. Although numerous validated HPLC-DAD methods exist for the quantification of benzodiazepines, none have been described in literature for the analysis of NPS-benzodiazepines [351,352].

The majority of this work to develop and validate an HPLC-DAD method for the analysis of NPS-benzodiazepines has already been published [353]. The HPLC-DAD method was validated according to ICH guidelines for linearity, limit of detection (LOD), limit of quantitation (LOQ), accuracy and precision [335]. Validation of analytical methods is important to ensure that reliable results are obtained through assessing the accuracy and precision of a method.

3.1.2 Results

Linearity

The linearity of an analytical method refers to the propensity of the measurements (e.g. peak area or peak height) to be proportional to the actual concentration of compound in the samples [354]. The method was linear over the concentration range 0.0004 - 0.25 mg mL^{-1} for all compounds. A high R^2 value for all compounds indicates a linear concentration-response and a suitable method (Table 3.1).

LOD and LOQ

The limit of quantitation is the lowest concentration that can be quantified with precision and accuracy while the limit of detection is the lowest concentration that can be detected although not quantified with accuracy and precision [354]. All compounds generally had comparable limits of detection and quantitation when compared with reported values in literature (Table 3.1). Pyrazolam exhibited the lowest response to the HPLC-DAD method, with a LOQ of 263.9 ng mL^{-1} and a LOD of 82.0 ng mL^{-1}. The observed LODs and LOQs were similar to that of other published HPLC-DAD methods for benzodiazepines such as alprazolam (LOQ 300 ng mL^{-1}) and diazepam, oxazepam and temazepam (LOD 50 ng mL^{-1}, LOQ 100 ng mL^{-1}) [355,356].

Accuracy and Precision

The accuracy of an analytical method refers to the closeness of a measured value to that of an accepted reference value [354]. Precision refers to the closeness of measured values of the same homogenous sample to one another and ensures that the same method will produce the same results with low variation [354]. Accuracy was determined through comparison of the percentage recovery at three concentrations; 0.25, 0.01 and 0.0004 mg mL^{-1} (n=3) as this covered the linear range assessed for this method. Percentage recovery was generally within 2 % (Table 3.2) and thus deemed to be acceptable as this was similar to reported accuracies for other HPLC-DAD methods for the quantitation of benzodiazepines [356]. Precision was determined from the calculation of the standard deviation and relative standard deviation (RSD) of the compound peak areas at three concentrations; 0.25, 0.01 and 0.0004 mg mL^{-1}

(n=3). High levels of precision for all benzodiazepines were recorded (Table 2) and were similar to levels of precision reported in literature previously for benzodiazepines with methods also using HPLC-DAD analysis [357,358].

3.1.3   Discussion

The HPLC-DAD analytical method described is suitable for the analysis of the NPS-benzodiazepines as judged by the linearity of the method in the established range and the high precision and accuracy obtained. The limits of quantitation and detection were similar to those reported elsewhere in literature.

Table 3.1: Linearity, LOQ and LOD data for benzodiazepines analysed using a HPLC-DAD method

Compound	Slope	Correlation coefficient	y intercept	Residual sum of squares	LOQ (ng mL^{-1})	LOD (ng mL^{-1})
3-Hydroxyphenazepam	4455.57	1.00	- 0.55	19.40	189	42.9
4'-Chlorodiazepam	4819.30	1.00	1.44	11.30	202	59.5
Alprazolam	4826.85	1.00	1.36	27.07	145	49.8
Clonazepam	4407.07	1.00	0.37	21.90	185	59.2
Desalkylflurazepam	4283.08	1.00	- 0.74	16.43	187	53.4
Deschloroetizolam	4072.89	1.00	0.86	13.00	206	62.5
Diazepam	4758.95	1.00	- 0.74	18.41	186	51.8
Diclazepam	4817.39	1.00	0.48	12.73	199	59.9
Etizolam	4007.71	1.00	0.51	13.20	194	57.0
Flubromazepam	4084.79	1.00	0.73	15.99	166	67.6
Flubromazolam	4168.69	1.00	- 0.42	10.68	177	47.2
Flunitrazepam	4223.77	1.00	- 0.92	13.05	159	51.5
Meclonazepam	4805.99	1.00	0.87	9.15	186	52.5
Nitrazepam	4367.07	1.00	- 0.37	10.82	179	49.4
Oxazepam	4466.93	1.00	- 0.53	7.17	160	50.2
Phenazepam	4149.34	1.00	- 0.17	11.76	191	65.3
Prazepam	4338.90	1.00	0.34	9.32	172	56.0
Pyrazolam	3967.82	1.00	- 0.31	14.76	264	82.0
Temazepam	4646.75	1.00	- 0.34	9.67	196	51.9

Table 3.2: Precision and accuracy data for benzodiazepines analysed using a HPLC-DAD method.

Compound	Concentration 0.0004 (n=3)			0.01 (n=3)			0.25 (n=3)		
	Precision SD	Precision RSD (%)	Accuracy (%)	Precision SD	Precision RSD (%)	Accuracy (%)	Precision SD	Precision RSD (%)	Accuracy (%)
3 - Hydroxyphenazepam	0.04	2.08	99.39	0.53	1.17	100.46	8.88	0.80	99.17
4' - Chlorodiazepam	0.06	1.72	101.35	0.47	0.93	101.85	10.29	0.85	100.54
Alprazolam	0.04	1.31	99.49	0.88	1.75	100.57	13.44	1.10	99.86
Clonazepam	0.05	1.53	101.11	0.81	1.62	99.25	6.91	1.77	99.98
Desalkylflurazepam	0.02	1.10	98.60	0.27	0.62	101.50	7.16	0.66	101.12
Deschloroetizolam	0.04	1.58	99.25	0.24	0.57	99.56	5.81	0.57	100.68
Diazepam	0.02	1.16	98.90	0.59	1.24	100.98	11.69	0.97	101.23
Diclazepam	0.02	0.70	98.92	0.54	1.07	101.49	6.46	0.54	99.10
Etizolam	0.04	1.74	98.99	0.72	1.78	99.57	9.95	1.00	99.73
Flubromazepam	0.03	1.16	99.21	0.66	1.56	101.76	5.36	0.52	101.34
Flubromazolam	0.03	2.15	100.41	0.55	1.13	100.89	17.93	1.71	100.74
Flunitrazepam	0.06	2.03	98.97	0.27	0.55	99.56	9.33	0.78	99.72
Meclonazepam	0.02	0.81	99.43	0.31	0.63	100.35	8.49	0.71	99.46
Nitrazepam	0.02	1.21	98.20	0.54	1.10	100.15	9.67	0.78	100.83
Oxazepam	0.02	1.44	101.76	0.70	1.56	101.68	7.48	0.68	99.21
Phenazepam	0.03	2.17	101.01	0.98	2.37	99.95	6.45	0.62	100.23
Prazepam	0.05	2.15	98.63	0.67	1.54	99.78	6.51	1.66	99.51

3.2 Validation of an GC-MS Analytical Method

3.2.1 Introduction

GC-MS is a common method used for the quantitation of drugs in forensic science [359]. GC-MS is widely-used and high accuracy and precision can be achieved with its use [360]. Validation of any analytical method is critical in order to ensure that any results obtained from it are reliable and the use of the method is appropriate [354]. For this analytical method this took place according to the ICH guidelines [335].

Quinine and chlorpromazine were included for the GC-MS method as they were used in the blood to plasma concentration ratio experiments, further details about this can be found in Section 8.

3.2.2 Results

The high sensitivity of the GC-MS towards benzodiazepines was evident by the large peak heights gained. This is exemplified by Figure 3.1; nitrazepam at a concentration of 250 μM or 70.3 μg mL^{-1}. High sensitivity is a typical characteristic of mass spectrometry methods and is a large factor behind their use.
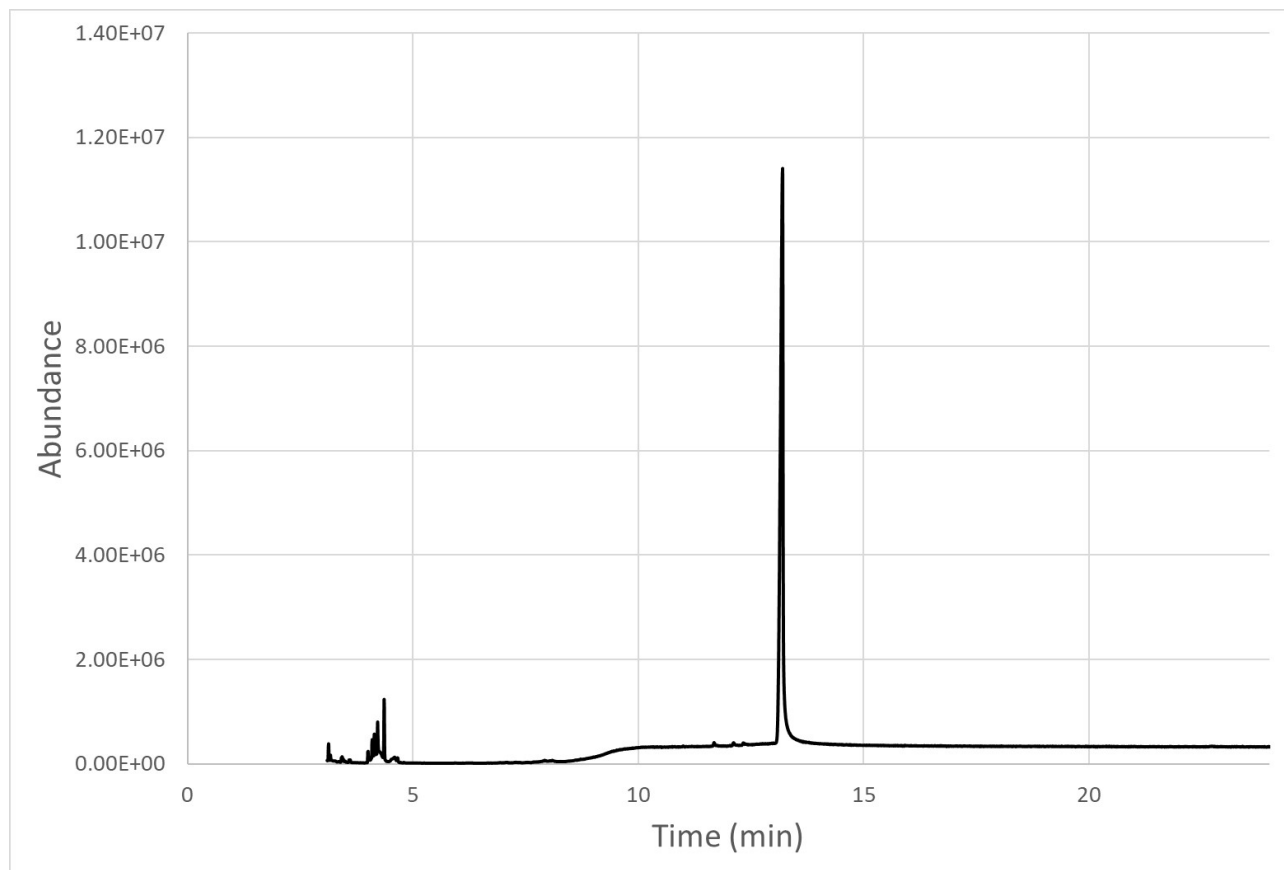
Figure 3.1: A chromatogram of nitrazepam at a concentration of 250 μM run using the method described in Section 2.3

Linearity

The linearity of an analytical method refers to whether a proportional response is obtained between the concentration of analyte in the sample and the resultant instrumental response (e.g. abundance) [361].

If a statistical difference exists between the variance at the highest concentration and the variance at the lowest concentration, then a weighting factor is typically applied to the data [336,337]. The variance is calculated as the square of the standard deviation. Using the Data Analysis tools in Microsoft Excel a two-sample F-test for variances can be performed, yielding a p value. If the p value was greater than 0.05 then this indicated that the difference in the variance at the highest concentration was not statistically significant when compared to the difference in the variance at the lowest concentration. If the p value was lower than 0.05 then this indicated that the difference in the variance at the highest concentration was statistically significant when compared to the difference in the variance at the lowest concentration. If the difference in variances was found to be statistically significant ($p < 0.05$) then a weighting factor was applied. This is typically a 1/x or $1/x^2$ weighting factor and can be performed in the Agilent software. A plot of the variance at each concentration versus the concentration was computed. If a linear relationship between variance and concentration is observed then a 1/x weighting factor is used, whereas if a parabolic relationship between variance and concentration is observed then a $1/x^2$ weighting factor is used.

An example of a parabolic relationship between variance and concentration is shown in Figure 3.2 for chlorpromazine and an example of a linear relationship between variance and concentration is shown in Figure 3.3.
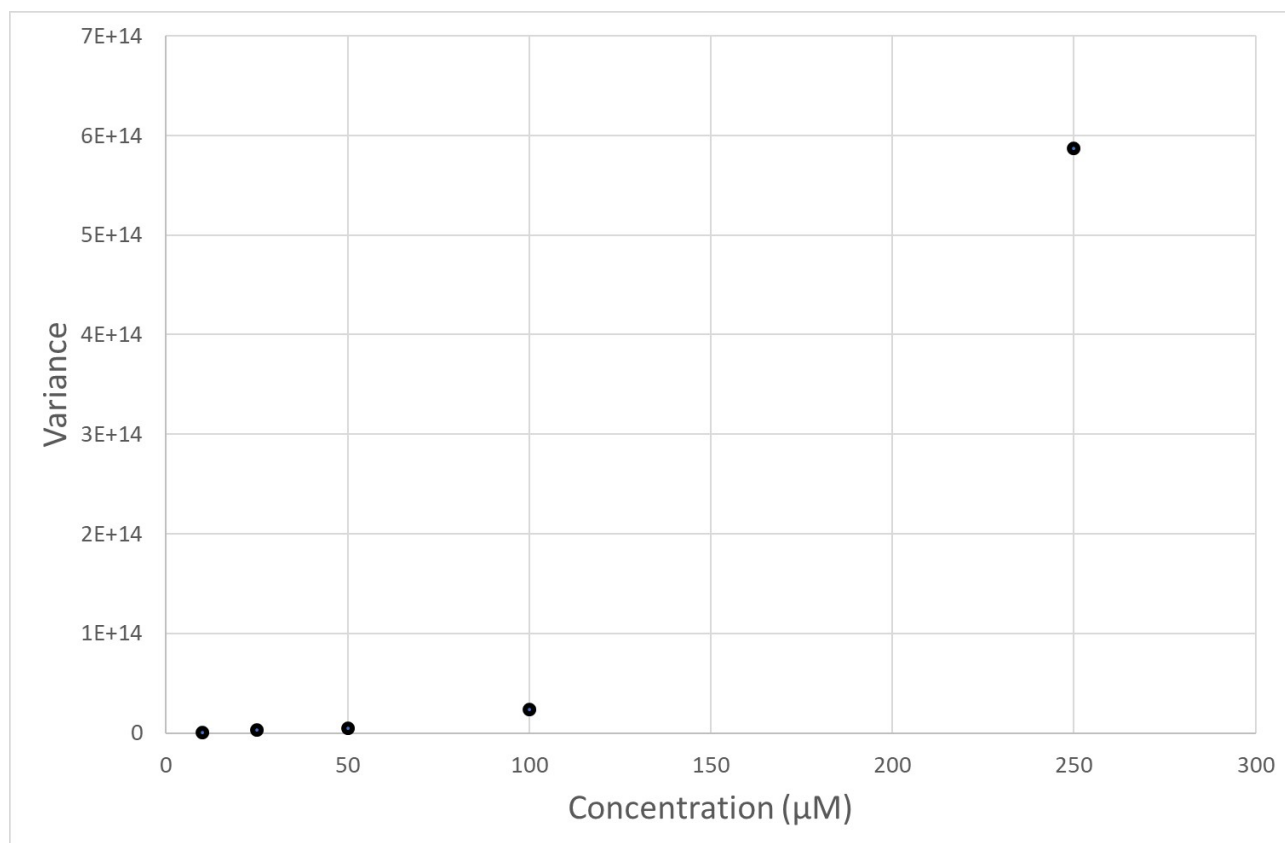
Figure 3.2: A plot of the variance against concentration for chlorpromazine
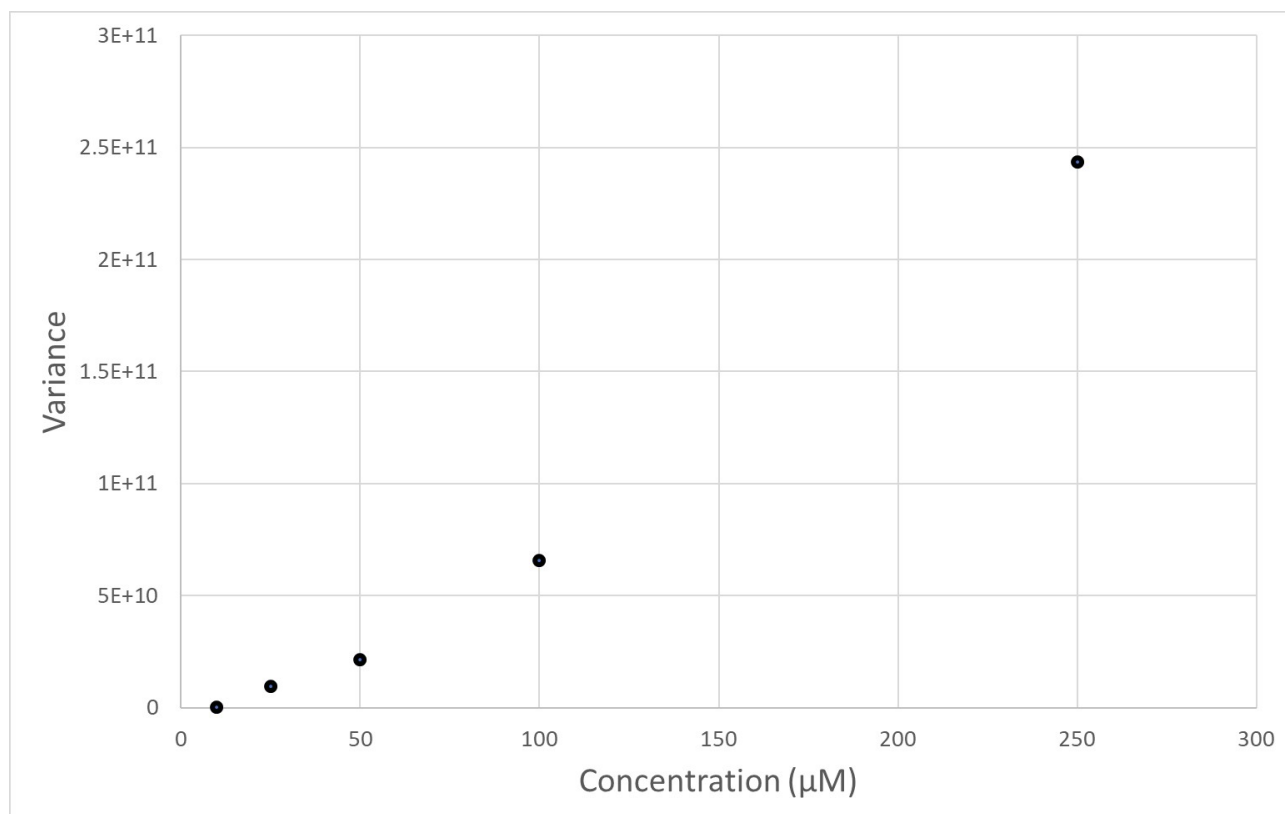
Figure 3.3: A plot of the variance against concentration for phenazepam

As discussed in Section 2.3, with knowledge of the weighting factor, the plot of data points can be fitted with either a linear (Equation 2.1) or quadratic (Equation 2.2) model.

The most appropriate model to use is the one that is the simplest but still adequately describes the relationship. The models can be compared using a two-way analysis of variation (ANOVA) test which can be performed using the Data Analysis tools in Microsoft Excel.

In this test, both linear and quadratic models are used to calculate a theoretical instrumental response for each of the five concentrations. The variation between the theoretical instrumental response and the experimental instrumental response (for both models) is then compared. A p value is obtained to describe the statistical significance of the models. If the p value is greater than 0.05 then the difference between models is not statistically significant and the quadratic model does not give a better fit to the data than the linear model. The purpose of this is to choose the simplest model to describe the data. The data used to determine the linearity is displayed in Table 3.3.

Table 3.3: Data used to validate the GC-MS method

Compound	p value for variance	Weighting required? ($p < 0.05$)	Weighting	p value between models	Chosen model	Slope	Correlation coefficient	y intercept	Standard deviation of the residuals (%)
Chlorpromazine	0.00114	Yes	$1/x^2$	0.37501	Linear	743565	0.9856	-133472	6.4
Diazepam	0.00693	Yes	$1/x$	0.33630	Linear	203406	0.9881	-27992	3.9
Nitrazepam	0.00253	Yes	$1/x$	0.44421	Linear	167529	0.9918	13515	3.5
Quinine	0.00085	Yes	$1/x^2$	0.27961	Linear	937503	0.9731	-98744	6.3
Diclazepam	0.00365	Yes	$1/x$	0.29428	Linear	211486	0.9771	-11163	5.7
Deschloroetizolam	0.00409	Yes	$1/x^2$	0.39600	Linear	94662	0.9898	5251	3.8
Etizolam	0.00169	Yes	$1/x^2$	0.89904	Linear	97205	0.9700	3408	5.8
Meclonazepam	0.00179	Yes	$1/x$	0.17453	Linear	96736	0.9755	-22642	5.7
Phenazepam	0.00109	Yes	$1/x$	0.40693	Linear	48633	0.9910	-14970	3.4
Pyrazolam	0.00037	Yes	$1/x^2$	0.19880	Linear	48493	0.9903	48493	3.4

Accuracy and Precision

The accuracy of an analytical method is the closeness of an experimental value to that of a reference value while the precision of an analytical method describes the closeness of replicates to one another [335]. Interday and intraday accuracy was assessed for each compound through three repetitions of three concentrations; 10, 50 and 250 μM and experimental instrument response was compared to the theoretical instrument response from a calibration plot. The results are displayed in Table 3.4.

The interday and intraday precision was measured at three concentrations as they spanned the analytical range of the method; 10, 50 and 250 μM. Three repetitions at each concentration were used and the relative standard deviation was calculated. The results are displayed in Table 3.4.

LOD and LOQ

The LOD is the lowest concentration of an analyte that is detectable by the analytical method, while the LOQ is the lowest concentration of an analyte that is detectable by the analytical while maintaining an acceptable level of accuracy and precision [382]. The values of the LOD and LOQ are displayed in Table 3.5.

Table 3.4: Interday (Inter) and Intraday (Intra) Precision (Prec) and Accuracy (Acc) Data for Compounds and Benzodiazepines in the GC-MS Method.

Compound	Concentration 250 μM ($n=3$)				Concentration 50 μM ($n=3$)				Concentration 10 μM ($n=3$)			
	Inter Prec RSD (%)	Intra Prec RSD (%)	Inter Acc (%)	Intra Acc (%)	Inter Prec RSD (%)	Intra Prec RSD (%)	Inter Acc (%)	Intra Acc (%)	Inter Prec RSD (%)	Intra Prec RSD (%)	Inter Acc (%)	Intra Acc (%)
Chlorpromazine	11.9	5.6	109.2	105.0	5.6	8.3	105.8	107.6	11.6	8.3	96.4	97.5
Diazepam	5.0	6.4	97.3	97.9	9.0	2.5	96.7	106.5	7.1	5.5	104.4	94.0
Nitrazepam	5.1	4.6	97.0	95.6	9.9	5.3	94.9	101.2	6.3	7.8	98.0	103.0
Quinine	12.7	3.7	107.0	108.7	10.3	5.3	106.9	95.2	9.7	4.4	103.4	104.4
Diclazepam	4.7	6.5	93.7	93.6	7.5	6.1	87.6	91.5	6.7	6.8	101.7	107.6
Deschloroetizolam	4.7	3.5	93.9	110.6	6.7	10.1	103.5	97.3	6.7	6.4	105.3	103.2
Etizolam	9.6	6.1	93.3	103.2	12.3	10.5	92.5	94.1	8.4	11.0	97.6	107.4
Meclonazepam	5.6	3.8	107.2	104.5	14.3	5.6	86.6	97.0	7.0	6.0	93.0	107.3
Phenazepam	3.9	6.2	104.9	106.0	7.0	8.4	87.2	96.9	3.8	6.7	90.0	95.2
Pyrazolam	8.6	2.4	100.9	98.1	6.4	8.1	100.3	104.3	3.8	4.7	108.9	103.5

Table 3.5: Limits of quantitation and detection for compounds using the GC-MS method

Compound	LOQ (ng mL^{-1})	LOD (ng mL^{-1})
Chlorpromazine	235.9	130.7
Diazepam	170.8	76.9
Nitrazepam	472.5	140.6
Quinine	525.6	159.0
Diclazepam	242.6	92.6
Deschloroetizolam	410.2	138.8
Etizolam	438.8	96.0
Meclonazepam	359.4	89.0
Phenazepam	262.2	73.4
Pyrazolam	492.4	134.6

3.2.3   Discussion

Thermal decomposition of nitrazepam has been observed when analysing with GC-MS and 7-aminonitrazepam is formed through reduction [362]. Peak shoulders or separate peaks are observed with this decomposition. However, no such peaks were observed in this work, possibly as a result of the lower temperature used in this method; 280 °C versus 300 °C described in literature [362]. This is evident in Figure 3.1, a chromatogram of the instrumental response against time for nitrazepam at a concentration of 250 μM (70.3 μg mL^{-1}).

Linearity

Parabolic responses of the variance per concentration were identified for chlorpromazine, quinine, deschloroetizolam, etizolam and pyrazolam. Therefore a $1/x^2$ weighting factor was used. All other compounds had a $1/x$ weighting factor applied. Linearity was good, with the lowest R^2 being 0.9700 for etizolam and the highest being an R^2 of 0.9918 for nitrazepam. These R^2 values for the linearity of the concentration-response plots were similar to those seen in literature for the GC-MS analysis of benzodiazepines [359,362-364].

Accuracy and Precision

The best interday accuracy was 100.3 % for pyrazolam at a concentration of 50 μM and the lowest interday accuracy was 109.2 % for chlorpromazine at 250 μM. The best intraday accuracy was 101.2 % for nitrazepam at 10 μM and the lowest intraday accuracy was 91.5 % for diclazepam at a concentration of 50 μM.

The lowest interday precision observed was a relative standard deviation of 14.3 % for meclonazepam at 50 μM and the highest interday precision was 3.8 % for phenazepam and pyrazolam both at 10 μM. The lowest intraday precision was a relative standard deviation of 11.0 % for etizolam at a concentration of 10 μM and the highest intraday precision was a relative standard deviation of 2.4 % for pyrazolam at a concentration of 250 μM.

All calculated values for accuracy and precision were within the previously-specified criteria of ± 15 % which is similar to other GC-MS methods described in literature [365].

LOD and LOQ

The limits of quantitation and detection can be found in Table 3.5.

The lowest LOD was 73.4 ng mL^{-1} for phenazepam while the highest was 159.0 ng mL^{-1} for quinine. The lowest LOQ was 170.8 ng mL^{-1} for diazepam while the highest was 525.6 ng mL^{-1} for quinine.

The limits of detection and quantitation were lower than those reported elsewhere in literature for similar GC-MS methods. Diazepam was determined as having an LOD of 76.9 ng mL^{-1} in this work versus 8 - 38.6 ng mL^{-1} elsewhere and an LOQ of 170.8 ng mL^{-1} in this work against an LOQ 103 - 116.9 ng mL^{-1} elsewhere [364].

Quinine has a reported LOD of 12.2 ng mL^{-1} versus 159.0 ng mL^{-1} in this work and an LOQ of 40.6 ng mL^{-1} versus 525.6 mg mL^{-1} in this work [366].

The differences in the limits of quantitation and detection can be explained by the lack of sensitivity of the mass spectrometer used. In addition the method was not fully optimised as obtaining low limits of detection and quantitation was not the primary aim of this validation process. The primary use of this method was to quantitate compound concentrations for the blood to plasma concentration ratio experiments as detailed in Section 8. Based upon the data presented regarding the good linearity of the method and the high accuracy and precision, the method was suitably validated.

Chapter 4

The log $D_{7.4}$ of NPS-benzodiazepines

4.1 Introduction

As discussed in Section 1.7.1, the log $D_{7.4}$ of a compound affects all pharmacokinetic parameters such as its absorption through biological membranes, its distribution within the body (e.g. plasma protein binding) and its metabolism and its excretion [112,113]. As a result of its effects on these pharmacokinetic processes, knowledge of the log $D_{7.4}$ is especially important for pharmacokinetic modelling [121,126]. Benzodiazepines are absorbed quickly within the body and distribute well into the brain because of their relatively high lipophilicity with the majority of benzodiazepines having a log $D_{7.4}$ between 2-3 [128-133].

Although high-throughput methods exist for the determination of log $D_{7.4}$, the shake-flask method is generally considered the 'gold standard' as it is accurate and precise and can be performed easily with standard laboratory equipment and reagents [136,137]. The shake-flask method typically only requires octanol, reagents for formulating an appropriate buffer, a method to separate the two phases (e.g. a centrifuge) and a method to analyse the compound concentrations (e.g. any of a variety of spectroscopic methods) [136]. The aims of the work in this Section were to develop and validate an appropriate shake-flask method for the benzodiazepines under investigation. This took place by comparing the log $D_{7.4}$ values obtained for eight test benzodiazepines that were equilibrated for three time periods; one, four or six hours.

Once an appropriate method of measuring log $D_{7.4}$ had been developed, the aim was to determine the log $D_{7.4}$ of 12 NPS-benzodiazepines. These experimental values could then be compared to theoretical values in order to evaluate whether theoretical predictions could replace experimentally-determined values. Log $D_{7.4}$ values play a crucial role in the prediction of pharmacokinetic parameters such as the volume of distribution at steady state [135]. The generation of log $D_{7.4}$ values in this Section will therefore also be used to predict this pharmacokinetic parameter. The majority of this work to determine the log $D_{7.4}$ values of NPS-benzodiazepines, compare them to theoretical predictions from software packages and subsequent analysis of the values has been published [353].

4.2 Results

4.2.1 Log $D_{7.4}$ Method Development

The calculated log $D_{7.4}$ values for the eight test benzodiazepines equilibrating for 1, 4 or 6 hours are listed in Table 4.1. An unpaired t test was used to compare the values calculated at 4 and 6 hours.

4.2.2 Theoretical log $D_{7.4}$ values of benzodiazepines

The most suitable length of equilibration was selected for the determination of the log $D_{7.4}$ of the NPS-benzodiazepines in the study. The experimental values are listed in Table 4.1.

4.2.3 Theoretical log $D_{7.4}$ of NPS-benzodiazepines

Following the experimental determination of log $D_{7.4}$, the theoretical values were generated and compared by means of the absolute error. This was performed for both the test benzodiazepines and the NPS-benzodiazepines.

Table 4.1: Benzodiazepine, literature log D$_{7.4}$ and experimental log D$_{7.4}$ values at a range of volumes and times

Benzodiazepine	Log D$_{7.4}$ 1 hour	Log D$_{7.4}$ 4 hours	Log D$_{7.4}$ 6 hours	p value (4 and 6 hours)	Log D$_{7.4}$ literature	References
Alprazolam	0.26 ±0.06	2.10 ±0.01	2.07 ±0.04	0.2761	2.12 - 2.16	[367,368]
Clonazepam	0.36 ±0.24	2.40 ±0.02	2.43 ±0.03	0.2230	2.41	[367,369]
Diazepam	0.69 ±0.31	2.81 ±0.03	2.87 ±0.13	0.4795	2.79 - 2.99	[367-370]
Flunitrazepam	0.37 ±0.13	2.05 ±0.01	2.07 ±0.05	0.5342	2.06 - 2.14	[367-369]
Nitrazepam	0.23 ±0.16	2.17 ±0.03	2.15 ±0.03	0.4601	2.13 - 2.16	[367,369]
Oxazepam	0.60 ±0.17	2.24 ±0.05	2.20 ±0.06	0.4252	2.13 - 2.24	[369,371]
Prazepam	0.51 ±0.19	3.74 ±0.04	3.68 ±0.02	0.0808	3.7 - 3.73	[367,369]
Temazepam	0.68 ±0.24	2.32 ±0.01	2.30 ±0.02	0.1963	1.79 - 2.19	[367,369]

Table 4.2: Benzodiazepine, literature, experimental and theoretical log $D_{7.4}$ values and absolute errors for 3 software packages; ACD/I-Lab (ACD), Marvin Sketch (MS) and ADMET Predictor (AP).

Compound	Literature log $D_{7.4}$	Experimental log $D_{7.4}$	Theoretical log $D_{7.4}$			Absolute Error			References
			ACD	MS	AP	ACD	MS	AP	
Test Benzodiazepines									
Alprazolam	2.12 - 2.16	2.10 ±0.01	2.44	3.02	2.63	0.34	0.85	0.53	[367,368]
Clonazepam	2.41	2.40 ±0.02	2.57	3.15	2.49	0.17	0.56	0.09	[367,369]
Diazepam	2.79 - 2.99	2.81 ±0.03	2.87	3.08	2.96	0.06	0.07	0.15	[367-370]
Flunitrazepam	2.06 - 2.14	2.05 ±0.01	2.20	2.55	1.87	0.15	0.25	0.18	[367-369]
Nitrazepam	2.13 - 2.16	2.17 ±0.03	2.03	2.55	2.49	0.14	0.14	0.32	[367-369]
Oxazepam	2.13 - 2.24	2.24 ±0.05	2.04	2.92	1.95	0.20	0.46	0.29	[369,371]
Prazepam	3.7 - 3.73	3.74 ±0.04	3.84	3.86	3.68	0.10	0.01	0.06	[367,369]
Temazepam	1.79 - 2.19	2.32 ±0.01	2.13	2.79	2.18	0.19	0.22	0.14	[367,369]
NPS-Benzodiazepines									
3-Hydroxyphenazepam	Not reported	2.54 ±0.01	2.67	3.69	2.40	0.13	1.15	0.14	Not reported
4'-Chlorodiazepam	Not reported	2.75 ±0.08	3.13	3.68	3.40	0.38	0.93	0.65	Not reported
Desalkylflurazepam	2.78	2.82 ±0.09	2.71	3.15	2.74	0.11	0.33	0.08	[367]
Deschloroetizolam	Not reported	2.60 ±0.03	2.43	3.45	2.82	0.17	0.85	0.22	Not reported
Diclazepam	Not reported	2.73 ±0.02	3.13	3.68	3.25	0.40	0.95	0.52	Not reported
Etizolam	Not reported	2.40 ±0.01	2.74	4.06	3.32	0.34	1.66	0.92	Not reported
Flubromazepam	Not reported	2.87 ±0.05	2.96	3.52	2.80	0.09	0.65	0.07	Not reported
Flubromazolam	Not reported	2.40 ±0.04	2.52	3.33	2.60	0.12	0.93	0.20	Not reported
Meclonazepam	Not reported	2.64 ±0.05	2.91	3.72	2.80	0.27	1.08	0.16	Not reported
Phenazepam	Not reported	3.25 ±0.04	3.52	3.98	3.19	0.27	0.73	0.06	Not reported
Pyrazolam	Not reported	0.97 ±0.01	1.76	2.36	2.03	0.79	1.39	1.06	Not reported

4.3   Discussion

4.3.1   Log D$_{7.4}$ method development

There are large variations in literature of experimentally-determined log D$_{7.4}$ values. For example, the compound nortriptyline has a reported log D$_{7.4}$ of both 1.1 and 2.05 with both methods using the shake-flask method; just under a ten-fold difference in lipophilicity [372,373]. Another compound, atenolol, has reported log D$_{7.4}$ values of -1.88 and -0.16 with both methods also using the shake-flask method [374,375]. This is approximately a 52-fold difference in reported lipophilicity. It is clear that factors exist that are responsible for the large variation in log D$_{7.4}$ values observed in literature. The composition of the buffer has long been known to play an important role in experimentally-determined log D$_{7.4}$ values [372]. However, experimental determination of log D$_{7.4}$ values is often not the primary focus of many studies; instead the majority of these studies are attempting to correlate log P or log D$_{7.4}$ values with other physiochemical properties and biological effects of the compounds. Thus it can be seen in literature that a selection of different buffers are often employed. A recent study calculated log D$_{7.4}$ values for 29 compounds using eight different buffers and found significant differences existed between the different buffer systems [376]. It was observed that although there was some relationship observed with polar surface area and molecular polarisability, the resulting differences in log D$_{7.4}$ values were unpredictable [376]. The large variation in published log D$_{7.4}$ values in literature is an observable effect of this. Use of a 0.01 M phosphate buffer has been shown to give an exact correlation of partition coefficients determined in the octanol-phosphate system for acidic and neutral drugs [377]. The use of a 0.01 M phosphate buffer is common and it is easily formulated using standard laboratory reagents [375].

The volume of 700 μL for each phase (1400 μL total) was chosen as this volume fits comfortably inside a 1500 μL microcentrifuge tube which was required for phase separation by centrifugation.

The values at one hour typically fell between log D$_{7.4}$ values of 0 - 1. A log D$_{7.4}$ value of 0 indicates an equal distribution between the octanol and buffer phases (i.e. a D value of 1 which would give a base-10 logarithm value of 0). Equal distribution between octanol and a buffer

phase for highly-lipophilic compounds such as the benzodiazepines indicates insufficient time for equilibration. The log $D_{7.4}$ obtained at 4 and 6 hours were more reasonable and either within the range of, or close to, established values in literature. The values observed at 4 and 6 hours were compared by means of an unpaired t test. The p values were not statistically significant for all eight test benzodiazepines. Therefore, to decrease the time taken for measurements, four hours was chosen and log $D_{7.4}$ at four hours was used.

4.3.2   Experimental log $D_{7.4}$

Alprazolam exhibited a slightly lower log $D_{7.4}$ of 2.10 compared to a literature range of 2.12 - 2.16 [367,368]. Clonazepam exhibited a similar log $D_{7.4}$ of 2.40 versus a single literature value that could be found of 2.41 [367,369]. Diazepam had a log $D_{7.4}$ of 2.81 within its literature range of 2.79 - 2.99 [367-370]. Flunitrazepam was slightly lower than literature range with a log $D_{7.4}$ of 2.05 versus 2.06 - 2.14 [367-369]. Nitrazepam had a similar log $D_{7.4}$ to its literature range of 2.13 - 2.16 [367,369]. Oxazepam was within its literature range of 2.13 - 2.24 with a log $D_{7.4}$ of 2.24 [369,371]. Prazepam was slightly above its literature range of 3.7 - 3.73 with a log $D_{7.4}$ of 3.74 [367,369]. Temazepam had a calculated log $D_{7.4}$ of 2.32 was versus literature values of 1.79 - 2.19 [367,369]. Although 0.13 log units higher than the greatest literature value there was a low standard deviation and all of the other experimental values for the benzodiazepines were in agreement with their literature values. In addition to this in the method development experiments, a value of 2.30 was observed for temazepam at 6 hours of equilibration. As discussed earlier, the log $D_{7.4}$ is dependent upon the method used to measure it including the choice of buffer and strength of the buffer. No such information was given for the reported values in literature and therefore it may be that the method in this work has a greater accuracy for measuring the log $D_{7.4}$ of benzodiazepines.

The experimental log $D_{7.4}$ values of the NPS-benzodiazepines under investigation are listed in Table 4.2. Similar to the test benzodiazepines, the NPS-benzodiazepines in this work were found to be highly lipophilic with the majority having log $D_{7.4}$ values above 2. Only one NPS-benzodiazepine had a previously-reported value in literature which was desalkylflurazepam

with 2.78 [367]. A value of 2.82 was returned in this work with a standard deviation of 0.09. The lowest log $D_{7.4}$ value observed was for pyrazolam, with 0.97. The highest log $D_{7.4}$ value observed was for phenazepam, with 3.25. The other ten benzodiazepines were in the range of 2.40 (etizolam and flubromazolam) to 2.87 (flubromazepam). These log $D_{7.4}$ values of between 2 and 3 are common for benzodiazepines, with seven of the eight test benzodiazepines falling into this range.

The only NPS-benzodiazepine in this work to return a log $D_{7.4}$ value of less than 2 was pyrazolam which was found to have a log $D_{7.4}$ of 0.97. This is an atypical benzodiazepine as it does not contain a phenyl ring at position 5 and rather contains a pyridin-2-yl ring. Analysing these molecular fragments in isolation reveals that a phenyl ring has a log $D_{7.4}$ of 1.56 versus a log $D_{7.4}$ of 0.62 for a pyridin-2-yl ring [378]. The presence of a bromine atom substituent at position 7 is also known to lead to a decreased log $D_{7.4}$ [133]. A prescription benzodiazepine, bromazepam, also contains a pyridin-2-yl ring and a 7-bromo substitution and has a reported log $D_{7.4}$ of 1.38 - 1.60 [367,369,370]. In contrast to bromazepam, pyrazolam is a triazolobenzodiazepine and thus contains an additional triazole ring. This is a known structural feature that has been well described as decreasing the apparent lipophilicity for other pharmaceutical compounds [379,380]. The structural features of a pyridin-2-yl ring, a 7-bromo substitution and a triazole ring are likely to have contributed to the low log $D_{7.4}$ of pyrazolam that was calculated in this work.

The lipophilicity (as log P) of ten NPS-benzodiazepines have already been published in literature with the stated aim of the authors being to make them available for the estimation of pharmacological and toxicological properties [134]. The work presented here adds to this.

4.3.3   Theoretical log $D_{7.4}$

Although a small dataset and thus more strongly influenced by the error in a single value, the average of the absolute errors was used to give a quick comparison between the generated values. ACD/I-Lab returned the closest values for the test benzodiazepines and the NPS-benzodiazepines with average absolute errors 0.18 and 0.28 respectively. ACD/I-Lab was

closely followed by ADMET Predictor which had average absolute errors of 0.24 for the test benzodiazepines and 0.37 for the NPS-benzodiazepines. MarvinSketch had an average absolute error of 0.39 for the test benzodiazepines and 0.97 for the NPS-benzodiazepines.

The greatest absolute errors were given by ACD/I-Lab for pyrazolam (0.79), MarvinSketch for etizolam (1.66) and by ADMET Predictor again for pyrazolam (1.06). Pyrazolam has a very low log $D_{7.4}$ value of 0.97 and the theoretical software packages may have failed to take into account the reduced lipophilicity likely as a result of the pyridine-2-yl ring it contains.

The second highest absolute error for MarvinSketch was for pyrazolam (1.39). The Consensus model used by MarvinSketch makes use of a model described in literature using multivariate regression [381]. This model is known to calculate a log P (octanol-water partition coefficient) for pyridine of 1.20 versus an experimental log P of 0.64, vastly overestimating the contribution of the pyridine group towards lipophilicity and this may be a factor behind the overestimation of lipophilicity [381].

However, this does not explain the large absolute error returned by MarvinSketch for etizolam (1.66). Although etizolam is a thienodiazepine the thiophene group is calculated in literature model as having a log p of of 1.63 versus an experimental log p of 1.81 [381]. Without knowing the specific calculations used to generate log $D_{7.4}$ values it is extremely difficult to attribute the errors generated in the theoretical log $D_{7.4}$ values to a specific cause. The inclusion of the experimental log $D_{7.4}$ values determined in this work in future predictive software may prove fruitful in order to improve their accuracy. For the moment it is clear that experimental log $D_{7.4}$ is more accurate than the available predictions from these three software packages. Evaluation of other software packages could prove useful in order to assess whether they hold any improvement in predicting log $D_{7.4}$ of NPS-benzodiazepines.

Chapter 5

The pK$_a$ of NPS-benzodiazepines

5.1   Introduction

Although pKa is often described as being of secondary importance as a physicochemical param-
eter when compared to log D$_{7.4}$, the use of pK$_a$ has still found great utility in pharmacokinetic
modelling such as predicting the volume of distribution at steady state, adipose tissue dis-
tribution and post-mortem redistribution of benzodiazepines [107,148-150]. pK$_a$ is especially
important when utilised in conjunction with other physicochemical parameters such as log
D$_{7.4}$ [106,141,143]. As the pK$_a$ of a compound affects factors such as its solubility in aqueous
media, it indirectly affects pharmacokinetic parameters such as absorption and distribution
[141,144,145].

The pK$_a$ values of benzodiazepines have been previously reported to aid correlation between
their log D$_{7.4}$, plasma protein binding and their volume of distribution at steady state [107,148].
This was discussed in greater detail in Section 1.8.2 but again highlights the importance of
accurate physicochemical knowledge.

In this study capillary electrophoresis was used to determine pK$_a$ values of benzodiazepines as
it is possibly the most common method and can be automated [154,155]. This facilitated quick
and easy determination of pK$_a$ values.

5.2 Results

5.2.1 Experimental pK$_a$ and Theoretical pK$_a$

The experimental results for pK$_a$ for the test benzodiazepines and NPS-benzodiazepines are given in Table 5.1.

ACD/I-Lab, MarvinSketch and ADMET Predictor were used to generate theoretical pK$_a$ values for both the test benzodiazepines and NPS-benzodiazepines and the values are provided in Table 5.1.

Table 5.1: Benzodiazepine, literature, experimental and theoretical pKa values and absolute errors for 3 software packages; ACD/I-Lab (ACD), Marvin Sketch (MS) and ADMET Predictor (AP).

Compound	Literature pKa		Experimental pKa		Theoretical pKa — ACD		Theoretical pKa — MS		Theoretical pKa — AP		References
	pKa1	pKa2	pKa1	pKa2	pKa1	pKa2	pKa1	pKa2	pKa1	pKa2	
Test Benzodiazepines											
Alprazolam	2.4	N/A	2.48 ±0.01	N/A	2.37	N/A	1.45, 5.01	N/A	0.93, 3.01	N/A	[382]
Clonazepam	1.49 - 1.52	10.37 - 10.51	1.55 ±0.02	10.45 ±0.05	1.55	11.21	1.89	11.65	1.43	10.77	[382-384]
Diazepam	3.17 - 3.31	N/A	3.10 ±0.00	N/A	3.40	N/A	2.92	N/A	2.96	N/A	[383,385]
Flunitrazepam	1.8	N/A	3.40 ±0.00	N/A	1.68	N/A	1.72	N/A	1.87	N/A	[382,386]
Flurazepam	N/A	N/A	1.82 ±0.04	N/A	2.55	N/A	2.65	N/A	2.49	N/A	[383,386]
Nitrazepam	2.94 - 3.2	10.8 - 11	3.11 ±0.06	11.02 ±0.05	2.65	11.35	2.49	11.66	2.57	11.02	[383,384]
Oxazepam	1.56 - 1.7	11.21 - 11.6	1.67 ±0.05	11.34 ±0.03	1.17	10.94, 12.75	1.66	10.65, 12.47	3.10	11.31	[383,384]
Prazepam	2.7 - 2.74	N/A	2.71 ±0.01	N/A	3.44	N/A	3.06	N/A	2.48	N/A	[382,383]
Temazepam	1.31 - 1.6	N/A	1.45 ±0.05	N/A	1.58	11.66	1.70	10.68	2.48	N/A	[383,387]
NPS-Benzodiazepines											
3-Hydroxyphenazepam	Not reported	Not reported	1.25 ±0.10	11.96 ±0.09	0.13	10.80, 12.68	N/A	10.61, 12.45	1.95	11.24	Not reported
4'-Chlorodiazepam	2.57	11.76	3.13 ±0.01	N/A	3.08	N/A	2.45	N/A	2.55	N/A	Not reported
Desalkylflurazepam	Not reported	Not reported	2.51 ±0.05	11.64 ±0.04	2.36	11.55	1.80	12.29	2.31	11.37	[388]
Deschloroetizolam	Not reported	Not reported	4.19 ±0.01	N/A	0.20, 2.45	N/A	1.31, 5.37	N/A	1.84, 3.96	N/A	Not reported
Diclazepam	Not reported	Not reported	2.31 ±0.07	N/A	1.75	N/A	2.13	N/A	1.95	N/A	Not reported
Etizolam	2.76	N/A	2.83 ±0.06	N/A	0.10, 2.37	N/A	1.33, 4.55	N/A	1.61, 3.31	N/A	[389]
Flubromazepam	Not reported	Not reported	3.25 ±0.10	10.74 ±0.05	2.32	11.55	1.8	12.28	2.70	11.45	Not reported
Flubromazolam	Not reported	Not reported	2.07 ±0.02	N/A	2.27	N/A	1.48, 4.01	N/A	0.96, 2.98	N/A	Not reported
Meclonazepam	Not reported	Not reported	2.10 ±0.09	11.45 ±0.07	1.70	11.24	1.65	11.57	2.10	10.88	Not reported
Phenazepam	Not reported	Not reported	2.19 ±0.05	11.21 ±0.04	2.18	11.58	2.06	12.28	2.44	11.43	Not reported
Pyrazolam	Not reported	Not reported	3.30 ±0.03	N/A	1.30, 2.18	N/A	1.79, 2.75	N/A	0.65, 2.47, 3.21	N/A	Not reported

5.3 Discussion

5.3.1 Method Development for Capillary Electrophoresis-PDA

Although the Beckman P/ACE MDQ capillary electrophoresis instrument was programmable and so therefore be automated, multiple problems arose with the use of it for this purpose. The capillary needle was fragile and during one repeat at one pH required four insertions into the vials (two rinses, one injection and one separation). For the compounds where two pK_a values were observed, 16 pH levels were needed; 1.5, 2.0, 2.5, 3.0, 3.5, 4.0, 5.0, 6.0, 7.0, 8.0, 9.0, 10.0, 10.5, 11.0, 11.5 and 12.5. Therefore 64 needle insertions were required for the repeat of one compound and 196 needle insertions for 3 repeats. The fragility of the capillary needle, coupled with the unyielding nature of the rubber caps for the vials caused frequent snapping of the needle. Therefore this could be alleviated to a certain extent by ceasing experiments once the compound and DMSO marker peaks had co-eluted at the same migration time. This meant that the compound was unionised and its pK_a value could be determined from the values already determined. For example, in the case of diazepam, both the DMSO marker and diazepam peaks had co-eluted by the injection at pH 5.0. Further experiments at higher pH levels up to 12.0 were not necessary; diazepam cannot have another pK_a value as there is no other deprotonation site on the molecule.

The 32 Karat Data Analysis Software was able to quickly identify and integrate peaks. The only information required from peak integration was the retention times of the compound and the DMSO marker. From this the migration times could be calculated and the Microsoft Excel add-in Solver could be used to calculate pK_a values.

The pK_a of a compound is not a constant and can be affected by temperature, ionic strength and the solvent dielectric constant [390]. Temperature can be controlled within the capillary electrophoresis instrument and was set at 20 °C. Ionic strength was also controlled, with all buffers having an ionic strength (I) of 0.05 as this is a standardised method [341]. As all the compounds were dissolved in methanol at the same concentration prior to capillary electrophoresis, the solvent dielectric constant was also kept constant.

The eight test benzodiazepines had pK$_a$ values determined in this work that were all within 0.20 pH units of their literature values with a standard deviation that was lower than of 0.07 pH units. These two values of 0.20 and 0.07 for accuracy and precision are the values typically held to be indicative of a suitable capillary electrophoresis method for determining pK$_a$ and further validation is not required [161].

5.3.2   Experimental pK$_a$

pK$_a$ values of 2.83 for etizolam and 2.51 and 11.64 for desalkylflurazepam were calculated in this work. These compared favourably to their literature values of 2.76 and of 2.57 and 11.76 [388,389].

The lowest value for pK$_a$1 was calculated as 1.25 for 3-hydroxyphenazepam. The presence of a hydroxyl group decreases the pK$_a$ of benzodiazepines as a result of the electron-withdrawing properties of this substituent [386]. The presence of a chlorine substituent at the R$_{2'}$ position is also known to decrease the pK$_a$1 value of 1,4-benzodiazepines [386]. Phenazepam, which is structurally similar to 3-hydroxyphenazepam except for the omission of a hydroxyl group, had a higher pK$_a$ of 2.19. The hydroxyl group on 3-hydroxyphenazepam led to a decrease in 0.94 pK$_a$ units when compared to phenazepam. A similar decrease was observed for temazepam which differs only from diazepam by the addition of a 3-hydroxyl group. The experimental pK$_a$ of temazepam was 1.45 compared to 3.10 for diazepam, a decrease of 1.65 pK$_a$ units. This relationship is also observed for nitrazepam and clonazepam. Nitrazepam does not contain a 2'-chloro substituent whereas clonazepam does. Nitrazepam has greater pK$_a$1 (3.11 versus 1.55) and pK$_a$2 (11.02 versus 1.45) values than clonazepam.

Another NPS-benzodiazepine that contains a substituent on the 3-position is meclonazepam. However, this substitution is a methyl group rather than a hydroxyl group. Meclonazepam is structurally similar to clonazepam, differing only by the addition of the 3-methyl group. Compared to the experimental pK$_a$1 and pK$_a$2 values of 1.55 and 10.45 for clonazepam, meclonazepam exhibited higher values of 2.10 and 11.45 respectively. This indicates that the 3-methyl substitution will increase the pK$_a$ values of benzodiazepines.

Deschloroetizolam has an increased pK_a1 (4.19) when compared to etizolam (2.83). Etizolam contains an additional 2'-chloro substituent and this has already been noted to produce a reduction in the pK_a1 value of 1,4-benzodiazepines [386]. A similar reduction also appears to occur for thienotriazolodiazepines.

4'-Chlorodiazepam and diazepam have similar pK_a values of 3.13 and 3.10 respectively, indicating that the addition of a chlorine substituent on the 4' position of a 1,4-benzodiazepine does not greatly affect its pK_a. In contrast however, the addition of a chlorine substituent on the 2' position causes the pK_a1 value to decrease from 3.10 (diazepam) to 2.31 (diclazepam).

The change of a 2′ substituent to one that is more electronegative appears to increase the pK_a1 and decrease the pK_a2 of 1,4-benzodiazepines. Flubromazepam has a 2'-fluoro substituent which is more electronegative than the 2'-chloro substituent of phenazepam. Flubromazepam has a higher pK_a1 (3.25 versus 2.19) and a lower pK_a2 (10.74 versus 11.21). Substituents with a greater electronegativity have a greater tendency to behave in an electron-withdrawing manner which can result in a partial deactivation of the aromatic system therefore leading to a reduction in the number of delocalised electrons. This in turn decreases the stability of negative charges in the system. As the pK_a2 values of 1,4-benzodiazepines are thought to be resonance-stabilised by delocalisation, any decreases in delocalisation have the effect of increasing the ease with which a species can be deprotonated. This therefore decreases the pK_a2 values which are resonance-stabilised negative charges on the nitrogen and oxygen atoms.

The change of 7- substituent to one that is less electronegative appears to increase the pK_a1 and decrease the pK_a2 of 1,4-benzodiazepines. Flubromazepam has a 7-bromo substituent which is less electronegative than the 7-chloro substituent of desalkylflurazepam. Flubromazepam has a higher pK_a1 (3.25 versus 2.51) and a lower pK_a2 (10.74 versus 11.64) than desalkylflurazepam. This is the opposite effect observed for substitution by a less electronegative substituent at the 2' position. The possible cause of this is that when a substituent at position 7 is less electronegative it reduces the propensity of that substituent to withdraw electrons. This means that a greater electron density exists in a more delocalised state in the molecule. The greater delocalisation stabilises negative charges and increases the ease by which a species can be

deprotonated.

A wider range of benzodiazepines with substituents at the 2' and 7 positions for 1,4-benzodiazepines would be required in order to more fully explore the observed differences between pK$_a$1 and pK$_a$2.

5.3.3   Theoretical pK$_a$

ADMET Predictor returned predicted values with the closest agreement to experimental pK$_a$ values, with an absolute average error of 0.4 for both the test set and the NPS set. This was closely followed by ACD/I-Lab which returned absolute average errors of 0.5 for both sets. MarvinSketch returned average absolute errors of 0.6 for the test set and 0.7 for the NPS set. MarvinSketch did not predict pK$_a$1 values for oxazepam and temazepam and instead predicted two pK$_a$2 values for oxazepam (only one of which exists) and one pK$_a$2 value for temazepam (only a pK$_a$1 value is observed). Large errors were observed in some of the pK$_a$ values returned by the software. For example; a pK$_a$ of 2.45 predicted by ACD/I-Lab for deschloroetizolam versus an experimental pK$_a$ of 4.19, a pK$_a$ of 1.33 predicted by MarvinSketch for etizolam versus an experimental pK$_a$ of 2.80 and a pK$_a$ of 2.98 predicted for flubromazolam by ADMET Predictor versus an experimental pK$_a$ of 2.07. Additionally, all three software packages predicted multiple other deprotonation sites for some of the benzodiazepines which are not experimentally observed. The importance of obtaining accurate experimental pK$_a$ values is therefore clear especially if these predictive models are to be improved upon.

Multiple versions of MarvinSketch exist and the accuracy of the pK$_a$ predictive software has been well-reviewed and compared to other programs for several of these versions. One study that looked at 261 protonation sites found that MarvinSketch 5.1.4. predicted 49.81 % of pK$_a$ values to within $\pm$ 0.5 log units and 14.94 % of pK$_a$ values to within $\pm$ 0.1 log units [162]. However the r^2 value was 0.763 which ranked MarvinSketch seventh out of nine programs.

In previous work no statistically-significant difference between the large errors given in pK$_a$ predictions by MarvinSketch 5.2. and pK$_a$ predictions given by ACD/I-Lab [391]. However

other research suggests that ACD/I-Lab is more accurate than MarvinSketch for predicting pK_a values [392]. In this work ACD/I-Lab was more accurate than MarvinSketch for predicting pK_a values. However, at present, none of the software packages were able to generate pK_a values that are as reliable as experimental pK_a values.

Chapter 6

The Plasma Protein Binding of NPS-benzodiazepines

6.1   Introduction

As discussed in Section 1.8.1, the fraction of a compound not bound to plasma proteins is responsible for the pharmacological effect and it is the unbound fraction that undergoes metabolism and elimination [166]. Plasma protein binding is therefore an important determinant of pharmacokinetic parameters such as the volume of distribution as steady state [166,177].

Plasma protein binding can be easily determined *in vitro*, requiring only equilibrium dialysis equipment and an analytical method capable of quantifying compound concentrations such as HPLC-DAD or LC-MS [176].

The work described in this Section to determine the plasma protein binding values of NPS-benzodiazepines, compare them to theoretical predictions from software packages and subsequent analysis of the values has previously been published in a peer-reviewed publication [353].

6.2   Results

6.2.1   Method Development

The eight benzodiazepines chosen for the method development (alprazolam, clonazepam, diazepam, flunitrazepam, oxazepam, nitrazepam, prazepam and temazepam) were chosen as they represent a range of benzodiazepine structures (diazepam is a 1,4-benzodiazepine, alprazolam is a triazolobenzodiazepine) and have a range of substitutions (prazepam has a bulky substituent on position 1, flunitrazepam has an NO_2 substitution, temazepam has a 3-hydroxy substituent).

The extraction efficiency of the eight benzodiazepines chosen to test the method is shown in Table 6.1. The average extraction efficiency was 94.9 $\pm$ 1.6 % (standard deviation).

The experimental plasma protein binding values after 6 hours and 24 hours, with standard deviations, are shown in Table 6.2, as are the p values.

Table 6.1: Extraction efficiencies for eight benzodiazepines.

Benzodiazepine	Extraction Efficiency (%) (n=3)
Alprazolam	94.2 $\pm$0.3
Clonazepam	94.9 $\pm$0.8
Diazepam	96.1 $\pm$0.7
Flunitrazepam	96.9 $\pm$1.1
Oxazepam	93.6 $\pm$1.3
Nitrazepam	95.9 $\pm$0.5
Prazepam	93.7 $\pm$2.9
Temazepam	94.0 $\pm$0.4

Table 6.2: Benzodiazepine, literature and experimental plasma protein binding (PPB) for 6 and 24 hours as well as standard deviations.

Compound	Literature PPB	Experimental PPB (n=3)		p value (6 and 24 hours)	References
		6 hours	24 hours		
Alprazolam	68.4 - 76.7	90.2 $\pm$9.3	71.6 $\pm$0.5	0.0258	[189,192]
Clonazepam	85.4 - 86.1	93.2 $\pm$3.3	85.5 $\pm$1.1	0.0186	[189,192]
Diazepam	98.4 - 99	98.6 $\pm$3.9	99.0 $\pm$0.2	0.8678	[192,342]
Flunitrazepam	77.5 - 84.5	88.4 $\pm$4.9	78.9 $\pm$1.2	0.0310	[189,192]
Nitrazepam	82.1 - 88.9	94.6 $\pm$2.3	88.4 $\pm$1.8	0.0213	[393,394]
Oxazepam	89.0 - 98.4	99.4 $\pm$1.2	96.9 $\pm$0.1	0.0228	[189,192]
Prazepam	97	98.8 $\pm$1.2	97.4 $\pm$0.5	0.1356	[395]
Temazepam	92 - 96.8	89.9 $\pm$4.3	94.3 $\pm$0.1	0.1511	[189,192]

Table 6.3: A comparison of the plasma pH at 6 hours and at 24 hours (n=5).

Plasma pH at 0 hours	Plasma pH at 24 hours	Difference	p value
7.41 ±0.03	7.48 ±0.09	+0.07	0.1376

The pH of five blank aliquots of plasma was measured prior to and after 24 hours of equilibration. The pH increased from 7.41 to 7.48 over the course of 24 hours. An unpaired t test was performed on the two values and the p value was found to be 0.1376 (Table 6.3).

6.2.2   Experimental and Theoretical Plasma Protein Binding

The most suitable length of equilibration for the determination of plasma protein binding was determined to be 24 hours. 24 hours was the equilibration time used to determine the plasma protein binding of 12 NPS-benzodiazepines.

The three software packages ACD/I-Lab, ADMET Predictor and PreADMET generated theoretical plasma protein binding values. These values were compared by means of the absolute error to the experimental values determined previously.

Table 6.4: Benzodiazepine, literature, experimental and theoretical plasma protein binding (PPB) values and absolute errors for 3 software packages; ACD/I-Lab (ACD), ADMET Predictor (AP) and PreADMET (PA).

Compound	Literature PPB	Experimental PPB	Theoretical PPB			Absolute Error			References
			ACD	AP	PA	ACD	AP	PA	
Test Benzodiazepines									
Alprazolam	68.4 - 76.7	71.6 ±0.5	89.5	91.2	95.2	17.9	19.6	23.60	[189,192]
Clonazepam	85.4 - 86.1	85.5 ±1.2	91.9	90.9	93.3	6.4	5.4	7.80	[189,192]
Diazepam	98.4 - 99	99.0 ±0.2	96.5	93.2	98.7	2.5	5.8	0.30	[192,342]
Flunitrazepam	77.5 - 84.5	78.9 ±1.2	84.4	86.5	98.9	5.5	7.6	20.00	[189,192]
Nitrazepam	82.1 - 88.9	88.4 ±1.8	88.5	84.3	92.0	0.1	4.1	3.60	[393,394]
Oxazepam	89.0 - 98.4	96.9 ±0.1	95.6	88.9	96.7	1.3	8.0	0.20	[189,192]
Prazepam	97	97.4 ±0.5	97.7	96.5	94.0	0.3	0.9	3.40	[395]
Temazepam	92 - 96.8	94.3 ±0.1	95.4	91.1	74.3	1.1	3.2	20.00	[189,192]
NPS-Benzodiazepines									
3-Hydroxyphenazepam	Not reported	97.7 0.6	92.5	93.8	90.1	5.2	7.60	3.9	Not reported
4'-Chlorodiazepam	Not reported	98.2 0.5	96.5	96.2	93.2	1.7	5.00	2.0	Not reported
Desalkylflurazepam	96.1 - 96.5	95.5 1.5	96.1	92.8	91.4	0.6	4.13	2.7	[396]
Deschloroetizolam	Not reported	87.2 1.5	85.8	91.5	89.8	1.4	2.56	4.3	Not reported
Diclazepam	Not reported	93.8 1.2	96.5	95.7	97.7	2.7	3.94	1.9	Not reported
Etizolam	Not reported	92.8 0.6	90.2	94.7	90.8	2.6	2.05	1.9	Not reported
Flubromazepam	Not reported	96.4 0.9	89.0	93.2	93.9	7.4	2.45	3.2	Not reported
Flubromazolam	89	89.5 0.4	87.4	91.1	92.2	2.1	2.73	1.6	[222]
Meclonazepam	Not reported	88.2 0.5	93.0	93.0	92.3	4.8	4.10	4.8	Not reported
Phenazepam	Not reported	98.3 1.2	94.6	95.6	93.6	3.7	4.68	2.7	Not reported
Pyrazolam	Not reported	78.7 0.4	77.6	86.5	94.8	1.1	16.07	7.8	Not reported

6.3 Discussion

6.3.1 Method Development

The extraction efficiency from plasma was calculated as being 94.9 %. This was high and had a low standard deviation of 1.6 % across the eight test benzodiazepines. The extraction efficiency was only required for calculation of an estimated concentration in the buffer, for those benzodiazepines that were highly-protein-bound and who had buffer concentrations below the LOQ determined in Section 2.2.

After six hours of equilibration the plasma protein binding values of all benzodiazepines other than temazepam were greater than their literature values. Temazepam had a plasma protein binding value of 89.9 % versus a literature range of 92 - 96.8 % [189,192]. As the compounds were spiked into the plasma, it is suggested that the passage of the compounds across the cellulose membranes was extremely slow and required a longer equilibration time of 24 hours. Although the dialysis apparatus was placed in a shaking waterbath to facilitate equilibration, there may not have been enough mechanical motion to encourage diffusion across the cellulose membrane. The result of this lack of equilibration time would have been a greater than expected concentration in the plasma phase and therefore overestimating plasma protein binding. However in literature an equilibrium dialysis time of 20 hours has been reported for alprazolam, diazepam, flunitrazepam oxazepam and temazepam [189,192]. There was no information on the method used for the determination of the plasma protein binding for prazepam [395]. Plasma protein binding for nitrazepam was obtained from *in vivo* data [393,394].

The p values for alprazolam, clonazepam, flunitrazepam, nitrazepam and oxazepam were all statistically significant when comparing 6 hours and 24 hours of equilibration. For diazepam, prazepam and temazepam the p values were not statistically significant. These three benzodiazepines are all highly-bound to plasma proteins and the potential lack of equilibration did not have an effect. For benzodiazepines with lower plasma protein binding, 6 hours of equilibration was in sufficient. After 24 hours of equilibration, the plasma protein binding values calculated were closer to the values stated in the literature. 24 hours has also been used for equilibration in

other plasma protein binding experiments, as reported for the NPS-benzodiazepine flubromazolam [222]. For equilibrium dialysis experiments with semipermeable membranes such as the cellulose membrane used in this work, equilibration times of up to 16 hours have been reported [211].

After 24 hours, all experimental plasma protein binding values generated were within literature ranges other than for prazepam. Only one literature value of 97 % for plasma protein binding was found for prazepam and an experimental value of 97.4 % was determined in this work. Age and sex of the donor have both been observed as causing differences in the plasma protein binding of drugs which could explain the ranges observed for plasma protein binding in literature [397,398]. The experimentally derived values for the test benzodiazepines were typically within literature ranges with low variations.

The pH of plasma naturally increases throughout the course of equilibrium dialysis experiments as a result of the loss of CO_2 from carbonic acid which acts as a buffer within plasma [399]. The increase in pH during the course of plasma protein binding experiments has been previously reported for 96-well equilibrium dialysis microplates [399]. These 96-well microplates are an alternative, high-throughput method of measuring plasma protein binding and consist of two chambers separated by a membrane, similar to the Harvard Apparatus Micro-Equilibrium Dialysers used in this work. However, they differ as they are sealed only by a thin adhesive film over the top which is gas-permeable [400]. The change in pH was also reportedly minimised when equilibration was conducted in an atmosphere containing 10 % CO_2 [399]. It has been reported that pH changes during equilibrium dialysis are minimised by the use of equipment consisting of thick polytetrafluoroethylene (PTFE) chambers [399]. The Harvard Apparatus Micro-Equilibrium Dialysers used in this work were thick (10 mm) PFTE dialysers which were able to be completely sealed in contrast to the 96-well equilibrium dialysis microplates. In this work the pH of five blank aliquots of plasma was measured prior to and after 24 hours of equilibration. The pH increased from 7.41 to 7.48 (n=5) over the course of 24 hours, although with only five samples the statistical power of this test could be improved upon . An unpaired t test was performed on the two values and the p value was found to be 0.1376 and thus the variance between the two values was not statistically significant. The thickness of these Micro-

Equilibrium Dialysers coupled with their ability to be completely sealed may have reduced the propensity of the plasma pH to change. In addition, the Micro-Equilibrium Dialysers were submerged in water which may have further limited the ability of CO_2 to diffuse out of the apparatus.

Although pH does affect the plasma protein binding during equilibrium dialysis, the plasma protein binding of diazepam has been observed to be very similar over the pH range from 7.2 - 7.8, decreasing by 0.25 % throughout this range and only decreasing by 0.63 % from pH 7.2 to pH 8.5 [401]. A difference of 0.25 % would be slightly above the standard deviation measured for diazepam (0.20 %) in this work and a difference of 0.63 % would be well within the standard deviation measured for other benzodiazepines such as nitrazepam (1.8 %) in this work.

The low standard deviation and closeness to literature values indicates that the proposed method of equilibrating for 24 hours was therefore found to be suitable for the determination of plasma protein binding and could be applied to find the plasma protein binding of NPS-benzodiazepines.

6.3.2   Experimental Plasma Protein Binding

The majority of the NPS-benzodiazepine whose plasma protein binding had not been determined had a high degree of plasma protein binding (> 90 %) similar to the test benzodiazepines (data for which can be viewed in Table 6.4). Three NPS-benzodiazepines had literature values for plasma protein binding. The plasma protein binding values derived in this work agreed with those found in literature; desalkylflurazepam (experimental 95.5 % versus 96.1 - 96.5 % literature), etizolam (experimental 92.8 % versus 93 % literature) and flubromazolam (experimental 89.5 % versus literature 89 %) [222,248,396,402].

Pyrazolam had an experimental plasma protein binding of 78.7 % which was far lower than the next lowest plasma protein binding of 87.2 % for deschloroetizolam. Although low compared to the rest of the benzodiazepines, some benzodiazepines have even lower plasma protein binding; for example bromazepam is 60 % bound to plasma proteins [403]. Bromazepam contains a
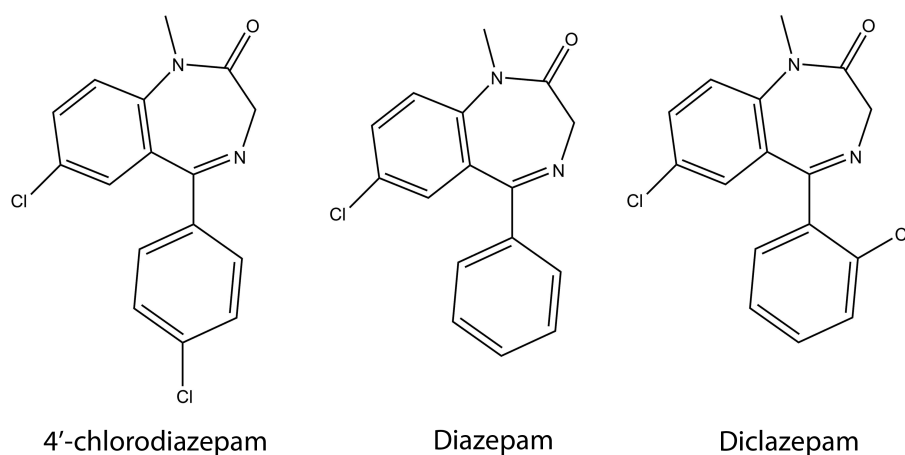
Figure 6.1: Molecular structures of diazepam, diclazepam and 4′-chlorodiazepam.

pyridin-2-yl ring rather than a phenyl ring at position 5. This substitution leads to a decrease in plasma protein binding for 1,4-benzodiazepines [402]. Although pyrazolam is a triazolobenzodiazepine the same effect and decrease in plasma protein binding could also occur as it also contains a pyridin-2-yl ring rather than a phenyl ring at position 5 (Figure 1.2A).

Two NPS-benzodiazepines in this work are structural isomers, 4′-chlorodiazepam and diclazepam. Both compounds are structurally related to a test benzodiazepine, diazepam, differing only by the substitution of a chlorine atom on the 2' position for diclazepam and the 4' position for 4′-chlorodiazepam.

4′-Chlorodiazepam exhibits similarly high plasma protein binding compared to diazepam; 98.2 % versus 99.0 %, however diclazepam has a reduced plasma protein binding of 93.8 %. The most likely reason for this is that substitution of a chlorine atom at the 4′ position is not thought to greatly affect the plasma protein binding of 1,4-benzodiazepines hence a similar plasma protein binding is observed for diazepam and 4′-chlorodiazepam [402]. However if this substitution is present at the 2′ position instead then a decrease in plasma protein binding is observed as a result of the change in the rotation and orientation of the phenyl ring; such a decrease is noted in this work for diclazepam [402].

Phenazepam also contains a chlorine atom on the 2' position and has a plasma protein binding of 98.3 %. Flubromazepam is structurally identical other than containing a fluorine atom on the 2' position instead and has a plasma protein binding of 96.4 %. This decrease in plasma

protein binding when a 2′-chloro substituent is replaced by a 2′-fluoro substituent is consistent with previous observations in literature [402].

Another structural feature leading to a decrease in plasma protein binding for 1,4-benzodiazepines is the addition of a hydroxyl group at position 3 [350]. 3-Hydroxyphenazepam has this substitution and exhibits a lower plasma protein binding of 97.7 % versus 98.3 % for phenazepam.

Replacement of a bromine atom at position 7 on 1,4-benzodiazepines by a chlorine atom is reported to lead to a decrease in plasma protein binding and this is confirmed here with de-salkylflurazepam containing a 7-chloro substituent and having a plasma protein binding of 95.5 % versus flubromazepam containing a 7-bromo substituent and having a plasma protein binding of 96.4 % [402].

Deschloroetizolam differs from etizolam by the removal of a chlorine atom on the 2' position. It has a lower plasma protein binding of 87.2 % versus 92.8 % whereas the opposite effect would be expected for the removal of a 2′-chloro substituent from a 1,4-benzodiazepine [402]. Substitution on the 2′ position may therefore be an important structural feature for thienotriazolodiazepine plasma protein binding in contrast to 1,4-benzodiazepines.

6.3.3   Theoretical Plasma Protein Binding

Theoretical plasma protein binding values were calculated using the three software packages; ACD/I-Lab, ADMET Predictor and PreADMET, are provided in Table 6.4. The differences between the experimental values and the theoretical values were calculated as average absolute errors.

Plasma protein binding was best predicted by ACD/I-Lab which returned average absolute errors of 4.4 % for the test benzodiazepines and 3.0 % for the NPS-benzodiazepines. ADMET Predictor followed closely behind with average absolute errors of 6.8 % for the test benzodi-azepines and 3.4 % for the NPS-benzodiazepines. PreADMET returned average absolute errors of 9.9 % for the test benzodiazepines and 5.0 %, compared to experimental determined data

for the NPS-benzodiazepines. The software packages appeared to be less effective at predicting plasma protein binding of the test benzodiazepines than the NPS-benzodiazepines (Table 6.4). However, an important caveat is that the average absolute error values for the test benzodiazepines were influenced heavily by the small dataset and the presence of alprazolam; the experimental plasma protein binding was determined as being 71.6 % and the predicted values were 89.5 % (ACD/I-Lab), 91.2 % (ADMET Predictor) and 95.2 % (PreADMET). It should be noted that all three predicted values are also outside the range found in literature which terminates at 76.7 % [189,192]. This is surprising as alprazolam is well-characterised and is the most widely-prescribed benzodiazepine and psychotropic drug in the United States although it is only available under private prescription in the United Kingdom [404].

The large errors observed for predictions for benzodiazepines such as alprazolam, which is widely-prescribed, highlights the necessity for the publication of reliable experimental data as it improves the accuracy of pharmacokinetic modelling and, if used to build predictive models, can improve predictive software for parameters such as plasma protein binding. At present the performance of the three software packages is not a suitable replacement for the experimental measurement of plasma protein binding.

Chapter 7

The Volume of Distribution at Steady State of NPS-Benzodiazepines

7.1   Introduction

In Sections 4, 5 and 6, the log $D_{7.4}$, the pK_a and the plasma protein binding of NPS-benzodiazepines were determined. As mentioned in Section 1.8.2, these three parameters are critical in predicting the volume of distribution at steady state [107,148]. Together these three parameters will be used to calculate the fraction of a compound unbound in the tissues of the body. From the unbound fraction in tissues, the volume of distribution at steady state can be calculated from the Øie-Tozer equation [208]. The volume of distribution at steady state has reported to have been calculated for 12 benzodiazepines with a mean-fold error of 1.86 [107,148]. The mean-fold error indicates that a predicted Vd_{ss} would be within 0.86 L kg^{-1} of its experimental value. The work in this Section aims to improve on the error in these pharmacokinetic predictions.

There are currently 35 benzodiazepines under international control although this is only a small proportion of the total benzodiazepine structures possible. Pharmacokinetic data is limited even for these 35 benzodiazepines, thus limiting the size of the dataset that could be gathered [6]. The fraction unbound in tissues is not a routine pharmacokinetic measurement, nor is the Vd_{ss}

as benzodiazepines are typically administered orally. For some benzodiazepines, no values for log $D_{7.4}$ or pK_a could be found in literature. As a result these were predicted using ACD/I-Lab for log $D_{7.4}$ (α-hydroxymidazolam, adinazolam and brotizolam) and ADMET Predictor for pK_a (adinazolam) as they were found to be the most reliable in previous research (Sections 4.3.3 and 5.3.3). In total seventeen benzodiazepines were included in the training dataset for the theoretical model. The training dataset was known experimental data from which theoretical relationships could be derived through nonlinear regression.

The training benzodiazepines and the values found in the literature or calculated theoretically are shown in Table 7.1.

Table 7.1: Parameters used to predict the Volume of Distribution at Steady State

Benzodiazepine	Vd_{ss} (L kg^{-1})	f_u	Log $D_{7.4}$	pK_a	$f_{i7.4}$	f_{ut}	References
α-Hydroxymidazolam	0.77	0.106	2.03[a]	4.2[a]	0.00126	0.061	[403,405,406]
Adinazolam	0.98	0.31	1.41[a]	6.2	0.05935	0.146	[407,408]
Alprazolam	0.80	0.272b	2.01b	2.48b	0.00001	0.165	[409,410]
Bromazepam	0.85	0.477	1.38	pK_a1 2.76,pK_a2 11.78	0.00002	0.240	[351,367,369,370,383,402,409,411]
Brotizolam	0.75	0.092	2.75[a]	2.76	0.00002	0.076	[405,409,412-414]
Clonazepam	2.9	0.145b	2.41b	pK_a1 1.55b,pK_a2 10.45b	0.00000	0.020	[383,405,409,410]
Delorazepam	2.2	0.05	3.16	2.17	0.00001	0.010	[107,409,415]
Desmethyldiazepam	1.1	0.032	2.97	3.48	0.00005	0.034	[415,416]
Diazepam	1.0	0.01b	2.81b	3.10b	0.00000	0.007	[107,148,383,385,409,412,417]
Flunitrazepam	1.9	0.211b	2.05b	1.82b	0.00000	0.036	[409,410]
Lorazepam	1.3	0.090	2.39	pK_a1 1.53,pK_a2 10.92	0.00000	0.023	[107,369,384,409,412]
Lormetazepam	1.6	0.12	2.50	1.30	0.00000	0.032	[107,369,409,415]
Midazolam	1.1	0.017	1.53	6.15	0.05324	0.008	[107,369,403,409,418]
Nitrazepam	1.7	0.116b	2.17b	pK_a1 3.11b,pK_a2 11.02b	0.00005	0.025	[153,409,412]
Oxazepam	0.59	0.042b	2.24b	pK_a1 1.67b,pK_a2 11.34b	0.00000	0.028	[107,153,383,384,409,419]
Temazepam	1.63	0.057b	2.32b	1.45b	0.00000	0.010	[383,387,412]
Triazolam	0.58	0.10	1.64	1.52	0.11182	0.074	[405,409,420]

[a]Predicted using ACD/I-Lab available at ilab.cds.rsc.org
[b]Experimentally derived in this research

7.2 Results

7.2.1 Method Development

The multiple linear regression in the R language programming environment varied the numerical values in equation 7.1 to give the highest correlation between the known fraction unbound in tissues $log(f_{ut})$ obtained from experimental data and the fraction unbound in tissues $log(f_{ut})$ theoretically calculated using the log $D_{7.4}$, the fraction unbound in plasma, $log(f_u)$, and the fraction ionised at pH 7.4, $f_{i7.4}$.

The following relationship was obtained (Equation 7.1).

$$log(f_{ut}) = (-0.33478 \times log(D_{7.4}) + (0.70562 \times log(f_u)) + (0.55955 \times f_{i7.4}) \qquad (7.1)$$

Equation 7.1 Relationship between $log(f_{ut})$, $log(D_{7.4})$, $log(f_u)$ and $f_{i7.4}$

The $log(f_{ut})$ was calculated for the seventeen benzodiazepines using Equation 7.1 from their $log(D_{7.4})$, $log(f_u)$ and $f_{i7.4}$

and compared against their $log(f_{ut})$ values calculated using Equation 7.1 (i.e. from experimental Vd$_{ss}$ data). A correlation of 0.8641 was obtained (Figure 7.1).
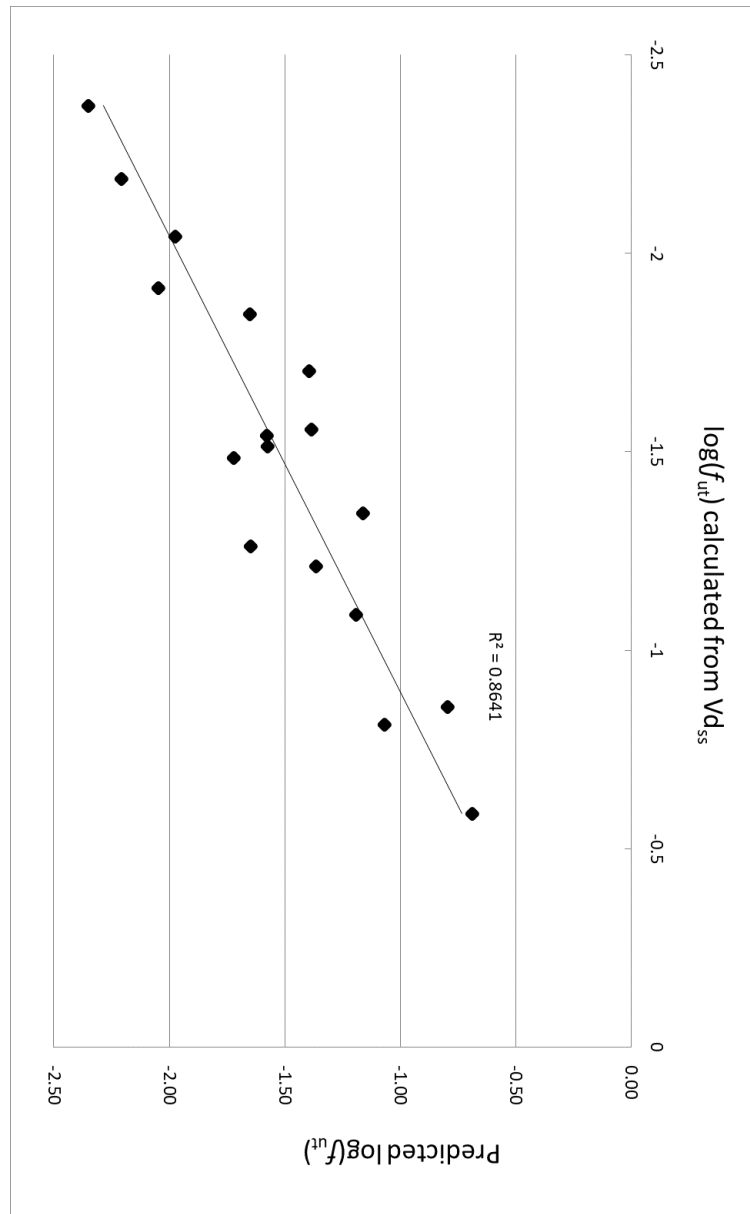
Figure 7.1: A graph of predicted $log(f_{ut})$ values versus calculated $log(f_{ut})$ values.

7.2.2 Calculation of the Vd$_{ss}$ for NPS-benzodiazepines

With knowledge of the relationship between $\log(f_{ut})$, $\log(f_u)$, $f_{i7.4}$ and $\log D_{7.4}$, the Vd$_{ss}$ could be predicted for the NPS-benzodiazepines whose values for these parameters were previously determined (Table 7.2).

7.3 Discussion

7.3.1 Method Development

The plot of the $\log(f_{ut})$ calculated from Vd$_{ss}$ versus the predicted $\log(f_{ut})$ returned an R^2 of 0.8641 (Figure 7.1). In other literature an R^2 of 0.8737 has been reported for this correlation between 12 benzodiazepines [107]. The same source in literature reported a 1.86 mean-fold error for Vd$_{ss}$ predictions [107]. In this work an improved mean-fold error of 1.11 was returned for the prediction of Vd$_{ss}$ values meant that, on average, each Vd$_{ss}$ value would be accurate to within 0.11 L kg^{-1}. The highest fold error was observed for brotizolam (2.21). This was the only thienotriazolodiazepine in the dataset and additionally its $\log D_{7.4}$ value was predicted using the ACD/I-lab software. The possibility of an error in this value cannot be ruled out and experimental data would be vastly preferable. Greater knowledge of experimental Vd$_{ss}$ and physicochemical values of benzodiazepines would be valuable in order to provide greater accuracy in the prediction of future Vd$_{ss}$ values.

7.3.2   The Vd$_{ss}$ of NPS-benzodiazepines

Table 7.2: The log D$_{7.4}$, plasma protein binding (PPB), fraction ionised at pH 7.4 (f$_{i7.4}$) and predicted steady state volume of distribution values for 11 NPS-benzodiazepines.

Compound	Log D$_{7.4}$	PPB (%)	f$_{i7.4}$	Predicted Vd$_{ss}$ (L kg^{-1})
3-Hydroxyphenazepam	2.54	94.9	0.00000	1.21
4′-Chlorodiazepam	2.75	98.2	0.00005	0.95
Desalkylflurazepam	2.82	95.5	0.00001	1.43
Deschloroetizolam	2.60	81.1	0.00062	1.81
Diclazepam	2.73	93.8	0.00001	1.47
Etizolam	2.40	92.8	0.00003	1.21
Flubromazepam	2.87	96.2	0.00007	1.33
Flubromazolam	2.40	89.5	0.00000	1.35
Meclonazepam	2.64	88.2	0.00001	1.65
Phenazepam	3.25	97.2	0.00001	1.44
Pyrazolam	0.97	78.7	0.00008	0.60

The lowest predicted Vd$_{ss}$ was 0.60 L kg^{-1} for pyrazolam. Such a low value was not unexpected as it had the lowest measured log D$_{7.4}$ of 0.97 and the lowest plasma protein binding of 78.7 %. A Vd$_{ss}$ of 0.60 $^{-1}$ or less is considered a low volume of distribution at steady state [144]. The rest of the NPS-benzodiazepines were considered to have medium volumes of distribution at steady state. The highest predicted Vd$_{ss}$ was 1.81 L kg^{-1} for deschloroetizolam. This is a thienodiazepine and as discussed earlier only one thienodiazepine (brotizolam) was included in the training set thus potentially affecting the accuracy of this prediction. The rest of the NPS-benzodiazepines had predicted Vd$_{ss}$ values that were broadly similar to the training-set benzodiazepines.

The NPS-benzodiazepines with the highest Vd$_{ss}$ values were deschloroetizolam with 1.81 L kg^{-1} and meclonazepam with 1.65 L kg^{-1}. As a result these benzodiazepines would likely have a greater distribution within the tissues of the body and this fraction will be unavailable for elimination from the body. They would therefore be expected to have a lower clearance from the body.

An important exception for these predicted values should be noted for 4′-chlorodiazepam. In contract to other benzodiazepines in this dataset, this atypical benzodiazepine does not bind to the GABA$_A$ receptor in contrast to the other benzodiazepines in this dataset. Instead it

binds to the translocator protein (18kDa) (TSPO) which is extensively distributed throughout the body including in the circulatory and lymphatic systems [421]. Therefore, the fraction unbound in tissue may not be able to be accurately predicted using this method hence affecting the accuracy of the obtained Vd_{ss} of 0.95 L kg^{-1}. A future NPS-benzodiazepine to emerge that, in a similar manner to 4′-chlorodiazepam, does not experience a great deal of binding to the GABA$_A$ receptor may have Vd_{ss} values that cannot be predicted by the current method. Compilation of *in vivo* data would be necessary in order to assess whether Vd_{ss} values can be accurately predicted by this method.

The work presented in this Section provides proof of concept that pharmacokinetic parameters such as the volume of distribution at steady state can be predicted with a reasonable reliability from parameters derived *in vitro*, as judged by the high correlation obtained (R^2=0.8641 between the $\log(f_{ut})$ calculated from the Vd_{ss} and the predicted $\log(f_{ut})$ predicted by use of the $\log D_{7.4}$, plasma protein binding (PPB), fraction ionised at pH 7.4 ($f_{i7.4}$) of the benzodiazepine.

Chapter 8

The Blood to Plasma Ratios of NPS-Benzodiazepines

8.1 Introduction

Analytes that have a high blood to plasma concentration ratio ($K_{b/p}$) will have a greater sensitivity to an analytical method that is purely analysing the separated plasma. Knowledge of the $K_{b/p}$ can therefore provide reliable data to determine whether a quantitative method should analyse whole blood or plasma. Post-mortem investigations often analyse total blood concentrations while medical laboratories often analyse plasma concentrations [212]. Knowledge of the $K_{b/p}$ of a compound can therefore aid in the interpretation of toxicological results and allow equivalences to be drawn regarding the concentration of a compound in plasma or blood [213]. The method used in this work and described previously in the literature requires only analysis of the concentration of a compound in the plasma [223]. This removes the necessity of matrix-matching samples and improves the ease and speed of determination of a particular benzodiazepine. When partitioning into the plasma fraction of the blood is low, an analytical method utilising the plasma may struggle to quantitate the compound.

As mentioned in Section 1.8.3, many of the benzodiazepines described in the literature have similar blood to plasma concentration ratios of around 1.00. Therefore additional compounds

were required to validate a method to calculate the $K_{b/p}$. The two compounds chosen were chlorpromazine and quinine, as they have blood to plasma concentration ratios of 0.80 - 1.48 and 0.97 - 2.00 respectively depending on the literature source (Table 8.1).

8.2 Results

8.2.1 Method Development

The blood to plasma partition coefficients were calculated for four test compounds in this work; chlorpromazine, diazepam, nitrazepam and quinine and are listed in Table 8.1. They were then compared to literature values. As some literature values were reported as either blood to plasma partition coefficients or blood to plasma concentration ratios, conversion was required with the use of Equation 8.1. The haematocrit was not listed for any of literature values and therefore the haematocrit value that was reported for the blood in this work (41 %) was used.

$$K_{b/p} = (K_{e/p} \times H) + (1 - H) \tag{8.1}$$

Equation 8.1 Conversion between the blood to plasma partition coefficient ($K_{e/p}$) and the blood to plasma concentration ratio ($K_{b/p}$) with the haematocrit (H).

Table 8.1: The blood to plasma concentration ratios and partition coefficients for four test compounds.

Compound	$K_{e/p}$ literature	$K_{b/p}$ literature	$K_{e/p}$ this work (n=3)	$K_{b/p}$ this work (n=3)	Reference(s)
Chlorpromazine	0.52 ±0.20[a] 1.15 ±0.57[a] 2.17[c]	0.80 ±0.08b[b] 1.06 ±0.23[b] 1.48[a]	2.04 ±0.79	1.43 ±0.32	[422] [423] [424]
Diazepam	-0.15[c] -0.02[c]	0.53 ±0.12[c] 0.58[c]	0.00± 0.05	0.59 ±0.02	[425] [212,426]
Nitrazepam	-0.05[a]	0.57 ±0.27[a]	0.09 ±0.06	0.63 ±0.02	[425]
Quinine	0.93 ±0.02[a] 3.44[c]	0.97[c] 2.00[a]	2.60 ±1.28	1.66 ±0.52	[427] [428]

[a] Literature value
[b] Calculated from $K_{e/p}$ assuming a haematocrit of 41 %
[b] Calculated from $K_{b/p}$ assuming a haematocrit of 41 %

8.2.2 The Blood to Plasma Partition Coefficients of NPS-benzodiazepines

Following development of a suitable method in the Section 8.2.1, the blood to plasma concentration ratios of six benzodiazepines defined as new psychoactive substances were then calculated from experimentally derived data (Table 8.2).

Table 8.2: Blood to plasma partition coefficient and concentration ratios of six NPS-benzodiazepines calculated from experimental data using Equations 2.9 and 8.1

Compound	$K_{e/p}$ (n=3)	$K_{b/p}$ (n=3)
Deschloroetizolam	0.23 ±0.15	0.68 ±0.06
Diclazepam	0.55 ±0.12	0.82 ±0.05
Etizolam	0.27 ±0.08	0.70 ±0.03
Meclonazepam	0.57 ±0.20	0.83 ±0.08
Phenazepam	-0.05 ±0.32	0.57 ±0.13
Pyrazolam	1.44 ±0.08	1.18 ±0.03

8.3   Discussion

8.3.1   Method Development

Nitrazepam was chosen as one of the four test compounds as its $K_{b/p}$ was stated to be 1.00 in humans in literature [135,221]. Using Equation 8.1, this would convert to a $K_{e/p}$ of 1.00. However, a large discrepancy was observed following experimental determination in this work and a $K_{e/p}$ of 0.09 was obtained. Upon further investigation of the source of the literature value (of 1.00) it appeared to be based on the results of experiments using the whole blood of rabbits [429]. Analysis of an additional literature source in humans provide a $K_{b/p}$ for nitrazepam of 0.57 ±0.27 [425]. With Equation 8.1 this would provide a $K_{e/p}$ of -0.05. The same source reports a $K_{b/p}$ of 0.53 ±0.12 for diazepam [94]. This is similar to the reported $K_{b/p}$ of 0.58 for diazepam from other literature sources [212,426]. Therefore, the decision was made to disregard the literature $K_{b/p}$ of 1.00 for nitrazepam and used the reported ratio of 0.57 instead [425]. This was also similar to the $K_{b/p}$ of 0.63 derived in this work.

Large variations exist in literature for blood to plasma concentration ratios and blood to plasma partition coefficients. For example, chlorpromazine had a $K_{e/p}$ range of 0.52 - 2.17 and quinine had a $K_{e/p}$ range of 0.93 - 3.44 [422-424,427,428]. Quinine is an anti-malarial drug and in patients who have malaria the concentration of quinine in red blood cells is much greater than normal therefore affecting blood to plasma concentration ratios [430]. This is one potential explanation for the large ranges for blood to plasma partition coefficients observed in literature for this drug as they may have been unknowingly measured in patients with malaria. The range for diazepam for the $K_{e/p}$ was far smaller at -0.15 - -0.02 [212,425,426].

8.3.2 The Blood to Plasma Ratios of NPS-benzodiazepines

As a result of earlier experiments, only six NPS-benzodiazepines remained in a great enough quantity to allow the blood to plasma concentration ratio experiments to be conducted.

The measured blood to plasma concentration ratios for the six NPS-benzodiazepines ranged from 0.57 for phenazepam to 1.18 for pyrazolam. The value of 0.57 for phenazepam indicates extensive partitioning into the plasma and an extremely low association with red blood cells. This is similar to diazepam which has a blood to plasma concentration ratio of 0.58 reported in literature and 0.59 reported in this work [426].

The value of 1.18 for pyrazolam is typical of a more even distribution between the blood cells and plasma. A similar value for the $K_{b/p}$ of 1.14 has been reported for lorazepam, however a far lower value of 0.60 for lorazepam has also been additionally been published in literature [431]. The large variations in blood to plasma concentration ratios and partition coefficients was previously noted in Section 8.2.1 for chlorpromazine and quinine and the experimental determination of more values will help to reliably identify a more accurate value.

Deschloroetizolam and etizolam had similar blood to plasma concentration ratios of 0.68 and 0.70 respectively. Meclonazepam had a blood to plasma concentration ratio of 0.83 which is close to the value for clonazepam (0.65), a structurally-similar compound which lacks only the 3-methyl group on position 3 (Figure 1.2A) [426].

Published values of the blood to plasma concentration ratios for benzodiazepines could only be found for 12 benzodiazepines. Those values that are available are 0.53 - 0.56 for midazolam, 0.58 for diazepam, 0.62 for triazolam, 0.70 for adinazolam, 0.75 for flunitrazepam, 0.78 - 0.81 for alprazolam, 0.90 - 1.00 for oxazepam and 1.00 for nitrazepam [210,219,221,406,432-4351]. Additional data from a dissertation (non peer-reviewed, dissertation submitted for a Bachelor of Health Science) reports blood to plasma ratios of 0.58 for diazepam, 0.58 for desmethyldiazepam (nordiazepam), 0.62 for temazepam, 0.64 for oxazepam, 0.65 for clonazepam and 0.74 for alprazolam [426]. The limited experimental data determined for the six NPS-benzodiazepines in this study shows that they have similar blood to plasma ratios to those published in literature for

related benzodiazepines, however there is a large range observed even with the small number of compounds used in this work.

As mentioned previously knowledge of the blood to plasma ratio of a compound is important for the prediction of *in vivo* clearance from *in vitro* data from human hepatocytes or human liver microsome studies [221]. Where blood to plasma ratios are unavailable, it is often assumed that the blood to plasma ratio is 1.0 [221]. However, such an approach has been demonstrated to be unreliable for NPS-benzodiazepines in this study.

Although only six NPS-benzodiazepines were studied in this work, a large range of blood to plasma concentration ratios was observed from 0.57 for phenazepam to 1.18 for pyrazolam. This work highlights the importance of accurate pharmacokinetic data as equivalences cannot be drawn between different benzodiazepines.

Chapter 9

Metabolic Characterisation of the C3A and HepaRG Cell Lines

9.1 Introduction

Since different hepatocellular carcinoma cell lines express differing levels of phase I drug metabolising enzymes, careful evaluation is required to determine the most suitable cell line for use in drug metabolism studies [278]. This process involves incubation of the different cell lines with substrates for the six phase I cytochrome P450 (CYP450) enzymes which are responsible for the majority of phase I metabolism for pharmaceutical compounds [119,120,231]. The aim of the work in this chapter intended to serve three purposes. Firstly, to characterise the C3A cell line fully for six key drug metabolising enzymes (CYP1A2, CYP2B6, CYP2C19, CYP2C9, CYP2D6 and CYP3A4/5) as this has not yet been reported in literature; secondly to induce the expression of CYP450 enzymes via incubation with DMSO since this has previously been reported to be an effective method of inducing enzyme expression [271,272] and finally to repeat this characterisation with the HepaRG cell line and determine the most suitable cell line for the determination of the metabolic pathways of NPS-benzodiazepines.

The protocols for the incubation of the test substrates with the cell lines and the analysis with LC-MS are reported in Section 2.10.

9.2   Results

9.2.1   CYP1A2

C3A Cells

Following incubation with the C3A cell line, phenacetin was detected at 29.256 minutes (m/z 180.1013 $[\text{M+H}]^{+}$) with a mass difference of 2.93 ppm. The known metabolite of phenacetin, paracetamol (acetaminophen) was observed with the same retention time of 29.256 minutes (m/z 152.0705 $[\text{M+H}]^{+}$) with a mass difference of 0.13 ppm. However, there was no chromatographic separation of the phenacetin and paracetamol (Figure 9.2). Phenacetin has been observed to undergo ESI-source fragmentation which produces an ion that is structurally identical to paracetamol [436]. In-source fragmentation is often observed in mass spectrometers and has been noted for metabolic studies on sugar-phosphates in yeast cultures [437]. It is thought to occur in the area of the mass spectrometer between the ion source and the vacuum chamber [437]. It is therefore more likely that no paracetamol was observed and CYP1A2 is inactive in this particular cell culture. CYP1A2 has been reported to be expressed in the C3A cell line [269]. However other research suggests CYP1A2 activity only occurs in the presence of an inducer [438]. The overlaid extracted ion chromatogram (EICs) of phenazepam and the in-source degradation product, showing the overlap in retention times are shown in Figure 9.1.
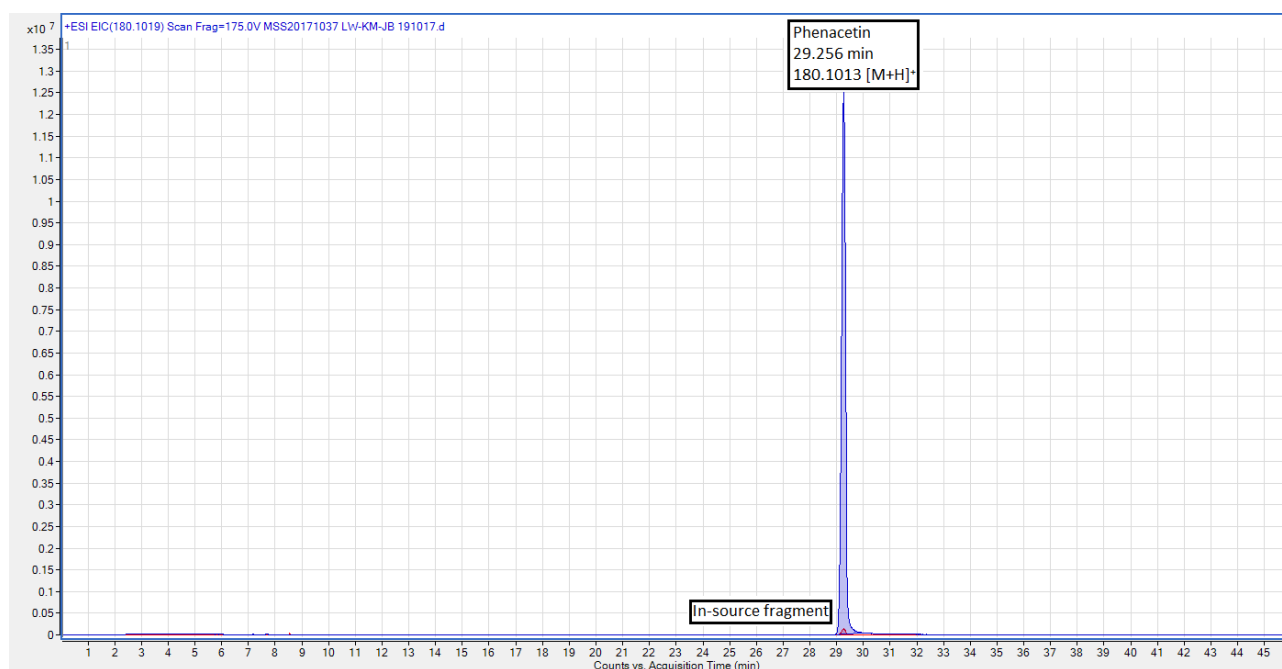
Figure 9.1: Overlaid EICs for phenacetin and its in-source degradation product following incubation with the C3A cell line.
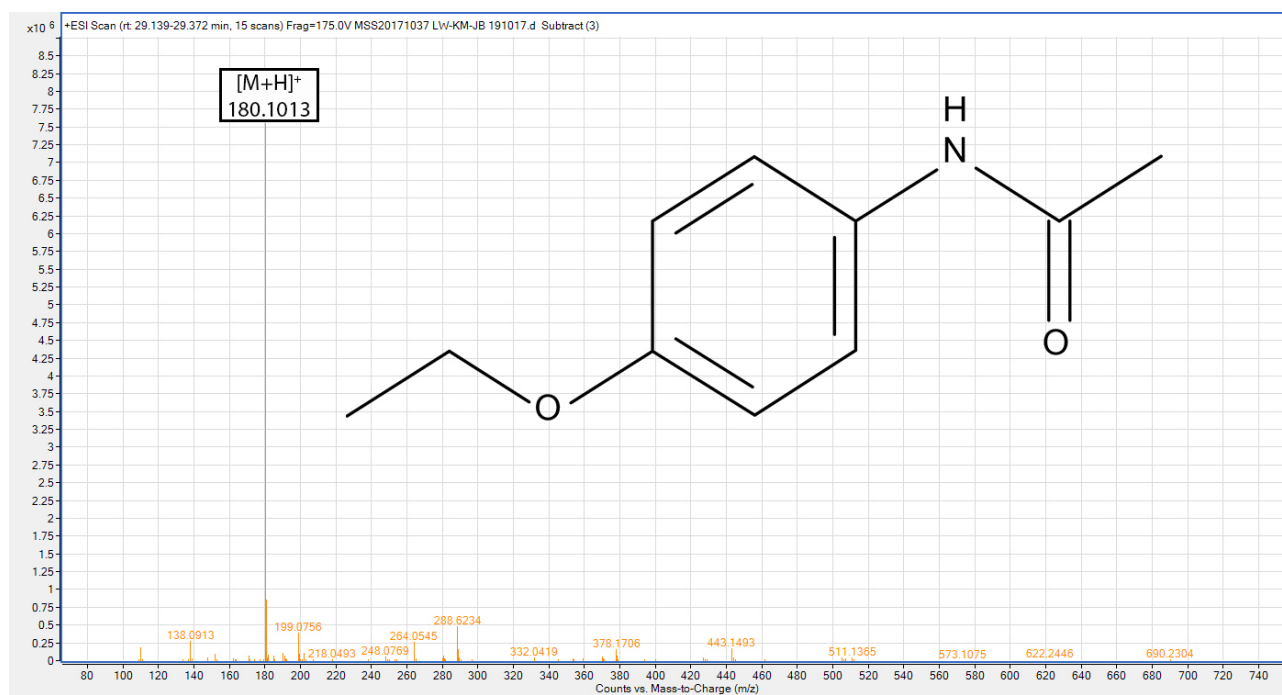
Figure 9.2: LC-MS analysis and structure of phenacetin following incubation with the C3A cell line.

DMSO-treated C3A Cells

Following incubation with the DMSO-treated cell line, phenacetin was again was detected at 28.977 minutes (m/z 180.1017 [M+H]$^+$) (Figure 9.4) with a mass difference of 1.51 ppm. The metabolite of phenacetin, paracetamol (acetaminophen) was again also observed with the same retention time of 28.977 minutes (m/z 152.0688 [M+H]$^+$) and a mass difference of 0.38 ppm. As there was also no chromatographic separation in this sample it is therefore likely that this was an in-source fragmentation and both the metabolite and CYP1A2 were not present in the samples (Figure 9.3).
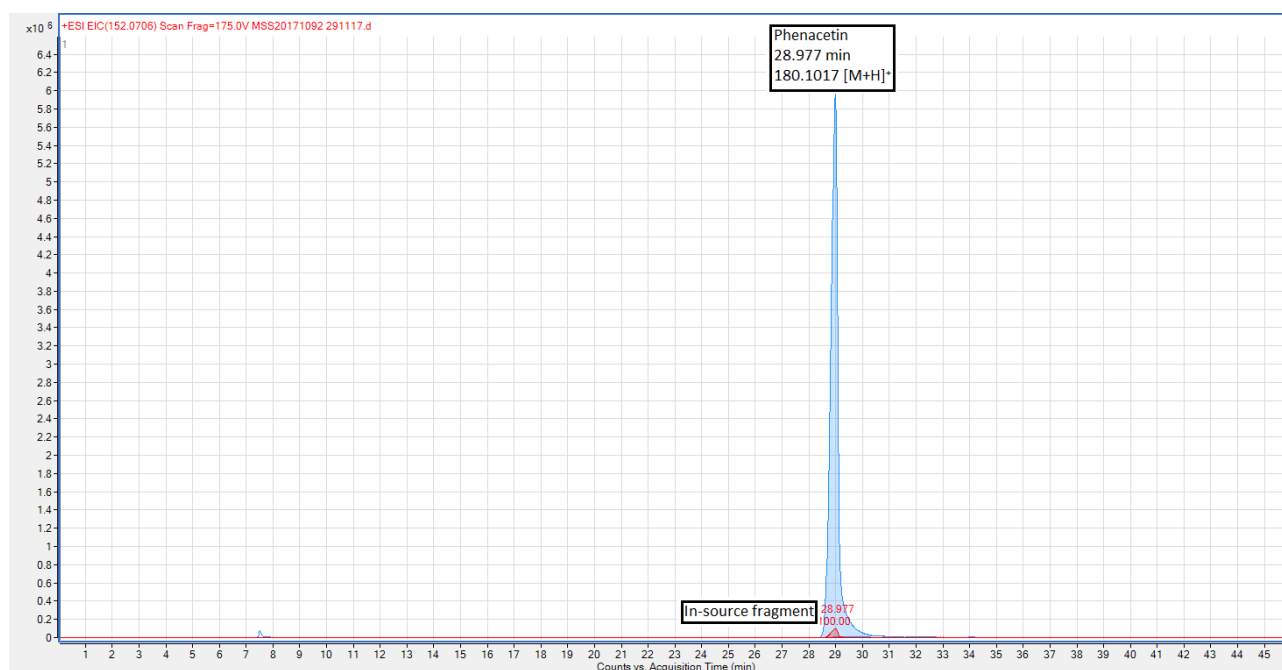
Figure 9.3: Overlaid EICs of phenacetin and its in-source degradation product following incubation with the DMSO-treated C3A cell line.
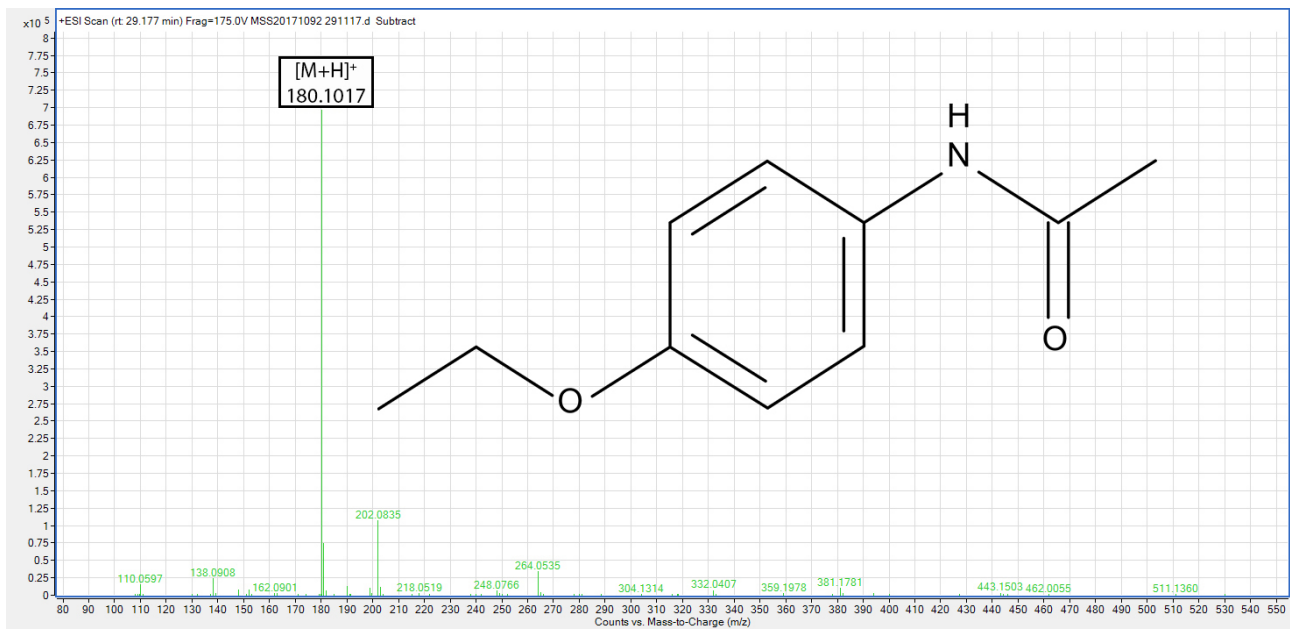
Figure 9.4: LC-MS analysis and structure of phenacetin following incubation with the DMSO-treated C3A cell line.

HepaRG Cells

In the HepaRG cell line, phenacetin was detected at 28.991 minutes (m/z 180.1018 [M+H]$^+$) with a mass difference of 0.26 ppm (Figure 9.6). The metabolite paracetamol was detected at 6.098 minutes (m/z 152.0695 [M+H]$^+$) with a mass difference of 7.11 ppm (Figure 9.8). Although a large difference was observed in the retention times for phenacetin and its paracetamol this is not uncommon; one study in the literature using an HPLC method reports a retention time of 5.28 minutes for paracetamol and 19.50 minutes for phenacetin [439]. Another reports a retention time of 3.791 minutes for paracetamol and 9.094 minutes for phenacetin [440]. Additional supporting evidence was provided by the presence of the [M+NH$_4$]$^+$ adduct (m/z 169.0971) with a mass difference of 0.26 ppm, indicating the presence of paracetamol at 6.098 minutes (Figure 9.8). This data suggests that CYP1A2 was present in the HepaRG cell line.

For the phenacetin that was incubated with the C3A and DMSO-treated C3A cell lines, paracetamol was observed at the same retention time as phenacetin and was potentially an ESI-source fragmentation product. No paracetamol was observed at the retention time for phenacetin incubated with the HepaRG cells. A potential reason behind this could be because of the lower fragmentor voltage used in the LC-MS method, 150 V compared to 175 V.

The total ion chromatogram (TIC) with the EIC for phenacetin is shown in Figure 9.5 and the TIC with the EIC for paracetamol is shown in Figure 9.7. The other peaks are likely to be contaminants from the cell culture media and extraction procedure.
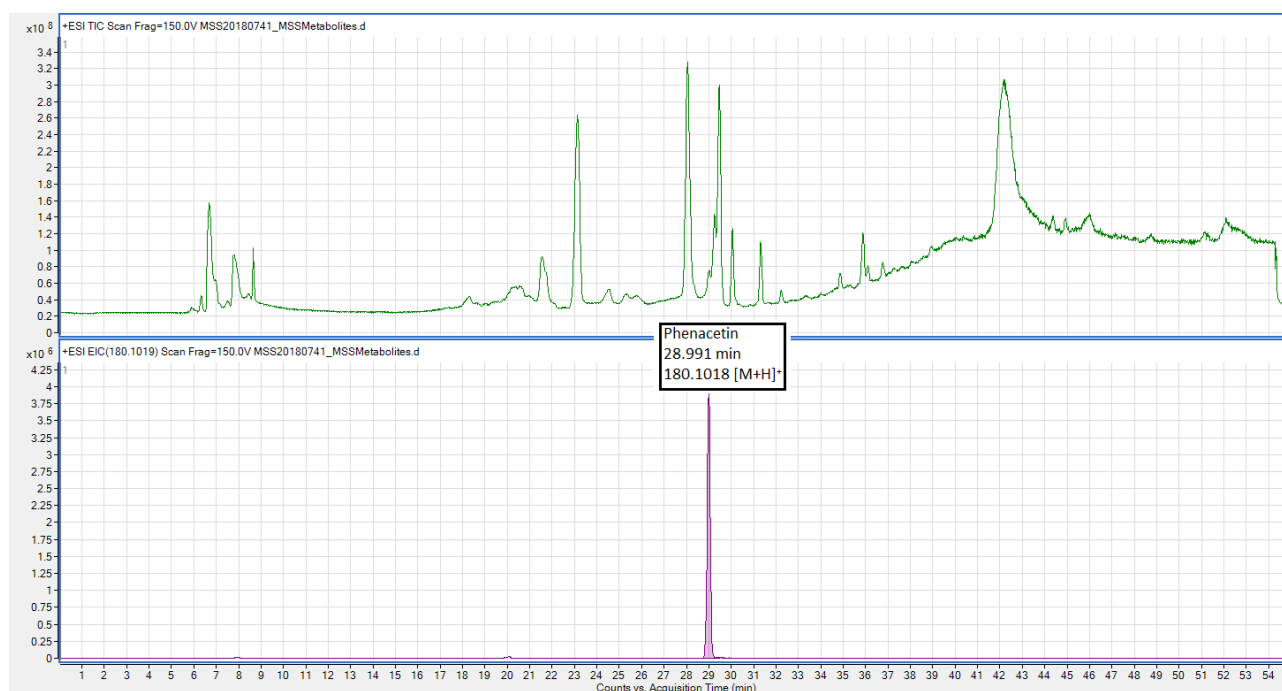
Figure 9.5: TIC and EIC of phenacetin following incubation with the HepaRG cell line.
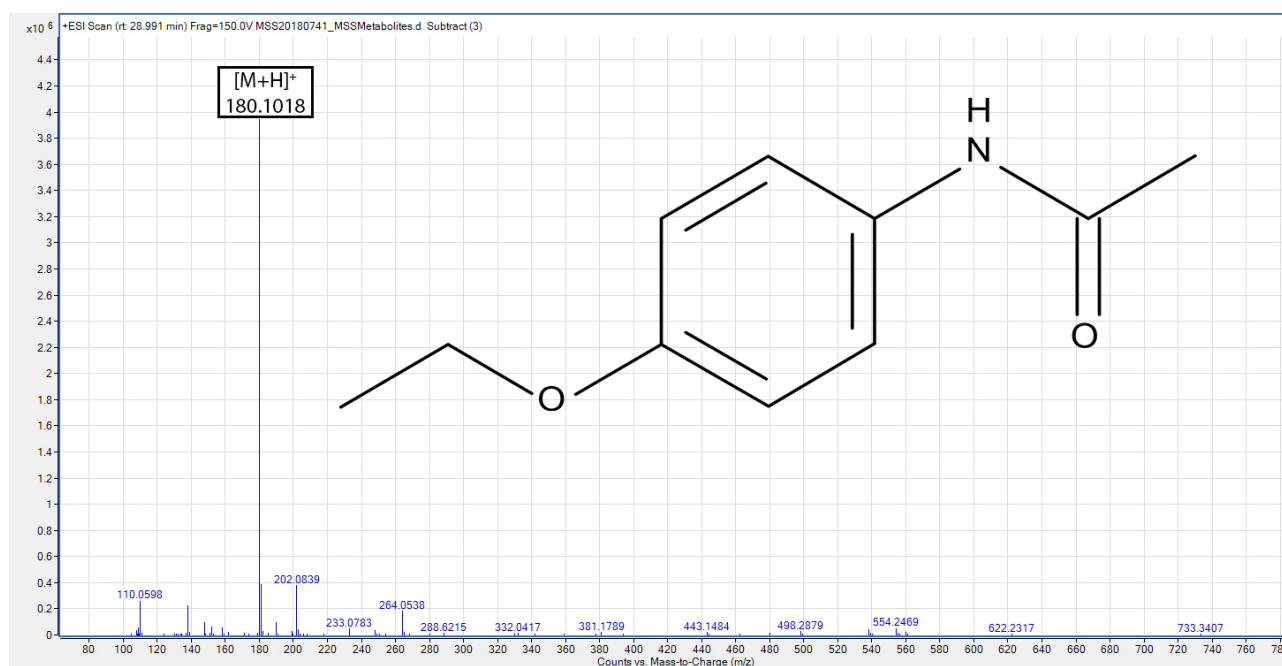
Figure 9.6: LC-MS analysis and structure of phenacetin following incubation with the HepaRG cell line.
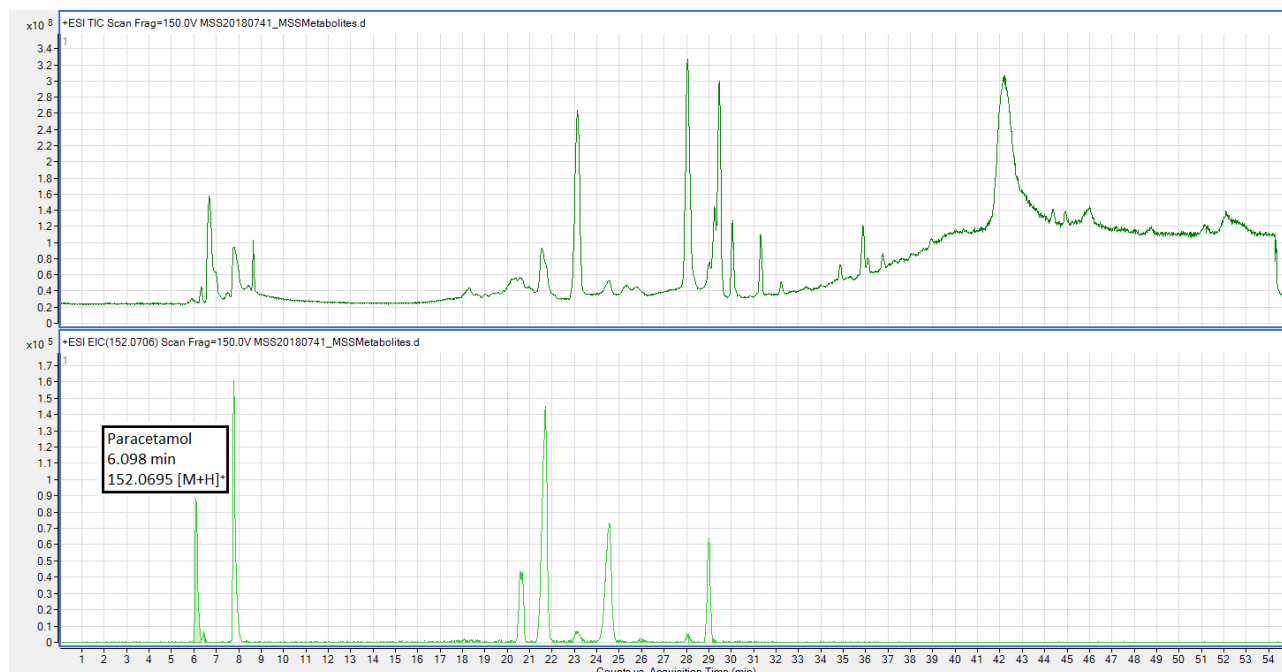
Figure 9.7: TIC and EIC of paracetamol following incubation with the HepaRG cell line.
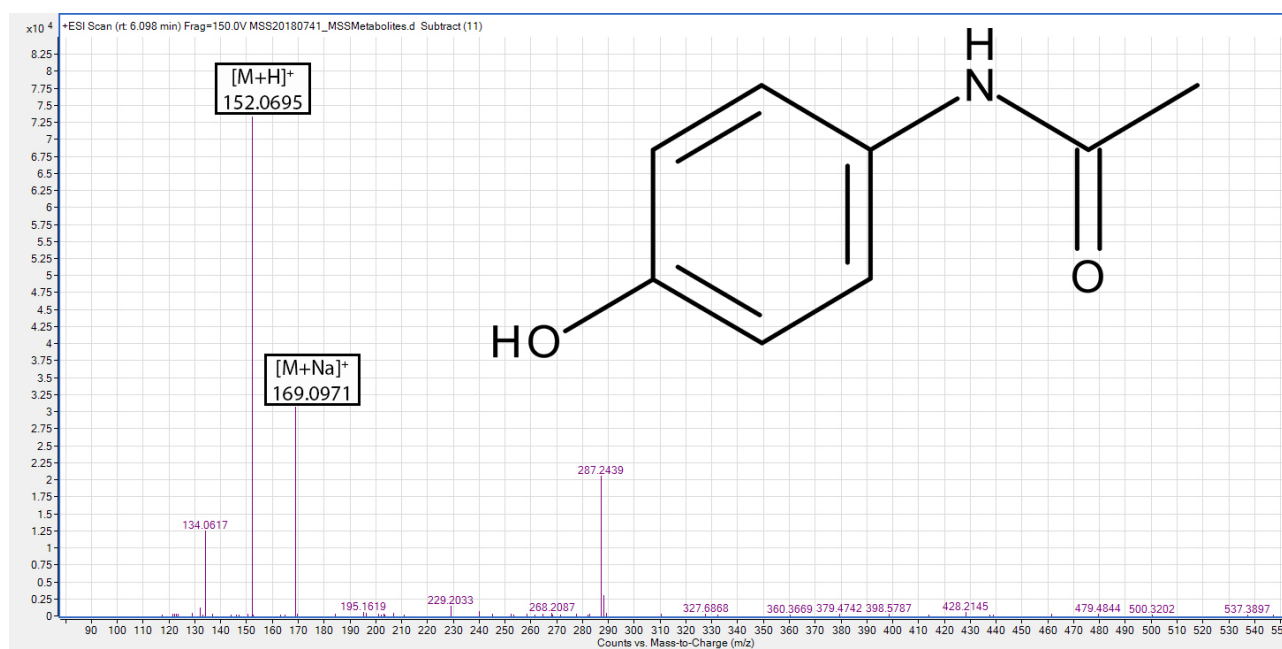
Figure 9.8: LC-MS analysis and structure of paracetamol following incubation with the HepaRG cell line.

9.2.2 CYP2B6

C3A Cells

In the C3A cell line bupropion was detected at 27.263 minutes (m/z 240.1153 [M+H]$^+$) with a mass difference of -9.07 ppm (Figure 9.10). The expected metabolite resulting from the metabolic activity of CYP2B6, 2-hydroxybupropion, was not observed in the mass spectra. However two other compounds were detected at 26.880 minutes (m/z 242.1315 [M+H]$^+$) and at 27.380 minutes (m/z 242.1295 [M+H]$^+$) with mass differences of -3.49 and 4.79 ppm respectively (Figure 9.11 and Figure 9.12).

The EICs of these compounds, overlaid with one another, are shown in Figure 9.9.

The likely structure of these compounds corresponds to two ketone-reduced derivatives of bupropion being present existing as an isomeric pair and exhibiting some separation on the chromatograph. Bupropion is formulated as a racemic mixture; (R)-bupropion and (S)-bupropion. Reduction of bupropion to an isomeric pair of metabolites, threohydrobupropion and erythrohydrobupropion, is known to be a metabolic pathway in the human liver [441]. Threohydrobupropion is formed by the 11-hydroxysteroid dehydrogenase 1 (11β-HSD1) and erythrohydrobupropion by an additional carbonyl reductase [442]. These reactions have been previously observed to occur in human liver cytosol and microsomes and it is therefore likely that this C3A cell line expressed 11β-HSD1 and an additional carbonyl reductases responsible for the formation of threo- and erythro- hydrobupropion [443]. Further metabolism of this enantiomeric pair is then conducted by CYP2C19. As this further biotransformation was not observed it is therefore likely that there is no expression of CYP2C19 in this cell line.
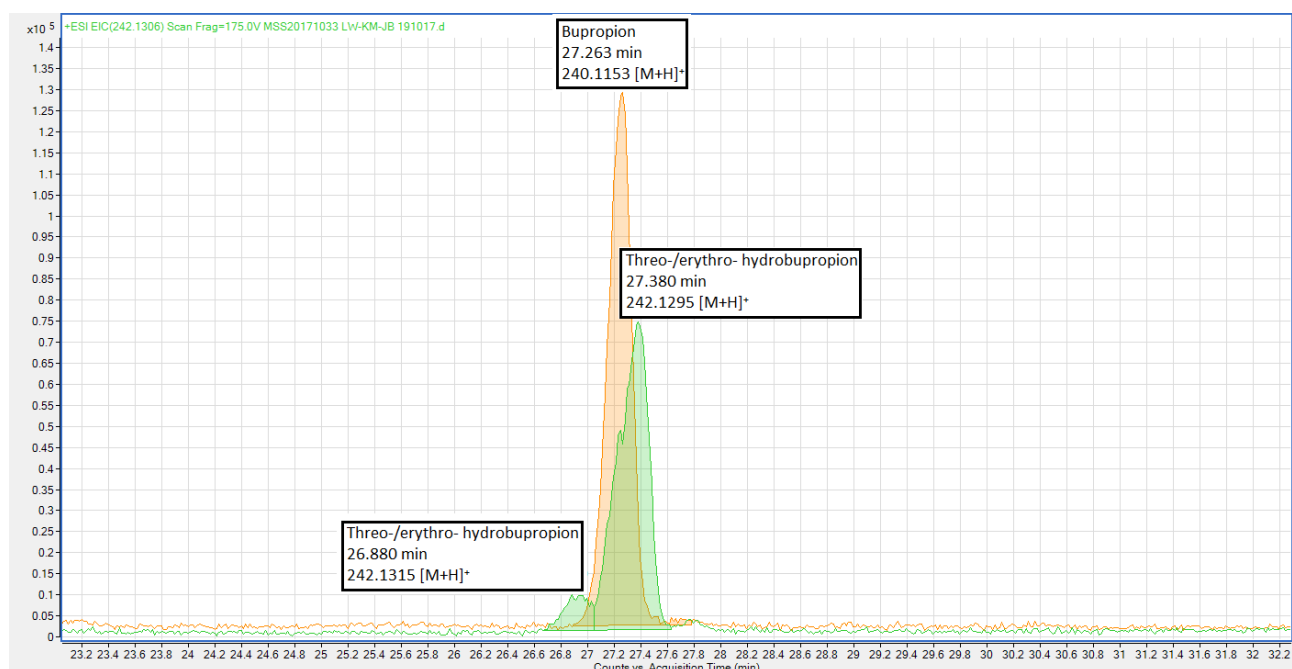
Figure 9.9: Overlaid EICs of bupropion, erythrohydrobupropion and threohydrobupropion following incubation with the C3A cell line.

Figure 9.10: LC-MS analysis and structure of bupropion following incubation with the C3A cell line.

Figure 9.11: LC-MS analysis and structure of erythro-/threo- hydrobupropion following incubation with the C3A cell line.

Figure 9.12: LC-MS analysis and structure of erythro-/threo- hydrobupropion following incubation with the C3A cell line.

DMSO-treated C3A Cells

Following incubation with the DMSO-treated cell line, bupropion was detected at 27.219 minutes (m/z 240.1161 [M+H]$^+$ with a mass difference of -4.72 ppm (Figure 9.13). The expected hydroxylated metabolite was not found to be present. The ketone-reduced derivatives that were observed in the non-treated cells were also not present. This indicates a decrease in the metabolic activities of the 11β-HSD1/carbonyl reductase responsible for the formation of threo-/erythro- hydrobupropion [442].
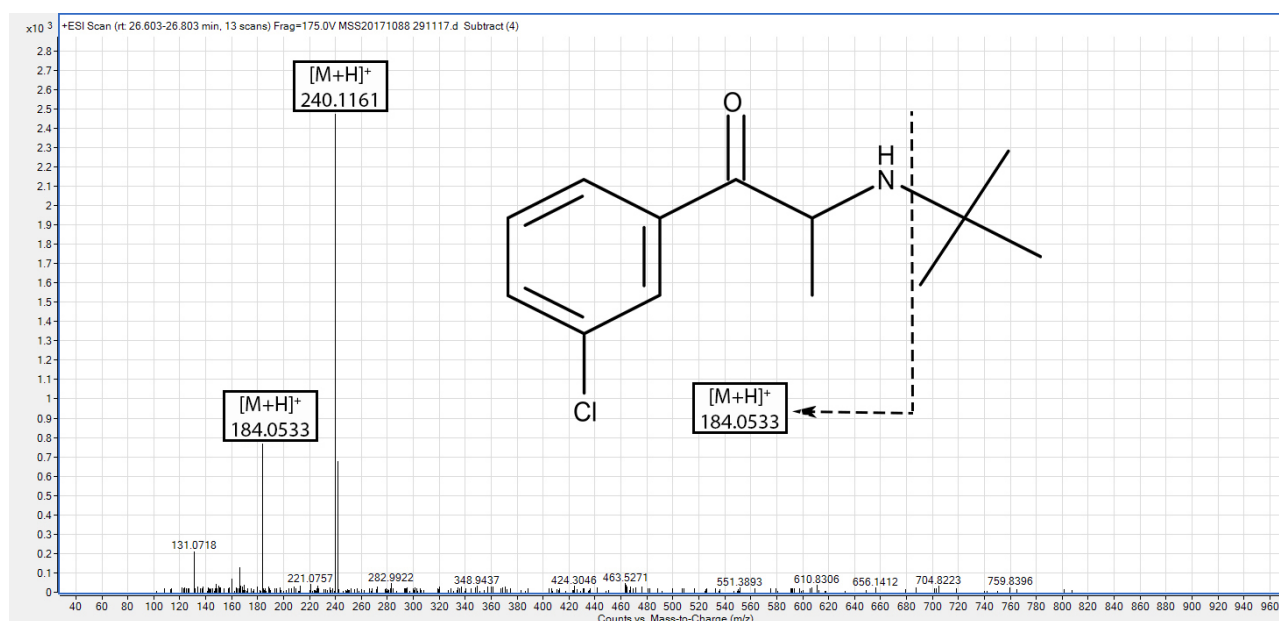
Figure 9.13: LC-MS analysis and structure of bupropion following incubation with the DMSO-treated C3A cell line.

HepaRG Cells

Following incubation with the HepaRG cell line, bupropion was detected at 26.644 minutes (m/z 240.1152 [M+H]$^+$) with a mass difference of -1.04 ppm (Figure 9.15).

Two hydroxybupropion compounds were detected on the mass spectra at 21.012 minutes (m/z 256.1110 [M+H]$^+$ with a mass difference of -4.21 ppm, Figure 9.16) and 21.178 minutes (m/z 256.1102 [M+H]$^+$ with a mass difference of -1.37 ppm, Figure 9.17).

Another two hydroxybupropion compounds were detected at 22.023 minutes (m/z 256.1101 [M+H]$^+$ with a mass difference of 0.90 ppm, Figure 9.18) and 22.188 minutes (m/z 256.1100

$[M+H]^+$ with a mass difference of -0.57 ppm, Figure 9.19).

These pairs of hydroxybupropion compounds can be tentatively detected as two enantiomeric pairs, with one pair consisting of S,S-hydroxybupropion and R,R-hydroxybupropion. The formation of S,S-hydroxybupropion and R,R-hydroxybupropion is characterised by the formation of a morpholine ring system containing both nitrogen and oxygen atoms (Figure 9.20). Therefore two chiral centres are present. As two chiral centres exist in S,S-hydroxybupropion and R,R-hydroxybupropion, the possibility exists of four diastereoisomers with the addition of S,R- and R,S- hydroxybupropion. However only the R,R- and S,S- enantiomers have been observed to be formed metabolically from R-/S-bupropion and it is postulated that this is a result of steric hindrance in the molecule [444]. The second pair of enantiomers is likely to correspond to S-4'-hydroxybupropion and R-4'-hydroxybupropion (Figure 9.20). The $[M+H]^+$ adducts with a m/z of 238.0993 and of 238.0995 (Figures 9.18 and 9.19 respectively) are likely to correspond to the loss of water from the molecule (Figure 9.20).

These hydroxybupropion metabolites have been previously detected and reported in human plasma and at least some of them are thought to be formed by CYP2B6 [445-447]. Research has shown that bupropion (100 μM) is metabolised to S,S-hydroxybupropion and R,R-hydroxybupropion by CYP2C19, CYP3A4 and CYP1A2 although at levels of 2, 0.4 and 0.1 % respectively when compared to CYP2B6 [448]. Bupropion (1 μM) is metabolised to S,S-hydroxybupropion and R,R-hydroxybupropion by CYP2C19, CYP3A4 and CYP1A2 at levels of 7, 10 and 2 % respectively when compared to CYP2B6 [448]. The formation of 4'-hydroxybupropion is thought to be mainly conducted by CYP2C19 with a very minor contribution from CYP2B6 [448]. Therefore, it is likely that both CYP2B6 and CYP2C19 are present in the HepaRG cell line.

Two ketone-reduced bupropion derivatives were detected at 26.230 minutes (m/z 242.1304 $[M+H]^+$ with a mass difference of 2.01 ppm, Figure 9.21) and 26.777 minutes (m/z 242.1305 $[M+H]^+$ with a mass difference of 0.38 ppm, Figure 9.22). This pair of ketone-reduced bupropion derivatives are again likely to correspond to the isomeric pair of metabolites, threo- and erythro- hydrobupropion, that were detected in the C3A cells and are thought to be formed by

11β-HSD-1 [442,448,449].

A ketone-reduced hydroxylated bupropion derivative was detected at 29.593 minutes (m/z 258.1263 [M+H]$^+$ with a mass difference of 0.38 ppm, Figure 9.23). This metabolic pathway follows the formation of erythro- and threo- hydrobupropion (which was observed in these cells) and has been previously reported [442,448,449]. However, whilst a pair of diastereoisomers is typically detected, only one compound was observed here and it may be that chromatographic separation of the pair of diastereoisomers did not occur in this analysis. The formation of erythro-/threo- hydrobupropion is thought to be catalysed by CYP2C19 [448]. This provides further evidence that CYP2C19 is present in the HepaRG cell line as well as CYP2B6.

The stacked EICs for bupropion and the metabolites observed can be viewed in Figure 9.14.

The metabolic pathways observed in this Section for bupropion can be visualised in Figure 9.24.
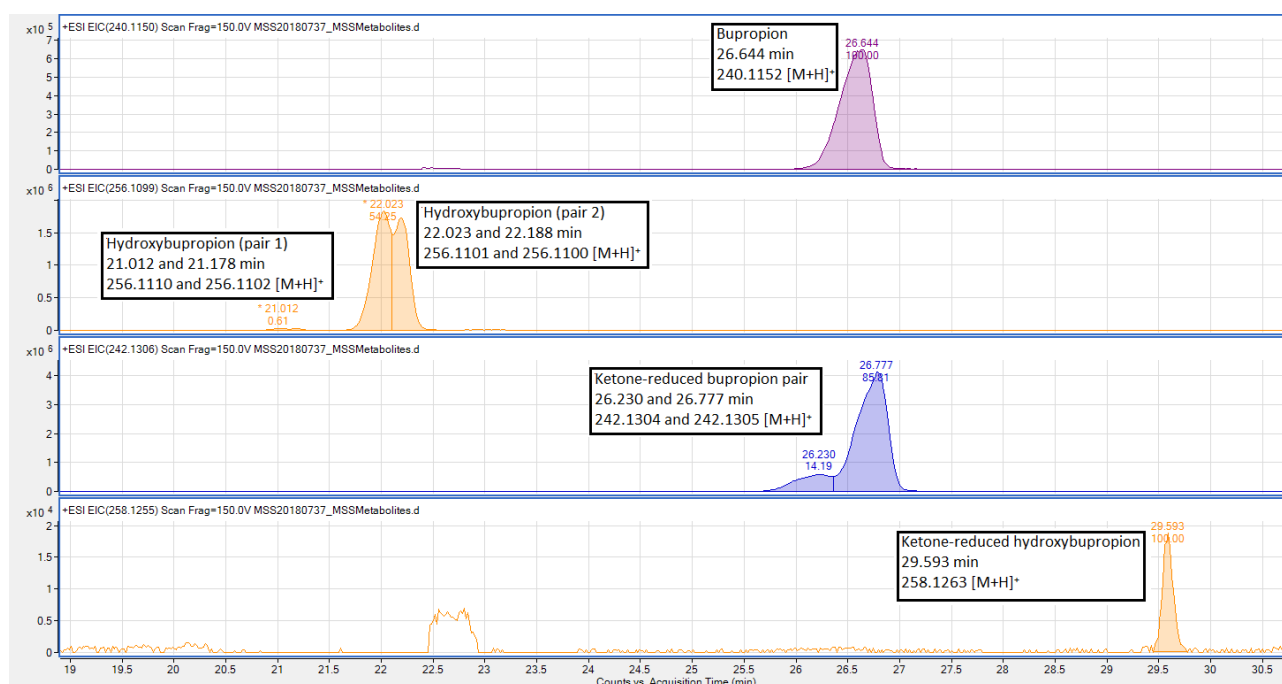
Figure 9.14: Stacked EICs for bupropion and its metabolites following incubation with the HepaRG cell line.
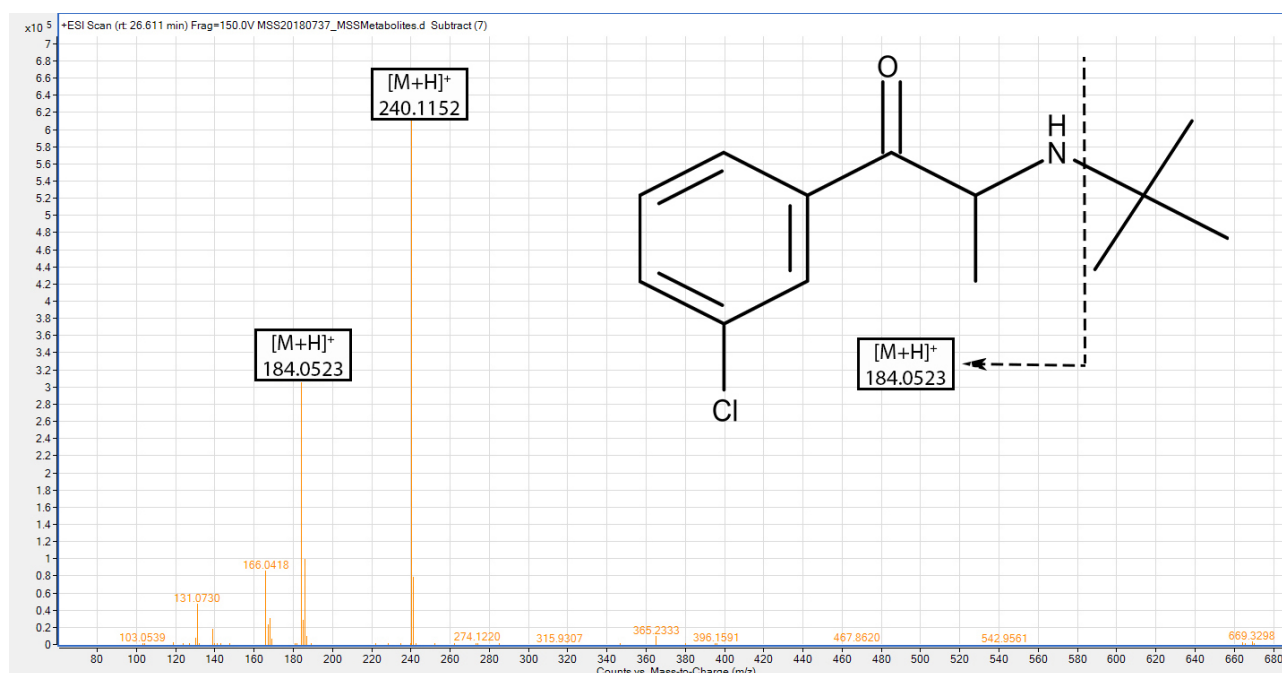
Figure 9.15: LC-MS analysis and structure of bupropion following incubation with the HepaRG cell line.
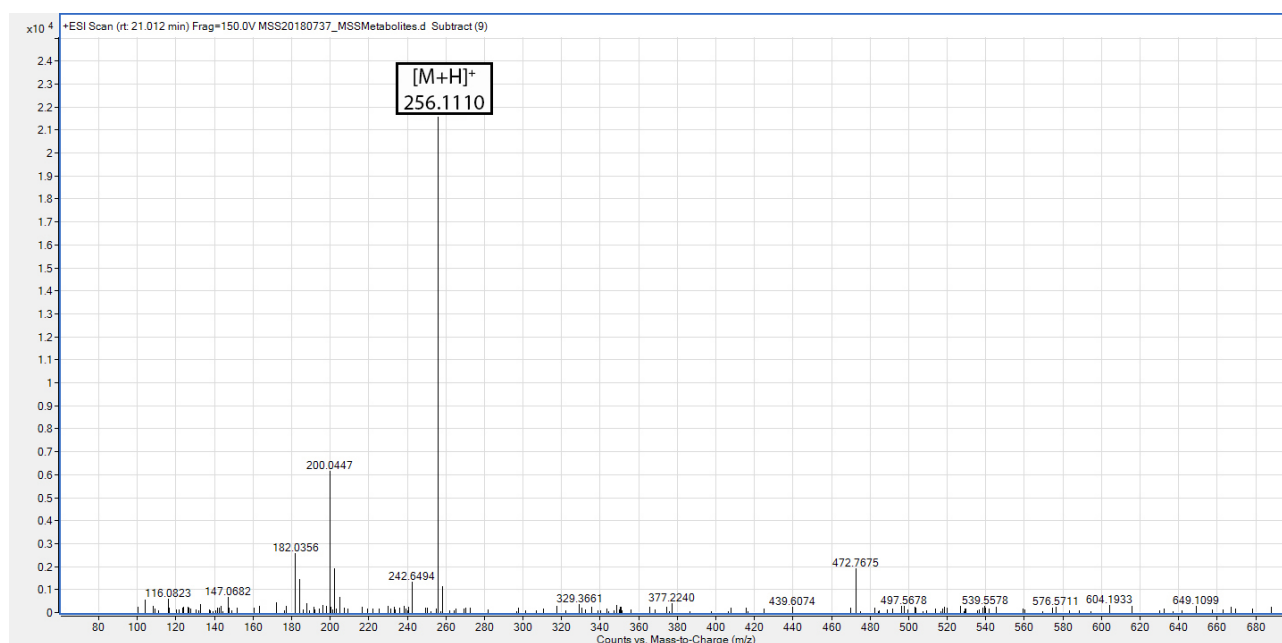

Figure 9.16: LC-MS analysis of R,R-hydroxybupropion or S,S-hydroxybupropion (Figure 9.16 and Figure 9.17) or S-4'-hydroxybupropion or R-4'-hydroxybupropion (Figure 9.18 and Figure 9.19) following incubation with the HepaRG cell line.
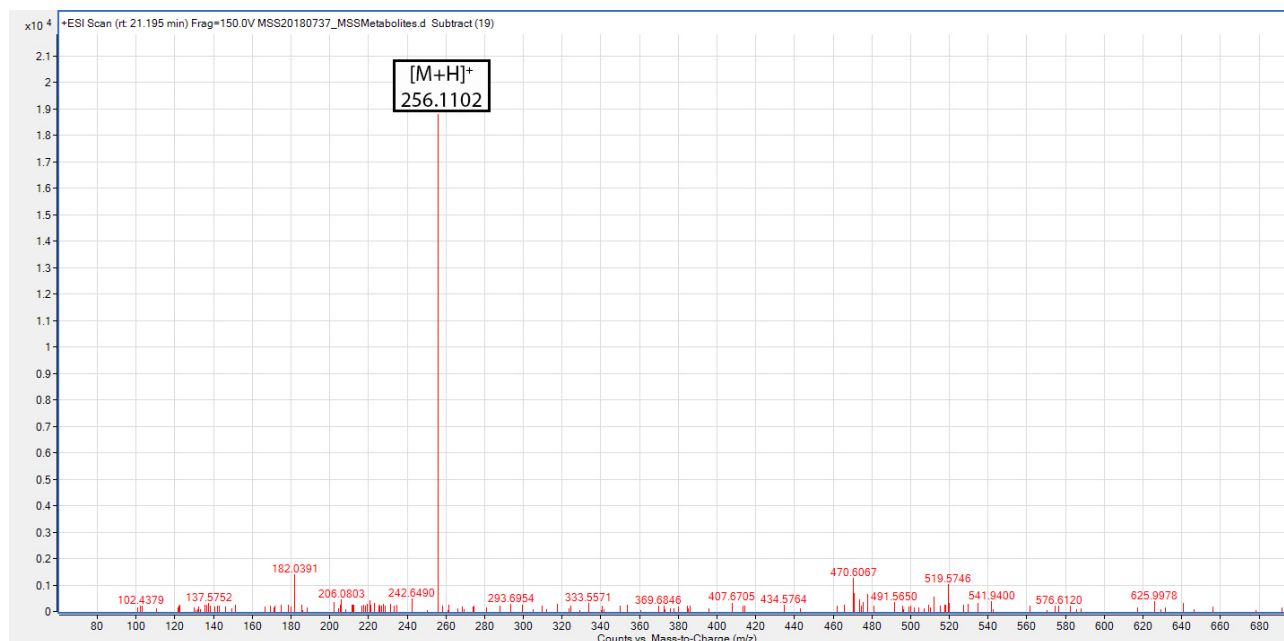
Figure 9.17: LC-MS analysis of R,R-hydroxybupropion or S,S-hydroxybupropion (Figure 9.16 and Figure 9.17) or S-4'-hydroxybupropion or R-4'-hydroxybupropion (Figure 9.18 and Figure 9.19) following incubation with the HepaRG cell line.
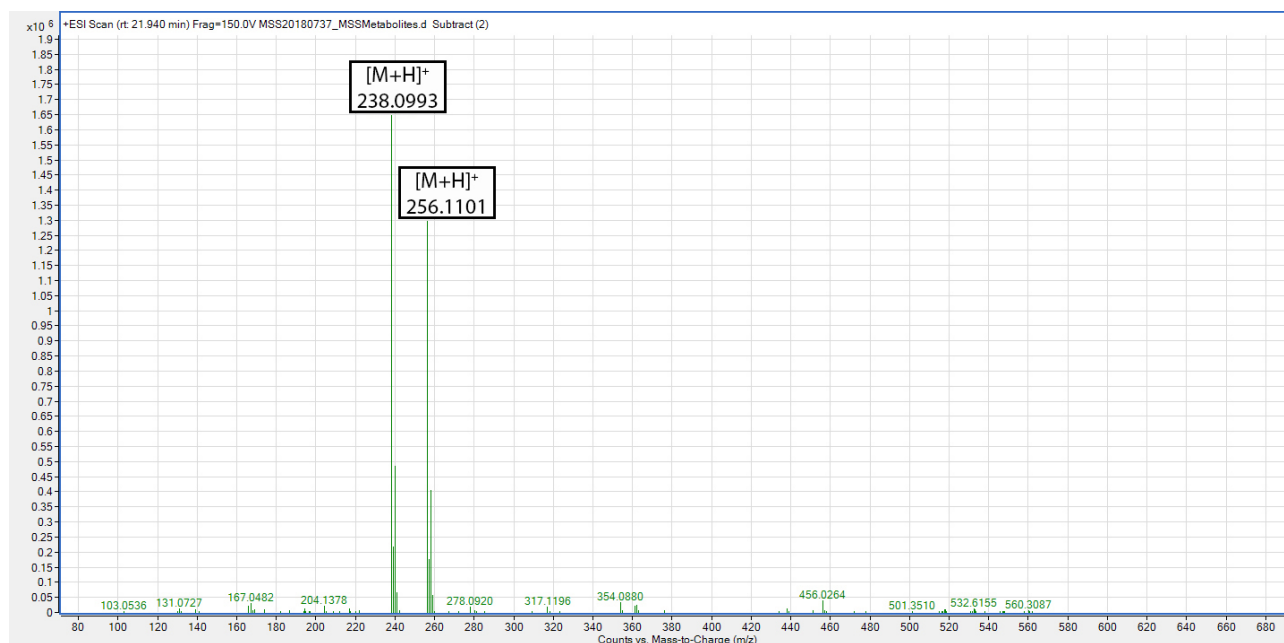
Figure 9.18: LC-MS analysis of R,R-hydroxybupropion or S,S-hydroxybupropion (Figure 9.16 and Figure 9.17) or S-4'-hydroxybupropion or R-4'-hydroxybupropion (Figure 9.18 and Figure 9.19) following incubation with the HepaRG cell line.
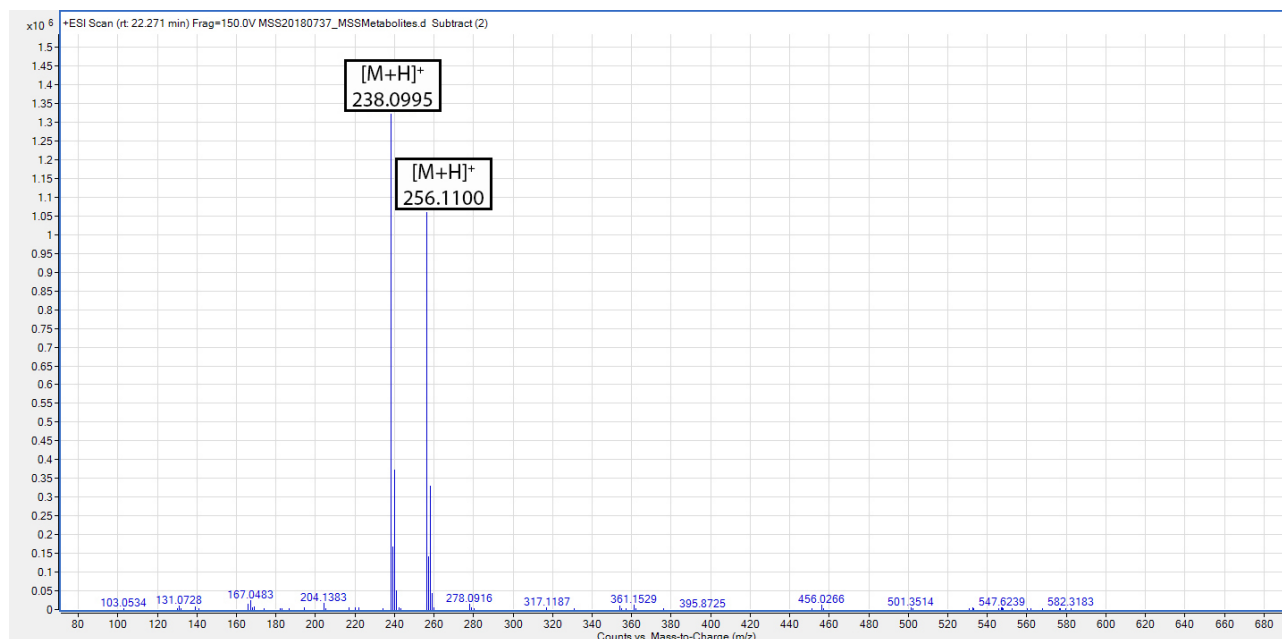
Figure 9.19: LC-MS analysis of R,R-hydroxybupropion or S,S-hydroxybupropion (Figure 9.16 and Figure 9.17) or S-4'-hydroxybupropion or R-4'-hydroxybupropion (Figure 9.18 and Figure 9.19) following incubation with the HepaRG cell line.
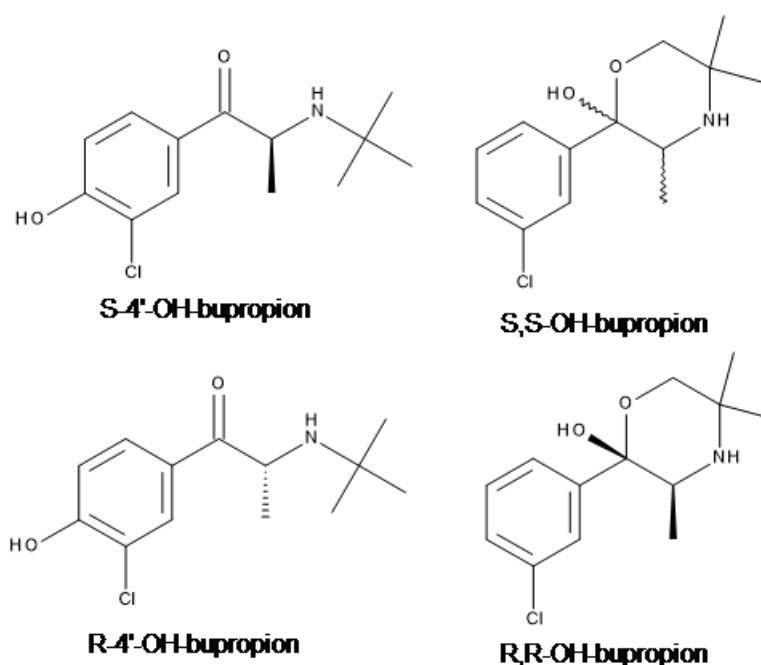
Figure 9.20: Structures of the two pairs of diastereoisomers observed in the LC-MS analysis in Figures 9.16, 9.17, 9.18 and 9.19 following incubation with the HepaRG cell line.
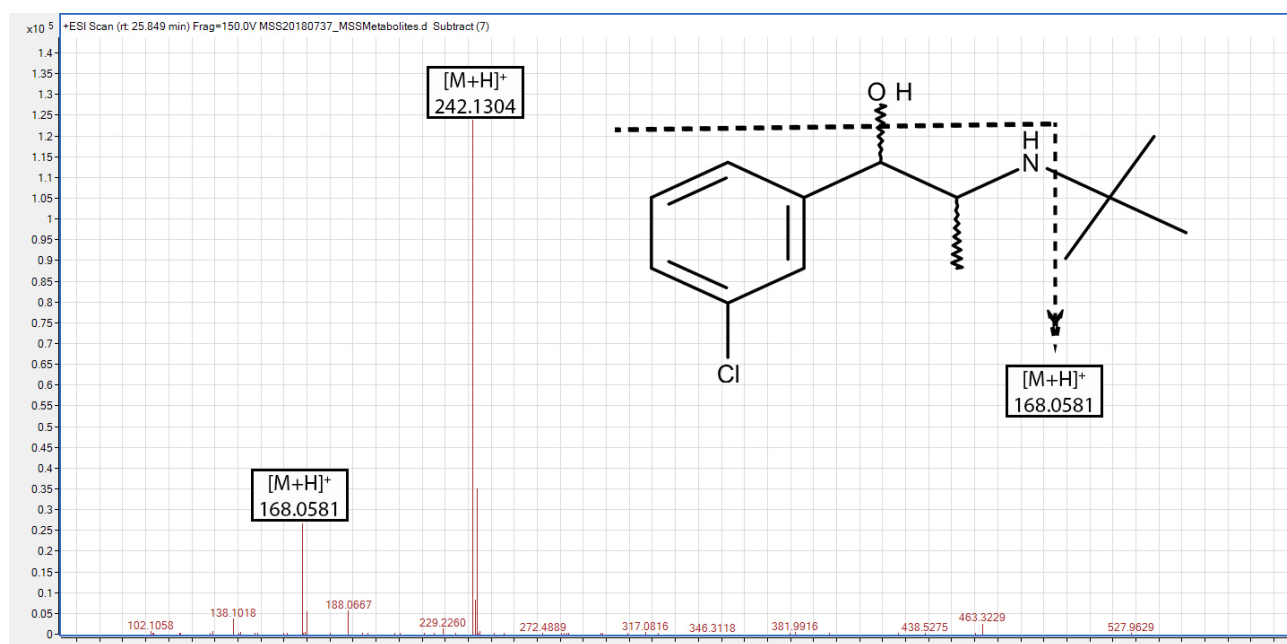
Figure 9.21: LC-MS analysis of S,S-threohydrobupropion or R,S-erythrohydrobupropion or S,R-erythrohydrobupropion or R,R-threohydrobupropion following incubation with the HepaRG cell line.
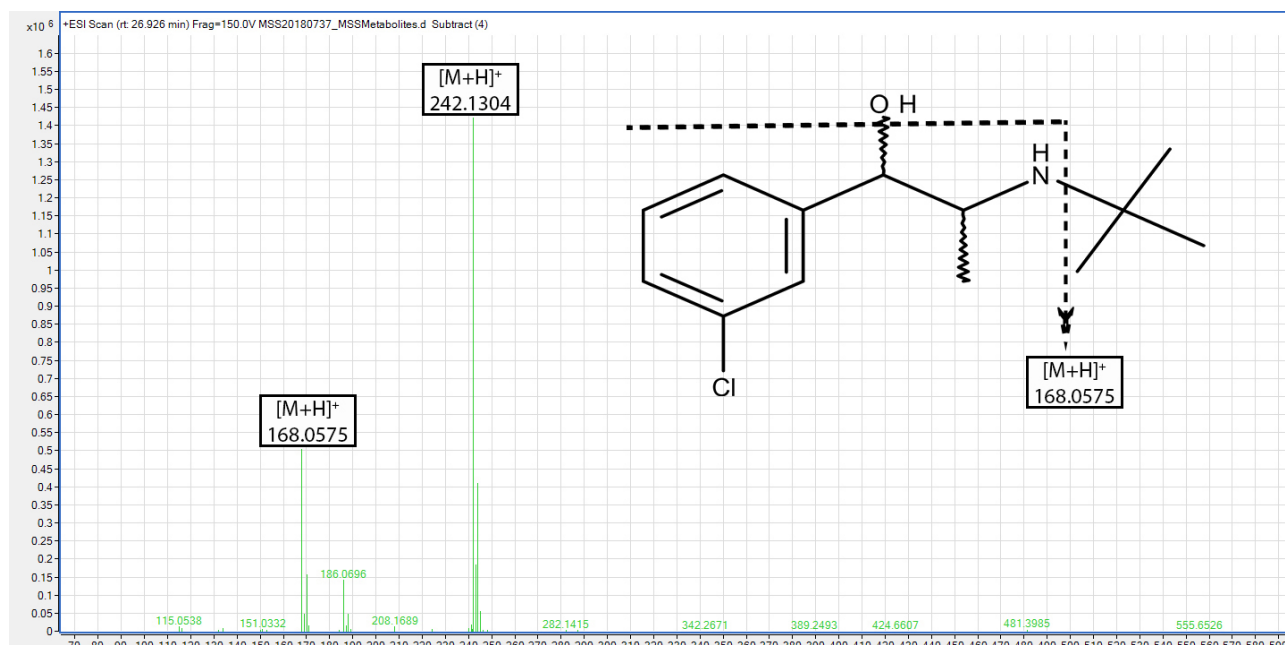
Figure 9.22: LC-MS analysis of S,S-threohydrobupropion or R,S-erythrohydrobupropion or S,R-erythrohydrobupropion or R,R-threohydrobupropion following incubation with the HepaRG cell line.
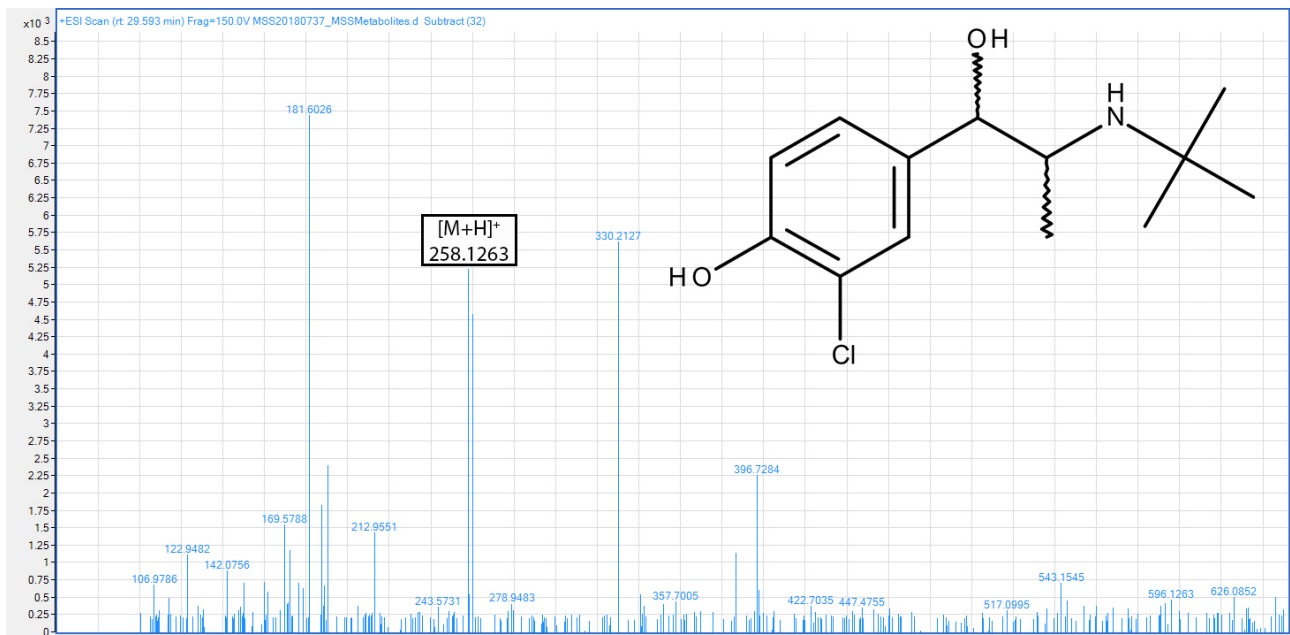
Figure 9.23: LC-MS analysis and structure of erythro- or threo- 4'-OH-hydrobupropion following incubation with the HepaRG cell line.

Figure 9.24: Metabolic pathways and structures of bupropion and its metabolites as observed in this work.

9.2.3   CYP2C19

C3A Cells

Following incubation with the C3A cell line, omeprazole was detected at 23.884 minutes (m/z 346.1224 [M+H]$^+$ with a mass difference of -3.40 ppm, Figure 9.26). An adduct with a m/z of 368.1048 and a mass difference of 2.22 ppm was also observed, corresponding to the [M+Na]$^+$ species.

No hydroxylated metabolite was observed. However, a deoxygenated compound was observed at 28.462 minutes (m/z 330.1266 [M+H]$^+$ with a mass difference of 1.17 ppm,Figure 9.27). This was tentatively detected as omeprazole sulfide, with the loss of an oxygen atom from the sulfoxide group.

The TIC and the extracted EICs for omeprazole and omeprazole sulfide can be viewed in Figure 9.25.

Omeprazole sulfide was an unexpected byproduct of cell culture and to identify the source of this compound, omeprazole was incubated in cell culture media for 24 hours in the absence of cells. Following analysis with a dual-ESI-TOF both omeprazole (m/z 346.1218 [M+H]$^+$ with a mass difference of 0.78 ppm) and omeprazole sulfide (m/z 330.1264 [M+Na]$^+$ with a mass difference of 1.82 ppm) were observed (Figure 9.28). This indicates that it is a degradation product formed. The potentially confounding and unwanted presence of this compound, means that omeprazole is unlikely to be a suitable probe for CYP2C19. As a result of this sample being run on a less-sensitive mass spectrometer with no liquid-chromatography separation, the mass spectrum had poor sensitivity. Details of the analysis of these two compounds can be found in Section 2.10.6.
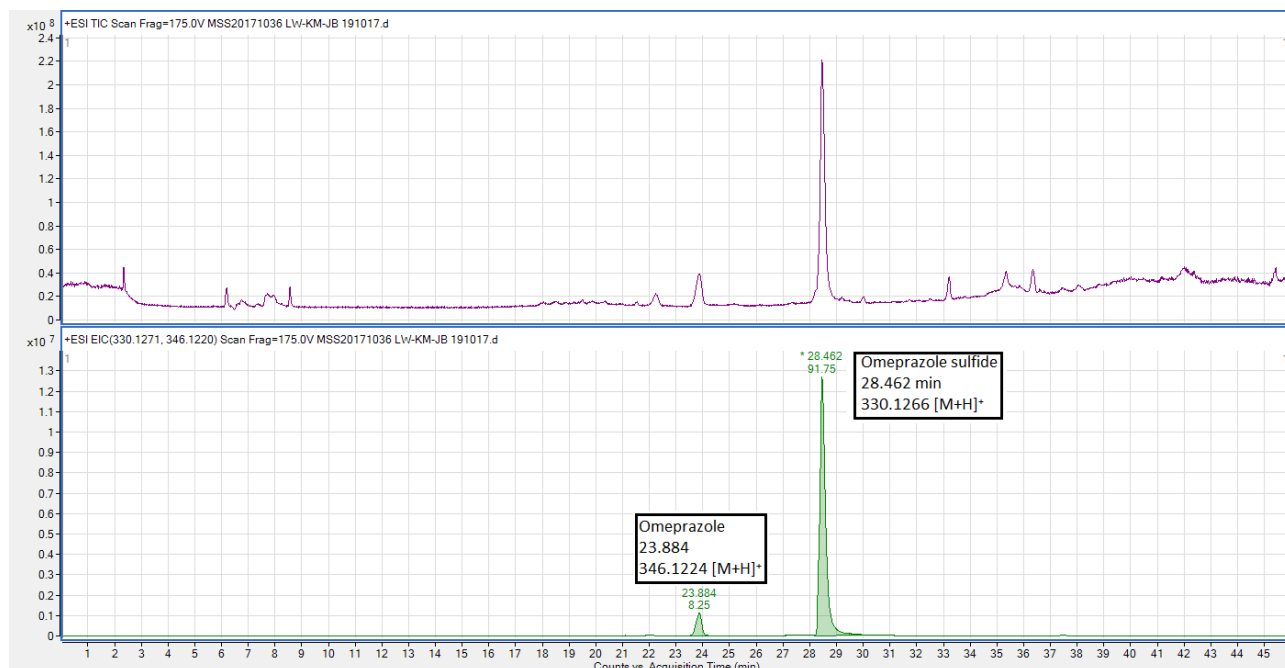
Figure 9.25: TIC and overlaid EICs for omeprazole and omeprazole sulfide following incubation with the C3A cell line.
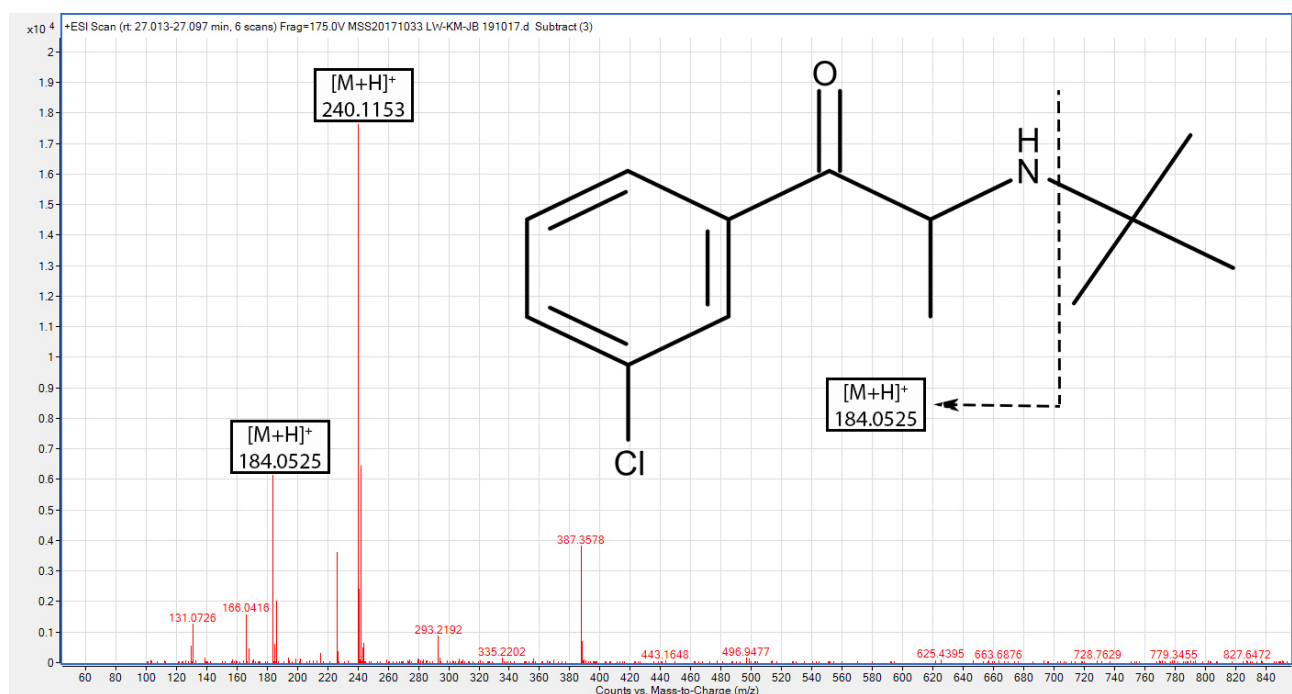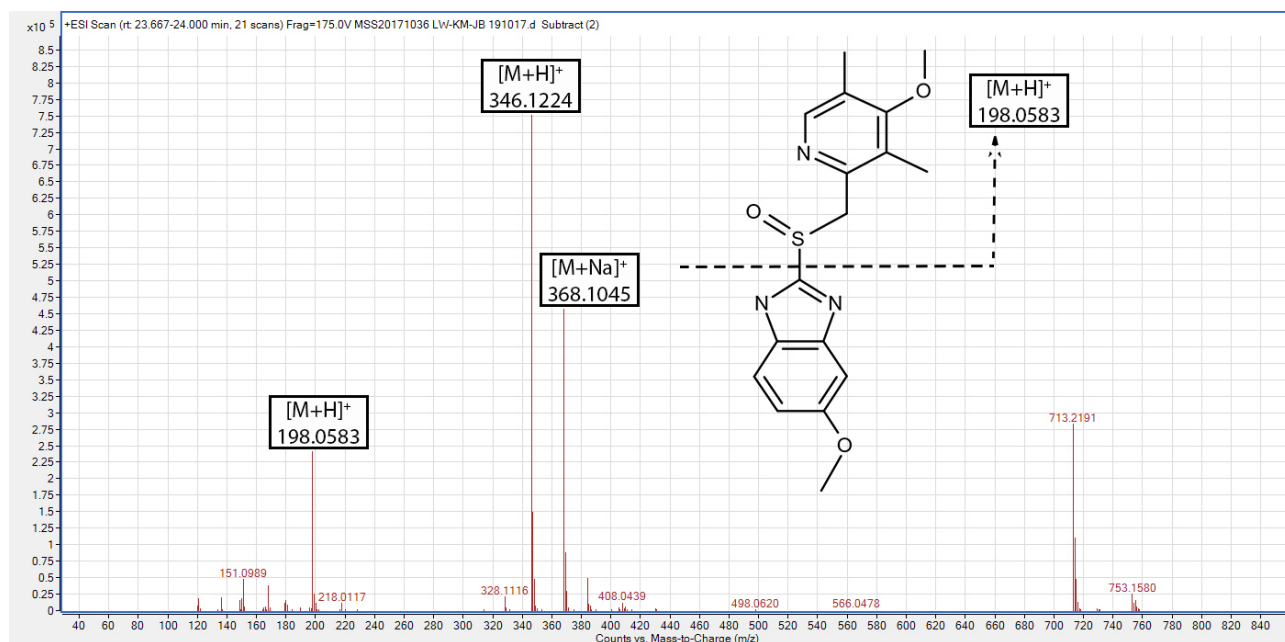

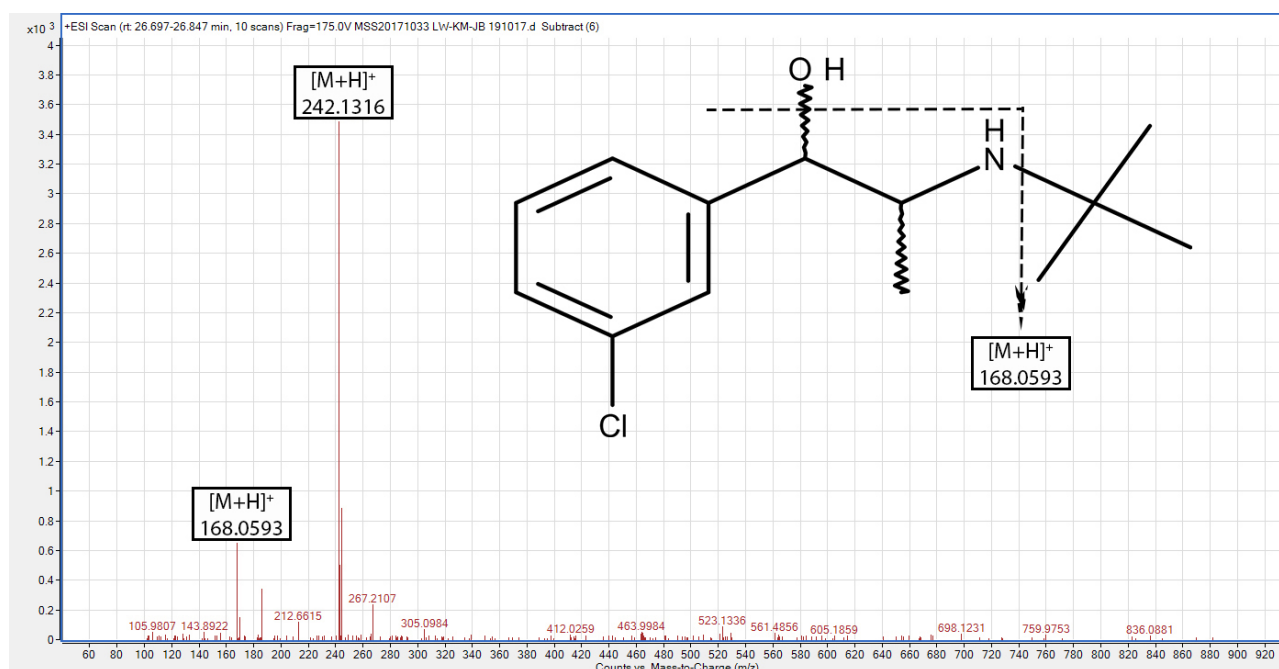Figure 9.26: LC-MS analysis and structure of omeprazole following incubation with the C3A cell line.
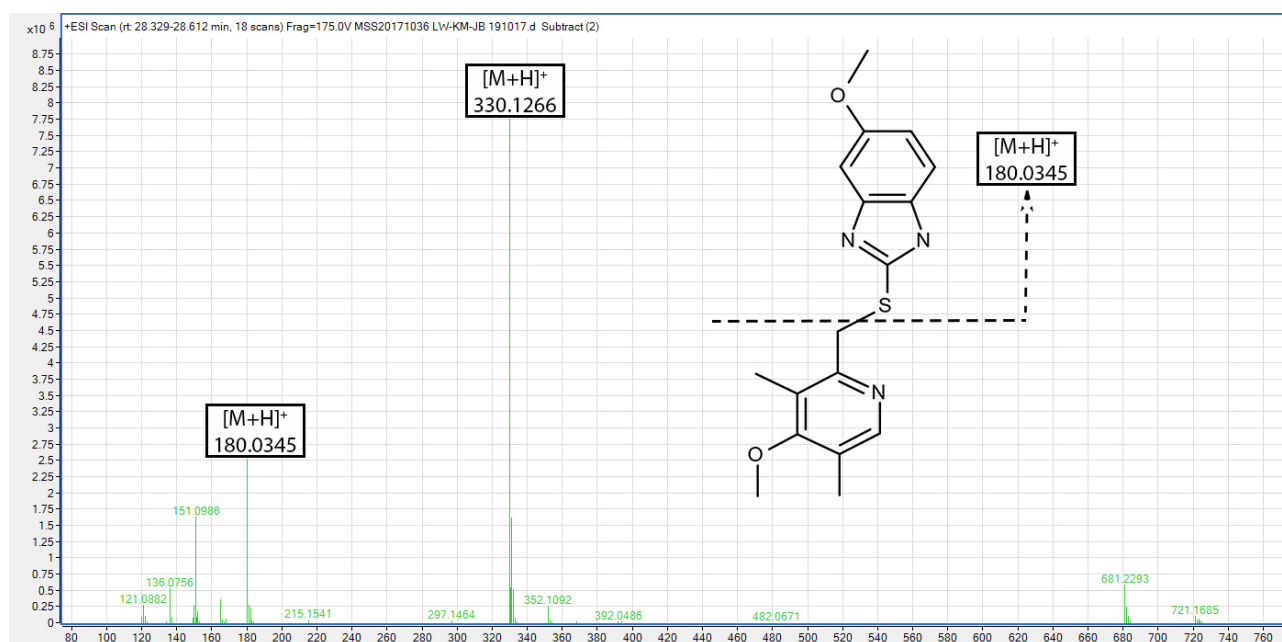
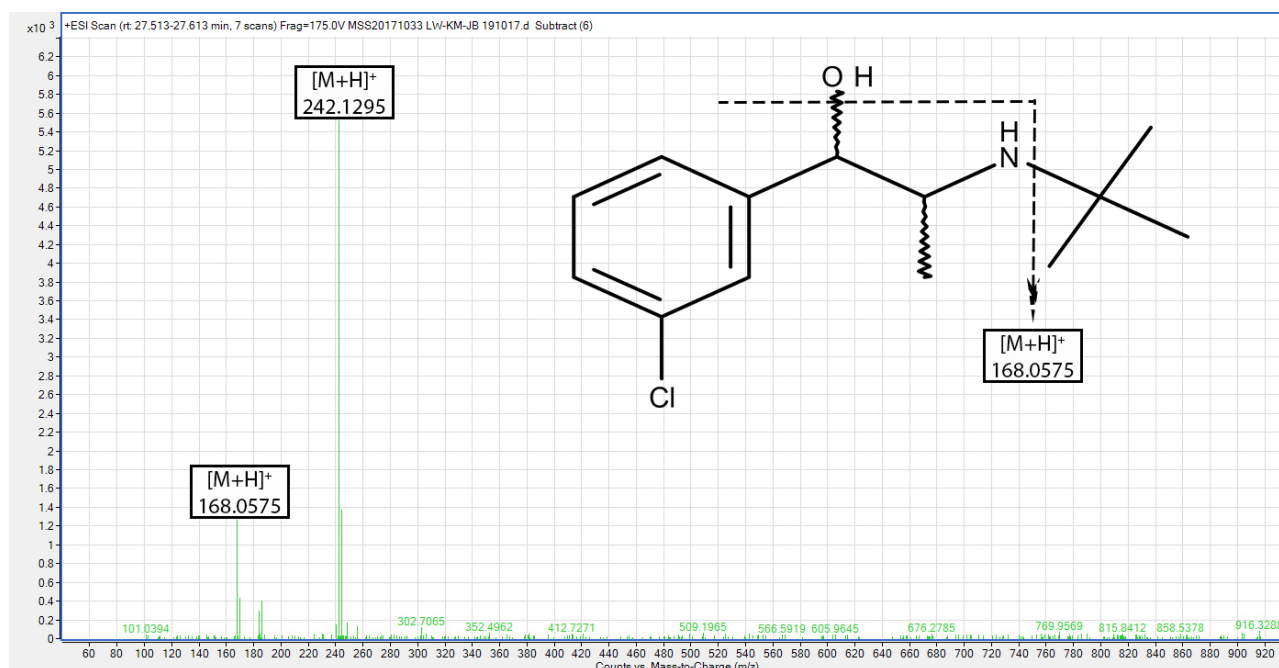Figure 9.27: LC-MS analysis and structure of omeprazole sulfide following incubation with the C3A cell line.

Figure 9.28: Expanded (m/z 308 - 362) MS analysis and structures of omeprazole and omeprazole sulfide in cell culture medium.

DMSO-Treated C3A Cells

Following incubation with the DMSO-treated cell line omeprazole was detected at 24.768 minutes (m/z 346.1231 $[M+H]^+$ with a mass difference of -2.57 ppm, Figure 9.30). An adduct with a m/z of 368.1038 and a mass difference of -1.09 ppm corresponding to the $[M+Na]^+$ was also observed.

The expected metabolite of omeprazole formed by CYP2C19, 5-hydroxyomeprazole, was not observed. Omeprazole sulfide was again detected at 28.797 minutes (m/z 330.1266 $[M+H]^+$ with a mass difference of -0.12 ppm, Figure 9.31) and is likely to be a degradation product.

The TIC and overlaid EICs for omeprazole and omeprazole sulfide can be seen in Figure 9.29.
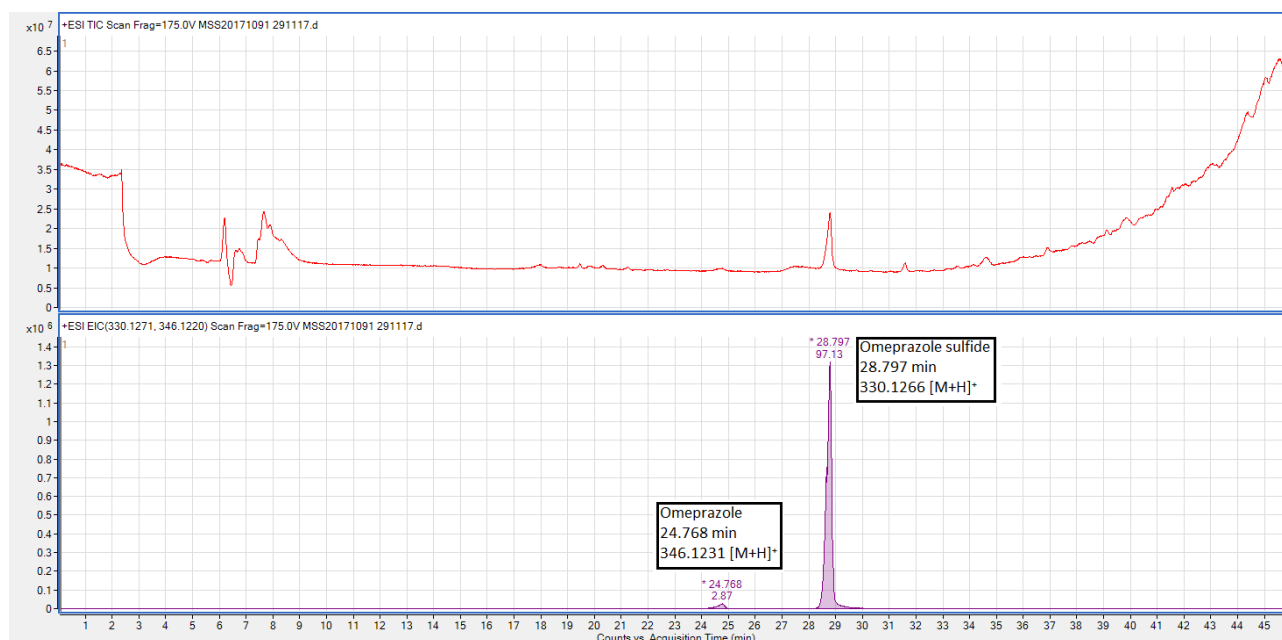
Figure 9.29: TIC and overlaid EICs for omeprazole and omeprazole sulfide following incubation with the DMSO-treated C3A cell line.

Figure 9.30: LC-MS analysis and structure of omeprazole following incubation with the DMSO-treated C3A cell line.
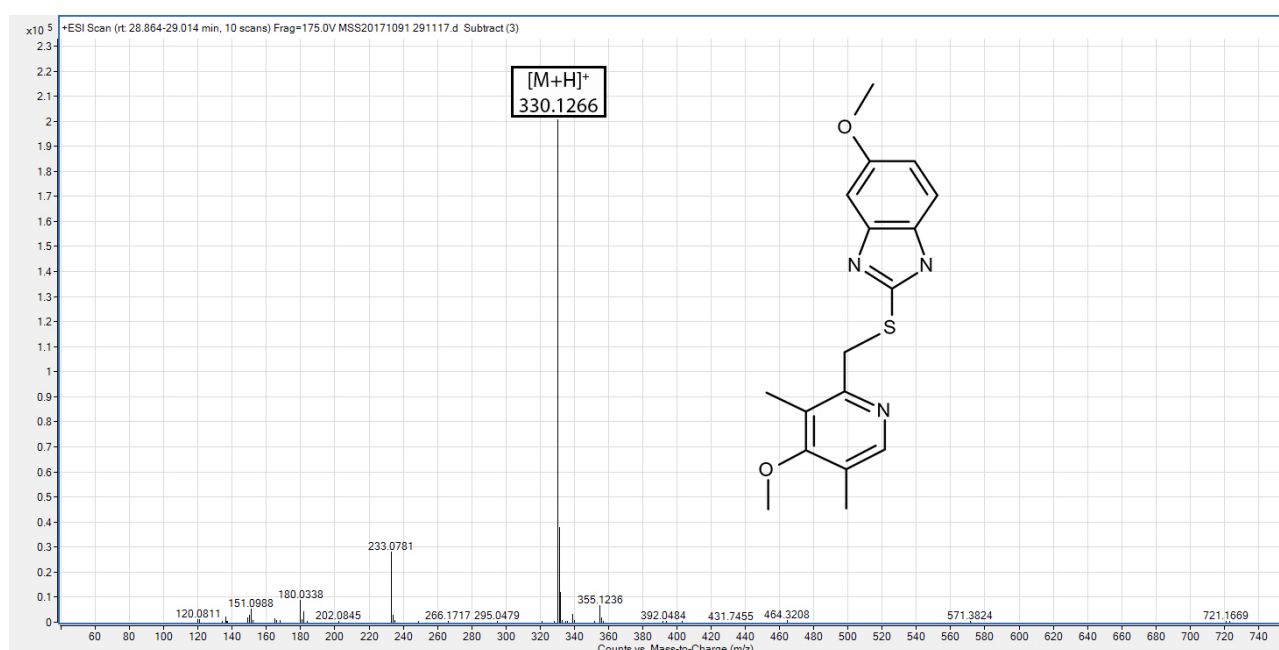
Figure 9.31: LC-MS analysis and structure of omeprazole sulfide following incubation with the DMSO-treated C3A cell line.

HepaRG Cells

In the HepaRG cells, omeprazole was detected at 23.139 minutes (m/z 346.1231 [M+H]$^+$ with a mass difference of -3.50 ppm, Figure 9.33). An [M+Na]$^+$ adduct with a m/z of 368.1048 and a mass difference of 2.22 ppm was also observed.

Omeprazole sulfide was observed at 28.059 minutes (m/z 330.1270 [M+H]$^+$, with a mass difference of -0.23 ppm, Figure 9.34). A peak at 29.235 minutes corresponding to an adduct with a m/z of 362.1154 ([M+H]$^+$) and a mass difference of 4.19 ppm was also observed (Figure 9.35). Both omeprazole sulfone and 5-hydroxyomeprazole share the same molecular mass of 361 g mol^{-1}. Therefore both compounds would be expected to produce the same m/z of 362 ([M+H]$^+$). The formation of omeprazole sulfone is thought to be mediated by CYP3A4 and the formation of 5-hydroxyomeprazole by CYP2C19 [450].

When omeprazole sulfone was injected as a standard onto the LC-MS instrument it eluted at 30.250 minutes (m/z 362.1169 [M+H]$^+$) rather than 29.235 minutes as observed in the HepaRG sample. In addition, when pure omeprazole sulfone was run as a sample (see Section 2.10.6 it produced a peak on the m/z spectrum that had an m/z 384.0986 (Figure 9.36). This m/z corresponds to the [M+Na]$^+$ adduct. No such adduct was observed to form in the HepaRG cells, making it likely that 5-hydroxyomeprazole was observed in the HepaRG cells rather than omeprazole sulfone. The formation of 5-hydroxyomeprazole is therefore suggestive of the presence of CYP2C19.

The TIC and overlaid EIcs for omeprazole sulfide and 5-hydroxyomeprazole can be seen in Figure 9.32.
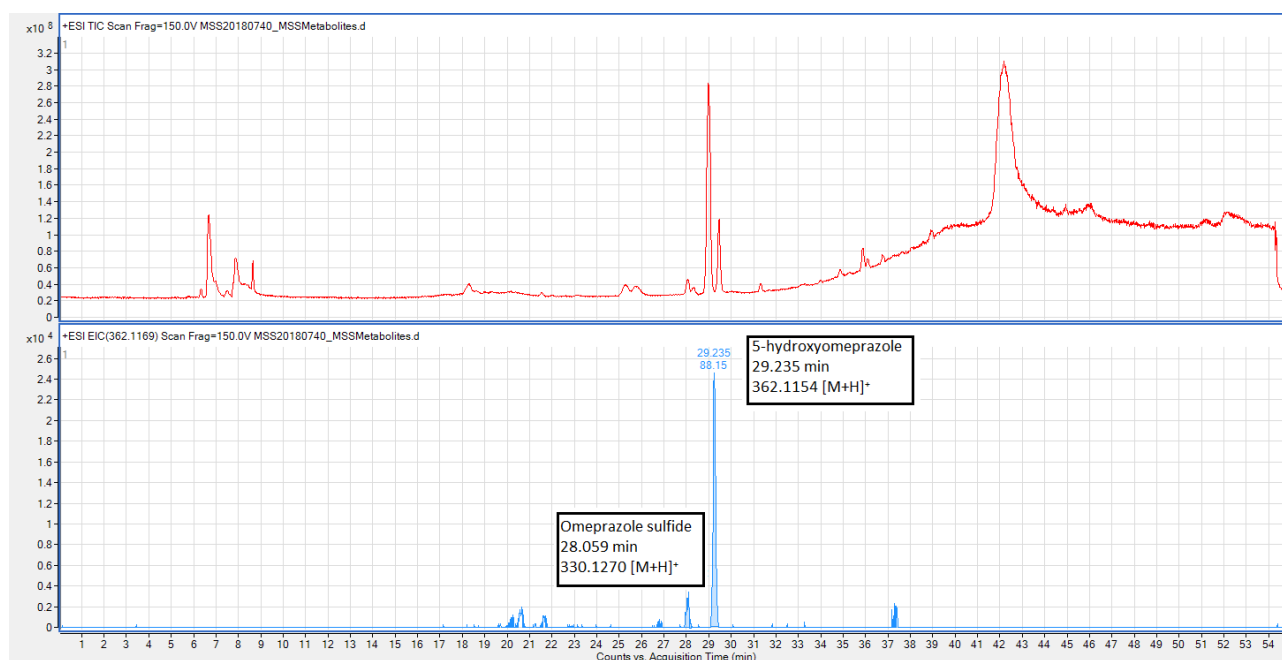
Figure 9.32: TIC and overlaid EICs for omeprazole sulfide and 5-hydroxyomeprazole following incubation with the HepaRG cell line.

Figure 9.33: LC-MS analysis and structure of omeprazole following incubation with the HepaRG cell line.
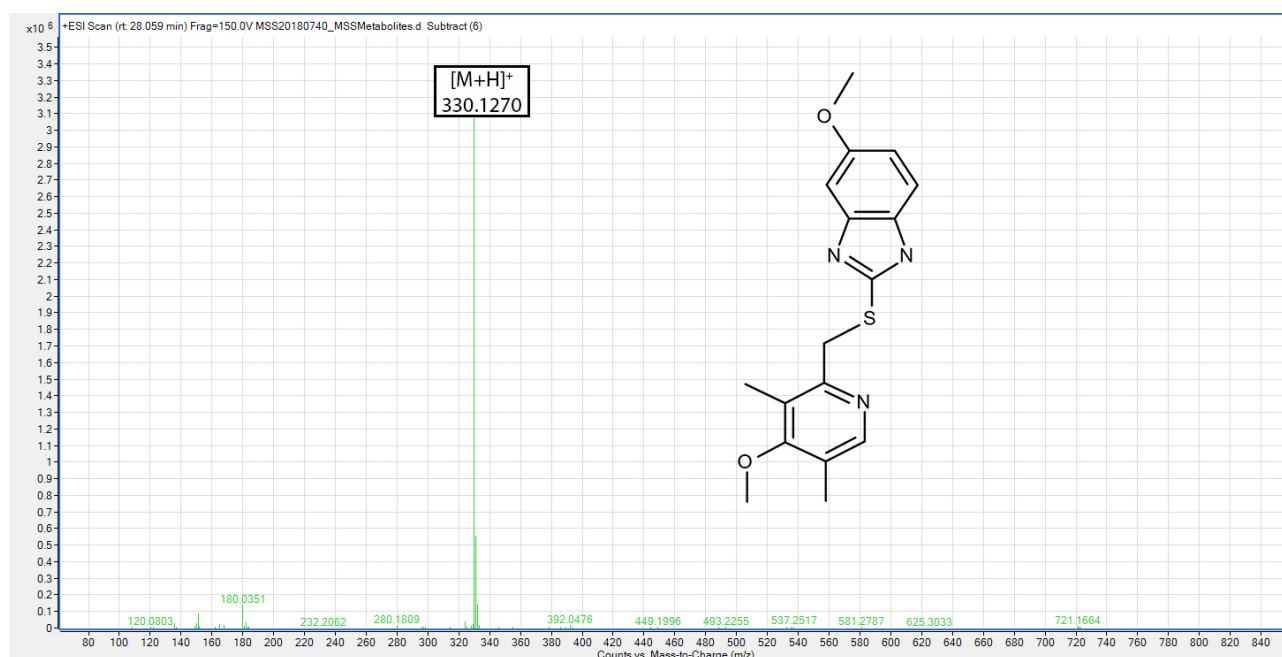
Figure 9.34: LC-MS analysis and structure of omeprazole sulfide following incubation with the HepaRG cell line.
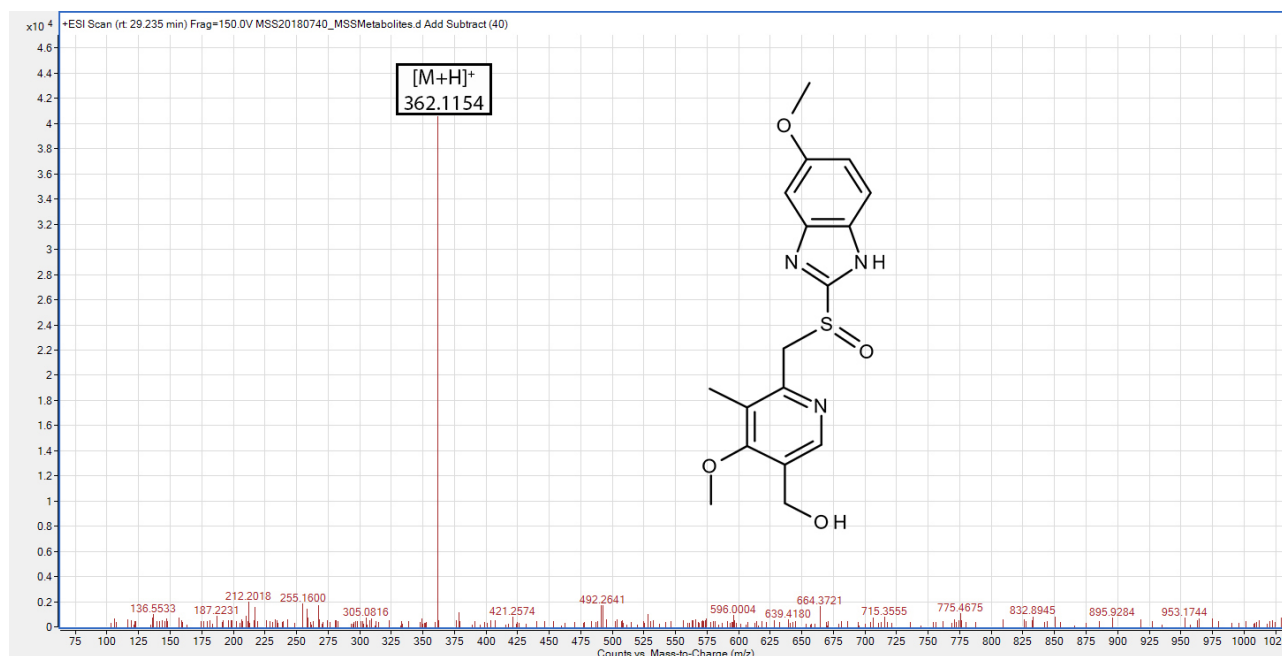
Figure 9.35: LC-MS analysis and structure of 5-hydroxyomeprazole following incubation with the HepaRG cell line.
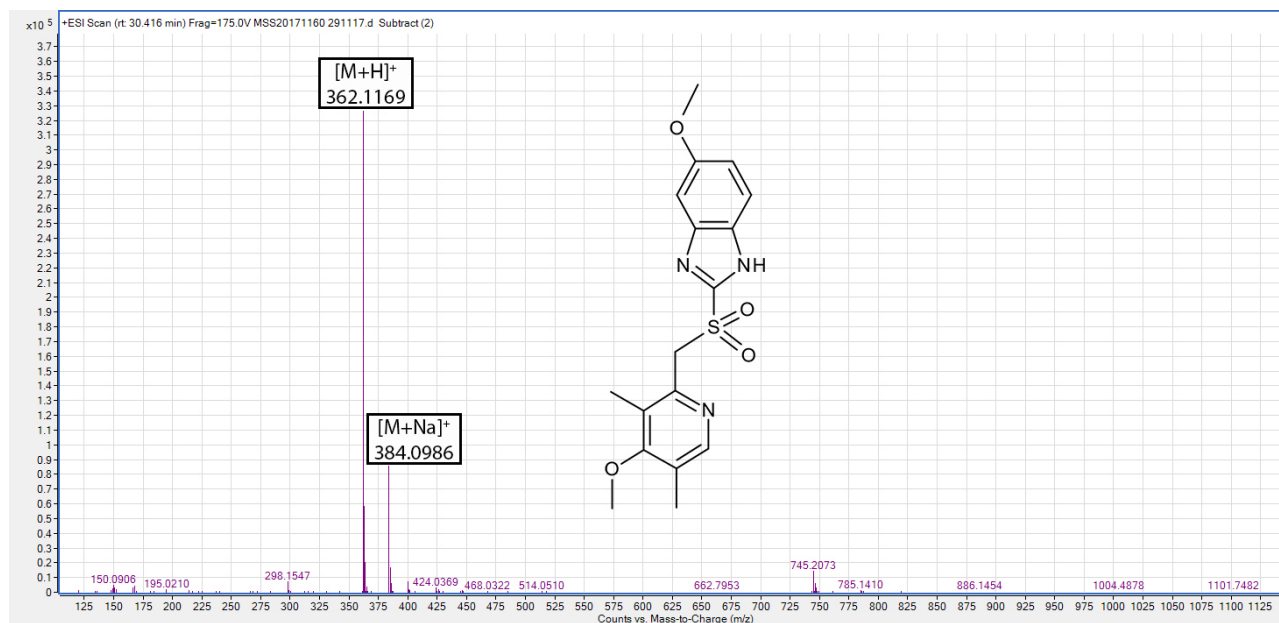
Figure 9.36: LC-MS analysis and spectra of omeprazole sulfone as a standard in the absence of cells.

9.2.4   CYP2C9

C3A Cells

Following incubation with the C3A cell line, diclofenac was detected at 38.818 minutes (m/z 296.0243 [M+H]$^+$ with a mass difference of -1.08 ppm, Figure 9.37). No metabolite was observed for diclofenac. Two ions with m/zs of 250.0185 and 215.0492 (both [M+H]$^+$) corresponding to loss of the carboxylic acid group and further loss of hydrogen chloride respectively were also observed.
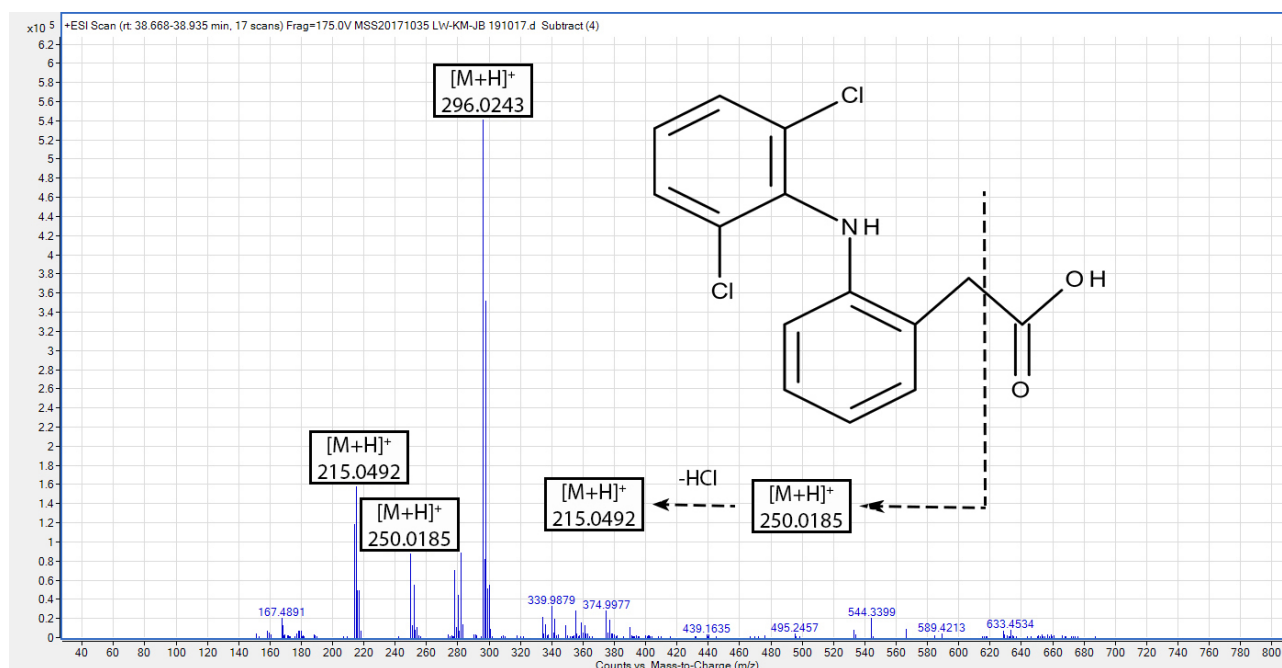
Figure 9.37: LC-MS analysis and structure of diclofenac following incubation with the C3A cell line.

DMSO-treated C3A Cells

Following incubation with the DMSO-treated cell line diclofenac was detected at 38.601 minutes (m/z 296.0239 [M+H]$^+$ with a mass difference of 0.51 ppm, Figure 9.38). In similarity to the untreated C3A cells, no metabolite was observed for diclofenac. Two ions with m/zs of 250.0183 and 215.0439 (both [M+H]$^+$) corresponding to loss of the carboxylic acid group and further loss of hydrogen chloride respectively were also observed.
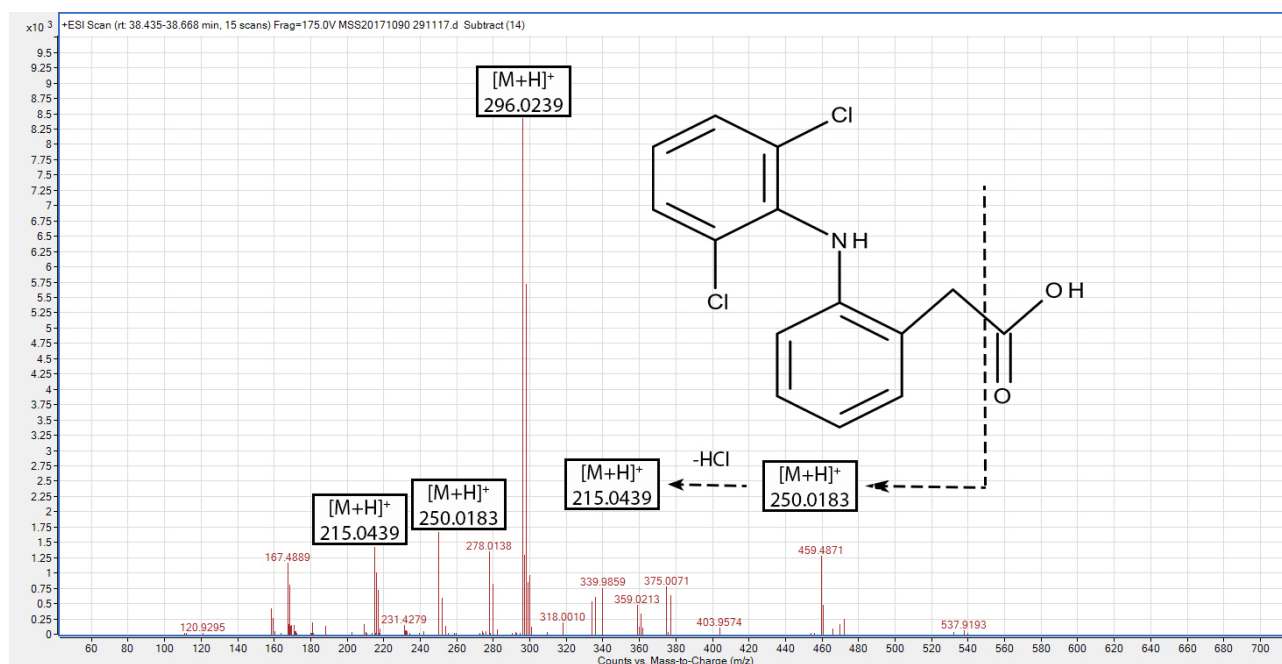
Figure 9.38: LC-MS analysis and structure of diclofenac following incubation with the DMSO-treated C3A cell line.

HepaRG Cells

In the HepaRG cells diclofenac was detected at 38.425 minutes (m/z 296.0240 [M+H]$^+$) with no metabolite present (Figure 9.39). CYP2C9 has previously been reported to be expressed in the HepaRG cell line using diclofenac as a substrate with a concentration of 20 μM [277]. The use of diclofenac as a CYP2C9 probe at a concentration of 90 μM in primary human hepatocytes and 1 μM in human liver microsomes has also been reported [451,452]. In this work a concentration of 5 μM was used as this is both common and close to determined Km values for diclofenac [453]. Concentrations of 5 and 10 μM are the most commonly used concentrations according to a review of cytochrome P450 substrates [454]. Nonetheless the substrate concentration used in this work may simply have been too low to allow sufficient quantity of the hydroxylated metabolite to be produced. Two ions with m/zs of 250.0170 and 215.0501 (both [M+H]$^+$) corresponding to loss of the carboxylic acid group and further loss of hydrogen chloride respectively were also observed.
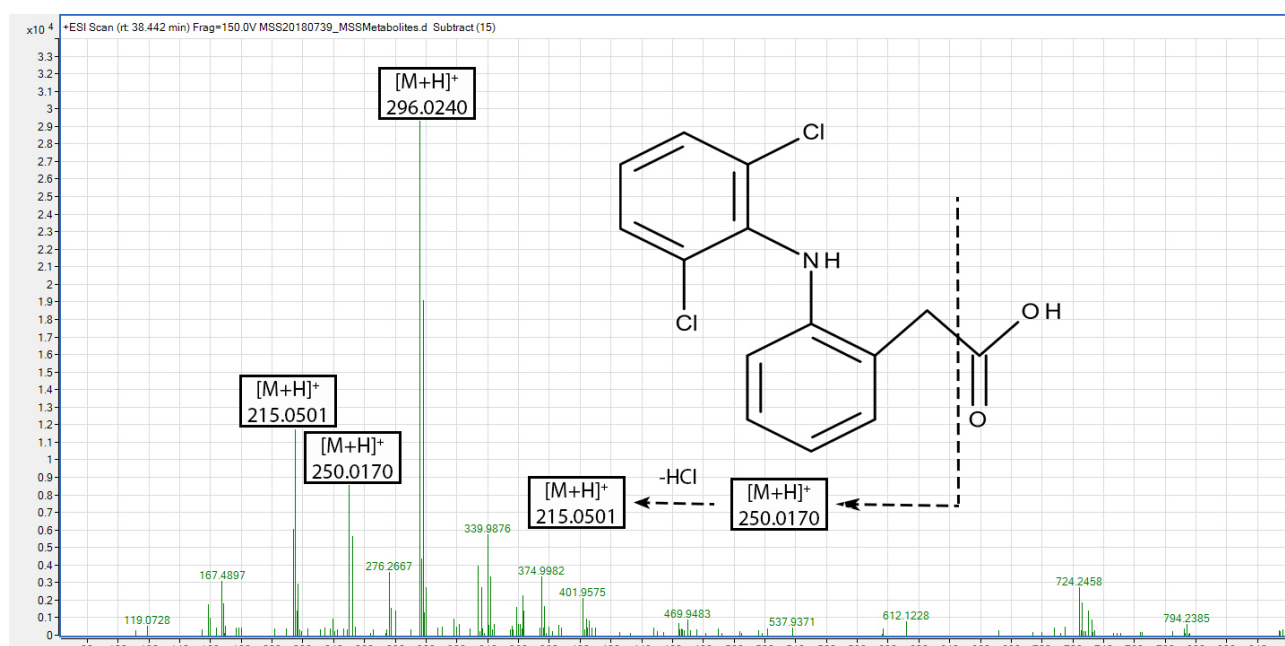
Figure 9.39: LC-MS analysis and structure of diclofenac in HepaRG C3A cells.

9.2.5 CYP2D6

C3A Cells

Following incubation with the C3A cell line, dextromethorphan was detected at 29.997 minutes (m/z 272.1997 $[M+H]^+$ with a mass difference of 2.72 ppm, Figure 9.41). Its O-demethylated metabolite, dextrorphan, was detected at 29.464 minutes (m/z 258.1844 $[M+H]^+$ with a mass difference of 4.06 ppm, Figure 9.42). The dextromethorphan to dextrorphan ratio was 3:1 indicating the presence of CYP2D6. The overlaid EICs for dextromethorphan and dextorphan can be seen in Figure 9.40.
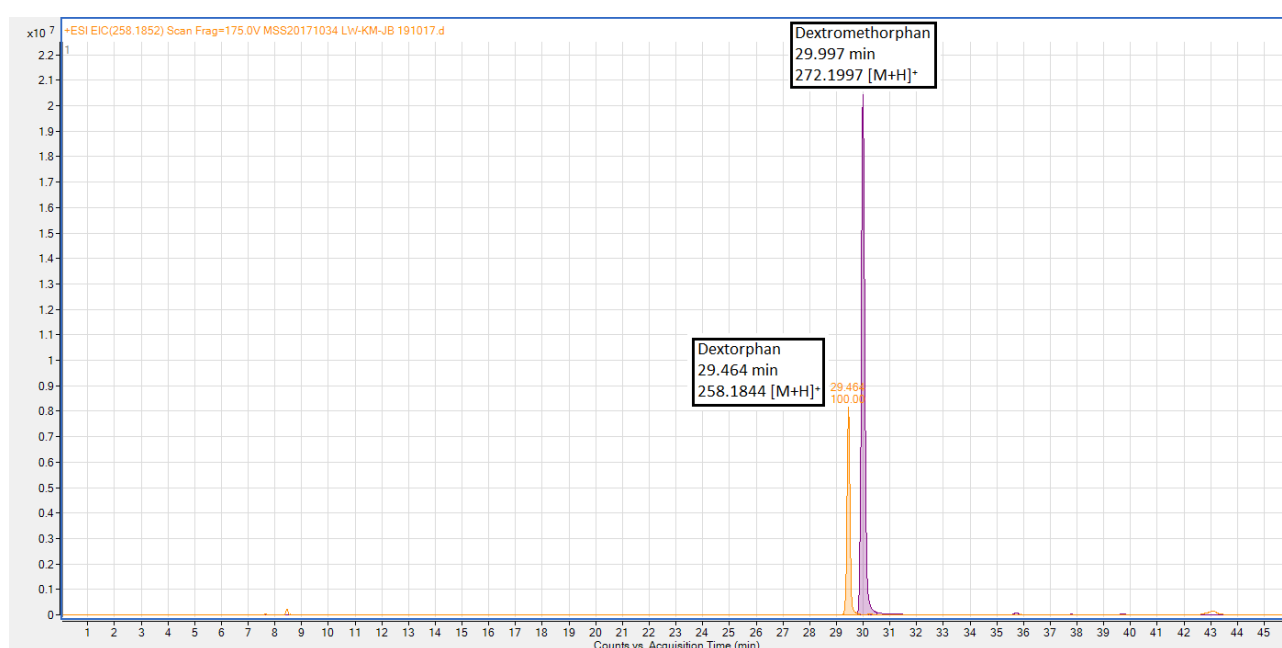
Figure 9.40: Overlaid EICs of dextromethorphan and dextrorphan following incubation with the C3A cell line.
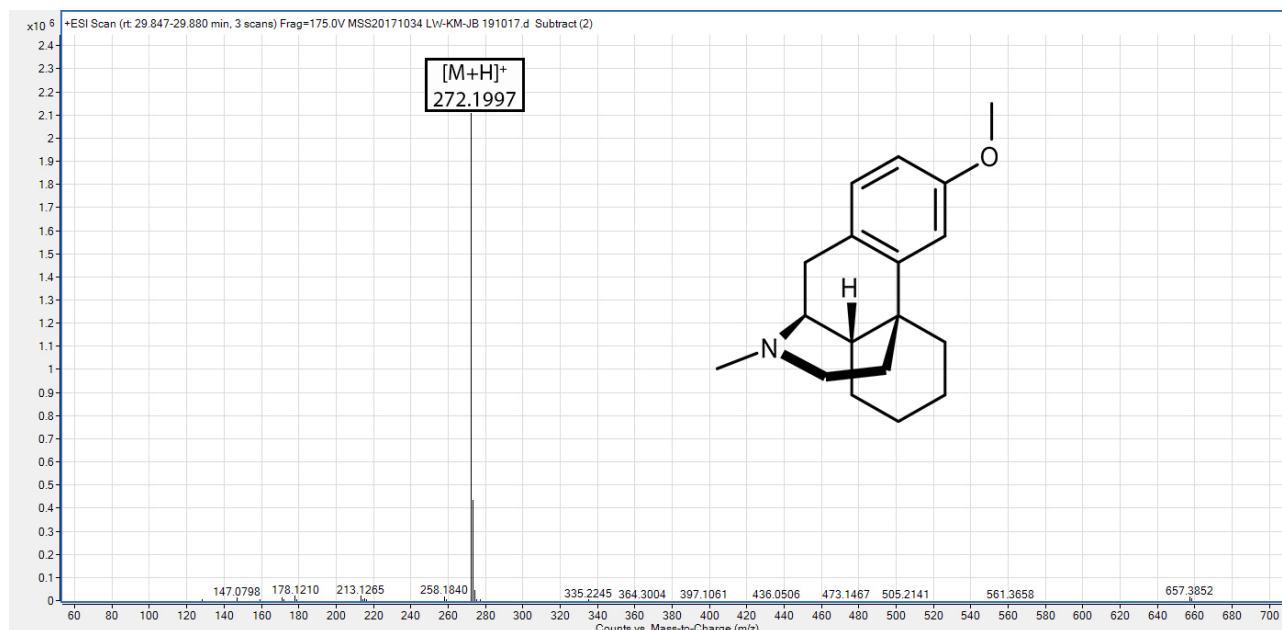
Figure 9.41: LC-MS analysis and structure of dextromethorphan following incubation with the C3A cell line.
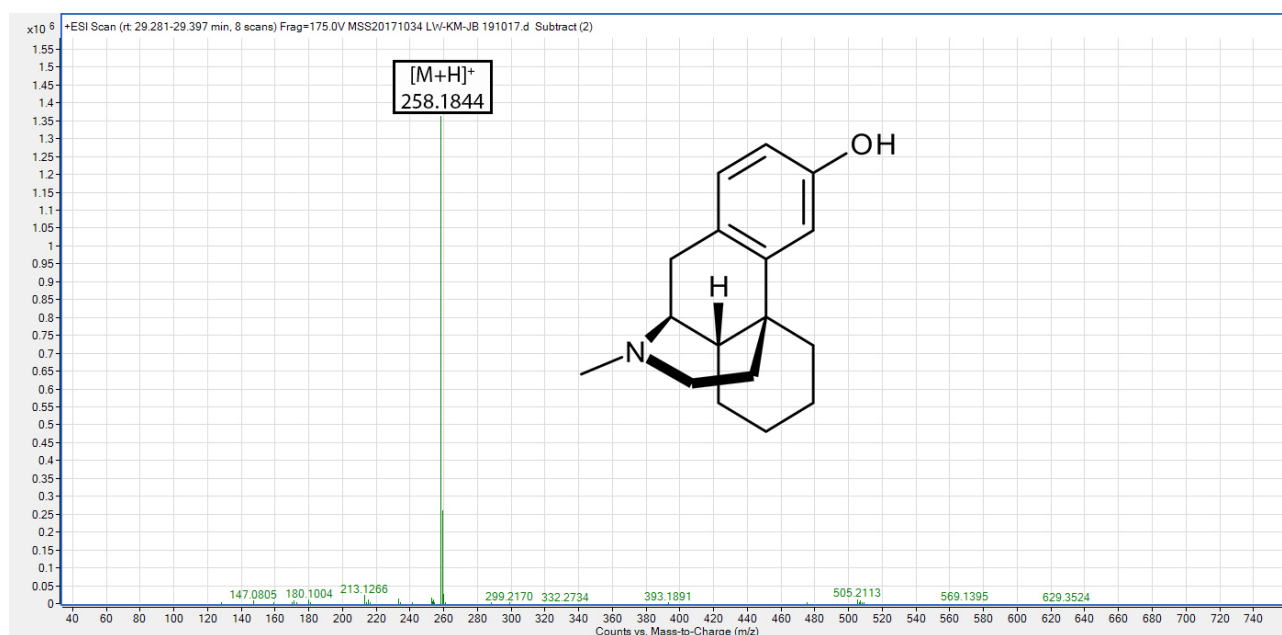
Figure 9.42: LC-MS analysis and structure of dextrorphan following incubation with the C3A cell line.

DMSO-treated C3A Cells

Following incubation with the DMSO-treated C3A cell line, dextromethorphan was detected at 29.997 minutes (m/z 272.2013 [M+H]$^+$ with a mass difference of -0.99 ppm, Figure 9.44). Dextorphan was detected at 29.431 minutes (m/z 258.1853 [M+H]$^+$ with a mass difference of 1.31 ppm, Figure 9.45). The area ratio was approximately 255:1 in favour of the dextromethorphan. This in contrast to the 3:1 ratio detected in the untreated set. The indication of this is a reduction in the metabolic activity observed for the DMSO-treated C3A cells. A potentially similar reduction in metabolic activity was also observed for the metabolism of bupropion to threo-/erythro- hydrobupropion. The overlaid EICs for dextromethorphan and dextorphan can be seen in Figure 9.43.
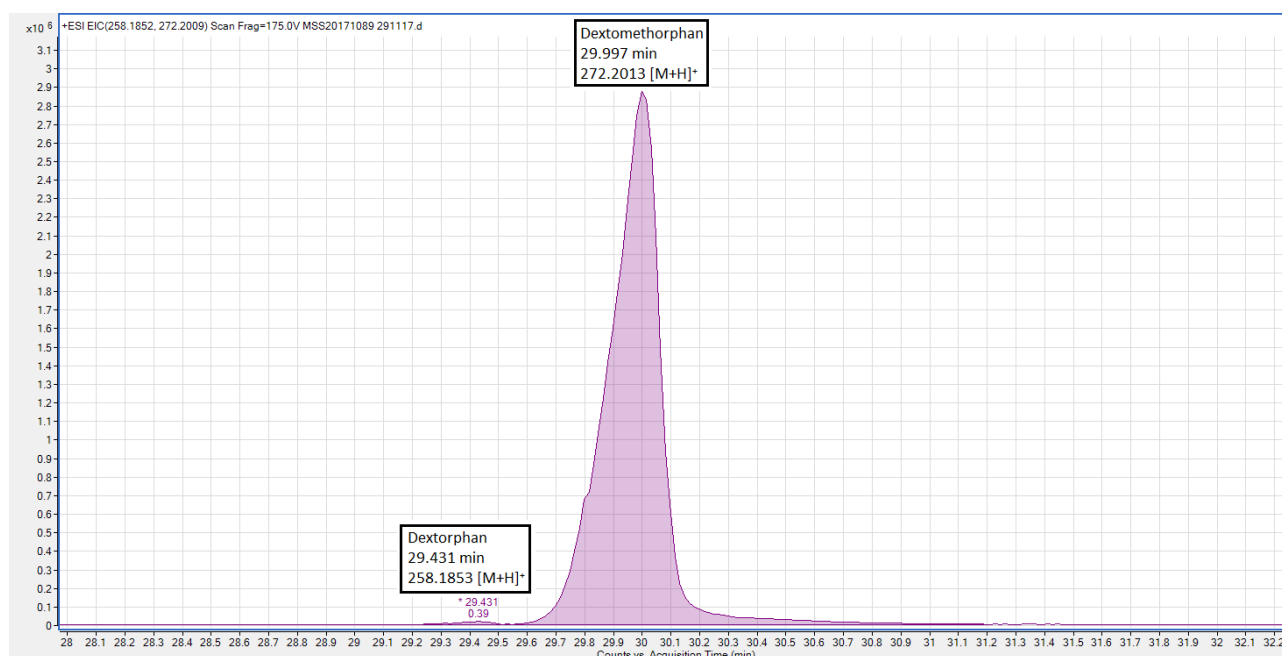
Figure 9.43: Overlaid EICs of dextromethorphan and dextrorphan following incubation with the DMSO-treated C3A cell line.
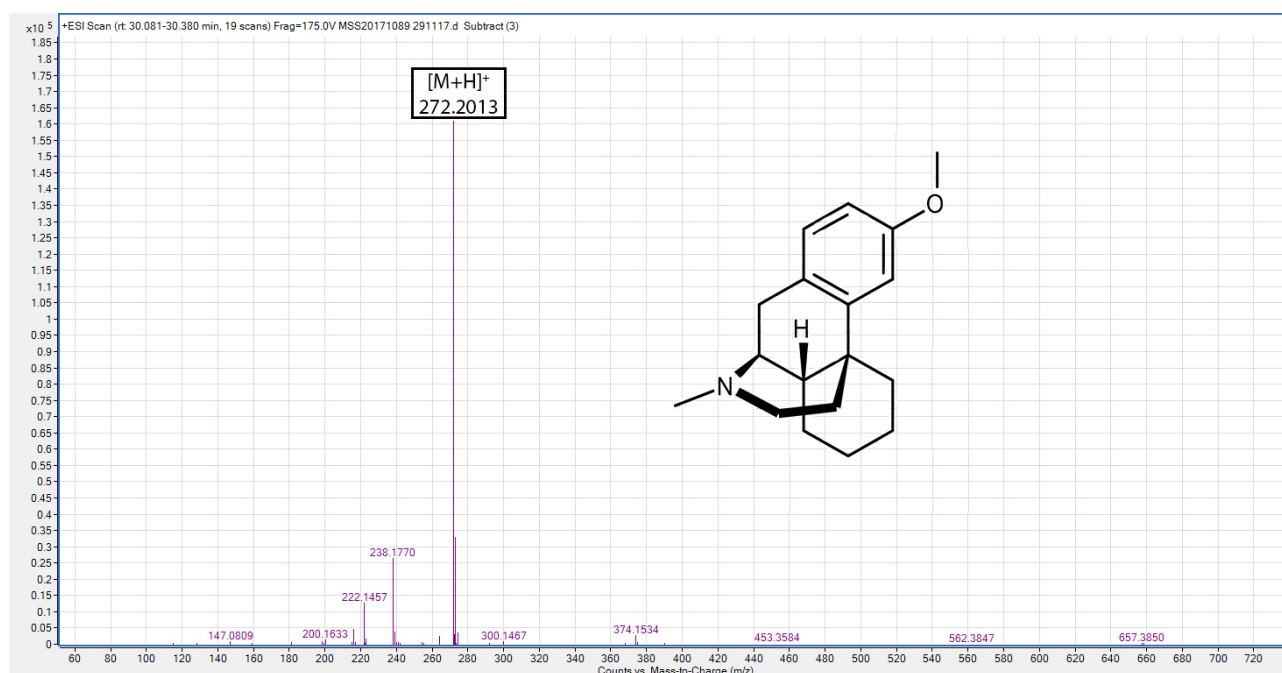
Figure 9.44: LC-MS analysis and structure of dextromethorphan following incubation with the DMSO-treated C3A cell line.
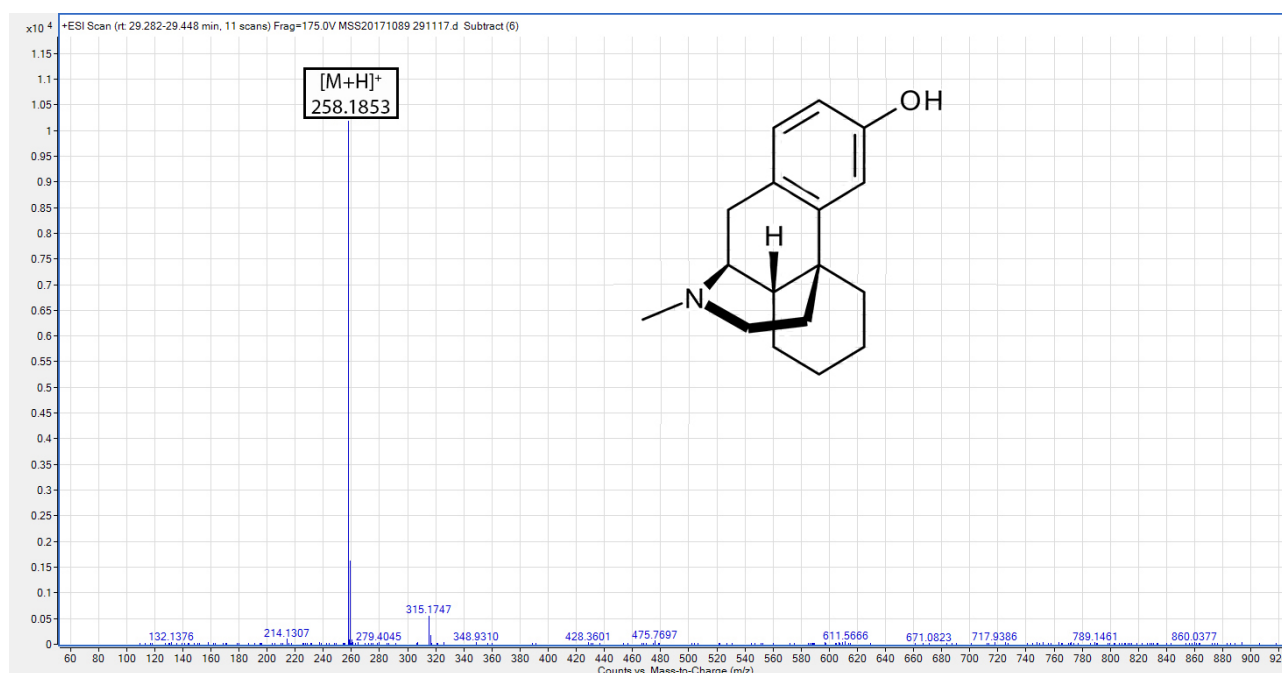
Figure 9.45: LC-MS analysis and structure of dextrorphan following incubation with the DMSO-treated C3A cell line.

HepaRG Cells

In the HepaRG cells, dextromethorphan was detected at 29.682 minutes (m/z 272.2012 [M+H]$^+$) and its metabolite dextrorphan was detected at 29.119 minutes (m/z 258.1853 [M+H]$^+$) (Figures 9.48 and 9.48 respectively). The ratio of dextromethorphan to dextorphan was approximately 5:1. The HepaRG cell line is derived from an individual who reportedly had a low expression of CYP2D6 resulting in a relatively low proportion of this enzyme compared to the other CYP enzymes it expresses [274,277]. Nonetheless it was found to be expressed in this work. The overlaid EICs for dextromethorphan and dextorphan can be seen in Figure 9.46.
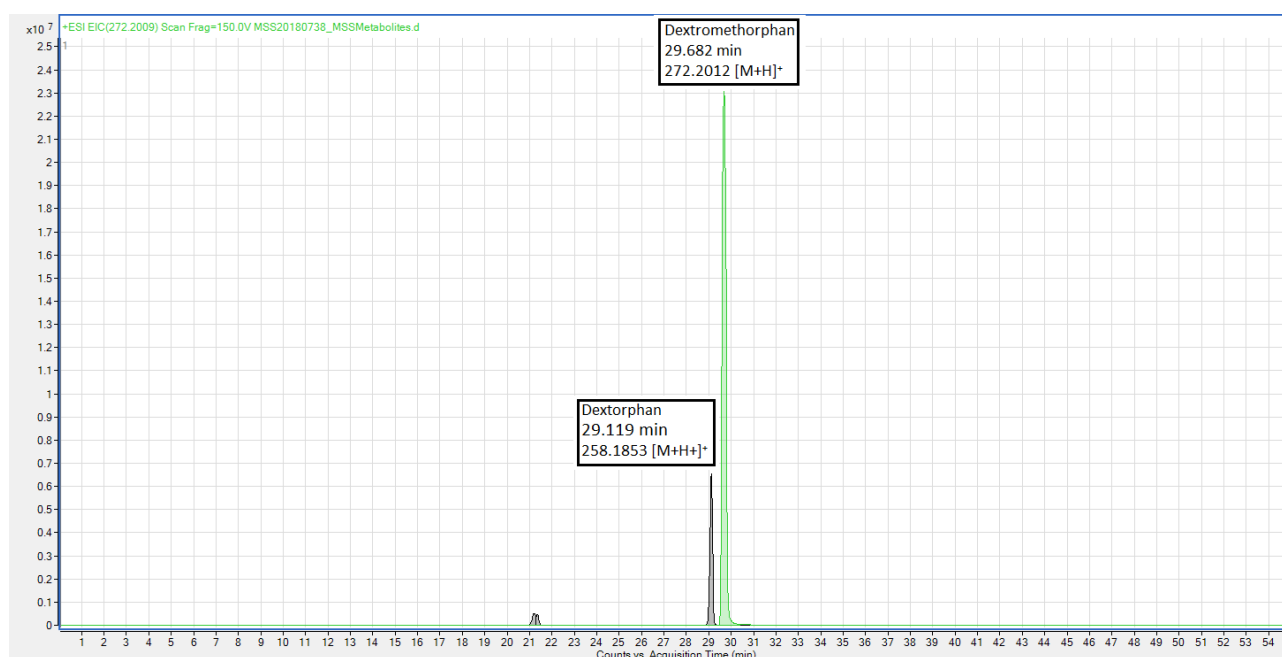
Figure 9.46: Overlaid EICs of dextromethorphan and dextrorphan following incubation with the HepaRG cell line.
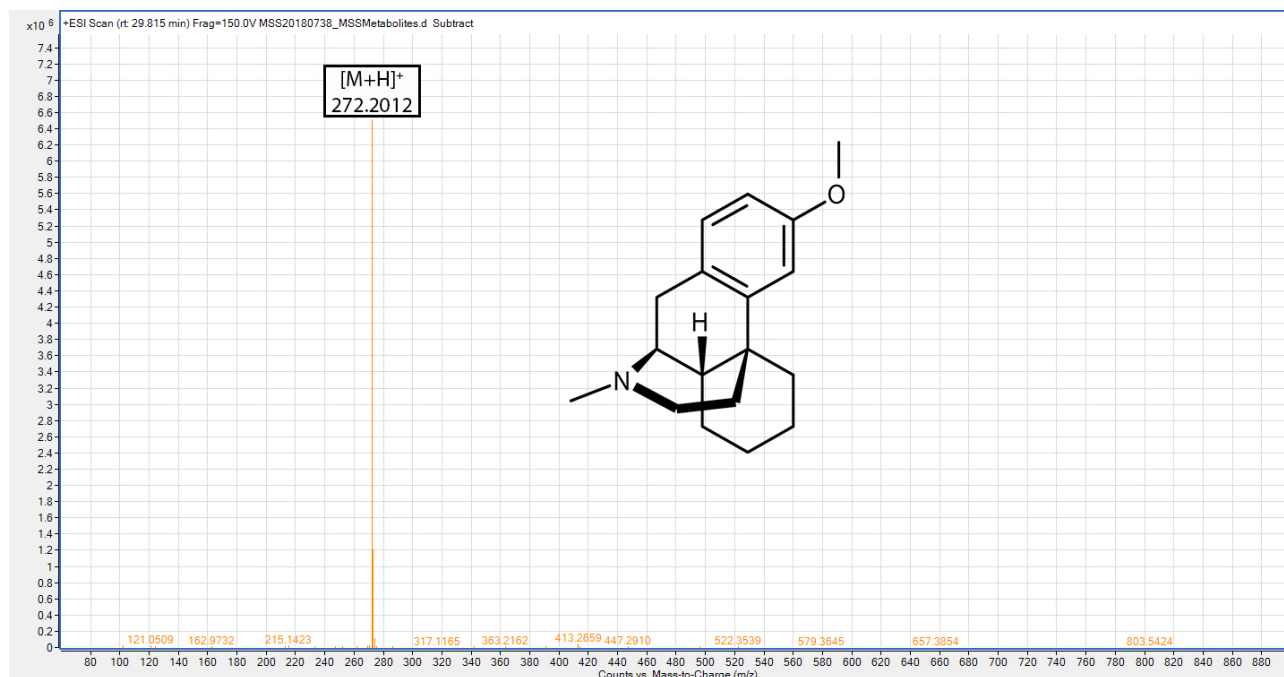
Figure 9.47: LC-MS analysis and structure of dextromethorphan following incubation with the HepaRG cell line.
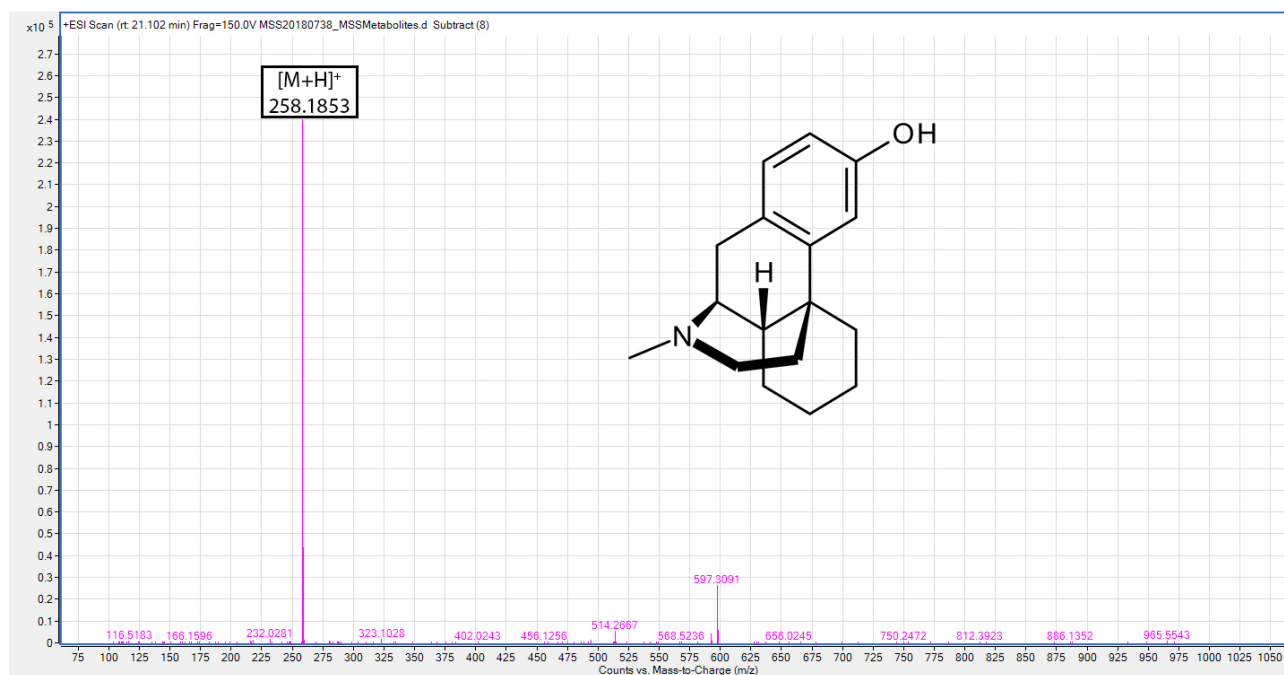
Figure 9.48: LC-MS analysis and structure of dextrorphan following incubation with the HepaRG cell line.

9.2.6 CYP3A4/5

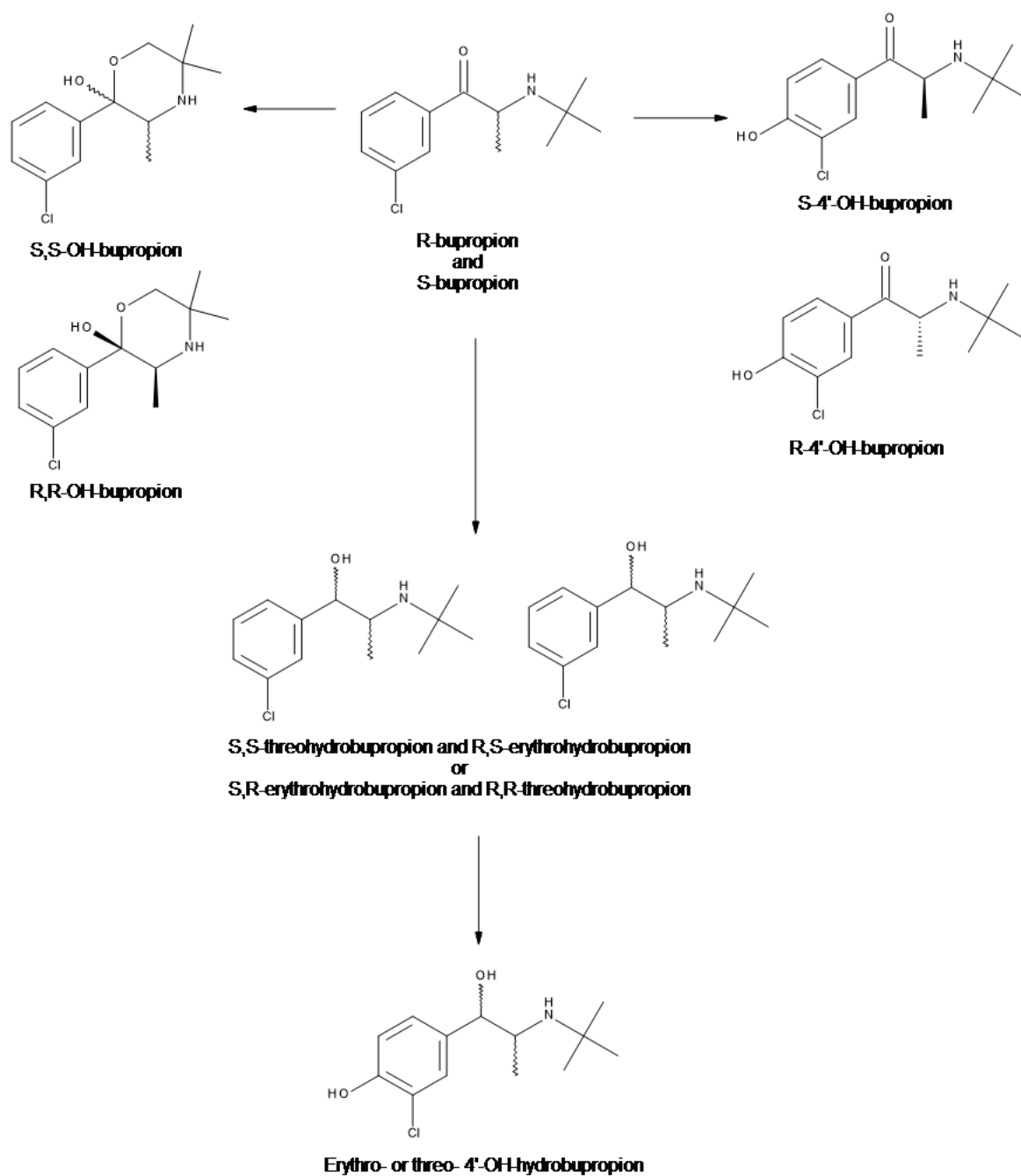**C3A Cells**

Following incubation with the C3A cell line, testosterone was detected at 36.787 minutes (m/z 289.2155 [M+H]$^+$ with a mass difference of 1.8 ppm, Figure 9.49). No metabolite was observed for testosterone. Other published work has reported the presence of CYP3A4 in the C3A cell line [269]. However following incubation with testosterone, the metabolites produced were 16 β -hydroxytesterone and androstenedione rather than the expected CYP3A4 metabolite, 6β-hydroxytestosterone [269]. CYP3A4 activity in C3A cells has also been reported to be minimal and below the detection limit when measured with the P450-Glo assay (Promega). This utilises a luminescent method to detect CYP3A4 activity [455].
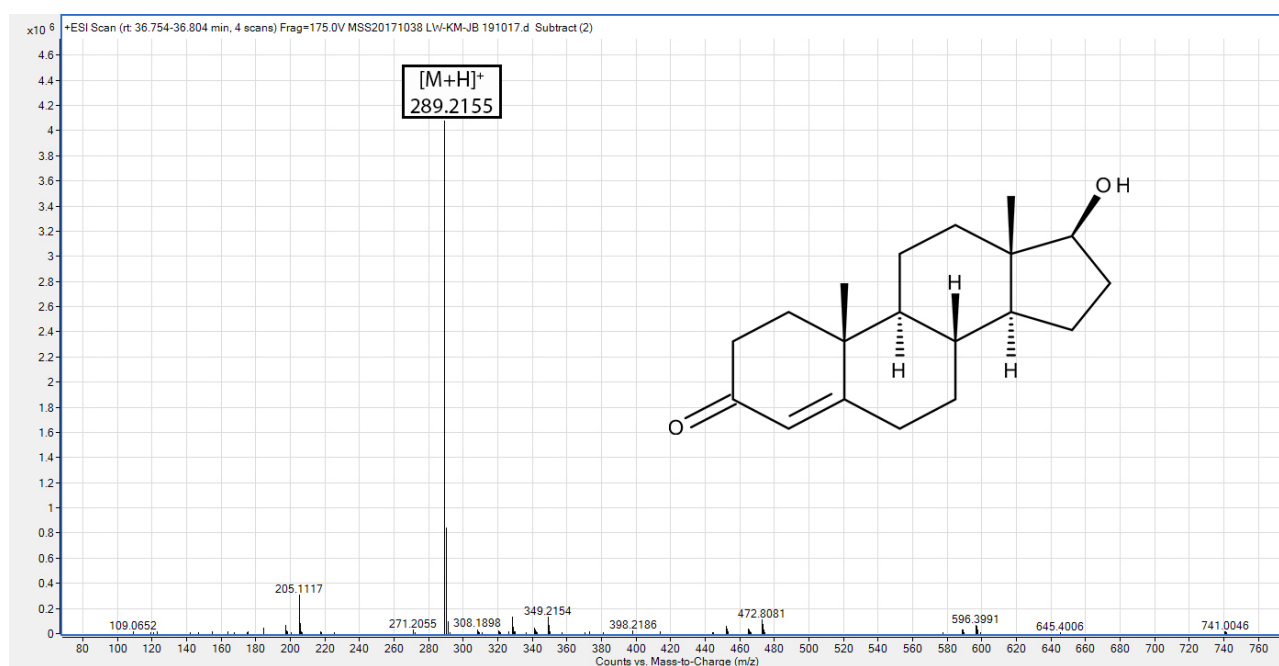
Figure 9.49: LC-MS analysis and structure of testosterone following incubation with the C3A cell line.

DMSO-treated C3A Cells

Following incubation with the DMSO-treated C3A cell line, testosterone was detected at 36.787 minutes (m/z 289.2161 [M+H]$^+$ with a mass difference of 0.34 ppm, Figure 9.50). There was no observation of the hydroxylated metabolite.
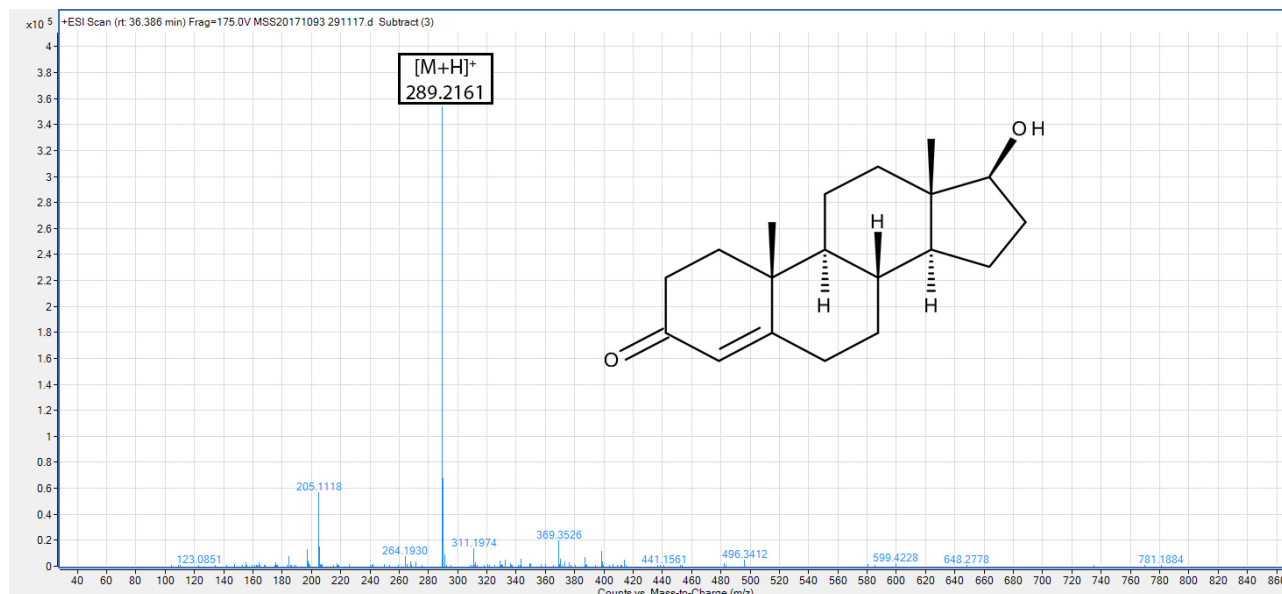
Figure 9.50: LC-MS analysis and structure of testosterone following incubation with the DMSO-treated C3A cell line.

HepaRG Cells

In the HepaRG cells testosterone was detected at 36.553 minutes (m/z 289.2162 [M+H]$^+$ with a mass difference of -0.17 ppm, Figure 9.54). A metabolite was detected at 38.129 minutes (m/z 287.2004 [M+H]$^+$ with a mass difference of -7.99 ppm) and was tentatively detected as androstenedione (Figure 9.55). Androstenedione is known to be formed from testosterone by 17-hydroxysteroid dehydrogenase (HSD) [456]. Additionally CYP2C19 and CYP2C9 are known to catalyse the oxidation of testosterone to androstenedione [458]. Another metabolite, detected as a hydroxylated metabolite of testosterone, was detected at 27.559 minutes (m/z 305.2108 [M+H]$^+$ with a mass difference of 0.84 ppm, m/z 327.1933 [M+Na]$^+$ with a mass difference of -1.20 ppm) (Figure 9.56).

The TIC and EIC for testosterone can be seen in Figure 9.51, for andronstenedione in Figure 9.52 and for a hydroxytestosterone metabolite in Figure 9.53. Although multiple peaks were

observed on the EIC for a *m/z* of 305, only the peak at 27.559 minutes had an additional $[M+Na]^+$ adduct with a *m/z* of 327.1933 to provide additional confirmation of the presence of a hydroxylated metabolite. However it is entirely possible that other hydroxylated metabolites were produced from testosterone by the HepaRG cell line.

The majority of testosterone metabolites (88.2 %) are thought to be produced by CYP3A4 [459]. The other contributory enzymes are thought to be CYP3A5 and CYP3A7, responsible for 7.1 % and 2.2 % of testosterone metabolism respectively [459]. Of the metabolites produced by CYP3A4, 6β-hydroxytestosterone is the most prominent followed by 15β-hydroxytesterone and 2β-hydroxytesterone [459]. Without further analysis using NMR it is impossible to assign an exact site of hydroxylation on testosterone in this work. However, given that 6β-hydroxytesterone is the most prominent metabolite it can be tentatively assumed that this is the metabolite observed in this work. As all hydroxylated metabolites are mainly formed by CYP3A4 this indicates that CYP3A4 was present in the HepaRG cells used in this study. Another method of identifying the exact metabolite produced would have been to run all expected hydroxylated metabolites as standards on the LC-MS and match the compound observed here to a mass spectra/retention time. Unfortunately standards were not readily available when this work was conducted and this confirmatory step was not carried out. Therefore only one hydroxylated metabolite with both $[M+H]^+$ and $[M+Na]^+$ adducts was postulated as being present in this study.
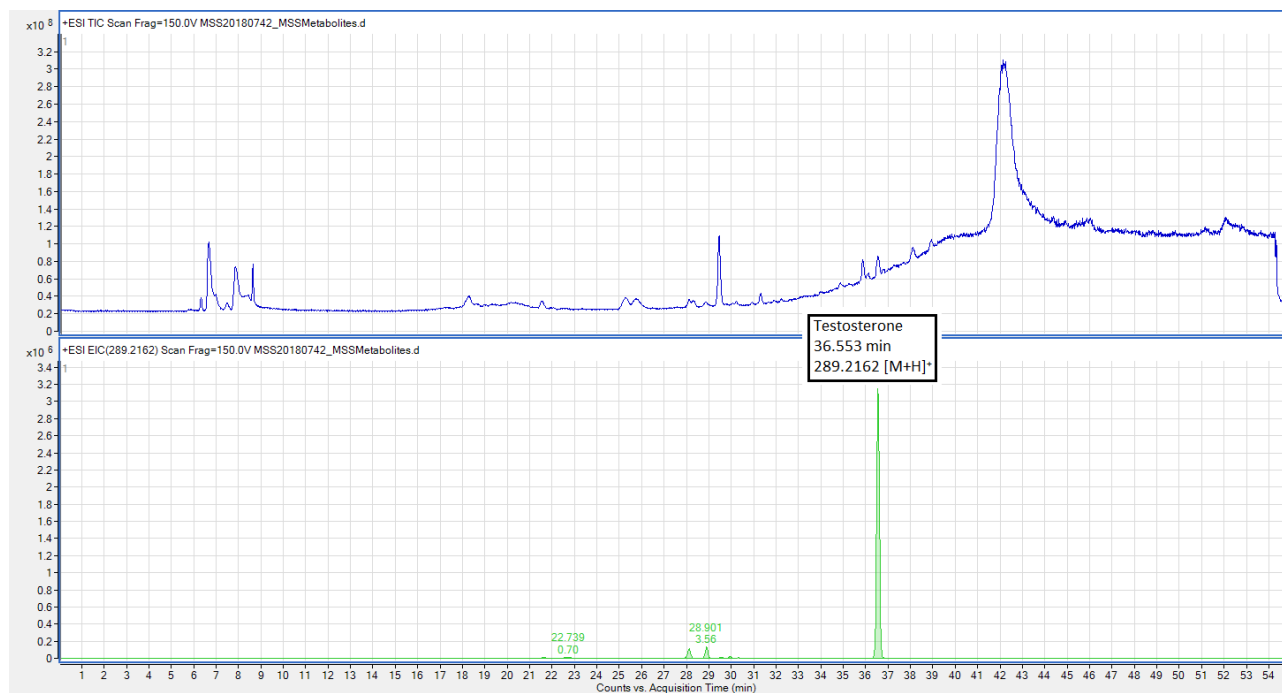
Figure 9.51: TIC and EIC of testosterone following incubation with the HepaRG cell line.
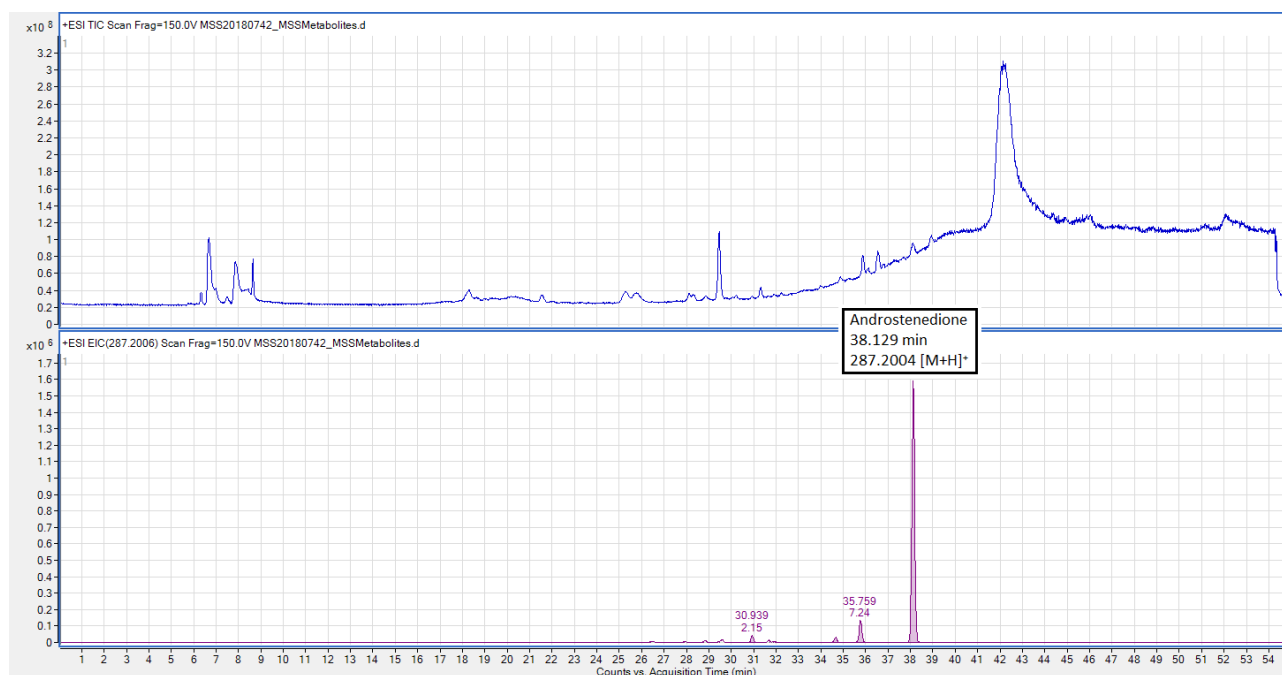
Figure 9.52: TIC and EIC of andronstenedione following incubation with the HepaRG cell line.
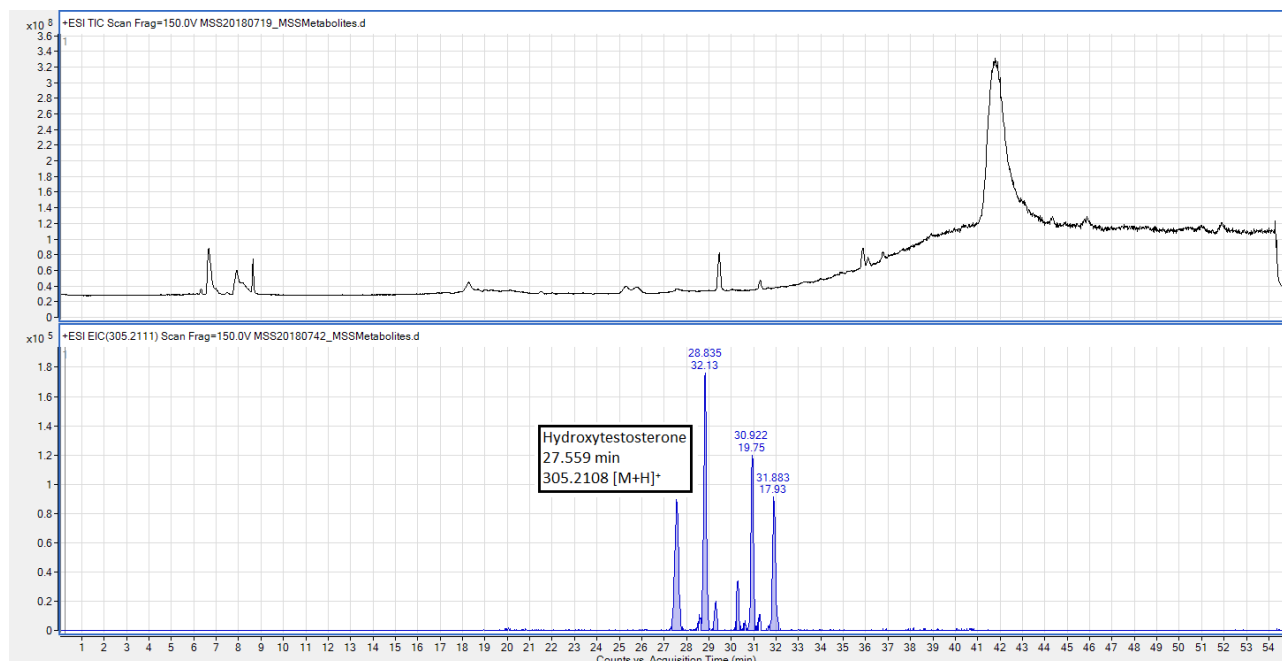
Figure 9.53: TIC and EIC of a hydroxytestosterone metabolite following incubation with the HepaRG cell line.
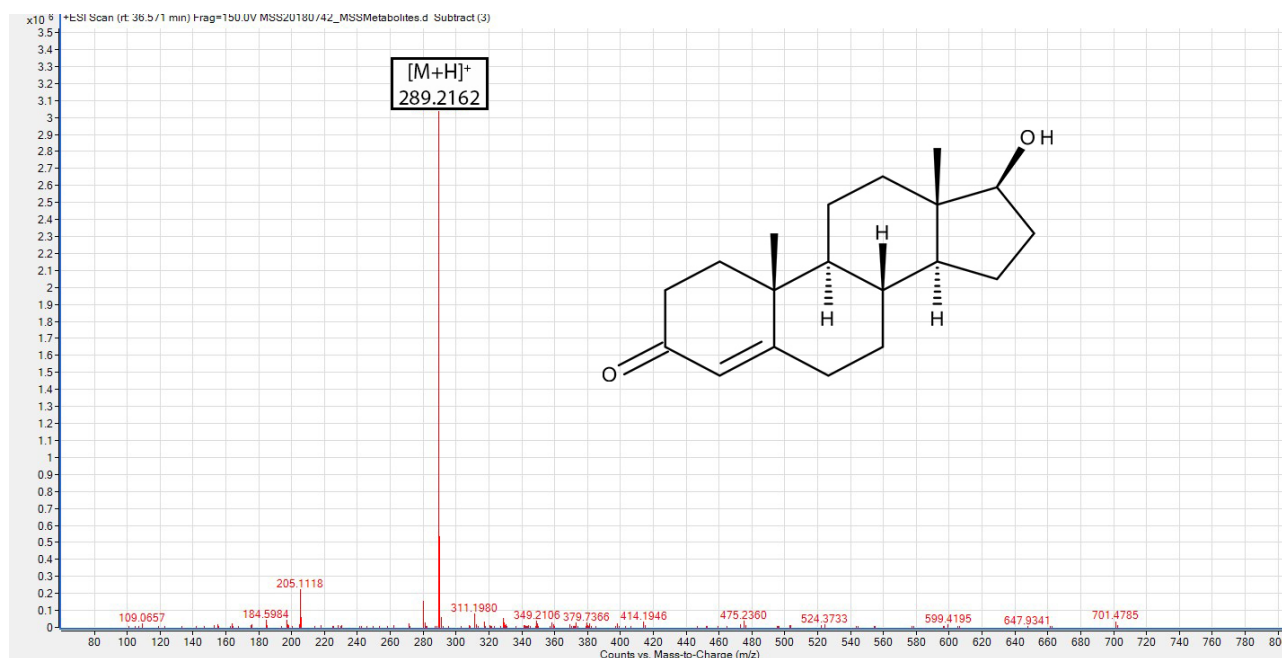
Figure 9.54: LC-MS analysis and structure of testosterone following incubation with the HepaRG cell line.
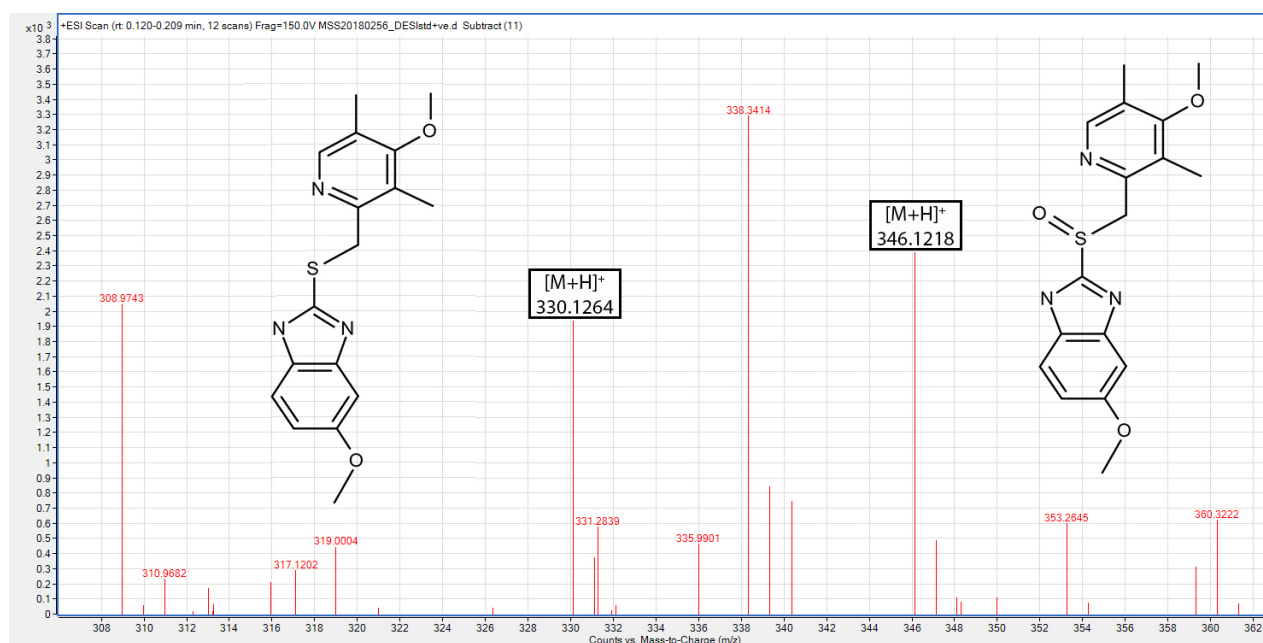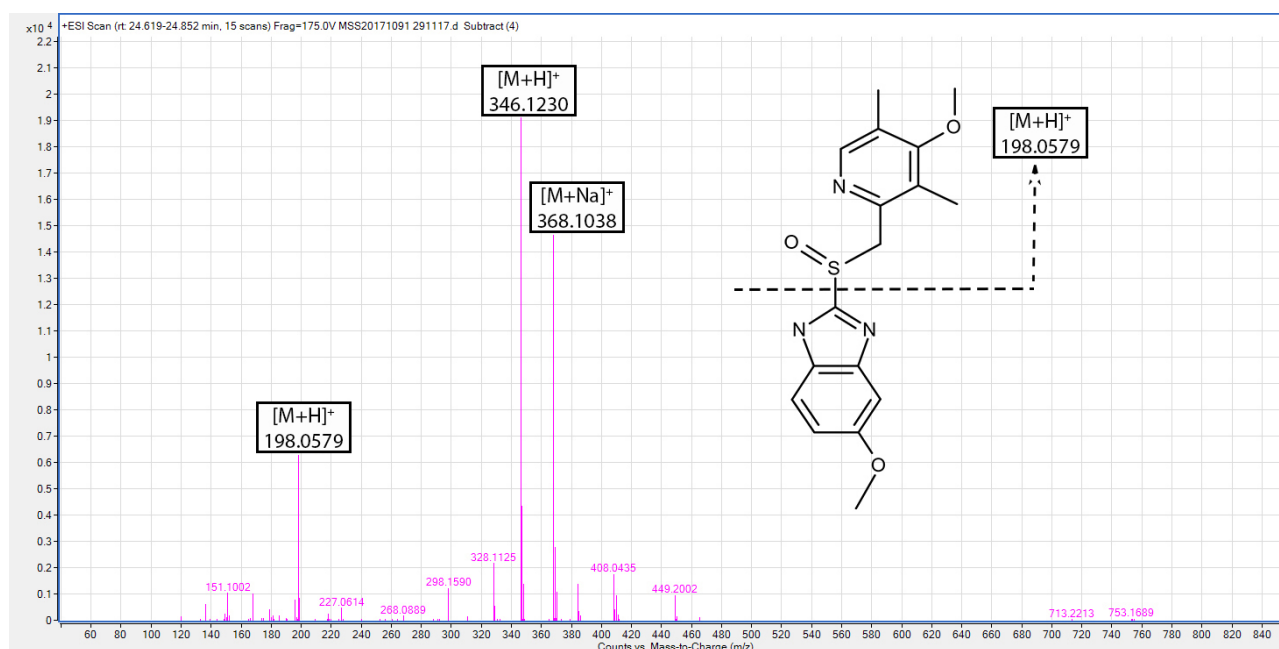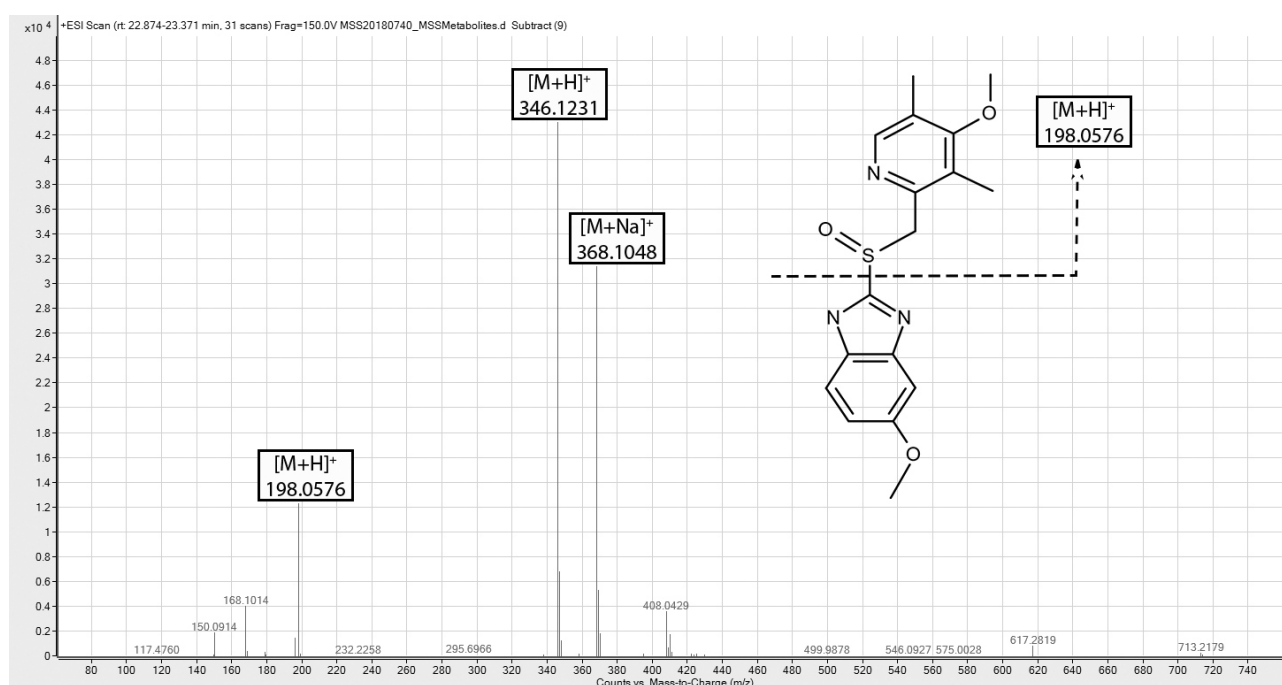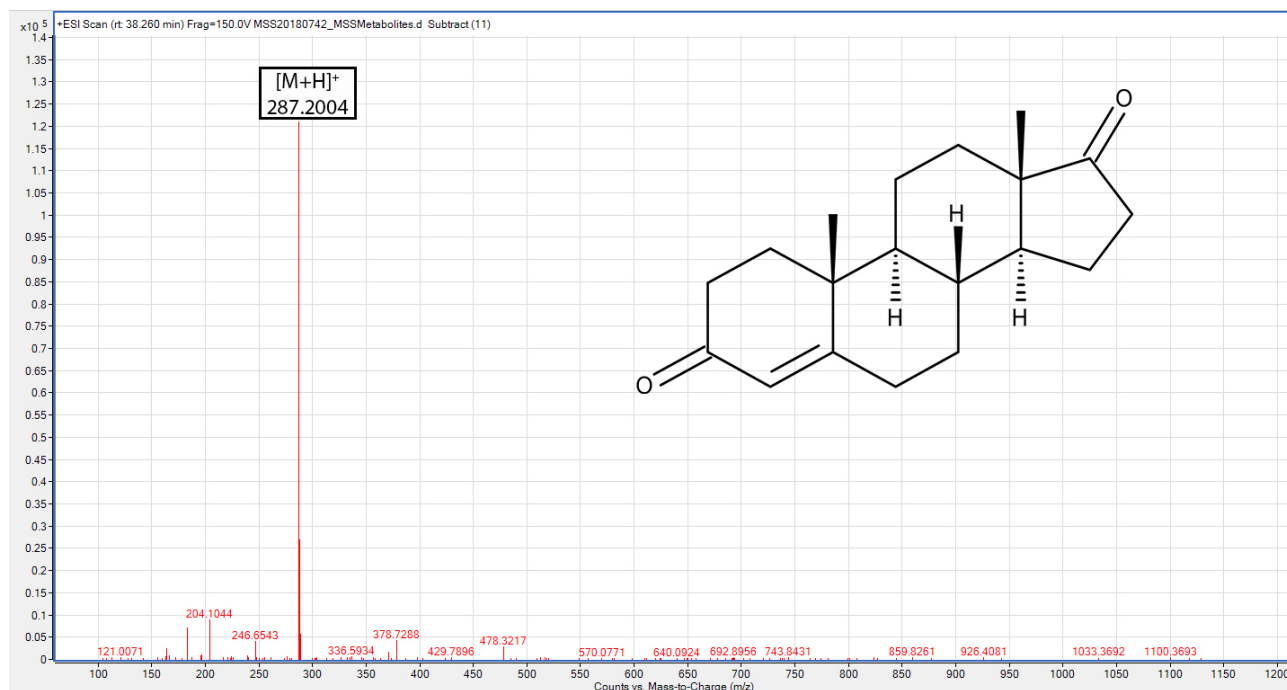
Figure 9.55: LC-MS analysis and structure of andronstenedione following incubation with the HepaRG cell line.
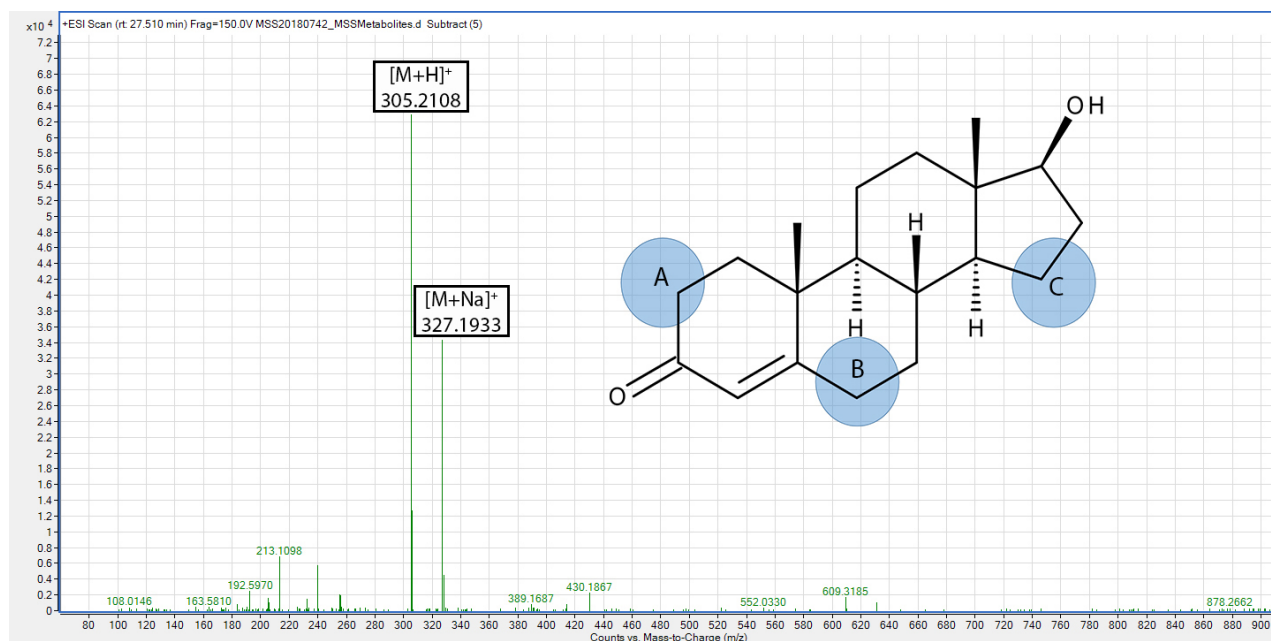

Figure 9.56: LC-MS analysis, structure and possible hydroxylation sites for hydroxytestosterone following incubation with the HepaRG cell line, A (6β), B (15β) and C (2β).

Table 9.1: LC-MS data for compounds observed following the incubation of test substrates in the C3A, DMSO-treated and HepaRG cell lines

Test substrate	Cell line	Compounds observed	Retention time (min)	m/z	Most likely adduct	Observed neutral mass	Theoretical mass	Mass difference (ppm)
Phenacetin	C3A	Phenacetin	29.256	180.1013	$[M+H]^+$	179.0941	179.0946	2.93
		Paracetamol		152.0705	$[M+H]^+$	151.0633	151.0633	0.13
	DMSO-C3A	Phenacetin	28.977	180.1013	$[M+H]^+$	179.0944	179.0946	1.51
		Paracetamol	28.977	152.0688	$[M+H]^+$	151.0633	151.0633	0.38
	HepaRG	Phenacetin	28.991	180.1018	$[M+H]^+$	179.0946	179.0946	0.26
		Paracetamol		152.0695	$[M+H]^+$	151.0623	151.0633	7.11
		Paracetamol	6.098	169.0971	$[M+NH_4]^+$	151.0633	151.0633	0.26
		Bupropion	27.263	240.1153	$[M+H]^+$	239.1099	239.1077	-9.07
	C3A	Erythro/threo bupropion	26.880	242.1315	$[M+H]^+$	241.1242	241.1233	-3.49
		Erythro/threo bupropion	27.380	242.1295	$[M+H]^+$	241.1222	241.1233	4.79
	DMSO-C3A	Bupropion	27.219	240.1161	$[M+H]^+$	239.1088	239.1077	-4.72
		Bupropion	26.644	184.0523	$[M\text{-}^tBu+H]^+$	183.0450	183.0451	0.28
		Bupropion		240.1152	$[M+H]^+$	239.1079	239.1077	-1.04
		Hydroxybupropion	21.012	256.1110	$[M+H]^+$	255.1037	255.1026	-4.21
		Hydroxybupropion	21.178	256.1102	$[M+H]^+$	255.1030	255.1026	-1.37
Bupropion		Hydroxybupropion	22.023	238.0993	$[M\text{-}H_2O+H]^+$	237.0921	237.0920	-0.32
		Hydroxybupropion		256.1101	$[M+H]^+$	255.1028	255.1026	-0.90
	HepaRG	Hydroxybupropion	22.188	238.0995	$[M\text{-}H_2O+H]^+$	237.0922	237.0920	-0.59
		Hydroxybupropion		256.1100	$[M+H]^+$	255.1028	255.1026	-0.57
		Ketone-reduced bupropion	26.230	242.1304	$[M+H]^+$	241.1229	241.1233	2.01
		Ketone-reduced bupropion		168.0575	$[M\text{-}^tBu\text{-}H_2O+H]^+$	167.0502	167.0502	-0.14
		Ketone-reduced bupropion	26.277	186.0696	$[M\text{-}^tBu+H]^+$	185.0618	185.0607	-5.96
				242.1305	$[M+H]^+$	241.1233	241.1233	0.38
		Ketone-reduced hydroxybupropion	29.593	258.1263	$[M+H]^+$	257.1190	257.1183	-3.03
	C3A	Omeprazole	23.884	346.1224	$[M+H]^+$	345.1151	345.1147	-1.22
		Omeprazole		368.1045	$[M+Na]^+$	345.1152	345.1147	-1.43
		Omeprazole sulfide	28.462	330.1266	$[M+H]^+$	329.1194	329.1198	1.17
Omeprazole	DMSO-C3A	Omeprazole	24.768	346.1230	$[M+H]^+$	345.1156	345.1147	-2.57
		Omeprazole		368.1038	$[M+Na]^+$	345.1151	345.1147	-1.09
		Omeprazole sulfide	28.797	330.1266	$[M+H]^+$	329.1198	329.1198	-0.12
		Omeprazole	23.139	346.1231	$[M+H]^+$	345.1159	345.1147	-3.50
	HepaRG	Omeprazole		368.1048	$[M+Na]^+$	345.1155	345.1147	2.22
		Hydroxyomeprazole	29.235	362.1154	$[M+H]^+$	361.1081	361.1096	4.19
		Omeprazole sulfide	28.059	330.1270	$[M+H]^+$	329.1199	329.1198	-0.23
	C3A	Diclofenac	38.818	296.0243	$[M+H]^+$	295.017	295.0167	-1.08
Diclofenac	DMSO-C3A	Diclofenac	38.601	296.0239	$[M+H]^+$	295.0165	295.0167	0.51
	HepaRG	Diclofenac	38.425	296.0240	$[M+H]^+$	295.0165	295.0167	0.67
	C3A	Dextromethorphan	29.997	272.1997	$[M+H]^+$	271.1925	271.1936	4.06
		Dextrorphan	29.464	258.1844	$[M+H]^+$	257.1773	257.178	2.72
Dextromethorphan	DMSO-C3A	Dextromethorphan	29.997	272.2013	$[M+H]^+$	271.1939	271.1936	-0.99
		Dextrorphan	29.431	258.1853	$[M+H]^+$	257.1783	257.1780	-1.31
	HepaRG	Dextromethorphan	29.682	272.2012	$[M+H]^+$	271.1939	271.1936	-1.12
		Dextrorphan	29.119	258.1853	$[M+H]^+$	257.1780	257.1780	-0.17
	C3A	Testosterone	36.787	289.2155	$[M+H]^+$	288.2084	288.2089	1.8
	DMSO-C3A	Testosterone	36.787	289.2161	$[M+H]^+$	288.2088	288.2089	0.34
Testosterone		Testosterone	36.553	289.2162	$[M+H]^+$	288.2090	288.2089	-0.17
	HepaRG	Hydroxytestosterone	22.520	305.2108	$[M+H]^+$	304.2036	304.2038	0.84
		Hydroxytestosterone		327.1933	$[M+Na]^+$	304.2042	304.2038	1.20
		Androstenedione	38.129	287.2004	$[M+H]^+$	264.2110	264.2089	-7.99

9.3   Discussion

Following the administration of 1 % DMSO and subsequent culturing, the hepatocellular carcinoma cell line Huh7 has been previously observed to cease division and enter a terminally differentiated state [460]. In this research no cessation of cellular division was observed. The DMSO-treated C3A cell line continued to divide and required passaging, although at a lower rate of every 4 - 5 days rather than 2 - 3 days. Both the C3A cells and DMSO-treated cells were seeded at a density of 3.3×10^5 cells mL^{-1}. Estimated cell counts were 6.0×10^5 cells mL^{-1} for the C3A cells and 4.5×10^5 cells mL^{-1} for the DMSO-treated C3A cells after 48 hours of incubation. Cells were counted using a haemocytometer as detailed in Section 2.10.3. This indicates that despite the rate of cellular division decreasing, cell growth and viability were not completely inhibited.

CYP1A2 was not found to be expressed in the C3A cells or the DMSO-treated C3A cells. However its expression was evident in the HepaRG cells as a result of the biotransformation of phenacetin to paracetamol. In addition the $[M+NH_4]^+$ adduct was also observed for paracetamol, providing further evidence for the presence of paracetamol in the samples and demonstrating CYP1A2 activity in the HepaRG cells.

Following culture of the C3A cells with bupropion, metabolites were observed indicating CYP2B6 metabolism. The metabolites were tentatively detected as an isomeric pair corresponding to threo- and erythro-hydrobupropion. The formation of these metabolites in known to be facilitated by 11β-HSD1 and a carbonyl reductase [442,443]. Further metabolism was expected by CYP2C19, however this was not observed in this work. Threo- and erythro- hydrobupropion were not detected following incubation with the DMSO-treated C3A cell line, indicating a reduction in metabolic activity. In contrast to the C3A cells, the HepaRG cell line was metabolically-active as indicated by the presence of the seven metabolites observed. Two pairs of products, tentatively detected as diastereoisomers, of hydroxylated bupropion metabolites were observed. S,S-hydroxybupropion and R,R-hydroxybupropion metabolites are believed to be produced by CYP2B6 [445-447]. CYP2C19 is thought to contribute to the majority of the formation of 4'-hydroxybupropion [448]. This provides evidence for the presence of CYP2C19 as

well as CYP2B6 in these HepaRG cells. Metabolites 5 and 6 were detected as ketone-reduced bupropion derivatives corresponding to the threo- and erythro- hydrobupropion metabolites observed in the C3A cell line and formed by 11-HSD-1 [442,448,449]. Further hydroxylation of threo-/erythro- hydrobupropion is known to be mediated by CYP2C19 [448]. This did not occur in the C3A cell line but in the HepaRG cell line a single erythro-/threo- hydrobupropion metabolite was observed although chromatographic separation of an isomeric pair may not have occurred. Therefore, based on the CYP2B6 probe, bupropion, CYP2C19 is also likely to be present in the HepaRG cell line.

After CYP3A4, CYP2C19 is perhaps the second most important enzyme for benzodiazepine metabolism [234-242]. Although S-mephenytoin is the recommended probe for CYP2C19, difficulties were encountered in sourcing this substrate [279]. Therefore it was substituted for omeprazole which is a commonly-used CYP2C19 probe [461,462]. Omeprazole is known to undergo a sulfoxidation pathway via CYP3A4, thereby making it a dual probe for these enzymes [463].

The CYP2C9 probe, diclofenac, was not observed to undergo metabolism in the C3A cells, the DMSO-treated C3A cells or the HepaRG cells. The metabolism of diclofenac has previously been reported in HepaRG cells although with a greater substrate concentration of 20 μM compared to the concentration of 5 μM in this work [277]. The concentration of 5 μM diclofenac was chosen as it is close to the K_m value for diclofenac and is commonly used [453,454]. The K_m value is often used as a guideline for the concentration of a substrate for metabolic studies [453,454]. However this concentration may have been too low to generate a detectable level of and any future studies should aim to test a higher concentration. CYP2C9 is known to be involved in the demethylation of benzodiazepines such as flunitrazepam and diazepam although it plays a minor role when compared to other enzymes such as CYP3A4, CYP2C19 and CYP2B6 [240,464].

CYP2D6 was found to be present in the C3A cell line and the DMSO-treated C3A cell line as a result of the detection of the dextromethorphan metabolite, dextorphan. A potential decrease in the metabolic activity of CYP2D6 was observed, as assessed by the ratio of dextromethorphan

to its metabolite dextorphan which decreased following incubation with the DMSO-treated cell line. A similar decrease was also noted following incubation with the DMSO-treated cell line for the conversion of bupropion to erythro-/hydro-bupropion by the 11β-HSD1 and/or a carbonyl reductase.

In previously published work, culturing the HepG2 cell line (the parent cell line of the C3A cell line) with 1 % DMSO did not increase the levels of CYP3A4 [465]. No metabolites for the substrate for CYP3A4, testosterone, were detected in either the C3A or the DMSO-treated C3A cells in this study. However hydroxylation to a hydroxytestosterone metabolite was observed in the HepaRG cell line as was the reductive metabolic formation of androstenedione was also observed. The majority of benzodiazepine metabolism is thought to be mediated by CYP3A4 and therefore the HepaRG cell line represents the best choice for studying the *in vitro* metabolism of NPS-benzodiazepines [234-242]. The exact position of hydroxylation on the testosterone metabolite could not be assigned, however it is likely the 6-hydroxytesterone metabolite given that this is the most common [459]. In addition, the formation of omeprazole sulfoxide from omeprazole (the CYP2C19 probe) provides supporting evidence for the presence of CYP3A4 [454].

Although the HepaRG cell line did not appear to express CYP2C9, this cell line likely represents the best choice in order to study the *in vitro* metabolic pathways of NPS-benzodiazepines.

Chapter 10

The *in vitro* Characterisation of the Metabolism of NPS-benzodiazepines

10.1 Introduction

Prior knowledge of the metabolites formed from new psychoactive substances is valuable as it can aid in the detection of these compounds and interpretation of toxicological results in biological samples submitted for testing [255]. Although parallels between metabolic pathways of structurally similar benzodiazepines can be drawn in order to predict metabolites of NPS- *in silico*, unexpected metabolites can still be observed. One such example is the debromination of the NPS-benzodiazepine flubromazepam as reported in the literature [251]. Characterisation of metabolites formed *in vitro* is often conducted with human liver microsomes and cryopreserved human hepatocytes. NPS-benzodiazepines have been routinely assessed using cryopreserved human hepatocytes, human liver microsomes and self-ingestion experiments [247,257,315]. However the evaluation of NPS-benzodiazepine metabolism in human hepatocellular carcinoma cell lines has not yet been reported. The work presented in this Section represents the first attempt at characterising the metabolism of NPS-benzodiazepines with a human hepatocellular carcinoma cell line. The HepaRG cell line was found to be extremely metabolically active in the work in Section 9 and therefore the investigation NPS-benzodiazepine metabolism was con-

ducted using this cell line. Differences between the metabolites produced by the HepaRG cell line and those produced in studies using other methods will be valuable in order to judge which, if any, of the *in vitro* methods is the most suitable for assessing the formation of metabolites from NPS-benzodiazepines.

The NPS-benzodiazepines chosen for the metabolic study are listed below. These NPS-benzodiazepines were chosen as they represent a range of generic benzodiazepine structures including thieno-triazolodiazepines (deschloroetizolam and etizolam) and triazolobenzodiazepines (flubromazolam, nitrazolam and pyrazolam), with the rest being 1,4-benzodiazepines. Additionally they exhibit a wide range of different structural features such as hydroxylation at position 3 (3-hydroxyphenazepam), methylation at position 3 (meclonazepam), a pyridine ring rather than a phenyl ring (pyrazolam), nitro substitutions (nitrazolam and meclonazepam) and a substitution at position 4' on the phenyl ring (4'-chlorodiazepam).

1. 3-Hydroxyphenazepam

2. 4'-Chlorodiazepam

3. Desalkylflurazepam

4. Deschloroetizolam

5. Diclazepam

6. Etizolam

7. Flubromazepam

8. Flubromazolam

9. Meclonazepam

10. Nitrazolam

11. Phenazepam

12. Pyrazolam

10.2 Results

10.2.1 3-Hydroxyphenazepam

3-Hydroxyphenazepam is an active metabolite of the NPS-benzodiazepine phenazepam, contributing to its pharmacological effect in humans, however it is also an NPS-benzodiazepine itself. 3-Hydroxyphenazepam was detected at 33.594 minutes (m/z 364.9684 [M+H]$^+$ with a mass difference of 0.82 ppm, Figure 10.1). An adduct with a m/z of 386.9499 and a mass difference of 1.27 ppm, corresponding to the [M+Na]$^+$ adduct was also detected. No metabolites were observed in this work. In the literature an *in vitro* study using human liver microsomes have also reported the absence of phase I metabolites of 3-hydroxyphenazepam [81]. Other 3-hydroxylated benzodiazepines such as oxazepam, lorazepam and temazepam are metabolised via phase II metabolic pathways such as glucuronidation [81,363].
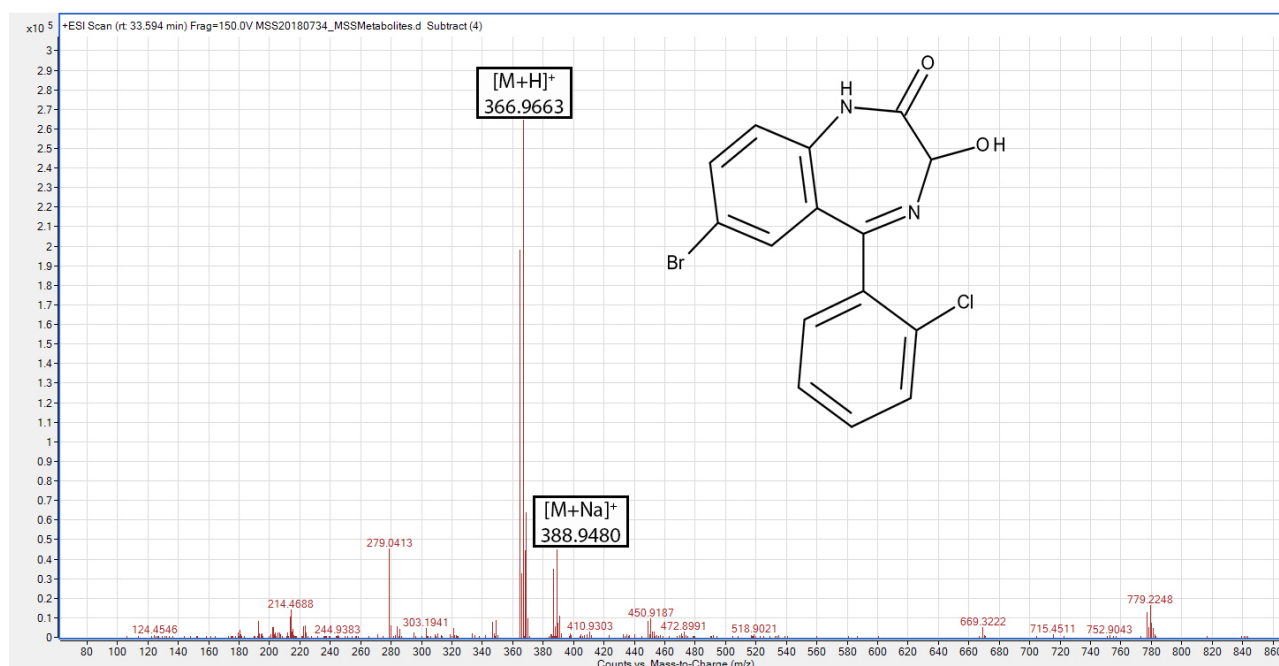
Figure 10.1: LC-MS analysis and structure of 3-hydroxyphenazepam following incubation with the HepaRG cell line.

10.2.2   4′-Chlorodiazepam

4'-Chlorodiazepam was detected at 40.884 minutes (m/z 319.0402 [M+H]$^+$ with a mass difference of -1.24 ppm, Figure 10.4). A demethylated metabolite was detected at 38.168 minutes (m/z 305.0241 [M+H]$^+$ with a mass difference of 0.10 ppm) and a hydroxylated metabolite was detected at 38.135 minutes (m/z 335.0362 [M+H]$^+$ with a mass difference of -4.03 ppm) (Figures 10.5 and 10.6 respectively). Demethylation of 4'-chlorodiazepam is likely to occur on the N_1 nitrogen atom and hydroxylation on the C_3 carbon atom in a similar manner to diazepam [466]. 4'-Chlorodiazepam is structurally similar to diazepam, differing only by the addition of a chlorine atom on the 4' position. Diazepam produces three metabolites, a 3-hydroxylated metabolite, a 1-demethylated metabolite and a metabolite that is both 3-hydroxylated and 1-demethylated, oxazepam [466]. However a metabolite that was both 3-hydroxylated and 1-demethylated was not observed in this work for 4'-chlorodiazepam.

The EICs for 4'-chlorodiazepam and its metabolites can be seen in Figure 10.2 with an enlarged version in Figure 10.3 to view the separation of the demethylated and hydroxylated metabolites.
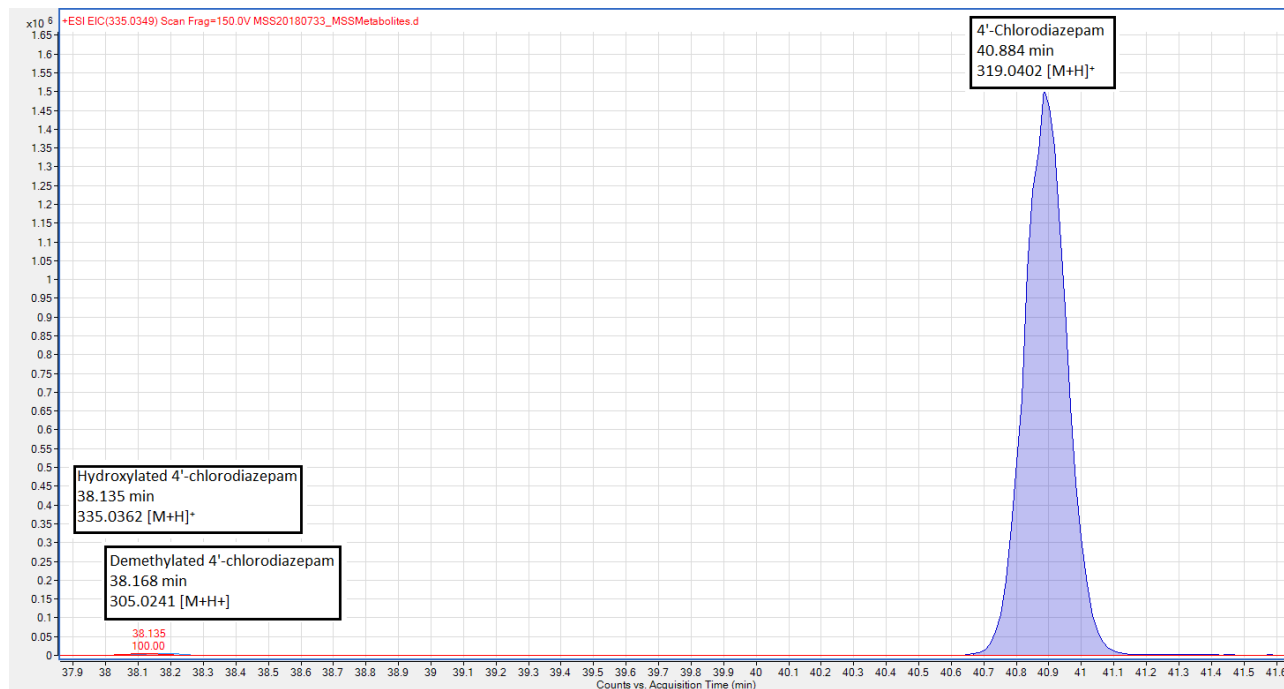
Figure 10.2: Overlaid EICs of 4′-chlorodiazepam and its demethylated and hydroxylated metabolites following incubation with the HepaRG cell line.
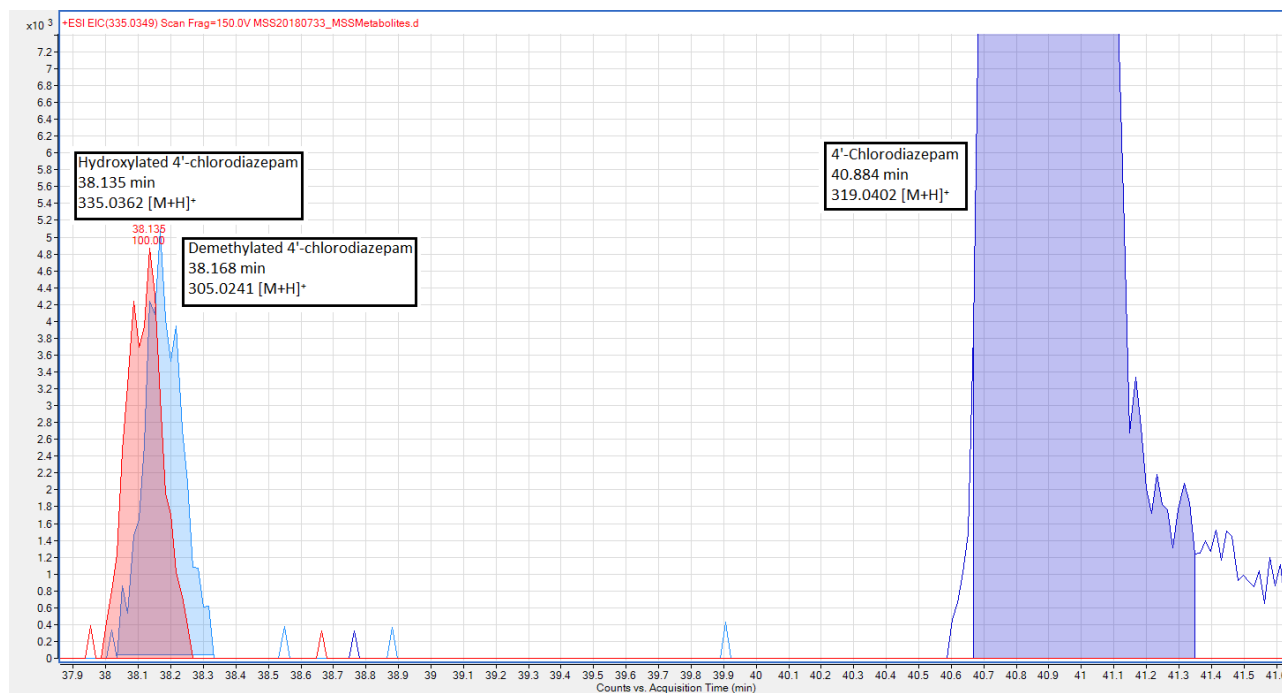
Figure 10.3: Enlarged, overlaid EICs of 4′-chlorodiazepam and its demethylated and hydroxylated metabolites following incubation with the HepaRG cell line.
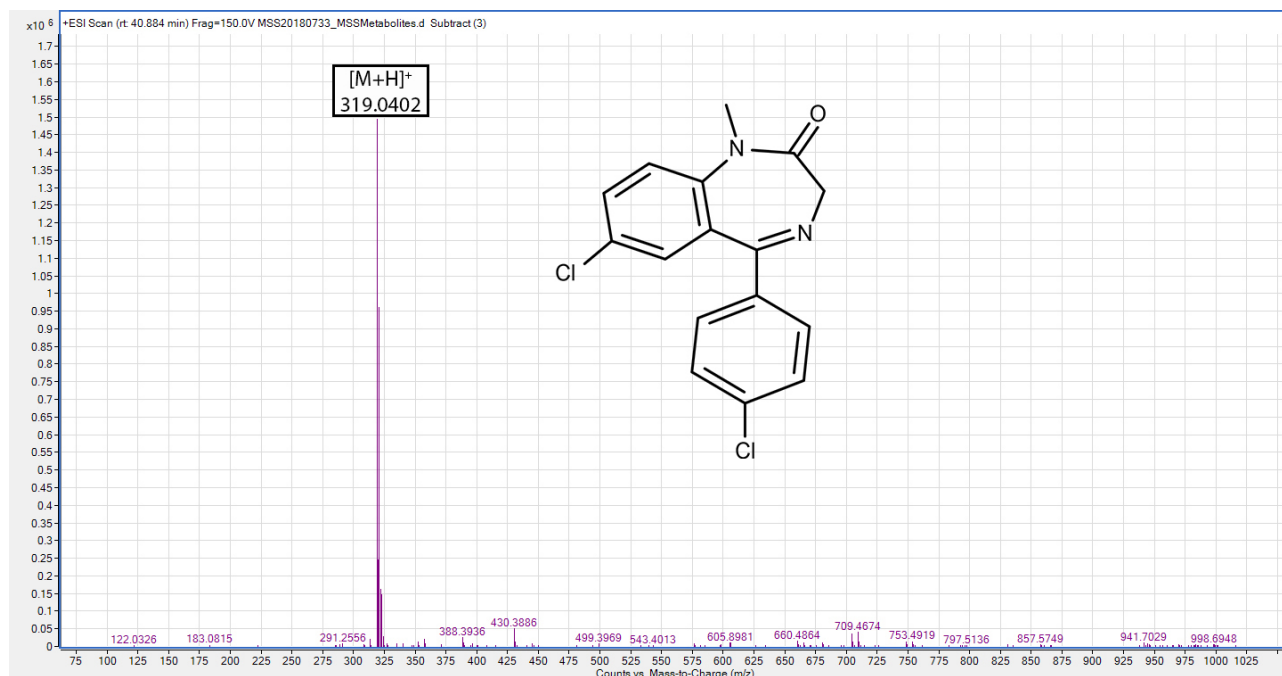
Figure 10.4: LC-MS analysis and structure of 4′-chlorodiazepam following incubation with the HepaRG cell line.
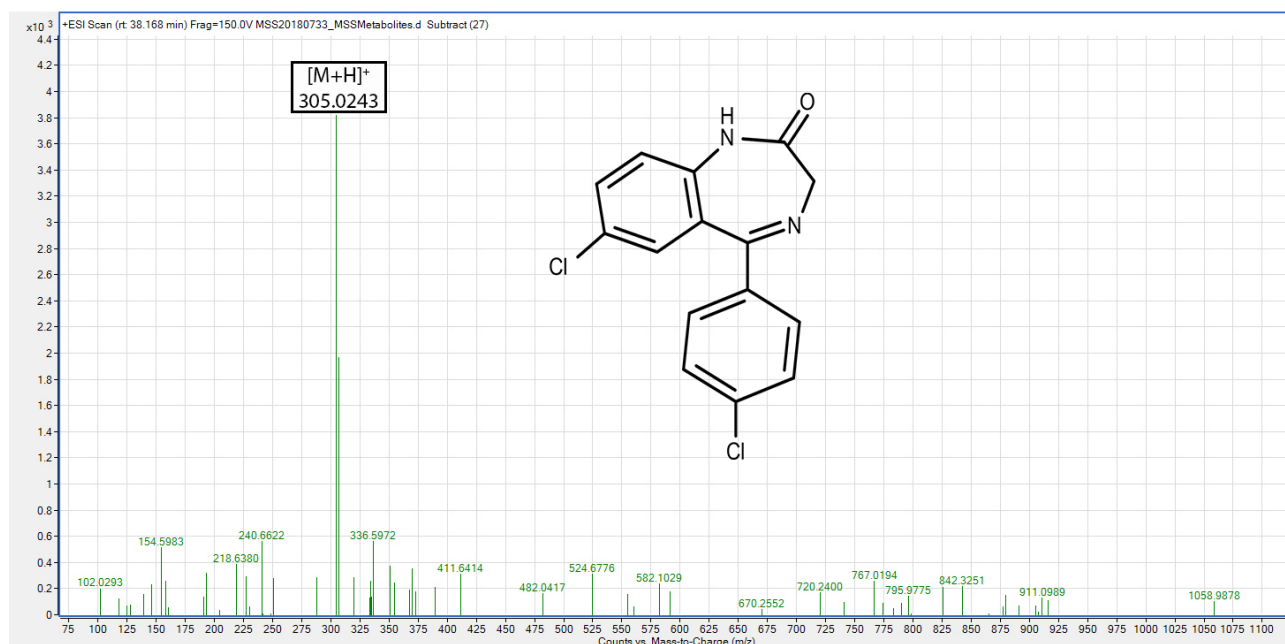
Figure 10.5:   LC-MS analysis and structure of an N-demethylated metabolite of 4′-chlorodiazepam following incubation with the HepaRG cell line.
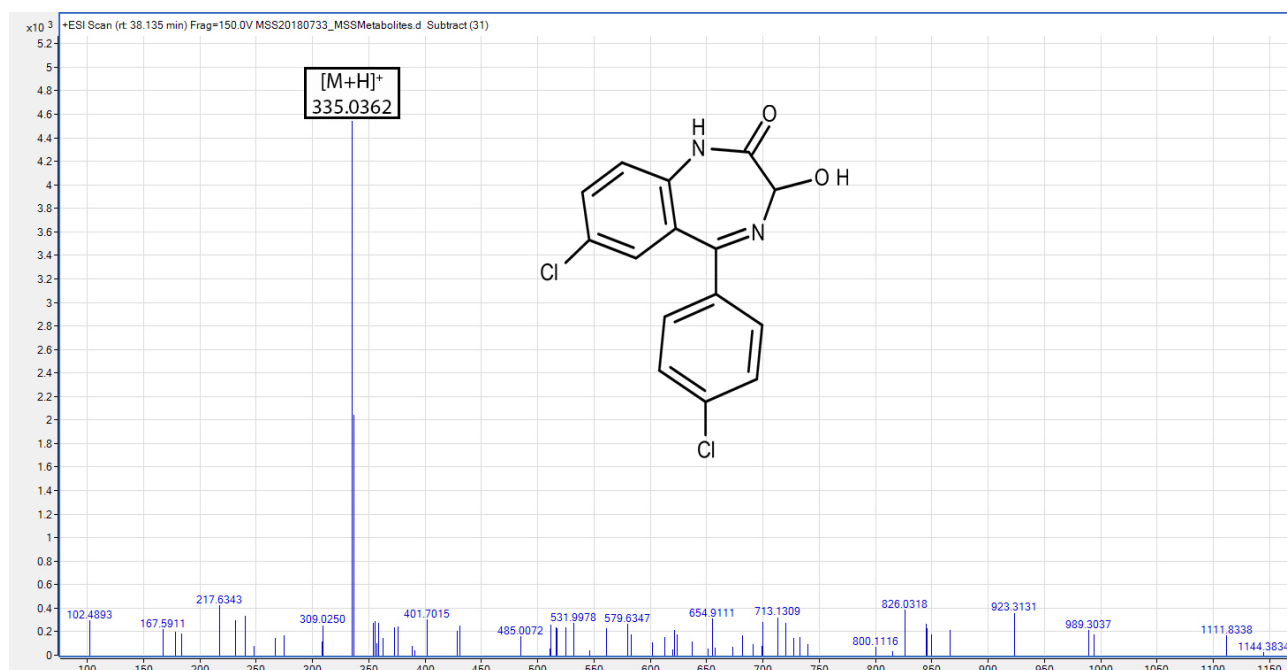
Figure 10.6: LC-MS analysis and structure of a hydroxylated metabolite of 4'-chlorodiazepam following incubation with the HepaRG cell line.

10.2.3 Desalkylflurazepam

Desalkylflurazepam was detected at 34.433 minutes (m/z 289.0538 [M+H]$^+$ with a mass difference of 0.02 ppm, Figure 10.7). No further metabolites were detected. Desalkylflurazepam is itself a pharmacologically active metabolite of several benzodiazepines including flurazepam and flutoprazepam [467,468]. A hydroxylated (position 3) metabolite of desalkylflurazepam has been reported to occur in trace amounts following ingestion of flurazepam or flutoprazepam [467,468]. This hydroxylated metabolite was not observed although the possibility of occurrence cannot be ruled out as it is the likely step prior to glucuronide conjugation via phase II metabolism [467,468]. This may be a limitation of the use of the hepatocellular carcinoma cell line used in this work and in similarity to the work presented in Section 9, the concentration used (10 μM) may have been too low to produce a significant concentration of a potential metabolite.
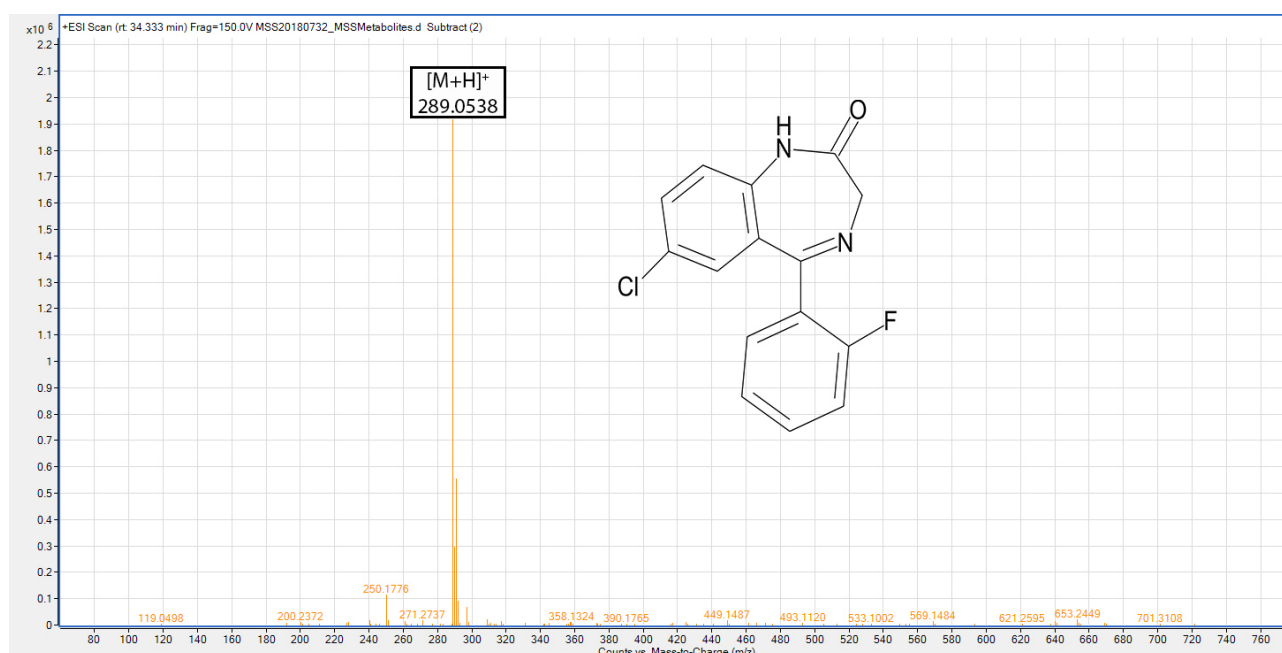
Figure 10.7: LC-MS analysis and structure of desalkylflurazepam following incubation with the HepaRG cell line.

10.2.4   Deschloroetizolam

Deschloroetizolam eluted at 34.269 minutes (m/z 309.1176 $[M+H]^+$ with a mass difference of -2.48 ppm, Figure 10.9). An adduct with a m/z of 331.0990 and mass difference of -0.70 ppm, corresponding to the $[M+Na]^+$ adduct, was also detected. A hydroxylated metabolite was observed at 22.276 minutes (m/z 325.1139 $[M+H]^+$ with a mass difference of -6.51 ppm, Figure 10.10). A sodiated $[M+Na]^+$ adduct with a (m/z) of 347.0926 and a mass difference of -1.07 ppm was also detected. Deschloroetizolam has previously been reported as being metabolised to three hydroxylated metabolites and one dihydroxylated metabolite [257]. Only one hydroxylated metabolite was observed here with the exact position of hydroxylation unable to be detected without NMR. It has been suggested that hydroxylation could take place on either the 9-methyl, 2-ethyl or 6 positions [257]. The deschloroetizolam:hydroxydeschloroetizolam ratio was 1:35 showing that metabolism was significant. Multiple hydroxylated metabolites could have potentially been formed and produced no separation on the LC-MS. As they would all have the same masses, being singularly hydroxylated, they would also have the same m/z ratios.

The overlaid EIC of deschloroetizolam and its hydroxylated metabolite observed here can be seen in Figure 10.8.
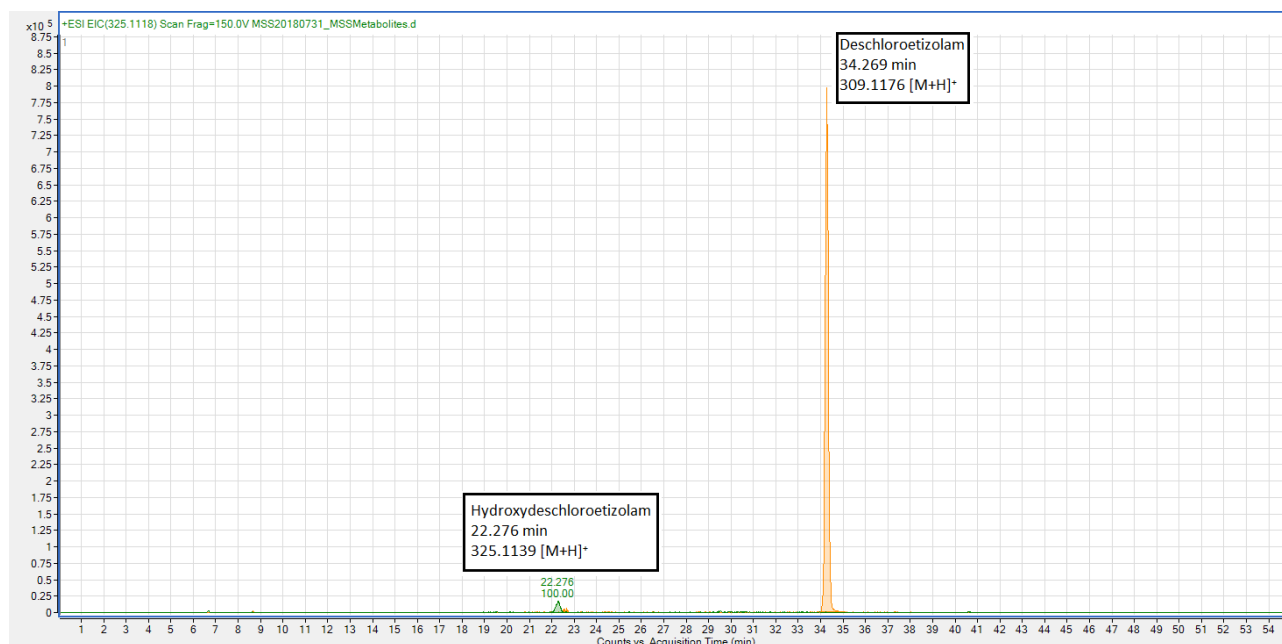
Figure 10.8: Overlaid EICs of deschloroetizolam and its hydroxylated metabolite following incubation with the HepaRG cell line.
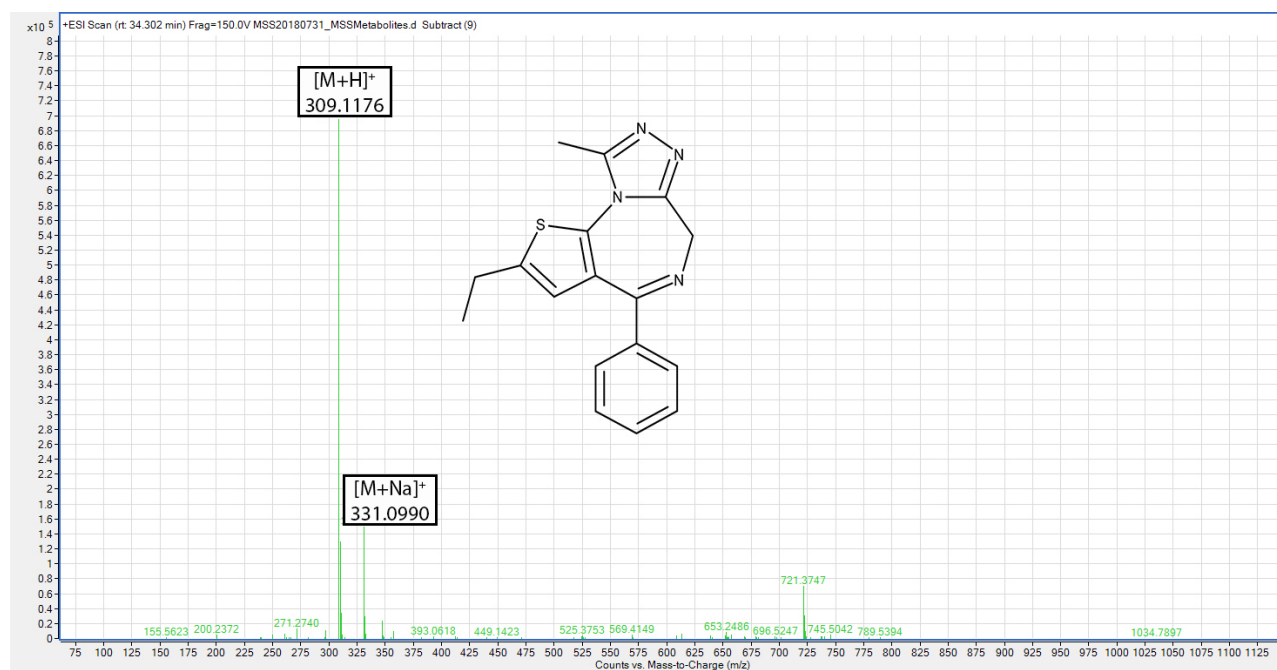
Figure 10.9: LC-MS analysis and structure of deschloroetizolam following incubation with the HepaRG cell line.
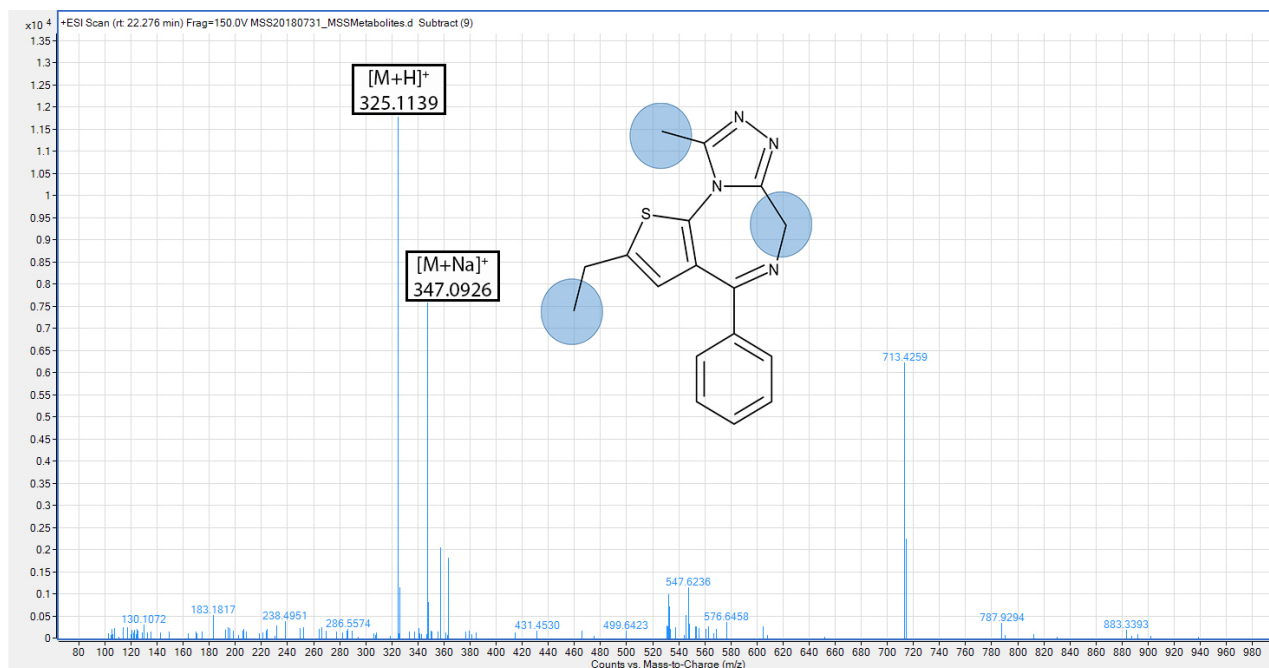
Figure 10.10: LC-MS analysis and structure of a hydroxylated metabolite of deschloroetizolam following incubation with the HepaRG cell line with the potential sites of hydroxylation circled.

10.2.5   Diclazepam

Diclazepam was detected at 37.901 minutes (m/z of 319.0399 [M+H]$^+$ with a mass difference of -0.94 ppm, Figure 10.12). A hydroxylated metabolite was detected at 35.631 minutes (m/z 335.0349 [M+H]$^+$ with a mass difference of -0.41 ppm, Figure 10.13). The probable site of hydroxylation was position 3 to form the benzodiazepine lormetazepam, as reported previously in the literature [247]. A demethylated metabolite (with demethylation occurring on position 1), delorazepam, was also detected at 35.267 minutes (m/z 305.0243 [M+H]$^+$ with a mass difference of -0.41 ppm, Figure 10.14). Both of these metabolites have been previously reported in a study involving self-ingestion [247]. Diclazepam is a structural isomer of another NPS-benzodiazepine in this work, 4'-chlorodiazepam, differing only by the placement of the chlorine atom on the phenyl ring. It follows a similar pattern of metabolism with one hydroxylated metabolite and one demethylated metabolite.

The overlaid EICs of diclazepam, delorazepam and lormetazepam can be seen in Figure 10.11.
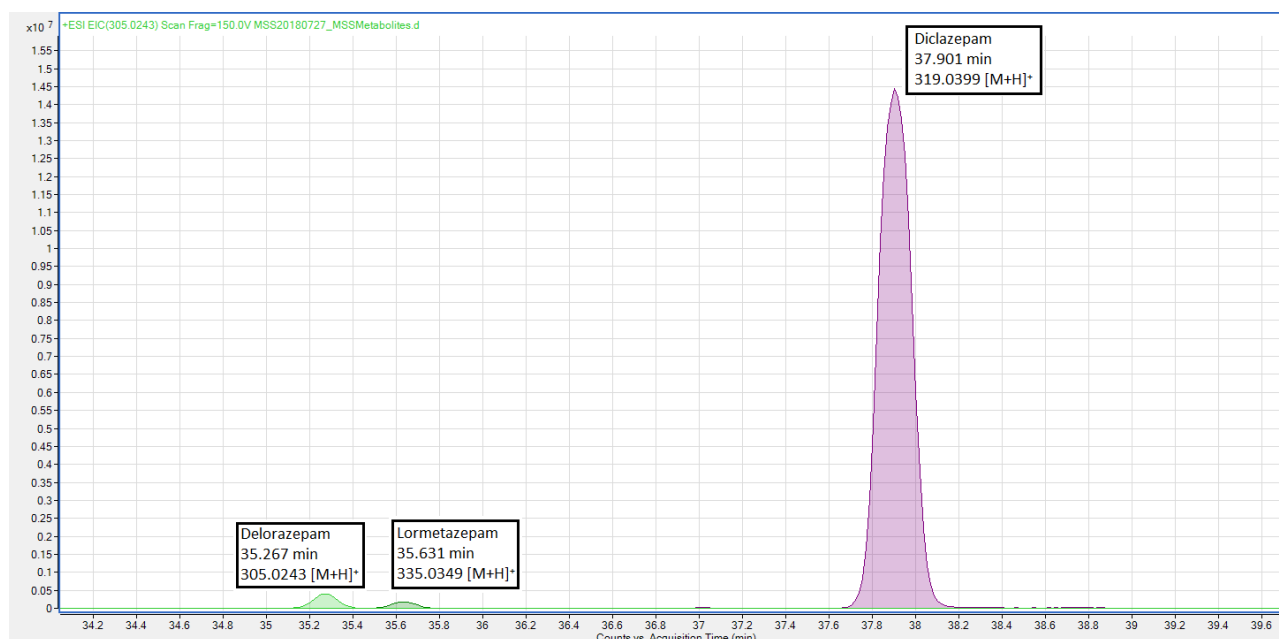
Figure 10.11: Overlaid EICs of diclazepam, delorazepam and lormetazepam following incubation with the HepaRG cell line.
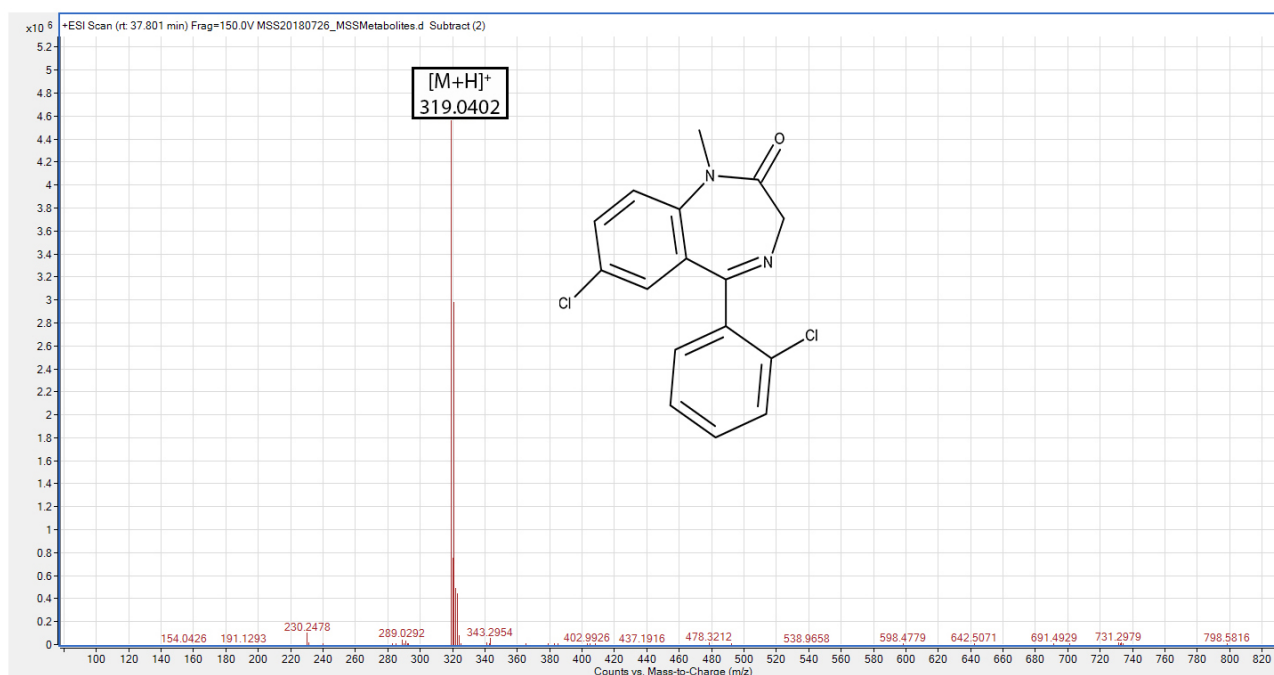
Figure 10.12: LC-MS analysis and structure of diclazepam following incubation with the Hep-aRG cell line.
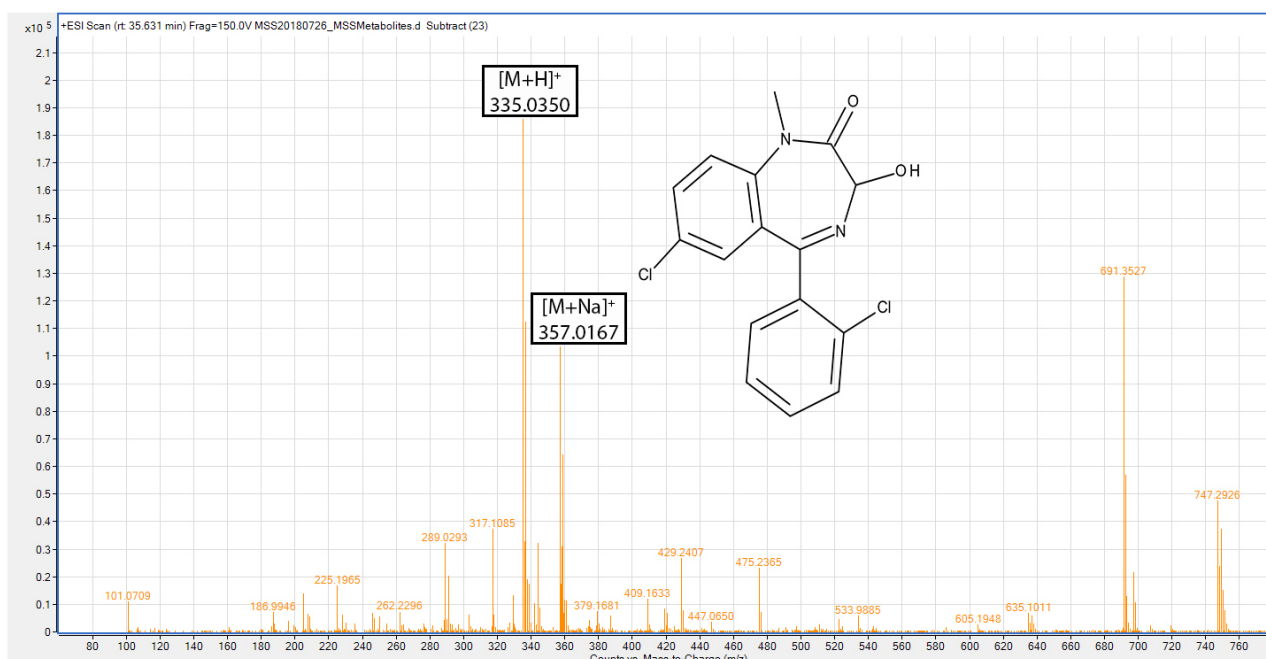
Figure 10.13: LC-MS analysis and structure of lormetazepam following incubation with the HepaRG cell line.
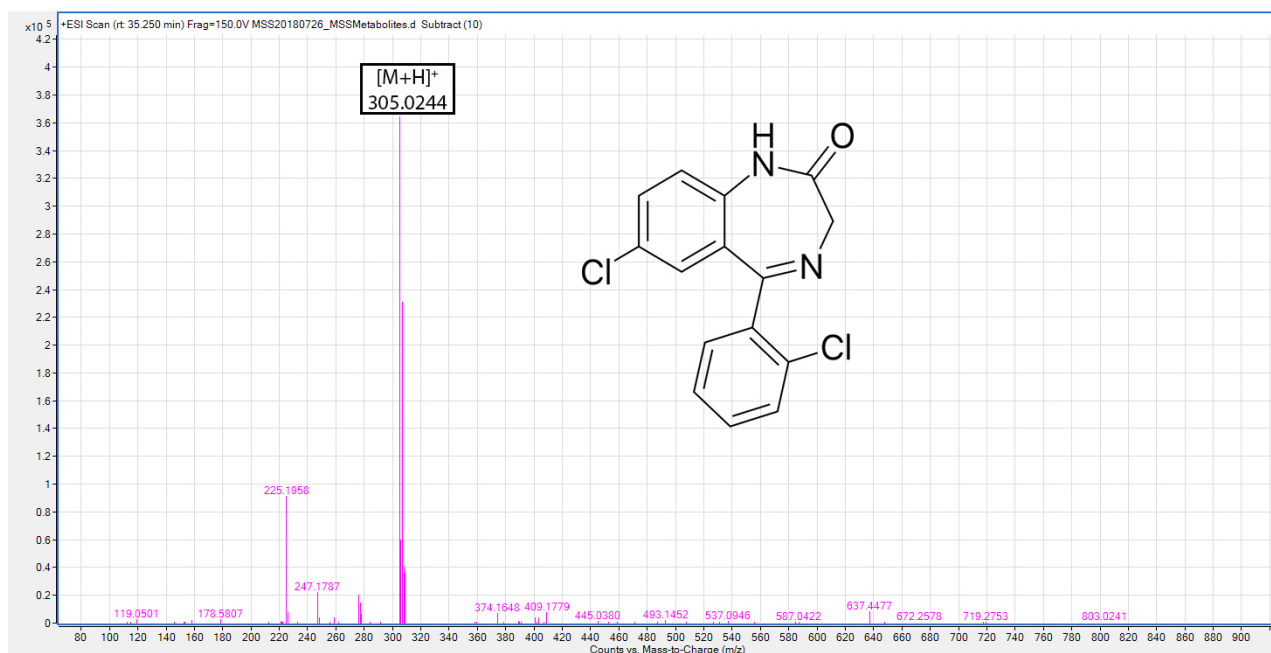
Figure 10.14: LC-MS analysis and structure of delorazepam following incubation with the HepaRG cell line.

10.2.6   Etizolam

Etizolam was detected at 36.649 minutes (m/z 343.0784 [M+H]$^+$ with a mass difference of 1.20 ppm, Figure 10.15). An adduct with a m/z of 365.0592 and a mass difference of 0.49 ppm, corresponding to the [M+Na]$^+$ ion was also observed.

Three monohydroxylated products were also detected. The first of these was at 28.466 minutes with adducts corresponding to the [M+H]$^+$ (m/z 359.0730 with a mass difference of -0.48 ppm), [M+Na]$^+$ (m/z 381.0547 with a mass difference of 0.21 ppm) and the [M+K]$^+$ (m/z 397.0283 with a mass difference of 0.91 ppm) species (10.17).

The second monohydroxylated product was observed at 32.358 minutes with adducts corresponding to the [M+H]$^+$ (m/z 359.0729 with a mass difference of 2.66 ppm) and the [M+Na]$^+$ (m/z 381.0547 with a mass difference of 0.21 ppm) species (10.18).

The final monohydroxylated product was observed at 32.789 minutes with adducts corresponding to the [M+H]$^+$ (m/z 359.0725 with a mass difference of 0.80 ppm) and the [M+Na]$^+$ (m/z 381.0577 with a mass difference of -8.37 ppm) species (10.19).

The overlaid EICs of the three hydroxylated metabolites of etizolam can be seen in Figure 10.16.

Etizolam has previously been reported as producing two monohydroxylated metabolites with hydroxylation occurring on the 2-ethyl and 9-methyl groups [317]. Another potential site for hydroxylation on etizolam exists on position 6 (Figure 1.2D) and is thought to occur for structurally-similar thienodiazepines such as metizolam and deschloroetizolam [81,257]. Hydroxylation has also been suggested to occur on a triazole nitrogen atom for metizolam [469].

The aforementioned metabolites for structurally-similar thienodiazepines to etizolam suggest that hydroxylation at position 6 is possible and that this may be a cause behind the three monohydroxylated metabolites observed.
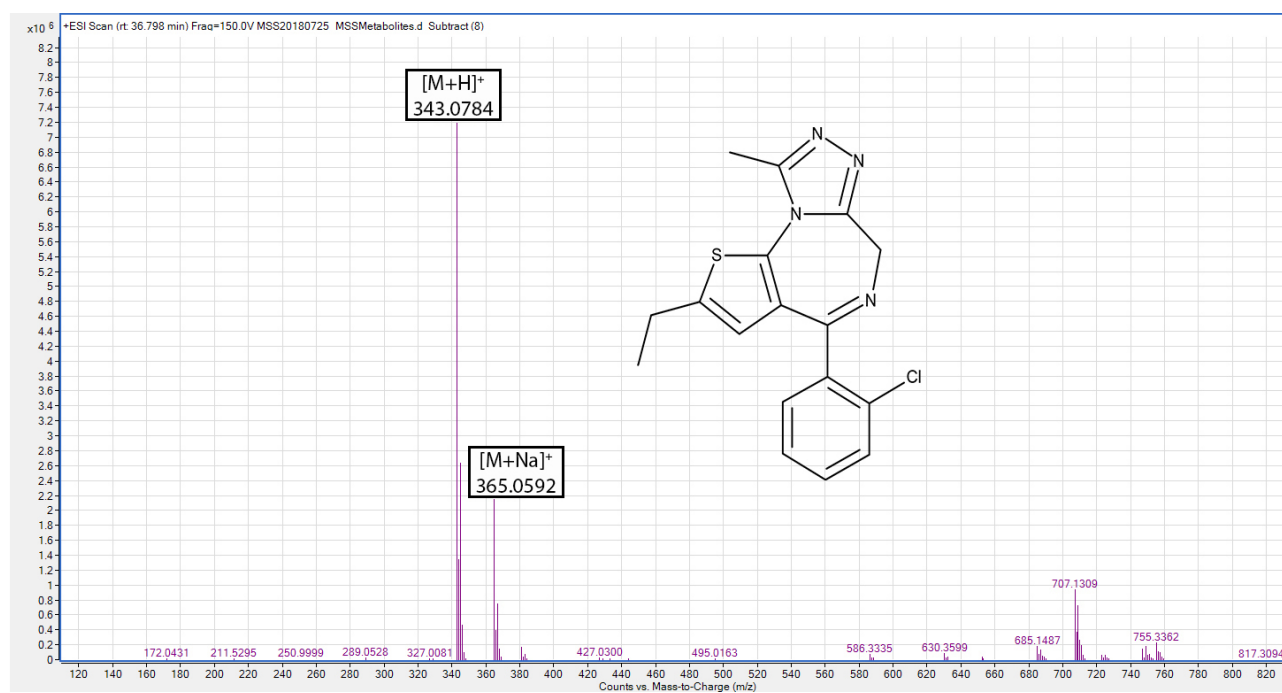
Figure 10.15: LC-MS analysis and structure of etizolam following incubation with the HepaRG cell line.
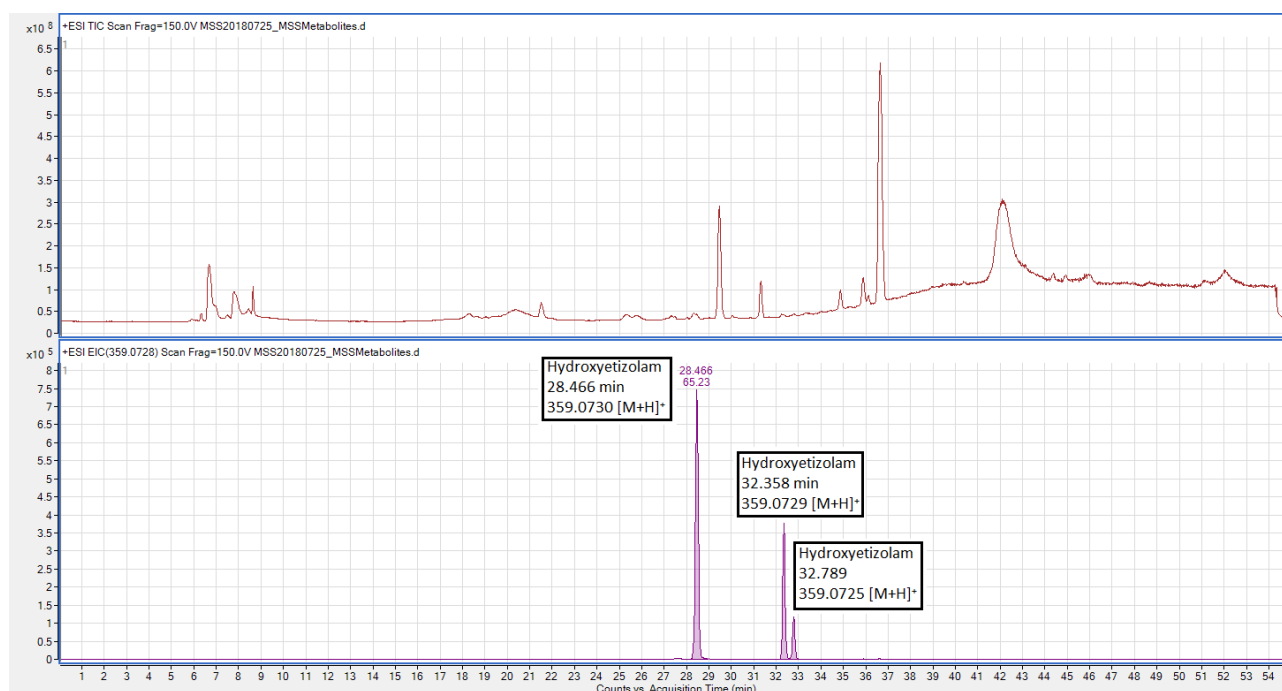
Figure 10.16: Overlaid EICs of the three hydroxylated metabolites of etizolam following incubation with the HepaRG cell line.
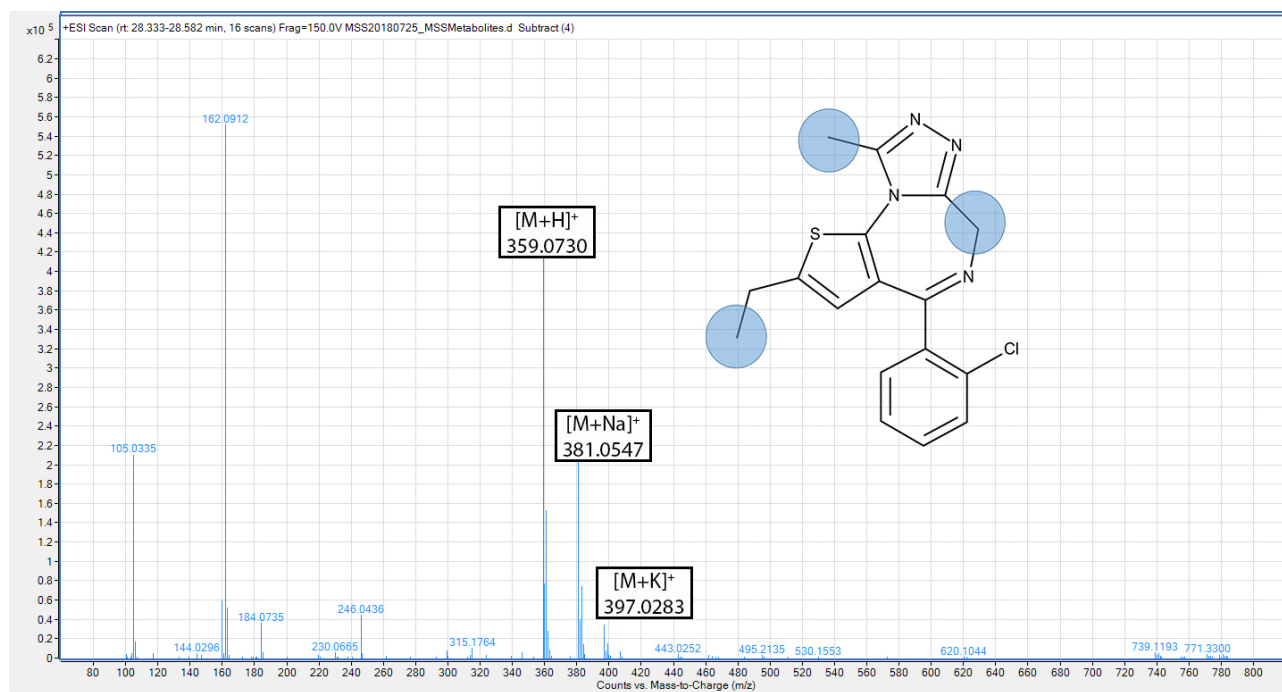
Figure 10.17: LC-MS analysis of a hydroxylated metabolite of etizolam following incubation with the HepaRG cell line with the potential sites of hydroxylation circled.
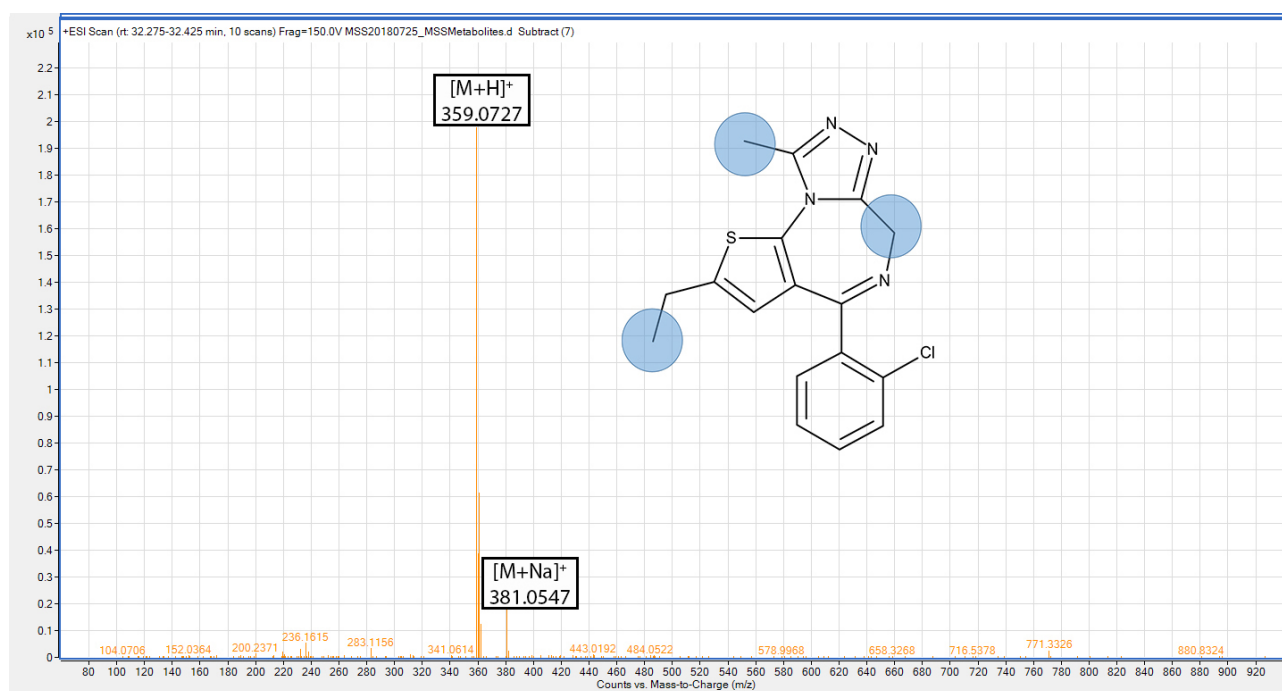
Figure 10.18: LC-MS analysis of a hydroxylated metabolite of etizolam following incubation with the HepaRG cell line with the potential sites of hydroxylation circled.
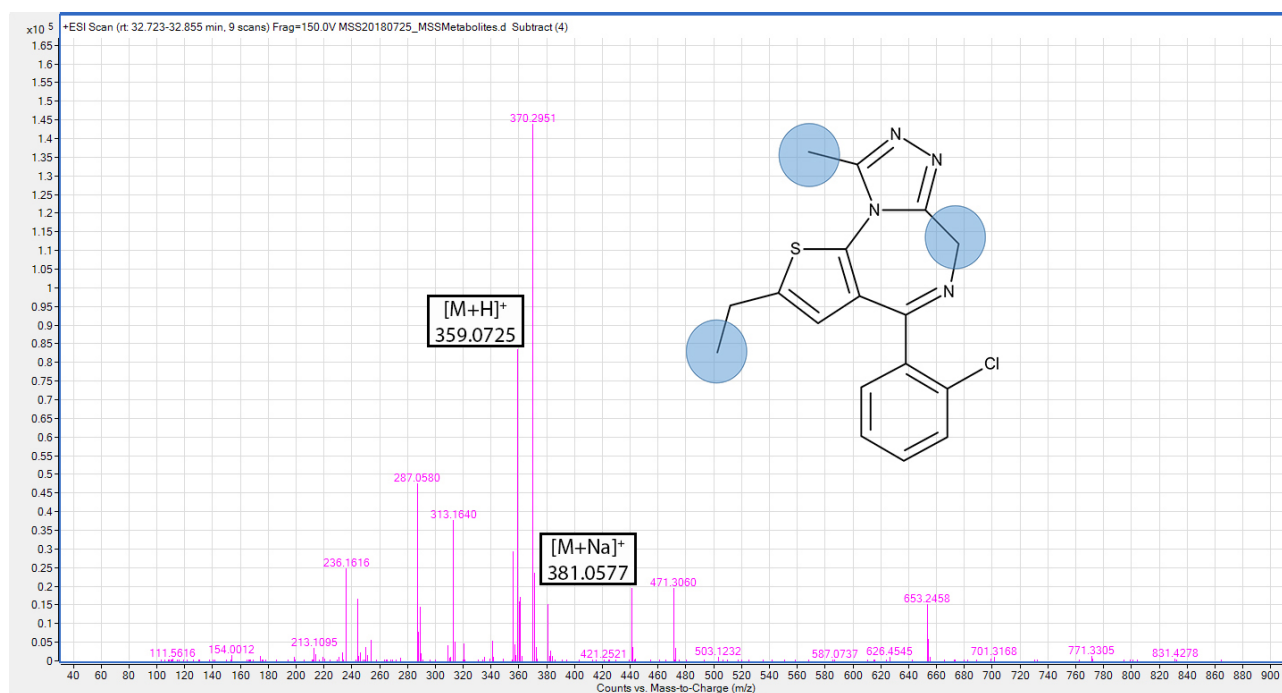
Figure 10.19: LC-MS analysis of a hydroxylated metabolite of etizolam following incubation with the HepaRG cell line with the potential sites of hydroxylation circled.

10.2.7   Flubromazepam

Flubromazepam was detected with at 34.894 minutes (m/z 333.0038 [M+H]$^+$ with a mass difference of -1.44 ppm,   10.22).A hydroxylated metabolite was detected at 32.790 minutes (m/z 348.9973 [M+H]$^+$ with a mass difference of 2.59 ppm, Figure   10.23) and a potential debrominated metabolite was detected at 34.894 minutes (m/z 255.0928 [M+H]$^+$ with a mass difference of 0.55 ppm, Figure   10.24). Both of these metabolites have been reported in the literature [251]. In common with other 1,4-benzodiazepines, hydroxylation is thought to occur at position 3 [251].

The peak areas for flubromazepam and debrominated flubromazepam can be seen in the overlaid EICs in Figure 10.20. An enlarged EIC to show the hydroxylated metabolite is shown in Figure 10.20.
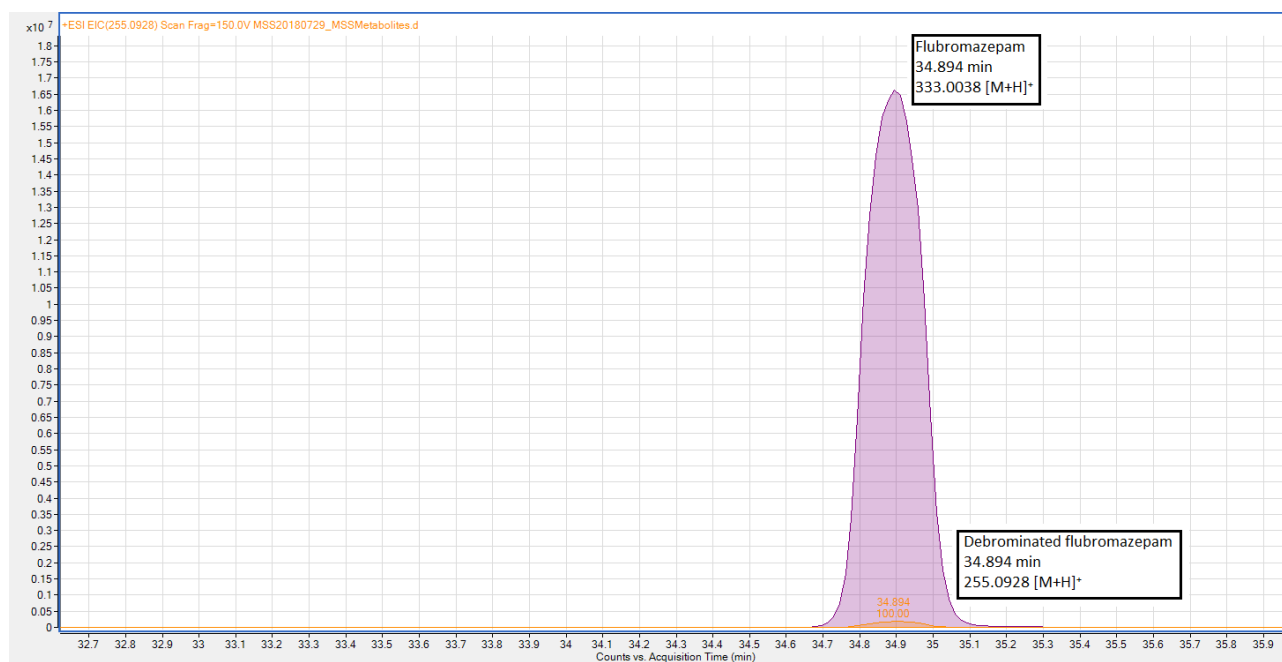
Figure 10.20: Overlaid EICs of flubromazepam and debrominated flubromazepam following incubation with the HepaRG cell line.
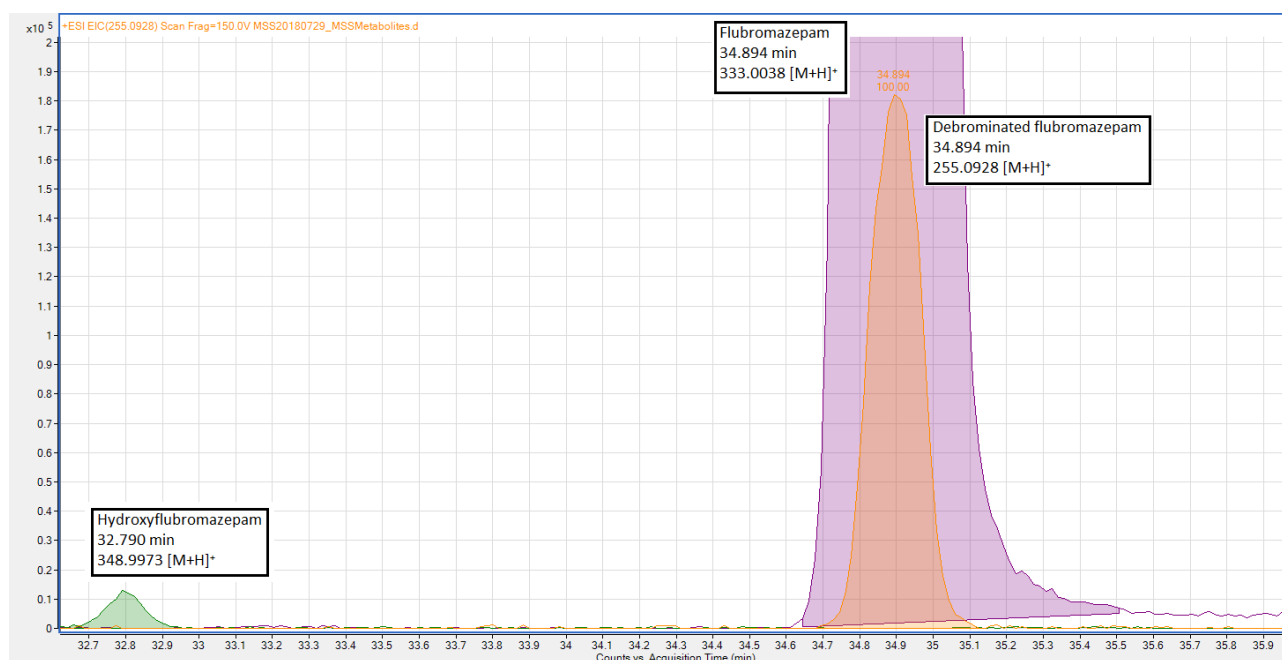
Figure 10.21: Enlarged, overlaid EICs of flubromazepam and its metabolites following incubation with the HepaRG cell line.
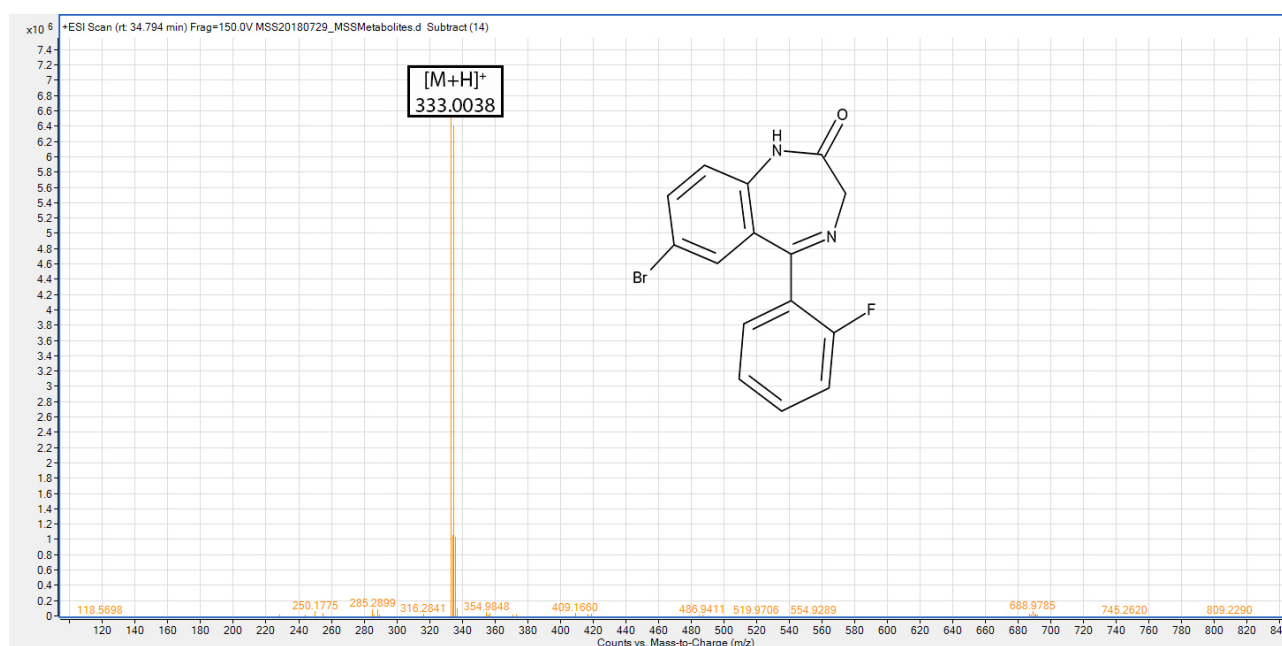
Figure 10.22: LC-MS analysis of flubromazepam following incubation with the HepaRG cell line.
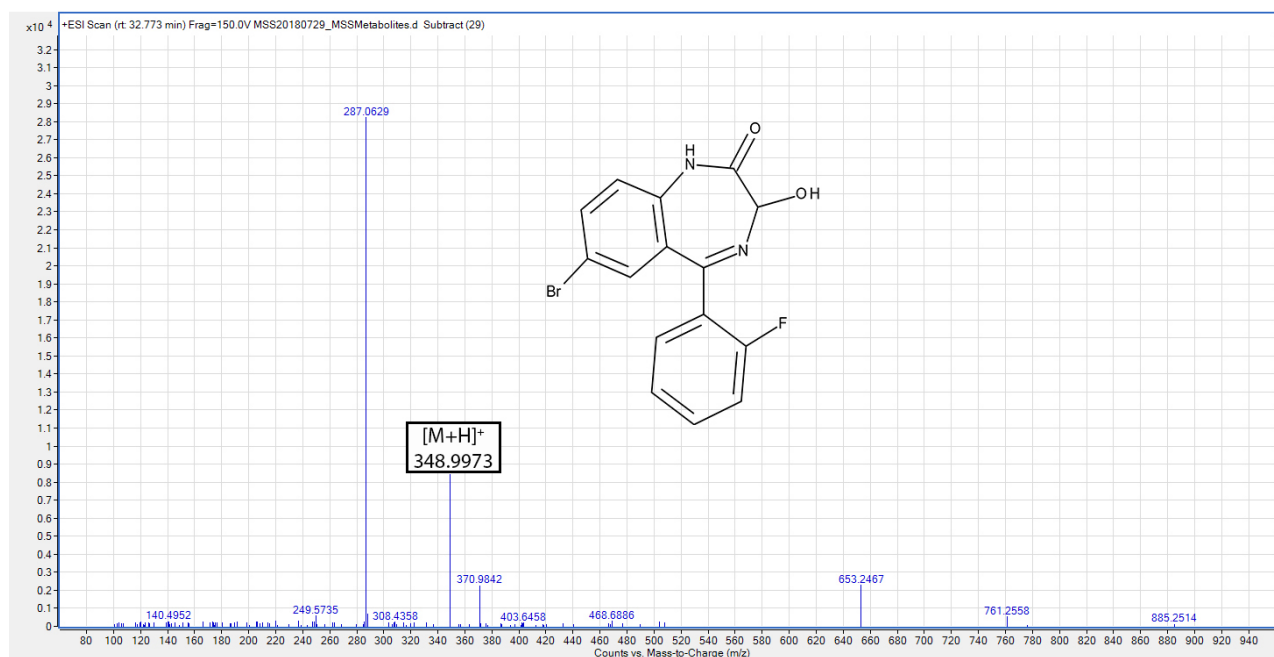
Figure 10.23: LC-MS analysis of a hydroxylated metabolite of flubromazepam following incubation with the HepaRG cell line.
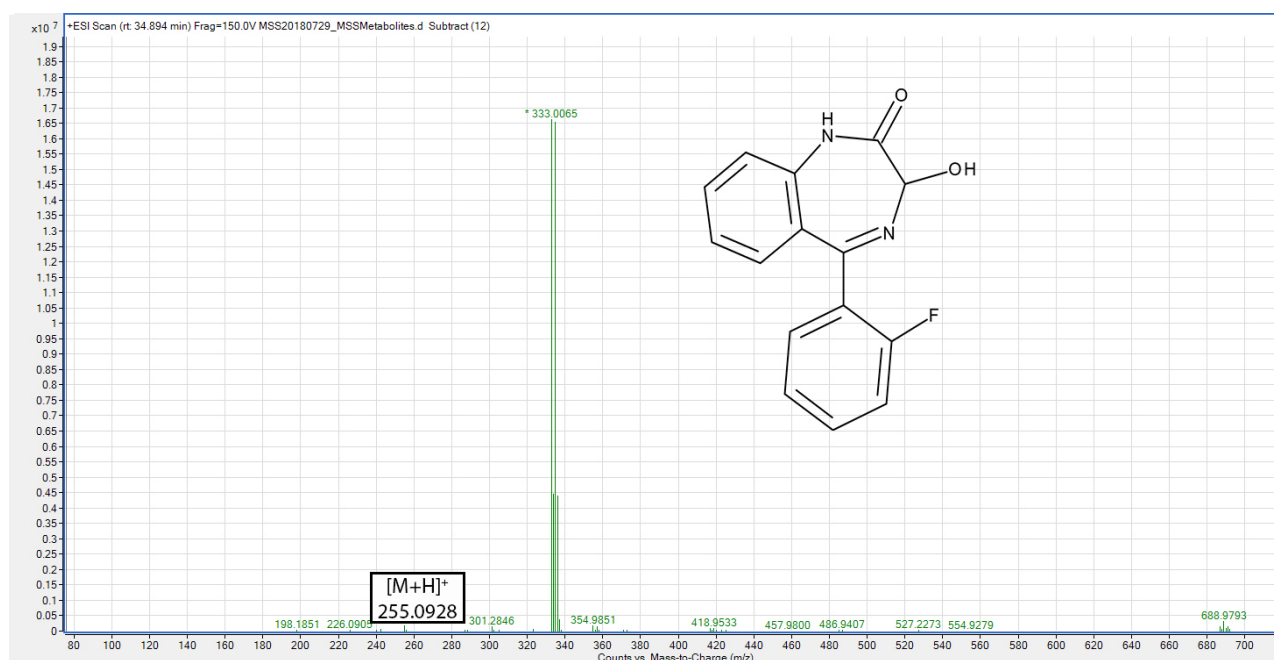
Figure 10.24: LC-MS analysis of debrominated flubromazepam following incubation with the HepaRG cell line.

10.2.8 Flubromazolam

Flubromazolam eluted at 35.057 minutes (m/z 371.0306 [M+H]$^+$ with a mass difference of -0.86 ppm, Figure 10.25). A sodiated adduct with a m/z of 393.0120 ([M+Na]$^+$) and a mass difference of 0.16 ppm was also observed. No metabolites were detected following incubation with the HepaRG cells. Minor amounts of two monohydroxylated metabolites for flubromazolam have been reported following incubation with cryopreserved human hepatocytes [[315]. A monohydroxylated and a dihydroxylated metabolite have also been reported following incubation with HLMs [257]. A single monohydroxylated metabolite has been reported following a study involving self-ingestion [470].
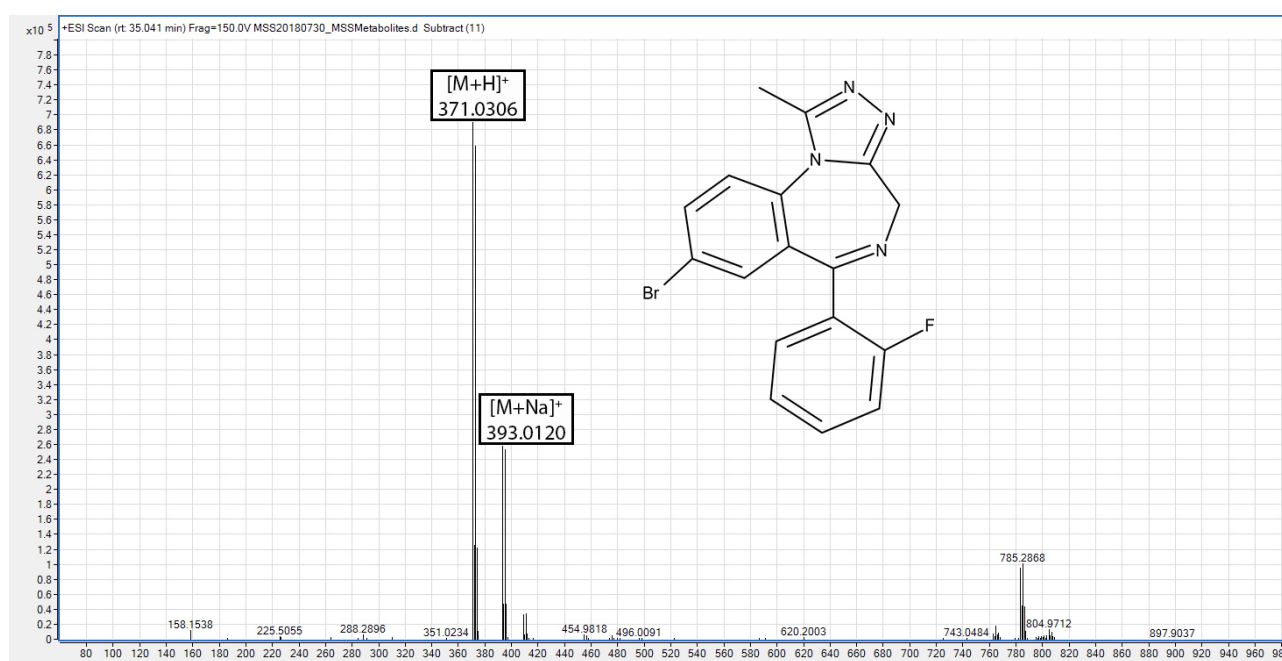
Figure 10.25: LC-MS analysis of flubromazolam following incubation with the HepaRG cell line.

10.2.9   Meclonazepam

Following incubation with the HepaRG cell line, meclonazepam was detected at 35.631 minutes (m/z 330.0640 [M+H]$^+$ with a mass difference of 0.32 ppm) with no metabolites detected (Figure 10.26). A nitro-reduced derivative, 7-aminomeclonazepam, has been previously reported [314]. A monohydroxylated metabolite, with hydroxylation thought to occur on the 3-methyl group has also been reported [257]. This monohydroxylated metabolite has only been reported in human liver microsomes and is not thought to occur in incubations with primary human hepatocytes [471]. In a study involving authentic human urine samples monohydroxylated metabolites of meclonazepam were not reported and only the 7-aminomecloanzepam was observed [472].

Clonazepam is a structurally-similar benzodiazepine to meclonazepam, lacking only the 3-methyl substituent. In experiments involving human ingestion, cryopreserved human hepatocytes and HLMs, 7-aminomeclonazepam was most abundant in human urine followed by cryopreserved human hepatocytes [314]. Following incubation with HLMs only minimal amounts of 7-aminomeclonazepam were formed under standard conditions (NADPH regenerating system in potassium phosphate buffer, 0.1 M, pH 7.4, at 37 °C). When the HLMs were incubated in an atmosphere containing nitrogen, the amount of 7-aminomeclonazepam produced was 140 times greater [311].

In reported incubations with HLMs, the benzodiazepine flunitrazepam, also containing a 7-nitro substitution, failed to produce a reduced 7-amino metabolite [241,473,474]. However this 7-amino metabolite of flunitrazepam has been observed to occur in both human urine and blood [475,476].

Following incubation with the HepaRG cell line, meclonazepam may not be metabolised to detectable concentrations of 7-aminomeclonazepam.

Nitro-containing benzodiazepines are known to be unstable when stored in biological matrices for long periods of time. For example, levels of meclonazepam decrease when it is stored in glass tubes at -20 °C for three months but the same decrease is not observed when meclonazepam

stored in polypropylene tubes at -20 °C [477]. Decreases are also observed when stored at ambient temperatures of 20 °C for one day in both glass and polypropylene tubes [477]. The 7-amino metabolites of the benzodiazepines clonazepam, nitrazepam and flunitrazepam have been found to be unstable in blood and water when stored at -20 °C for two months [478]. After eight months of storage at -20 °C in a liver homogenate matrix, the levels of 7-aminoclonazepam and 7-aminoflunitrazepam decreased by 90 % and 75 % respectively [479]. The samples in this study were initially collected in polypropylene tubes and then transferred to glass tubes for solvent evaporation. This extended period of time at ambient temperature, some of it in glass tubes may have hastened the decomposition of metabolites.

The nitro-group on the structurally-related benzodiazepine clonazepam is thought to be reduced by CYP3A4 [235]. However CYP3A4 was clearly present in the HepaRG cells as judged by the metabolism of the testosterone control.
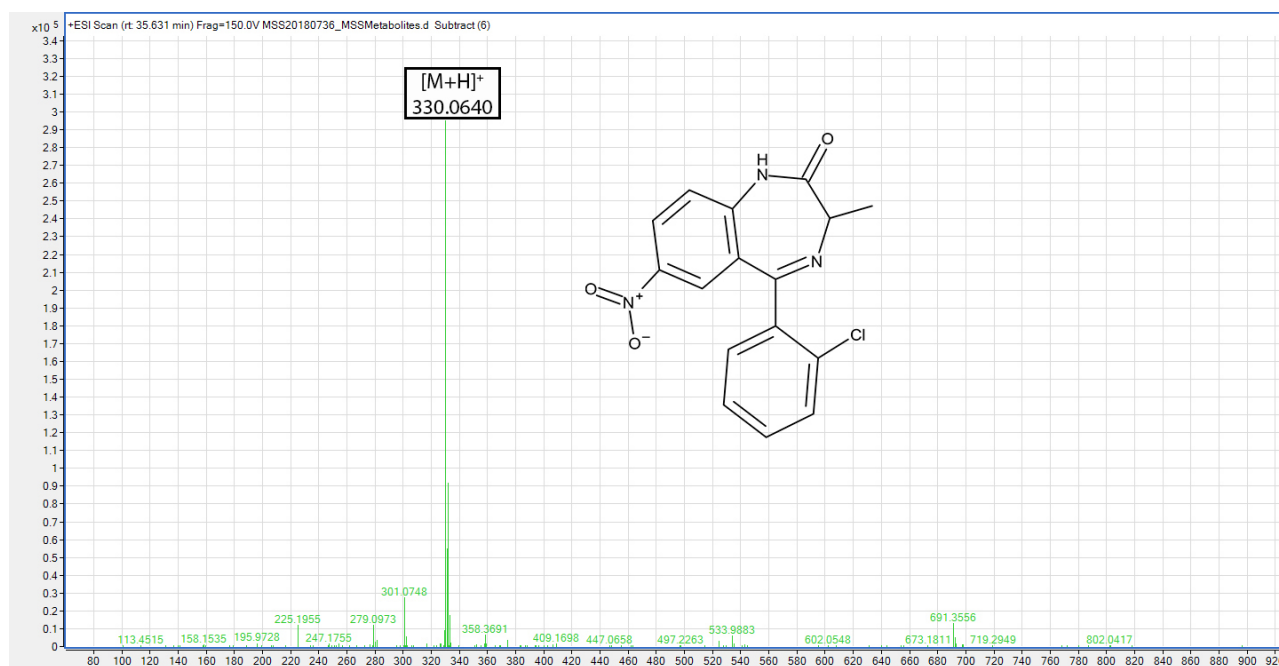
Figure 10.26: LC-MS analysis of meclonazepam following incubation with the HepaRG cell line.

10.2.10   Nitrazolam

Nitrazolam was detected at 32.804 minutes (m/z 320.1143 [M+H]$^+$ with a mass difference of -0.29 ppm and m/z 342.0969 [M+Na]$^+$ with a mass difference of -2.38 ppm, Figure 10.28) and a metabolite corresponding to the 8-nitro reduction was detected at 23.892 minutes (m/z 290.1409 [M+H]$^+$ with a mass difference of -3.05 ppm, Figure 10.29 respectively). 8-Aminonitrazolam has been previously reported in HLMs [81]. A monohydroxylated metabolite has also been reported in HLMs, with hydroxylation thought to occur on the 4- or α (1-methyl) position, however no such metabolite was observed here [81].

The overlaid EICs for nitrazolam and its 8-amino metabolite can be seen in Figure 10.27.

For a similar triazolobenzodiazepine containing a nitro group, flunitrazolam, no hydroxylated metabolite was detected in either human urine or following incubation with HLMs and only the 8-aminoflunitrazolam was observed in HLMs [480]. Another similar triazolobenzodiazepine, clonazolam, produces both hydroxylated and nitro-reduced metabolites in human urine [481].

Only two benzodiazepines in this work contained a nitro group; meclonazepam and nitrazolam. Whilst no nitro-reduced metabolite of meclonazepam was detected, the nitro-reduced (8-amino) metabolite of nitrazolam was detected in this study. If it can be tentatively assumed that the same enzyme is responsible for the metabolic reduction of the amino moiety, then some other factor may have been responsible for the lack of an amino metabolite for meclonazepam. This could possibly be related to the issue of benzodiazepine stability during storage, as discussed previously for meclonazepam. However, the exact reason is unclear and may be related to extra stability conferred upon the molecule by the presence of a triazole ring.
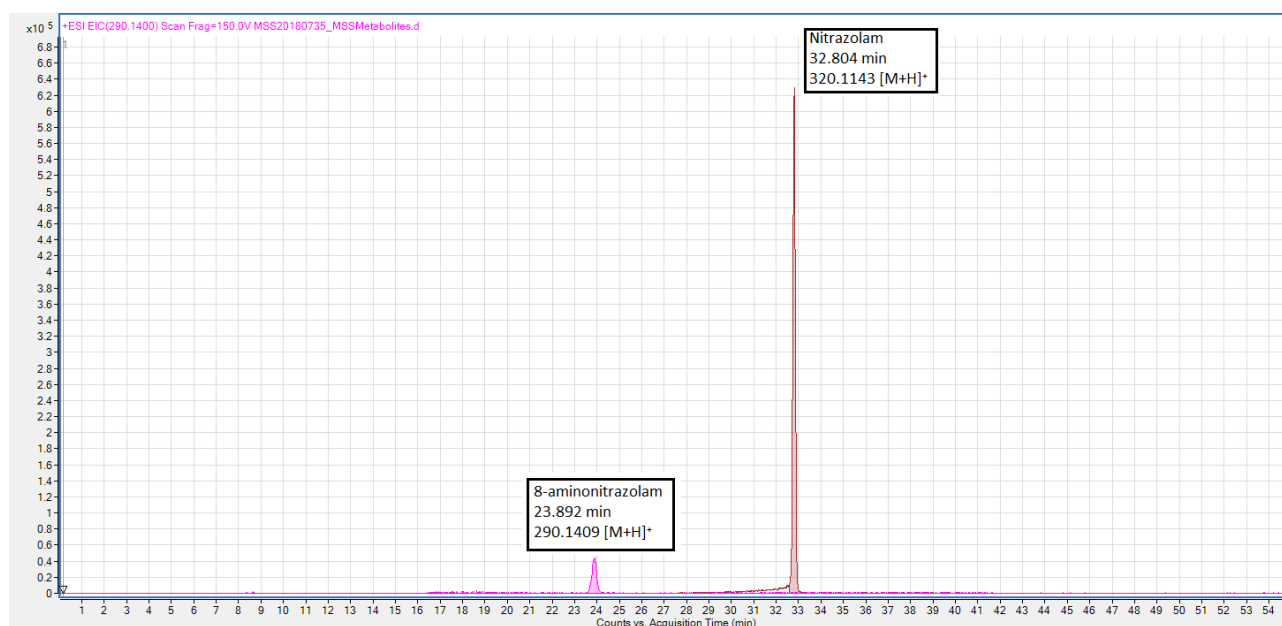
Figure 10.27: Overlaid EICs of nitrazolam and its 8-amino metabolite following incubation with the HepaRG cell line.
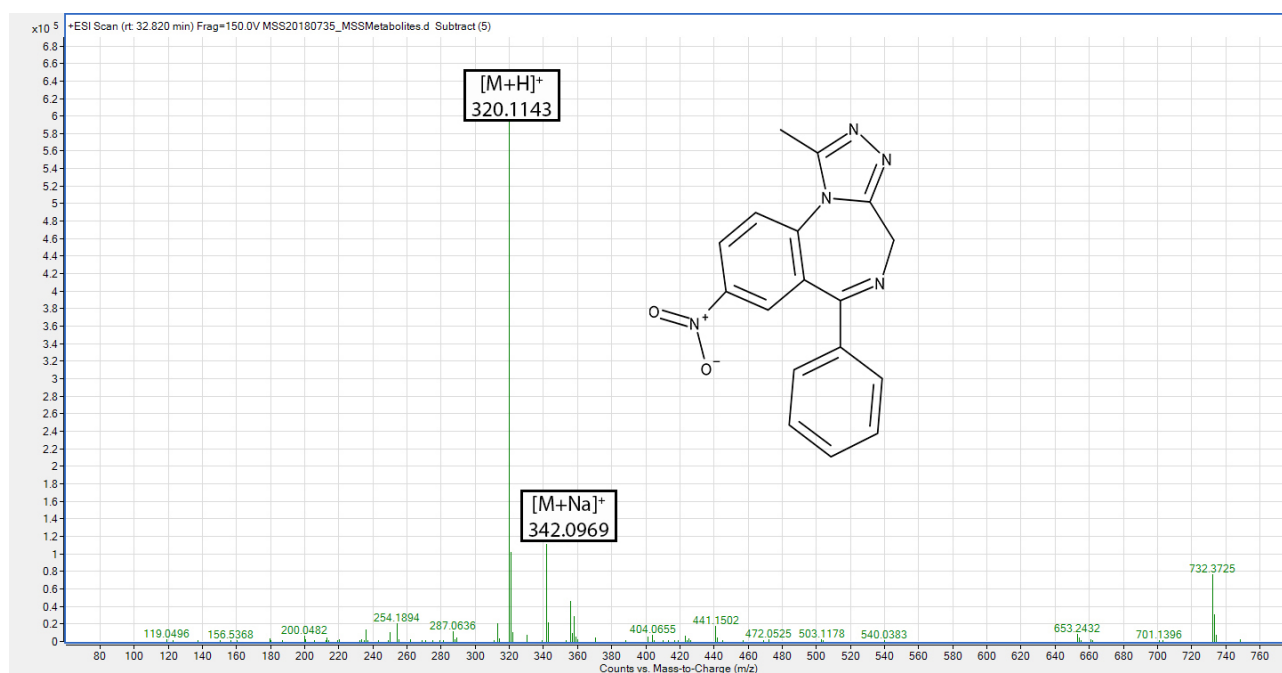
Figure 10.28: LC-MS analysis of nitrazolam following incubation with the HepaRG cell line.
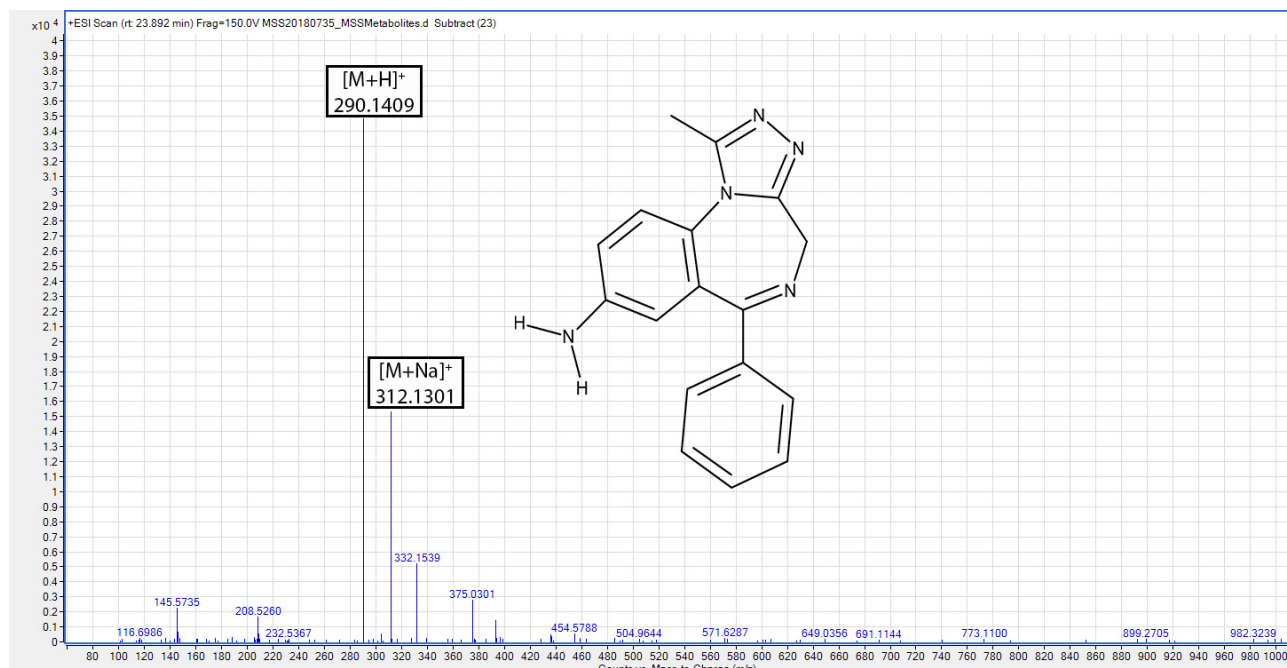
Figure 10.29: LC-MS analysis of 8-aminonitrazolam following incubation with the HepaRG cell line.

## 10.2.11   Phenazepam

Phenazepam was detected as the $[M+H]^+$ adduct at 35.788 minutes with an m/z ratio of 348.9741 and a mass difference of -1.33 ppm (Figure 10.30). The expected phase I hydroxylated metabolite, 3-hydroxyphenazepam, was not detected. In one study involving oral ingestion in humans, no significant amounts of 3-hydroxyphenazepam (detection limit 3 ng mL^{-1}) have been reported to occur [482]. Another study suggests the presence of 3-hydroxyphenazepam and another metabolite, 2-amino-5-bromo,chloro-aminobenzophenone, in human urine following oral ingestion [483]. The main metabolite of phenazepam, 3-hydroxyphenazepam, is known to be thermally unstable leading to sensitivity issues when using analytical techniques such as GC-MS [484]. Degradation during storage may well have occurred leading to a level of 3-hydroxyphenazepam that would be undetectable with the current analytical method.
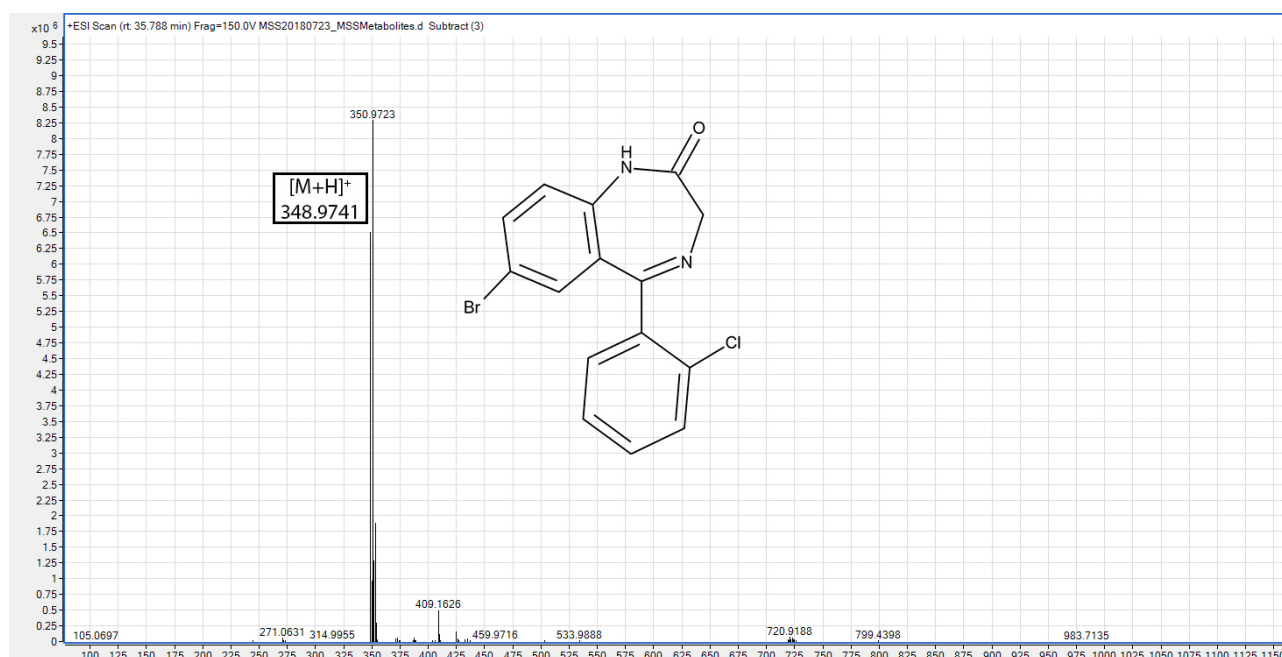
Figure 10.30: LC-MS analysis of phenazepam following incubation with the HepaRG cell line.

10.2.12 Pyrazolam

Pyrazolam was detected at 30.809 minutes (m/z 354.0346 [M+H]$^+$ with a mass difference of 0.23 ppm and m/z 376.0164 [M+Na]$^+$ with a mass difference of 0.95 ppm, Figure 10.31). No metabolites were detected in the mass spectra. Experiments involving self-ingestion in humans have reported no metabolites for pyrazolam and it was postulated that this because the individual involved in the study had a low expression of CYP2D6 [485]. However other research suggests that two metabolites are observed in human urine involving hydroxylation on the diazepine ring at position 4 and hydroxylation on the methyl group at position 1 [258]. Neither of these metabolites were observed in this work.
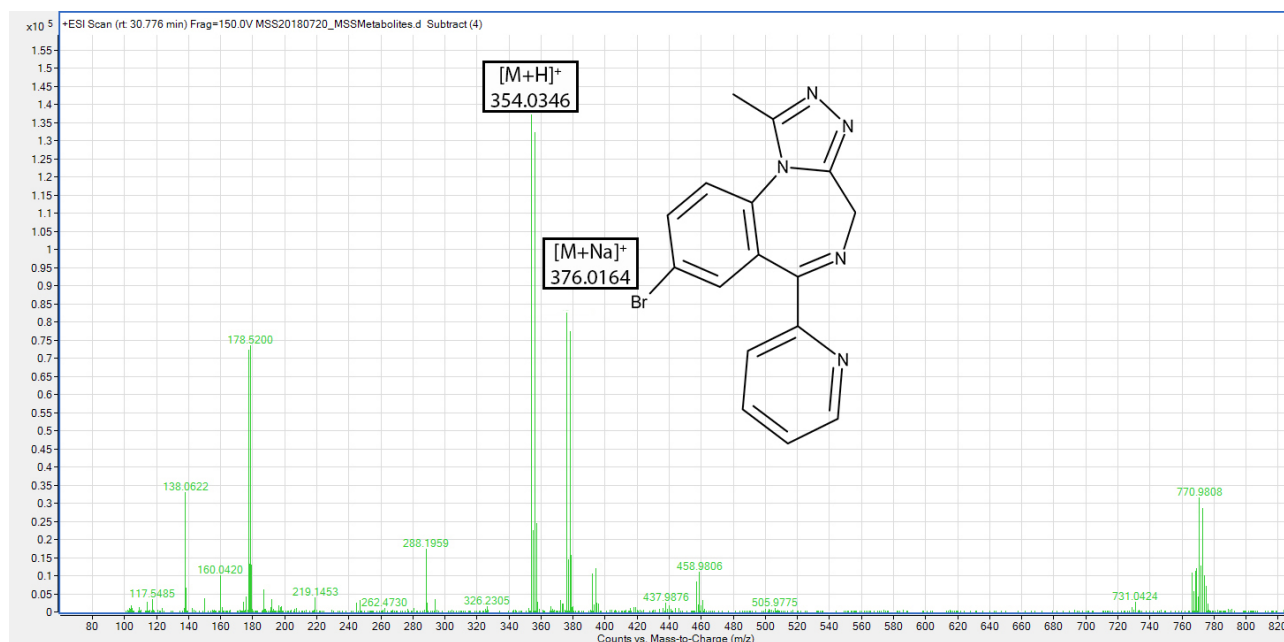
Figure 10.31: LC-MS analysis of pyrazolam following incubation with the HepaRG cell line.

Table 10.1: LC-MS data for compounds observed following the incubation of NPS-benzodiazepines with the HepaRG cell line

NPS-benzodiazepine	Compounds observed	Retention time (min)	m/z	Most likely adduct	Observed neutral mass	Theoretical mass	Mass difference (ppm)
3-Hydroxyphenazepam	3-Hydroxyphenazepam	33.594	364.9684	[M+H]$^+$	363.9611	363.9614	0.82
	3-Hydroxyphenazepam		386.9499	[M+Na]$^+$	363.9610	363.9614	1.27
4'-Chlorodiazepam	4'-Chlorodiazepam	40.884	319.0402	[M+H]$^+$	318.0331	318.0327	-1.24
	Demethylated 4'-Chlorodiazepam	38.168	305.0243	[M+H]$^+$	304.0170	304.0170	0.10
	Hydroxylated 4'-Chlorodiazepam	38.135	335.0362	[M+H]$^+$	334.0289	334.0276	-4.03
Desalkylflurazepam	Desalkylflurazepam	34.433	289.0538	[M+H]$^+$	288.0466	288.0466	0.02
Deschloroetizolam	Deschloroetizolam	34.269	309.1176	[M+H]$^+$	308.1103	308.1096	-2.48
	Deschloroetizolam		331.0990	[M+Na]$^+$	308.1098	308.1096	-0.70
	Hydroxydeschloroetizolam	22.276	325.1139	[M+H]$^+$	324.1066	324.1045	-6.51
	Hydroxydeschloroetizolam		347.0926	[M+Na]$^+$	324.1048	324.1045	-1.07
Diclazepam	Diclazepam	37.901	319.0402	[M+H]$^+$	318.0330	318.0327	-0.94
	Delorazepam	35.267	305.0245	[M+H]$^+$	304.0171	304.0170	-0.41
	Lormetazepam	35.631	335.0350	[M+H]$^+$	334.0277	334.0276	-0.41
Etizolam	Etizolam	36.649	343.0784	[M+H]$^+$	342.0710	342.0706	1.20
	Etizolam		365.0592	[M+Na]$^+$	342.0708	342.0706	0.49
	Hydroxyetizolam	28.466	359.0730	[M+H]$^+$	358.0657	358.0655	-0.48
	Hydroxyetizolam		381.0547	[M+Na]$^+$	358.0654	358.0655	0.21
	Hydroxyetizolam		397.0283	[M+K]$^+$	358.0652	358.0655	0.91
	Hydroxyetizolam	32.358	359.0729	[M+H]$^+$	358.0665	358.0655	2.66
	Hydroxyetizolam		381.0547	[M+Na]$^+$	358.0654	358.0655	0.21
	Hydroxyetizolam	32.789	359.0725	[M+H]$^+$	358.0652	358.0655	0.80
	Hydroxyetizolam		381.0577	[M+Na]$^+$	358.0685	358.0655	-8.37
Flubromazepam	Flubromazepam	34.894	333.0038	[M+H]$^+$	331.9965	331.9961	-1.44
	Hydroxyflubromazepam	32.790	348.9973	[M+H]$^+$	347.9901	347.9910	2.59
	Debrominated flubromazepam	34.894	255.0928	[M+H]$^+$	254.0854	254.0855	0.55
Flubromazolam	Flubromazolam	35.057	371.0306	[M+H]$^+$	370.0233	370.0229	-0.86
	Flubromazolam		393.0120	[M+Na]$^+$	370.0229	370.0229	0.16
Meclonazepam	Meclonazepam	35.631	330.0640	[M+H]$^+$	329.0566	329.0567	0.32
Nitrazolam	Nitrazolam	32.804	320.1143	[M+H]$^+$	319.1070	319.1069	-0.29
	Nitrazolam		342.0969	[M+Na]$^+$	319.1077	319.1069	-2.38
	8-Aminonitrazolam	23.892	290.1409	[M+H]$^+$	289.1336	289.1327	-3.05
Phenazepam	Phenazepam	35.788	348.9741	[M+H]$^+$	347.9670	347.9665	-1.33
Pyrazolam	Pyrazolam	35.057	354.0346	[M+H]$^+$	353.0275	353.0276	0.23
	Pyrazolam		376.0164	[M+Na]$^+$	353.0273	353.0276	0.95

10.3   Discussion

Although metabolites were observed for eight of the twelve benzodiazepines following incubation with the HepaRG cell line, the metabolites detected were different from those previously reported. A substrate concentration of 10 μM was utilised in this work and this concentration has been reported previously for flubromazolam and meclonazepam in cryopreserved human hepatocytes and human liver microsomes [314,315]. A greater concentration of 20 μM for clonazolam, deschloroetizolam, flubromazolam and meclonazepam in human liver microsomes has also been utilised and reported in literature [257]. For the thienodiazepine metizolam, a concentration of 90 μM has been reported in human liver microsomes [469]. None of the previous studies in the literature were conducted using human hepatocellular carcinoma cell lines such as the HepaRG cell line used in this work. A potential reason for the lack of metabolites observed in this work may have been that the concentration of 10 μM produced metabolite concentrations that were below the limits of detection. Unfortunately the limits of detection were not calculated in this study and determining these would be valuable in any future work. The stability of some of the benzodiazepines, especially those containing a nitro group, may have affected the observed results as decomposition may have occurred prior to analysis, reducing the analytes to an undetectable concentration with the current method. Although the samples were stored at -20 °C prior to analysis, a lower storage temperature may have reduced any decomposition that occurred. Alternatively, a shorter time between extraction and analysis may have reduced the likelihood of decomposition, however this was an external factor not subject to control in this study.

Unfortunately, as HepaRG is a single-use cell line, the metabolic characterisation experiments were unable to be repeated. This is a potential limitation behind their use *in vitro* to determine the metabolic pathways of new psychoactive substances. A hepatocellular carcinoma cell line such as the C3A cell line would be more suitable as they can undergo regular cellular division and passaging. However in this study (Section 9) the C3A cell line did not produce suitable levels of CYP450 enzymes for use in a phase I metabolic study.

Only two of the 12 NPS-benzodiazepines in this work, diclazepam and flubromazepam, followed

the exact metabolic patterns that have been observed previously [247,251].

Three of the NPS-benzodiazepines in this work produced no metabolites in contrast to reports in the literature of them producing *in vitro* metabolites (flubromazolam, meclonazepam and pyrazolam) [257,258,314,315,471]. Both of these benzodiazepines had only been characterised in human urine and human liver microsomes and the use of hepatocytes in this work may have affected the metabolites produced.

Two of the NPS-benzodiazepines produced a lower number of metabolites than have been previously reported (deschloroetizolam and nitrazolam) [81,257]. Deschloroetizolam produced one hydroxylated metabolite compared to the four metabolites reported in literature [257]. Nitrazolam only produced one nitro-reduced metabolite in contrast to the additional hydroxylated metabolite reported in literature [81]. However meclonazepam, also containing a nitro-group, did not produce a nitro-reduced metabolite. The observed difference could be as a result of the differing structures, nitrazolam is a triazolobenzodiazepine while meclonazepam is a 1,4-benzodiazepine. The enzyme(s) responsible for metabolism may have had a greater affinity for the nitro-containing triazolobenzodiazepines.

Two of the NPS-benzodiazepines, desalkylflurazepam and phenazepam, did not produce the expected hydroxylated metabolites (position 3). Neither of these two NPS-benzodiazepines have undergone *in vitro* studies previously with both having a hydroxylated metabolite observed *in vivo* [467,468,482,483].

The differences in the various techniques used (human liver microsomes, authentic *in vivo* samples in human urine, cryopreserved human hepacotyes and the HepaRG cell line in this work) may have contributed to the lack of metabolites observed for some benzodiazepines.

As mentioned earlier, cryopreserved human hepatocytes are often considered the 'gold standard' for *in vitro* metabolic studies and express a range of phase I and phase II enzymes that are more akin to those found in the human body. The analysis of NPS-benzodiazepines and their metabolites in human urine, following self-ingestion, is of course also likely to produce the expected metabolites depending on the metabolic phenotype of the individual. Compared to

these methods, human hepatocellular carcinoma cell lines be deficient in some phase I enzymes or they may have a lower activity in cell culture.

However, the stability issues mentioned, especially for nitro-containing benzodiazepines (e.g. meclonazepam and nitrazolam) and their metabolites could also have played a role.

Another factor mentioned previously was the substrate concentration, with 20 μM being reported for NPS-benzodiazepines incubated with HLMs. Further experiments incubating the NPS-benzodiazepines with the HepaRG cell line over a larger concentration range would be desirable in order to confirm these results.

Chapter 11

Final Discussion and Future Work

11.1 Final Discussion

The aim of the work presented in this thesis was to investigate the physicochemical and pharmacokinetic properties of emerging benzodiazepines that have appeared as new psychoactive substances. The emergence and spread of these NPS-benzodiazepines has necessitated investigation of their properties in order to predict their pharmacokinetics and explain their effects through understanding their pharmacodynamics [16].

As with any compound, whether it be a pharmaceutical drug or a new psychoactive substance, suitable analytical methods are required for their detection, identification and quantitation [351,352]. In order for results to be reliable full validation is required. The HPLC-DAD and GC-MS methods in Section 3 were suitably validated for the analysis of a variety of NPS-benzodiazepines. Although these methods were only utilised as intermediate steps in order to calculate log $D_{7.4}$, plasma protein binding and the blood to plasma ratio, their versatility indicates that they could find utility in future investigations of the pharmacokinetics or physiochemical properties of NPS-benzodiazepines, however this would be dependent upon them achieving sufficient chromatographic separation of emerging NPS-benzodiazepines. The HPLC-DAD method in Section 3 had limits of detection and quantitation that were similar to those previously published in the literature for benzodiazepines such as alprazolam (LOQ 300

ng mL^{-1} versus 144.6 ng mL^{-1} in this work) and diazepam, oxazepam and temazepam (LOD 50 ng mL^{-1}, LOQ 100 ng mL^{-1}) [355,356]. The methods described in the literature also used HPLC-DAD [355,356]. In addition, the simplicity of the method was advantageous as it consisted of an isocratic flow used and mobile phases of acetonitrile and a phosphate buffer.However the disadvantage of these methods are that gradient elutions are often more appropriate for the chromatographic separation of compounds.

The method presented in Section 4 for determining log D$_{7.4}$ was found to be suitable upon comparison with published values in the literature. Although not a high-throughput method, the high accuracy (as assessed by the closeness of experimental to literature values) and precision (as assessed by the repeatability of the measurements) of the method are indicative of its appropriateness in this case. Precision was excellent with the greatest standard deviation for test benzodiazepines being 0.05 log units. All test benzodiazepines had similar experimental values to their literature values such as a log D$_{7.4}$ of 2.81 for diazepam versus a literature range of 2.79 - 2.99 [367-370]. Temazepam produced the greatest difference between experimental and literature values with a log D$_{7.4}$ of 2.32 in this work versus reported values of 1.79 - 2.19 in the literature [367,369]. As a result of the various methods employed there is known to be a large variation in literature values and a standardised method is desirable for comparison [372,375]. The proposed method of using a sodium phosphate buffer with a concentration of 0.01 M for future determinations was found to be suitable in this instance and appears to be one of the most common methods in the literature; therefore it may be suitable for this method to be used more-widely in future [375,377]. The log D$_{7.4}$ of a compound affects several pharmacokinetic parameters such as its absorption and plasma protein binding and knowledge of this parameter allows for more accurate predictions and interpretations of pharmacokinetics [110,112,116-118,486]. A large variation in lipophilicity values was observed for the NPS-benzodiazepines in question; pyrazolam was the least lipophilic with a log D$_{7.4}$ of 0.97 and phenazepam was the most lipophilic with a log D$_{7.4}$ of 3.25. The apparent low lipophilicity for pyrazolam was postulated to be as a result of its molecular structure including a pyridin-2-yl ring system. Incorporation of benzodiazepines with a range of structures and log D$_{7.4}$ values into future predictive software packages may prove useful in order to accurately

predict the log $D_{7.4}$ of these compounds. ACD/I-Lab returned the closest predicted values to experimental values for log $D_{7.4}$ average absolute errors 0.18 and 0.28 for the test benzodiazepines and NPS-benzodiazepines respectively. Errors of 0.18 and 0.28 on a logarithmic scale are fairly large errors and to date experimental values would prove more useful than theoretical values.

The pK_a of a compound is important as it aids in the formation of a larger picture of the pharmacokinetic properties of a compound when used with other parameters such as log $D_{7.4}$ and pK_a values for a set of NPS-benzodiazepines were determined in Section 5 [106,141,143]. The determination of the pK_a of compounds using capillary electrophoresis is widely-used and can be automated thus improving its efficiency [156,157]. The use of capillary electrophoresis in pK_a determinations has been well reviewed and measurements from different instruments are directly comparable [154,155]. Furthermore, capillary electrophoresis instruments are common in analytical laboratories rather than specific instruments that can only measure pK_a. The measured pK_a values had values comparable to those in the literature with an accuracy of under 0.20 units and a precision of under 0.07 units [161]. 3-Hydroxyphenazepam had the lowest pK_a1 value of 1.25 while deschloroetizolam had the highest pK_a1 value of 4.19. Phenazepam had the lowest pK_a2 value of 11.24 and 3-hydroxyphenazepam had the highest of 11.96. Several relationships between pK_a values and atomic substitutions were postulated, such as the addition of a chlorine substituent on the 4 position of a 1,4-benzodiazepine does not greatly affect its pK_a. These relationships may prove useful in any future model capable of accurately predicting the pK_a of NPS-benzodiazepines. ADMET Predictor returned the closest predicted values to experimental values for pK_a with an absolute average error of 0.4 for both the test benzodiazepines and the NPS-benzodiazepines set. However several errors were too large for the theoretical values to be of any use; for example a pK_a of 2.98 predicted for flubromazolam by ADMET Predictor versus an experimental pK_a of 2.07. In addition, multiple erroneous sites of protonation were theorised by all three software packages. The derivation of relationships between molecular substitutions and pK_a is therefore important if future predictive models are to be improved.

Section 6 of this work dealt with the experimental determination of the plasma protein binding.

The plasma protein binding of a compound is one of the most important pharmacokinetic parameters that can be determined *in vitro* and equilibrium dialysis is often considered the gold-standard for this measurement [176]. Plasma protein binding is important both from a standalone point of view but also to aid in the prediction of pharmacokinetic properties such as the volume of distribution [168]. As a result of the concentration-independence of plasma protein binding for benzodiazepines, greater concentrations of 20 μM were used as these were detectable by the previously-discussed and validated HPLC-DAD method in Section 3. The low standard deviation and high-precision for the experimental plasma protein binding values when compared to the literature values indicates that the proposed method with a concentration of 20 μM and an equilibration time of 24 hours was suitable. All plasma protein binding values for the test benzodiazepines were within their literature ranges, other than for prazepam where an experimental value of 97.4 % was determined versus a single literature value of 97 % [395]. The maximum standard deviation for the test benzodiazepines was 1.8 % for nitrazepam. Pyrazolam experienced the lowest plasma protein binding of 78.7 % while phenazepam had a plasma protein binding of 98.3 % and the majority of the plasma protein binding values were explainable by comparison of their molecular structures and substitutions. With regards to the predictive software, ACD/I-Lab returned the closest predicted values to experimental values for both plasma protein binding with average absolute errors of 4.4 % for the test benzodiazepines and 3.0 % for the NPS-benzodiazepines. Larger errors were observed, for example ACD/I-Lab predicted a plasma protein binding of 89.5 % for alprazolam whereas its experimental plasma protein binding was 71.6 %. The large variations in individual errors, as exemplified by alprazolam, means that experimental data for these NPS-benzodiazepines is currently of greater utility than that generated from predictive software.

Following on from the determination of log $D_{7.4}$, pK_a and plasma protein binding in Sections 4, 5 and 6 respectively, these values were used to predict the volume of distribution at steady state in Section 7. This was performed using the Øie-Tozer equation [208]. A low mean-fold error of 1.11 was derived in this work compared to a 1.86 mean-fold error reported elsewhere in the literature [107]. However a much higher error was observed for the only thienotriazolodiazepine in the dataset, brotizolam, which was 2.21. Again, as with the parameters used to predict the

volume of distribution at steady state, inclusion of a wider dataset may improve the predictive power of this model.

The blood to plasma ratio of six NPS-benzodiazepines was experimentally determined in Section 8. One problem encountered was that errors were observed in the literature for the stated blood to plasma concentration ratio; for example the commonly quoted value of 1.00 for nitrazepam appeared to be derived from experiments performed with rabbits [429]. Large variations also existed in the literature for blood to plasma concentration ratios and blood to plasma partition coefficients, even for the selected test compounds. For example, chlorpromazine had a Ke/p range of 0.52 - 2.17 and quinine had a $K_{e/p}$ range of 0.93 - 3.44 [422-424,427,428]. This again highlights the difficulty of gathering accurate pharmacokinetic data. Despite this, the values determined for NPS-benzodiazepines were similar to benzodiazepine blood to plasma concentration values listed in the literature. The lowest blood to plasma concentration ratio found was 0.57 for phenazepam which is similar to other benzodiazepines that experience a great degree of plasma protein binding such as diazepam [426]. The highest value observed was 1.18 for pyrazolam and it was theorised that this was as a result of its low plasma protein binding.

In order to detect illicit compounds and interpret toxicological results, knowledge of the metabolic pathways of compounds is necessary [255]. The metabolic pathways are often determined *in vitro* using human hepatocellular carcinoma cell lines. However the metabolic capacities of any cell line must be determined prior to their incubation with new substances amd in Section 9 of this work, the metabolic activities of the HepaRG and C3A cell lines were compared [278]. The C3A cell line had previously only been characterised with regards to the CYP3A4 and CYP1A2 enzymes in the literature and characterisation with the six key metabolic enzymes (CYP1A2, CYP2B6, CYP2C9, CYP2C19, CYP2D6 and CYP3A4) was conducted. Only the CYP2D6 enzyme was found to be expressed in the C3A cell line. Metabolic expression of enzymes is known to be inducible by DMSO and such an attempt was made in this work with the C3A cell line [271,272]. Unfortunately no apparent increase in metabolic capability was observed and instead a potential decrease was observed. The HepaRG cell line was found to be much more suitable than the C3A cell line for the study of the metabolic pathways of NPS-benzodiazepines as a result of its expression of the CYP1A2, CYP2D6, CYP3A4,

CYP2C19, CYP2B6 enzymes. The CYP2C9 was not observed but a contributing factor may have been the low concentration of the substrate, diclofenac, used in the incubation.

The metabolic pathways of a range of NPS-benzodiazepines were investigated in Section 10. Knowledge of these metabolic pathways is important for interpretation of forensic and toxicological analyses and prediction of future metabolic activity [255]. Although a number of the NPS-benzodiazepines followed previously-observed metabolic pathways, a number of them did not. They either failed to produce metabolites or produced previously-unobserved metabolites (e.g. etizolam). This serves to highlight a potential limitation of only using one method of studying the *in vitro* metabolism of new psychoactive substances.

11.2   Future Work

From the discussed problems with the theoretical predictions from various software packages, experimental data for the log $D_{7.4}$, pK_a and plasma protein binding of NPS-benzodiazepines is currently of greater use. Experimental values are more reliable and accurate than those generated in a theoretical manner. The determination of log $D_{7.4}$, pK_a and plasma protein binding for more NPS-benzodiazepines, for example the other 21 NPS-benzodiazepines reported to the EMCDDA, could be evaluated in future. A suitably-large dataset could then be utilised in order to derive a theoretical model more capable of accurately predicting these values. This would allow for a more rapid prediction of pharmacokinetic parameters such as the volume of distribution.

In a similar manner to the log $D_{7.4}$, pK_a and plasma protein binding, compilation of a larger dataset for the volume of distribution at steady state could increase the predictive capability of the discussed model. However this comes with limitations as experimental volume of distribution values for the benzodiazepines are lacking. The incorporation of compounds with a similar structure into the model, which also have experimental volume of distribution values, could be a potential solution to improving the model.

The HepaRG cell line appeared to express five of the six key CYP450 enzymes under investiga-

tion but the CYP2C9 enzyme did not appear to be present based upon the lack of turnover of diclofenac into its metabolite. Although unrelated to the investigation of NPS-benzodiazepines, if the metabolic experiments in the HepaRG cell line were to be repeated with a range of different diclofenac concentrations then an optimum concentration could be determined and it could be seen whether this enzyme was present.

It may prove useful to repeat the HepaRG metabolic experiments in order to determine whether they are truly suitable for investigating the metabolic pathways of NPS-benzodiazepines. Repeating the experiments with a range of concentrations to study whether a concentration of 10 μM either inhibited metabolism or produced too-low a concentration of metabolite to be detected. Comparison of the metabolism of NPS-benzodiazepines in the HepaRG cell line with their metabolism in human liver microsomes could additionally be performed.

Although the HepaRG cells are known to express phase II enzymes such as UDP-glucuronosyltransferase, no phase II metabolites were detected in this work [487,488]. As benzodiazepines are further transformed by phase II reactions such as glucuronidation and acetylation, knowledge of these processes for NPS-benzodiazepines is important [489,490]. Greater incubation times at a higher substrate concentration could provide these phase II metabolic products *in vitro*.

As cell culture has already been successfully utilised in this research to study the metabolic pathways of NPS-benzodiazepines, it could also be used to assess other parameters. Once of these parameters could be the permeability of the intestinal wall to the NPS-benzodiazepines and study their absorption through this membrane. This can be performed *in vitro* using the Caco-2 cell line [491,492]. This has been performed for other drugs of abuse such as cannabinoids, alkaloids from the psychoactive plant khat, 3-methylenedioxyamphetamine (MDMA) and other amphetamine derivatives [493-496]. The apparent permeability of a compound through the Caco-2 cell line is often considered a gold-standard for assessing compound absorption in the body [497,498].

As discussed in Section 1.9 regarding the pharmacology of benzodiazepines, their mechanism of action lies with their ability to bind to the GABA$_A$ receptor and modulate its response

to the neurotransmitter GABA. As the majority of GABA$_A$ receptors lie within the brain, benzodiazepines must firstly cross the blood-brain barrier in order to bind to these receptors. The Madin Darby canine kidney (MDCK) cell line is commonly used to assess the propensity of a compound to cross the blood-brain barrier because of its expression of the MDR1 gene which encodes for the P-glycoprotein. Although only one protein is assessed, the P-glycoprotein is one of the most important efflux transporters in the brain and therefore this assay allows a good estimation of blood-brain barrier penetration [499-502].

The clearance of NPS-benzodiazepines from the human body could also be investigated with an *in vitro* approach. This has been shown previously for multiple drugs where the rate of clearance is firstly calculated for the compound in human liver microsomes or hepatocytes and then scaled up to calculate the clearance for the human body [503].

From the previous discussion it is clear that there are still a large amount of parameters that could be determined *in vitro* such as phase II metabolism, in-depth phase I metabolic comparison, clearance, intestinal permeability and blood-brain barrier penetration. Additionally, increased knowledge of the log $D_{7.4}$, pK_a and plasma protein binding of benzodiazepines could allow for more-detailed structure-activity relationships to be formed. If such parameters could be accurately predicted then this would greatly reduce the time required for experimental measurements and greatly increase the size of datasets available for the prediction of more complex parameters such as the volume of distribution.

References

[1] APA. Diagnostic and Statistical Manual of Mental Disorders (4th Ed.)1994.

[2] Crocq MA. Historical and cultural aspects of mans relationship with addictive drugs. Dialogues Clin. Neurosci. 2007; 9: 355-361.

[3] Barratt MJ, Seear K, Lancaster K. A critical examination of the definition of psychoactive effect in Australian drug legislation. Int. J. Drug Policy 2017; 40: 16-25., doi: 10.1016/j.drugpo.2016.10.002.

[4] European Monitoring Centre for Drugs and Drug Addiction. New psychoactive substances in Europe. EU early Warn. Syst. 2015; 12., doi: 10.2810/372415.

[5] Lande A. The Single Convention on Narcotic Drugs, 1961. Int. Organ. 1962; 16: 776-797., doi: 10.1017/S0020818300011620.

[6] UNODC. Schedules of the Convention on Psychotropic Substances of 1971, as at 25 September 2013.2013.

[7] Banning Psychoactive Substances: A Slippery Slope. EBioMedicine 2015; 2: 613-614., doi: 10.1016/j.ebiom.2015.07.016.

[8] Brandt SD, King LA, Evans-Brown M. The new drug phenomenon. Drug Test. Anal. 2014; 6: 587-597., doi: 10.1002/dta.1686.

[9] UNODC. The challenge of new psychoactive substances. A Report from the Global SMART Programme March 2013. 2013;

[10] Prosser JM, Nelson LS. The Toxicology of Bath Salts: A Review of Synthetic Cathinones. J. Med. Toxicol. 2012; 8: 33-42., doi: 10.1007/s13181-011-0193-z.

[11] Dean BV, Stellpflug SJ, Burnett AM, Engebretsen KM. 2C or Not 2C: Phenethylamine Designer Drug Review. J. Med. Toxicol. 2013; 9: 172-178., doi: 10.1007/s13181-013-0295-x.

[12] Arbo MD, Bastos ML, Carmo HF. Piperazine compounds as drugs of abuse. Drug Alcohol Depend. 2012; 122: 174-185., doi: 10.1016/j.drugalcdep.2011.10.007.

[13] Arajo AM, Carvalho F, Bastos M de L, Guedes de Pinho P, Carvalho M. The hallucinogenic world of tryptamines: an updated review. Arch. Toxicol. 2015; 89: 1151-1173., doi: 10.1007/s00204-015-1513-x.

[14] Seely KA, Lapoint J, Moran JH, Fattore L. Spice drugs are more than harmless herbal blends: A review of the pharmacology and toxicology of synthetic cannabinoids. Prog. Neuro-Psychopharmacology Biol. Psychiatry 2012; 39: 234-243., doi: 10.1016/j.pnpbp.2012.04.017.

[15] Prekupec MP, Mansky PA, Baumann MH. Misuse of Novel Synthetic Opioids. J. Addict. Med. 2017; 11: 256-265., doi: 10.1097/ADM.0000000000000324.

[16] Manchester KR, Lomas EC, Waters L, Dempsey FC, Maskell PD. The emergence of new psychoactive substance (NPS) benzodiazepines: A review. Drug Test. Anal. 2018; 10: 37-53., doi: 10.1002/dta.2211.

[17] El-Menyar A, Mekkodathil A, Al-Thani H, Al-Motarreb A. Khat use: History and heart failure. Oman Med. J. 2015; 30: 77-82., doi: 10.5001/omj.2015.18.

[18] Singh D, Müller CP, Vicknasingam BK. Kratom (Mitragyna speciosa) dependence, withdrawal symptoms and craving in regular users. Drug Alcohol Depend. 2014; 139: 132-137., doi: 10.1016/j.drugalcdep.2014.03.017.

[19] Feng LY, Battulga A, Han E, Chung H, Li JH. New psychoactive substances of natural origin: A brief review. J. Food Drug Anal. 2017; 25: 461-471., doi:

10.1016/j.jfda.2017.04.001.

[20] EMCDDA. EMCDDA-Europol 2007 Annual Report on the Implementation of Council Decision 2005/387/JHA2008.

[21] EMCDDA. EMCDDA-Europol 2014 Annual Report on the Implementation of Council Decision 2005/387/JHA,2015.

[22] EMCDDA. EMCDDA-Europol 2015 Annual Report on the Implementation of Council Decision 2005/387/JHA,2016.

[23] EMCDDA. EMCDDA-Europol 2016 Annual Report on the Implementation of Council Decision 2005/387/JHA2017.

[24] EMCDDA-Europol. EMCDDA-Europol 2017 Annual Report on the Implementation of Council Decision 2005/387/JHAn.d.

[25] EMCDDA. EMCDDA-Europol 2005 Annual Report on the Implementation of Council Decision 2005/387/JHA2006.

[26] EMCDDA. EMCDDA-Europol 2008 Annual Report on the Implementation of Council Decision 2005/387/JHA2009.

[27] EMCDDA. EMCDDA-Europol 2011 Annual Report on the Implementation of Council Decision 2005/387/JHA2012.

[28] EMCDDA. EMCDDA-Europol 2012 Annual Report on the Implementation of Council Decision 2005/387/JHA2013.

[29] EMCDDA. EMCDDA-Europol 2013 Annual Report on the Implementation of Council Decision 2005/387/JHA2014.

[30] EMCDDA. EMCDDA-Europol 2009 Annual Report on the Implementation of Council Decision 2005/387/JHA2010.

[31] EMCDDA. EMCDDA-Europol 2016 Annual Report on the Implementation of Council Decision 2005/387/JHA2017.

[32] Mehdi T. Benzodiazepines Revisited. Br. J. Med. Pract. 2012; 5: a501., doi: 10.1093/jat/bkt075.

[33] López-Munoz F, álamo C, García-García P. The discovery of chlordiazepoxide and the clinical introduction of benzodiazepines: Half a century of anxiolytic drugs. J. Anxiety Disord. 2011; 25: 554-562.

[34] Riemann D, Perlis ML. The treatments of chronic insomnia: A review of benzodiazepine receptor agonists and psychological and behavioral therapies. Sleep Med. Rev. 2009; 13: 205-214.

[35] Schaefer TJ, Hafner JW. Are Benzodiazepines Effective for Alcohol Withdrawal? Ann. Emerg. Med. 2013; 62: 2013.

[36] Sirven JI, Waterhouse E. Management of Status Epilepticus. Am. Fam. Physician 2003; 68: 469-476.

[37] Rund DA, Ewing JD, Mitzel K, Votolato N. The use of intramuscular benzodiazepines and antipsychotic agents in the treatment of acute agitation or violence in the emergency department. J. Emerg. Med. 2006; 31: 317-324.

[38] Ashton H. Guidelines for the Rational Use of Benzodiazepines: When and What to Use. Drugs 1994; 48: 25-40., doi: 10.2165/00003495-199448010-00004.

[39] Ashton H. The diagnosis and management of benzodiazepine dependence. Curr. Opin. Psychiatry 2005; 18: 249-255.

[40] Longo LP, Johnson B. Addiction: Part I. Benzodiazepines–side effects, abuse risk and alternatives. Am. Fam. Physician 2000; 61: 2121-2128., doi: 10.1016/j.osfp.2012.10.001.

[41] Uzun S, Kozumplik O, Jakovljevi M, Sedi B. Side effects of treatment with benzodiazepines inPsychiatr. Danub. 2010 pp.90-93.

[42] Ashton H. Protracted withdrawal syndromes from benzodiazepines. J. Subst. Abuse Treat. 1991; 8: 19-28., doi: 10.1016/0740-5472(91)90023-4.

[43] Busto U, Sellers EM, Naranjo CA, Cappell H, et al. Withdrawal reaction after long-term therapeutic use of benzodiazepines. N. Engl. J. Med. 1986; 315: 854-859., doi: 10.1056/nejm198610023151403.

[44] Morgan WW. Abuse liability of barbiturates and other sedative-hypnotics. Adv. Alcohol Subst. Abus. 1990; 9: 67-82., doi: 10.1080/J251v09n0105.

[45] Brett J, Murnion B. Management of benzodiazepine misuse and dependence. Aust. Prescr. 2015; 38: 152-155., doi: 10.18773/austprescr.2015.055.

[46] Cole JO, Chiarello RJ. The benzodiazepines as drugs of abuse. J. Psychiatr. Res. 1990; 24: 135-144., doi: 10.1016/0022-3956(90)90045-R.

[47] Obrien CP. Benzodiazepine use, abuse, and dependence. J. Clin. Psychiatry 2005; 66 Suppl 2: 28-33., doi: papers3://publication/uuid/17204236-1A80-46FE-81A4-0A5D2339D7CA.

[48] Jones JD, Mogali S, Comer SD. Polydrug abuse: A review of opioid and benzodiazepine combination use. Drug Alcohol Depend. 2012; 125: 8-18., doi: 10.1016/j.drugalcdep.2012.07.004.

[49] Vogel M, Knöpfli B, Schmid O, Prica M, et al. Treatment or high: benzodiazepine use in patients on injectable heroin or oral opioids. Addict. Behav. 2013; 38: 2477-2484.

[50] Navaratnam V, Foong K. Opiate dependence–the role of benzodiazepines. Curr. Med. Res. Opin. 1990; 11: 620-630., doi: 10.1185/03007999009112688.

[51] Lintzeris N, Mitchell TB, Bond A, Nestor L, Strang J. Interactions on mixing diazepam with methadone or buprenorphine in maintenance patients. J. Clin. Psychopharmacol. 2006; 26: 274-283., doi: 10.1097/01.jcp.0000219050.33008.61.

[52] Backmund M, Meyer K, Henkel C, Soyka M, et al. Co-consumption of benzodiazepines in heroin users, methadone-substituted and codeine-substituted patients. J. Addict. Dis. 2005; 24: 17-29., doi: 10.1300/J069v24n0402.

[53] Pick CG. Antinociceptive interaction between alprazolam and opioids. Brain Res. Bull. 1997; 42: 239-243., doi: 10.1016/S0361-9230(96)00265-1.

[54] Primeaux SD, Wilson SP, McDonald AJ, Mascagni F, Wilson MA. The role of delta opioid receptors in the anxiolytic actions of benzodiazepines. Pharmacol. Biochem. Behav. 2006; 85: 545-554., doi: 10.1016/j.pbb.2006.09.025.

[55] Cox RF, Collins MA. The effects of benzodiazepines on human opioid receptor binding and function. Anesth. Analg. 2001; 93: 354-358., doi: 10.1213/00000539-200108000-00024.

[56] Poisnel G, Dhilly M, Le Boisselier R, Barre L, Debruyne D. Comparison of five benzodiazepine-receptor agonists on buprenorphine-induced mu-opioid receptor regulation. J. Pharmacol. Sci. 2009; 110: 36-46., doi: 10.1254/jphs.08249FP.

[57] Walker BM, Ettenberg A. Benzodiazepine modulation of opiate reward. Exp. Clin. Psychopharmacol. 2001; 9: 191-197., doi: 10.1037/1064-1297.9.2.191.

[58] Chen KW, Berger CC, Forde DP, DAdamo C, et al. Benzodiazepine use and misuse among patients in a methadone program. BMC Psychiatry 2011; 11:, doi: 10.1186/1471-244X-11-90.

[59] White JM, Irvine RJ. Mechanisms of fatal opioid overdose. Addiction 1999; 94: 961-972., doi: 10.1046/j.1360-0443.1999.9479612.x.

[60] Mégarbane B, Hreiche R, Pirnay S, Marie N, Baud FJ. Does high-dose buprenorphine cause respiratory depression? Possible mechanisms and therapeutic consequences. Toxicol. Rev. 2006; 25: 79-85., doi: 10.2165/00139709-200625020-00002.

[61] Webster LR. Considering the Risks of Benzodiazepines and Opioids Together. Pain Med. 2010; 11: 801-802., doi: 10.1111/j.1526-4637.2010.00873.x.

[62] Kalyuzhny AE, Dooyema J, Wessendorf MW. Opioid- and GABA(A)-receptors are co-expressed by neurons in rat brain. Neuroreport 2000; 11: 2625-2628., doi: 10.1097/00001756-200008210-00004.

[63] Hollister LE. Interactions between alcohol and benzodiazepines. Recent Dev. Alcohol. 1990; 8: 233-9.

[64] Jedeikin R, Bruderman I, Menutti D, Hoffman S. Prolonged respiratory center depression after alcohol and benzodiazepines. Chest 1985; 87: 262-264., doi: 10.1378/chest.87.2.262.

[65] National Records of Scotland, Drug-related Deaths in Scotland in 2017, 2018.

[66] SA Handley, JD Ramsey RF. Substance misuse-related poisoning deaths, England and Wales, 1993-2016. Drug Sci. Policy Law 2018; 4: 1-18., doi: 10.1177/2050324518767445.

[67] Weaver MF. Prescription sedative misuse and abuse. Yale J. Biol. Med. 2015; 88: 247-256.

[68] Pedersen W, Lavik NJ. Adolescents and benzodiazepines: prescribed use, selfmedication and intoxication. Acta Psychiatr. Scand. 1991; 84: 94-98., doi: 10.1111/j.1600-0447.1991.tb01427.x.

[69] Kapil V, Green JL, Lait C Le, Wood DM, Dargan PI. Misuse of benzodiazepines and Z-drugs in the UK. Br. J. Psychiatry 2014; 205: 407-408.

[70] Clarify AW. Diazepam, Alcohol, and Barbiturate Abuse. Br. Med. J. 1971; 4: 340., doi: 10.1136/bmj.4.5783.340.

[71] Hanna SM. A case of oxazepam (serenid D) dependence. Br. J. Psychiatry 1972; 120: 443-445., doi: 10.1192/bjp.120.557.443.

[72] Glatt MM. Benzodiazepines. Br. Med. J. 1967; 2: 444.

[73] Nutt D, King LA, Saulsbury W, Blakemore C. Development of a rational scale to assess the harm of drugs of potential misuse. Lancet 2007; 369: 1047-1053., doi: 10.1016/S0140-6736(07)60464-4.

[74] Gitto R, Zappalà M, Sarro G De, Chimirri A. Design and development of 2,3-benzodiazepine (CFM) noncompetitive AMPA receptor antagonists. Farm. 2002; 57: 129-134.

[75] Brogden RN, Heel RC, Speight TM, Avery GS. Clobazam: A Review of its Pharmacological Properties and Therapeutic Use in Anxiety. Drugs 1980; 20: 161-178., doi: 10.2165/00003495-198020030-00001.

[76] Hammer H, Ebert B, Jensen HS, Jensen AA. Functional characterization of the 1,5-benzodiazepine clobazam and its major active metabolite n-desmethylclobazam at human GABA$_A$ receptors expressed in xenopus laevis oocytes. PLoS One 2015; 10:, doi: 10.1371/journal.pone.0120239.

[77] Sanna E, Pau D, Tuveri F, Massa F, et al. Molecular and Neurochemical Evaluation of the Effects of Etizolam on GABA$_A$ Receptors under Normal and Stress Conditions. Arzneimittelforschung 2011; 49: 88-95., doi: 10.1055/s-0031-1300366.

[78] Maskell PD, De Paoli G, Nitin Seetohul L, Pounder DJ. Phenazepam: The drug that came in from the cold. J. Forensic Leg. Med. 2012; 19: 122-125., doi: 10.1016/j.jflm.2011.12.014.

[79] OConnell CW, Sadler CA, Tolia VM, Ly BT, et al. Overdose of etizolam: the abuse and rise of a benzodiazepine analog. Ann. Emerg. Med. 2015; 65: 465-466.

[80] Mitsushima T, Ueki S. [Psychopharmacological effects of flutazolam (MS-4101) (authors transl)]. Nihon Yakurigaku Zasshi. 1978; 74: 959-979., doi: 10.1254/fpj.74.959.

[81] Moosmann B, Bisel P, Franz F, Huppertz LM, Auwarter V. Characterization and in vitro phase I microsomal metabolism of designer benzodiazepines - an update comprising adinazolam, cloniprazepam, fonazepam, 3-hydroxyphenazepam, metizolam and nitrazolam. J. Mass Spectrom. 2016; 51: 1080-1089., doi: 10.1002/jms.3840.

[82] Katselou M, Papoutsis I, Nikolaou P, Spiliopoulou C, Athanaselis S. Metabolites replace the parent drug in the drug arena. The cases of fonazepam and nifoxipam. Forensic Toxicol. 2017; 35: 1-10., doi: 10.1007/s11419-016-0338-5.

[83] US Patent. US 3136815, 1964.

[84] Hester JBJ, Rudzik AD, VonVoigtlander PF. 1-(Aminoalkyl)-6-aryl-4-H-s-triazolo[4,3-a][1,4]benzodiazepines with antianxiety and antidepressant activity. J. Med. Chem. 1980; 23: 392-402., doi: 10.1021/jm00178a009.

[85] German Patent, DE2005276C3, 1978.

[86] Medical Products Agency Sweden. https://lakemedelsverket.se/overgripande/Lagar–regler/Yttranden-enligt-lagen-om-forstorande-av-vissa-halsofarliga-missbrukssubstanser/, 2018.

[87] Hester JB, Von Voigtlander P. 6-Aryl-4H-s-Triazolo[4,3-a][1,4]benzodiazepines. Influence of 1-Substitution on Pharmacological Activity. J. Med. Chem. 1979; 22: 1390-1398., doi: 10.1021/jm00197a021.

[88] Hester Jr. JB, Rudzik AD, Kamdar B V. 6-phenyl-4H-s-triazolo[4,3-a][1,4]benzodiazepines which have central nervous system depressant activity. J Med Chem 1971; 14: 1078-1081.

[89] Medical Products Agency Sweden. https://lakemedelsverket.se/overgripande/Lagar–regler/Yttranden-enligt-lagen-om-forstorande-av-vissa-halsofarliga-missbrukssubstanser/, 2018.

[90] Weber K H, Daniel H. Heteroaromaten mit anellierten Siebenringen, IV Thieno[3,2f][1,2,4]triazolo[4,3a[1,4]diazepin6on und Folgeprodukte. Liebigs Ann. der Chemie 1979; 1979: 328-333., doi: 10.1002/jlac.197919790305.

[91] European Patent. EP 0158267, 1985.

[92] Patent U. US 3523939, 1970.

[93] Gesundheit österreich GmbH. EWS-EU: new psychoactive substances.

[94] Tahara T, Araki K, Shiroki M, Matsuo H MT. Syntheses and structure-activity relationships of 6-aryl-4H-s-triazolo[3,4-c]thieno[2,3-e] [1,4]diazepines. Arzneimittelforschung1 978; 28: 1153-1158.

[95] Belgian Early Warning System on Drugs. NPS detected in EU 2018.

[96] Sternbach LH, Fryer RI, Metlesics W, Sach G, Stempel A. Quinazolines and 1,4-Benzodiazepines. V. o-Aminobenzophenones. J. Org. Chem. 1962; 27: 3781-3788.

[97] Hester JB, Rudzik AD, Kamdar B V. 6-phenyl-4H-s-triazolo[4,3-a][1,4]benzodiazepines which have central nervous system depressant activity. J. Med. Chem. 1971; 14: 1078-1081.

[98] US Patent. US 4155913, 1979.

[99] German Patent. DE 1812252A1, 1969.

[100] US Patent. US 4031078, 1977.

[101] US Patent. US 3904641, 1975.

[102] US Patent. US 3987052, 1976.

[103] US Patent. US 3954728, 1979.

[104] US Patent. US 3678036, 1963.

[105] Gesundheit österreich GmbH. EWS-EU: new psychoactive substances.

[106] Kerns EH, Di L. Physicochemical profiling: overview of the screens. Drug Discov. Today. Technol. 2004; 1: 343-348.

[107] Lombardo F, Obach RS, Shalaeva MY, Gao F. Prediction of Human Volume of Distribution Values for Neutral and Basic Drugs. 2. Extended Data Set and Leave-Class-Out Statistics. J. Med. Chem. 2004; 47: 1242-1250., doi: 10.1021/jm030408h.

[108] IUPAC. Compendium of Chemical Terminology. 2014.

[109] Xing L, Glen RC. Novel Methods for the Prediction of logP, pK_a, and logD. J. Chem. Inf. Model. 2002; 42: 796-805.

[110] Lipinski CA, Lombardo F, Dominy BW, Feeney PJ. Experimental and computational approaches to estimate solubility and permeability in drug discovery and development settings. Adv. Drug Deliv. Rev. 1997; 23: 3-25.

[111] Spector AA, Yorek MA. Membrane lipid composition and cellular function. J. Lipid Res. 1985; 26: 1015-1035.

[112] Liu X, Testa B, Fahr A. Lipophilicity and its relationship with passive drug permeation. Pharm. Res. 2011; 28: 962-977.

[113] Leeson PD, Springthorpe B. The influence of drug-like concepts on decision-making in medicinal chemistry. Nat. Rev. Drug Discov. 2007; 6: 881-890.

[114] Sanguinetti MC, Jiang C, Curran ME, Keating MT. A Mechanistic Link between an Inherited and an Acquired Cardiac Arrhythmia: HERG Encodes the IKr Potassium Channel. Cell 1995; 81: 299-307.

[115] Kawai Y, Tsukamoto S, Ito J, Akimoto K, Takahashi M. A Risk Assessment of Human Ether-a-Go-Go-Related Gene Potassium Channel Inhibition by Using Lipophilicity and Basicity for Drug Discovery. Chem. Pharm. Bull. 2011; 59: 1110-1116.

[116] Lázníček M, Lázníčková A. The effect of lipophilicity on the protein binding and blood cell uptake of some acidic drugs. J. Pharm. Biomed. Anal. 1995; 13: 823-828.

[117] Begley DJ. ABC transporters and the blood-brain barrier. Curr. Pharm. Des. 2004; 10: 1295-312., doi: 10.2174/1381612043384844.

[118] Schinkel AH. P-Glycoprotein, a gatekeeper in the blood-brain barrier. Adv. Drug Deliv. Rev. 1999; 36: 176-194.

[119] Tanaka E. Clinically important pharmacokinetic drug-drug interactions: role of cytochrome P450 enzymes. J. Clin. Pharm. Ther. 1998; 23: 403-416.

[120] Guengerich FP. Cytochrome p450 and chemical toxicology. Chem. Res. Toxicol. 2008; 21: 70-83.

[121] Lewis DF V, Lake BG, Dickins M. Quantitative structure-activity relationships (QSARs) in inhibitors of various cytochromes P450: The importance of compound lipophilicity. J. Enzyme Inhib. Med. Chem. 2007; 22: 1-6.

[122] Lewis DF V, Jacobs MN, Dickins M. Compound lipophilicity for substrate binding to human P450s in drug metabolism. Drug Discov. Today 2004; 9: 530-537.

[123] Testa B, Crivori P, Reist M, Carrupt PA. The influence of lipophilicity on the pharmacokinetic behavior of drugs: Concepts and examples. Perspect. Drug Discov. Des. 2000; 19: 179-211., doi: 10.1023/A:1008741731244.

[124] Arnott JA, Planey SL. The influence of lipophilicity in drug discovery and design. Expert Opin. Drug Discov. 2012; 7: 863-875., doi: 10.1517/17460441.2012.714363.

[125] Grassy G, Chavanieu A. Molecular Lipophilicity: A Predominant Descriptor for QSAR inChemogenomics Chem. Genet. (Eds: E. Marechal, S. Roy, L. Lafanechère) Springer, Berlin 2011 pp.153-170.

[126] Dearden JC. Partitioning and lipophilicity in quantitative structure-activity relationships. Environ. Health Perspect. 1985; VOL. 61: 203-228., doi: 10.2307/3430073.

[127] Roy K, Das RN. A Review on Principles, Theory and Practices of 2D-QSAR.2014.

[128] Griffin CE, Kaye AM, Bueno FR, Kaye AD. Benzodiazepine pharmacology and central nervous system-mediated effects. Ochsner J. 2013; 13: 214-23.

[129] García DA, Perillo MA. Benzodiazepine localisation at the lipid-water interface: Effect of membrane composition and drug chemical structure. Biochim. Biophys. Acta - Biomembr. 1999; 1418: 221-231., doi: 10.1016/S0005-2736(99)00040-1.

[130] Aaltonne L, Kanto J, Iisalo E, Koski K, et al. The Passage of Flunitrazepam into Cerebrospinal Fluid in Man. Acta Pharmacol. Toxicol. (Copenh). 1981; 48: 364-368., doi: 10.1111/j.1600-0773.1981.tb01633.x.

[131] Arendt RM, Greenblatt DJ, Liebisch DC, Luu MD, Paul SM. Determinants of benzodi-
azepine brain uptake: lipophilicity versus binding affinity. Psychopharmacology (Berl).
1987; 93: 72-76., doi: 10.1007/BF02439589.

[132] Nilsson A. Pharmacokinetics of benzodiazepines and their antagonists. Baillieres. Clin.
Anaesthesiol. 1991; 5: 615-634.

[133] Litvin AA, Kolyvanov GB, Zherdev VP, Arzamastsev AP. Relationship between physic-
ochemical characteristics and pharmacokinetic parameters of 1,4-benzodiazepine deriva-
tives. Pharm. Chem. J. 2004; 38: 583-586., doi: 10.1007/s11094-005-0034-y.

[134] Tomková J, Švidrnoch M, Maier V, Ondra P. Analysis of selected designer benzodiazepines
by ultra high performance liquid chromatography with high-resolution time-of-flight mass
spectrometry and the estimation of their partition coefficients by micellar electrokinetic
chromatography. J. Sep. Sci. 2017; 40: 2037-2044., doi: 10.1002/jssc.201700069.

[135] Poulin P, Theil FP. Prediction of pharmacokinetics prior to in vivo studies. 1. Mechanism-
based prediction of volume of distribution. J. Pharm. Sci. 2002; 91: 129-156., doi:
10.1002/jps.10005.

[136] Lu D, Chambers P, Wipf P, Xie XQ, et al. Lipophilicity screening of novel drug-like
compounds and comparison to clogP. J. Chromatogr. A 2012; 1258: 161-167., doi:

[137] Wenlock MC, Potter T, Barton P, Austin RP. A method for measuring the lipophilic-
ity of compounds in mixtures of 10. J. Biomol. Screen. 2011; 16: 348-355., doi:
10.1177/1087057110396372.

[138] Csizmadia F, Tsantili-Kakoulidou A, Panderi I, Darvas F. Prediction of distribution co-
efficient from structure. 1. Estimation method. J. Pharm. Sci. 1997; 86: 865-871., doi:
10.1021/js960177k.

[139] Mannhold R, Poda GI, Ostermann C, Tetko I V. Calculation of molecular lipophilicity:
State-of-the-art and comparison of log P methods on more than 96,000 compounds. J.
Pharm. Sci. 2009; 98: 861-893., doi: 10.1002/jps.21494.

[140] Kah M, Brown CD. Log D: Lipophilicity for ionisable compounds. Chemosphere 2008; 72: 1401-1408., doi: 10.1016/j.chemosphere.2008.04.074.

[141] Manallack DT. The pK$_a$ Distribution of Drugs: Application to Drug Discovery. Perspect. Medicin. Chem. 2007; 1: 25-38.

[142] Jelfs S, Ertl P, Selzer P. Estimation of pK$_a$ for druglike compounds using semiempirical and information-based descriptors. J. Chem. Inf. Model. 2007; 47: 450-459., doi: 10.1021/ci600285n.

[143] Avdeef a. Physicochemical profiling (solubility, permeability and charge state). Curr. Top. Med. Chem. 2001; 1: 277-351., doi: 10.2174/1568026013395100.

[144] Smith DA, Beaumont K, Maurer TS, Di L. Volume of Distribution in Drug Design. J. Med. Chem. 2015; 58: 5691-5698., doi: 10.1021/acs.jmedchem.5b00201.

[145] Tracy TS. Drug Absorption and Distrubition inMod. Pharmacol. with Clin. Appl. 2004 pp.20-47.

[146] Kirch W, Görg KG. Clinical pharmacokinetics of atenolol-a review. Eur. J. Drug Metab. Pharmacokinet. 1982; 7: 81-91.

[147] Pichette V, P du Souich. Role of the kidneys in the metabolism of furosemide: its inhibition by probenecid. J. Am. Soc. Nephrol. 1996; 7: 345-349.

[148] Lombardo F, Obach RS, Shalaeva MY, Gao F. Prediction of Volume of Distribution Values in Humans for Neutral and Basic Drugs Using Physicochemical Measurements and Plasma Protein Binding Data. J. Med. Chem. 2002; 45: 2867-2876., doi: 10.1021/jm0200409.

[149] Giaginis C, Tsantili-Kakoulidou A, Theocharis S. Applying Quantitative Structure-Activity Relationship (QSAR) Methodology for Modeling Postmortem Redistribution of Benzodiazepines and Tricyclic Antidepressants. J. Anal. Toxicol. 2014; 38: 242-248., doi: 10.1093/jat/bku025.

[150] Xie X, Steiner SH, Bickel MH. Kinetics of distribution and adipose tissue storage as a function of lipophilicity and chemical structure. II. Benzodiazepines. Drug Metab. Dispos. 1991; 19: 15-19.

[151] Simpson NJK, Martha WJM. Introduction to Solid-Phase Extraction.2000.

[152] Moffat AC, Osselton DM, Widdop B, Watts J. Clarkes Analysis of Drugs and Poison2011.

[153] Barrett J, Smyth WF, Davidson IE. An examination of acidbase equilibria of 1,4benzodiazepines by spectrophotometry. J. Pharm. Pharmacol. 1973; 25: 387-393., doi: 10.1111/j.2042-7158.1973.tb10033.x.

[154] Reijenga J, A van Hoof, A van Loon, Teunissen B. Development of Methods for the Determination of pK$_a$ Values. Anal. Chem. Insights 2013; 8: 53-71.

[155] Babi S, Horvat AJM, Pavlovi DM, Ka štelan-Macan M. Determination of pK$_a$ values of active pharmaceutical ingredients. Trends Anal. Chem. 2007; 26: 1043-1061.

[156] Nowak P, Woniakiewicz M, Kocielniak P. Application of capillary electrophoresis in determination of acid dissociation constant values. J. Chromatogr. A 2015; 1377: 1-12.

[157] Poole SK, Patel S, Dehring K, Workman H, Poole CF. Determination of acid dissociation constants by capillary electrophoresis. J. Chromatogr. A 2004; 1037: 445-454., doi: 10.1016/j.chroma.2004.02.087.

[158] Gluck S, Cleveland Jr. JA. Investigation of experimental approaches to the determination of pK$_a$ values by capillary electrophoresis. J. Chromatogr. A 1994; 680: 49-56., doi: 10.1016/0021-9673(94)80051-0.

[159] IUPAC. Compendium of Chemical Terminology2014.

[160] Gluck S, Cleveland Jr. JA. Investigation of experimental approaches to the determination of pK$_a$ values by capillary electrophoresis. J. Chromatogr. A 1994; 680: 49-56., doi: 10.1016/0021-9673(94)80051-0.

[161] Poole SK, Patel S, Dehring K, Workman H, Poole CF. Determination of acid dissociation constants by capillary electrophoresis. J. Chromatogr. A 2004; 1037: 445-454., doi: 10.1016/j.chroma.2004.02.087.

[162] Liao C, Nicklaus MC. Comparison of Nine Programs Predicting pK_a Values of Pharmaceutical Substances. J. Chem. Inf. Model. 2009; 49: 2801-2812.

[163] Stang PJ, Anderson AG. Hammett and Taft Substituent Constants for the Mesylate, Tosylate, and Triflate Groups. J. Org. Chem. 1976; 41: 781-785., doi: 10.1021/jo00867a007.

[164] Darke SG, Ross JE, Hall WD. Benzodiazepine use among injecting heroin users. Med. J. Aust. 1995; 162: 645-647.

[165] Dobbin M, Martyres RF, Clode D, De Crespigny FEC. Association of benzodiazepine injection with the prescription of temazepam capsules. Drug Alcohol Rev. 2003; 22: 153-157., doi:

[166] Colmenarejo G. In Silico Prediction of Plasma and Tissue Protein Binding inRef. Modul. Chem. Mol. Sci. Chem. Eng. 2014.

[167] Colmenarejo G. In Silico Prediction of Plasma and Tissue Protein Binding inRef. Modul. Chem. Mol. Sci. Chem. Eng. 2014.

[168] Schmidt S, Gonzalez D, Derendorf H. Significance of protein binding in pharmacokinetics and pharmacodynamics. J. Pharm. Sci. 2010; 99: 1107-1122., doi: 10.1002/jps.21916.

[169] Bohnert T, Gan L-S. Plasma protein binding: From discovery to development. J. Pharm. Sci. 2013; 102: 2953-2994., doi: 10.1002/jps.23614.

[170] Routledge PA. The plasma protein binding of basic drugs. Br. J. Clin. Pharmacol. 1986; 22: 499-506.

[171] Tamura A, Kawase F, Sato T, Fujii T. Binding of chlorpromazine, phenytoin and aspirin to the erythrocytes and lipoproteins in whole human blood. J. Pharm. Pharmacol. 1987; 39: 740-742.

[172] Piafsky KM, Borgá O, Odar-Cederlöf I, Johansson C, Sjöqvist F. Increased plasma protein binding of propranolol and chlorpromazine mediated by disease-induced elevations of plasma alpha1 acid glycoprotein. N. Engl. J. Med. 1978; 299: 1435-1439.

[173] Bickel MH. Binding of chlorpromazine and imipramine to red cells, albumin, lipoproteins and other blood components. J. Pharm. Pharmacol. 1975; 27: 733-738.

[174] Bailey DN, Briggs JR. The binding of selected therapeutic drugs to human serum alpha-1 acid glycoprotein and to human serum albumin in vitro. Ther. Drug Monit. 2004; 26: 40-43.

[175] Gibaldi M, Levy G, McNamara PJ. Effect of plasma protein and tissue binding on the biologic half-life of drugs. Clin. Pharmacol. Ther. 1978; 24: 1-4., doi: 10.1002/cpt19782411.

[176] Ghafourian T, Amin Z. QSAR Models for the Prediction of Plasma Protein Binding. BioImpacts 2013; 3: 21-27.

[177] Pellegatti M, Pagliarusco S, Solazzo L, Colato D. Plasma protein binding and blood-free concentrations: which studies are needed to develop a drug? Expert Opin. Drug Metab. Toxicol. 2011; 7: 1009-1020., doi: 10.1517/17425255.2011.586336.

[178] Arendt RM, Greenblatt DJ, deJong RH, Bonin JD, et al. In vitro correlates of benzodiazepine cerebrospinal fluid uptake, pharmacodynamic action and peripheral distribution. J Pharmacol Exp Ther 1983; 227: 98-106.

[179] Bohnert T, Gan L-S. Plasma protein binding: From discovery to development. J. Pharm. Sci. 2013; 102: 2953-2994., doi: 10.1002/jps.23614.

[180] Fanali G, Cao Y, Ascenzi P, Trezza V, et al. Binding of 9-tetrahydrocannabinol and Diazepam to Human Serum Albumin. IUBMB Life 2011; 63: 446-451.

[181] Fasano M, Curry S, Terreno E, Galliano M, et al. The Extraordinary Ligand Binding Properties of Human Serum Albumin. IUBMB Life 2005; 57: 787-796.

[182] Sudlow G, Birkett DJ, Wade DN. The Characterization of Two Specific Drug Binding Sites on Human Serum Albumin. Mol. Pharmacol. 1975; 11: 824-832.

[183] Sudlow G, Birkett DJ, Wade DN. Further characterization of specific drug binding sites on human serum albumin. Mol. Pharmacol. 1976; 12: 1052-1061.

[184] Dockal M, Carter DC, Rüker F. The Three Recombinant Domains of Human Serum Albumin. J. Biol. Chem. 1999; 274: 29303-29310., doi: 10.1074/jbc.274.41.29303.

[185] Zsila F, Bikadi Z, Malik D, Hari P, et al. Evaluation of drug-human serum albumin binding interactions with support vector machine aided online automated docking. Bioinformatics 2011; 27: 1806-1813.

[186] Müller W, Wollert U. Characterization of the Binding of Benzodiazepines to Human Serum Albumin . Naunyn Schmiedebergs Arch. Pharmacolology 1973; 280: 229-237.

[187] Chuang VT, Otagiri M. Flunitrazepam, a 7-nitro-1,4-benzodiazepine that is unable to bind to the indole-benzodiazepine site of human serum albumin. Biochim. Biophys. Acta 2001; 1546: 337-345.

[188] Maruyama T, Furuie MA, Hibino S, Otagiri M. Comparative Study of Interaction Mode of Diazepines with Human Serum Albumin and a,-Acid Glycoprotein . J. Pharm. Sci. 1992; 81: 16-20.

[189] Moschitto LJ, Greenblatt DJ. Concentration-independent plasma protein binding of benzodiazepines. J. Pharm. Pharmacol. 1983; 35: 179-180., doi: 10.1111/j.2042-7158.1983.tb04302.x.

[190] Klotz U, Antonin KH, Bieck PR. Pharmacokinetics and plasma binding of diazepam in man, dog, rabbit, guinea pig and rat. J. Pharmacol. Exp. Ther. 1976; 199: 67-73.

[191] Greenblatt DJ, Wright CE. Clinical pharmacokinetics of alprazolam. Therapeutic implications. Clin. Pharmacokinet. 1993; 24: 453-471.

[192] Zhang F, Xue J, Shao J, Jia L. Compilation of 222 drugs plasma protein binding data and guidance for study designs. Drug Discov. Today 2012; 17: 475-485., doi: 10.1016/j.drudis.2011.12.018.

[193] Divoll M, Greenblatt DJ. Binding of diazepam and desmethyldiazepam to plasma protein: Concentration-dependence and interactions. Psychopharmacology (Berl). 1981; 75: 380-382., doi: 10.1007/BF00435857.

[194] Barré J, Chamouard JM, Houin G, Tillement JP. Equilibrium dialysis, ultrafiltration, and ultracentrifugation compared for determining the plasma-protein-binding characteristics of valproic acid. Clin. Chem. 1985; 31: 60-64.

[195] Ghafourian T, Amin Z. QSAR models for the prediction of plasma protein binding. Bioimpacts 2013; 3: 21-7., doi: 10.5681/bi.2013.011.

[196] Kratochwil NA, Huber W, Müller F, Kansy M, Gerber PR. Predicting plasma protein binding of drugs: a new approach. Biochem. Pharmacol. 2002; 64: 1355-1374., doi: 10.1016/S0006-2952(02)01074-2.

[197] Sun L, Yang H, Li J, Wang T, et al. In Silico Prediction of Compounds Binding to Human Plasma Proteins by QSAR Models. ChemMedChem 2017;, doi: 10.1002/cmdc.201700582.

[198] Rodgers SL, Davis a M, van de Waterbeemd H. Time-series QSAR analysis of human plasma protein binding data. Qsar Comb. Sci. 2007; 26: 511-521., doi: 10.1002/qsar.200630114.

[199] Colmenarejo G, Alvarez-Pedraglio A, Lavandera JL. Cheminformatic models to predict binding affinities to human serum albumin. J. Med. Chem. 2001; 44: 4370-4378., doi: 10.1021/jm010960b.

[200] Votano JR, Parham M, Hall LM, Hall LH, et al. QSAR modeling of human serum protein binding with several modeling techniques utilizing structure-information representation. J. Med. Chem. 2006; 49: 7169-7181., doi: 10.1021/jm051245v.

[201] Toutain PL, Bousquet-Mélou A. Volumes of distribution inJ. Vet. Pharmacol. Ther. 2004 pp.441-453.

[202] Jones DR, Hall SD, Jackson EK, Branch R a, Wilkinson GR. Brain uptake of benzodiazepines: effects of lipophilicity and plasma protein binding. J. Pharmacol. Exp. Ther.

1988; 245: 816-822.

[203] Treiman DM. Pharmacokinetics and clinical use of benzodiazepines in the management of status epilepticus. Epilepsia 1989; 30 Suppl 2: S4-S10., doi: 10.1111/j.1528-1157.1989.tb05824.x.

[204] Lin JH. Tissue distribution and pharmacodynamics: a complicated relationship. Curr. Drug Metab. 2006; 7: 39-65., doi: 10.2174/138920006774832578.

[205] Benet LZ, Zia-Amirhosseini P. Basic principles of pharmacokinetics inToxicol. Pathol. 1995 pp.115-123.

[206] Berry LM, Li C, Zhao Z, Al BET. Species Differences in Distribution and Prediction of Human Vss from Preclinical Data. Drug Metab. Dispos. 2011; 39: 2103-2116., doi: 10.1124/dmd.111.040766.for.

[207] Freitas AA, Limbu K, Ghafourian T. Predicting volume of distribution with decision tree-based regression methods using predicted tissue:plasma partition coefficients. J. Cheminform. 2015; 7:, doi: 10.1186/s13321-015-0054-x.

[208] Jones R Do, Jones HM, Rowland M, Gibson CR, et al. PhRMA CPCDC initiative on predictive models of human pharmacokinetics, part 2: Comparative assessment of prediction methods of human volume of distribution. J. Pharm. Sci. 2011; 100: 4074-4089., doi: 10.1002/jps.22553.

[209] Valkó KL, Nunhuck SB, Hill AP. Estimating unbound volume of distribution and tissue binding by in vitro HPLC-based human serum albumin and immobilised artificial membrane-binding measurements. J. Pharm. Sci. 2011; 100: 849-862., doi: 10.1002/jps.22323.

[210] Jantos R, Schuhmacher M, Veldstra JL, Bosker WM, Klöpping-Ketelaars I, Touliou K, Sardi GM, Brookhuis KA, Ramaekers JG, Mattern R SG. Determination of blood/serum ratios of different forensically relevant analytes in authentic samples. Arch. Kriminol. 2011; 227: 188-203.

[211] Hinderling PH. Red blood cells: a neglected compartment in pharmacokinetics and phar-macodynamics. Pharmacol. Rev. 1997; 49: 279-295.

[212] Jones AW, Larsson H. Distribution of diazepam and nordiazepam between plasma and whole blood and the influence of hematocrit. Ther. Drug Monit. 2004; 26: 380-385., doi: 10.1097/00007691-200408000-00007.

[213] Launiainen T, Ojanper?? I. Drug concentrations in post-mortem femoral blood compared with therapeutic concentrations in plasma. Drug Test. Anal. 2014; 6: 308-316., doi: 10.1002/dta.1507.

[214] Boy RG, Henseler J, Ramaekers JG, Mattern R, Skopp G. A comparison between ex-perimental and authentic blood/serum ratios of 3,4-methylenedioxymethamphetamine and 3,4-methylenedioxyamphetamine. J. Anal. Toxicol. 2009; 33: 283-286., doi: 10.1093/jat/33.5.283.

[215] Hanson VW, Buonarati MH, Baselt RC, Wade NA, et al. Comparison of 3H- and 125I-radioimmunoassay and gas chromatography/mass spectrometry for the determination of delta 9-tetrahydrocannabinol and cannabinoids in blood and serum. J. Anal. Toxicol. 1983; 7: 96-102.

[216] Widman M, Agurell S, Ehrnebo M, Jones G. Binding of (+)- and (-)-delta-1-tetrahydrocannabinols and (minus)-7-hydroxy-delta-1-tetrahydrocannabinol to blood cells and plasma proteins in man. J. Pharm. Pharmacol. 1974; 26: 914-916., doi: 10.1111/j.2042-7158.1974.tb09207.x.

[217] Schwilke EW, Karschner EL, Lowe RH, Gordon AM, et al. Intra-and intersub-ject whole blood/plasma cannabinoid ratios determined by 2-dimensional, electron impact GC-MS with cryofocusing. Clin. Chem. 2009; 55: 1188-1195., doi: 10.1373/clinchem.2008.114405.

[218] Cook CE, Brine DR, Jeffcoat AR, Hill JM, et al. Phencyclidine disposition after intra-venous and oral doses. Clin. Pharmacol. Ther. 1982; 31: 625-34.

[219] Ye M, Nagar S, Korzekwa K. A physiologically based pharmacokinetic model to predict the pharmacokinetics of highly protein-bound drugs and the impact of errors in plasma protein binding. Biopharm. Drug Dispos. 2016; 37: 123-141., doi: 10.1002/bdd.1996.

[220] Yang J, Jamei M, Yeo KR, Rostami-Hodjegan A, Tucker GT. Misuse of the well-stirred model of hepatic drug clearance. Drug Metab. Dispos. 2007;, doi: 10.1124/dmd.106.013359.

[221] Uchimura T, Kato M, Saito T, Kinoshita H. Prediction of human blood-to-plasma drug concentration ratio. Biopharm. Drug Dispos. 2010; 31: 286-97., doi: 10.1002/bdd.711.

[222] Noble C, Mardal M, Bjerre Holm N, Stybe Johansen S, Linnet K. In vitro studies on flubromazolam metabolism and detection of its metabolites in authentic forensic samples. Drug Test. Anal. 2017; 9: 1182-1191., doi: 10.1002/dta.2146.

[223] Yu S, Li S, Yang H, Lee F, et al. A novel liquid chromatography/tandem mass spectrometry based depletion method for measuring red blood cell partitioning of pharmaceutical compounds in drug discovery. Rapid Commun. Mass Spectrom. 2005; 19: 250-254., doi: 10.1002/rcm.1777.

[224] Almazroo OA, Miah MK, Venkataramanan, Almazroo, O. A., Miah, M. K., Venkataramanan R (2017). DM in the LC in LD https://doi. org/10. 1016/j. cld. 2016. 08. 00. R. Drug Metabolism in the Liver. Clin. Liver Dis. 2017; 21: 1-20., doi: 10.1016/j.cld.2016.08.001.

[225] Griffin CE, Kaye AM, Bueno FR, Kaye AD. Benzodiazepine pharmacology and central nervous system-mediated effects. Ochsner J. 2013; 13: 214-23.

[226] Xu C, Li CY-T. Induction of Phase I, II and III Drug Metabolism/Transport by Xenobiotics . Arch. Pharm. Res. 2005; 28: 249-268.

[227] Omiecinski CJ, Heuvel JP Vanden, Perdew GH, Peters JM. Xenobiotic Metabolism, Disposition, and Regulation by Receptors: From Biochemical Phenomenon to Predictors of Major Toxicities. Toxicol. Sci. 2011; 120: S49-S75.

[228] Jancova P, Anzenbacher P, Anzenbacherova E. PHASE II DRUG METABOLIZING EN-ZYMES. Biomed. Pap. Med. Fac. Univ. Palacky, Olomouc, Czechoslov. 2010; 154: 103-116.

[229] Rendic S, F J di Carlo. Human cytochrome P450 enzymes: a status report summarizing their reactions, substrates, inducers, and inhibitors. Drug Metab. Rev. 1997; 29: 413-580.

[230] McKinnon RA, Sorich MJ, Ward MB. Cytochrome P450 Part 1: Multiplicity and Function. J. Pharm. Pract. Res. 2008; 38: 55-57.

[231] Zanger UM, Schwab M. Cytochrome P450 enzymes in drug metabolism: Regulation of gene expression, enzyme activities, and impact of genetic variation. Pharmacol. Ther. 2013; 138: 103-141.

[232] Riner TL, Penning TM. Role of aldo-keto reductase family 1 (AKR1) enzymes in human steroid metabolism. Steroids 2014; 79: 49-63., doi: 10.1016/j.steroids.2013.10.012.

[233] Casey Laizure S, Herring V, Hu Z, Witbrodt K, Parker RB. The role of human car-boxylesterases in drug metabolism: Have we overlooked their importance? Pharma-cotherapy 2013; 33: 210-222., doi: 10.1002/phar.1194.

[234] Fukasawa T, Suzuki A, Otani K. Effects of genetic polymorphism of cytochrome P450 enzymes on the pharmacokinetics of benzodiazepines. J. Clin. Pharm. Ther. 2007; 32: 333-341.

[235] Seree EJ, Pisano PJ, Placidi M, Rahmani R, Barra YA. Identification of the human and animal hepatic cytochromes P450 involved in clonazepam metabolism. Fundam. Clin. Pharmacol. 1993; 7: 69-75.

[236] Miura M, Otani K, Ohkubo T. Identification of human cytochrome P450 enzymes involved in the formation of 4-hydroxyestazolam from estazolam. Xenobiotica. 2005; 35: 455-465., doi: 10.1080/00498250500111612.

[237] Molanaei H, Stenvinkel P, Qureshi AR, Carrero JJ, et al. Metabolism of alprazolam (a marker of CYP3A4) in hemodialysis patients with persistent inflammation. Eur. J. Clin.

Pharmacol. 2012; 68: 571-577.

[238] Park JY, Kim KA, Park PW, Lee OJ, et al. Effect of CYP3A5*3 genotype on the pharmacokinetics and pharmacodynamics of alprazolam in healthy subjects. Clin. Pharmacol. Ther. 2006; 79: 590-599.

[239] Patki KC, L L Von Moltke, Greenblatt DJ. In vitro metabolism of midazolam, triazolam, nifedipine, and testosterone by human liver microsomes and recombinant cytochromes p450: role of cyp3a4 and cyp3a5. Drug Metab. Dispos. 2003; 31: 938-944.

[240] Hesse LM, Venkatakrishnan K, L L von Moltke, Shader RI, Greenblatt DJ. CYP3A4 Is the Major CYP Isoform Mediating the in Vitro Hydroxylation and Demethylation of Flunitrazepam. Drug Metab. Dispos. 2001; 29: 133-140.

[241] Kilicarslan T, Haining RL, Rettie AE, Busto U, et al. Flunitrazepam Metabolism by Cytochrome P450s 2C19 and 3A4. Drug Metab. Dispos. 2001; 29: 460-465.

[242] Venkatakrishnan K, Von Moltke LL, Duan SX, Fleishaker JC, et al. Kinetic characterization and identification of the enzymes responsible for the hepatic biotransformation of adinazolam and N-desmethyladinazolam in man. J. Pharm. Pharmacol. 1998; 50: 265-274., doi: 10.1111/j.2042-7158.1998.tb06859.x.

[243] Coller JK, Somogyi AA, Bochner F. Flunitrazepam oxidative metabolism in human liver microsomes: involvement of CYP2C19 and CYP3A4. Xenobiotica 1999; 29: 973-986.

[244] Mandrioli R, Mercolini L, Raggi M. Benzodiazepine Metabolism: An Analytical Perspective. Curr. Drug Metab. 2008; 9: 827-844., doi: 10.2174/138920008786049258.

[245] Oda M, Kotegawa T, Tsutsumi K, Ohtani Y, et al. The effect of itraconazole on the pharmacokinetics and pharmacodynamics of bromazepam in healthy volunteers. Eur. J. Clin. Pharmacol. 2003; 59: 615-619., doi: 10.1007/s00228-003-0681-4.

[246] Onof S, Hatanaka T, Miyazawa S, Tsutsui M, et al. Human liver microsomal diazepam metabolism using cDNA-expressed cytochrome P450s: Role of CYP2B6, 2C19 and the 3A subfamily. Xenobiotica 1996; 26: 1155-1166., doi: 10.3109/00498259609050260.

[247] Moosmann B, Bisel P, Auwärter V. Characterization of the designer benzodiazepine diclazepam and preliminary data on its metabolism and pharmacokinetics. Drug Test. Anal. 2014; 6: 757-763., doi: 10.1002/dta.1628.

[248] Fracasso C, Confalonieri S, Garattini S, Caccia S. Single and multiple dose pharmacokinetics of etizolam in healthy subjects. Eur. J. Clin. Pharmacol. 1991; 40: 181-185., doi: 10.1007/BF00280074.

[249] Meyer MR, Bergstrand MP, Helander A, Beck O. Identification of main human urinary metabolites of the designer nitrobenzodiazepines clonazolam, meclonazepam, and nifoxipam by nano-liquid chromatography-high-resolution mass spectrometry for drug testing purposes. Anal. Bioanal. Chem. 2016; 408: 3571-3591.

[250] Peppers MP. Benzodiazepines for alcohol withdrawal in the elderly and in patients with liver disease. Pharmacotherapy 1996; 16: 49-57.

[251] Moosmann B, Huppertz LM, Hutter M, Buchwald A, et al. Detection and identification of the designer benzodiazepine flubromazepam and preliminary data on its metabolism and pharmacokinetics. J. Mass Spectrom. 2013; 48: 1150-1159.

[252] Wells PG, Mackenzie PI, Chowdhury JR, Guillemette C, et al. Glucuronidation and the UDP-Glucuronosyltransferases in health and disease. Drug Metab. Dispos. 2004; 32: 281-290.

[253] Mandrioli R, Mercolini L, Raggi M. Benzodiazepine Metabolism: An Analytical Perspective. Curr. Drug Metab. 2008; 9: 827-844., doi: 10.2174/138920008786049258.

[254] Olivera M, Martínez C, Gervasini G, Carrillo JA, et al. Effect of common NAT2 variant alleles in the acetylation of the major clonazepam metabolite, 7-aminoclonazepam. Drug Metab. Lett. 2007; 1: 3-5.

[255] Ekins S, Ring BJ, Grace J, McRobie-Belle DJ, Wrighton S a. Present and future in vitro approaches for drug metabolism. J. Pharmacol. Toxicol. Methods 2001; 44: 313-24., doi: S1056-8719(00)00110-6 [pii].

[256] Vikingsson S, Wohlfarth A, Andersson M, Gréen H, et al. Identifying Metabolites of Meclonazepam by High-Resolution Mass Spectrometry Using Human Liver Microsomes, Hepatocytes, a Mouse Model, and Authentic Urine Samples. AAPS J. 2017; 19: 736-742., doi: 10.1208/s12248-016-0040-x.

[257] Huppertz LM, Bisel P, Westphal F, Franz F, et al. Characterization of the four designer benzodiazepines clonazolam, deschloroetizolam, flubromazolam, and meclonazepam, and identification of their in vitro metabolites. Forensic Toxicol. 2015; 33: 388-395.

[258] Pettersson Bergstrand M, Meyer MR, Beck O, Helander A. Human urinary metabolic patterns of the designer benzodiazepines flubromazolam and pyrazolam studied by liquid chromatography-high resolution mass spectrometry. Drug Test. Anal. 2018; 10: 496-506., doi: 10.1002/dta.2243.

[259] Moosmann B, Bisel P, Auwärter V. Characterization of the designer benzodiazepine diclazepam and preliminary data on its metabolism and pharmacokinetics. Drug Test. Anal. 2014; 6: 757-763.

[260] Bergstrand M, Richter L, Maurer H, Wagmann L, Meyer M. In vitro glucuronidation of designer benzodiazepines by human UDP glucuronyltransferases. Drug Test. Anal. 2018;, doi: 10.1002/dta.2463.

[261] Gerets HHJ, Tilmant K, Gerin B, Chanteux H, et al. Characterization of primary human hepatocytes, HepG2 cells, and HepaRG cells at the mRNA level and CYP activity in response to inducers and their predictivity for the detection of human hepatotoxins. Cell Biol. Toxicol. 2012; 28: 69-87.

[262] Donato MT, Lahoz A, Castell J V, Gómez-Lechón MJ. Cell lines: a tool for in vitro drug metabolism studies. Curr Drug Metab. 2008; 9: 1-11., doi: 10.2174/138920008783331086.

[263] Shulman M, Nahmias Y. Long-term culture and coculture of primary rat and human hepatocytes. Methods Mol. Biol. 2013; 945: 287-302., doi: 10.1007/978-1-62703-125-717.

[264] Lee J, Liu X. The conduct of drug metabolism studies considered good practice (II): in vitro experiments. Curr Drug Metab. 2007 2007; 8: 822-829., doi: 10.2174/138920007782798207.

[265] Westerink WMA, Schoonen WGEJ. Cytochrome P450 enzyme levels in HepG2 cells and cryopreserved primary human hepatocytes and their induction in HepG2 cells. Toxicol. Vitr. 2007; 21: 1581-1591.

[266] Wilkening S, Stahl F, Bader A. Comparison of primary human hepatocytes and hepatoma cell line Hepg2 with regard to their biotransformation properties. Drug Metab. Dispos. 2003; 31: 1035-1042.

[267] U.S. Permanent Human Hepatocyte Cell Line and Its Use in a Liver Assist Device (LAD) , 1994.

[268] Gaskell H, Sharma P, Colley HE, Murdoch C, et al. Characterization of a functional C3A liver spheroid model. Toxicol. Res. (Camb). 2016; 5: 1053-1065.

[269] Nelson LJ, Morgan K, Treskes P, Samuel K, et al. Human Hepatic HepaRG Cells Maintain an Organotypic Phenotype with High Intrinsic CYP450 Activity/Metabolism and Significantly Outperform Standard HepG2/C3A Cells for Pharmaceutical and Therapeutic Applications. Basic Clin. Pharmacol. Toxicol. 2017; 120: 30-37.

[270] Wenum M van, Adam AAA, Hakvoort TBM, Hendriks EJ, et al. Selecting Cells for Bioartificial Liver Devices and the Importance of a 3D Culture Environment: A Functional Comparison between the HepaRG and C3A Cell Lines. Int. J. Biol. Sci. 2016; 12: 964-978., doi: 10.7150/ijbs.15165.

[271] Choi S, B. Sainz J, Corcoran P, Uprichard S, Jeong H. Characterization of increased drug metabolism activity in dimethyl sulfoxide (DMSO)-treated Huh7 hepatoma cells. Xenobiotica 2009; 39: 205-217.

[272] Nikolaou N, Green CJ, Gunn PJ, Hodson L, Tomlinson JW. Optimizing human hepatocyte models for metabolic phenotype and function: effects of treatment with dimethyl sulfoxide (DMSO). Physiol. Rep. 2016; 4: e12944.

[273] Gripon P, Rumin S, Urban S, Seyec J Le, et al. Infection of a human hepatoma cell line by hepatitis B virus. Proc. Natl. Acad. Sci. U. S. A. 2002; 99: 15655-15660.

[274] Guillouzo A, Corlu A, Aninat C, Glaise D, et al. The human hepatoma HepaRG cells: A highly differentiated model for studies of liver metabolism and toxicity of xenobiotics. Chem. Biol. Interact. 2007; 168: 66-73.

[275] Kanebratt KP, Andersson TB. HepaRG cells as an in vitro model for evaluation of cytochrome P450 induction in humans. Drug Metab. Dispos. 2008; 36: 137-145.

[276] Lambert CB, Spire C, Claude N, Guillouzo A. Dose- and time-dependent effects of phenobarbital on gene expression profiling in human hepatoma HepaRG cells. Toxicol. Appl. Pharmacol. 2009; 234: 345-360.

[277] Lübberstedt M, Müller-Vieira U, Mayer M, Biemel KM, et al. HepaRG human hepatic cell line utility as a surrogate for primary human hepatocytes in drug metabolism assessment in vitro. J. Pharmacol. Toxicol. Methods 2011; 63: 59-68.

[278] Hewitt NJ, Hewitt P. Phase I and II enzyme characterization of two sources of HepG2 cell lines. Xenobiotica 2004; 34: 243-256.

[279] Huang SM, Strong JM, Zhang L, Reynolds KS, et al. Drug interactions/review: New era in drug interaction evaluation: US Food and Drug Administration update on CYP enzymes, transporters, and the guidance process. J. Clin. Pharmacol. 2008; 48: 662-670., doi: 10.1177/0091270007312153.

[280] Kirchmair J, Göller AH, Lang D, Kunze J, et al. Predicting drug metabolism: experiment and/or computation? Nat. Rev. Drug Discov. 2015; 14: 387-404.

[281] Olsen RW, Sieghart W. GABA A receptors: subtypes provide diversity of function and pharmacology. Neuropharmacology 2009; 56: 141-148.

[282] Olsen RW, Sieghart W. International Union of Pharmacology. LXX. Subtypes of gamma-aminobutyric acid(A) receptors: classification on the basis of subunit composition, pharmacology, and function. Update. Pharmacol. Rev. 2008; 60: 243-260.

[283] Baumann SW, Baur R, Sigel E. Individual properties of the two functional agonist sites in GABA$_A$ receptors. J. Neurosci. 2003; 23: 11158-11166., doi: 23/35/11158 [pii].

[284] Sigel E. Mapping of the Benzodiazepine Recognition Site on GABA-A Receptors. Curr. Top. Med. Chem. 2002; 2: 833-839.

[285] Wang Q, Han Y, Xue H. Ligands of the GABA$_A$ Receptor Benzodiazepine Binding Site. CNS Drug Rev. 2006; 5: 125-144.

[286] Sieghart W, Sperk G. Subunit Composition, Distribution and Function of GABA-A Receptor Subtypes. Curr. Top. Med. Chem. 2002; 2: 795-816., doi: 10.2174/1568026023393507.

[287] Hosie AM, Wilkins ME, Smart TG. Neurosteroid binding sites on GABA$_A$ receptors. Pharmacol. Ther. 2007; 116: 7-19., doi: 10.1016/j.pharmthera.2007.03.011.

[288] Carpenter TS, Lau EY, Lightstone FC. Identification of a possible secondary picrotoxin-binding site on the GABA$_A$ receptor. Chem. Res. Toxicol. 2013; 26: 1444-1454., doi: 10.1021/tx400167b.

[289] Sigel E, Steinmann ME. Structure, Function, and Modulation of GABA$_A$ Receptors. J. Biol. Chem. 2012; 287: 40224-40231.

[290] McCormick DA. GABA as an inhibitory neurotransmitter in human cerebral cortex. J. Neurophysiol. 1989; 62: 1018-1027., doi: 10.1152/jn.1989.62.5.1018.

[291] Gallager DW, Mallorga P, Thomas JW, Tallman JF. GABA-benzodiazepine interactions: physiological, pharmacological and developmental aspects. Fed Proc 1980; 39: 3043-3049.

[292] Haefely W. Benzodiazepine interactions with GABA receptors. Neurosci. Lett. 1984; 47: 201-206., doi: 10.1016/0304-3940(84)90514-7.

[293] Bianchi MT, Botzolakis EJ, Lagrange AH, Macdonald RL. Benzodiazepine modulation of GABA$_A$receptor opening frequency depends on activation context: A patch clamp and simulation study. Epilepsy Res. 2009; 85: 212-220., doi: 10.1016/j.eplepsyres.2009.03.007.

[294] Bateson AN. The benzodiazepine site of the GABA$_A$ receptor: an old target with new potential? Sleep Med. 2004; 5: S9-S15., doi: 10.1016/S1389-9457(04)90002-0.

[295] Maddalena DJ, Johnston GA. Prediction of receptor properties and binding affinity of ligands to benzodiazepine/GABA$_A$ receptors using artificial neural networks. J Med Chem 1995; 38: 715-724.

[296] Holmes P V, Drugan RC. Differential effects of anxiogenic central and peripheral benzo-diazepine receptor ligands in tests of learning and memory. Psychopharmacology (Berl). 1991; 104: 249-254.

[297] Papadopoulos V, Baraldi M, Guilarte TR, Knudsen TB, et al. Translocator protein (18 kDa): new nomenclature for the peripheral-type benzodiazepine receptor based on its structure and molecular function. Trends Pharmacol. Sci. 2006; 27: 402-409.

[298] Papadopoulos V, Lecanu L. Translocator protein (18 kDa) TSPO: An emerging thera-peutic target in neurotrauma. Exp. Neurol. 2009; 219: 53-57.

[299] Rupprecht R, Rammes G, Eser D, Baghai TC, et al. Translocator protein (18 kD) as target for anxiolytics without benzodiazepine-like side effects. Science (80-.). 2009; 325: 490-493.

[300] Rupprecht R, Papadopoulos V, Rammes G, Baghai TC, et al. Translocator protein (18 kDa) (TSPO) as a therapeutic target for neurological and psychiatric disorders. Nat. Rev. Drug Discov. 2010; 9: 971-988.

[301] Casellas P, Galiegue S, Basile AS. Peripheral benzodiazepine receptors and mitochondrial function. Neurochem. Int. 2002; 40: 475-486.

[302] Gavish M, Katz Y, Bar-Ami S, Weizman R. Biochemical, Physiological, and Pathological Aspects of the Peripheral Benzodiazepine Receptor. J. Neurochem. 1992; 58: 1589-1601.

[303] Gavish M, Bachman I, Shoukrun R, Katz Y, et al. Enigma of the Peripheral Benzodi-azepine Receptor. Pharmacol. Rev. 1999; 51: 629-650.

[304] Persona K, Madej K, Knihnicki P, Piekoszewski W. Analytical methodologies for the determination of benzodiazepines in biological samples. J. Pharm. Biomed. Anal. 2015; 113: 239-264., doi: 10.1016/j.jpba.2015.02.017.

[305] Segura M, Barbosa J, Torrens M, Farré M, et al. Analytical methodology for the detection of benzodiazepine consumption in opioid-dependent subjects. J. Anal. Toxicol. 2001; 25: 130-136., doi: 10.1093/jat/25.2.130.

[306] Nasir Uddin M. An Overview on Total Analytical Methods for the Detection of 1,4-Benzodiazepines. Pharm. Anal. Acta 2014; 05:, doi: 10.4172/2153-2435.1000303.

[307] Kim J, Lee S, In S, Choi H, Chung H. Validation of a simultaneous analytical method for the detection of 27 benzodiazepines and metabolites and zolpidem in hair using LC-MS/MS and its application to human and rat hair. J. Chromatogr. B Anal. Technol. Biomed. Life Sci. 2011; 879: 878-886., doi: 10.1016/j.jchromb.2011.02.038.

[308] Ashri NY, Abdel-Rehim M. Sample treatment based on extraction techniques in biological matrices. Bioanalysis 2011; 3: 2003-2018., doi: 10.4155/bio.11.201.

[309] Toninandel L, Seraglia R. Matrix effect, signal suppression and enhancement in LC-ESI-MS. Adv. LC-MS Instrum. 2007; 72: 193.

[310] Buszewski B, Szultka M. Past, Present, and Future of Solid Phase Extraction: A Review. Crit. Rev. Anal. Chem. 2012; 42: 198-213., doi: 10.1080/07373937.2011.645413.

[311] Andrade-Eiroa A, Canle M, Leroy-Cancellieri V, Cerdà V. Solid-phase extraction of organic compounds: A critical review (Part I). TrAC - Trends Anal. Chem. 2016; 80: 641-654., doi: 10.1016/j.trac.2015.08.015.

[312] El Balkhi S, Chaslot M, Picard N, Dulaurent S, et al. Characterization and identification of eight designer benzodiazepine metabolites by incubation with human liver microsomes and analysis by a triple quadrupole mass spectrometer. Int. J. Legal Med. 2017; 10.1007/s00414-017-1541-6.

[313] Mortelé O, Vervliet P, Gys C, Degreef M, et al. In vitro Phase I and Phase II metabolism of the new designer benzodiazepine cloniprazepam using liquid chromatography coupled to quadrupole time-of-flight mass spectrometry. J. Pharm. Biomed. Anal. 2018; 153: 158-167., doi: 10.1016/j.jpba.2018.02.032.

[314] Vikingsson S, Wohlfarth A, Andersson M, Green H, et al. Identifying Metabolites of Meclonazepam by High-Resolution Mass Spectrometry Using Human Liver Microsomes, Hepatocytes, a Mouse Model, and Authentic Urine Samples. AAPS J. 2017;, doi: 10.1208/s12248-016-0040-x.

[315] Wohlfarth A, Vikingsson S, Roman M, Andersson M, et al. Looking at flubromazolam metabolism from four different angles: metabolite profiling in human liver microsomes, human hepatocytes, mice and authentic human urine samples with liquid chromatography high-resolution mass spectrometry . Forensic Sci. Int. 2017; 274: 55-63., doi: 10.1016/j.forsciint.2016.10.021.

[316] Inoue H, Maeno Y, Iwasa M, Matoba R, Nagao M. Screening and determination of benzodiazepines in whole blood using solid-phase extraction and gas chromatography/mass spectrometry. Forensic Sci.Int. 2000; 113: 367-373., doi: 10.1016/S0379-0738(00)00226-7.

[317] Nakamae T, Shinozuka T, Sasaki C, Ogamo A, et al. Case report: Etizolam and its major metabolites in two unnatural death cases. Forensic Sci. Int. 2008; 182: e1-e6., doi: 10.1016/j.forsciint.2008.08.012.

[318] Morini L, Vignali C, Polla M, Sponta A, Groppi A. Comparison of extraction procedures for benzodiazepines determination in hair by LC-MS/MS. Forensic Sci. Int. 2012; 218: 53-56., doi: 10.1016/j.forsciint.2011.10.013.

[319] Kaliszan R. High Performance Liquid Chromatographic Methods and Procedures of Hydrophobicity Determination. Quantitative Structure-Activity Relationships. 1990; 9: 83-87., doi: 10.1002/qsar.19900090202.

[320] Aguilar M-I. Reversed-Phase High-Performance Liquid Chromatography. HPLC Pept. Proteins Methods Protoc. 2004; 251: 9-22., doi: 10.1385/1-59259-742-4:9.

[321] Šuleková M, Hudák A, Smcová M. The determination of food dyes in vitamins by RP-HPLC. Molecules 2016; 21:, doi: 10.3390/molecules21101368.

[322] Swartz M. HPLC detectors: A brief review. J. Liq. Chromatogr. Relat. Technol. 2010; 33: 1130-1150., doi: 10.1080/10826076.2010.484356.

[323] Hussain SZ, Maqbool K. GC-MS: Principle, Technique and its application in Food Science. INT J CURR SCI 2014; 13: 116-126.

[324] Gunnar T, Ariniemi K, Lillsunde P. Determination of 14 benzodiazepines and hydroxy metabolites, zaleplon and zolpidem as tert-butyldimethylsilyl derivatives compared with other common silylating reagents in whole blood by gas chromatography-mass spectrometry. J. Chromatogr. B Anal. Technol. Biomed. Life Sci. 2005; 818: 175-189., doi: 10.1016/j.jchromb.2004.12.032.

[325] Tiscione N, Shan X, Alford I, Yeatman D. Quantitation of benzodiazepines in whole blood by electron impact-gas chromatography-mass spectrometry. J. Anal. Toxicol. 2008; 32: 644-652.

[326] Siuzdak G. An Introduction to Mass Spectrometry Ionization: An Excerpt from The Expanding Role of Mass Spectrometry. Biotechnology 2004; 50-63., doi: 10.1016/j.jala.2004.01.004.

[327] Mbughuni MM, Jannetto PJ, Langman LJ. Mass Spectrometry Applications for Toxicology. Ejifcc 2016; 27: 272-287.

[328] Ho CS, Lam CWK, Chan MHM, Cheung RCK, et al. Electrospray ionisation mass spectrometry: principles and clinical applications. Clin. Biochem. 2003; 24: 3-12., doi: 10.1146/annurev.bi.64.070195.001531.

[329] Mbughuni MM, Jannetto PJ, Langman LJ. Mass Spectrometry Applications for Toxicology. Ejifcc 2016; 27: 272-287.

[330] Chernushevich I V., Loboda A V., Thomson BA. An introduction to quadrupole-time-of-flight mass spectrometry. J. Mass Spectrom. 2001; 36: 849-865., doi: 10.1002/jms.207.

[331] El-Aneed A, Cohen A, Banoub J. Mass spectrometry, review of the basics: Electrospray, MALDI, and commonly used mass analyzers. Appl. Spectrosc. Rev. 2009; 44: 210-230., doi: 10.1080/05704920902717872.

[332] Boesl U. Time-of-flight mass spectrometry: Introduction to the basics. Mass Spectrom. Rev. 2017; 36: 86-109., doi: 10.1002/mas.21520.

[333] Roman M, Strom L, Tell H, Josefsson M. Liquid chromatography/time-of-flight mass spectrometry analysis of postmortem blood samples for targeted toxicological screening. Anal. Bioanal. Chem. 2013; 405: 4107-4125., doi: 10.1007/s00216-013-6798-0.

[334] Mandema JW, Sansom LN, Dios-Vièitez MC, Hollander-Jansen M, Danhof M. Pharmacokinetic-pharmacodynamic modeling of the electroencephalographic effects of benzodiazepines. Correlation with receptor binding and anticonvulsant activity. J. Pharmacol. Exp. Ther. 1991; 257: 472-8.

[335] ICH guidelines. Q2(R1): Validation of Analytical Procedures: Text and Methodology. Int. Conf. Harmon. 2005; 1994: 17., doi: http://www.ich.org/fileadmin/PublicWebSite/ICHProducts/Guidelines/Quality/Q2R1/Step4/Q2R

[336] Gu H, Liu G, Wang J, Aubry AF, Arnold ME. Selecting the correct weighting factors for linear and quadratic calibration curves with least-squares regression algorithm in bioanalytical LC-MS/MS assays and impacts of using incorrect weighting factors on curve stability, data quality, and assay perfo. Anal. Chem. 2014;, doi: 10.1021/ac5018265.

[337] Duer WC, Ogren PJ, Meetze A, Kitchen CJ, et al. Comparison of ordinary, weighted, and generalized least-squares straight-line calibrations for LC-MS-MS, GC-MS, HPLC, GC, and enzymatic assay. J. Anal. Toxicol. 2008;, doi: 10.1093/jat/32.5.329.

[338] ACD/I-Lab. https://ilab.acdlabs.com/iLab2/. 2018.

[339] ChemAxon MarvinSketch. https://chemaxon.com/products/marvin. 2018.

[340] Simulations Plus ADMET Predictor. https://www.simulations-plus.com/software/admetpredictor/. 2018.

[341] Miller JM, Blackburn AC, Shi Y, Melzak AJ, Ando HY. Semi-empirical relationships between effective mobility, charge, and molecular weight of pharmaceuticals by pressure-assisted capillary electrophoresis: Applications in drug discovery. Electrophoresis 2002; 23: 2833-2841., doi: 10.1002/1522-2683(200209)23:17¡2833::AID-ELPS2833¿3.0.CO;2-7.

[342] Banker MJ, Clark TH, Williams JA. Development and validation of a 96-well equilibrium dialysis apparatus for measuring plasma protein binding. J. Pharm. Sci. 2003; 92: 967-974., doi: 10.1002/jps.10332.

[343] Atherton JC. Acid-base balance: maintenance of plasma pH. Anaesth. Intensive Care Med. 2009; 10: 557-561., doi: 10.1016/j.mpaic.2009.08.005.

[344] PreADMET. https://preadmet.bmdrc.kr/. 2018

[345] Ihaka K, Gentleman R. R: A language for data analysis and graphics. J. Comput. Graph. Stat. 1996; 5: 299-314.

[346] Dixit V, Hariparsad N, Desai P, Unadkat JD. In vitro LC-MS cocktail assays to simultaneously determine human cytochrome P450 activities. Biopharm. Drug Dispos. 2007;, doi: 10.1002/bdd.552.

[347] Wang JJ, Guo JJ, Zhan J, Bu HZ, Lin JH. An in-vitro cocktail assay for assessing compound-mediated inhibition of six major cytochrome P450 enzymes. J. Pharm. Anal. 2014;, doi: 10.1016/j.jpha.2014.01.001.

[348] Schaefer N, Peters B, Schmidt P, Ewald AH. Development and validation of two LC-MS/MS methods for the detection and quantification of amphetamines, designer amphetamines, benzoylecgonine, benzodiazepines, opiates, and opioids in urine using turbulent flow chromatography. Anal. Bioanal. Chem. 2013; 405: 247-258., doi: 10.1007/s00216-012-6458-9.

[349] Miraghaei S, Mohammadi B, Babaei A, Keshavarz S, Bahrami G. Development and validation of a new HPLC-DAD method for quantification of sofosbuvir in human serum and its comparison with LC-MS/MS technique: Application to a bioequivalence study. J. Chromatogr. B 2017; 1063: 118-122., doi: https://doi.org/10.1016/j.jchromb.2017.06.047.

[350] Erni F, Steuer W, Bosshardt H. Automation and validation of HPLC-systems. Chromatographia 1987; 24: 201-207., doi: 10.1007/BF02688481.

[351] Al-Hawasli H, Al-Khayat MA, Al-Mardini MA. Development of a validated HPLC method for the separation and analysis of a Bromazepam, Medazepam and Midazolam mixture. J. Pharm. Anal. 2012; 2: 484-491., doi: 10.1016/j.jpha.2012.05.001.

[352] Uddin MN, Samanidou VF, Papadoyannis IN. Development and validation of an HPLC method for the determination of benzodiazepines and tricyclic antidepressants in biological fluids after sequential SPE. J. Sep. Sci. 2008;, doi: 10.1002/jssc.200800079.

[353] Manchester KR, Maskell PD, Waters L. Experimental versus theoretical log $D_{7.4}$, pK_a and plasma protein binding values for benzodiazepines appearing as new psychoactive substances. Drug Test. Anal. 2018;, doi: 10.1002/dta.2387.

[354] Bridwell H, Dhingra V, Peckman D, Roark J, Lehman T. Perspectives on Method Validation: Importance of Adequate Method Validation. Qual. Assur. J. n.d.; 13: 72-77., doi: 10.1002/qaj.473.

[355] Pérez-Lozano P, García-Montoya E, Orriols A, Miarro M, et al. Development and validation of a new HPLC analytical method for the determination of alprazolam in tablets. J. Pharm. Biomed. Anal. 2004;, doi: 10.1016/j.jpba.2003.12.012.

[356] M. El-Gizawy S. Simultaneous Determination of Diazepam, Oxazepam and Temazepam in Spiked Urine By Hplc. Anal. Lett. - ANAL LETT 2000; 33: 629-638.

[357] Mercolini L, Mandrioli R, Amore M, Raggi MA. Separation and HPLC analysis of 15 benzodiazepines in human plasma. J. Sep. Sci. 2008;, doi: 10.1002/jssc.200800212.

[358] Bazmi E, Behnoush B, Akhgari M, Bahmanabadi L. Quantitative analysis of benzodiazepines in vitreous humor by high-performance liquid chromatography. SAGE Open Med. 2016;, doi: 10.1177/2050312116666243.

[359] Perez ER, Knapp JA, Horn CK, Stillman SL, et al. Comparison of LC-MS-MS and GC-MS analysis of benzodiazepine compounds included in the drug demand reduction

urinalysis program. J. Anal. Toxicol. 2016;, doi: 10.1093/jat/bkv140.

[360] Krone N, Hughes BA, Lavery GG, Stewart PM, et al. Gas chromatography/mass spectrometry (GC/MS) remains a pre-eminent discovery tool in clinical steroid investigations even in the era of fast liquid chromatography tandem mass spectrometry (LC/MS/MS). J. Steroid Biochem. Mol. Biol. 2010;, doi: 10.1016/j.jsbmb.2010.04.010.

[361] Araujo P. Key aspects of analytical method validation and linearity evaluation. J. Chromatogr. B Anal. Technol. Biomed. Life Sci. 2009;, doi: 10.1016/j.jchromb.2008.09.030.

[362] Blachut D, Bykas-Strêkowska M, Taracha E, Szukalski B. Application of Gas Chromatography/mass spectrometry (GC/MS) to the analysis of benzodiazepines. Probl. Forensic Sci. 2004; 59: 5-37.

[363] Valentine JL, Middleton R, Sparks C. Identification of urinary benzodiazepines and their metabolites: Comparison of automated HPLC and GC-MS after immunoassay screening of clinical specimens. J. Anal. Toxicol. 1996; 20: 416-424., doi: 10.1093/jat/20.6.416.

[364] Papoutsis II, Athanaselis SA, Nikolaou PD, Pistos CM, et al. Development and validation of an EI-GC-MS method for the determination of benzodiazepine drugs and their metabolites in blood: Applications in clinical and forensic toxicology. J. Pharm. Biomed. Anal. 2010;, doi: 10.1016/j.jpba.2010.01.027.

[365] Lakshmi HimaBindu MR, Angala Parameswari S, Gopinath C. A review on GC-MS and method development and validation. Int. J. Pharm. Qual. Assur. 2013;

[366] Damien R, Daval S, Souweine B, Deteix P, et al. Rapid gas chromatography/mass spectrometry quinine determination in plasma after automated solid-phase extraction. Rapid Commun. Mass Spectrom. 2006;, doi: 10.1002/rcm.2625.

[367] Benet LZ, Broccatelli F, Oprea TI. BDDCS Applied to Over 900 Drugs. AAPS J. 2011; 13: 519-547., doi: 10.1208/s12248-011-9290-9.

[368] Giaginis C, Theocharis S, Tsantili-Kakoulidou A. Contribution to the standardization of the chromatographic conditions for the lipophilicity assessment of neutral and basic

drugs. Anal. Chim. Acta 2006; 573-574: 311-318., doi: 10.1016/j.aca.2006.03.074.

[369] Hansch C, Björkroth JP, Leo A. Hydrophobicity and central nervous system agents: On the principle of minimal hydrophobicity in drug design. J. Pharm. Sci. 1987; 76: 663-687., doi: 10.1002/jps.2600760902.

[370] Lombardo F, Shalaeva MY, Tupper KA, Gao F. ElogD o ct: A Tool for Lipophilicity Determination in Drug Discovery. 2. Basic and Neutral Compounds. J. Med. Chem. 2001; 44: 2490-2497., doi: 10.1021/jm0100990.

[371] Di L, Kerns EH. Drug-Like Properties: Concepts, Structure Design and Methods from ADME to Toxicity OptimizationElsevier, London, U.K.,2016.

[372] Unger SH, Chiang GH. Octanol-Physiological Buffer Distribution Coefficients of Lipophilic Amines by Reversed-Phase High-Performance Liquid Chromatography and Their Correlation with Biological Activity. J. Med. Chem. 1981; 24: 262-270., doi: 10.1021/jm00135a006.

[373] McLure JA, Miners JO, Birkett DJ. Nonspecific binding of drugs to human liver microsomes. Br. J. Clin. Pharmacol. 2000; 49: 453-461.

[374] Alimuddin M, Grant D, Bulloch D, Lee N, et al. Determination of log D via Automated Microfluidic Liquid-Liquid Extraction. J. Med. Chem. 2008; 51: 5140-5142.

[375] Alelyunas YW, Pelosi-Kilby L, Turcotte P, Kary M-B, Spreen RC. A high throughput dried DMSO Log D lipophilicity measurement based on 96-well shake-flask and atmospheric pressure photoionization mass spectrometry detection. J. Chromatogr. A 2010; 1217: 1950-1955.

[376] Ferreira LA, Chervenak A, Placko S, Kestranek A, et al. Effect of ionic composition on the partitioning of organic compounds in octanol-buffer systems. RSC Adv. 2015; 5: 20574-20582., doi: 10.1039/c5ra01402f.

[377] Wang P H, Lien EJ. Effects of different buffer species on partition coefficients of drugs used in quantitative structure-activity relationships. J. Pharm. Sci. 1980; 69: 662-668.,

doi: 10.1002/jps.2600690614.

[378] Sangster J. OctanolWater Partition Coefficients of Simple Organic Compounds. J. Phys. Chem. Ref. Data 1989; 18: 1111-1229., doi: 10.1063/1.555833.

[379] Costa EC, Cassamale TB, Carvalho DB, Bosquiroli LSS, et al. Antileishmanial activity and structure-activity relationship of triazolic compounds derived from the neolignans grandisin, veraguensin, and machilin G. Molecules 2016; 21:, doi: 10.3390/molecules21060802.

[380] Chu W, Rothfuss J, Zhou D, MacH RH. Synthesis and evaluation of isatin analogs as caspase-3 inhibitors: Introduction of a hydrophilic group increases potency in a whole cell assay. Bioorganic Med. Chem. Lett. 2011; 21: 2192-2197., doi: 10.1016/j.bmcl.2011.03.015.

[381] Klopman G, Li JY, Wang S, Dimayuga M, et al. Computer Automated log P Calculations Based on an Extended Group Contribution Approach. J. Chem. Inf. Comput. Sci. 1994; 34: 752-781., doi: 10.1021/ci00020a009.

[382] Moffat AC, Osselton MD, Widdop B, Watts J. Clarkes Analysis of Drugs and PoisonsPharmaceutical Press, London, U.K.,2011.

[383] Graf E, El-Menshawy M. pK- und Vk-Messungen an Benzodiazepinen. Pharm. Unserer Zeit 1977; 6: 171-178., doi: 10.1002/pauz.19770060602.

[384] Shayesteh TH, Radmehr M, Khajavi F, Mahjub R. Application of chemometrics in determination of the acid dissociation constants (pK_a) of several benzodiazepine derivatives as poorly soluble drugs in the presence of ionic surfactants. Eur. J. Pharm. Sci. 2015; 69: 44-50., doi: 10.1016/j.ejps.2014.12.013.

[385] Bacalum E, Cheregi M, David V. Retention behaviour of some benzodiazepines in solid-phase extraction using modified silica adsorbents having various hydrophobicities. Rev. Roum. Chim. 2015; 60: 891-898.

[386] Barrett J, Smyth WF, Davidson IE. An examination of acid-base equilibria of 1,4-benzodiazepines by spectrophotometry. J. Pharm. Pharmacol. 1973; 25: 387-393., doi: 10.1111/j.2042-7158.1973.tb10033.x.

[387] Gautam L, Sharratt SD, Cole MD. Drug facilitated sexual assault: Detection and stability of benzodiazepines in spiked drinks using gas chromatography-mass spectrometry. PLoS One 2014; 9:, doi: 10.1371/journal.pone.0089031.

[388] Groves JA, Smyth WF. Polarographic study of flurazepam and its major metabolites. Analyst 1981; 106: 890., doi: 10.1039/an9810600890.

[389] World Health Organisation (WHO). Expert Committee on Drug Dependence Thirty-Seventh Meeting: Etizolam Pre-Review ReportGeneva2015.

[390] Reijenga J, van Hoof A, van Loon A, Teunissen B. Development of Methods for the Determination of pK_a Values. Anal. Chem. Insights 2013;, doi: 10.4137/ACI.S12304.

[391] Manchester J, Walkup G, Rivin O, You Z. Evaluation of pK_a Estimation Methods on 211 Druglike Compounds. J. Chem. Inf. Model. 2010; 50: 565-571.

[392] Meloun M, Bordovská S. Benchmarking and validating algorithms that estimate pK a values of drugs based on their molecular structures. Anal. Bioanal. Chem. 2007; 389: 1267-1281., doi: 10.1007/s00216-007-1502-x.

[393] Abernethy D, Greenblatt D, Locniskar A, Ochs H, et al. Obesity effects on nitrazepam disposition. Br. J. Clin. Pharmacol. 1986; 22: 551-557., doi: 10.1111/j.1365-2125.1986.tb02934.x.

[394] Kangas L, Allonen H, Lammintausta R, Salonen M, Pekkarinen A. Pharmacokinetics of Nitrazepam in Saliva and Serum after a Single Oral Dose. Acta Pharmacol. Toxicol. (Copenh). 1979; 45: 20-24., doi: 10.1111/j.1600-0773.1979.tb02354.x.

[395] G. Seyffart. Drug Dosage in Renal InsufficiencySpringer Science Business Media, New York, USA2012.

[396] Miller LG, Greenblatt DJ, Abernethy DR, Friedman H, et al. Kinetics, brain uptake, and receptor binding characteristics of flurazepam and its metabolites. Psychopharmacology (Berl). 1988; 94: 386-391., doi: 10.1007/BF00174694.

[397] Verbeeck RK, Cardinal JA, Wallace SM. Effect of age and sex on the plasma binding of acidic and basic drugs. Eur. J. Clin. Pharmacol. 1984; 27: 91-97., doi: 10.1007/BF00553161.

[398] Grainger-Rousseau TJ, McElnay JC, Collier PS. The influence of disease on plasma protein binding of drugs. Int. J. Pharm. 1989; 54: 1-13., doi: 10.1016/0378-5173(89)90159-2.

[399] Kochansky CJ, McMasters DR, Lu P, Koeplinger KA, et al. Impact of pH on plasma protein binding in equilibrium dialysis. Mol. Pharm. 2008; 5: 438-448., doi: 10.1021/mp800004s.

[400] Curran RE, Claxton CRJ, Hutchison L, Harradine PJ, et al. Control and Measurement of Plasma pH in Equilibrium Dialysis: Influence on Drug Plasma Protein Binding. Drug Metab. Dispos. 2011; 39: 551 LP - 557.

[401] Wanwimolruk S, Birkett DJ. The effects of NB transition of human serum albumin on the specific drug-binding sites. Biochim. Biophys. Acta (BBA)/Protein Struct. Mol. 1982; 709: 247-255., doi: 10.1016/0167-4838(82)90467-8.

[402] Lucek RW, Coutinho CB. The role of substituents in the hydrophobic binding of the 1,4-benzodiazepines by human plasma proteins. Mol. Pharmacol. 1976; 12: 612-619.

[403] Mandona JW, Tuk B, Steveninck AL van, Breimer DD, et al. Pharmacokinetic-pharmacodynamic modeling of the central nervous system effects of midazolam and its main metabolite α-hydroxymidazolam in healthy volunteers. Clin. Pharmacol. Ther. 1992; 51: 715-728.

[404] Ait-Daoud N, Hamby AS, Sharma S, Blevins D. A Review of Alprazolam Use, Misuse, and Withdrawal. J. Addict. Med. 2018;, doi: 10.1097/ADM.0000000000000350.

[405] Lombardo F, Jing Y. In Silico Prediction of Volume of Distribution in Human. Extensive Data Set and the Exploration of Linear and Non-linear Methods Coupled with Molecular Interaction Fields Descriptors. J. Chem. Inf. Model. 2016; 56: 2042-2052.

[406] Heizmann P, Eckert M, Ziegler W. Pharmacokinetics and bioavailability of midazolam in man. Br. J. Clin. Pharmacol. 1983; 16: 43S-49S., doi: 10.1111/j.1365-2125.1983.tb02270.x.

[407] Fleishaker JC, Friedman H, Pollock SR. Extent and variability of the first-pass elimination of adinazolam mesylate in healthy male volunteers. Pharm. Res. 1991; 8: 162-167.

[408] Ogata M, Tahara T, Nishimura T. NMR Spectroscopic Characterization of Adinazolam Mesylate: pH-Dependent Structure Change in Aqueous Solution and Active Methylene. J. Pharm. Sci. 1995; 84: 786-790.

[409] Obach RS, Lombardo F, Waters NJ. Trend Analysis of a Database of Intravenous Pharmacokinetic Parameters in Humans for 670 Drug Compounds. Drug Metab. Dispos. 2008; 36: 1385-1405.

[410] Moffat AC, Osselton DM, Widdop B, Watts J. Clarkes Analysis of Drugs and Poison2011.

[411] Pfendt LB, Popovi G V., Damjanovi T, Sladi DM. Protolytic equilibria of bromazepam. J. Serbian Chem. Soc. 2002; 67: 187-195., doi: 10.2298/JSC0203187P.

[412] Yamada Y, Sakurai K, Nakamura K, Sawada Y, Iga T. Prediction of Alteration of Apparent Volume of Distribution of Drugs in Hepatic Disease. Drug Metab. Pharmacokinet. 1993; 8: 283-293.

[413] Jochemsen R, Joeres RP, Wesselman JGJ, Richter E, Breimer DD. Pharmacokinetics of oral brotizolam in patients with liver cirrhosis. Br. J. Clin. Pharmacol. 1983; 16 Supplem: 315S-322S.

[414] Gallo B, Alonso RM, Madariaga JM, Patriarche GJ, Viré JC. Spectrophotometric Study of Acid-Base Equilibrium of a Thienotriazolodiazepine, Brotizolam, Determination in Pharmaceutical Formulations. Anal. Lett. 1986; 19: 1853-1865.

[415] Hilal SH, Y El-Shabrawy, Carreira LA, Karickhoff SW, et al. Estimation of the ionization pK$_a$ of pharmaceutical substances using the computer program SPARC. Talanta 1996; 43: 607-619.

[416] Tognoni G, Gomeni R, Maio D De, Alberti GG, et al. Pharmacokinetics of N-demethyldiazepam in patients suffering from insomnia and treated with nortriptyline. Br. J. Clin. Pharmacol. 1975; 2: 227-232.

[417] Kyburz E. New trends in minor tranquilizers inMed. Chem. Adv. (Eds: F. G. De Las Heras, S. Vega) Pergamon, Oxford and New York, 1981 pp.355-368.

[418] Gerecke M. Chemical structure and properties of midazolam compared with other benzodiazepines. Br. J. Clin. Pharmacol. 1983; 16 Supplem: 11S-16S.

[419] Shayesteh TH, Radmehr M, Khajavi F, Mahjub R. Application of chemometrics in determination of the acid dissociation constants (pK$_a$) of several benzodiazepine derivatives as poorly soluble drugs in the presence of ionic surfactants. Eur. J. Clin. Pharmacol. 2015; 10: 44-50.

[420] Konishi M, Hirai K, Mori Y. Kinetics and mechanism of the equilibrium reaction of triazolam in aqueous solution. J. Pharm. Sci. 1982; 71: 1328-1334.

[421] Lan N, Chen J. Differential Effects of 4-Chlorodiazepam on Expressed Human GABA$_A$ Receptors. J. Neurochem. 1995; 1-5.

[422] Lund A. The Distribution of Chlorpromazine between Plasma and Erythrocytes. Acta Pharmacol. Toxicol. (Copenh). n.d.; 47: 300-304., doi: 10.1111/j.1600-0773.1980.tb03658.x.

[423] Linnoila M, Dorrity F. Measurement of Plasma and Erythrocyte Chlorpromazine and NMonodesmethylchlorpromazine Levels by Gas Chromatography with a Nitrogen Sensitive Detector. Acta Pharmacol. Toxicol. (Copenh). 1978; 42: 264-270., doi: 10.1111/j.1600-0773.1978.tb02199.x.

[424] Shibata Y, Takahashi H, Ishii Y. A convenient in vitro screening method for predicting in vivo drug metabolic clearance using isolated hepatocytes suspended in serum. Drug Metab. Dispos. 2000; 28: 1518-1523.

[425] Hand CW, Rutterford M, Smith RF, Moore RA. Analysis of Benzodiazepines in Whole Blood, Plasma and Urine by 125-1 Immunoassay in11th Int. Counc. Alcohol, Drugs Traffic Saf. Conf. 1989 pp.893-897.

[426] Säilä J. Comparing the Concentrations of Drugs and Medicines In Whole Blood, Plasma and Oral Fluid Samples of Drivers Suspected of Driving Under the Influence, 2009.

[427] Kwakye RA, Kuntworbe N, Ofori-Kwakye K, Osei YA. Detection, quantification, and investigation of the red blood cell partitioning of cryptolepine hydrochloride. J. Pharm. Pharmacogn. Res. 2018; 6: 260-270.

[428] Imawaka H, Ito K, Kitamura Y, Sugiyama K, Sugiyama Y. Prediction of human bioavailability from human oral administration data and animal pharmacokinetic data without data from intravenous administration of drugs in humans. Pharm. Res. 2009; 26: 1881-1889., doi: 10.1007/s11095-009-9902-6.

[429] Yokogawa K, Nakashima E, Ishizaki J, Maeda H, et al. Relationships in the Structure–Tissue Distribution of Basic Drugs in the Rabbit. Pharm. Res. 1990; 7: 691-696., doi: 10.1023/A:1015803202857.

[430] Grayson ML, Cosgrove SE, Crowe S, Hope W, et al. Anti-Parasitic Drugs inKucers Use Antibiot. Sixth Ed. A Clin. Rev. Antibacterial, Antifung. Antivir. Drugs CRC Press, Boca Raton, Florida, U.S., 2010 p.2014.

[431] Deguchi T, Watanabe N, Kurihara A, Igeta K, et al. Human pharmacokinetic prediction of UDP-glucuronosyltransferase substrates with an animal scale-up approach. Drug Metab. Dispos. 2011; 39: 820-829., doi: 10.1124/dmd.110.037457.

[432] Fleishaker JC, Friedman H, Pollock SR. Extent and Variability of the First-Pass Elimination of Adinazolam Mesylate in Healthy Male Volunteers. Pharm. Res. An Off. J. Am. Assoc. Pharm. Sci. 1991; 8: 162-167., doi: 10.1023/A:1015875516834.

[433] Smink B, Hofman BJ, Dijkhuizen A, Lusthof KJ, de Gier JJ, Egberts AC UD. The concentration of oxazepam and oxazepam glucuronide in oral fluid, blood and serum after controlled administration of 15 and 30 mg oxazepam. Br. J. Clin. Pharmacol. 2008; 66: 556-560., doi: 10.1111/j.1365-2125.2008.03252.x.

[434] Barceloux D. Medical Toxicology of Drug Abuse: Synthetized Chemicals and Psychoactive Plants. Med. Toxicol. Drug Abus. 2012; 788-804., doi: 10.1002/9781118105955.

[435] Salamone SJ, Ed. . Benzodiazepines and GHB: Detection and PharmacologyHumana Press, New York, USA2001.

[436] Weaver R, Graham KS, Beattie IG, Riley RJ. Cytochrome P450 inhibition using recombinant proteins and mass spectrometry/multiple reaction monitoring technology in a cassette incubation. Drug Metab. Dispos. 2003;, doi: 10.1124/dmd.31.7.955.

[437] Xu YF, Lu W, Rabinowitz JD. Avoiding misannotation of in-source fragmentation products as cellular metabolites in liquid chromatography-mass spectrometry-based metabolomics. Anal. Chem. 2015;, doi: 10.1021/ac504118y.

[438] Elkayam T, Amitay-Shaprut S, Dvir-Ginzberg M, Harel T, Cohen S. Enhancing the Drug Metabolism Activities of C3A A Human Hepatocyte Cell LineBy Tissue Engineering Within Alginate Scaffolds. Tissue Eng. 2006; 12: 1357-1368., doi: 10.1089/ten.2006.12.1357.

[439] Cox SK, Hamner T, Bartges J. Determination of acetaminophen and phenacetin in porcine microsomal samples. J. Liq. Chromatogr. Relat. Technol. 2003; 26: 925-935., doi: 10.1081/JLC-120018893.

[440] Zhai X, Lu Y. Development and validation of a simple LC method for the determination of phenacetin, coumarin, tolbutamide, chlorzoxazone, testosterone and their metabolites as markers of cytochromes 1A2, 2A6, 2C11, 2E1 and 3A2 in rat microsomal medium. Pharmazie 2013; 68: 19-26., doi: 10.1691/ph.2013.2108.

[441] Masters AR, McCoy M, Jones DR, Desta Z. Stereoselective method to quantify bupropion and its three major metabolites, hydroxybupropion, erythro-dihydrobupropion, and

threo-dihydrobupropion using HPLC-MS/MS. J. Chromatogr. B Anal. Technol. Biomed. Life Sci. 2016; 1015-1016: 201-208., doi: 10.1016/j.jchromb.2016.02.018.

[442] Meyer A, Vuorinen A, Zielinska AE, Strajha P, et al. Formation of threohydrobupropion from bupropion is dependent on 11β-hydroxysteroid dehydrogenase 1. Drug Metab. Dispos. 2013; 41: 1671-1678.

[443] Molnari JC, Myers AL. Carbonyl reduction of bupropion in human liver. Xenobiotica 2012; 42: 550-561.

[444] Coles R, Kharasch ED. Stereoselective metabolism of bupropion by cytochrome P4502B6 (CYP2B6) and human liver microsomes. Pharm. Res. 2008; 25: 1405-1411., doi: 10.1007/s11095-008-9535-1.

[445] Sager JE, Choiniere JR, Chang J, Stephenson-Famy A, et al. Identification and Structural Characterization of Three New Metabolites of Bupropion in Humans. ACS Med. Chem. Lett. 2016; 7:, doi: 10.1021/acsmedchemlett.6b00189.

[446] Faucette SR, Hawke RL, Lecluyse EL, Shord SS, et al. Validation of bupropion hydroxylation as a selective marker of human cytochrome P450 2B6 catalytic activity. Drug Metab. Dispos. 2000; 28: 1222-1230.

[447] Hesse LM, Venkatakrishnan K, Court MH, Von Moltke LL, et al. CYP2B6 mediates the in vitro hydroxylation of bupropion: Potential drug interactions with other antidepressants. Drug Metab. Dispos. 2000; 28: 1176-1183.

[448] Sager JE, Price LSL, Isoherranen N. Stereoselective metabolism of bupropion to OH-bupropion, threohydrobupropion, erythrohydrobupropion, and 49-OH-bupropion in vitro. Drug Metab. Dispos. 2016; 44: 1709-1719., doi: 10.1124/dmd.116.072363.

[449] Connarn JN, Zhang X, Babiskin A, Sun D. Metabolism of Bupropion by carbonyl reductases in liver and intestine. Drug Metab. Dispos. 2015; 43: 1019-1027., doi: 10.1124/dmd.115.063107.

[450] Tassaneeyakul W, Tassaneeyakul W, Vannaprasaht S, Yamazoe Y. Formation of omeprazole sulphone but not 5-hydroxyomeprazole is inhibited by grapefruit juice. Br. J. Clin. Pharmacol. 2000;, doi: 10.1046/j.1365-2125.2000.00122.x.

[451] Pillai VC, Strom SC, Caritis SN, Venkataramanan R. A sensitive and specific CYP cocktail assay for the simultaneous assessment of human cytochrome P450 activities in primary cultures of human hepatocytes using LC-MS/MS. J. Pharm. Biomed. Anal. 2013; 74: 126-132.

[452] Liu LY, Han YL, Zhu JH, Yu Q, et al. A sensitive and high-throughput LC-MS/MS method for inhibition assay of seven major cytochrome P450s in human liver microsomes using an in vitro cocktail of probe substrates. Biomed. Chromatogr. 2015; 29: 437-444., doi: 10.1002/bmc.3294.

[453] Wang J-J, Guo J-J, Zhan J, Bu H-Z, Lin JH. An in-vitro cocktail assay for assessing compound-mediated inhibition of six major cytochrome P450 enzymes . J. Pharm. Anal. 2014; 4: 270-278.

[454] Spaggiari D, Geiser L, Daali Y, Rudaz S. A cocktail approach for assessing the in vitro activity of human cytochrome P450s: An overview of current methodologies. J. Pharm. Biomed. Anal. 2014; 101: 221-237., doi: 10.1016/j.jpba.2014.03.018.

[455] Liu Y, Flynn TJ, Xia M, Wiesenfeld PL, Ferguson MS. Evaluation of CYP3A4 inhibition and hepatotoxicity using DMSO-treated human hepatoma HuH-7 cells. Cell Biol. Toxicol. 2015; 31: 221-230., doi: 10.1007/s10565-015-9306-9.

[456] Fouad Mansour M, Pelletier M, Boulet MM, Mayrand D, et al. Oxidative activity of 17-hydroxysteroid dehydrogenase on testosterone in male abdominal adipose tissues and cellular localization of 17-HSD type 2. Mol. Cell. Endocrinol. 2015;, doi: 10.1016/j.mce.2015.06.016.

[457] Yamazaki H, Shimada T. Progesterone and testosterone hydroxylation by cytochromes P450 2C19, 2C9, and 34 in human liver microsomes. Arch. Biochem. Biophys. 1997;, doi: 10.1006/abbi.1997.0302.

[458] Choi MH, Skipper PL, Wishnok JS, Tannenbaum SR. Characterization of Testosterone 11 -Hydroxylation Catalyzed By Human Liver Microsomal Cytochromes P450. Pharmacology 2005;, doi: 10.1124/dmd.104.003327.mors.

[459] Usmani KA, Tang J. Human Cytochrome P450: Metabolism of Testosterone by CYP3A4 and Inhibition by Ketoconazole inCurr. Protoc. Toxicol. 2004.

[460] Sainz B, Chisari F V. Production of Infectious Hepatitis C Virus by Well-Differentiated, Growth-Arrested Human Hepatoma-Derived Cells. J. Virol. 2006; 80: 10253-10257.

[461] Tolonen A, Petsalo A, Turpeinen M, Uusitalo J, Pelkonen O. In vitro interaction cocktail assay for nine major cytochrome P450 enzymes with 13 probe reactions and a single LC/MSMS run: Analytical validation and testing with monoclonal anti-CYP antibodies. J. Mass Spectrom. 2007;, doi: 10.1002/jms.1239.

[462] Testino SA, Patonay G. High-throughput inhibition screening of major human cytochrome P450 enzymes using an in vitro cocktail and liquid chromatography-tandem mass spectrometry. J. Pharm. Biomed. Anal. 2003; 30: 1459-1467., doi: 10.1016/S0731-7085(02)00480-6.

[463] Abelo A, Andersson TB, Antonsson M, Naudot AK, et al. Stereoselective metabolism of omeprazole by human cytochrome P450 enzymes. Drug Metab. Dispos. 2000;

[464] Onof S, Hatanaka T, Miyazawa S, Tsutsui M, et al. Human liver microsomal diazepam metabolism using cDNA-expressed cytochrome P450s: Role of CYP2B6, 2C19 and the 3A subfamily. Xenobiotica 1996; 26: 1155-1166., doi: 10.3109/00498259609050260.

[465] Mowbray CA, Howard A, Morsman J, Hirst BH. Differentiation of HepG2 and Huh7 cells using dimethyl sulfoxide. FASEB J. 2010; 24: lb654.

[466] Hooper WD, Watt JA, Mckinnon GE, Reelly PEB. Metabolism of diazepam and related benzodiazepines by human liver microsomes. Eur. J. Drug Metab. Pharmacokinet. 1992; 17: 51-59., doi: 10.1007/BF03189988.

[467] Weinfeld RE, Miller KF. Determination of the major urinary metabolite of flurazepam in man by high-performance liquid chromatography. J. Chromatogr. 1981; 223: 123-130.

[468] Barzaghi N, Leone L, Monteleone M, Tomasini G, Perucca E. Pharmacokinetics of flutoprazepam, a novel benzodiazepine drug, in normal subjects. Eur. J. Drug Metab. Pharmacokinet. 1989; 14: 293-298.

[469] Kintz P, Richeval C, Jamey C, Ameline A, et al. Detection of the designer benzodiazepine metizolam in urine and preliminary data on its metabolism. Drug Test. Anal. 2016;, doi: 10.1002/dta.2099.

[470] Huppertz LM, Moosmann B, Auwärter V. Flubromazolam - Basic pharmacokinetic evaluation of a highly potent designer benzodiazepine. Drug Test. Anal. 2018; 10: 206-211., doi: 10.1002/dta.2203.

[471] Richter LHJ, Maurer HH, Meyer MR. New psychoactive substances: Studies on the metabolism of XLR-11, AB-PINACA, FUB-PB-22, 4-methoxy--PVP, 25-I-NBOMe, and meclonazepam using human liver preparations in comparison to primary human hepatocytes, and human urine. Toxicol. Lett. 2017;, doi: 10.1016/j.toxlet.2017.07.901.

[472] Meyer MR, Bergstrand MP, Helander A, Beck O. Identification of main human urinary metabolites of the designer nitrobenzodiazepines clonazolam, meclonazepam, and nifoxipam by nano-liquid chromatography-high-resolution mass spectrometry for drug testing purposes. Anal Bioanal Chem 2016; 408: 3571-3591., doi: 10.1007/s00216-016-9439-6.

[473] Coller JK, Somogyi AA, Bochner F. Quantification of flunitrazepams oxidative metabolites, 3-hydroxyflunitrazepam and desmethylflunitrazepam, in hepatic microsomal incubations by high-performance liquid chromatography. J. Chromatogr. B Biomed. Appl. 1998; 719: 87-92., doi: 10.1016/S0378-4347(98)00383-1.

[474] Tanaka E, Nakamura T, Terada T, Shinozuka T, Honda K. Preliminary study of the in vitro interaction between alcohol, high-dose flunitrazepam and its three metabolites using human liver microsomes. Basic Clin. Pharmacol. Toxicol. 2005; 96: 88-90., doi: 10.1111/j.1742-7843.2005.pto960113.x.

[475] Negrusz a, Moore CM, Stockham TL, Poiser KR, et al. Elimination of 7-aminoflunitrazepam and flunitrazepam in urine after a single dose of Rohypnol. J. Forensic Sci. 2000; 45: 1031-40.

[476] Hasegawa K, Wurita A, Minakata K, Gonmori K, et al. Postmortem distribution of flunitrazepam and its metabolite 7-aminoflunitrazepam in body fluids and solid tissues in an autopsy case: Usefulness of bile for their detection. Leg. Med. 2015; 17: 394-400., doi: 10.1016/j.legalmed.2015.06.002.

[477] Coassolo P, Aubert C, Cano JP. Plasma determination of 3-methylclonazepam by capillary gas chromatography. J. Chromatogr. 1985; 338: 347-355.

[478] Robertson MD, Drummer OH. Stability of nitrobenzodiazepines in postmortem blood. J. Forensic Sci. 1998; 43: 5-8.

[479] Mata DC. Stability of 26 sedative hypnotics in six toxicological matrices at different storage conditions. J. Anal. Toxicol. 2016;, doi: 10.1093/jat/bkw084.

[480] Ameline A, Richeval C, Gaulier J-M, Raul J-S, Kintz P. Detection of the designer benzodiazepine flunitrazolam in urine and preliminary data on its metabolism. Drug Test. Anal. n.d.; 0:, doi: 10.1002/dta.2480.

[481] Meyer MR, Bergstrand MP, Helander A, Beck O. Identification of main human urinary metabolites of the designer nitrobenzodiazepines clonazolam, meclonazepam, and nifoxipam by nano-liquid chromatography-high-resolution mass spectrometry for drug testing purposes. Anal. Bioanal. Chem. 2016; 408: 3571-3591., doi: 10.1007/s00216-016-9439-6.

[482] Zherdev VP, Caccia S, Garattini S, Ekonomov AL. Species differences in phenazepam kinetics and metabolism. Eur. J. Drug Metab. Pharmacokinet. 1982; 7: 191-196.

[483] Ekonomov AL, Zherdev VP, Rodionov AP, Vikhlyaev YI. Metabolism of the new psychotropic agent phenazepam. Pharm. Chem. J. 1980; 13: 681-685., doi: 10.1007/BF00789513.

[484] Crichton ML, Shenton CF, Drummond G, Beer LJ, et al. Analysis of phenazepam and 3-hydroxyphenazepam in post-mortem fluids and tissues. Drug Test. Anal. 2015; 7: 926-936., doi: 10.1002/dta.1790.

[485] Moosmann B, Hutter M, Huppertz LM, Ferlaino S, et al. Characterization of the designer benzodiazepine pyrazolam and its detectability in human serum and urine. Forensic Toxicol. 2013; 31: 263-271., doi: 10.1007/s11419-013-0187-4.

[486] Tetko I V., Poda GI. Application of ALOGPS 2.1 to predict log D distribution coefficient for pfizer proprietary compounds. J. Med. Chem. 2004; 47: 5601-5604., doi: 10.1021/jm049509l.

[487] Hoekstra R, Nibourg GAA, Van Der Hoeven T V., Plomer G, et al. Phase 1 and phase 2 drug metabolism and bile acid production of HepaRG cells in a bioartificial liver in absence of dimethyl sulfoxide. Drug Metab. Dispos. 2013;, doi: 10.1124/dmd.112.049098.

[488] Kanebratt KP, Andersson TB. Evaluation of HepaRG cells as an in vitro model for human drug metabolism studies. Drug Metab. Dispos. 2008;, doi: 10.1124/dmd.107.020016.

[489] Miller ME, Garland WA, Min BH, Ludwick BT, et al. Clonazepam acetylation in fast and slow acetylators. Clin. Pharmacol. Ther. 1981;, doi: 10.1038/clpt.1981.170.

[490] Court MH, Duan SX, Guillemette C, Journault K, et al. Stereoselective conjugation of oxazepam by human UDP-glucuronosyltransferases (UGTS): S-oxazepam is glucuronidated by UGT2B15, while R-oxazepam is glucuronidated by UGT2B7 and UGT1A9. Drug Metab. Dispos. 2002;, doi: 10.1124/dmd.30.11.1257.

[491] de Angelis I, Turco L. Caco-2 cells as a model for intestinal absorption. Curr. Protoc. Toxicol. 2011;, doi: 10.1002/0471140856.tx2006s47.

[492] van Breemen RB, Li Y. Caco-2 cell permeability assays to measure drug absorption. Expert Opin. Drug Metab. Toxicol. 2005;, doi: 10.1517/17425255.1.2.175.

[493] Alhamoruni A, Lee AC, Wright KL, Larvin M, OSullivan SE. Pharmacological Effects of Cannabinoids on the Caco-2 Cell Culture Model of Intestinal Permeability. J. Pharmacol.

Exp. Ther. 2010;, doi: 10.1124/jpet.110.168237.

[494] Atlabachew M, Combrinck S, Viljoen AM, Hamman JH, Gouws C. Isolation and in vitro permeation of phenylpropylamino alkaloids from Khat (Catha edulis) across oral and intestinal mucosal tissues. J. Ethnopharmacol. 2016;, doi: 10.1016/j.jep.2016.09.012.

[495] Kuwayama K, Inoue H, Kanamori T, Tsujikawa K, et al. Uptake of 3,4-methylenedioxymethamphetamine and its related compounds by a proton-coupled transport system in Caco-2 cells. Biochim. Biophys. Acta - Biomembr. 2008;, doi: 10.1016/j.bbamem.2007.08.023.

[496] Crowe A, Diep S. pH dependent efflux of methamphetamine derivatives and their reversal through human Caco-2 cell monolayers. Eur. J. Pharmacol. 2008;, doi: 10.1016/j.ejphar.2008.06.090.

[497] Bittermann K, Goss KU. Predicting apparent passive permeability of Caco-2 and MDCK cell-monolayers: A mechanistic model. PLoS One 2017;, doi: 10.1371/journal.pone.0190319.

[498] Alsenz J, Haenel E. Development of a 7-Day, 96-Well Caco-2 Permeability Assay with High-Throughput Direct UV Compound Analysis. Pharm. Res. 2003;, doi: 10.1023/B:PHAM.0000008043.71001.43.

[499] Czupalla CJ, Liebner S, Devraj K. In vitro models of the blood-brain barrier. Methods Mol. Biol. 2014;, doi: 10.1016/j.fsi.2018.05.062.

[500] Dolghih E, Jacobson MP. Predicting efflux ratios and blood-brain barrier penetration from chemical structure: Combining passive permeability with active efflux by P-glycoprotein. ACS Chem. Neurosci. 2013;, doi: 10.1021/cn3001922.

[501] Doan KMM. Passive Permeability and P-Glycoprotein-Mediated Efflux Differentiate Central Nervous System (CNS) and Non-CNS Marketed Drugs. J. Pharmacol. Exp. Ther. 2002;, doi: 10.1124/jpet.102.039255.

[502] Wang Q, Rager JD, Weinstein K, Kardos PS, et al. Evaluation of the MDR-MDCK cell line as a permeability screen for the blood-brain barrier. Int. J. Pharm. 2005;, doi: 10.1016/j.ijpharm.2004.10.007.

[503] Lu C, Li P, Gallegos R, Uttamsingh V, et al. Comparison of intrinsic clearance in liver microsomes and hepatocytes from rats and humans: Evaluation of free fraction and uptake in hepatocytes. Drug Metab. Dispos. 2006;, doi: 10.1124/dmd.106.010793.

Appendix A

Publications

WILEY

REVIEW

The emergence of new psychoactive substance (NPS) benzodiazepines: A review

Kieran R. Manchester[1] | Emma C. Lomas[1] | Laura Waters[1] | Fiona C. Dempsey[2] |
Peter D. Maskell[3] 🄳

[1] School of Applied Sciences, Queensgate Campus, University of Huddersfield, Huddersfield, UK

[2] MedAnnex Ltd, 1 Summerhall Place, Techcube 3.5, Edinburgh, EH9 1PL, UK

[3] School of Science, Engineering and Technology, Abertay University, Dundee, UK

Correspondence
Peter D. Maskell, School of Science, Engineering and Technology, Abertay University, Dundee, UK.
Email: p.maskell@abertay.ac.uk

The market for new psychoactive substances has increased markedly in recent years and there is now a steady stream of compounds appearing every year. Benzodiazepines consist of only a fraction of the total number of these compounds but their use and misuse has rapidly increased. Some of these benzodiazepines have only been patented, some of them have not been previously synthesised, and the majority have never undergone clinical trials or tests. Despite their structural and chemical similarity, large differences exist between the benzodiazepines in their pharmacokinetic parameters and metabolic pathways and so they are not easily comparable. As benzodiazepines have been clinically used since the 1960s, many analytical methods exist to quantify them in a variety of biological matrices and it is expected that these methods would also be suitable for the detection of benzodiazepines that are novel psychoactive substances. Illicitly obtained benzodiazepines have been found to contain a wide range of compounds such as opiates which presents a problem since the use of them in conjunction with each other can lead to respiratory depression and death. This review collates the available information on these benzodiazepines and provides a starting point for the further investigation of their pharmacokinetics which is clearly required.

KEYWORDS

benzodiazepine, drug abuse, legal highs, NPS

1 | THE USE AND MISUSE OF BENZODIAZEPINES

The use and misuse of new psychoactive substances (or 'legal highs') has increased significantly around the world in the past 10 years[1] and has to date showed no signs of slowing. In Europe alone, the total number of new compounds reported by the European Monitoring Centre for Drugs and Drug Addiction (EMCDDA) has risen rapidly since 2007 with 101 new psychoactive substances reported to the EMCDDA in 2014[2] and 98 in 2015.[3] The majority of these compounds have been synthetic cannabinoids, cathinones, and phenylethylamines.[2] One group of these compounds, the benzodiazepines, has received limited attention but their use has increased significantly in the past few years. The abuse potential for benzodiazepines was recognised early in their use and led to 35 benzodiazepines being placed under control by the UN Convention on Psychotropic Substances 1971.[4] Benzodiazepines are one of the most prescribed groups of drugs around the world with the limited available data suggesting that 5.6% of Americans filled a benzodiazepine prescription in 2013.[5] In England, over 5 million doses of diazepam alone were dispensed in 2014, whilst the total number of prescriptions issued for benzodiazepines stood at more than 10.4 million, indicating their widespread use.[6] Benzodiazepines are also linked to a significant number of deaths, both via abuse as a drug in their own right and as part of a deliberate polypharmacy regime.[7] They are commonly implicated in cases of opioid overdoses, where benzodiazepines are detected in 50–80% of heroin-related deaths and in 40–80% of methadone-related deaths in various countries around the world.[7] Benzodiazepines also account for around 28–45% of drug-induced deaths in Europe.[2] A study of 1500 people in 2014 used an internet-based survey to investigate the reasons for the abuse of benzodiazepines and Z-drugs in the United Kingdom (Z-drugs such as zopiclone and zolpidem are structurally different from benzodiazepines but also act via the γ-aminobutyric acid type-A (GABA$_A$) receptor). The study found that most abuse of Z-drugs and benzodiazepines occurred because users were trying to alleviate stress, to help with sleep, or to get high.[8] Unfortunately, the study did not differentiate between benzodiazepines or Z-drugs but because of their similar effects it is

likely that they are used interchangeably. When used in combination with other drugs (such as opioids/opiates) the aim of benzodiazepine use is typically to enhance and/or prolong the high or to reduce the withdrawal effects of the other drugs.[9]

Outside normal prescription methods, benzodiazepines are obtained via various routes such as diversion of prescriptions, the illicit market, and internet purchasing, which is thought to be a rising trend.[10] In 2016, the Research and Development (RAND) corporation published a report suggesting that the UK had the second largest number of online vendors of illegal drugs on the darknet (with the USA first) but that UK vendors averaged the most transactions per month.[11]

In recent years, an increasing number of NPS-benzodiazepines have appeared for sale in various countries. Novel psychoactive substances are defined by the United Nations Office on Drugs and Crime as 'substances of abuse, either in a pure form or a preparation, that are not controlled by the 1961 Single Convention on Narcotic Drugs or the 1971 Convention on Psychotropic Substances, but which may pose a public health threat'.[12] These novel psychoactive substances are often sold online and labelled for use as 'research chemicals' only, even though they are implicitly intended for human consumption. Many of these NPS-benzodiazepines have never undergone the clinical testing that is required of licensed medicines and the increasing availability of them may therefore pose serious health risks to polydrug users and benzodiazepine-dependent patients who can no longer obtain their prescription and may turn to other means of obtaining benzodiazepines. We introduce the general classification of benzodiazepines (duration of action, half-life and chemical structure), their mechanism of action and review what is known to date about these NPS-benzodiazepines including user experiences, their pharmacology, pharmacokinetics, and analytical detection. This data is summarised in Table 1 and was obtained from a variety of published journal articles except the user experiences which were obtained from chat and comments on internet forums such as Reddit,[13] Bluelight,[14] Flashback,[15] and UK Chemical Research.[16] Caution should be taken when interpreting these user experiences as any experiences are subjective and users may have ingested other compounds at the same time. Instead they serve as a rough guide as to the likely effects that may be expected.

2 | THE RISE OF THE NPS-BENZODIAZEPINES

The first illicit benzodiazepines identified in Europe to the EMCDDA were phenazepam (fenazepam) and nimetazepam in 2007.[17] Phenazepam is a prescription drug in the former Soviet bloc.[18] In the intervening years, it was detected in an increasing number of cases around the world.[19-25] This led to it being scheduled in the UK and other countries.[26-28] Recently, phenazepam was placed in schedule VI of the 1971 UN Drug Control Convention.[29] The benzodiazepine-derivative etizolam was the next compound to be detected to the EMCDDA in 2011.[30] It belongs to a class of compounds known as thienodiazepines and is commonly prescribed in Japan.[31] The naming of benzodiazepines and their derivatives is discussed in the next section of this review – Classification of benzodiazepines. Its

appearance mirrored that of phenazepam; a prescription drug in a country outside the UK which subsequently found its way to the UK market. Pyrazolam was the next benzodiazepine to appear on the market and was notable as this was the first benzodiazepine to appear that was not a prescription drug in any country.[32] Following this, multiple benzodiazepines were reported to the EMCDDA that have not been licensed for clinical use anywhere in the world. These benzodiazepines include flubromazepam and diclazepam in 2013[33] along with meclonazepam, nifoxipam, and deschloroetizolam (a thienodiazepine) in 2014.[34] Clonazolam and flubromazolam are also thought to have first appeared in 2014[10] and were subsequently reported to the EMCDDA. Various other benzodiazepines such as adinazolam, nitrazolam, and metizolam (another thienodiazepine) have all been reported to the EMCDDA in the 2015 implementation report.[35] Two other benzodiazepines, 3-hydroxyphenazepam (a metabolite of phenazepam[18]) and flutazolam (a Japanese prescription drug[36]) have been detected separately in tablets seized in Sweden in 2015 by the Medical Products Agency (MPA), with the use and spread of flutazolam being monitored and 3-hydroxyphenazepam being subject to an investigation by the MPA.[37] Flunitrazolam, desmethylflunitrazepam (also known as fonazepam), and cloniprazepam were also detected by the MPA in 2016.[38] Bromazolam,[39] desalkylflurazepam (also known as norflurazepam),[39] and 4-chlorodiazepam (also known as Ro5–4864)[40] are also thought to have appeared at various points in 2016. The years that these benzodiazepines appeared and their year of patent (if available) has been summarised in Table 2 and the timeline can be viewed in Figure 1. Currently hundreds of benzodiazepines have been patented and described in the scientific literature and these are not expected to be the last benzodiazepines that are detected in the so-called explosion of novel psychoactive substances.

NPS-benzodiazepines and thienodiazepines were implicated in nine drug-related deaths in England and Wales between 2013 and 2014 as either being the cause of death or as having contributed to death.[41] In 2016, the Psychoactive Substances Act was introduced in the UK[42] with the aim of stopping the cat and mouse game of an NPS being produced to circumvent legislation, being controlled, and then another being produced. This legislation restricts the production, sale, and supply of drugs that are psychoactive. Following the introduction of this Act, that a fall in supply and use of NPS-benzodiazepines may be expected. However, phenazepam and etizolam are now both controlled benzodiazepines in the UK under the Misuse of Drugs Act (1971)[43] but are still regularly identified in post-mortem cases and in drug-impaired drivers in the UK.[21,22]

2.1 | Classification of benzodiazepines

Benzodiazepines have traditionally been classified in one of three ways, either by:

1. Their duration of action. Benzodiazepines that have durations of action under 24 h are short-acting while those with durations of action above 24 h are long-acting.[44]

2. Their elimination half-life (t½). Typically, this consists of four classifications: ultra-short (t½, <6 h), short (t½, 6 h), intermediate (t½ 6–24 h), and long (t½ > 24 h). The reason for these four

TABLE 1 Pharmacological details of NPS-benzodiazepines

Drug	Formula	mW (g mol⁻¹)	Typical recreational dose (mg)	'therapeutic'/DUID range in blood (mg l⁻¹)	T1/2 (h)	Vd (l kg⁻¹)	User reports of effects	Refs
3-hydroxyphenazepam	$C_{15}H_{10}BrClN_2O_2$	365.6	0.5–2	–	–	–	Anxiolytic, slight muscle relaxant, strongly sedating	Bluelight[14], Crichton[88]
4-chlorodiazepam	$C_{16}H_{12}Cl_2N_2O$	319.2	–	–	–	–	No reports	–
Adinazolam	$C_{19}H_{18}ClN_5$	351.8	20	0.1–0.46	1–3	2.2	No reports	Aijr[89], Fleishaker[90], Fleishaker[91], Fleishaker[92], Venkatakrishnan[93]
Bromazolam	$C_{17}H_{13}BrN_4$	353.2	1	–	–	–	No reports	–
Clonazolam	$C_{17}H_{12}ClN_5O_2$	353.1	0.5–1	0.0019–0.011	–	–	Slight euphoria, strongly sedating	Bluelight[94], Høiseth[95]
Cloniprazepam	$C_{19}H_{16}ClN_3O_3$	369.8	2.5	–	–	–	Slight anxiolytic, higher doses (>5–10 mg) required for muscle relaxation, sedation in most users	Bluelight[96]
Desalkylflurazepam	$C_{15}H_{10}ClFN_2O$	288.7	5	–	–	–	Strongly sedating and long lasting effects	UK Chemical Research[16]
Deschloroetizolam	$C_{17}H_{16}N_4S$	308.4	4–6	–	–	–	Effects lasting 12–24 hours, anxiolytic, sedative effect, slight euphoria	Bluelight[14]
Desmethylflunitrazepam (fonazepam)	$C_{15}H_{10}FN_3O_3$	299.3	0.6	–	–	–	Anxiolytic, muscle relaxant, sedation	Reddit[97], Bluelight[98]
Diclazepam	$C_{16}H_{12}Cl_2N_2O$	319.2	1–2	0.0021–0.057	42	–	Effects lasting 5–12 hours, anxiolytic, useful for 'tapering' dependence of other benzodiazepines, low cognitive impairment, low recreational value.	Moosmann[81], Crichton[88], Høiseth[95]
Etizolam	$C_{17}H_{15}ClN_4S$	342.1	0.25–3	0.019–0.17	3.4–7.1	0.91	Anxiolytic, euphoric, muscle relaxant, used as a sleep-aid	Høiseth[95]
Flubromazepam	$C_{15}H_{10}BrFN_2O$	333.1	4	0.0047–1.2	106.4	–	Effects lasting 18–24 hours, anxiolytic, mild euphoria, blackouts, sedating and muscle relaxant effects, short-term memory loss	Høiseth[95], Xu[99], Kintz[100]
Flubromazolam	$C_{17}H_{12}BrFN_4$	371.2	0.15–0.25	0.0048–0.10	–	–	Effects lasting 12–18 hours, anxiolytic, high tolerance to lower doses quickly observed, blackouts and memory loss, strongly sedating, higher doses of 2.5–4 mg have effects reported to last up to 3 days and strong memory loss and cognitive impairment. Ingestion of 3 mg of flubromazolam 19 hours prior to hospitalization has been reported in a patient. Severe respiratory failure, hypotension, central nervous system depression and brain damage were observed.	Moosmann[79], Høiseth[95], Lukasik-Glebocka[101]
Flunitrazolam	$C_{17}H_{12}FN_5O_2$	337.3	0.1	–	–	–	Strong sedative, slight amnesia reported, anxiolytic	Bluelight[94]
Flutazolam	$C_{19}H_{18}ClFN_2O_3$	376.8	4–12	0.014	~3.3	690 L	Strong anxiolytic, hypnotic, short acting (3–4 hours)	Mitsubishi-Tanabe-Pharma-Corporation[102]
Meclonazepam	$C_{16}H_{12}ClN_3O_3$	329.7	2–3	0.01–0.1	80	100 L	Low sedation, anxiolytic, muscle relaxant	Huppertz[10], UK Chemical Research[103], El Balkhi[104]
Metizolam (desmethyletizolam)	$C_{16}H_{13}ClN_4S$	328.8	2	0.000011	–	–	Anxiolytic and muscle relaxant, effects not as strong as etizolam	Kintz[100]
Nifoxipam	$C_{15}H_{10}FN_3O_4$	315.3	0.5–2	–	–	–	Effects lasting 12–18 hours, anxiolytic, moderately sedating, mild euphoric, high doses can cause users to feel sleep-deprived, muscle relaxant	Katselou[105]

(Continues)

TABLE 1 (Continued)

Drug	Formula	mW (g mol⁻¹)	Typical recreational dose (mg)	'therapeutic'/DUID range in blood (mg l⁻¹)	T1/2 (h)	Vd (l kg⁻¹)	User reports of effects	Refs
Nimetazepam	$C_{16}H_{13}N_3O_3$	295.3	5	0.0000134	12–21	—	No reports	PMDA Japan [106], JAPIC [107], Yakuzaishiharowa [108]
Nitrazolam	$C_{17}H_{13}N_5O_2$	319.3	0.5–2	—	—	—	Anxiolytic, hypnotic, strongly sedating	UK Chemical Research [109]
Phenazepam	$C_{15}H_{10}BrClN_2O$	349.6	0.5–1	0.030–0.070	6–80	4.7–6.0	Anxiolytic, extremely sedating, short-term memory loss often leads to users redosing, blackouts at higher doses, psychotic episodes, insomnia	Bluelight [94], Maskell [110], Lomas [112]
Pyrazolam	$C_{16}H_{12}BrN_5$	354.2	1	0.074	17	—	Effects lasting 6–7 hours, anxiolytic, low sedation, low hypnotic effect, low recreational value	Høiseth [95], Moosmann [113]

TABLE 2 Benzodiazepine patent years and EMCDDA report years

Compound	Year patented	Year reported to the EMCDDA
3-hydroxyphenazepam	Not reported	2016 [37,46]
4-chlorodiazepam (Ro5–4864)	1964 [131]	2016 [40]
Adinazolam	1976 [132]	2015 [35]
Bromazolam	1976 [133]	2016 [39]
Clonazolam	1971 [194]	2014 [35]
Cloniprazepam	Not reported	2015 [134]
Desalkylflurazepam	Not reported	2016 [39]
Deschloroetizolam	1998 [196]	2014 [34]
Desmethylflunitrazepam (fonazepam)	1963 [197]	2016 [38]
Diclazepam	1964 [198]	2013 [33]
Etizolam	1978 [199]	2011 [30]
Flubromazepam	1962 [200]	2013 [33]
Flubromazolam	1978 [201]	2014 [34]
Flunitrazolam	Not reported	2016 [38]
Flutazolam	1970 [202]	2015 [37]
Meclonazepam	1975 [203]	2014 [34]
Metizolam	1988 [204]	2015 [35]
Nifoxipam	1985 [205]	2014 [34]
Nimetazepam	1963 [206]	2007 [17]
Nitrazolam	1971 [194]	2015 [35]
Phenazepam	1974 [207]	2007 [17]
Pyrazolam	1979 [208]	2012 [32]

classifications is because the duration of action of the benzodiazepines can be extended by active metabolites.[45-47]

3. Their chemical structure. The core structure of benzodiazepines is a diazepine ring fused to a benzene ring. A phenyl ring is usually attached to the diazepine ring (Figure 2). Most common benzodiazepines are 1,4-benzodiazepines (Figure 2A) (e.g. diazepam[46]) but 1,5-benzodiazepines (Figure 2B) (e.g. clobazam[48]) also exist. A whole host of derivatives of this basic benzodiazepine structure are possible. Some of them involve the addition of another cyclic system to the molecule, for example a triazole ring (Figure 2C) (e.g. alprazolam[49]), imidazole ring (Figure 2D) (e.g. midazolam[50]) or oxazole ring (Figure 2E) (e.g. cloxazolam[51]). Others involve replacement of the benzene ring with a thiophene or pyridine ring. One such group of benzodiazepine derivatives are the thienodiazepines (e.g. etizolam[52]) (Figure 2F). They differ in structure by the replacement of a benzene ring with a thiophene ring but they have similar anticonvulsant, anxiolytic and sedative properties.[52-54] Thienotriazolodiazepines (Figure 2G) (e.g. brotizolam[54]) have a triazole ring fused to the diazepine ring, much like the triazolobenzodiazepines. 2,3-benzodiazepines such as tofisopam exist[55] (Figure 2H) but despite them having the benzodiazepine ring structure they exhibit different pharmacological properties compared with the other benzodiazepines; they act via the 2-amino-3-(3-hydroxy-5-methylisoxazol-4-yl)propionic acid (AMPA) glutamate receptor but still exhibit anxiolytic

Date of Reporting to EMCDDA

2017   Desalkylflurazepam
4-chlorodiazepam (Ro5-4864)

2016
3-hydroxyphenazepam
Cloniprazepam
Desmethylflunitrazepam (fonazepam)
Flunitrazolam
Flutazolam
Bromazolam

2015   Adinazolam
Metizolam
Nitrazolam

2014
Clonazolam
Deschloroetizolam
Flubromazolam
Meclonazepam
Nifoxipam

2013   Diclazepam
Flubromazepam

2012   Pyrazolam

2011   Etizolam

2007
Phenazepam
Nimetazepam

FIGURE 1 Timeline of the reporting of NPS-benzodiazepines to the EMCDDA

activity.[56,57] To the best of the authors' knowledge there are no reports of abuse of 2,3-benzodiazepines. It may only be possible to classify the NPS-benzodiazepines by structure until more information becomes available. Despite being structurally different, thienodiazepines will be grouped together with benzodiazepines as NPS-benzodiazepines in this review.

FIGURE 2 Structure of benzodiazepines and derivatives

3 | MECHANISM OF ACTION OF BENZODIAZEPINES

The main sites of action of benzodiazepines in the human body are *gamma*-Aminobutyric acid A (GABA$_A$) receptors. GABA$_A$ receptors are ligand-gated ion channels which are endogenously activated by *gamma*-Aminobutyric acid (GABA), the major inhibitor neurotransmitter in the central nervous system (CNS).[58] Their structure consists of five protein subunits that surround a central pore through which Cl$^-$ ions can permeate.[58] Binding of GABA to the receptor triggers the chloride ion pore to open leading to an inhibition of neural signals. There are seven receptor subunit families (α 1–6, β 1–3 γ 1–3, δ, ε, π, θ) but the most common GABA$_A$ receptor combination is α2β2γ, which comprises around 43% of all GABA$_A$ receptors in the CNS, with 10 other combinations also identified.[59,60] These isoforms are preferentially distributed within specific regions of the CNS.[61] As a result, the receptors have different pharmacological properties and this helps to explain the differing pharmacological effects observed with the benzodiazepines. The role of GABA$_A$ receptor subunits and addiction has been reviewed by Tan et al.,[62] with the α1 subunit containing GABA$_A$ receptors thought to be those that are involved in the addictive properties of benzodiazepines.[62-64] Benzodiazepines bind between the α1 and γ2 subunits at a site that is distinct from the GABA binding site. They act as positive allosteric modulators, increasing the affinity of GABA to the receptor and potentiating the response of the receptor to GABA.[65] Ethanol also binds to the GABA$_A$ receptor[66] as do another class of drugs, the barbiturates.[67] An exception to the benzodiazepines binding to the GABA$_A$ receptor can be found for 4-chlorodiazepam (Ro5–4864) which recently appeared as an NPS-benzodiazepine.[40] 4-chlorodiazepam binds exclusively to the translocator protein (18 kDa) (TSPO 18 kDa),[68] initially known as the peripheral benzodiazepine receptor.[69] TSPO (18 kDa) is found throughout the body and has a variety of biological functions which have been extensively reviewed[69-71] and it is thought to have considerable potential
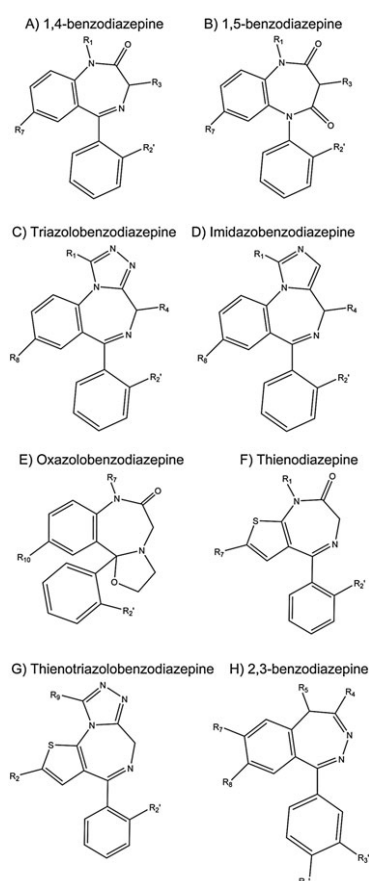
therapeutic value as a pharmacological target.[72,73] Certain compounds that bind to TSPO (18 kDa) can exhibit typical benzodiazepine effects such as being anxiolytic without causing some side effects associated with benzodiazepine use such as sedation.[74] However 4-chlorodiazepam has been found to induce anxiety and cause convulsions in rats despite being a sedative.[75,76] Other benzodiazepines such as diazepam also experience some binding to TSPO (18 kDa)[70,77] but the majority of their pharmacological effects result from the binding of them to $GABA_A$ receptors.[71]

3.1 | Benzodiazepine pharmacokinetics

The pharmacokinetics of benzodiazepines vary widely. The most common route of administration for prescription benzodiazepines is oral but they are also given intramuscularly, intravenously, or rectally.[44] When administered orally, there is a wide variation between the time taken to reach t_{max}.[44] For example, the NPS-benzodiazepine phenazepam reaches a t_{max} between 2 and 4 h following a 2 mg dose[78] while flubromazepam is only thought to reach t_{max} after 11.8 h following a 4 mg dose.[79] The time of day that benzodiazepines are administered can affect t_{max}; triazolam exhibits a t_{max} of ~13 min when taken in the morning compared with ~22 min when taken in the evening. The half-life ($t_{1/2}$) was similarly affected (2.94 h in the morning versus 3.77 h in the evening).[80] It was thought that this is because of the longer fasting period prior to the dose.[80]

Benzodiazepines can have vastly differing half-lives and this has been well reviewed.[44] An important point of note is that the half-life of active benzodiazepine metabolites can be far greater than that of the parent benzodiazepine. For example, desmethyldiazepam (also known as nordazepam) is an active metabolite of several benzodiazepines and can have a half-life of 96 ± 34 h following oral administration of prazepam[45] or 120 h following diazepam.[46] Similarly, desalkylflurazepam is the active metabolite of flurazepam and can have a half-life of 40–144 h following oral administration.[47] Desalkylflurazepam is now known to be sold as a NPS.[39] The main monohydroxylated metabolite of the NPS-benzodiazepine flubromazepam can be detected in urine up to 28 days following ingestion compared to 6 days and 20 h for the parent compound indicating a higher half-life for the metabolite.[79] Similarly, diclazepam is found only in very low concentrations in serum and urine for just over four days. However, its metabolites are detectable for longer time periods: delorazepam is detectable for 6 days in urine and 10 days in serum; lorazepam is detectable for 19 days in both serum and urine; and lormetazepam is detectable for 11 days in urine.[81]

As well as the variations discussed for maximum plasma concentrations and half-lives, other pharmacokinetic parameters exhibit large differences for the benzodiazepines. For example, triazolam has a bioavailability of 44%[82] versus a bioavailability of 97% for diazepam,[83] diazepam is 97% bound to plasma proteins[84] while alprazolam is only 70% bound to plasma proteins.[85] Volumes of distribution also differ; oxazepam and the NPS-benzodiazepine flubromazepam have relatively low volumes of distribution (0.27 l kg^{-1}[86] and 0.73 l kg^{-1},[79] respectively) versus a high volume of distribution of 4.4 l kg^{-1} for flunitrazepam.[87]

The differences briefly mentioned mean that the pharmacokinetics of benzodiazepines cannot be easily compared and specific knowledge of their individual pharmacokinetic parameters is required to understand how they behave in the body. Typical blood concentrations, half-lives, and volumes of distribution (where known) for the NPS-benzodiazepines is provided in Table 1.

The majority of drug metabolism occurs in the liver, primarily by oxidative metabolism mediated by the cytochrome P450 (CYP450) family of enzymes.[99] CYP3A4 is the enzyme most commonly involved in the metabolism of benzodiazepines.[114] However other enzymes are also involved in the metabolism of benzodiazepines such as CYP3A5, CYP2C19, CYP2B6, CYP2C18, and CYP2C9.[115] The CYP3A4 enzyme can also conjugate benzodiazepines containing a nitro group with a glutathione group which can result in cytotoxicity in the liver.[114] Polymorphisms in metabolic enzymes can lead to an alteration in the metabolism of specific drugs. There is only limited evidence that polymorphisms of CYP3A4/5 clinically affect benzodiazepine metabolism.[116] However, CYP2C19 polymorphisms have been shown to influence the metabolism of benzodiazepines to a significant degree particularly with clobazam,[117] etizolam,[118] and diazepam.[119,120] In one study subjects who were CYP2C19 poor metabolisers exhibited an elimination half-life for diazepam which was twice that of normal metabolisers.[121] The effect of polymorphisms could not only lead to greater toxicity but also a longer detection window after administration. The phase II metabolic pathways of benzodiazepines have been less widely studied but are thought to involve uridine 5′-diphospho-glucuronosyltransferase (UGT) enzymes particularly UGT2B15,[122] UGT1A9,[123] UGT2B7,[123] and UGT1A4.[124] Polymorphisms in N-acetyltransferase 2 (NAT2) enzymes can affect the metabolism of benzodiazepines that undergo N-acetylation. This has been observed for a metabolite of clonazepam, 7-aminoclonazepam, where variant NAT2 polymorphisms caused a reduction in the rate of its metabolism.[125]

To detect benzodiazepine use, it is important to be able to detect the parent drug as well as any metabolites. Depending on the type of benzodiazepine 'class' and the additional chemical substituent groups on the core structure the benzodiazepines undergo similar phase I metabolism. The common metabolic pathways for 1,4-benzodiazepines and some triazolo/imidazobenzodiazepines are shown in Figures 3 and 4, respectively. Oxidation is the primary phase I metabolic pathway observed for most benzodiazepines. Typically, this involves hydroxylation on the same carbon atom on the diazepine ring, either labelled as position-3 (e.g. phenazepam[110]) or position 4 (e.g. clonazolam[10]). Hydroxylation at the α-position is also thought to occur for some benzodiazepines (e.g. flubromazolam[10]). N-demethylation of the tertiary amine located on the diazepine ring of diclazepam has been described[81] whilst benzodiazepines containing a nitro group (e.g. meclonazepam[10]) undergo reduction. For phase II metabolism, benzodiazepines that contain hydroxyl groups typically undergo phase II glucuronide conjugation (e.g. lorazepam and oxazepam[126]) without any phase I metabolism. Benzodiazepines containing a 3-hydroxy group typically have a shorter duration of action as they are directly metabolised to glucuronidated forms that are inactive.[127] Some benzodiazepines can be detected as benzophenones (they are either directly metabolised to these compounds or experience some form
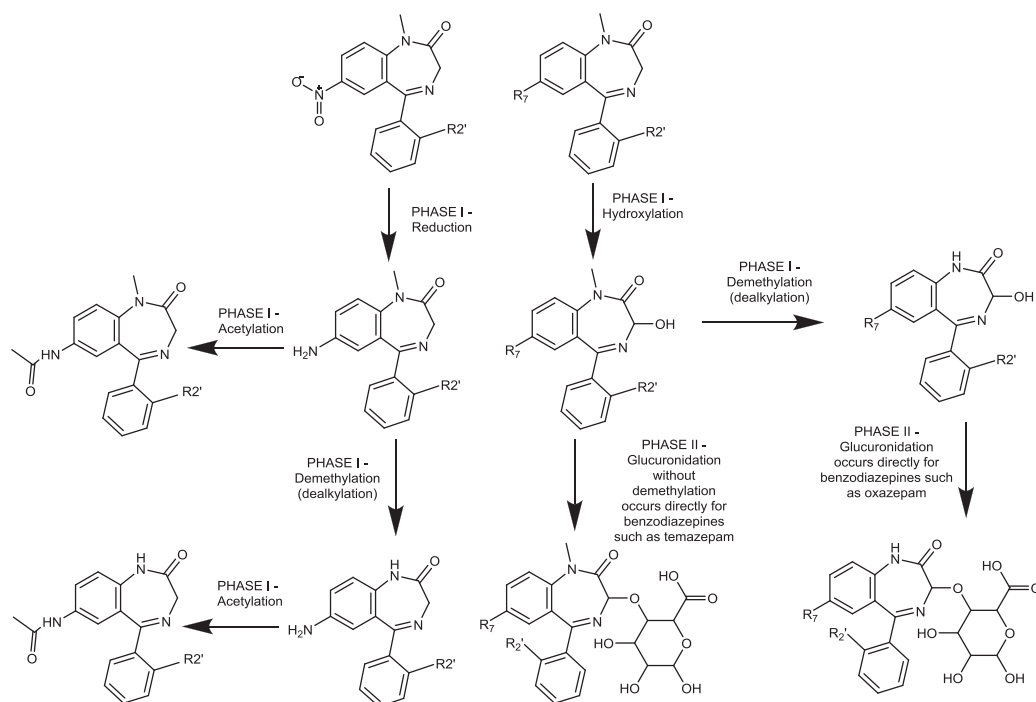
FIGURE 3 General metabolic pathways for 1,4-benzodiazepines

of physical degradation) in urine after administration of the parent drug (e.g. alprazolam,[128] nitrazepam,[129] and phenazepam[130]). The structures of the NPS-benzodiazepines are provided in Figures 2A–2H and Tables 2–6 and their metabolic routes are provided in Figures 3 and 4, and Table 8.

FIGURE 4 General metabolic pathways for triazolobenzodiazepines (also applies to imidazobenzodiazepines)

Once benzodiazepines are metabolised they are mainly eliminated in urine with between <1% and ~20% of the parent drug excreted unchanged with glucuronidated forms being the most common metabolites.[44] As benzodiazepines follow common patterns it should be possible to predict the likely metabolites and routes of elimination of the NPS-benzodiazepines.

To detect the use of NPS-benzodiazepines, give appropriate clinical treatment people who have been exposed to the NPS-benzodiazepines, and interpret their blood/plasma concentrations, it is important to have pharmacokinetic, analytical, and clinical data. With this in mind, we have collated the current available data on the NPS-benzodiazepines within this review.

4 | ANALYTICAL DETECTION OF NPS-BENZODIAZEPINES

It is important in toxicological analysis that analytical methodology can detect, identify, and quantify drugs in a large number of matrices. As benzodiazepines are routinely used in clinical practice throughout the world, many methods exist for their detection and quantification. The analytical methodologies for the determination of benzodiazepines in biological samples (blood, plasma, vitreous, oral fluid, hair, nails, and others) have been recently reviewed.[137,138] It is also important to understand whether analytical methodologies are likely to detect previously unknown benzodiazepines. The common methodological sequence during systematic toxicological analysis is detection, identification and then finally quantitation.[139] Toxicology laboratories commonly utilise immunoassays for presumptive detection before confirmation with other analytical techniques because of the large numbers of samples they may acquire. The advantage of the use of an immunoassay for screening is the lack of absolute selectivity of

TABLE 3 1,4-benzodiazepine-based NPS structures

Compound	From Figure 2A				
	R_1	$R_{2'}$	R_3	R_7	
3-hydroxyphenazepam	H	Cl	OH	Br	
4-chlorodiazepam (Ro5–4864)	CH_3	H	H	Cl	Note: 4-chlorophenyl ring instead of phenyl ring at position 6
Cloniprazepam	Methylcyclopropane	Cl	H	NO_2	
Desalkylflurazepam	H	F	H	Cl	
Desmethylflunitrazepam (fonazepam)	H	F	H	NO_2	
Diclazepam	CH_3	Cl	H	NO_2	
Flubromazepam	H	F	H	Br	
Meclonazepam	H	Cl	CH_3	NO_2	
Nifoxipam	H	F	OH	NO_2	
Nimetazepam	H	H	OH	NO_2	
Phenazepam	H	Cl	H	Br	

TABLE 4 Triazolobenzodiazepine-based NPS structures

	From Figure 2C			
Compound	R1	R2'	R8	
Adinazolam	CH2N(CH¬3)2	H	Cl	
Bromazolam	CH3	H	Br	
Clonazolam	CH3	Cl	NO2	
Flubromazolam	CH3	F	Br	
Flunitrazolam	CH3	F	NO2	
Nitrazolam	CH3	H	NO2	
Pyrazolam				
	CH3	None	Br	Note: Pyridine ring instead of phenyl ring at position 6

TABLE 5 Thienotriazolodiazepine-based NPS structures

	From Figure 2G		
Compound	R2	R2'	R9
Deschloroetizolam	CH2CH3	H	CH3
Etizolam	CH2CH3	Cl	CH3
Metizolam	CH2CH3	Cl	H

TABLE 6 Oxazolobenzodiazepine-based NPS structures

	From Figure 2E		
Compound	$R_{2'}$	R_7	R_{10}
Flutazolam	F	CH_2CH_2OH	Cl

immunoassay antibodies that target the general structure of drug (such as benzodiazepines) rather that the specific drug (such as diazepam or phenazepam).[140] Two recent publications investigating the cross reactivity of standard commercial immunoassay drug screening to new NPS-benzodiazepines in both blood and urine have shown that new NPS-benzodiazepines would be detected by current immunoassay screens.[141,142] Potential misidentification could occur however for structural isomers such as diclazepam and 4-chlorodiazepam

(Ro5–4864).[143] It is likely that new, as yet unknown, benzodiazepines would be detected by current commercial benzodiazepine immunoassays. This hypothesis was backed up by data from the Swedish STRADA project (a project that monitors the occurrence and trends of new psychoactive substances) where 390 clinical samples tested positive in a benzodiazepine immunoassay screen and subsequently tested negative in a classical LC–MS/MS benzodiazepine screen. Later, 40% of these samples were confirmed as containing NPS-benzodiazepines.[144] Following the presumptive detection of benzodiazepines confirmation and quantitation are needed. Typically, high performance liquid chromatography (HPLC)[145,146] with or without a mass spectrometer is used but gas chromatography–mass spectrometry (GC–MS)[111,147] and capillary electrophoresis[148] have been utilised. As the NPS-benzodiazepines are extremely similar in structure to clinically used benzodiazepines, it is expected that they would be able to be detected using similar methods. Liquid chromatography-time of flight-mass spectrometry (LC-TOF-MS) currently gives the best methodology for the detection of any emerging NPS-benzodiazepines, as it is possible to search for compounds based on the molecular formula alone,[149] although care needs to be taken with any isomers that may lead to misidentification. Sample preparation is an important step in the detection and quantitation of NPS-benzodiazepines. The two common techniques used are that of liquid–liquid extraction (LLE) and solid-phase extraction

(SPE).[139] SPE gives advantages amongst others of higher selectivity and increased extraction efficiency and recovery over LLE.[150] This could, however, be a disadvantage when trying to identify new compounds that have not previously been detected and may not elute from a specific SPE column.

One extraction technique that is becoming increasingly popular is quick, easy, cheap, effective, rugged, safe (QuEChERS) a hybrid LLE-SPE method.[151] The use of a primary and secondary amine phase (PSA) allows easier removal of complex matrix components such as blood.[152] The QuEChERS technique has been shown to increase the recoveries of benzodiazepines extracted from various biological matrices such as blood and urine[153] and from milk-based alcoholic drinks (where benzodiazepines are often added illicitly) which provides a complex matrix for extraction as a result of the high number of proteins and fatty acids.[154]

The methods that are currently available for the detection and quantitation of NPS-benzodiazepines in body fluids are listed in Table 7. LC–MS has been used to detect both flubromazepam and its metabolites in urine and serum[79] and also pyrazolam.[113] Pyrazolam does not appear to produce metabolites according to one study[113] but is detectable in serum for up to 50 h but it is excreted in urine for up to 6 days following ingestion of 1 mg which provides a fairly large window of detection for analysis.[113] Diclazepam is found only in very low concentrations for just over four days following ingestion of 1 mg.[81] However its metabolites are discernible for longer time periods with delorazepam detectable for 6 days in urine and 10 days in serum, lorazepam 19 days in both serum and urine and lormetazepam 11 days in urine.[81] Flubromazepam and its metabolites also exhibit a low level of detection in urine using immunoassays.[79,142,161] However, using LC–MS, the monohydroxylated metabolite was detectable for 28 days following ingestion in the urine samples, compared with 23 days in the plasma samples providing an extremely long window of detection for the drug.[79] Other NPS-benzodiazepines would be expected to be similarly detectable.

The metabolic pathways for benzodiazepines are fairly similar (Figures 3 and 4) and this allows metabolites to be predicted and actively searched for when analyzing samples using techniques such as LC–MS.[157,162] As a result of the aforementioned similar metabolic pathways, care must be taken when interpreting the apparent presence of a metabolite. For example, diclazepam is metabolised to lorazepam, lormetazepam, and delorazepam which are all prescription drugs.[81] Likewise, 3-hydroxyphenazepam has been sold on its own as an NPS-benzodiazepine but is a metabolite from both phenazepam[18] and a Russian prescription benzodiazepine cinazepam.[163] Desalkylflurazepam is a metabolite of several drugs including flurazepam,[164] midazolam,[165] and the Japanese prescription drugs flutoprazepam[166] and fludiazepam.[167]

5 | NPS-BENZODIAZEPINE STABILITY

With any detection, identification, and quantification of a drug, it is important to have information on the stability of the drug and any possible changes in the drug concentration that may happen during transportation and/or storage.[168] There have been numerous studies on the stability of benzodiazepines in matrices such as blood and urine at temperatures from 20°C to −80°C.[169-172] Nitrobenzodiazepines (such as flunitrazepam, clonazepam, and nitrazepam) and chlordiazepoxide have been found to be the most unstable especially in bacterially-contaminated specimens.[169,173] Two studies have been carried out investigating the stability of NPS-benzodiazepines (pyrazolam, diclazepam, flubromazepam, meclonazepam, phenazepam, etizolam, nifoxipam, deschloroetizolam, clonazolam, flubromazolam and flutazolam) but only in urine for 1 month and 7 months.[157,174] These studies showed that flubromazepam, clonazolam, nifoxipam, and meclonazepam (the latter three are nitrobenzodiazepines) were unstable in urine (at ambient temperature and at −4°C). Meclonazepam was only detected at 8% of its original concentration after 4 weeks at −4°C and −20°C after 4 weeks). Meclonazepam has also been shown to be unstable in plasma in glass, but not in polypropylene tubes at −20°C.[159] These studies indicate that any future nitrobenzodiazepines are likely to be unstable and suggest that all NPS-benzodiazepines should be investigated for stability and that they should all be collected in tubes containing fluoride oxalate (1%) and then stored at the lowest temperature possible (ideally −20°C or lower) before analysis.

6 | PREDICTION OF THE PHARMACOLOGICAL, TOXICOLOGICAL, AND PHARMACOKINETIC PROPERTIES OF BENZODIAZEPINES

The lack of both *in vivo* and *in vitro* pharmacological testing of the new psychoactive substances that are emerging can be overcome to an extent with the use of quantitative structure activity relationship (QSAR) modelling. This technique creates a model that relates biological activity to structural descriptors of the compound and is based on a learning set with known biological activity. Systematic *in vivo* and *in vitro* work has also been carried out to investigate the structural characteristics that relate to pharmacological activity. From these studies estimations of activity of novel 1,4–benzodiazepines (Figure 2A) can be estimated for half-life (t½), volume of distribution (V_D), bioavailability (F)[175] as well as the potential toxicity of benzodiazepines,[176] showing that hydrazone fragments, primary amines and saturated heterocyclic ring systems lead to increases in toxicity.[176] The biological activity of benzodiazepines was initially studied by Hester who determined the effects of substituents on the biological activity. This determined that triazolobenzodiazepines (Figure 2C) were more potent than the corresponding 1,4-benzodiazepine.[177,178] As for the 1,4–benzodiazepines, the R1, R3, R7 and R2' positions (Figure 2A) are important for biological activity.[179,180] The removal of the phenyl group removes the GABA potentiation by the compound but it can still bind to the GABA site.[181] QSAR studies identified the relative importance of each site to activity and which functional groups could be added at various positions for optimal biological activity. The R7 position was the most important position for increasing receptor affinity (30% in the QSAR model) with the 10 optimal functional groups being CH_2CF_3 > I > Br > CF_3 > Cl > $C(CH_3)_3$ > NO_2 > F > N_3 > CH = CH_2.[182] At the R1 position (37% in the QSAR model) the most optimal groups

TABLE 7 Analytical methods for the analysis of NPS-benzodiazepines in biological matrices

Analyte	Matrix	Analytical method	Internal standard	Extraction	Limit of detection (ng ml⁻¹)	Linear range (ng ml⁻¹)	Limit of quantitation (ng ml⁻¹)	Ref.
Adinazolam	Plasma	HPLC–UV	Alprazolam	LLE (ethyl acetate)	~5	10–800	10	Peng [155]
3-hydroxyphenazepem Phenazepam	Blood Urine Vitreous Muscle Brain Liver	LC–MS/MS	Diazepam-d5	LLE (hexane:Ethylacetate 7:3)	0.3 7	16–100 0.7–200	0.7 16	Crichton [88]
Clonazolam Meclonazepam Nifoxipam	Urine	LC–MS	Methamphetamine-d5 Pethidine-d4	LLE	Not provided	Not provided	Not provided	Vikingsson [156]
Clonazolam, Diclazepam Etizolam Flubormazepam Flubromazolam Pyrazolam	Blood	UPLC–MS/MS	Diazepam-d5	LLE (ethyl acetate:Heptane 4:1)	Same as LOQ	Not provided	1.4 1.6 1.4 3.3 0.37 3.5	Høiseth [95]
Pyrazolam Diclazepam Flubormazepam Meclonazepam Phenazepam Etizolam Nifoxipam Deschloroetizolam Clonazolam Flubromazolam Flutazolam	Urine	LC–MS/MS	Temazepam-d5 Estazolam-d5	B-glucuronidation followed by dilute and shoot	4 2 2.5 1 5 2 10 2 5 2 5	10–1000 2–200 2.5–250 1–100 5–500 5–500 10–1000 5–500 5–500 5–500 5–500	10 2 2.5 1 5 5 10 5 5 5 5	Bergstrand [157]
Desmethylflunitrazepam (fonazepam)	Numerous methods reviewed by Katselou[105]							
Diclazepam	Plasma/ urine	LC–MS	Diazepam-d5 Lorazepam-d4 Nordazepam-d5 Temazepam-d5	B-glucuronidation then LLE using 1-chlorobutane and borate buffer (pH 9)	0.25	0.25–100	Not provided	Moosmann [81]
Etizolam	Plasma/ urine	HPLC	Alprazolam	LLE	1	1–100	Not provided	Fracasso [135]
Etizolam	Plasma	HPLC	N/A	N/A	0.3	Not provided	0.6 ng/ml	Fukasawa [118]
Etizolam	Plasma/ urine	GC–MS/MS	Fludiazepam	SPE	Not provided	5–50	Not provided	Nakamae [158]
Flubromazepam	Plasma/ urine	LC–MS/MS	Nordazepam	LLE (1-chlorobutane)	1	1–100	Not provided	Moosmann [79]
Meclonazepam	Plasma	GC	None	LLE (butyl acetate)	0.1	0.6–20	0.6	Coassolo [159]
Meclonazepam	Urine	LC-MS-QTOF	None	B-glucuronidation	Not provided	Not provided	Not provided	Vikingsson [156]

(Continues)

TABLE 7 (Continued)

Analyte	Matrix	Analytical method	Internal standard	Extraction	Limit of detection (ng ml⁻¹)	Linear range (ng ml⁻¹)	Limit of quantitation (ng ml⁻¹)	Ref.
Metizolam	Urine	LC–MS/MS	Methyl-clonazepam & □-OH-ethylthoethophyllin	LLE (dichloromethane/n-heptane/isopropanol (25/65/20))	0.025	0.05–50	0.05	Kintz[100]
Nifoxipam		Numerous methods reviewed by Katselou[105]						
Nitrazepam	Urine	LC–MS/MS	Nitrazepam-d5	SPE	0.05	0.05–100	0.1	Wang[136]
Phenazepam	Plasma	GC	7-bromo-5-(2-bromophenyl)-1,3-dihydro-1,4-benzodiazepin-2-one	LLE (diethyl ether)	1–2	1–150	Not provided	Ékonomov[160]
Phenazepam	Plasma	GC–MS	Prazepam	SPE	Not provided	Not provided	1	Kerrigan[111]
Phenazepam	Plasma/plasma	LC–MS/MS	Diazepam	SPE	1.44	5–1000	3.06	Kriiku[24]
Phenazepam	Plasma	Dual-column GC	Norclobazam	LLE (ethyl acetate)	5 ng g⁻¹	10–500 ng g⁻¹	10 ng g⁻¹	Rasanen[131]
Phenazepam	Plasma	LC–MS/MS	Diazepam	LLE (acetone)	12	100–1600	28	Stephenson[25]
Pyrazolam	Plasma/urine	LC–MS/MS	Alprazolam	LLE (1-chlorobutane)	1	1–100	Not provided	Moosmann[113]

were OH > F > NH_2 > H > NHOH > C_2H_5 > Cl > CF_3 > Br > CH_3[183] and the *tert*-butyl substitution led to inactivity.[184] At the R2' position (15% in the QSAR model) the order of the most optimal groups was NO_2 > F > CN > Cl > CF_3.[182,185] The influence that substitution at the R3 position has on biological activity is unclear and difficult to predict because of the formation of enantiomeric forms[186,187] but it is thought to have limited influence on the biological activity.[188] In the literature, there are measured binding affinities for desmethylflunitrazepam (fonazepam) and meclonazepam (log IC_{50}) of 0.176 and 0.079 respectively with predicted values of 0.565 and 0.357, respectively.[186,187] These results show that although QSAR can be useful for prediction it is not a replacement for traditional *in vivo* and *in vitro* testing.

7 | THE COMPOSITION OF ILLICITLY-SOLD NPS-BENZODIAZEPINES

A major issue with the purchase of drugs online is that there is no guarantee of the quality of composition. Alprazolam is one of the most widely-prescribed benzodiazepines in the world therefore it is not surprising that it is often illicitly sold. However, the wide variety of drugs that are sold and stated to contain alprazolam is both remarkable and concerning. Mimic alprazolam tablets have been found to contain melatonin[189] or the opioid fentanyl.[183] EcstasyData.org is an independent testing laboratory, created primarily to reduce the potential harm of illicit ecstasy by providing data on the composition of ecstasy tablets.[184] However, a variety of other drugs are often sent in and tested. This independent testing laboratory utilise GC–MS, thin layer chromatography (TLC) and colour tests for analysing and identifying the materials that are supplied to them.[184] Other drugs that have been found in alprazolam tablets include other clinically-used benzodiazepines, synthetic cannabinoids, synthetic opiates, Z-drugs, piperazines, barbiturates and clinically-used anaesthetics and antihistamines. Clonazepam tablets have been identified as containing the NPS-benzodiazepine clonazolam.[184] Etizolam tablets have been found to contain alprazolam, flubromazepam (an NPS-benzodiazepine) and diphenylprolinol, a compound used as a designer drug.[184] Diclazepam tablets have been identified as containing nimetazepam,[184] a widely prescribed and abused drug in southeast Asia[190] and an NPS-benzodiazepine in Europe itself[17] and some illicit tablets of nimetazepam (also known as Ermin 5) have been found to contain phenazepam.[191] In addition, in the 2016 EMCDDA drug report it was noted that alprazolam tablets had been identified as containing flubromazolam and diazepam tablets had been identified to contain phenazepam.[3] This is a huge problem for drug users as they may be inadvertently taking a drug potentially many times more harmful than expected because of the lack of information regarding drug–drug interactions. As mentioned previously, it is well known that the concurrent use of opioids, opiates and benzodiazepines can increase the risk of death.[7,192] There have been sporadic reports of the use of benzodiazepines as either diluents or adulterants in heroin however this does not appear to be as common.[193] The majority of the data from EcstasyData.org is from the United States but samples are sent in from across the world with many appearing to have been purchased online in China.[184] With the increase of NPS-benzodiazepines in recent years, this may become even more problematic.

TABLE 8 Metabolic pathways and metabolites of NPS-benzodiazepines

Compound	Major phase I metabolites (both *in vivo* and *in vitro*)	Reference(s)
3-hydroxyphenazepam	None known	Moosmann [134]
4-chlorodiazepam (Ro5–4864)	There appears to be a lack of information on the metabolic routes of this benzodiazepine but they are possibly similar to those observed for diclazepam such as N-demethylation and 3-hydroxylation	No reference
Adinazolam	N-desmethyladinazolam N,N-didesmethyladinazolam α-hydroxyadinazolam, Estazolam	Moosmann [134] Fraser [132]
Bromazolam	No experimental studies to date but possible metabolites are hydroxylation at the α or 4 positions as is the case with other triazolobenzodiazepines	No reference
Clonazolam	7-aminoclonazolam, 7-acetaminoclonazolam Hydroxyclonazolam	Huppertz [10], Meyer [133]
Cloniprazepam	Monohydroxylated cloniprazepam Clonazepam (dealkylation) Reduction of the 7-nitro to a 7-amino group 7-aminoclonazepam (dealkylation and reduction) Hydroxylation and dealkylation Hydroxylation and dealkylation Oxidation of the 3-hydroxy group to a 3-keto group	Moosmann [134]
Desalkylflurazepam	It is unclear as to whether this would go further phase I metabolism or instead proceed directly to phase II metabolism as is the case when it is a metabolite from flurazepam	Breimer [47]
Deschloroetizolam	Monohydroxylation (probable 9-methyl) Monohydroxylation (probable 2-ethyl) Monohydroxylation (probable position 6) Dihydroxylation (positions undetermined)	Huppertz [10], El Balkhi [104]
Desmethylflunitrazepam (fonazepam)	3-hydroxynorflunitrazepam Monohydroxylation (position undetermined) 7-aminonorflunitrazepam	Moosmann [134]
Diclazepam	Delorazepam, lorazepam Lormetazepam	Moosmann [81], El Balkhi [104]
Etizolam	Hydroxylation on the α-carbon of the 9-methyl group (also known as α-hydroxyetizolam) Hydroxylation on the α-carbon of the 2-ethyl group (also known as 8-hydroxyetizolam)	El Balkhi [104], Fracasso [135]
Flubromazepam	Monohydroxylation (possibly 3-hydroxy, undetermined) Debromination and monohydroxylation (possibly 3-hydroxy, undetermined) Monohydroxylation (either on the phenyl ring or the benzene ring, undetermined)	Moosmann [79], El Balkhi [104]
Flubromazolam	α-hydroxyflubromazepam 4-hydroxyflubromazepam Dihydroxylation (α-hydroxy and 4-hydroxy)	Huppertz [10], El Balkhi [104]
Flunitrazolam	No experimental studies to date but possible metabolites are reduction of the 8-nitro group to an 8-amino group and hydroxylation at position 4 of the diazepine ring.	No reference
Flutazolam	Oxazole ring-opening and elimination The above metabolite is thought to be the main metabolite present in plasma but other metabolic pathways do exist: N1-dealkylation (loss of CH$_2$CH$_2$OH), 3-hydroxylation Hydroxylation on either the fluorophenyl or chlorophenyl ring Both N1-dealkylation and 3-hydroxylation	Mitsubishi-Tanabe-Pharma-Corporation [36]
Meclonazepam	7-aminomeclonazepam, 7-acetaminomeclonazepam	El Balkhi [104], Meyer [133]
Metizolam	2 mono-hydroxylated compounds Di-hydroxylated compound Hydroxylation (likely to be 2-ethyl or 6- position)	Kintz [100], Moosmann [134]
Nifoxipam	7-aminonifoxipam, 7-acetaminonifoxipam	El Balkhi [104], Meyer [133]
Nimetazepam	Nitrazepam, 7-aminonimetazepam	Wang [136]
Nitrazolam	8-aminonitrazolam Mono hydroxylated metabolite (likely either 4- or α- position)	Moosmann [134]
Phenazepam	3-hydroxyphenazepam Hydroxylation and methoxy addition (positions undetermined)	Zherdev [18], Maskell [110]
Pyrazolam	No detectable metabolites in serum or urine	Moosmann [113]

8 | SUMMARY

The use and abuse of benzodiazepines is already common throughout the world. In recent years, there has been a large increase in the number of novel psychoactive substances. Benzodiazepines are only a small subsection of the total number of novel psychoactive substances but that number is steadily increasing. NPS-benzodiazepines are appearing in a variety of countries across the world. NPS-thienodiazepines are appearing at a much slower rate, perhaps because of a lower usage clinically and the already widespread availability of benzodiazepines. NPS-benzodiazepines have been implicated in deaths in England and Wales and the increasing availability of all novel psychoactive substances led to the introduction of the Psychoactive Substances Act within the UK in 2016. It remains to be seen whether this will affect the supply and use of NPS-benzodiazepines because phenazepam and etizolam were placed under control in the UK under the Misuse of Drugs Act 1971 but are still regularly identified in post-mortem cases and in drug-impaired drivers within the UK. The same may be expected for the NPS-benzodiazepines. The pharmacokinetics and metabolic pathways of NPS-benzodiazepines are not currently well understood and there can be huge variation in pharmacokinetic parameters between individual compounds. Further investigation is clearly needed to establish the exact pharmacology of these novel psychoactive substances.

REFERENCES

1. UNODC (United Nations Office on Drugs and Crime). World drug report 2016. Available at: https://www.unodc.org/documents/colombia/2016/WDR/WORLD_DRUG_REPORT_2016_web.pdf [March 2017].

2. EMCDDA (European Monitoring Centre for Drugs and Drug Addiction)-Europol. European drug report: Trends and Developments 2015. Available at: http://www.emcdda.europa.eu/attachements.cfm/att_239505_EN_TDAT15001ENN.pdf [March 2017].

3. EMCDDA (European Monitoring Centre for Drugs and Drug Addiction)-Europol. European drug report: Trends and Developments 2016. Available at: http://www.emcdda.europa.eu/system/files/publications/2637/TDAT16001ENN.pdf [March 2017].

4. UNODC (United Nations Office on Drugs and Crime). The International drug control conventions, schedules of the Convention on psychotropic substances of 1971 as at 4 November 2015.

5. Bachhuber MA, Hennessy S, Cunningham CO, Starrels JL. Increasing benzodiazepine prescriptions and overdose mortality in the United States 1996–2013. Am J Public Health. 2016;106:686-688.

6. Health and Social Care Information Centre. Prescriptions dispensed in the community, Statistics for England - 2004-2014. 2015.

7. Jones JD, Mogali S, Comer SD. Polydrug abuse: A review of opioid and benzodiazepine combination use. Drug Alcohol Depend. 2012;125:8-18.

8. Kapil V, Green JL, Lait CL, Wood DM, Dargan PI. Misuse of benzodiazepines and Z-drugs in the UK. Brit J Psychiat. 2014;205:407-408.

9. Vogel M, Knöpfli B, Schmid O, et al. Treatment or "high": Benzodiazepine use in patients on injectable heroin or oral opioids. Addict Behav. 2013;38:2477-2484.

10. Huppertz L, Bisel P, Westphal F, Franz F, Auwärter V, Moosmann B. Characterization of the four designer benzodiazepines clonazolam, deschloroetizolam, flubromazolam, and meclonazepam, and identification of their in vitro metabolites. Forensic Toxicol. 2015;33:388-395.

11. RAND Corporation, Internet-facilitated drugs trade: An analysis of the size, scope and the role of the Netherlands, 2016, Available from http://www.rand.org/pubs/research_reports/RR1607.html [31 May 2017]

12. UNODC (United Nations Office on Drugs and Crime). The challenge of new psychoactive substances. Available at: https://www.unodc.org/documents/scientific/NPS_2013_SMART.pdf [31 May 2017].

13. Reddit. Available at: www.reddit.com [31 May 2017].

14. Bluelight. Available at: www.bluelight.org [31 May 2017].

15. Flashback. Available at: https://www.flashback.org/t2805464 [31 May 2017].

16. UK chemical research. Available at: https://www.ukchemicalresearch.org/Thread-N-Desalkylflurazepam-Norflurazepam [31 May 2017].

17. EMCDDA (European Monitoring Centre for Drugs and Drug Addiction). EMCDDA–Europol 2007 Annual report on the implementation of Council Decision 2005/387/JHA. Available at: http://www.emcdda.europa.eu/system/files/publications/503/2007_Implementation_report_281403.pdf [31 May 2017].

18. Zherdev VP, Caccia S, Garattini S, Ekonomov AL. Species differences in phenazepam kinetics and metabolism. Eur J Drug Metab Pharmacokinet. 1982;7:191-196.

19. Чекулаев МИ, Владимировна МТ, Барсегян СС. Опасность феназепама как уличного наркотика. Здоровье и образование в XXI веке. 2015;17:85-86.

20. Zhu B-L, Meng L, Zheng K-F. Analysis of the new psychoactive substance of phenazepam. Chin J Forensic Sci. 2014;6:44

21. McAuleya A, Hecht G, Barnsdale L, et al. Mortality related to novel psychoactive substances in Scotland, 2012: An exploratory study. Int J Drug Policy. 2015;26:461-467.

22. Shearer K, Bryce C, Parsons M, Torrance H. Phenazepam: A review of medico-legal deaths in south Scotland between 2010 and 2014. Forensic Sci Int. 2015;254:197-204.

23. Simonsen KW, Edvardsen HME, Thelander G, et al. Fatal poisoning in drug addicts in the Nordic countries in 2012. Forensic Sci Int. 2015;248:172-180.

24. Kriikku P, Wilhelm L, Rintatalo J, Hurme J, Kramer J, Ojanperä I. Phenazepam abuse in Finland: Findings from apprehended drivers, post-mortem cases and police confiscations. Forensic Sci Int. 2012;10:1-3.

25. Stephenson JB, Golz DE, Brasher MJ. Phenazepam and its effects on driving. J Anal Toxicol. 2013;37:25-29.

26. Government of Finland, Valtioneuvoston asetus huumausaineina pidettävistä aineista, valmisteista ja kasveista annetun valtioneuvoston asetuksen liitteen IV muuttamisesta, Available at: http://www.finlex.fi/fi/laki/alkup/2014/20140589 [31 May 2017].

27. Government of China, 关于印发《非药用类麻醉药品和精神药品列管办法》的通知. Available at: http://www.sfda.gov.cn/WS01/CL0056/130753.html [31 May 2017].

28. U.K. Government, Import ban of new 'legal high' phenazepam introduced, Available at: https://www.gov.uk/government/news/import-ban-of-new-legal-high-phenazepam-introduced [31 May 2017].

29. UN Commission on Narcotic Drugs. Inclusion of Phenazepam in schedule iv of the Convention on psychotropic substances of 1971. 2016

30. EMCDDA (European Monitoring Centre for Drugs and Drug Addiction)-Europol. EMCDDA–Europol 2011 Annual report on the implementation of Council Decision 2005/387/JHA, 2011. Available at: http://www.emcdda.europa.eu/system/files/publications/689/EMCDDA-Europol_Annual_Report_2011_2012_final_335568.pdf [31 May 2017].

31. Mitsubishi-Tanabe-Pharma-Corporation, 2016. Available at: https://medical.mt-pharma.co.jp/di/file/if/f_dep.pdf [31 May 2017].

32. EMCDDA. (European Monitoring Centre for Drugs and Drug Addiction)-Europol. EMCDDA–Europol 2012 Annual report on the implementation of Council Decision 2005/387/JHA, 2012. Available at: http://www.emcdda.europa.eu/system/files/publications/734/

EMCDDA-Europol_2012_Annual_Report_final_439477.pdf [31 May 2017].

33. EMCDDA (European Monitoring Centre for Drugs and Drug Addiction)-Europol. EMCDDA-Europol 2013 Annual report on the implementation of Council Decision 2005/387/JHA, 2013. Available at: http://www.emcdda.europa.eu/system/files/publications/814/TDAN14001ENN_475519.pdf [31 May 2017].

34. EMCDDA (European Monitoring Centre for Drugs and Drug Addiction)-Europol. EMCDDA-Europol 2014 Annual report on the implementation of Council Decision 2005/387/JHA, 2014. Available at: http://www.emcdda.europa.eu/system/files/publications/1018/TDAN15001ENN.pdf [31 May 2017].

35. EMCDDA (European Monitoring Centre for Drugs and Drug Addiction)-Europol. EMCDDA–Europol 2015 Annual report on the implementation of Council Decision 2005/387/JHA, 2016. Available at: http://www.emcdda.europa.eu/system/files/publications/1018/TDAN15001ENN.pdf [31 May 2017].

36. Mitsubishi-Tanabe-Pharma-Corporation, 2009. Available at: https://medical.mt-pharma.co.jp/di/file/if/f_crm.pdf [31 May 2017].

37. Medical Products Agency Sweden, 2016. Available at: https://lakemedelsverket.se/overgripande/Lagar--regler/Yttranden-enligt-lagen-om-forstorande-av-vissa-halsofarliga-missbrukssubstanser/ [31 May 2017].

38. Medical Products Agency Sweden, 2016. Available at: https://www.folkhalsomyndigheten.se/documents/tillsyn-regelverk/klassificering-missbrukssubstanser/substanser/n-desmetylflunitrazepam.pdf [31 May 2017].

39. Austrian Public Health Institute, 2016. Available at: https://forum.goeg.at/EwsForum/default.aspx?g=posts&m=270 [31 May 2017].

40. National forensic laboratory Slovenia, 2016. Available at: http://www.policija.si/apps/nfl_response_web/0_Analytical_Reports_final/Ro5-4864_(Chlorodiazepam)-ID-1567-16_rpt-110816.pdf [31 May 2017].

41. Office for National Statistics, Deaths Related to Drug Poisoning in England and Wales: 2014 registrations, 2014. Available from: http://www.ons.gov.uk/ons/rel/subnational-health3/deaths-related-to-drug-poisoning/england-and-wales---2014/index.html [31 May 2017].

42. UK Government. Psychoactive substances bill. 2015, Available at: https://www.gov.uk/government/collections/psychoactive-substances-bill-2015 [31 May 2017].

43. UK government. Misuse of drugs act, 1971.

44. Drummer OH. *The Forensic Pharmacology of Drugs of Abuse.* Arnold, UK; 2001.

45. Smith MT, Evans LEJ, Eadie MJ, Tyre JH. Pharmacokinetics of prazepam in man. *Eur J Clin Pharmacol.* 1979;16:141-147.

46. Mandelli M, Tognoni G, Garattini S. Clinical pharmacokinetics of diazepam. *Clin Pharmacokinet.* 1978;3:72-91.

47. Breimer DD, Jochemsen R. Clinical pharmacokinetics of hypnotic benzodiazepines. *Brit J Clin Pharmacol.* 1983;16:277S-278S.

48. Gerhards HJ. Neuropharmacological profile of clobazam, a new 1′,5′-benzodiazepine. *Psychopharmacol.* 1978;58:27-33.

49. Greenblatt DJ, Moltke LLv, Harmatz JS, Ciraulo DA, Shader RI. Alprazolam pharmacokinetics, metabolism, and plasma levels: Clinical implications. *J Clin Psychiatry.* 1993;54:4-14.

50. Smith MT, Eadie MJ, Brophy TOR. The pharmacokinetics of midazolam in man. *Eur J Clin Pharmacol.* 1981;19:271-278.

51. Fischer-Cornelssen KA. Multicenter trials and complementary studies of cloxazolam, a new anxiolytic drug. *Arzneimittelforschung.* 1981;31:1757-1765.

52. Bertolino A, Mastucci E, Porro V, et al. Etizolam in the treatment of generalized anxiety disorder: A controlled clinical trial. *J Int Med Res.* 1989;17:455-460.

53. Casacchiaa M, Bolinoa F, Ecarib U. Etizolam in the treatment of generalized anxiety disorder: A double-blind study versus placebo. *Curr Med Res Op.* 1990;12:215-223.

54. Langley MS, Clissold SP. Brotizolam. A review of its pharmacodynamic and pharmacokinetic properties, and therapeutic efficacy as an hypnotic. *Drugs.* 1988;35:104-122.

55. Rundfeldt C, Socała K, Wlaź P. The atypical anxiolytic drug, tofisopam, selectively blocks phosphodiesterase isoenzymes and is active in the mouse model of negative symptoms of psychosis. *J Neural Transm.* 2010;117:1319-1325.

56. Gitto R, Zappalà M, Sarro GD, Chimirri A. Design and development of 2,3-benzodiazepine (cfm) noncompetitive ampa receptor antagonists. *Il Farmaco.* 2002;57:129-134.

57. Horváth EJ, Horváth K, Hámori T, Fekete MI, Sólyom S, Palkovits M. Anxiolytic 2,3-benzodiazepines, their specific binding to the basal ganglia. *Prog Neurobiol.* 2000;60:309-342.

58. GABAA (Γ-aminobutyric acid). *Brit J Clin Pharmacol.* 2009;158(Suppl 1):S110-S112.

59. Olsen RW, Sieghart W. International Union of Pharmacology. Lxx. Subtypes of gamma-aminobutyric acid(a) receptors: Classification on the basis of subunit composition, pharmacology, and function. Update. *Pharmacol Rev.* 2008;60:243-260.

60. Olsen RW, Sieghart W. GABAA receptors: Subtypes provide diversity of function and pharmacology. *Neuropharmacology.* 2009;56:141-148.

61. Sieghart W, Sperk G. Subunit composition, distribution and function of GABAA receptor subtypes. *Curr Top Med Chem.* 2002;2:795-816.

62. Tan KR, Rudolph U, Lüscher C. Hooked on benzodiazepines: GABAA receptor subtypes and addiction. *Trends Neurosci.* 2011;34:188-197.

63. Heikkinen AE, Möykkynen TP, Korpi ER. Long-lasting modulation of glutamatergic transmission in Vta dopamine neurons after a single dose of benzodiazepine agonists. *Neuropsychopharmacology.* 2009;34:290-298.

64. Tan KR, Brown M, Labouèbe G, et al. Neural bases for addictive properties of benzodiazepines. *Nature.* 2010;463:769-774.

65. Sigel E, Steinmann ME. Structure, function, and modulation of GABAA receptors. *J Biol Chem.* 2012;287:40224-40231.

66. Grobin AC, Matthews DB, Devaud LL, Morrow AL. The role of GABAA receptors in the acute and chronic effects of ethanol. *Psychopharmacol.* 1998;139:2-19.

67. Olsen RW. GABA-benzodiazepine-barbiturate receptor interactions. *J Neurochem.* 1981;37:1-13.

68. Holmes PV, Drugan RC. Differential effects of anxiogenic central and peripheral benzodiazepine receptor ligands in tests of learning and memory. *Psychopharmacol.* 1991;104:249-254.

69. Papadopoulos V, Baraldi M, Guilarte TR, et al. Translocator protein (18 Kda): New nomenclature for the peripheral-type benzodiazepine receptor based on its structure and molecular function. *Trends Pharmacol Sci.* 2006;27:402-409.

70. Casellas P, Galiegue S, Basile AS. Peripheral benzodiazepine receptors and mitochondrial function. *Neurochem Int.* 2002;40:475-486.

71. Gavish M, Bachman I, Shoukrun R, et al. Enigma of the peripheral benzodiazepine receptor. *Pharmacol Rev.* 1999;51:629-650.

72. Rupprecht R, Papadopoulos V, Rammes G, et al. Translocator protein (18 Kda) (Tspo) as a therapeutic target for neurological and psychiatric disorders. *Nat Rev Drug Discov.* 2010;9:971-988.

73. Papadopoulos V, Lecanu L. Translocator protein (18 Kda) Tspo: An emerging therapeutic target in neurotrauma. *Exp Neurol.* 2009;219:53-57.

74. Rupprecht R, Rammes G, Eser D, et al. Translocator protein (18 Kd) as target for anxiolytics without benzodiazepine-like side effects. *Science.* 2009;325:490-493.

75. Pellow S, File SE. Anxiolytic and anxiogenic drug effects on exploratory activity in an elevated plus-maze: A novel test of anxiety in the rat. *Pharmacol Biochem Behav.* 1986;24:525-529.

76. File SE, Green AR, Nutt DJ, Vincent ND. On the convulsant action of Ro 5-4864 and the existence of a micromolar benzodiazepine binding site in rat brain. *Psychopharmacol*. 1984;82:199-202.

77. Gavish M, Katz Y, Bar-Ami S, Weizman R. Biochemical, physiological, and pathological aspects of the peripheral benzodiazepine receptor. *J Neurochem*. 1991;58:1589-1601.

78. Lomas EC, Maskell PD. Phenazepam: More information coming in from the cold. *J Forensic Leg Med*. 2015;36:61-62.

79. Moosmann B, Huppertz L, Hutter M, Buchwald A, Ferlaino S, Auwärter V. Detection and identification of the designer benzodiazepine flubromazepam and preliminary data on its metabolism and pharmacokinetics. *J Mass Spectrom*. 2013;48:1150-1159.

80. Smith RB, Kroboth PD, Phillips JP. Temporal variation in triazolam pharmacokinetics and pharmacodynamics after oral administration. *J Clin Pharmacol*. 1986;26:120-124.

81. Moosmann B, Bisel P, Auwärter V. Characterization of the designer benzodiazepine diclazepam and preliminary data on its metabolism and pharmacokinetics. *Drug Test Anal*. 2014;6:757-763.

82. Kroboth PD, McAuley JW, Kroboth FJ, Bertz RJ, Smith RB. Triazolam pharmacokinetics after intravenous, oral, and sublingual administration. *J Clin Psychopharmacol*. 1995;15:259-262.

83. Ochs HR, Otten H, Greenblatt DJ, Dengler HJ. Diazepam absorption: Effects of age, sex, and billroth gastrectomy. *Dig Dis Sci*. 1982;27:225-230.

84. Klotz U, Antonin KH, Bieck PR. Pharmacokinetics and plasma binding of diazepam in man, dog, rabbit, guinea pig and rat. *J Pharmacol Exp Therapeut*. 1976;199:67-73.

85. Garzone PD, Kroboth PD. Pharmacokinetics of the newer benzodiazepines. *Clin Pharmacokinet*. 1989;16:337-364.

86. Sonne J, Loft S, Døssing M, et al. Bioavailability and pharmacokinetics of oxazepam. *Eur J Clin Pharmacol*. 1988;35:385-389.

87. Boxenbaum HG, Posmanter HN, Macasieb T, et al. Pharmacokinetics of Flunitrazepam following single- and multiple-dose oral administration to healthy human subjects. *J Pharmacokinet Biopharm*. 1978;6:283-293.

88. Crichton ML, Shenton CF, Drummond G, Beer LJ, Seetohul LN, Maskell PD. Analysis of phenazepam and 3-hydroxyphenazepam in post-mortem fluids and tissues. *Drug Test Anal*. 2015;7:926-936.

89. Ajir K, Smith M, Lin KM, et al. The pharmacokinetics and pharmacodynamics of adinazolam: Multi-ethnic comparisons. *Psychopharmacol*. 1997;129:265-270.

90. Fleishaker JC, Hulst LK, Smith TC, Friedman H. Clinical pharmacology of adinazolam and N-desmethyladinazolam mesylate following single intravenous infusions of each compound in health volunteers. *Eur J Clin Pharmacol*. 1992;42:287-294.

91. Fleishaker JC, Phillips JP. Adinazolam pharmacokinetics and behavioral effects following administration of 20-60 mg oral doses of its Mesylate salt in healthy volunteers. *Psychopharmacol*. 1989;99:34-39.

92. Fleishaker JC, Wright CE. Pharmacokinetic and Pharmacodynamic comparison of immediate-release and sustained-release adinazolam mesylate tablets after single- and multiple-dose administration. *Pharm Res*. 1992;9:457-463.

93. Venkatakrishnan K, Culm KE, Ehrenberg BL, et al. Kinetics and dynamics of intravenous adinazolam, n-desmethyl adinazolam, and alprazolam in healthy volunteers. *J Clin Pharmacol*. 2005;45:529-537.

94. Bluelight. Available at: http://www.bluelight.org/vb/threads/791664-Flunitrazolam [31 May 2017].

95. Høiseth G, Tuv SS, Karinen R. Blood concentrations of new designer benzodiazepines in forensic cases. *Forensic Sci Int*. 2016;268:35-38.

96. Bluelight. Available at: http://www.bluelight.org/vb/threads/775400-Cloniprazolam [31 May 2017].

97. Reddit. Available at: https://www.reddit.com/r/researchchemicals/comments/5gciof/fonazepam_first_thoughts/ [31 May 2017].

98. Flashback. [cited 2017 January]; Available from: https://www.flashback.org/t2650660 [31 May 2017].

99. Xu C, Li CY-T, Kong A-NT. Induction of phase I, ii and iii drug metabolism/transport by xenobiotics. *Arch Pharm Res*. 2005;28:249-268.

100. Kintz P, Richeval C, Jamey C, et al. Detection of the designer benzodiazepine metizolam in urine and preliminary data on its metabolism. *Drug Test Anal*. 2016. https://doi.org/10.1002/dta.2099.

101. Lukasik-Glebocka M, Sommerfeld K, Tezyk A, Zielinska-Psuja B, Panienski P, Zaba C. Flubromazolam--a new life-threatening designer benzodiazepine. *Clin Toxicol (Phila)*. 2016;54:66-68.

102. Mitsubishi Tanabe Pharma Corporation. Available at: https://medical.mt-pharma.co.jp/di/file/if/f_crm.pdf [31 May 2017].

103. UK chemical research. Available at: https://www.ukchemicalresearch.org/Thread-meclonazepam [31 May 2017].

104. El Balkhi S, Chaslot M, Picard N, et al. Characterization and identification of eight designer benzodiazepine metabolites by incubation with human liver microsomes and analysis by a triple quadrupole mass spectrometer. *Int J Leg Med*. 2017; https://doi.org/10.1007/s00414-00017-01541-00416

105. Katselou M, Papoutsis I, Nikolaou P, Spiliopoulou C, Athanaselis S. Metabolites replace the parent drug in the drug arena. The cases of fonazepam and nifoxipam. *Forensic Toxicol*. 2017;35:1-10.

106. PMDA (Pharmaceutical and medical devices Agency) Japan. 2017. Available at: http://www.info.pmda.go.jp/go/pack/1124004F1042_2_09/ [31 May 2017].

107. JAPIC (Japan Pharmaceutical information center). 2005. Available at: http://www.japic.or.jp/service/whats_new/japicnews/pdf/254.pdf [31 May 2017].

108. Yakuzaishiharowa. 2017. Available at: http://yakuzaishiharowa.com/medical_pharmacy/bz-medicine.html [31 May 2017].

109. UK chemical research. Available at: https://www.ukchemicalresearch.org/Thread-Nitrazolam [31 May 2017].

110. Maskell PD, De-Paoli G, Seetohul LN, Pounder DJ. Phenazepam: The drug that came in from the cold. *J Forensic Leg Med*. 2012;19:122-125.

111. Kerrigan S, Mellon MB, Hinners P. Detection of phenazepam in impaired driving. *J Anal Toxicol*. 2013;37:605-610.

112. Lomas EC, Maskel PD. Phenazepam: More information coming in from the cold. *J Forensic Leg Med*. 2015;36:61-62.

113. Moosmann B, Hutter M, Huppertz LM, Ferlaino S, Redlingshöfer L, Auwärter V. Characterization of the designer benzodiazepine pyrazolam and its detectability in human serum and urine. *Forensic Toxicol*. 2013;31:263-271.

114. Mizuno K, Katoh M, Okumura H, et al. Metabolic activation of benzodiazepines by Cyp3a4. *Drug Metab Dispos*. 2009;37:345-351.

115. Fukasawa T, Suzuki A, Otani K. Effects of genetic polymorphism of cytochrome P450 enzymes on the pharmacokinetics of benzodiazepines. *J Clin Pharm Therapeut*. 2007;32:333-341.

116. Whirl-Carrillo M, McDonagh EM, Hebert JM, et al. Pharmacogenomics knowledge for personalized medicine. *Clin Pharmacol Therapeut*. 2012;92:414-417.

117. Parmeggiani A, Posar A, Sangiorgi S, Giovanardi-Rossi P. Unusual sideeffects due to clobazam: A case report with genetic study of Cyp2c19. *Brain Dev*. 2004;26:63-66.

118. Fukasawa T, Yasui-Furukori N, Suzuki A, Inoue Y, Tateishi T, Otani K. Pharmacokinetics and pharmacodynamics of etizolam are influenced by polymorphic Cyp2c19 activity. *Eur J Clin Pharmacol*. 2005;61:791-795.

119. Sohn DR, Kusaka M, Ishizaki T, et al. Incidence of S-mephenytoin hydroxylation deficiency in a Korean population and the interphenotypic differences in diazepam pharmacokinetics. *Clin Pharmacol Therapeut*. 1992;52:160-169.

120. Goldstein JA. Clinical relevance of genetic polymorphisms in the human Cyp2c subfamily. *Brit J Clin Pharmacol*. 2001;52:349-355.

121. Bertilsson L, Henthorn TK, Sanz E, Tybring G, Säwe J, Villén T. Importance of genetic factors in the regulation of diazepam metabolism: Relationship to S-Mephenytoin, but not debrisoquin, hydroxylation phenotype. *Clin Pharmacol Therapeut*. 1989;45:348-355.

122. Court MH, Hao Q, Krishnaswamy S, et al. Udp-glucuronosyltransferase (Ugt) 2b15 pharmacogenetics: Ugt2b15 D85y genotype and gender are major determinants of oxazepam glucuronidation by human liver. *J Pharmacol Exp Therapeut*. 2004;310:656-665.

123. Court MH, Duan SX, Guillemette C, et al. Stereoselective conjugation of oxazepam by human udp-glucuronosyltransferases (Ugts): S-oxazepam is glucuronidated by Ugt2b15, while R-oxazepam is glucuronidated by Ugt2b7 and Ugt1a9. *Drug Metab Dispos*. 2002;30:1257-1265.

124. Bourcier K, Hyland R, Kempshall S, et al. Investigation into Udp glucuronosyltransferase (Ugt) enzyme kinetics of imidazole- and triazole containing antifungal drugs in human liver microsomes and recombinant Ugt enzymes. *Drug Metab Dispos*. 2010;38:923-929.

125. Olivera M, Martínez C, Gervasini G, et al. Effect of common Nat2 variant alleles in the acetylation of the major clonazepam metabolite, 7-Aminoclonazepam. *Drug Metab Lett*. 2007;1:3-5.

126. Peppers MP. Benzodiazepines for alcohol withdrawal in the elderly and in patients with liver disease. *Pharmacotherapy*. 1996;16:49-57.

127. Mozayani A, Raymon L. *Handbook of Drug Interactions: A Clinical and Forensic Guide*. New York: Springer Science & Business Media; 2003.

128. Fraser AD, Bryan W, Isner AF. Urinary screening for alprazolam and its major metabolites by the Abbott Adx and Tdx analyzers with confirmation by GC/MS. *J Anal Toxicol*. 1991;15:25-29.

129. Inoue T, Niwaguchi T. Determination of nitrazepam and its main metabolites in urine by thin-layer chromatography and direct densitometry. *J Chromatogr*. 1985;339:163-169.

130. Kopanitsa MV, Zhuk OV, Zinkovsky VG, Krishtal OA. Modulation of GABAA receptor-mediated currents by phenazepam and its metabolites. *Naunyn Schmiedebergs Arch Pharmacol*. 2001;364:1-8.

131. Rasanen I, Ojanperä I, Vuori E. Quantitative screening for benzodiazepines in blood by dual-column gas chromatography and comparison of the results with urine immunoassay. *J Anal Toxicol*. 2000;24:46-53.

132. Fraser AD, Isner AF, Bryan W. Urinary screening for adinazolam and its major metabolites by the emit D.A.U. And FPIA benzodiazepine assays with confirmation by HPLC. *J Anal Toxicol*. 1993;17:427-431.

133. Meyer MR, Bergstrand MP, Helander A, Beck O. Identification of main human urinary metabolites of the designer nitrobenzodiazepines clonazolam, meclonazepam, and nifoxipam by nano-liquid chromatography-high-resolution mass spectrometry for drug testing purposes. *Anal Bioanal Chem*. 2016;408:3571-3591.

134. Moosmann B, Bisel P, Franz F, Huppertz LM, Auwarter V. Characterization and in vitro phase I microsomal metabolism of designer benzodiazepines - an update comprising adinazolam, clonizprazepam, fonazepam, 3-hydroxyphenazepam, metizolam and nitrazolam. *J Mass Spectrom*. 2016;51:1080-1089.

135. Fracasso C, Confalonieri S, Garattini S, Caccia S. Single and multiple dose pharmacokinetics of etizolam in healthy subjects. *Eur J Clin Pharmacol*. 1991;40:181-185.

136. Wang KC, Cheng MC, Hsieh CL, Hsu JF, Wu JD, Lee CK. Determination of nimetazepam and 7-aminonimetazepam in human urine by using liquid chromatography-tandem mass spectrometry. *Forensic Sci Int*. 2013;224:84-89.

137. Uddin MN, Samanidou VF, Papadoyannis IN. An overview on total analytical methods for the detection of 1,4-benzodiazepines. *Pharmaceutica Analytica Acta*. 2014;5:1-13.

138. Persona K, Madej K, Knihnicki P, Piekoszewski W. Analytical methodologies for the determination of benzodiazepines in biological samples. *J Pharm Biomed Anal*. 2015;113:239-264.

139. Moffat AC, Osselton MD, Widdop B, Watts J. *Clarke's Analysis of Drugs and Poisons*. Fourth ed. London, UK: Pharmaceutical Press; 2011.

140. Krasowski MD, Pizon AF, Siam MG, Giannoutsos S, Iyer M, Ekins S. Using molecular similarity to highlight the challenges of routine immunoassay-based drug of abuse/toxicology screening in emergency medicine. *BMC Emerg Med*. 2009;9:5

141. O'Connor LC, Torrance HJ, McKeown DA. Elisa detection of phenazepam, etizolam, pyrazolam, flubromazepam, diclazepam and delorazepam in blood using Immunalysis® benzodiazepine kit. *J Anal Toxicol*. 2016;40:159-161.

142. Pettersson Bergstrand M, Helander A, Hansson T, Beck O. Detectability of designer benzodiazepines in Cedia, emit ii plus, Heia, and Kims ii immunochemical screening assays. *Drug Test Anal*. 2016;9:640.

143. Pellow S, File SE. Behavioural actions of Ro 5-4864: A peripheral-type benzodiazepine? *Life Sci*. 1984;35:229-240.

144. Pettersson Bergstrand M, Helander A, Beck O. Development and application of a multi-component LC–Ms/Ms method for determination of designer benzodiazepines in urine. *J Chromatogr B*. 2016;1035:104-110.

145. Lambert WE, Meyer E, Xue-Ping Y, Leenheer APD. Screening, identification, and quantitation of benzodiazepines in postmortem samples by HPLC with photodiode array detection. *J Anal Toxicol*. 1995;19:35-40.

146. Akerman KK, Jolkkonen J, Parviainen M, Penttilä I. Analysis of lowdose benzodiazepines by HPLC with automated solid-phase extraction. *Clin Chem*. 1996;42:1412-1416.

147. Yegles M, Mersch F, Wennig R. Detection of benzodiazepines and other psychotropic drugs in human hair by GC/MS. *Forensic Sci Int*. 1997;84:211-218.

148. McClean S, O'Kane E, Hillis J, Smyth WF. Determination of 1,4-benzodiazepines and their metabolites by capillary electrophoresis and high-performance liquid chromatography using ultraviolet and electrospray ionisation mass spectrometry. *J Chromatogr A*. 1999;838:273-291.

149. Roman M, Strom L, Tell H, Josefsson M. Liquid chromatography/time-of-flight mass spectrometry analysis of postmortem blood samples for targeted toxicological screening. *Anal Bioanal Chem*. 2013;405:4107-4125.

150. Soriano T, Jurado C, Menendez M, Repetto M. Improved solid-phase extraction method for systematic toxicological analysis in biological fluids. *J Anal Toxicol*. 2001;25:137-143.

151. Anzillotti L, Odoardi S, Strano-Rossi S. Cleaning up blood samples using a modified "Quechers" procedure for the determination of drugs of abuse and benzodiazepines by UPLC–MSMS. *Forensic Sci Int*. 2014;243:99-106.

152. Usui K, Hayashizaki Y, Hashiyada M, Funayama M. Rapid drug extraction from human whole blood using a modified Quechers extraction method. *Leg Med*. 2012;14:286-296.

153. Westland JL, Dorman FL. Quechers extraction of benzodiazepines in biological matrices. *J Pharmaceut Anal*. 2013;3:509-517.

154. Famiglini G, Capriotti F, Palma P, Termopoli V, Cappiello A. The rapid measurement of benzodiazepines in a milk-based alcoholic beverage using Quechers extraction and GC-MS analysis. *J Anal Toxicol*. 2015;39:306-312.

155. Peng GW. Assay of adinazolam in lasma by liquid chromatography. *J Pharm Sci*. 1984;73:1173-1175.

156. Vikingsson S, Wohlfarth A, Andersson M, et al. Identifying metabolites of meclonazepam by high-resolution mass spectrometry using human liver microsomes, hepatocytes, a mouse model, and authentic urine samples. *AAPS J*. 2017;19:736.

157. Bergstrand MP, Helander A, Beck O. Development and application of a multi-component LC–MS/MS method for determination of designer benzodiazepines in urine. *J Chromatogr B*. 2016;1035:104-110.

158. Nakamae T, Shinozuka T, Sasaki C, et al. Case report: Etizolam and its major metabolites in two unnatural death cases. *Forensic Sci Int*. 2008;182:e1-e6.

159. Coassolo P, Aubert C, Cano JP. Plasma determination of 3-methylclonazepam by capillary gas chromatography. *J Chromatogr.* 1985;338:347-355.

160. Ékonomov AL, Zherdev VP. Method of quantitative gas-chromatographic determination of phenazepam and its metabolite 3-hydroxyphenazepam in plasma. *Pharmaceut Chem J.* 1980;14:579-582.

161. O'Connor LC, Torrance HJ, McKeown DA. Elisa detection of phenazepam, etizolam, pyrazolam, flubromazepam, diclazepam and delorazepam in blood using Immunalysis benzodiazepine kit. *J Anal Toxicol.* 2016;40:159-161.

162. El Balkhi S, Chaslot M, Picard N, et al. Characterization and identification of eight designer benzodiazepine metabolites by incubation with human liver microsomes and analysis by a triple quadrupole mass spectrometer. *Int J Leg Med.* 2017. https://doi.org/10.1007/s00414-017-1541-6.

163. Zhuk OV, Zinkovsky VG, Schukin SI, Sivachenko AV. Biotransformation, pharmacokinetics and pharmacodynamics of cinazepam. *Pharmacol Rep.* 2007;59:60-61.

164. Schwartz MA, Postma E. Metabolism of flurazepam, a benzodiazepine, in man and dog. *J Pharm Sci.* 1970;59:1800-1806.

165. Heizmann P, Eckert M, Ziegler WH. Pharmacokinetics and bioavailability of midazolam in man. *Brit J Clin Pharmacol.* 1983;16:43S-49S.

166. Barzaghi N, Leone L, Monteleone M, Tomasini G, Perucca E. Pharmacokinetics of flutoprazepam, a novel benzodiazepine drug, in normal subjects. *Eur J Drug Metab Pharmacokinet.* 1989;14:293-298.

167. Nakatsuka I, Shimizu H, Asami Y, Katoh T, Hirose A, Yoshitake A. Benzodiazepines and their metabolites: Relationship between binding affinity to the benzodiazepine receptor and pharmacological activity. *Life Sci.* 1985;36:113-119.

168. Skopp G. Preanalytic aspects in postmortem toxicology. *Forensic Sci Int.* 2004;142:75-100.

169. Robertson MD, Drummer OH. Stability of nitrobenzodiazepines in postmortem blood. *J Forensic Sci.* 1998;43:5-8.

170. El Mahjoub A, Staub C. Stability of benzodiazepines in whole blood samples stored at varying temperatures. *J Pharm Biomed Anal.* 2000;23:1057-1063.

171. Skopp G, Potsch L, Konig I, Mattern R. A preliminary study on the stability of benzodiazepines in blood and plasma stored at 4 degrees C. *Int J Leg Med.* 1998;111:1-5.

172. Melo P, Bastos ML, Teixeira HM. Benzodiazepine stability in postmortem samples stored at different temperatures. *J Anal Toxicol.* 2012;36:52-60.

173. Levine B, Blanke RV, Valentour JC. Postmortem stability of benzodiazepines in blood and tissues. *J Forensic Sci.* 1983;28:102-115.

174. Watson SSKH, O'Connor L, McKeown DA. Determination of the stability of 10 novel benzodiazepines and 3 metabolites in urine using LC-MS/MS. 6th Annual Meeting of the United Kingdom and Ireland Association of Forensic Toxicologists (UKIAFT), Manchester, UK, 2016 [31 May 2017].

175. Artemenko AG, Kuz'min VE, Muratov EN, Polishchuk PG, Borisyuk IY, Golovenko NY. Influence of the structure of substituted benzodiazepines on their pharmacokinetic properties. *Pharmaceut Chem J.* 2009;43:454-462.

176. Kar S, Roy K. Predictive toxicity modelling of benzodiazepine drugs using multiple in silico approaches: Descriptor-based Qstr, groupbased Qstr and 3d-toxicophore mapping. *Mol Simul.* 2015;41:345-355.

177. Hester JB, Duchamp DJ, Chidester CG. A synthetic approach to new 1,4-benzodiazepine derivatives. *Tetrahedron Lett.* 1971;12:1609-1612.

178. Meguro K, Kuwada Y. Syntheses and structures of 7-chloro-2-hydrazino-5-phenyl-3h-1,4-benzodiazepines and some isomeric 1,4,5-benzotriazocines. *Tetrahedron Lett.* 1970;11:4039-4042.

179. Sternbach LH. The benzodiazepine story. *J Med Chem.* 1979;22:1-7.

180. Childress SJ, Gluckman MI. 1,4-benzodiazepines. *J Pharm Sci.* 1964;53:577-590.

181. Whitwam JG, Amrein R. Pharmacology of flumazenil. *Acta Anaesthesiol Scand Suppl.* 1995;108:3-14.

182. Maddalena DJ, Johnston GAR. Prediction of receptor properties and binding affinity of ligands to benzodiazepine/GABAA receptors using artificial neural networks. *J Med Chem.* 1995;38:715-724.

183. Zalkind S. 'Death pill': Fentanyl disguised as other drugs linked to spike in US overdoses. 2016. Available at: https://www.theguardian.com/society/2016/may/10/fentanyl-drug-overdoses-xanax-pain-killers [31 May 2017].

184. Ecstasydata.Org. Available at: https://www.ecstasydata.org/resultsphp?start=0&search_field=all&s=etizolam [31 May 2017].

185. Oilman NW, Sternbach LH. Quinazolines and 1,4-benzodiazepines. Li. The synthesis of the T-butyl analog of diazepam. *J Heterocycl Chem.* 1971;8:297-300.

186. Borea PA. De novo analysis of receptor binding affinity data of benzodiazepines. *Arzneimittelforschung.* 1983;33:1086-1088.

187. Haefely EKW, Gerecke M, Mohler H. Recent advances in the molecular pharmacology of benzodiazepine receptors and in the structure activity relationships of their agonists and antagonists. *Adv Drug Res.* 1985;14:165-322.

188. So SS, Karplus M. Genetic neural networks for quantitative structure activity relationships: Improvements and application of benzodiazepine affinity for benzodiazepine/GABAA receptors. *J Med Chem.* 1996;39:5246-5256.

189. The Drug Enforcement Administration (DEA). Mimic alprazolam tablet (actually containing melatonin) seized in New York. *Microgram Bulletin.* 2009;42:80

190. Chong YK, Kaprawi MM, Chan KB. The quantitation of nimetazepam in erimin-5 tablets and powders by reverse-phase HPLC. *Microgram Journal.* 2004;2:27-33.

191. Lim WJL, Yap ATW, Mangudi M, Koh HB, Tang ASY, Chan KB. Detection of phenazepam in illicitly manufactured erimin 5 tablets. *Drug Test Anal.* 2016;9:293-305.

192. Megarbane B, Pirnay S, Borron SW, et al. Flunitrazepam does not alter cerebral distribution of buprenorphine in the rat. *Toxicol Lett.* 2005;157:211-219.

193. Broséus J, Gentile N, Esseiva P. The cutting of cocaine and heroin: A critical review. *Forensic Sci Int.* 2016;262:73-83.

The use of a quantitative structure-activity relationship (QSAR) model to predict GABA-A receptor binding of newly emerging benzodiazepines

Laura Waters[a],[*], Kieran R. Manchester[a], Peter D. Maskell[b], Caroline Haegeman[c], Shozeb Haider[c]

[a] School of Applied Sciences, University of Huddersfield, Huddersfield, UK
[b] School of Science, Engineering and Technology, Abertay University, Dundee, UK
[c] School of Pharmacy, University College London, London, UK

ARTICLE INFO

ABSTRACT

The illicit market for new psychoactive substances is forever expanding. Benzodiazepines and their derivatives are one of a number of groups of these substances and thus far their number has grown year upon year. For both forensic and clinical purposes it is important to be able to rapidly understand these emerging substances. However as a consequence of the illicit nature of these compounds, there is a deficiency in the pharmacological data available for these 'new' benzodiazepines. In order to further understand the pharmacology of 'new' benzodiazepines we utilised a quantitative structure-activity relationship (QSAR) approach. A set of 69 benzodiazepine-based compounds was analysed to develop a QSAR training set with respect to published binding values to $GABA_A$ receptors. The QSAR model returned an R^2 value of 0.90. The most influential factors were found to be the positioning of two H-bond acceptors, two aromatic rings and a hydrophobic group. A test set of nine random compounds was then selected for internal validation to determine the predictive ability of the model and gave an R^2 value of 0.86 when comparing the binding values with their experimental data. The QSAR model was then used to predict the binding for 22 benzodiazepines that are classed as new psychoactive substances. This model will allow rapid prediction of the binding activity of emerging benzodiazepines in a rapid and economic way, compared with lengthy and expensive in vitro/in vivo analysis. This will enable forensic chemists and toxicologists to better understand both recently developed compounds and prediction of substances likely to emerge in the future.

1. Introduction

Benzodiazepines and their derivatives are routinely prescribed for a variety of medical conditions as anxiolytic, anti-insomnia and anticonvulsant drugs, acting on the gamma-aminobutyric acid type A ($GABA_A$) receptor [1,2]. The endogenous neurotransmitter for the $GABA_A$ receptor is gamma-aminobutyric acid (GABA), the binding of which reduces the excitability of the cell [3]. Benzodiazepines potentiate the response of the $GABA_A$ receptor to GABA which results in far less cellular excitability which, in physiological terms, results in sedation and relaxation [1].

In these circumstances benzodiazepines are medically beneficial by alleviating stress and agitation in patients through their anxiolytic effects. However, as a result of their psychoactive effects, benzodiazepines have a long history of abuse and are often illicitly obtained [4–6]. In more recent years a steady stream of benzodiazepines have appeared on the illicit market that have either been newly-synthesised or are licensed as prescription drugs in another country but not in the home

country [7–10]. These are termed 'new psychoactive substances' (NPS) [11,12]. The majority of these emerging benzodiazepines have not undergone standard pharmaceutical trials and can be quite variant in their effects and potentially dangerous in their activity [13]. Although relatively safe when used as medically prescribed, concurrent use of benzodiazepines and opioids (either prescribed or abused) can lead to respiratory depression and death [4,14,15]. When benzodiazepines are not carefully prescribed and monitored, they can cause a variety of side effects including tolerance and dependency if taken long-term and sudden withdrawal can cause medical problems including anxiety and insomnia [16–18]. These NPS benzodiazepines have already been reported in a number of overdose cases, driving under the influence of drugs (DUID) cases and hospital admissions [8,19–22]. The lack of control and safety over these illicit benzodiazepines is a prevalent issue and it is likely that it will become an even more worrying trend as their misuse continues to rise.

Benzodiazepines are a diverse group of psychoactive compounds with a central structural component consisting of a benzene ring and a
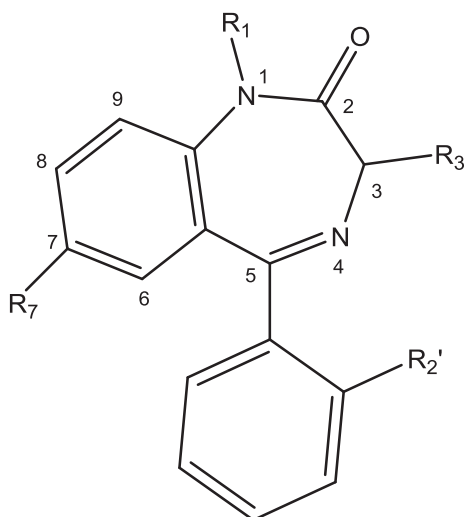
Fig. 1. The basic structural formula for benzodiazepines considered in this work.

diazepine ring (Fig. 1). A whole host of derivatives exist which include triazolobenzodiazepines, thienotriazolobenzodiazepines and imidazo-benzodiazepines (see Supplementary information Fig. S1 and Table S1).

Quantitative structure-activity relationship (QSAR) models attempt to correlate molecular structure to biological activity, often using a variety of molecular descriptors such as physiochemical, topological, electronic and steric properties [23]. Typically, a set of compounds whose biological activity is known is used to create a 'training' dataset and a model. This model can then be used to predict the unknown biological activity of compounds with a similar structure or to explore the structural features that are important for the specific biological activity in question. QSAR has been extensively used for a variety of reasons such as compound development in the pharmaceutical industry and the pharmacological interpretation of drug-related deaths [24–26]. In terms of applications towards new psychoactive substances, the predictive power of QSAR has been mainly applied to cannabinoid binding to the CB_1 and CB_2 receptors [27–29] but has also been used to examine the biological activity of hallucinogenic phenylalkylamines [30], the binding of phenylalkylamines, tryptamines and LSD to the 5-HT_{2A} receptor [31] and methcathinone selectivity for dopamine (DAT), norepinephrine (NAT) and serotonin transporters (SERT) [32]. Currently, the majority of novel benzodiazepines have not been analysed to determine their physicochemical and biological properties as this would require a substantial investment in both time and money. It is for this reason that a fast, yet economical method to predict their properties is desirable.

QSAR has previously been applied to benzodiazepines to predict bioavailability, absorption rate, clearance, half-life and volume of distribution for a group of benzodiazepines. This study included phena-zepam [33], a benzodiazepine that appeared as an NPS in 2007 [34]. Other benzodiazepines (such as etizolam) only appeared as new psychoactive substances in the years following the publication of this study. Furthermore, the application of a QSAR methodology has been used for modelling post-mortem redistribution of benzodiazepines where a good model was obtained ($R^2 = 0.98$) in which energy, ionisation and molecular size were found to exert significant impact [35]. Quantitative structure-toxicity relationships (QSTR) have been used to correlate the toxicity of benzodiazepines to their structure in an attempt to predict the toxicity of these compounds [36]. More recently, a study reported the use of QSTR whereby it was concluded that it is possible to identify structural fragments responsible for toxicity (the presence of amine and hydrazone substitutions as well as saturated heterocyclic ring systems resulted in a greater toxicity) and potentially use this information to create new, less toxic benzodiazepines for medical use

[37].

Various QSAR models have been used to correlate benzodiazepine structure to $GABA_A$ receptor binding and tease apart the complex relationship between various substituents and their effect on activity [38–43] although none have specifically attempted to predict binding values for benzodiazepines that are new psychoactive substances.

In this study we focus on the relationship between the structure of characterised benzodiazepines and $GABA_A$ receptor binding, expressed as the logarithm of the reciprocal of concentration (log 1/c) where c is the molar inhibitory concentration (IC_{50}) required to displace 50% of [3H]-diazepam from rat cerebral cortex synaptosomal preparations [41]. The purpose of this work is to create a QSAR model that can be used to predict the potential biological activity of the newly-emerging benzodiazepines to help understand, and therefore minimise their harmful potential in a faster time scale compared with in vitro/in vivo testing.

2. Methods and materials

2.1. Selection of the dataset

The binding data for the benzodiazepines was used as obtained from the literature, experimentally determined using spectrometric measurements of [3H]-diazepam displacement [44]. Benzodiazepines were selected from four categories; 1,4-benzodiazepines, triazolobenzodiazepines, imidazobenzodiazepines and thienotriazolobenzodiazepines. Benzodiazepines that did not have definitive binding values (i.e. listed values were simply stated as > 1000 or > 5000) were excluded. For simplicity benzodiazepines with atypical atoms or substituents (e.g. Ro 07-9238 which contained a sodium atom and Ro 05-5065 which contained a naphthalene ring) were also excluded. Benzodiazepines that also had atypical substitutions (i.e. positions R6, R8 and R9 from Fig. 1 which are not found in medically-used benzodiazepines or indeed those that are new psychoactive substances) were also excluded. In total, 88 benzodiazepines were selected for the training dataset.

2.2. QSAR/software and data analysis method

The 88 benzodiazepines were converted from SMILES to 3D structures based on Merck Molecular Force Field (MMFF) atom type and force field optimisation. These compounds were then aligned by common substructure and confirmation to Ro 05-306. Subsequently, the aligned compounds were clustered by Atomic Property Fields (APF) to identify benzodiazepines with poor alignment. The APF method, designed by MolSoft, uses the assignment of a 3D pharmacophore potential on a continuously distributed grid using physio-chemical properties of the selected compound(s) to classify or superimpose compounds. These properties include: hydrogen bond donors, acceptors, Sp2 hybridisation, lipophilicity, size, electropositivity/negativity and charge [45,46]. Poorly aligned benzodiazepines identified by APF clustering were subjected to re-alignment using APF-based flexible superimposition. At this point, 10 benzodiazepines with poor alignment were removed to improve model accuracy. (Supplementary information Table S1).

From the remaining 78 aligned compounds, 9 compounds were selected using a random number generator based on atmospheric noise. These compounds were removed from the training set and used for final model validation. The residual 69 compounds were used as the training set to build a 3D QSAR model, as shown in Fig. 2.

The APF 3D QSAR method was used where, for each of the 69 aligned compounds, the seven physicochemical properties were calculated and pooled together. Based on the activity data obtained from literature and the 3D aligned structures for the known compounds, weighted contributions for each APF component were obtained to allow quantitative activity predictions for unknown compounds. The optimal weight distributions were assigned by partial least-squares (PLS)
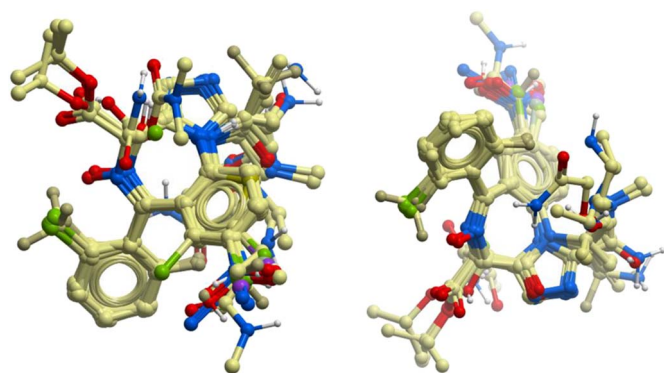
Fig. 2. Alignment of 69 training set benzodiazepines shown in two orientations.
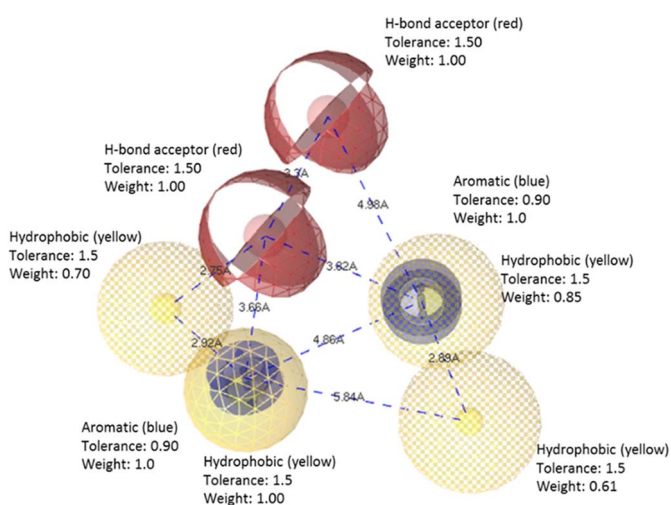
Fig. 3. Pharmacophore model of 33 compounds with binding values 8.0–9.0.
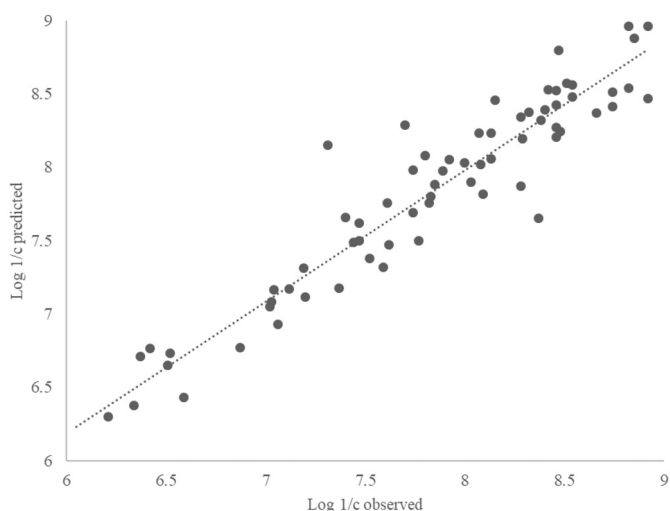
Fig. 4. Literature (i.e. observed) binding values (log 1/c) vs. QSAR predicted binding values fit with a partial least squares (PLS) regression ($R^2 = 0.90$).

methodology, where the optimal number of latent vectors for PLS was established by leave-one-out cross-validation on the training set. Then the weighted contributions were added together. The 9 compounds for validation and unknown compounds were assigned predicted binding values by calculating their fit within the combined QSAR APF. Any unknown benzodiazepines were subjected to the conversion and alignment protocol before predicted binding data was obtained. The above steps were conducted using Molsoft's ICM Pro software [47].
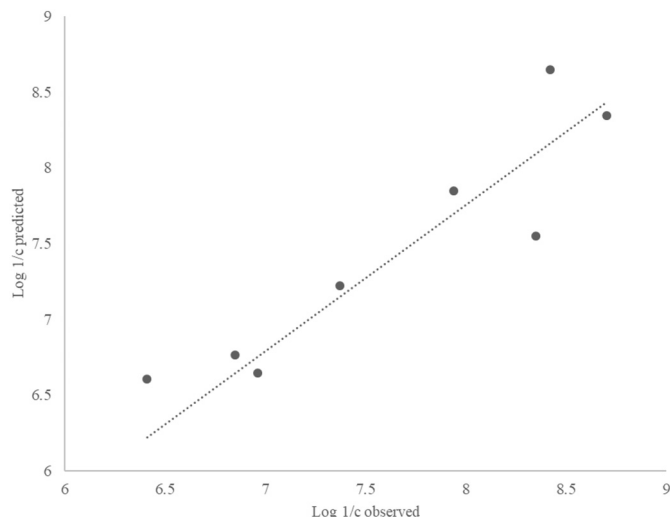
Fig. 5. Literature (i.e. observed) binding values (log 1/c) vs. QSAR predicted binding values for 9 compounds randomly selected for internal validation ($R^2 = 0.86$).

Further analysis of the PLS model fragment contributions from the 69 compounds was conducted using SPCI software. Here, a 2D QSAR model was built using the same PLS methodology as above. Additionally, a consensus model was created from averaging the predictions of PLS, gradient boosting, support vector machine and random forest modelling methods. The compounds were then subjected to automatic fragmentation and contribution calculations, which resulted in information on 11 key contributing groups [48]. Using Ligand Scout with default settings, four ligand-based pharmacophore models were created using compounds with binding values of 6.0–9.0, 7.0–9.0, 8.0–9.0 and 8.5–9.0, as exemplified in Fig. 3.

Ten benzodiazepines that had the highest predicted binding values were docked into a modelled GABA$_{A5}$ receptor using ICM software. The GABA$_{A5}$ receptor model was generated by homology modelling, using the crystal structure of a human GABA(A)R-beta3 homopentamer (PDB id 4COF) as a template. A pre-defined binding site containing co-crystallised benzodiazepine is already present in the template, which was retained in the final model. Modeller software was used to generate the homology models [49]. The final chosen model was energy minimized using the ACEMD software [50]. The stereochemistry was checked using Procheck and ProSA software [51,52]. The benzodiazepine in the allosteric binding site on the GABA$_{A5}$ receptor was used as a chemical template to dock NPS-benzodiazepines and the best-scoring conformations were analysed.

The distances between principle physiochemical properties and their weights in the pharmacophore model were calculated using the software LigandScout [53].

3. Results and discussion

The data that was used to create the QSAR model (i.e. benzodiazepine structural substitutions and experimentally-observed binding values) is provided in the Supplementary information (Table S1).

From the pharmacophore model visualised in Fig. 3 for highly bound benzodiazepines (log 1/c of 8.0–9.0), it is evident that important binding features for the benzodiazepines were the positioning of two H-bond acceptors, two aromatic rings and a hydrophobic group all with weights of 1.0.

The predicted binding values are not presented here but are listed in Supplementary Information (Table S1). They can be visualised in Fig. 4 as a plot of the observed binding value versus the predicted binding value.

Nine compounds were selected at random from the QSAR training set and their binding values estimated using the model as a system of

Table 1
Structural information and predicted binding values for 1,4-benzodiazepines.

Name	Substitutions				Log 1/c predicted	Basic structure
	R_7	R_1	R_2'	R_3		
Diclazepam	Cl	CH_3	Cl	–	8.39	
Desalkylflurazepam	Cl	–	F	–	8.44	
Meclonazepam	NO_2	–	Cl	CH_3	8.52	
Phenazepam	Br	–	Cl	–	8.12	
Desmethylflunitrazepam	NO_2	–	F	–	8.46	
3-hydroxyphenazepam	Br	–	Cl	OH	8.42	
Flubromazepam	F	–	Br	–	8.37	
Nifoxipam	NO_2	–	F	OH	8.63	
Cloniprazepam	NO_2	–	Cl	$C_3H_5CH_3$	7.83	
Nimetazepam	NO_2	CH_3	–	–	7.87	
4-chlorodiazepam[a]	Cl	CH_3	–	–	7.88	

[a] 4-chlorodiazepam has a Cl substituted on the R_4' position of the phenyl ring.

Table 2
Structural information and predicted binding values for triazolobenzodiazepines.

Name	Substitutions				Log 1/c predicted	Basic structure
	R_8	R_1	R_2'	R_4		
Flubromazolam	Br	CH_3	F	–	8.77	
Clonazolam	NO_2	CH_3	Cl	–	8.86	
Flunitrazolam	NO_2	CH_3	F	–	8.88	
Bromazolam	NO_2	CH_3	–	–	8.25	
Adinazolam	Cl	$CH_3N(CH_3)_2$	–	–	7.18	
Pyrazolam[a]	Br	CH_3	–	–	7.79	
Nitrazolam	NO_2	CH_3	–	–	8.34	

[a] Pyrazolam has a 2-pyridyl ring at position 6 rather than a phenyl ring.

Table 3
Structural information and predicted binding values for thienotriazolodiazepines.

Name	Substitutions			Log 1/c predicted	Basic structure
	R_9	R_2	R_2'		
Deschloroetizolam	CH_3	CH_2CH_3	–	7.96	
Etizolam	CH_3	CH_2CH_3	Cl	8.64	
Metizolam	–	CH_2CH_3	Cl	8.34	

Table 4
Structural information and a predicted binding value for an oxazolobenzodiazepine.
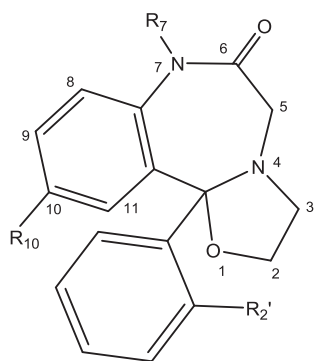
Name	Substitutions			Log 1/c predicted	Basic structure
	R_{10}	R_7	R_2'		
Flutazolam	Cl	CH_2CH_2OH	F	6.83	

Table 5
Observed and predicted binding values for new psychoactive substances.

Compound	Log 1/c observed	Log 1/c predicted	% (log 1/c obs.) / (log 1/c pred.)
Adinazolam	6.87	7.18	95.9%
Desalkylflurazepam	8.70	8.44	103.1%
Desmethylflunitrazepam (fonazepam)	8.82	8.46	104.3%
Etizolam	8.51	8.64	98.5%
Meclonazepam	8.92	8.52	104.7%
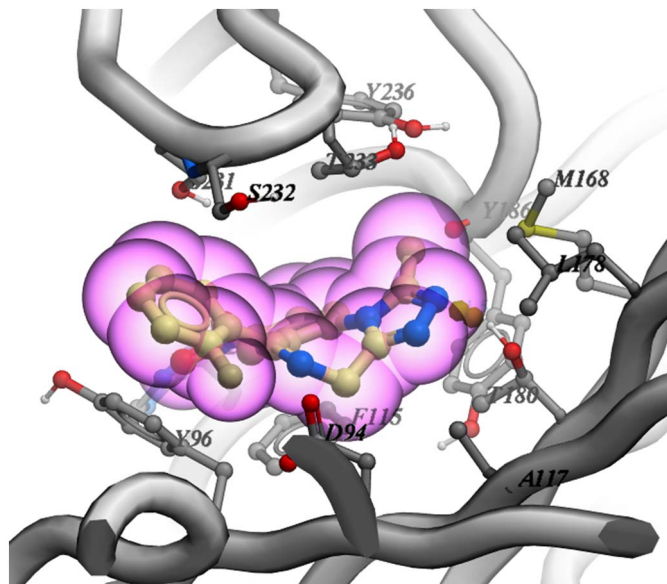
Fig. 6. Visualisation of the NPS-benzodiazepine flunitrazolam binding to the allosteric site of the GABA$_{A5}$ receptor.

internal validation. These estimated values were then compared to the experimental binding values (Fig. 5).

The QSAR model was then used to predict the binding for 22 benzodiazepines that are classed as new psychoactive substances. The results are divided in to four categories depending upon the nature of the substitutions, as shown in Tables 1, 2, 3 and 4.

Five compounds were present in the training dataset but have also appeared as new psychoactive substances; adinazolam, desalkylflurazepam, desmethylflunitrazepam (fonazepam), etizolam and meclonazepam. The experimental binding values from the literature and the predicted binding values are displayed in Table 5.

The NPS-benzodiazepine with the highest predicted log 1/c value was flunitrazolam with 8.88, closely followed by clonazolam with 8.86. However, based upon experimental data, meclonazepam with a log 1/c value of 8.92 (8.52 predicted) actually exhibited the greatest binding affinity. Only two benzodiazepines in the training set experimental values had a log 1/c value of 8.92; these were meclonazepam and brotizolam with the rest falling below this point. In general, the limitations to this model are most likely caused by the small size of the data set. It is widely reported that QSAR models have poorer predictive capabilities with training sets under 100 compounds [54,55]. Moreover, the diversity of substitutions within the small set of training compounds, created difficulties with APF superimposition and therefore may have reduced the accuracy of the model predictors. Secondary modelling with SPCI highlighted these limitations and demonstrated the existing dataset was less suitable for PLS 2D QSAR modelling [48]. However, the consensus from multiple modelling methods improves the predictive power of the 2D QSAR model. Additionally, as experimental errors in the training set are amplified both by the logarithmic scale and when calculating the weighted contributions, consistency and accuracy in the initial experimental values are essential for a strong QSAR model. Ideally, further improvements to the model could be made by using a larger training dataset with lower diversity yet this cannot be achievable as a consequence of limitations on literature data available.

From these docking studies with the modelled GABA$_{A5}$ receptor it can be seen that they only partially occupy the available volume at the allosteric binding site (exemplified in Fig. 6 for flunitrazolam). From the ten compounds that had the greatest binding affinity, four had non-bonded interactions with the T80 region within the receptor, two had non-bonded interactions with the K182 and S231 regions respectively. There were also stacking interactions with the Y96 region for four of the compounds. Therefore the possibility is that the binding is not completely optimal for these benzodiazepines and that with a modified chemical structure, a greater binding affinity could be theoretically possible. The reality exists that a benzodiazepine with an optimised binding affinity could emerge onto the illicit drugs market and could potentially (but not necessarily) exhibit a greater potency.

The 10 compounds with the greatest binding affinity for the receptor are listed in Table 6 (lower scores indicate a greater binding effect).

There are 35 benzodiazepines and their derivatives currently subject to international control, 30 of these compounds had binding values listed in the original source [44]. The average log 1/c value for these 30

Table 6
Binding scores and molecular descriptors of the 10 compounds exhibiting the greatest binding affinity for the receptor.

Compound name	Score	Number of atoms in ligand	Number of rotatable torsions	Hydrogen bond energy	Hydrophobic energy in exposing a surface to water	Van der Waals interaction energy	Internal conformation energy of the ligand	Desolvation of exposed h-bond donors and acceptors	Solvation electrostatics energy change upon binding	Potential of mean force score
Flunitrazolam	− 17.9003	37	1	− 1.55071	− 6.12229	− 27.3992	4.10324	10.7377	13.4407	− 158.403
Clonazolam	− 15.4617	37	1	− 1.53992	− 6.124	− 27.9233	7.64508	11.6698	16.8309	− 154.162
Flubromazolam	− 18.2738	35	0	− 1.61755	− 6.89366	− 25.8773	3.57746	11.0855	12.122	− 151.357
Etizolam	− 18.7025	38	1	− 2.03733	− 7.14073	− 25.5154	7.89581	11.8052	11.0572	− 101.516
Nifoxipam	− 20.836	33	2	− 5.90608	− 4.9646	− 22.352	6.0639	12.5432	13.905	− 129.57
Meclonazepam	− 13.4447	35	1	− 2.27939	− 5.98463	− 21.8787	5.69717	10.6159	14.6192	− 124.257
Desmethylflunitrazepam	− 15.5192	32	2	− 0.82246	− 5.27009	− 26.2114	2.37454	10.376	11.0938	− 144.474
Desalkylflurazepam	− 21.7837	30	0	− 2.01574	− 5.82939	− 27.462	0.691701	9.53716	11.4106	− 154.372
Diclazepam	− 16.8002	33	0	− 0.60989	− 6.76567	− 25.688	2.00693	10.3028	10.9647	− 121.093
Metizolam	− 13.7614	35	1	− 1.78622	− 6.65559	− 24.7768	3.51234	14.5321	12.8708	− 138.056

controlled compounds was 7.57. Out of these compounds, 43% (13 out of 30) had a log 1/c value that was > 8.00. The average log 1/c value for the whole training dataset was 7.81 and 48% of the compounds (33 out of 69) had a log 1/c value that was > 8.00. These values are fairly similar, however when comparing the results of the benzodiazepines that are new psychoactive substances, the average log 1/c value that was predicted was 8.22 and 68% of the compounds (15 out of 22) had a log 1/c value that was > 8.00. From this it is appears that benzodiazepines that are appearing as new psychoactive substances are more likely to have a greater binding affinity at the GABA$_A$ receptor. Whether this trend is deliberate is unclear.

A log 1/c value of 7.88 was obtained for 4-chlorodiazepam (Ro 5-4864). This suggests a relatively high affinity for the GABA$_A$ receptor when compared with the log 1/c values for clinically-used benzodiazepines; the binding value for diazepam is 8.09 and 8.40 for triazolam. However it has been reported that the experimental value for 4-chlorodiazepam (Ro-4864) is actually 3.79 (i.e. an IC$_{50}$ value of 160,500 nM) in one dataset when compared with a log 1/c of 7.80 for diazepam and 8.72 for triazolam in the same dataset [56]. There are obvious impracticalities with comparing different datasets as a result of differences in methods (e.g. the use of [^{3}H]-diazepam versus [^{3}H]-flunitrazepam as a radioligand), the differences in the species used (rat vs. mouse) and the differences in GABA$_A$ receptor expression between different brain homogenates. Despite this it is clear that 4-chlorodiazepam observes an extremely low affinity for GABA$_A$ receptors and one that this model did not accurately predict. This most likely results from the deficit of compounds in the training dataset that had a similar substitution on the R$_4'$ position of the phenyl ring. Indeed, this model focused upon the 'classical' 1,4-benzodiazepine, triazolobenzodiazepine, imidazobenzodiazepine and thienotriazolodiazepine substitutions. Substitutions on the R$_4'$ position of the phenyl ring are known to exhibit strong steric repulsion at the GABA$_A$ receptor interface and therefore compound binding is severely inhibited [40,57]. 4-chlorodiazepam is an outlier and atypical benzodiazepine as it does not act upon the GABA$_A$ receptor; instead exerting its pharmacological effects through the translocator protein 18 kDa (TSPO), previously known as the peripheral benzodiazepine receptor [58,59].

The oxazolobenzodiazepine flutazolam, a prescription drug in Japan, had a predicted log 1/c binding value of 6.83 which seems extremely low compared with the other benzodiazepines in this dataset. To the best of the authors' knowledge there exists no experimental GABA$_A$ receptor binding data for flutazolam. However other oxazolobenzodiazepines have low affinities for the GABA$_A$ receptor such as ketazolam with a log 1/c value of 5.89 [60] and oxazolam with a log 1/c value of 5.00 [61]. These log 1/c binding values are from additional sources – the previous paragraph discusses the difficulties in comparing binding values from different datasets. Nonetheless it is clear that oxazolobenzodiazepines exhibit a much lower affinity for the GABA$_A$

receptor. If the value for flutazolam is correct then this QSAR model successfully predicted the low binding affinity of flutazolam despite having no oxazolobenzodiazepines in the training dataset which serves as an indicator to the potential strength of the model.

4. Conclusions

The emergence of benzodiazepines and their derivatives as new psychoactive substances necessitates the investigation of their pharmacological attributes. The use of a QSAR model is ideal to gain an understanding into the binding properties of these substances. In this work a QSAR model has been successfully developed to predict the binding data for NPS-benzodiazepines. Benzodiazepines that have emerged as new psychoactive substances appear to have a greater binding affinity to GABA$_A$ receptors than those benzodiazepines that are used medically and are under international control. Whether this trend will continue is uncertain. Further in vitro work would allow the compilation of more data to improve the accuracy of this model. However, this model does allow a rapid estimation of the binding affinity of emerging benzodiazepines before more detailed studies can be carried out.

Appendix A. Supplementary data

Supplementary data to this article can be found online at https://doi.org/10.1016/j.scijus.2017.12.004.

References

[1] M. Lader, Benzodiazepines revisited-will we ever learn? Addiction 106 (2011) 2086–2109.
[2] Z. Tashma, L. Raveh, H. Liani, et al., Bretazenil, a benzodiazepine receptor partial agonist, as an adjunct in the prophylactic treatment of op poisoning, J. Appl. Toxicol. 21 (Suppl. S1) (2001) S115–S119.
[3] I. Restrepo-Angulo, A.D.V. Ruiz, J. Camacho, Ion channels in toxicology, J. Appl. Toxicol. 30 (2010) 497–512.
[4] J.D. Jones, S. Mogali, S.D. Comer, Polydrug abuse: a review of opioid and benzodiazepine combination use, Drug Alcohol Depend. 125 (2012) 8–18.
[5] O. Boeuf, M. Lapeyre-Mestre, Survey of forged prescriptions to investigate risk of psychoactive medications abuse in France: results of Osiap survey, Drug Saf. 30 (2007) 265–276.
[6] U. Bergman, M.L. Dahl-Puustinen, Use of prescription forgeries in a drug abuse surveillance network, Eur. J. Clin. Pharmacol. 36 (1989) 621–623.
[7] Bjoern Moosmann, Philippe Bisel, V. Auwärter, Characterization of the designer benzodiazepine Diclazepam and preliminary data on its metabolism and pharmacokinetics, Drug Testing and Analysis. 6 (2014) 757–763.
[8] M. Łukasik-Głębocka, K. Sommerfeld, A. Teżyk, et al., Flubromazolam-a new life-threatening designer benzodiazepine, Clin. Toxicol. 54 (2016) 66–68.
[9] M.P. Bergstrand, A. Helander, T. Hansson, O. Beck, Detectability of designer benzodiazepines in Cedia, emit ii plus, Heia, and Kims ii immunochemical screening assays, Drug Testing and Analysis 9 (2017) 640–645.
[10] P. Kintz, C. Richeval, C. Jamey, et al., Detection of the designer benzodiazepine Metizolam in urine and preliminary data on its metabolism, Drug Testing and Analysis. 9 (2016) 1026–1033.

[11] K.R. Manchester, E.C. Lomas, L. Waters, F.C. Dempsey, P.D. Maskell, The emergence of new psychoactive substance (nps) benzodiazepines: a review, Drug Testing and Analysis (2017) [Epub ahead of print].

[12] B. Moosmann, L.A. King, V. Auwärter, Designer benzodiazepines: a new challenge, World. Psychiatry. 14 (2015) 248.

[13] G. Høiseth, S.S. Tuv, R. Karinen, Blood concentrations of new designer benzodiazepines in forensic cases, Forensic Sci. Int. 268 (2016) 35–38.

[14] M. Jann, W.K. Kennedy, G. Lopez, Benzodiazepines: a major component in unintentional prescription drug overdoses with opioid analgesics, J. Pharm. Pract. 27 (2014) 5–16.

[15] J.A. Gudin, S. Mogali, J.D. Jones, S.D. Comer, Risks, management, and monitoring of combination opioid, benzodiazepines, and/or alcohol use, Postgrad. Med. 125 (2013) 115–130.

[16] A. Higgitt, P. Fonagy, M. Lader, The natural history of tolerance to the benzodiazepines, Psychol. Med. Monogr. Suppl. 13 (1988) 1–55.

[17] C.H. Vinkers, B. Olivier, Mechanisms underlying tolerance after long-term benzodiazepine use: a future for subtype-selective Gabaa receptor modulators? Adv. Pharmacol. Sci. 416864 (2012).

[18] H. Pétursson, The benzodiazepine withdrawal syndrome, Addiction 89 (1994) 1455–1459.

[19] K. Shearer, C. Bryce, M. Parsons, H. Torrance, Phenazepam: a review of medicolegal deaths in South Scotland between 2010 and 2014, Forensic Sci. Int. 254 (2015) 197–204.

[20] P. Kriikku, L. Wilhelm, J. Rintatalo, et al., Phenazepam abuse in Finland: findings from apprehended drivers, post-mortem cases and police confiscations, Forensic Sci. Int. 220 (2012) 111–117.

[21] J.M. Corkery, F. Schifano, A.H. Ghodse, Phenazepam abuse in the Uk: an emerging problem causing serious adverse health problems, including death, Human Psychopharmacology. 27 (2012) 254–261.

[22] C.W. O'Connell, C.A. Sadler, V.M. Tolia, et al., Overdose of Etizolam: the abuse and rise of a benzodiazepine analog, Ann. Emerg. Med. 65 (2014) 465–466.

[23] C. Nantasenamat, C. Isarankura-Na-Ayudhya, V.T. Naenna, A. Prachayasittikul, Practical overview of quantitative structure-activity relationship, EXCLI J. 8 (2009) 74–88.

[24] L.G. Valerio Jr, S. Choudhuri, Chemoinformatics and chemical genomics: potential utility of in silico methods, J. Appl. Toxicol. 31 (2012) 880–889.

[25] A.G. Leach, Predicting the activity and toxicity of new psychoactive substances: a pharmaceutical industry perspective, Drug Testing and Analysis. 6 (2013) 739–745.

[26] A.C. Moffat, A.T. Sullivan, The use of quantitative structure-activity relationships as an aid to the interpretation of blood levels in gases of fatal barbiturate poisoning, J. Forensic Soc. 21 (1981) 239–248.

[27] M. Fichera, G. Cruciani, A. Bianchi, G. Musumarra, A 3d-Qsar study on the structural requirements for binding to Cb1 and Cb2 cannabinoid receptors, J. Med. Chem. 43 (2000) 2300–2309.

[28] S. Durdagi, A. Kapou, T. Kourouli, et al., The application of 3d-Qsar studies for novel cannabinoid ligands substituted at the C1' position of the alkyl side chain on the structural requirements for binding to cannabinoid receptors Cb1 and Cb2, J. Med. Chem. 50 (2007) 2875–2885.

[29] S. Durdagi, M.G. Papadopoulos, D.P. Papahatjis, T. Mavromoustakos, Combined 3d Qsar and molecular docking studies to reveal novel cannabinoid ligands with optimum binding activity, Bioorg. Med. Chem. Lett. 17 (2007) 6754–6763.

[30] Z. Zhang, L. An, W. Hu, Y. Xiang, 3d-Qsar study of hallucinogenic Phenylalkylamines by using Comfa approach, J. Comput. Aided Mol. Des. 21 (2007) 145–153.

[31] M. Schulze-Alexandru, K.-A. Kovar, A. Vedani, Quasi-atomistic receptor surrogates for the 5-Ht2a receptor: a 3d-Qsar study on hallucinogenic substances, Molecular Informatics. 18 (1999) 548–560.

[32] S.S. Negus, M.L. Banks, Decoding the structure of abuse potential for new psychoactive substances: structure–activity relationships for abuse-related effects of 4-substituted Methcathinone analogs, Curr. Top. Behav. Neurosci. 32 (2016) 119–131.

[33] A.G. Artemenko, V.E. Kuz'min, E.N. Muratov, et al., Influence of the structure of substituted benzodiazepines on their pharmacokinetic properties, Pharm. Chem. J. 43 (2009) 454–462.

[34] P.D. Maskell, G.D. Paoli, L.N. Seetohul, D.J. Pounder, Phenazepam: the drug that came in from the cold, J. Forensic Legal Med. 19 (2012) 122–125.

[35] C. Giaginis, A. Tsantili-Kakoulidou, S. Theocharis, Applying quantitative structure-activity relationship (Qsar) methodology for modeling postmortem redistribution of benzodiazepines and tricyclic antidepressants, J. Anal. Toxicol. 38 (2014) 242–248.

[36] S. Funar-Timofei, D. Ionescu, T. Suzuki, A tentative quantitative structure–toxicity relationship study of benzodiazepine drugs, Toxicol. in Vitro 24 (2010) 184–200.

[37] S. Kar, K. Roy, Predictive toxicity modelling of benzodiazepine drugs using multiple in silico approaches: descriptor-based Qstr, group-based Qstr and 3d-Toxicophore mapping, Mol. Simul. 41 (2014) 345–355.

[38] P.A. Borea, De novo analysis of receptor binding affinity data of benzodiazepines, Arzneimittelforschung 33 (1983) 1086–1088.

[39] G. Greco, E. Novellino, C. Silipo, A. Vittoria, Study of benzodiazepines receptor sites using a combined Qsar-Comfa approach, Molecular Informatics. 11 (1993) 461–477.

[40] A.K. Ghose, G.M. Crippen, Modeling the benzodiazepine receptor binding site by the general three-dimensional structure-directed quantitative structure-activity relationship method Remotedisc, Mol. Pharmacol. 37 (1990) 725–734.

[41] D. Hadjipavlou-Litinat, C. Hansch, Quantitative structure-activity relationships of the benzodiazepines. A review and reevaluation, Chem. Rev. 94 (1994) 1483–1505.

[42] S.-S. So, M. Karplus, Genetic neural networks for quantitative structure-activity relationships: improvements and application of benzodiazepine affinity for benzodiazepine/Gabaa receptors, J. Med. Chem. 39 (1996) 5246–5256.

[43] D.J. Maddalena, G.A.R. Johnston, Prediction of receptor properties and binding affinity of ligands to benzodiazepine/Gabaa receptors using artificial neural networks, J. Med. Chem. 38 (1995) 715–724.

[44] W. Haefely, E. Kyburz, M. Gerecke, H. Möhler, Recent advances in the molecular pharmacology of benzodiazepine receptors and in the structure-activity relationships of their agonists and antagonists, in: B. Testa (Ed.), Advances in Drug Research, Academic Press, London, 1984, pp. 165–322.

[45] M. Totrov, Atomic property fields: generalized 3d Pharmacophoric potential for automated ligand superposition, pharmacophore elucidation and 3d Qsar, Chem. Biol. Drug Des. 71 (2008) 15–27.

[46] M. Totrov, Ligand binding site superposition and comparison based on atomic property fields: identification of distant homologues, convergent evolution and Pdb-wide clustering of binding sites, BMC Bioinformatics. 12 (Supplement 1) (2011) S35.

[47] R. Abagyan, M. Totrov, D. Kuznetsov, Icm—a new method for protein modeling and design: applications to docking and structure prediction from the distorted native conformation, J. Comput. Chem. 15 (1994) 488–506.

[48] P. Polishchuk, O. Tinkov, T. Khristova, et al., Structural and Physico-chemical interpretation (Spci) of Qsar models and its comparison with matched molecular pair analysis, J. Chem. Inf. Model. 56 (2016) 1455–1469.

[49] A. Fiser, A. Sali, Modeller: generation and refinement of homology-based protein structure models, Methods Enzymol. 374 (2003) 461–491.

[50] S. Doerr, M.J. Harvey, F. Noé, G. De Fabritiis, Htmd: high-throughput molecular dynamics for molecular discovery, J. Chem. Theory Comput. 12 (2016) 1845–1852.

[51] R.A. Laskowski, M.W. MacArthur, D.S. Moss, J.M. Thornton, Procheck: a program to check the Stereochemical quality of protein structures, J. Appl. Crystallogr. 26 (1993) 283–291.

[52] M. Wiederstein, M.J. Sippl, Prosa-web: interactive web Service for the Recognition of errors in three-dimensional structures of proteins, Nucleic Acids Res. 35 (2007) W407–410.

[53] G. Wolber, T. Langer, Ligandscout: 3-D pharmacophores derived from protein-bound ligands and their use as virtual screening filters, J. Chem. Inf. Model. 45 (2005) 160–169.

[54] A. Cherkasov, E.N. Muratov, D. Fourches, et al., Qsar modeling: where have you been? Where are you going to? J. Med. Chem. 57 (2014) 4977–5010.

[55] A. Golbraikh, E. Muratov, D. Fourches, A. Tropsha, Data set Modelability by Qsar, J. Chem. Inf. Model. 54 (2014) 1–4.

[56] C. Braestrup, M. Nielsen, Benzodiazepine receptors, in: L.L. Iversen, S.D. Iversen, S.H. Snyder (Eds.), Handbook of Psychopharmacology: Biochemical Studies of Cns Receptors, Plenum Press, New York, 1983, pp. 285–384.

[57] A. Hempel, N. Camerman, A. Camerman, Benzodiazepine stereochemistry: crystal structures of the diazepam antagonist Ro 15-1788 and the anomalous benzodiazepine Ro 5-4864, Can. J. Chem. 65 (1987) 1608–1612.

[58] F. Li, J. Liu, N. Liu, et al., Translocator protein 18 Kda (Tspo): an old protein with new functions? Biochemistry 55 (2016) 2821–2831.

[59] J. Choi, M. Ifuku, M. Noda, T.R. Guilarte, Translocator protein (18kda) (Tspo)/peripheral benzodiazepine receptor (Pbr) specific ligands induce microglia functions consistent with an activated state, Glia 59 (2011) 219–230.

[60] G. Blaschke, H. Kley, W.E. Müller, Racemation of the benzodiazepines Camazepam and Ketazolam and receptor binding of enantiomers, Arzneimittelforschung 36 (1986) 893–894.

[61] C. Braestrup, M. Nielsen, T. Honoré, L.H. Jensen, E.N. Petersen, Benzodiazepine receptor ligands with positive and negative efficacy, Neuropharmacology 22 (1983) 1451–1457.

Experimental versus theoretical log $D_{7.4}$, pK_a and plasma protein binding values for benzodiazepines appearing as new psychoactive substances

Kieran R Manchester[1], Peter D Maskell[2], Laura Waters[1*]

[1]School of Applied Sciences, University of Huddersfield, Huddersfield, UK.
[2]School of Science, Engineering and Technology, Abertay University, Dundee, UK.

*Author for correspondence. E-Mail: l.waters@hud.ac.uk

Abstract

The misuse of benzodiazepines as new psychoactive substances is an increasing problem around the world. Basic physicochemical and pharmacokinetic data is required on these substances in order to interpret and predict their effects upon humans. Experimental log $D_{7.4}$, pK_a and plasma protein binding values were determined for 11 benzodiazepines that have recently appeared as new psychoactive substances (3-hydroxyphenazepam, 4'-chlorodiazepam, desalkylflurazepam, deschloroetizolam, diclazepam, etizolam, flubromazepam, flubromazolam, meclonazepam, phenazepam and pyrazolam) and compared with values generated by various software packages (ACD/I-lab, MarvinSketch, ADMET Predictor and PreADMET). ACD/I-LAB returned the most accurate values for log $D_{7.4}$ and plasma protein binding while ADMET Predictor returned the most accurate values for pK_a. Large variations in predictive errors were observed between compounds. Experimental values are currently preferable and desirable as they may aid with the future 'training' of predictive models for these new psychoactive substances.

Keywords: logD; pKa; plasma; benzodiazepines; NPS

1. Introduction

New psychoactive substances (NPS) are an increasing problem around the world[1]. Benzodiazepines are one of a number of groups of NPS that have appeared on the illicit drug market[2]. They also exist as common prescription drugs for anxiety, insomnia and other medical conditions[3]. Benzodiazepines were misused long before emerging as new psychoactive substances and a recent report highlighted the increasing illicit availability and misuse of a clinically-used benzodiazepine, alprazolam, often purchased from the dark web[4]. The new psychoactive substance benzodiazepines (referred to in this work as NPS-benzodiazepines) have already been reported in a number of overdose cases, driving under the influence of drugs (DUID) cases and hospital admissions [5–8]. The lack of control and safety over these NPS-benzodiazepines is a prevalent issue and it is predicted that it will become an even more worrying trend as their misuse continues to rise. A number of these compounds were originally prescription drugs such as phenazepam (Russia) as well as etizolam and flutazolam (Japan) [9–11]. Some of these compounds never gained marketing approval (e.g. adinazolam) but the majority were simply patented and never brought to market and, as such, there is a deficit of physiochemical and pharmacokinetic data that would otherwise exist if they had undergone clinical trials [12]. However, such information is essential to fully understand the pharmacological behaviour of these compounds, especially as they are becoming more and more prevalent on the illicit drug market. This paper focuses on two physiochemical properties (log $D_{7.4}$ and pKa) and one pharmacokinetic property (plasma protein binding).

The lipophilicity of a compound is often expressed by the term log $D_{7.4}$, this is the distribution coefficient and represents the relative ratios of a compound in an organic and aqueous solvent at the physiologically-relevant pH of 7.4 [13]. Lipophilicity has various pharmacokinetic implications such as affecting a compound's absorption through cell

membranes and its distribution in biological tissues and accordingly is important for the prediction of many of these pharmacokinetic parameters [14,15]. Highly-lipophilic compounds typically exhibit greater plasma protein binding and can generally cross the blood-brain barrier with greater ease [16,17]. The majority of the well-known, from herein referred to as 'classic', benzodiazepines have comparatively high values for lipophilicity and can therefore partition with ease across cellular membranes and accumulate in areas of the body that are high in lipids [18,19]. Furthermore, benzodiazepines also have high volumes of distribution (V_d) such as diazepam with a V_d at steady state of $0.88 – 1.39$ L kg^{-1} [20–23]. The lipophilicity (as log P) of some NPS-benzodiazepines has already been published in literature [24].

The acid-base dissociation constant (pK_a) of a compound is typically investigated during pharmaceutical development and plays an important role when used in conjunction with other parameters such as molecular weight and lipophilicity [25]. pK_a can affect the site in the body where compounds are absorbed [26] and can also assist with the development of extraction methods from biological samples [27].

Upon administration to the body, compounds bind to proteins present within the plasma, this is reflected through measurement of plasma protein binding values [28,29]. The fraction that is not bound (known as the unbound or free fraction) is responsible for the pharmacological effect and it is this fraction that undergoes metabolism and excretion [18]. The majority of the classic benzodiazepines are highly protein-bound such as diazepam (99 % bound) but some experience vastly lower binding, for example bromazepam (60 % bound) [30,31]. Reducing clearance (Cl) and increased plasma protein binding generally correlates with an increase in half-life ($t_{1/2}$) of a drug [32]. Knowledge of plasma protein binding is therefore important to help characterise pharmacokinetics of drugs without *in vivo* studies. There has already been interest in the determination of these properties for new psychoactive substances, for example the plasma protein binding of flubromazolam (89 %) has recently been published in the

literature [33]. Yet for many of the more recently synthesised benzodiazepines the percentage bound is as yet unknown.

As many of these compounds have never undergone clinical trials, and are unlikely to as a result of the time and expense involved, it is critical that such analysis is undertaken, especially for the future prediction of any newly emerging psychoactive substances. The use of predictive software could be an attractive alternative to *in vitro* experiments to calculate these properties and this research will focus upon comparison of some predictive software packages with experimental values.

2. Materials and methods

Eight benzodiazepines that had values available in the literature for log $D_{7.4}$, pK_a and plasma protein binding were chosen to examine the suitability of the devised methods (alprazolam, clonazepam, diazepam, flunitrazepam, nitrazepam, oxazepam, prazepam and temazepam). These three properties were then investigated experimentally for a further 11, as yet, uncharacterised benzodiazepines, recently appearing as new psychoactive substances (3-hydroxyphenazepam, 4'-chlorodiazepam, desalkylflurazepam, deschloroetizolam, diclazepam, etizolam, flubromazepam, flubromazolam, meclonazepam, phenazepam and pyrazolam). The chemical structures of this latter group of compounds can be found in the Supplementary Information.

2.1. Materials

4'-Chlorodiazepam, alprazolam, clonazepam, desalkylflurazepam, diazepam, flunitrazepam, nitrazepam, oxazepam, prazepam and temazepam were obtained from Sigma-Aldrich (Dorset, UK). 3-Hydroxyphenazepam, deschloroetizolam, diclazepam, etizolam, flubromazepam, flubromazolam, meclonazepam, phenazepam and pyrazolam were obtained from Chiron (Trondheim, Norway). All compounds were received as powdered solids.

Dimethyl sulfoxide (DMSO), methanol, phosphoric acid, sodium hydrogen phosphate heptahydrate, sodium dihydrogen phosphate, disodium hydrogen phosphate, acetic acid, sodium acetate trihydrate, boric acid, sodium hydroxide, hydrochloric acid, sodium chloride and octan-1-ol were purchased from Fisher Scientific (Leicestershire, UK). Phosphate buffered saline (PBS) tablets were purchased from Sigma-Aldrich (Dorset, UK).

Human plasma (pooled, from three male donors and three female donors) was obtained from Seralab (West Sussex, UK). Plasma was received frozen with sodium citrate as an anticoagulant.

2.2. Methods
2.2.1. Determination of log $D_{7.4}$

The shake-flask method is commonly used in determining log $D_{7.4}$ values [34]. The compound of interest is dissolved in equal volumes of a buffer at a specified pH and an organic solvent, such as octanol. Following equilibration the octanol and buffer are separated and the concentration of the compound in each is determined. The log $D_{7.4}$ is then calculated using Equation 1.

$$logD = \frac{Compound\ concentration\ in\ aqueous\ phase}{Compound\ concentration\ in\ organic\ phase} \qquad (1)$$

Sodium phosphate buffer (0.01 M) was formulated using deionised water (Barnstead UltraPure) and filtered through a 0.45 µm Nylon Phenex filter membrane (Phenomenex, Cheshire, UK) using a Millipore filtration apparatus (Merck Millipore, Hertfordshire, UK).

Compounds were dissolved in methanol at a concentration of 1 mg ml^{-1}. Aliquots of compound solution were evaporated with a flow of nitrogen using a TurboVap to yield 0.20 mg of compound. Equal volumes (700 µl) of sodium phosphate buffer (0.01 M, pH 7.4) and octan-1-ol were added and the samples were vortexed for 30 seconds.

The samples were transferred into 1.5 mL Eppendorf microcentrifuge tubes and placed on a Stuart SB3 rotator (Bibby Scientific, Staffordshire UK) and rotated at 40 rpm for four hours. Samples were then centrifuged at 10,000 rpm for 20 minutes. The separated octanol and buffer phases were collected and analysed using high performance liquid chromatography (HPLC) coupled to a diode array detector (DAD). Further details of the method employed are given in Section 2.4. Each log D determination was repeated in triplicate.

2.2.2. Determination of pK$_a$

Capillary electrophoresis is a common method of measuring pK$_a$ [35]. The basic principle behind this technique is an applied electrical voltage which separates ions according to their electrophoretic mobility. When the solute is unionised it has no mobility and when an electrical voltage is applied and it is fully ionised it has maximum electrophoretic mobility. The mobility of the solute between these two extremes is a function of the dissociation equilibrium. The effective electrophoretic mobility of a compound can be calculated by using the difference in migration time between the test compound and a neutral marker [35].

$$\mu_{eff} = \left(\frac{L_d L_t}{V}\right)\left(\frac{1}{t_a} - \frac{1}{t_m}\right) \tag{2}$$

In Equation , t_a is the migration time for the test compound (s), t_m is the migration time for the neutral marker (s), L_d is the total length from the capillary inlet to the detection window (cm), L_t is the total capillary length (cm) and V is the applied voltage (V). As a result of the differences in pH there can be variations in electroosmotic flow but these are corrected for by using a neutral compound as a marker and adjusting for this in the calculation of effective mobility.

$$\mu_{eff} = \frac{\alpha \times 10^{-pH}}{10^{-pK_a} + 10^{-pH}} \tag{3}$$

$$\mu_{eff} = \frac{b_1(10^{-pH})^2 + a_1 10^{-pK_{a1}} 10^{-pK_{a2}}}{(10^{-pH})^2 + 10^{-pK_{a1}} 10^{-pH} + 10^{-pK_{a1}} 10^{-pK_{a2}}} \qquad (4)$$

Equations (3) and (4) describe the relationship between the effective electrophoretic mobility of a compound and its pK$_a$ for benzodiazepines with one ionisable basic group and an ionisable basic and acidic group [36].

Phosphate, acetate and borate buffers were utilised as described elsewhere with a pH spacing of 0.5 pH units [36]. All buffers had an ionic strength of *I*=0.05 and a concentration of 0.05 M. Sodium chloride was used to adjust the ionic strength and hydrochloric acid (0.1 M) or sodium hydroxide (0.1 M) were used to adjust the pH values if necessary. The pH was measured with a Jenway 3505 pH meter (Jenway, Essex, UK) which was calibrated before use. Buffers were filtered prior to use through a 0.45 μm Nylon Phenex filter membrane (Phenomenex, Cheshire, UK) using a Millipore filtration apparatus (Merck Millipore, Hertfordshire, UK).

Compounds were dissolved in methanol at a concentration of 1 mg ml^{-1}. Solutions were diluted to 0.25 mg ml^{-1} with deionised water (Barnstead UltraPure) and contained DMSO as the electroosmotic flow marker (1 % v/v).

DMSO (1 % v/v) in deionised water (Barnstead UltraPure) was run at each pH before experimental repeats to ensure that an expected electrophoretic mobility was obtained.

Compound migration times were determined using a Beckman Coulter P/ACE MDQ Capillary Electrophoresis System with a diode array detector (Beckman-Coulter, High Wycombe, UK). The internal capillary temperature was set at 25 °C using the liquid cooling system. Sample injection was conducted at 1.0 psi for 10 seconds and then 20 kV voltage was applied during separations. The capillary was rinsed between each run in the following

manner; NaOH applied at 20 psi for 1.0 minute followed by the appropriate buffer for the next repeat at 20 psi for 2.0 minutes.

Experimentally determined μ_{eff} values were obtained using Equation 2. The Microsoft Excel add-in, Solver, was used to calculate the pK_a value using least-squares regression. An initial 'best-guess' estimate for the pK_a and α values were used to calculate theoretical effective mobilities and the squared difference (the residuals) between these theoretical values and experimental values was then calculated and then minimised by varying the values for pK_a and α.

For pK_a measurements, accuracy is defined as a measured value being within 0.20 units from the literature value and precision is defined as a measured value having a repeatability that is equal to or less than 0.07 units [35]. Each pK_a measurement was repeated in triplicate.

2.2.3. Determination of plasma protein binding

Plasma protein binding values in this work were determined using the commonly-used method of equilibrium dialysis [37]. In this method, the compound of interest is spiked into plasma. The plasma and an appropriate buffer (e.g. at desired physiological pH) are then left to equilibrate, separated by a semi-permeable membrane that allows free drug to pass through but has a molecular-weight cut off (MWCO) to prevent proteins from passing through. Following equilibration, the resultant concentrations of drug are determined and Equation (5) is used to calculate the plasma protein binding.

Frozen plasma was thawed at room temperature prior to the experiments. The pH was measured with a Jenway 3505 pH meter (Jenway, Essex, UK) which was calibrated before use. Plasma pH was found to be within the physiological range of 7.38 – 7.42 and adjustment was not required [38].

PBS tablets were dissolved in deionised water (Barnstead UltraPure) to yield a buffer solution that contained 0.01M phosphate, 0.0027M KCl, and 0.137M NaCl, pH 7.4 at 25 °C. Stock solutions of compounds in DMSO at a concentration of 10 mM were created and were diluted with PBS prior to the experiments to yield working solutions at a concentration of 200 μM.

Reusable Single-Sample Fast Micro-Equilibrium Dialyzers (500 μL volume) were obtained from Harvard Apparatus (Cambridge, UK), as were cellulose acetate membranes with a MWCO of 10,000 Da.

The membranes were soaked for 30 minutes in deionised water (Barnstead UltraPure) and rinsed thoroughly. Thirty μL of compound working solution was added to 270 μL of plasma to yield a final concentration of 20 μM of compound (final DMSO concentration 0.2 %). This was placed in one chamber and 500 μL of PBS was placed in the second chamber. The Micro-Equilibrium Dialyzers were then placed into a shaking waterbath held at 37 °C for 24 hours. The temperature was monitored with a Sentry Thermometer (Fisher Scientific, Leicestershire, UK). After 24 hours had elapsed, the samples were extracted from each chamber, matrix matched (with blank plasma or blank buffer). Ice-cold acetonitrile at a 4:1 ratio was then added to precipitate proteins. The samples were centrifuged at 10,000 rpm for 20 minutes and the supernatant was recovered and evaporated using a flow of nitrogen with a TurboVap. The samples were then reconstituted in 200 μL of acetonitrile and analysed using HPLC-DAD. Details of this analysis are given in Section 2.4. Each plasma protein binding measurement was repeated in triplicate.

Plasma protein binding (PPB) was calculated using the experimental plasma concentration (P_{exp}) and the experimental buffer concentration (B_{exp}) according to Equation (5).

$$PPB\ (\%) = 100 \times \frac{P_{exp} - B_{exp}}{P_{exp}} \qquad (5)$$

For those benzodiazepines that were highly protein bound and had a concentration in the buffer phase that was below the limit of quantitation (LOQ), the buffer concentration was calculated indirectly using Equation (6) which involved the experimental plasma concentration and the total expected concentration (P_{tot}), determined using a calibration plot. The total expected concentration was adjusted using a previously-determined correction factor (*CF*) for the extraction efficiency ($\approx$ 95 %). This indirectly-calculated buffer concentration was then input into Equation (5) to generate plasma protein binding values.

$$B_{exp} = (P_{tot} \times CF) - P_{exp} \qquad (6)$$

2.3.   Theoretical approaches

Theoretical log $D_{7.4}$ and pK_a values were generated using the free, online software ACD/I-Lab (which makes use of the EPSRC funded National Chemical Database Service hosted by the Royal Society of Chemistry) and two commercial software packages; MarvinSketch (version 17.28.0) (ChemAxon) and ADMET Predictor (Simulations Plus). Theoretical plasma protein binding values were obtained from two sources used for log $D_{7.4}$ and pK_a; ACD/I-Lab and ADMET Predictor (Simulations Plus) and one source available as a free online resource, PreADMET (version 2.0). These software packages are all commonly used for the prediction of physicochemical and pharmacokinetic parameters [39–42]. Theoretical values were compared with experimental values by means of the absolute difference in values.

2.4.   HPLC analysis for log $D_{7.4}$ and plasma protein binding

Analysis was achieved with a Dionex UltiMate 3000 HPLC system equipped with an UltiMate 3000 Pump, UltiMate 3000 Autosampler, UltiMate 3000 Column Compartment, UltiMate 3000 Photodiode Array Detector and Chromeleon software (Dionex, Surrey, UK). Separation was achieved with a Waters® Spherisorb® analytical cartridge, C18 5 µm 80 Å

(4.6 × 150 mm) with an attached guard cartridge identically packed to the analytical cartridge (Waters, Hertfordshire, UK). The internal column temperature was kept constant at 25 °C and a flow rate of 0.8 mL min^{-1} was set. Injection volumes for the log $D_{7.4}$ experiments were 25 µL for the octanol phase and 100 µL for the phosphate buffer phase so that a dilution step was not necessary. Compound concentrations were retrospectively corrected. Injection volumes of 100 µL were used for the plasma protein binding experiments. A 46:54 (v/v) ratio of acetonitrile and sodium phosphate buffer (pH 3.0, 25 mM) was applied for 25 minutes. All compounds eluted within this time. The eluent was monitored by UV detection at 230 nm.

The method was validated in terms of linearity, limit of quantitation (LOQ), limit of detection (LOD), accuracy and precision. This was performed according to the ICH guidelines.

2.4.1. Linearity

The linearity of this method was measured by constructing a five-point calibration plot of the area under the curve (AUC) of each compound against its concentration in mg ml^{-1} (n=3) from 0.25 – 0.0004 mg ml^{-1}.

2.4.2. Limit of detection (LOD) and limit of quantitation (LOQ)

The limits of detection and quantitation were determined from the signal-to-noise ratio. The baseline response of blank samples was recorded. A ratio of 10:1 for the compound response to the baseline response was used for the LOQ and a ratio of 3:1 for the LOD.

2.4.3. Accuracy and precision

Accuracy was determined through comparison of the percentage recovery at three concentrations (0.25, 0.01 and 0.0004 mg ml^{-1}). Precision was determined from the calculation of the standard deviation and relative standard deviation (RSD) of the compound peak areas at three concentrations (0.25, 0.01 and 0.0004 mg ml^{-1}).

3. Results and discussion

3.1.   Method validation

3.1.1. Linearity

The method was linear over the concentration range $0.0004 - 0.25$ mg ml^{-1} for all compounds. The residual sum of squares for each compound was reasonably low indicating linear concentration-response and a suitable method (Table 1).

3.1.2. LOD and LOQ

All compounds generally had good limits of detection and quantitation (Table 1). Pyrazolam exhibited the lowest response to the HPLC method, with a LOQ of 263.9 ng ml^{-1} and a LOD of 82.0 ng ml^{-1}.

3.1.3. Accuracy and precision

Accuracy was determined through comparison of the percentage recovery at three concentrations (0.25, 0.01 and 0.0004 mg ml^{-1}). Percentage recovery was generally within 2 % and thus deemed to be acceptable (Table 5). Precision was determined from the calculation of the standard deviation and relative standard deviation (RSD) of the compound peak areas at three concentrations (0.25, 0.01 and 0.0004 mg ml^{-1}). High levels of precision for all benzodiazepines were recorded (Table 2).

3.2. Experimental values

Experimental log $D_{7.4}$, pK_a and plasma protein binding values for all the classic and NPS-benzodiazepines were successfully determined and compared with theoretical values.

3.2.1. Log $D_{7.4}$

Buffer composition is important for the determination of log $D_{7.4}$ values. Use of a 0.01 M phosphate buffer has been shown to give an excellent correlation of distribution coefficients determined in the octanol-phosphate system for acidic and neutral compounds [43]. Despite the basic nature of the compounds in this study, a 0.01 M sodium phosphate buffer (pH 7.4) was chosen and its suitability evaluated by way of a comparison between the experimental log $D_{7.4}$ values and literature log $D_{7.4}$ values.

For the clinically-used (and previously characterised) benzodiazepines the experimental results obtained for log $D_{7.4}$ in this study were very close to those reported elsewhere in the literature, thus proving the suitability of this method and also the use of the 0.01 M sodium phosphate buffer (pH 7.4) (Table 3).

The majority of the NPS-benzodiazepines were fairly lipophilic with log $D_{7.4}$ values above 2 (Table 3). None of the NPS-benzodiazepines had literature-reported log $D_{7.4}$ values other than desalkylflurazepam with 2.78 versus a value of 2.82 in this work. Phenazepam (log $D_{7.4}$ of 3.25) was observed to be the most lipophilic NPS-benzodiazepine in this dataset while pyrazolam (log $D_{7.4}$ of 0.97) was the least lipophilic, a 190-fold difference. The reason behind the low lipophilicity for pyrazolam becomes more apparent when its structure is considered. Pyrazolam contains a pyridin-2-yl ring at position 7 rather than a phenyl ring, as is the case with the rest of the benzodiazepines in this study. The phenyl ring has a log $D_{7.4}$ value of 1.56 versus a log $D_{7.4}$ value of 0.62 for the pyridin-2-yl ring [44]. Replacement of a phenyl ring for a pyridin-2-yl ring could lead to a decrease in lipophilicity. The benzodiazepine bromazepam contains a pyridin-2-yl ring rather than a phenyl ring and has a log $D_{7.4}$ value of

1.60 [45]. The addition of a triazole ring to some compounds is also known to lead to a decrease in the partition coefficient [46 47]. The pyridin-2-yl ring and triazole ring addition appear to lead to a marked decrease in lipophilicity for pyrazolam. Previous research has used log $D_{7.4}$ values in a quantitative structure-activity relationship (QSAR) model which predicted the post-mortem distribution of benzodiazepines and was found to contribute significantly to their distributive potential [48]. Log $D_{7.4}$ has also been utilised, along with plasma protein binding and pK_a, to derive models capable of predicting the volume of distribution at steady state of a wide range of compounds [49,50].

3.2.2. pK_a

Experimental pK_a values were all within 0.20 units of their literature values for the classic benzodiazepines and had excellent repeatability, under 0.07 units for all the reference compounds (Table 4). Classic benzodiazepines either have one pK_a value, for example flunitrazepam (1.8), or two clonazepam (1.5 and 10.5) [51,52]. The first pK_a value refers to the deprotonation of the nitrogen cation at position 4 and the second pK_a refers to the deprotonation of the nitrogen atom at position 1 [51]. The deprotonation of the nitrogen atom at position 1 is thought to be resonance stabilised with the negatively-charged oxygen atom [51]. This can be visualised in Figure 1 for clonazepam. Values of 2.83 for etizolam and 2.51 and 11.64 for desalkylflurazepam were calculated in this work. These compared favourably to their previously-reported values of 2.76 for etizolam and of 2.57 and 11.76 for desalkylflurazepam [53,54].

The presence of an electron-withdrawing hydroxyl group decreases the pK_a2 value, as does the presence of an ortho-chlorine substituent on the phenyl ring [55]. Clonazepam has this ortho-chlorine substituent and has a calculated pK_a value of 1.55 in this work. 3-Hydroxyphenazepam, in addition to an ortho-chlorine substituent, also has a hydroxyl group and therefore its low pK_a value of 1.25 was not unexpected. Repeatability was generally good

for the NPS-benzodiazepines; 0.07 is typically the expected variance in capillary electrophoresis measurements [35]. However, a variance of up to ±0.10 was observed for some compounds including 3-hydroxyphenazepam. This could be as a result of its pK_a1 value (1.25) being lower than the pH of the lowest buffer used (1.50).

3.2.3. Plasma protein binding

A number of the benzodiazepines had concentrations in the buffer phase would have been below the limit of quantitation (LOQ), these were; diazepam, oxazepam, prazepam, 4'-chlorodiazepam, flubromazepam and phenazepam. All concentrations were higher than the limit of detection (LOD). As mentioned in the methods section the buffer phase concentrations were calculated indirectly. The use of a correction factor is less desirable than direct measurements however, it did not appear to affect the calculated values for plasma protein binding when compared with literature values (Table 5).

Values for plasma protein binding are listed in Table 5 for clinically used benzodiazepines; wide variations were reported in the literature for many of the benzodiazepines. Age and sex have both been observed as causing differences in the plasma protein binding of drugs which may have been a factor in these variations as many of them were determined *in vivo* [56–58]. The experimentally derived values for the reference benzodiazepines were typically within the literature ranges with low variations. The majority of the NPS-benzodiazepines were observed to exhibit a high degree of plasma protein binding (> 90 %), i.e. similar to the clinically used benzodiazepines (Table 5). Literature values for the plasma protein binding of three NPS-benzodiazepines were available and experimental values derived in this work returned a consensus with these; desalkylflurazepam (experimental 95.5 % versus 96.1 – 96.5 % literature), etizolam (experimental 92.8 % versus 93 % literature) and flubromazolam (experimental 89.5 % versus literature 89 %) [24,59–61].

The lowest plasma protein binding was observed for pyrazolam which was 78.7 %. Such a low value of plasma protein binding for a benzodiazepine is not unheralded as bromazepam has a reported 60 % plasma protein binding [31]. Substitution of the phenyl ring at position-5 for a pyridin-2-yl ring has been previously reported to lead to a large decrease in lipophilicity for 1,-4-benzodiazepines [59]. The same effect could well occur for triazolobenzodiazepines.

4'-Chlorodiazepam differs from diazepam by having an additional chlorine atom substituted at the 4'-position of the phenyl ring and exhibits similarly high plasma protein binding; 98.2 % versus 99.0 % for diazepam. Diclazepam is an isomer of 4'-chlorodiazepam; identical in chemical formula but differing in structure with the chlorine atom being substituted at the 2'-position of the phenyl ring. Its plasma protein binding value was calculated as being 93.8 %, lower than diazepam or 4'-chlorodiazepam. However diclazepam's demethylated metabolite has been reported as having a plasma protein binding of 94.9 % and demethylation at the 1-position is not thought to substantially affect plasma protein binding [59]. Therefore, it stands to reason that the decreased plasma protein binding observed is most likely as a result of the substitution of a chlorine atom at the 2'-position. Substitution at the 2'-position with a chlorine atom has been observed to decrease plasma protein binding but if this substitution instead occurs at the 4' position then no such decrease is observed [59]. This is thought to be as a result of the substitution at the 2'-position affecting the rotation and orientation of the benzene ring and resulting in lower binding.

3-Hydroxyphenazepam exhibited lower plasma protein binding than its parent compound, phenazepam; 97.7 % versus 98.3 % and this is consistent with observations that hydroxylation at the 3-position leads to a decrease in plasma protein binding [59]. Deschloroetizolam has a reduced plasma protein binding compared to the thienotriazolodiazepine etizolam (87.2 % versus 92.8%). Removal of a chlorine atom from

position-7 has been found to decrease plasma protein binding for 1,4-benzodiazepines and a similar relationship may hold true for thienotriazolodiazepines [59].

Desalkylflurazepam differs from flubromazepam by replacement of the bromine atom at the 7-position by a chlorine atom. Its plasma protein binding is lower (95.5 % versus 96.2 %) which is consistent with literature observations that this replacement causes a decrease in plasma protein binding [59].

Phenazepam differs from flubromazepam by replacement of the fluorine atom at the 2'-position with a chlorine atom and exhibits an increase in plasma protein binding from 96.4 % to 98.3 %. Again, this is consistent with previous literature observations on 1,4-benzodiazepines [59].

3.3. Theoretical values

3.3.1. Log $D_{7.4}$

ACD/I-Lab returned the closest predicted log $D_{7.4}$ values to the experimental values for both the eight test benzodiazepines (average absolute error 0.18) and the 11 NPS-benzodiazepines (average absolute error 0.28). ADMET Predictor returned the next-closest predicted values with average absolute errors of 0.24 for the test benzodiazepines and 0.37 for the NPS-benzodiazepines. MarvinSketch fared the worst, returning an average absolute error of 0.39 for the test benzodiazepines and 0.97 for the NPS-benzodiazepines. It is therefore clear that all three programs had a lower accuracy in predicting the log $D_{7.4}$ for the NPS-benzodiazepines and this highlights the importance of the collection of experimental data especially if these models are to be improved. An example of this is for pyrazolam, with an experimental value of 0.97 yet ACD/I-Lab returned a value of 1.76, i.e. approximately a six-fold difference in apparent lipophilicity. The atypical structure of pyrazolam, with its pyridin-2-yl ring, possibly led to these large differences. Inclusion of pyrazolam along with the other

NPS-benzodiazepines in any future training dataset for these predictive models could possibly assist in the prediction of log $D_{7.4}$.

3.3.2. pK_a

ADMET Predictor returned the closest predicted values to experimental values, with an absolute average error of 0.4 for both the test set and the NPS set. This was closely followed by ACD/I-Lab which returned absolute average errors of 0.5 for both sets. MarvinSketch returned average absolute errors of 0.6 for the test set and 0.7 for the NPS set. MarvinSketch did not predict pK_a1 values for oxazepam and temazepam and instead predicted two pK_a2 values for oxazepam (only one of which exists) and one pK_a2 value for temazepam (only a pK_a1 value is observed). Large errors were observed in some of the pK_a values returned by the software. For example; a pK_a of 2.45 predicted by ACD/I-Lab for deschloroetizolam versus an experimental pK_a of 4.19, a pK_a of 1.33 predicted by MarvinSketch for etizolam versus an experimental pK_a of 2.80 and a pK_a of 2.98 predicted for flubromazolam by ADMET Predictor versus an experimental pK_a of 2.07. Additionally, all three software packages predicted multiple other deprotonation sites for some of the benzodiazepines which are not experimentally observed. The importance of obtaining accurate experimental pK_a values is therefore clear especially if these predictive models wish to be improved upon.

3.3.3. Plasma protein binding

Plasma protein binding was best predicted by ACD/I-Lab which returned average absolute errors of 4.4 % for the test benzodiazepines and 3.0 % for the NPS-benzodiazepines. ADMET Predictor followed closely behind with average absolute errors of 6.8 % for the test benzodiazepines and 3.4 % for the NPS-benzodiazepines. PreADMET returned average absolute errors of 9.9 % for the test benzodiazepines and 5.0 % for the NPS-benzodiazepines. The software appeared to be less effective at predicting plasma protein binding of the test benzodiazepines than the NPS-benzodiazepines (Table 5). However an important caveat is that the average absolute errors for the test benzodiazepines were influenced heavily by the

small dataset and the presence of alprazolam; the experimental plasma protein binding was determined as being 71.6 % and the predicted values were 89.5 % (ACD/I-Lab), 91.2 % (ADMET Predictor) and 95.2% (PreADMET). Again, inclusion of a wider range of benzodiazepines (especially those with aberrant structures such as pyrazolam) in any training dataset may assist with their predictive power.

4. Conclusions

Log $D_{7.4}$, pK_a and plasma protein binding values were successfully determined in this work for a range of benzodiazepines that have emerged as novel psychoactive substances. The experimental methods presented were judged to be suitably accurate for the determination of these values.

Large variations in plasma protein binding and log $D_{7.4}$ were observed for the NPS-benzodiazepines. Pyrazolam was found to be the least lipophilic NPS-benzodiazepine with a log $D_{7.4}$ of 0.97 and experienced the lowest plasma protein binding of 78.7 %. Phenazepam was the most lipophilic NPS-benzodiazepine with a log $D_{7.4}$ of 3.25 and a plasma protein binding of 98.3 %. 3-Hydroxyphenazepam had the lowest pK_a1 value of 1.25 while deschloroetizolam had the highest pK_a1 value of 4.19. Phenazepam had the lowest pK_a2 value of 11.24 and 3-hydroxyphenazepam had the highest of 11.96.

ACD/I-Lab returned the closest predicted values to experimental values for both plasma protein binding and log $D_{7.4}$ while ADMET Predictor returned the closest predicted values to experimental values for pK_a. Although the average errors returned by each software package were often low, there were large variations in individual errors. It is therefore likely that experimental data for these novel psychoactive substances remains preferable to that generated from predictive software. The inclusion of experimental data for these NPS-benzodiazepines could aid the predictive capability of various software packages.

1   European Monitoring Centre for Drugs and Drug Addiction (EMCDDA)-Europol. *European Drug Report: Trends and Developments,*2016.

2   Manchester KR, Lomas EC, Waters L, Dempsey FC, Maskell PD. The emergence of new psychoactive substance (NPS) benzodiazepines: A review. *Drug Test. Anal.* 2018; 10: 37–53., doi: 10.1002/dta.2211.

3   Mehdi T. Benzodiazepines Revisited. *Br. J. Med. Pract.* 2012; 5: a501., doi: 10.1093/jat/bkt075.

4   Martin Dittus, Joss Wright MG. *Platform Criminalism: The "Last-Mile" Geography of the Darknet Market Supply Chain*2018.

5   Kerrigan S, Mellon MB, Hinners P. Detection of Phenazepam in Impaired Driving. *J. Anal. Toxicol.* 2013; 37: 605–610., doi: 10.1093/jat/bkt075.

6   Shearer K, Bryce C, Parsons M, Torrance H. Phenazepam: A review of medico-legal deaths in South Scotland between 2010 and 2014. *Forensic Sci. Int.* 2015; 254: 197–204., doi: 10.1016/j.forsciint.2015.07.033.

7   Łukasik-Głębocka M, Sommerfeld K, Teżyk A, Zielińska-Psuja B, et al. Flubromazolam – A new life-threatening designer benzodiazepine. *Clin. Toxicol.* 2016; 54: 66–68., doi: 10.3109/15563650.2015.1112907.

8   Valli A, Lonati D, Locatelli CA, Buscaglia E, et al. Analytically diagnosed intoxication by 2-methoxphenidine and flubromazepam mimicking an ischemic cerebral disease. *Clin. Toxicol.* 2017; 55: 611–612., doi: 10.1080/15563650.2017.1286016.

9   Maskell PD, De Paoli G, Nitin Seetohul L, Pounder DJ. Phenazepam: The drug that came in from the cold. *J. Forensic Leg. Med.* 2012; 19: 122–125., doi: 10.1016/j.jflm.2011.12.014.

10   Nakamae T, Shinozuka T, Sasaki C, Ogamo A, et al. Case report: Etizolam and its major metabolites in two unnatural death cases. *Forensic Sci. Int.* 2008; 182: e1–e6., doi: 10.1016/j.forsciint.2008.08.012.

11   Pettersson Bergstrand M, Helander A, Hansson T, Beck O. Detectability of designer benzodiazepines in CEDIA, EMIT II Plus, HEIA, and KIMS II immunochemical screening assays. *Drug Test. Anal.* 2016;, doi: 10.1002/dta.2003.

12   Moosmann B, Bisel P, Franz F, Huppertz LM, Auwarter V. Characterization and in vitro phase I microsomal metabolism of designer benzodiazepines - an update comprising adinazolam, cloniprazepam, fonazepam, 3-hydroxyphenazepam, metizolam and nitrazolam. *J. Mass Spectrom.* 2016; 51: 1080–1089., doi: 10.1002/jms.3840.

13   Arnott JA, Planey SL. The influence of lipophilicity in drug discovery and design. *Expert Opin. Drug Discov.* 2012; 7: 863–875., doi: 10.1517/17460441.2012.714363.

14   Testa B, Crivori P, Reist M, Carrupt P-A. No Title. *Perspect. Drug Discov. Des.* 2000; 19: 179–211., doi: 10.1023/A:1008741731244.

15   Hou T, Wang J, Zhang W, Wang W, Xu X. Recent Advances in Computational Prediction of Drug Absorption and Permeability in Drug Discovery. *Curr. Med. Chem.* 2006; 13: 2653–2667., doi: 10.2174/092986706778201558.

16   Begley DJ. ABC transporters and the blood-brain barrier. *Curr. Pharm. Des.* 2004; 10: 1295–312., doi: 10.2174/1381612043384844.

17   Di L, Kerns EH. *Drug-Like Properties: Concepts, Structure Design and Methods from ADME to Toxicity Optimization*Elsevier, London, U.K.,2016.

18   Greenblatt DJ, Arendt RM, Abernethy DR, Giles HG, et al. In vitro quantitation of benzodiazepine lipophilicity: Relation to in vivo distribution. *Br. J. Anaesth.* 1983; 55: 985–989., doi: 10.1093/bja/55.10.985.

19   García DA, Perillo MA. Benzodiazepine localisation at the lipid-water interface: Effect of membrane composition and drug chemical structure. *Biochim. Biophys. Acta - Biomembr.* 1999; 1418: 221–231., doi: 10.1016/S0005-2736(99)00040-1.

20   Arendt RM, Greenblatt DJ, Liebisch DC, Luu MD, Paul SM. Determinants of benzodiazepine brain uptake: lipophilicity versus binding affinity. *Psychopharmacology (Berl).* 1987; 93: 72–76., doi: 10.1007/BF02439589.

21   Litvin AA, Kolyvanov GB, Zherdev VP, Arzamastsev AP. Relationship between physicochemical characteristics and pharmacokinetic parameters of 1,4-benzodiazepine derivatives. *Pharm. Chem. J.* 2004; 38: 583–586., doi: 10.1007/s11094-005-0034-y.

22   Mandelli M, Tognoni G, Garattini S. Clinical Pharmacokinetics of Diazepam. *Clin. Pharmacokinet.* 1978; 3: 72–91., doi: 10.2165/00003088-197803010-00005.

23   Herman RJ, Wilkinson GR. Disposition of diazepam in young and elderly subjects after acute and chronic dosing. *Br. J. Clin. Pharmacol.* 1996; 42: 147–155., doi: 10.1046/j.1365-2125.1996.03642.x.

24   Noble C, Mardal M, Bjerre Holm N, Stybe Johansen S, Linnet K. In vitro studies on flubromazolam metabolism and detection of its metabolites in authentic forensic samples. *Drug Test. Anal.* 2017; 9: 1182–1191., doi: 10.1002/dta.2146.

25   Manallack DT. The pKa Distribution of Drugs: Application to Drug Discovery. *Perspect. Medicin. Chem.* 2007; 1: 25–38.

26   Avdeef A. Physicochemical Profiling (Solubility, Permeability and Charge State). *Curr. Top. Med. Chem.* 2001; 1: 277–351., doi: 10.2174/1568026013395100.

27   Chen XH, Franke JP, Wijsbeek J, de Zeeuw RA. Isolation of Acidic, Neutral, and Basic Drugs from Whole Blood Using A Single Mixed-Mode Solid-Phase Extraction Column. *J. Anal. Toxicol.* 1992; 16: 351–5., doi: 10.1093/jat/16.6.351.

28   Routledge PA. The plasma protein binding of basic drugs. *Br. J. Clin. Pharmacol.* 1986; 22: 499–506.

29   Kratochwil NA, Huber W, Müller F, Kansy M, Gerber PR. Predicting plasma protein binding of drugs: a new approach. *Biochem. Pharmacol.* 2002; 64: 1355–1374., doi: 10.1016/S0006-2952(02)01074-2.

30   Divoll M, Greenblatt DJ. Binding of diazepam and desmethyldiazepam to plasma protein: Concentration-dependence and interactions. *Psychopharmacology (Berl).* 1981; 75: 380–382., doi: 10.1007/BF00435857.

31   Zhang F, Xue J, Shao J, Jia L. Compilation of 222 drugs' plasma protein binding data and guidance for study designs. *Drug Discov. Today* 2012; 17: 475–485., doi: 10.1016/j.drudis.2011.12.018.

32   Gibaldi M, Levy G, McNamara PJ. Effect of plasma protein and tissue binding on the biologic half-life of drugs. *Clin. Pharmacol. Ther.* 1978; 24: 1–4., doi: 10.1002/cpt19782411.

33   Tomková J, Švidrnoch M, Maier V, Ondra P. Analysis of selected designer benzodiazepines by ultra high performance liquid chromatography with high-resolution time-of-flight mass spectrometry and the estimation of their partition coefficients by micellar electrokinetic chromatography. *J. Sep. Sci.* 2017; 40: 2037–2044., doi: 10.1002/jssc.201700069.

34   Di L, Kerns EH. Lipophilicity Methods in *Drug-Like Prop.* 2016 pp.299–306.

35   Poole SK, Patel S, Dehring K, Workman H, Poole CF. Determination of acid dissociation constants by capillary electrophoresis. *J. Chromatogr. A* 2004; 1037: 445–454., doi: 10.1016/j.chroma.2004.02.087.

36   Miller JM, Blackburn AC, Shi Y, Melzak AJ, Ando HY. Semi-empirical relationships between effective mobility, charge, and molecular weight of pharmaceuticals by pressure-assisted capillary electrophoresis: Applications in drug discovery. *Electrophoresis* 2002; 23: 2833–2841., doi: 10.1002/1522-2683(200209)23:17<2833::AID-ELPS2833>3.0.CO;2-7.

37   Banker MJ, Clark TH, Williams JA. Development and validation of a 96-well equilibrium dialysis apparatus for measuring plasma protein binding. *J. Pharm. Sci.* 2003; 92: 967–974., doi: 10.1002/jps.10332.

38   Atherton JC. Acid-base balance: maintenance of plasma pH. *Anaesth. Intensive Care Med.* 2009; 10: 557–561., doi: 10.1016/j.mpaic.2009.08.005.

39   Li XZ, Zhang SN, Yang XY. Combination of cheminformatics and bioinformatics to explore the chemical basis of the rhizomes and aerial parts of Dioscorea nipponica Makino. *J. Pharm. Pharmacol.* 2017; 69: 1846–18657., doi: 10.1111/jphp.12825.

40   S.K.Lee, I.H.Lee, H.J.Kim, G.S.Chang, J.E.Chung KTN. The PreADME Approach: Web-based program for rapid prediction of physico-chemical, drug absorption and drug-like properties in*EuroQSAR 2002 Des. Drugs Crop Prot. Process. Probl. Solut.* Blackwell Publishing, Massachusetts, USA 2003 pp.418–420.

41   Fraczkiewicz R, Lobell M, Goller AH, Krenz U, et al. Best of both worlds: Combining pharma data and state of the art modeling technology to improve in silico pKa prediction. *J. Chem. Inf. Model.* 2015; 55: 389–397., doi: 10.1021/ci500585w.

42   Ghosh J, Lawless MS, Waldman M, Gombar V, Fraczkiewicz R. Modeling ADMET. *Methods Mol. Biol.* 2016; 1425: 63–83., doi: 10.1007/978-1-4939-3609-0_4.

43   Ferreira LA, Chervenak A, Placko S, Kestranek A, et al. Effect of ionic composition on the partitioning of organic compounds in octanol–buffer systems. *RSC Adv.* 2015; 5: 20574–20582., doi: 10.1039/C5RA01402F.

44   Sangster J. Octanol- Water Partition Coefficients of Simple Organic Compounds. *J. Phys. Chem. Ref. Data* 1989; 18: 1111–1229., doi: 10.1063/1.555833.

45   Hansch C, Björkroth JP, Leo A. Hydrophobicity and central nervous system agents: On the principle of minimal hydrophobicity in drug design. *J. Pharm. Sci.* 1987; 76: 663–687., doi: 10.1002/jps.2600760902.

46   Costa EC, Cassamale TB, Carvalho DB, Bosquiroli LSS, et al. Antileishmanial activity and structure-activity relationship of triazolic compounds derived from the neolignans grandisin, veraguensin, and machilin G. *Molecules* 2016; 21:, doi: 10.3390/molecules21060802.

47   Chu W, Rothfuss J, Zhou D, MacH RH. Synthesis and evaluation of isatin analogs as caspase-3 inhibitors: Introduction of a hydrophilic group increases potency in a whole cell assay. *Bioorganic Med. Chem. Lett.* 2011; 21: 2192–2197., doi: 10.1016/j.bmcl.2011.03.015.

48   Giaginis C, Tsantili-Kakoulidou A, Theocharis S. Applying Quantitative Structure–Activity Relationship (QSAR) Methodology for Modeling Postmortem Redistribution of Benzodiazepines and Tricyclic Antidepressants. *J. Anal. Toxicol.* 2014; 38: 242–248., doi: 10.1093/jat/bku025.

49   Lombardo F, Obach RS, Shalaeva MY, Gao F. Prediction of Volume of Distribution Values in Humans for Neutral and Basic Drugs Using Physicochemical Measurements and Plasma Protein Binding Data. *J. Med. Chem.* 2002; 45: 2867–2876., doi: 10.1021/jm0200409.

50   Lombardo F, Obach RS, Shalaeva MY, Gao F. Prediction of Human Volume of Distribution Values for Neutral and Basic Drugs. 2. Extended Data Set and Leave-Class-Out Statistics. *J. Med. Chem.* 2004; 47: 1242–1250., doi: 10.1021/jm030408h.

51   Kaplan SA, Alexander K, Jack ML, Puglisi C V., et al. Pharmacokinetic profiles of clonazepam in dog and humans and of flunitrazepam in dog. *J. Pharm. Sci.* 1974; 63: 527–532., doi: 10.1002/jps.2600630407.

52   Deinl I, Mahr G, von Meyer L. Determination of Flunitrazepam and its Main Metabolites in Serum and Urine by HPLC after Mixed-Mode Solid-Phase Extraction. *J. Anal. Toxicol.* 1998; 22: 197–202., doi: 10.1093/jat/22.3.197.

53   Groves JA, Smyth WF. Polarographic study of flurazepam and its major metabolites. *Analyst* 1981; 106: 890., doi: 10.1039/an9810600890.

54   World Health Organisation (WHO). *Expert Committee on Drug Dependence Thirty-Seventh Meeting: Etizolam Pre-Review Report*Geneva2015.

55   BARRETT J, SMYTH WF, DAVIDSON IE. An examination of acid-base equilibria of 1,4-benzodiazepines by spectrophotometry. *J. Pharm. Pharmacol.* 1973; 25: 387–393., doi: 10.1111/j.2042-7158.1973.tb10033.x.

56   Soldin OP, Mattison DR. Sex Differences in Pharmacokinetics and Pharmacodynamics. *Clin. Pharmacokinet.* 2009; 48: 143–157., doi: 10.2165/00003088-200948030-00001.

57   Routledge PA, Stargel WW, Kitchell BB, Barchowsky A, Shand DG. Sex-related differences in the plasma protein binding of lignocaine and diazepam. *Br. J. Clin. Pharmacol.* 1981; 11: 245–250.

58   Verbeeck RK, Cardinal JA, Wallace SM. Effect of age and sex on the plasma binding of acidic and basic drugs. *Eur. J. Clin. Pharmacol.* 1984; 27: 91–97., doi: 10.1007/BF00553161.

59   Lucek RW, Coutinho CB. The role of substituents in the hydrophobic binding of the 1,4-benzodiazepines by human plasma proteins. *Mol. Pharmacol.* 1976; 12: 612–619.

60   Miller LG, Greenblatt DJ, Abernethy DR, Friedman H, et al. Kinetics, brain uptake, and receptor binding characteristics of flurazepam and its metabolites. *Psychopharmacology (Berl).* 1988; 94: 386–391., doi: 10.1007/BF00174694.

61   Fracasso C, Confalonieri S, Garattini S, Caccia S. Single and multiple dose pharmacokinetics of etizolam in healthy subjects. *Eur. J. Clin. Pharmacol.* 1991; 40: 181–185., doi: 10.1007/BF00280074.

62   Benet LZ, Broccatelli F, Oprea TI. BDDCS Applied to Over 900 Drugs. *AAPS J.* 2011; 13: 519–547., doi: 10.1208/s12248-011-9290-9.

63   Giaginis C, Theocharis S, Tsantili-Kakoulidou A. Contribution to the standardization of the chromatographic conditions for the lipophilicity assessment of neutral and basic drugs. *Anal. Chim. Acta* 2006; 573–574: 311–318., doi: 10.1016/j.aca.2006.03.074.

64   Lombardo F, Shalaeva MY, Tupper KA, Gao F. ElogD o ct : A Tool for Lipophilicity Determination in Drug Discovery. 2. Basic and Neutral Compounds. *J. Med. Chem.* 2001; 44: 2490–2497., doi: 10.1021/jm0100990.

65   Moffat AC, Osselton MD, Widdop B, Watts J. *Clarke's Analysis of Drugs and Poisons*Pharmaceutical Press, London, U.K.,2011.

66   Graf E, El-Menshawy M. pK- und Vk-Messungen an Benzodiazepinen. *Pharm. Unserer Zeit* 1977; 6: 171–178., doi: 10.1002/pauz.19770060602.

67   Shayesteh TH, Radmehr M, Khajavi F, Mahjub R. Application of chemometrics in

determination of the acid dissociation constants (pKa) of several benzodiazepine derivatives as poorly soluble drugs in the presence of ionic surfactants. *Eur. J. Pharm. Sci.* 2015; 69: 44–50., doi: 10.1016/j.ejps.2014.12.013.

68   Bacalum E, Cheregi M, David V. Retention behaviour of some benzodiazepines in solid-phase extraction using modified silica adsorbents having various hydrophobicities. *Rev. Roum. Chim.* 2015; 60: 891–898.

69   Gautam L, Sharratt SD, Cole MD. Drug facilitated sexual assault: Detection and stability of benzodiazepines in spiked drinks using gas chromatography-mass spectrometry. *PLoS One* 2014; 9:, doi: 10.1371/journal.pone.0089031.

70   Moschitto LJ, Greenblatt DJ. Concentration-independent plasma protein binding of benzodiazepines. *J. Pharm. Pharmacol.* 1983; 35: 179–180., doi: 10.1111/j.2042-7158.1983.tb04302.x.

71   Abernethy D, Greenblatt D, Locniskar A, Ochs H, et al. Obesity effects on nitrazepam disposition. *Br. J. Clin. Pharmacol.* 1986; 22: 551–557., doi: 10.1111/j.1365-2125.1986.tb02934.x.

72   Kangas L, Allonen H, Lammintausta R, Salonen M, Pekkarinen A. Pharmacokinetics of Nitrazepam in Saliva and Serum after a Single Oral Dose. *Acta Pharmacol. Toxicol. (Copenh).* 1979; 45: 20–24., doi: 10.1111/j.1600-0773.1979.tb02354.x.

73   G. Seyffart. *Drug Dosage in Renal Insufficiency* Springer Science & Business Media, New York, USA, 2012.

Table 1. Linearity, LOQ and LOD data for benzodiazepines

Compound	Slope	Correlation coefficient	y intercept	Residual sum of squares	LOQ (ng ml^{-1})	LOD (ng ml^{-1})
3-Hydroxyphenazepam	4455.57	1.00	-0.55	19.40	188.9	42.9
4'-Chlorodiazepam	4819.30	1.00	1.44	11.30	202.2	59.5
Alprazolam	4826.85	1.00	1.36	27.07	144.6	49.8
Clonazepam	4407.07	1.00	0.37	21.90	185.4	59.2
Desalkylflurazepam	4283.08	1.00	-0.74	16.43	187.2	53.4
Deschloroetizolam	4072.89	1.00	0.86	13.00	206.1	62.5
Diazepam	4758.95	1.00	-0.74	18.41	185.5	51.8
Diclazepam	4817.39	1.00	0.48	12.73	198.8	59.9
Etizolam	4007.71	1.00	0.51	13.20	194.2	57.0
Flubromazepam	4084.79	1.00	0.73	15.99	165.6	67.6
Flubromazolam	4168.69	1.00	-0.42	10.68	177.3	47.2
Flunitrazepam	4223.77	1.00	-0.92	13.05	159.0	51.5
Meclonazepam	4805.99	1.00	0.87	9.15	186.4	52.5
Nitrazepam	4367.07	1.00	-0.37	10.82	179.2	49.4
Oxazepam	4466.93	1.00	-0.53	7.17	159.8	50.2
Phenazepam	4149.34	1.00	-0.17	11.76	191.2	65.3
Prazepam	4338.90	1.00	0.34	9.32	172.3	56.0
Pyrazolam	3967.82	1.00	-0.31	14.76	263.9	82.0
Temazepam	4646.75	1.00	-0.34	9.67	195.6	51.9

Table 2. Precision and accuracy data for benzodiazepines

| Compound | Concentration (mg ml⁻¹) | | | | | | | | |
| | 0.0004 (n=3) | | | 0.01 (n=3) | | | 0.25 (n=3) | | |
	Precision SD	Precision RSD (%)	Accuracy (%)	Precision SD	Precision RSD (%)	Accuracy (%)	Precision SD	Precision RSD (%)	Accuracy (%)
3-Hydroxyphenazepam	0.04	2.08	99.39	0.53	1.17	100.46	8.88	0.80	99.17
4'-Chlorodiazepam	0.06	1.72	101.35	0.47	0.93	101.85	10.29	0.85	100.54
Alprazolam	0.04	1.31	99.49	0.88	1.75	100.57	13.44	1.10	99.86
Clonazepam	0.05	1.53	101.11	0.81	1.62	99.25	6.91	1.77	99.98
Desalkylflurazepam	0.02	1.10	98.60	0.27	0.62	101.50	7.16	0.66	101.12
Deschloroetizolam	0.04	1.58	99.25	0.24	0.57	99.56	5.81	0.57	100.68
Diazepam	0.02	1.16	98.90	0.59	1.24	100.98	11.69	0.97	101.23
Diclazepam	0.02	0.70	98.92	0.54	1.07	101.49	6.46	0.54	99.10
Etizolam	0.04	1.74	98.99	0.72	1.78	99.57	9.95	1.00	99.73
Flubromazepam	0.03	1.16	99.21	0.66	1.56	101.76	5.36	0.52	101.34
Flubromazolam	0.03	2.15	100.41	0.55	1.13	100.89	17.93	1.71	100.74
Flunitrazepam	0.06	2.03	98.97	0.27	0.55	99.56	9.33	0.78	99.72
Meclonazepam	0.02	0.81	99.43	0.31	0.63	100.35	8.49	0.71	99.46
Nitrazepam	0.02	1.21	98.20	0.54	1.10	100.15	9.67	0.78	100.83
Oxazepam	0.02	1.44	101.76	0.70	1.56	101.68	7.48	0.68	99.21
Phenazepam	0.03	2.17	101.01	0.98	2.37	99.95	6.45	0.62	100.23
Prazepam	0.05	2.15	98.63	0.67	1.54	99.78	6.51	1.66	99.51
Pyrazolam	0.03	2.14	99.47	0.53	1.33	101.53	2.95	0.30	100.73
Temazepam	0.03	2.05	101.74	0.65	1.40	101.27	13.64	1.18	99.55

Table 3. Literature, experimental (n= ≥3) and theoretical log $D_{7.4}$ values for a set of classic and NPS-benzodiazepines

Compound	Literature log $D_{7.4}$	Experimental log $D_{7.4}$	Theoretical log $D_{7.4}$			References
			ACD/I-LAB/I-lab	MarvinSketch	ADMET Predictor	
Benzodiazepines						
Alprazolam	2.12 – 2.16	2.10 ±0.01	2.44	3.02	2.63	[62,63]
Clonazepam	2.41	2.40 ±0.02	2.57	3.15	2.49	[45,62]
Diazepam	2.79 – 2.99	2.81 ±0.03	2.87	3.08	2.96	[45,62–64]
Flunitrazepam	2.06 – 2.14	2.05 ±0.01	2.20	2.55	1.87	[45,62,63]
Nitrazepam	2.13 – 2.16	2.17 ±0.03	2.03	2.55	2.49	[45,62]
Oxazepam	2.13 – 2.24	2.24 ±0.05	2.04	2.92	1.95	[17,45]
Prazepam	3.7 – 3.73	3.74 ±0.04	3.84	3.86	3.68	[45,62]
Temazepam	1.79 – 2.19	2.32 ±0.01	2.13	2.79	2.18	[45,62]
NPS-benzodiazepines						
3-Hydroxyphenazepam	Not reported	2.54 ±0.01	2.67	3.69	2.40	Not reported
4'-Chlorodiazepam	Not reported	2.75 ±0.08	3.13	3.68	3.40	Not reported
Desalkylflurazepam	2.70	2.82 ±0.09	2.71	3.15	2.74	[62]
Deschloroetizolam	Not reported	2.60 ±0.03	2.43	3.45	2.82	Not reported
Diclazepam	Not reported	2.73 ±0.02	3.13	3.68	3.25	Not reported
Etizolam	Not reported	2.40 ±0.01	2.74	4.06	3.32	Not reported
Flubromazepam	Not reported	2.87 ±0.05	2.96	3.52	2.80	Not reported
Flubromazolam	Not reported	2.40 ±0.04	2.52	3.33	2.60	Not reported
Meclonazepam	Not reported	2.64 ±0.05	2.91	3.72	2.80	Not reported
Phenazepam	Not reported	3.25 ±0.04	3.52	3.98	3.19	Not reported
Pyrazolam	Not reported	0.97 ±0.01	1.76	2.36	2.03	Not reported

Table 4. Literature, experimental (n= ≥3) and theoretical pK$_a$ values for a set of classic and NPS benzodiazepines

Compound	Literature pK$_a$		Experimental pK$_a$		Theoretical pK$_a$						References
					ACD/I-LAB/I-lab		MarvinSketch		ADMET Predictor		
	pK$_a$1	pK$_a$2	pK$_a$1	pK$_a$2	pK$_a$1	pK$_a$2	pK$_a$1	pK$_a$2	pK$_a$1	pK$_a$2	
Benzodiazepines											
Alprazolam	2.4	None	2.48 ±0.01	None	2.37	None	1.45, 5.01	None	0.93, 3.01	None	[65]
Clonazepam	1.49 – 1.52	10.37 – 10.51	1.55 ±0.02	10.45 ±0.05	1.55	11.21	1.89	11.65	1.43	10.77	[65–67]
Diazepam	3.17 – 3.31	None	3.10 ±0.00	None	3.40	None	2.92	None	2.96	None	[66,68]
Flunitrazepam	1.8	None	1.82 ±0.04	None	1.68	None	1.72	None	1.87	None	[65]
Nitrazepam	2.94 – 3.2	10.8 – 11	3.11 ±0.06	11.02 ±0.05	2.55	11.35	2.65	11.66	2.49	11.02	[55,66]
Oxazepam	1.56 – 1.7	11.21 – 11.6	1.67 ±0.05	11.34 ±0.03	1.17	10.94, 12.75	None	10.65, 12.47	2.57	11.31	[66,67]
Prazepam	2.7 – 2.74	None	2.71 ±0.01	None	3.44	None	3.06	None	3.10	None	[65,66]
Temazepam	1.31 – 1.6	None	1.45 ±0.05	None	1.58	11.66	None	10.68	2.48	None	[66,69]
NPS-benzodiazepines											
3-Hydroxyphenazepam	Not reported	Not reported	1.25 ±0.10	11.96 ±0.09	0.13	10.80, 12.68	None	10.61, 12.45	1.95	11.24	Not reported
4'-Chlorodiazepam	Not reported	Not reported	3.13 ±0.01	None	3.08	None	2.45	None	2.55	None	Not reported
Desalkylflurazepam	2.57	11.76	2.51 ±0.05	11.64 ±0.04	2.36	11.55	1.80	12.29	2.31	11.37	[53]
Deschloroetizolam	Not reported	Not reported	4.19 ±0.01	None	0.20, 2.45	None	1.31, 5.37	None	1.84, 3.96	None	Not reported
Diclazepam	Not reported	Not reported	2.31 ±0.07	None	1.75	None	2.13	None	1.95	None	Not reported
Etizolam	2.76	None	2.83 ±0.06	None	0.10, 2.37	None	1.33, 4.55	None	1.61, 3.31	None	[54]
Flubromazepam	Not reported	Not reported	3.25 ±0.10	10.74 ±0.05	2.32	11.55	1.8	12.28	2.70	11.45	Not reported
Flubromazolam	Not reported	Not reported	2.07 ±0.02	None	2.27	None	1.48, 4.01	None	0.96, 2.98	None	Not reported
Meclonazepam	Not reported	Not reported	2.10 ±0.09	11.45 ±0.07	1.70	11.24	1.65	11.57	2.10	10.88	Not reported
Phenazepam	Not reported	Not reported	2.19 ±0.05	11.21 ±0.04	2.18	11.58	2.06	12.28	2.44	11.43	Not reported
Pyrazolam	Not reported	Not reported	3.30 ±0.03	None	1.30, 2.18	None	1.79, 2.75	None	0.65, 2.47, 3.21	None	Not reported

Table 5. Literature, experimental (n= ≥3) and theoretical plasma protein binding (PPB) values for a set of classic and NPS benzodiazepines

| Compound	Literature PPB (%)	Experimental PPB (%)	Theoretical PPB (%)			References
			ACD/ I-lab	ADMET Predictor	PreADMET	
Benzodiazepines						
Alprazolam	68.4 – 76.7	71.6 ±0.5	89.5	91.2	95.2	31,70
Clonazepam	85.4 – 86.1	85.5 ±1.2	91.9	90.9	93.3	31,70
Diazepam	98.4 – 99	99.0 ±0.2	96.5	93.2	98.7	31,37
Flunitrazepam	77.5 – 84.5	78.9 ±1.2	84.4	86.5	98.9	31,70
Nitrazepam	82.1 – 88.9	88.4 ±1.8	88.5	84.3	92.0	71,72
Oxazepam	89.0 – 98.4	96.9 ±0.1	95.6	88.9	96.7	31,70
Prazepam	≈97	97.4 ±0.5	97.7	96.5	94.0	73
Temazepam	92 – 96.8	94.3 ±0.1	95.4	91.1	74.3	31,70
NPS-benzodiazepines						
3-Hydroxyphenazepam	Not reported	97.7 ±0.6	92.5	93.8	90.1	Not reported
4'-Chlorodiazepam	Not reported	98.2 ±0.5	96.5	96.2	93.2	Not reported
Desalkylflurazepam	96.1 – 96.5	95.5 ±1.5	96.1	92.8	91.4	60
Deschloroetizolam	Not reported	87.2 ±1.5	85.8	91.5	89.8	Not reported
Diclazepam	Not reported	93.8 ±1.2	96.5	95.7	97.7	Not reported
Etizolam	Not reported	92.8 ±0.6	90.2	94.7	90.8	Not reported
Flubromazepam	Not reported	96.4 ±0.9	89.0	93.2	93.9	Not reported
Flubromazolam	89	89.5 ±0.4	87.4	91.1	92.2	24
Meclonazepam	Not reported	88.2 ±0.5	93.0	93.0	92.3	Not reported
Phenazepam	Not reported	98.3 ±1.2	94.6	95.6	93.6	Not reported
Pyrazolam	Not reported	78.7 ±0.4	77.6	86.5	94.8	Not reported
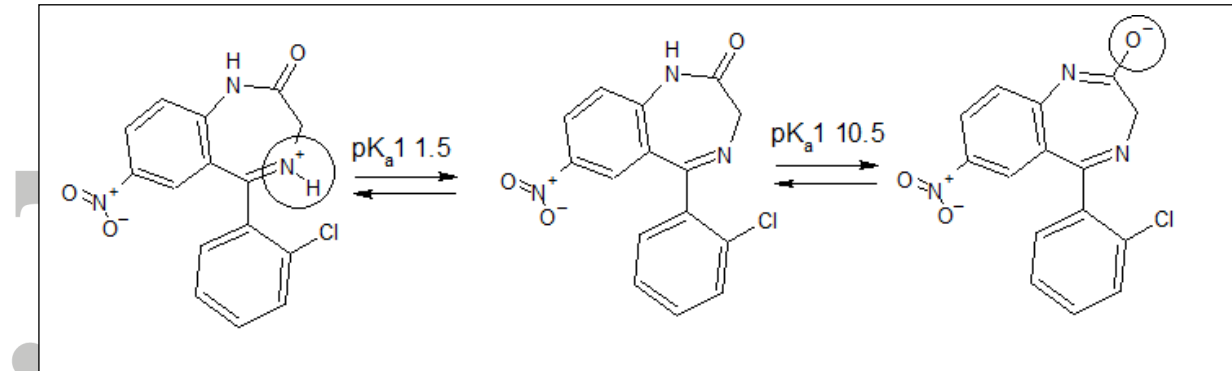
Figure 1. The two sites of deprotonation and corresponding pK$_a$ values for clonazepam